Using Flow Cytometry To Evaluate The Production Of Biopolymers In *Cupriavidus necator*.



UNIVERSITY OF BIRMINGHAM

John Rolley [redacted]

A thesis submitted to the University of Birmingham for the degree of Doctor of Philosophy

School of Chemical Engineering
College of Engineering and Physical Sciences
University of Birmingham
August 2021

UNIVERSITY OF
BIRMINGHAM

University of Birmingham Research Archive

e-theses repository

This unpublished thesis/dissertation is copyright of the author and/or third parties. The intellectual property rights of the author or third parties in respect of this work are as defined by The Copyright Designs and Patents Act 1988 or as modified by any successor legislation.

Any use made of information contained in this thesis/dissertation must be in accordance with that legislation and must be properly acknowledged. Further distribution or reproduction in any format is prohibited without the permission of the copyright holder.

Dedication

This thesis is dedicated to the memory of my Grandparents. Both of my Grandmothers passed away during my studies and I know how much they all would have loved to see me complete my PhD.



Barbara Rolley 1922 - 2014

Bill Rolley 1920 - 1989



Evelyn Glass 1926 - 2019

Tom Glass 1922 - 1985

Acknowledgements

I would like to thank Dr. Tim Overton for giving me the opportunity to do a PhD and for his support and guidance throughout.

I would also like to thank the biochemical engineering technical staff Elaine, Ronnie and David for their assistance.

I am also appreciative to Professor Izabela Radecka and Brian Lynden Johnston for providing me with *Cupriavidus necator* H16.

Thank you to the members of lab F3A for your friendship and support I will miss you all!

And finally, I would like to thank my family and friends without whom this would not have been possible.

COVID-19 statement

Unfortunately, the coronavirus pandemic has severely affected this study. Although a 6-month extension was granted due to the pandemic, difficulties in travelling to the University by train and the reduced oping hours of the University have reduced the amount of work possible. If the pandemic had not occurred experiments involving the evolution of PHA^{++} *C. necator* would have taken place in order to produce an optimised strain of *C. necator* which could have produced P3HB more quickly and in greater quantities. In addition, the COVID pandemic prevented the construction of a PhaP reporter plasmid which would have allowed for the PhaP protein to be quantified during experiments. This data could then have been related to P3HB accumulation and granule cell size determined by analytical disc centrifugation. The pandemic also prevented experiments in which the levels of fructose and gluconate would have been quantified in order to determine the effects of gluconate catabolite repression.

Abstract

Polyhydroxyalkanoates offer a credible solution to the environmental problems caused by non-biodegradable plastics and also have promising medical and consumer applications due to excellent biodegradable and biocompatible properties. This study has explored the production of P(3-hydroxybutyrate) (P3HB) using *Cupriavidus necator* grown in meat extract (ME) media supplemented with fructose and sodium gluconate. This study utilised flow cytometry in a novel manner which allowed the analysis of *C. necator* P3HB content, cell size and cell counts to take place simultaneously on a single-cell basis.

Overall experiments have failed to produce maximum P3HB in a reasonable timeframe of 72 hours due to a lag in P3HB biosynthesis which extends production well beyond 72 hours. The lag phase may have been due to the action of catabolite repression. This study reports for the first time that gluconate suppresses the metabolism of fructose by catabolite repression causing diauxic growth to take place as *C. necator* slowly adapts to fructose metabolism once gluconate is utilised. In comparison to fructose, sodium gluconate-supplemented *C. necator* produce more P3HB on average per cell and per mL of culture. This may be due to gluconate being co-transported across the cell membrane with sodium ions via secondary transport proteins. Fructose-supplemented *C. necator* cultures appear to favour cell division while cultures containing sodium gluconate favour cell expansion. It's likely the uptake of sodium ions also causes sodium gluconate-supplemented *C. necator* to expand by creating an osmotic gradient which causes an influx of H_2O into the cell, and by interacting with peptidoglycan precursors vital for cell expansion.

For the first time a $P3HB^{++}$ population of *C. necator* cells which produces up to 1000 times as much P3HB as the dominant phenotype and comprises less than 5% of the total population, is reported. Evidence shows that the production of $P3HB^{++}$ cells is sensitive to both nutrient and C concentrations. Due to this population's small proportion in cultures, production during exponential growth and small size, it's likely that $P3HB^{++}$ cells are a form of persister cell produced as a survival strategy in case the main population is unable to survive.

Contents

Chapter 1 Introduction 38

1.1 The life cycle of plastics 38

1.1.1 Crude oil distillation 39

1.1.2 Petrochemically derived plastics 41

1.1.3 Routes of plastic disposal 42

1.1.3.1 Recycling 42

1.1.3.2 Disposal to Landfill 44

1.1.3.3 Disposal as litter 44

1.1.3.4 Reuse 45

1.1.3.5 Biodegradation 45

1.1.4 Green alternatives to conventional plastic 46

1.1.4.1 Sustainably sourced non-biodegradable plastics 46

1.1.4.2 Biodegradable plastics derived from petrochemical sources 46

1.1.4.3 Biodegradable plastics derived from green sources 47

1.2 Polyhydroxyalkanoates 48

1.2.1 Intracellular PHA granule structure and function 48

1.2.2 The biosynthesis of P3HB in *C. necator* 50

1.2.3 Polyhydroxyalkanoate-associated proteins 52

1.2.3.1 Phasins - PhaP1 and its regulation by PhaR in *C. necator* 52

1.2.3.2 PhaM in *C. necator* 52

1.2.3.3 Poly-3-hydroxybutyrate synthase in *C. necator* 54

1.2.3.4 Poly-3-hydroxybutyrate depolymerase 54

1.2.3.5 Medium chain length PHA biosynthesis in *Pseudomonas putida* 55

1.2.3.6 Polyhydroxyalkanoate granule associated proteins in *P. putida* 56

1.2.4 Strategies for producing PHAs 58

1.2.4.1 Growth Media 58

1.2.4.2 Fermentation Strategy 58

1.2.4.3 Mechanical and thermal properties of P3HB 59

1.2.4.4 Co-Polymers containing P3HB 62

1.2.4.5 Co-polymers of P3HB genetically engineered *C. necator* and *E. coli* 65

1.2.4.6 Metabolic engineering approaches to *C. necator* 65

1.2.5 Applications of 3HB containing polymers 71

1.2.5.1 Medical Applications 71
1.2.5.2 Food Packaging Applications 73
1.2.5.3 Cosmetic Applications 74
1.2.5.4 Agricultural Applications 74
1.2.6 Extraction of PHAs 74
1.2.6.1 Pre-treatments 75
1.2.6.2 Solvent Extraction 75
1.2.6.3 Chemical Digestion 76
1.2.6.4 Supercritical Fluids 77
1.2.6.5 Enzymatic Digestion 77
1.2.6.6 Mechanical Disruption 78
1.2.7 Methods of PHA analysis 78
1.2.7.1 Dry weight 78
1.2.7.2 Flow Cytometry 79
1.2.7.3 Agar Plate Colony Screening 81
1.2.7.4 Microscopy 81
1.2.7.5 Fourier-transform infrared spectroscopy (FTIR) 82
1.2.7.6 Gas chromatography and GCMS 82
1.2.7.7 Nuclear magnetic resonance 83
1.2.7.8 Differential scanning caliometry 83
1.3 Aims and objectives 84
1.4 Outline of thesis 85
Chapter 2 Materials and Methods 86
2.1 Microbiological culture 86
2.1.1 General laboratory practice 86
2.1.2 Bacterial strains 86
2.1.3 General growth media and culture conditions 86
2.1.4 Long-term glycerol storage of *C. necator* 87
2.1.5 Short-term ME agar storage of *C. necator* 87
2.1.6 Growth of *C. necator* seed cultures 87
2.1.7 Experimental cultures 87
2.1.7.1 Experimental culture supplements 87
2.1.7.2 Batch cultures 88

2.1.7.3 Fed-batch cultures 88
2.1.7.4 Repeated-batch cultures 88
2.2 Analytical techniques 88
2.2.1 Measurements of OD_{600} 88
2.2.2 Flow cytometry 89
2.2.2.1 Flow cytometry staining protocol 1 89
2.2.2.2 Staining optimisation conditions 89
2.2.2.3 Flow cytometry staining protocol 2 90
2.2.3 Fluorescent Microscopy 90
2.2.3.1 Method 1 90
2.2.3.2 Method 2 90
2.3 Statistical Analysis 90
Chapter 3 Results and Discussion 92
3.1 Why does inoculation using a 12-hour seed culture produce multi-cell aggregates? 92
3.1.1 Initial studies use OD_{600} rather than flow cytometry cell counting 93
3.1.2 Seed culture cell density does not influence cell aggregation in experimental cultures. 93
3.1.3 Intracellular P3HB in seed cultures is not linked to persistent clumping in experimental cultures. 95
3.1.4 Seed culture cell size and aggregation are not linked 97
3.1.5 Various *C. necator* morphologies are observed during seed culture growth 98
3.1.6 The impact of cell morphology and nucleic acid staining on the flow cytometry threshold 101
3.1.7 Discussion 102
3.2 Initial *C. necator* ME experimental cultures 103
3.2.1 Increasing ME concentration correlates with increasing OD_{600} 103
3.2.2 More P3HB is produced by *C. necator* in 0.2% (w/v) ME that 0.6% and 0.8% after 48 hours. 105
3.2.3 Cultures of *C. necator* in 0.2% (w/v) ME do not form aggregates 107
3.2.4 Discussion 110

3.3 Growing *C. necator* in ME supplemented with fructose 111

3.3.1 Fructose supplementation significantly increases OD_{600} by a factor of 5 to 15 111

3.3.2 Supplementing with 0.5% (w/v) fructose increases P3HB production most for 0.2% (w/v) ME cultures 113

3.3.3 Cultures of *C. necator* contain a $P3HB^{++}$ super-producing population 118

3.3.4 Increasing the fructose to ME ratio leads to sustained larger cells 124

3.3.5 Cells in the $P3HB^{++}$ population are smaller than $P3HB^{+}$ cells 126

3.3.6 Discussion 128

3.4 Growth of *C. necator* in 0.08% and 0.2% (w/v) ME supplemented with 0.5% (w/v) fructose. 129

3.4.1 Supplementing 0.08% (w/v) ME with fructose increases OD_{600} 130

3.4.2 Reducing the ME concentration to 0.08% (w/v) does not increase P3HB 132

3.4.3 The $P3HB^{++}$ phenotype is influenced by the ME-to-fructose ratio 134

3.4.4 Fructose addition increases intracellular P3HB for the $P3HB^{++}$ population 136

3.4.5 Fructose supplemented 0.08% (w/v) ME cultures produce smaller cells at 4 hours, but larger cells after 24 hours 139

3.4.6 $PH3B^{++}$ cells are also smaller than $P3HB^{+}$ in fructose supplemented 0.08% (w/v) ME 142

3.4.7 Discussion 145

3.5 Increasing fructose concentration in 0.08% (w/v) ME 146

3.5.1 Increasing fructose concentration does not increase OD_{600} 146

3.5.2 Increasing fructose concentration does not increase intracellular P3HB 148

3.5.3 Increasing fructose concentration does not increase the proportion of $P3HB^{++}$ cells 150

3.5.4 Increasing fructose concentration has little impact on intracellular P3HB levels in $P3HB^{+}$ and $P3HB^{++}$ populations. 152

3.5.5 Increasing fructose concentration has little impact on cell size 154

3.5.6 Increasing fructose concentration above 0.5% (w/v) has little effect on cell size FSC 157

3.5.7 Discussion 159

3.6 *Cupriavidus necator* grown in 0.08% (w/v) ME with 0%, 0.6,% 1.2% and 1.6% (w/v) sodium gluconate. 160

3.6.1 At 48 hours,1.1 and 1.6% (w/v) sodium gluconate supplementation leads to higher OD_{600} values than fructose-supplemented cultures 161

3.6.2 Sodium gluconate media supplementation leads to significantly more P3HB than fructose at 48 hours 164
3.6.3 Cultures containing sodium gluconate produce more P3HB^{++} cells 167
3.6.4 Concentration of 0.6% and 1.1% (w/v) sodium gluconate produce increase P3HB per cell in the P3HB^{++} population 170
3.6.5 Sodium gluconate-supplemented cultures produce larger cells than fructose supplemented 173
3.6.6 Sodium gluconate supplementation increases P3HB^{+} cell size considerably 178
3.6.7 Discussion 182

3.7 Optimisation of SYTO62 and P-546 staining for flow cytometry experiments 183

3.7.1 Outcomes of flow cytometry staining optimisation 184
3.7.2 Discussion 186

3.8 Growing *C. necator* cultures for a longer period of time 187

3.8.1 Cell count determined by flow cytometry 188
3.8.2 Cultures supplemented with sodium gluconate produce more P3HB 189
3.8.3 Overall cell size decreases after 72 hours 193
3.8.4 Discussion 195

3.9 Growing *C. necator* in cultures supplemented with fructose for 10 days 196

3.9.1 Fructose-supplemented *C. necator* proliferates whereas sodium gluconate-supplemented *C. necator* elongates 197
3.9.2 After 168 hours sodium gluconate-supplemented cultures produce more P3HB per cell and per mL 200
3.9.3 The P3HB^{++} population likely produces more P3HB per mL but sample size restricts statistical outcomes 204
3.9.4 Cells in the P3HB^{++} population once again have a significantly smaller phenotype in most instances 208
3.9.5 Discussion 211

3.10 Conclusions 212

Chapter 4 Fed-batch *C. necator* cultures using fructose to increase cell number and sodium gluconate to produce P3HB.....213

4.1 Introduction 214

4.2 Does the addition of fructose at 0 hours and sodium gluconate to ME media at 24 hours increase P3HB production? 215

4.2.1 Cell proliferation does not occur in phase 3 215

4.2.2 Greater P-546 fluorescence is recorded in phase 3 217

4.2.3 Cells in 0.4% (w/v) ME cultures decrease in cell size in phase 3 223

4.2.4 Discussion 226

4.3 Attempting to reduce the P3HB production lag time by adding sodium chloride to growth media 227

4.3.1 No significant changes in cell counts are observed as sodium chloride concentration increases between 3 and 15g/L 228

4.3.2 The addition of sodium chloride to media does not prevent the lag time in P3HB production 229

4.3.3 Sodium chloride addition does not alter the influence of decreasing ME concentration on maintaining cell size 235

4.3.4 Discussion 238

4.4 Does changing the growth media at 24 hours move peak P3HB production from phase 3 to phase 2? 239

4.4.1 Increased pH is indicative of amino-acid deamination 239

4.4.2 Little cell proliferation occurs between 72 and 216 hours. 241

4.4.3 Changing to dilute ME media after 24 hours does not produce more P3HB in comparison to batch cultures. 243

4.4.4 Cultures which initially contained 0.2% (w/v) ME and sodium gluconate in changed media decrease mean cell size 249

4.4.5 Discussion 252

4.5 What effect on P3HB production does the simultaneous addition of fructose and sodium gluconate have? 253

4.5.1 Gluconate appears to prevent fructose usage through catabolite repression 254

4.5.2 Combining fructose and sodium gluconate addition leads to high P3HB production in phase 2. 258
4.5.3 Cell size generally decreases between 72 and 168 hours 263
4.5.4 Discussion 266
4.6 Conclusions 267
Chapter 5 Overall Discussion and conclusion 268
5.1 Initial studies varying the C to ME ratio and optimising cell staining for flow cytometry 268
5.2 Cultures of *C. necator* contain a population of P3HB^{++} cells which produce up to 1000 times more P3HB than the dominant P3HB^{+} phenotype 270
5.3 Supplementing cultures with fructose or sodium gluconate has implications on P3HB production, cell proliferation and cell expansion. 271
5.4 A delay causing P3HB production to extend beyond 72 hours may be due to catabolite regulation 273
5.5 Overall conclusions 275
Chapter 6 Future work 276
6.1 Scale-up experiments and different media supplementation 276
6.2 Biomass harvesting, P3HB separation, and P3HB characterisation 276
6.3 Separation of P3HB^{++} cells and directed evolution 276
6.4 Monitoring substrate usage 277
Chapter 7 Bibliography 278
Chapter 8 Appendix 1 314
8.1 Full data corresponding to section 3.1 314
8.2 Full data corresponding to section 3.2 315
8.3 Raw data corresponding to section 3.3 316

8.4 Full data corresponding to section 3.3 319

8.5 Full data corresponding to section 3.5 322

8.6 Full data corresponding to section 3.6 325

8.7 Full data corresponding to fructose and sodium gluconate comparisons in section 3.6 328

8.8 Full data corresponding to section 3.7 332

8.9 Full data corresponding to section 3.8 333

8.10 Full data corresponding to section 3.9 337

8.11 Comparisons between fructose and sodium gluconate supplementation corresponding to section 3.9 342

Chapter 9 - Appendix 2 (raw data corresponding to chapter 4) 344

9.1 Raw data corresponding to section 4.2 344

9.2 Raw data corresponding to section 4.3 349

9.3 Full data corresponding to section 4.4 354

9.4 Data corresponding to section 4.5..... 359

List of figures

Figure 1.1 - The distillation and application of crude oil fractions illustrate the relationship between hydrocarbon boiling point, chain length and application. Adapted from (PSAC, 2021). 39

Figure 1.2 - Example steam cracking reactions which produce by far the most common precursors for plastic production, ethylene and propene. 40

Figure 1.3 - General chemical structure of PHA monomer units where n is the number of repeating units. 49

Figure 1.4 - A diagram illustrating the gene positions and direction of transcription of the *C. necator phaCAB* operon responsible for the intracellular production of P3HB in addition to the genes responsible for the transcription of other key PGAPs in *C. necator*. 50

Figure 1.5 - The biosynthetic pathway of the *phaCAB* operon in *C. necator* responsible for the production of intracellular PH3B. n represents the number of repeating units. Adapted from Verlinden *et al*. (2007). 51

Figure 1.6 - The transcriptional regulation of PhaP1 in *C. necator* by PhaR during P3HB-promoting and non-P3HB-promoting conditions. (a) When growth-promoting levels of key nutrients are available PhaR binds to the promotor region of *phaP* and *phaR*. (b) During growth-limiting nutrient conditions, PhaR detaches from the *phaP* and *phaR* promotors migrate to the newly forming P3HB granules allowing transcription to proceed. (c) Granule formation with PGAP matrix dictating granule formation. (d) When nutrient-promoting conditions return P3HB granules are depolymerisation by PhaZ which releases bound PhaR which binds to the *phaP* and *phaR* promotors once again inhibiting transcription. 53

Figure 1.7 - Diagram illustrating the genomic positions and direction of translation of the genes involved in the *phaCIZC2D* (grey) and *phaFI* (blue) operons in *P. putida*. 56

Figure 1.8 - A summary of the molecular pathways linked to MCL-PHA production in *P. putida* K12440. PhaJ = (R)-specific enoyl-CoA hydratase. PhaG = transacylase. PhaC = PHA synthase I and II. Adapted from Magdouli *et al*. (2015) and Mozejko-Ciesielska *et al*., (2019). n represents the number of repeating units..... 57

Figure 1.9 - A simplified illustration of the BD Accuri™ C6 flow cytometer used in this study. 80

Figure 3.1 – Summary of mean OD_{600} for 0.8% (w/v) ME *C. necator* seed cultures, compared at 12 and 24-hour time points. Statistical significance was determined using a paired t-test to compare the same condition at different time points. NS = non-significant ($p \geq 0.05$). Error bars represent SD. n = 4 biological replicates. The full data can be found in Figure 8.1 (a) in Appendix 8.1. 94

Figure 3.2 – Summary of mean P-546 fluorescence (P3HB) of 0.8% (w/v) ME *C. necator* seed cultures compared at 12 and 24-hour time points. Statistical significance was determined using a paired t-test to compare the same condition at different time points. NS = non-significant ($p \geq 0.05$). Error bars represent SD. n = 4 biological replicates. The full data can be found in Figure 8.1 (b), Appendix 8.1. 96

Figure 3.3 – Summary of mean FSC of 0.8% (w/v) ME *C. necator* seed cultures compared at 12 and 24 hour time points. Statistical significance was determined using a paired t-test to compare the same condition at different time points. NS = non-significant ($p \geq 0.05$). Error bars represent SD. n = 4 biological replicates. The full data can be found in Figure 8.1 (c), Appendix 8.1. 97

FIGURE 3.4 - FLUORESCENT MICROSCOPY IMAGES AND THE CORRESPONDING FSC HISTOGRAMS DEPICTING DIFFERENT *C. NECATOR* MORPHOLOGIES OBSERVED IN 0.8% (W/V) ME SEED CULTURES. ON THE LEFT OF THE FIGURE ARE HISTOGRAMS SHOWING THE FSC OF EACH INDIVIDUAL REPLICATE. ON THE RIGHT ARE THE CORRESPONDING FLUORESCENT MICROSCOPE IMAGES OF *C. NECATOR* CELLS AT VARIOUS TIME POINTS. CELLS WERE STAINED WITH 1.33 MM SYTO9 FOR MICROSCOPY AND SEPARATELY STAINED WITH SYTO62 (5 MM) AND P-546 (1 MM) FOR FLOW CYTOMETRY. SCALE BARS REPRESENT 10 MM. FOR FSC HISTOGRAMS N=4 BIOLOGICAL REPLICATES. 100

FIGURE 3.5 - VISUALISING THE THEORETICAL IMPLICATIONS ON FLOW CYTOMETRY RESULTS USING THE SYTO62 FLUORESCENCE AS A THRESHOLD COMPARED TO FSC. SCALE BAR REPRESENTS 5 μM. CELLS WERE STAINED WITH 1.33 MM SYTO9. 101

FIGURE 3.6 - COMPARISON OF MEAN OD_{600} OF *C. NECATOR* CULTURES GROWN IN 0.2%, 0.4%, 0.6% AND 0.8% (W/V) ME AT 10 AND 48-HOUR TIME POINTS. PLOT (A) COMPARES OD_{600} AT 10 AND 48 HOURS AND INCLUDES ANNOTATIONS REPRESENTING STATISTICAL SIGNIFICANCE DETERMINED BY PAIRED T-TESTS. TABLE (B) CONTAINS STATISTICAL COMPARISONS BETWEEN EACH ME CONDITION AT 10 AND 48 HOURS, DETERMINED BY NON-PAIRED T-TESTS. NS = NON-SIGNIFICANT ($P \geq 0.05$), * = $P < 0.05$, ** = $P \leq 0.01$, *** = $P \leq 0.001$, **** = $P \leq 0.0001$. TREND LINES WERE CALCULATED USING LINEAR REGRESSION. R^2 REPRESENTS THE COEFFICIENT OF DETERMINATION. ERROR BARS REPRESENT SD. N = 3 BIOLOGICAL REPLICATES. THE FULL DATA IS DISPLAYED IN FIGURE 8.2 (A), APPENDIX 8.2. 104

FIGURE 3.7 - COMPARISON OF MEAN P-546 FLUORESCENCE (P3HB) PER CELL OF *C. NECATOR* CULTURES GROWN IN 0.2%, 0.4%, 0.6% AND 0.8% (W/V) ME AT 10 AND 48-HOUR TIME POINTS. PLOT (A) COMPARES P-546 FLUORESCENCE (P3HB) PER CELL AT 6 AND 48 HOURS AND INCLUDES ANNOTATIONS REPRESENTING STATISTICAL SIGNIFICANCE DETERMINED BY PAIRED T-TESTS. TABLE (B) CONTAINS STATISTICAL COMPARISONS BETWEEN EACH ME CONDITION AT EACH TIME POINT DETERMINED BY NON-PAIRED T-TESTS. NS = NON-SIGNIFICANT ($P \geq 0.05$), * = $P < 0.05$, ** = $P \leq 0.01$, *** = $P \leq 0.001$. ERROR BARS REPRESENT SD. N = 3 BIOLOGICAL REPLICATES. THE FULL DATA IS LOCATED IN FIGURE 8.2 (B), APPENDIX 8.2. 106

FIGURE 3.8 - COMPARISON OF MEAN FSC (CELL SIZE) OF *C. NECATOR* CULTURES GROWN IN 0.2%, 0.4%, 0.6% AND 0.8% (W/V) ME AT 6 AND 48-HOUR TIME POINTS. PLOT (A) COMPARES FSC AT 6 AND 48 HOURS AND INCLUDES ANNOTATIONS REPRESENTING STATISTICAL SIGNIFICANCE DETERMINED BY PAIRED T-TESTS. TABLE (B) CONTAINS STATISTICAL COMPARISONS BETWEEN EACH ME CONDITION AT EACH TIME POINT DETERMINED BY NON-PAIRED T-TESTS. NS = NON-SIGNIFICANT ($P \geq 0.05$), * = $P < 0.05$, ** = $P \leq 0.01$. ERROR BARS REPRESENT SD. N = 3 BIOLOGICAL REPLICATES. THE FULL DATA CAN BE FOUND IN FIGURE 8.2 (C), APPENDIX 8.2. 108

FIGURE 3.9 - FLUORESCENT MICROSCOPE IMAGES SHOWING VARIABLE *C. NECATOR* AGGREGATION AFTER 6 HOURS OF GROWTH IN 0.2%, 0.4%, 0.6% AND 0.8% (W/V) ME ACCOMPANIED BY CORRESPONDING FSC HISTOGRAMS. CELLS WERE STAINED WITH 1.33 MM SYTO9. SCALE BARS REPRESENT 10 μM. N=3 BIOLOGICAL REPLICATES FOR HISTOGRAMS. 109

FIGURE 3.10 - GRAPHS AND STATISTICAL ANALYSIS COMPARING THE OD_{600} OF *C. NECATOR* CULTURES GROWN IN 0.2%, 0.4%, 0.6% AND 0.8% (W/V) ME WITH AND WITHOUT 0.5% (W/V) FRUCTOSE. STATISTICAL ANALYSIS WAS PERFORMED USING UNPAIRED T-TESTS TO EVALUATE THE SAME ME CONCENTRATION WITH AND WITHOUT FRUCTOSE SUPPLEMENTATION AT 24 HOURS (ANNOTATIONS IN PLOT (A)) AND 48 HOURS (ANNOTATIONS IN PLOT (B)), AND ALSO TO COMPARE EACH FRUCTOSE-SUPPLEMENTED CONDITION AT EACH TIME POINT (C). ADDITIONAL STATISTICAL ANALYSIS WAS PERFORMED USING PAIRED T-TESTS IN ORDER TO COMPARE THE SAME CONDITION AT DIFFERENT TIME POINTS (D). NS = NON-SIGNIFICANT ($P \geq 0.05$), * = $P <$

0.05, ** = P ≤ 0.01, *** = P ≤ 0.001. ERROR BARS REPRESENT SD. N = 3 BIOLOGICAL REPLICATES. THE FULL DATA CAN BE FOUND IN FIGURE 8.3, APPENDIX 8.3. 112

FIGURE 3.11- GRAPHS AND STATISTICAL ANALYSIS COMPARING THE P-546 FLUORESCENCE (P3HB) PER CELL OF *C. NECATOR* CULTURES GROWN IN 0.2%, 0.4%, 0.6% AND 0.8% (W/V) ME AND WITH AND WITHOUT 0.5% (W/V) FRUCTOSE. STATISTICAL ANALYSIS WAS PERFORMED USING UNPAIRED T-TESTS TO EVALUATE THE SAME ME CONCENTRATION WITH AND WITHOUT FRUCTOSE SUPPLEMENTATION AT 4, 24 AND 48 HOURS (ANNOTATIONS IN PLOTS (A), (B) AND (C) RESPECTIVELY) AND ALSO TO COMPARE EACH FRUCTOSE-SUPPLEMENTED CONDITION (D). ADDITIONAL STATISTICAL ANALYSIS WAS PERFORMED USING A PAIRED T-TEST IN ORDER TO COMPARE THE SAME FRUCTOSE-SUPPLEMENTED CONDITION AT DIFFERENT TIME POINTS (E). NS = NON-SIGNIFICANT (P ≥ 0.05), * = P < 0.05, ** = P ≤ 0.01, *** = P ≤ 0.001. ERROR BARS REPRESENT SD. N = 3 BIOLOGICAL REPLICATES. THE FULL DATA CAN BE FOUND IN FIGURE 8.4 (A) APPENDIX 8.3. 115

FIGURE 3.12 – GRAPH DISPLAYING THE MEAN FSC AND MEAN P-546 FLUORESCENCE (P3HB) AT 24 HOURS FOR C. NECATOR CULTURES CONTAINING 0.2%, 0.4%, 0.6% AND 0.8% (W/V) ME AND SUPPLEMENTED WITH 0.5% FRUCTOSE. R^2 REPRESENTS THE COEFFICIENT OF DETERMINATION. ERROR BARS REPRESENT SD. N = 3 BIOLOGICAL REPLICATES. THE FULL DATA FOR MEAN P-546 FLUORESCENCE CAN BE FOUND IN FIGURE 8.4 (A), APPENDIX 8.3. THE FULL MEAN FSC DATA CAN BE FOUND IN FIGURE 8.5 (A), APPENDIX 8.3. 116

FIGURE 3.13 – FLUORESCENT MICROSCOPE IMAGES AND CORRESPONDING FSC HISTOGRAMS SHOWING *C. NECATOR* CELLS AFTER 24 HOURS OF GROWTH IN 0.2%, 0.4%, 0.6% AND 0.8% (W/V) ME AND SUPPLEMENTED WITH 0.5% FRUCTOSE. CELLS IN MICROSCOPE IMAGES WERE STAINED WITH 1.33 MM SYTO9. SCALE BARS REPRESENT 10 μM. N=3 BIOLOGICAL REPLICATES FOR FSC HISTOGRAMS. 117

FIGURE 3.14 - FLOW CYTOMETRY GATING STRATEGY USED TO MONITOR THE P3HB^{++} POPULATION. THIS EXAMPLE PLOT REPRESENTS THE FIRST REPLICATE OF THE 0.2% (W/V) ME SUPPLEMENTED WITH 0.5% (W/V) FRUCTOSE CONDITION SUMMARISED IN FIGURE 3.11 (B). 121

FIGURE 3.15 - GRAPHS AND STATISTICAL ANALYSIS COMPARING THE PROPORTION OF P3HB^{++} CELLS OF *C. NECATOR* CELLS CULTURED IN 0.2%, 0.4%, 0.6% AND 0.8% (W/V) ME AND SUPPLEMENTED WITH 0.5% (W/V) FRUCTOSE WITH COMPARISON TO CULTURES WITHOUT FRUCTOSE SUPPLEMENTATION. STATISTICAL ANALYSIS WAS PERFORMED USING UNPAIRED T-TESTS. IN PLOTS (A), (B) AND (C), ANNOTATIONS SHOW THE STATISTICAL COMPARISONS BETWEEN SAMPLES WITH AND WITHOUT 0.5% (W/V) FRUCTOSE ADDITION. TABLE (D) CONTAINS STATISTICAL COMPARISONS OF EACH FRUCTOSE-SUPPLEMENTED CONDITION. TABLE (E) STATISTICALLY COMPARES SAMPLES AT DIFFERENT TIME POINTS FOR FRUCTOSE-SUPPLEMENTED SAMPLES ONLY. NS = NON-SIGNIFICANT (P ≥ 0.05), * = P < 0.05, ** = P ≤ 0.01. ERROR BARS REPRESENT SD. N = 3 BIOLOGICAL REPLICATES. THE FULL DATA CAN BE FOUND IN FIGURE 8.4 (C), APPENDIX 8.3 122

FIGURE 3.16 - GRAPHS AND STATISTICAL ANALYSIS COMPARING THE MEAN P-546 FLUORESCENCE (P3HB) OF THE P3HB^{+} AND P3HB^{++} POPULATIONS FOR *C. NECATOR* CELLS CULTURED IN 0.2%, 0.4%, 0.6% AND 0.8% (W/V) ME AND SUPPLEMENTED WITH 0.5% FRUCTOSE. STATISTICAL ANALYSIS WAS PERFORMED USING UNPAIRED T-TESTS TO EVALUATE THE SAME ME CONCENTRATION WITH AND WITHOUT FRUCTOSE SUPPLEMENTATION (ANNOTATIONS IN PLOTS (A), (B) AND (C)) AND ALSO TO COMPARE EACH FRUCTOSE-SUPPLEMENTED CONDITION (D). ADDITIONAL STATISTICAL ANALYSIS WAS PERFORMED USING A PAIRED T-TEST IN ORDER TO COMPARE THE SAME CONDITION AT DIFFERENT TIME POINTS (E). NS = NON-SIGNIFICANT (P ≥

0.05), * = P < 0.05, ** = P ≤ 0.01, *** = P ≤ 0.001. ERROR BARS REPRESENT SD. N = 3 BIOLOGICAL REPLICATES. THE FULL DATA IS DISPLAYED IN FIGURE 8.4 (C), APPENDIX 8.3. 123

FIGURE 3.17 - GRAPHS AND STATISTICAL ANALYSIS COMPARING THE MEAN FSC (CELL SIZE) OF *C. NECATOR* CELLS CULTURED IN 0.2%, 0.4%, 0.6% AND 0.8% (W/V) ME AND SUPPLEMENTED WITH 0.5% FRUCTOSE WITH COMPARISON TO CULTURES WITHOUT FRUCTOSE SUPPLEMENTATION. STATISTICAL ANALYSIS WAS PERFORMED USING UNPAIRED T-TESTS TO EVALUATE THE SAME ME CONCENTRATION WITH AND WITHOUT FRUCTOSE SUPPLEMENTATION (ANNOTATIONS IN PLOTS (A), (B) AND (C)) AND ALSO TO COMPARE EACH FRUCTOSE-SUPPLEMENTED CONDITION (D). ADDITIONAL STATISTICAL ANALYSIS WAS PERFORMED USING A PAIRED T-TEST IN ORDER TO COMPARE THE SAME CONDITION AT DIFFERENT TIME POINTS (E). NS = NON-SIGNIFICANT (P ≥ 0.05), * = P < 0.05, ** = P ≤ 0.01, *** = P ≤ 0.001, **** = P ≤ 0.0001, ***** = P ≤ 0.00001. ERROR BARS REPRESENT SD. N = 3 BIOLOGICAL REPLICATES. LARGE ERROR BAR IN PLOT (B) FOR 0.8% (W/V) ME SAMPLES DUE TO AIR IN THE FLOW CYTOMETRY SYSTEM. THE FULL DATA CAN BE FOUND IN FIGURE 8.5 (A), APPENDIX 8.3. 125

FIGURE 3.18 - GRAPHS AND STATISTICAL ANALYSIS COMPARING THE MEAN FSC (CELL SIZE) OF THE $P3HB^{+}$ AND $P3HB^{++}$ POPULATIONS FOR *C. NECATOR* CELLS CULTURED IN 0.2%, 0.4%, 0.6% AND 0.8% (W/V) ME AND SUPPLEMENTED WITH 0.5% (W/V) FRUCTOSE. STATISTICAL ANALYSIS WAS PERFORMED USING UNPAIRED T-TESTS TO EVALUATE THE SAME ME CONCENTRATION WITH AND WITHOUT FRUCTOSE SUPPLEMENTATION (ANNOTATIONS IN PLOTS (A), (B) AND (C)) AND ALSO TO COMPARE EACH FRUCTOSE-SUPPLEMENTED CONDITION (D). ADDITIONAL STATISTICAL ANALYSIS WAS PERFORMED USING A PAIRED T-TEST IN ORDER TO COMPARE THE SAME CONDITION AT DIFFERENT TIME POINTS (E). NS = NON-SIGNIFICANT (P ≥ 0.05), * = P < 0.05, ** = P ≤ 0.01, *** = P ≤ 0.001, **** = P ≤ 0.0001, ***** = P ≤ 0.00001. ERROR BARS REPRESENT SD. N = 3 BIOLOGICAL REPLICATES. THE FULL DATA COLLECTED CAN BE FOUND IN FIGURE 8.5 (A), APPENDIX 8.3. 127

FIGURE 3.19 - GRAPHS AND STATISTICAL ANALYSIS COMPARING THE MEAN OD_{600} OF *C. NECATOR* CULTURES GROWN IN 0.08% AND 0.2% (W/V) ME WITH AND WITHOUT 0.5% (W/V) FRUCTOSE SUPPLEMENTATION. STATISTICAL ANALYSIS WAS PERFORMED USING UNPAIRED T-TESTS TO EVALUATE THE SAME ME CONCENTRATION WITH AND WITHOUT FRUCTOSE SUPPLEMENTATION (INDICATED BY) ANNOTATIONS IN PLOTS (A) AND (B)) AND ALSO TO COMPARE CONDITIONS AT EACH TIME POINT (D). ADDITIONAL STATISTICAL ANALYSIS WAS PERFORMED USING PAIRED T-TESTS IN ORDER TO COMPARE THE SAME CONDITION AT DIFFERENT TIME POINTS (D). NS = NON-SIGNIFICANT (P ≥ 0.05), * = P < 0.05, ** = P ≤ 0.01, *** = P ≤ 0.001, **** = P ≤ 0.0001, ***** = P ≤ 0.00001. ERROR BARS REPRESENT SD. N = 3 BIOLOGICAL REPLICATES. THE FULL DATA IS LOCATED IN FIGURE 8.6, APPENDIX 8.4. 131

FIGURE 3.20 - GRAPHS AND STATISTICAL ANALYSIS COMPARING THE MEAN P-546 FLUORESCENCE (P3HB) OF *C. NECATOR* CULTURES GROWN IN 0.08% AND 0.2% (W/V) ME WITH AND WITHOUT 0.5% (W/V) FRUCTOSE SUPPLEMENTATION. STATISTICAL ANALYSIS WAS PERFORMED USING UNPAIRED T-TESTS TO EVALUATE THE SAME ME CONCENTRATION WITH AND WITHOUT FRUCTOSE SUPPLEMENTATION (ANNOTATIONS IN PLOTS (A), (B) AND (C)) AND ALSO TO COMPARE CONDITIONS AT EACH TIME POINT (D). ADDITIONAL STATISTICAL ANALYSIS WAS PERFORMED USING A PAIRED T-TEST IN ORDER TO COMPARE THE SAME CONDITION AT DIFFERENT TIME POINTS (E). NS = NON-SIGNIFICANT (P ≥ 0.05), * = P < 0.05, ** = P ≤ 0.01, *** = P ≤ 0.001. ERROR BARS REPRESENT SD. N = 3 BIOLOGICAL REPLICATES. THE FULL DATA CAN BE FOUND IN FIGURE 8.7 (A) AND (B), APPENDIX 8.4. 133

FIGURE 3.21 - GRAPHS AND STATISTICAL ANALYSIS COMPARING THE MEAN PERCENTAGE OF P3HB^{++} CELLS IN *C. NECATOR* CULTURES GROWN IN 0.08% AND 0.2% (W/V) ME WITH AND WITHOUT 0.5% (W/V) FRUCTOSE SUPPLEMENTATION. STATISTICAL ANALYSIS WAS PERFORMED USING UNPAIRED T-TESTS TO EVALUATE THE SAME ME CONCENTRATION WITH AND WITHOUT FRUCTOSE SUPPLEMENTATION (ANNOTATIONS IN PLOTS (A), (B) AND (C)) AND ALSO TO COMPARE SAMPLES CONTAINING NON-SUPPLEMENTED 0.08% ME CULTURES TO OTHER CONDITIONS (D). ADDITIONAL STATISTICAL ANALYSIS WAS PERFORMED USING A PAIRED T-TEST IN ORDER TO COMPARE CONDITIONS AT EACH TIME POINT (E). NS = NON-SIGNIFICANT ($P \geq 0.05$), * = $P < 0.05$, ** = $P \leq 0.01$, *** = $P \leq 0.001$. ERROR BARS REPRESENT SD. N = 3 BIOLOGICAL REPLICATES. THE FULL DATA CAN BE FOUND IN FIGURE 8.4 (B) AND (C), APPENDIX 8.4. 135

FIGURE 3.22 - GRAPHS AND STATISTICAL ANALYSIS COMPARING THE MEAN P-546 FLUORESCENCE (P3HB) OF THE P3HB^{+} AND P3HB^{++} *C. NECATOR* POPULATIONS WHEN GROWN IN 0.08% AND 0.2% (W/V) ME WITH AND WITHOUT 0.5% (W/V) FRUCTOSE SUPPLEMENTATION. STATISTICAL ANALYSIS WAS PERFORMED USING UNPAIRED T-TESTS TO EVALUATE THE SAME ME CONCENTRATION WITH AND WITHOUT FRUCTOSE SUPPLEMENTATION (ANNOTATIONS IN PLOTS (A), (B) AND (C)) AND ALSO TO COMPARE EACH CONDITION (D). ADDITIONAL STATISTICAL ANALYSIS WAS PERFORMED USING A PAIRED T-TEST IN ORDER TO COMPARE THE SAME CONDITIONS AT EACH TIME POINT (E). NS = NON-SIGNIFICANT ($P \geq 0.05$), * = $P < 0.05$, ** = $P \leq 0.01$, *** = $P \leq 0.001$.THE FULL DATA CAN BE FOUND IN FIGURE 8.7 (E) AND (F), APPENDIX 8.4. 138

FIGURE 3.23 - GRAPHS AND STATISTICAL ANALYSIS COMPARING THE MEAN FSC OF *C. NECATOR* CULTURES GROWN IN 0.08% AND 0.2% (W/V) ME WITH AND WITHOUT 0.5% (W/V) FRUCTOSE SUPPLEMENTATION. STATISTICAL ANALYSIS WAS PERFORMED USING UNPAIRED T-TESTS TO EVALUATE THE SAME ME CONCENTRATION WITH AND WITHOUT FRUCTOSE SUPPLEMENTATION (ANNOTATIONS IN PLOTS (A), (B) AND (C)) AND ALSO TO COMPARE EACH CONDITION (D). ADDITIONAL STATISTICAL ANALYSIS WAS PERFORMED USING A PAIRED T-TEST IN ORDER TO COMPARE THE SAME COMPARE CONDITIONS AT EACH TIME POINT (E). NS = NON-SIGNIFICANT ($P \geq 0.05$), * = $P < 0.05$, ** = $P \leq 0.01$, *** = $P \leq 0.001$, **** = $P \leq 0.0001$. ERROR BARS REPRESENT SD. N = 3 BIOLOGICAL REPLICATES. THE FULL DATA CAN BE FOUND IN FIGURE 8.8 (A) AND (B), APPENDIX 8.4. 141

FIGURE 3.24 - GRAPHS AND STATISTICAL ANALYSIS COMPARING THE MEAN FSC OF THE P3HB^{+} AND P3HB^{++} *C. NECATOR* POPULATIONS WHEN GROWN IN 0.08% AND 0.2% (W/V) ME WITH AND WITHOUT 0.5% (W/V) FRUCTOSE SUPPLEMENTATION. STATISTICAL ANALYSIS WAS PERFORMED USING UNPAIRED T-TESTS TO EVALUATE THE SAME ME CONCENTRATION WITH AND WITHOUT FRUCTOSE SUPPLEMENTATION (ANNOTATIONS IN PLOTS (A), (B) AND (C)) AND ALSO TO COMPARE EACH CONDITION (D). ADDITIONAL STATISTICAL ANALYSIS WAS PERFORMED USING A PAIRED T-TEST IN ORDER TO COMPARE THE SAME CONDITION AT DIFFERENT TIME POINTS (E). NS = NON-SIGNIFICANT ($P \geq 0.05$), * = $P < 0.05$, ** = $P \leq 0.01$, *** = $P \leq 0.001$, **** = $P \leq 0.0001$ ERROR BARS REPRESENT SD. N = 3 BIOLOGICAL REPLICATES. THE FULL DATA CAN BE FOUND IN FIGURE 7.8 (C) AND (D), APPENDIX 8.4. 144

FIGURE 3.25 - GRAPHS AND STATISTICAL ANALYSIS COMPARING THE MEAN OD_{600} OF *C. NECATOR* CULTURES GROWN IN 0.08% (W/V) ME AND SUPPLEMENTED WITH 0%, 0.5%, 1% AND 1.5% (W/V) FRUCTOSE. MEAN OD_{600} AT 24 (A) AND 48 HOURS (B) IS ANALYSED STATISTICALLY USING UNPAIRED T-TESTS TO COMPARE CONDITIONS AT THE SAME TIME POINT (C), AND PAIRED T-TESTS TO COMPARE CONDITIONS AT DIFFERENT TIME POINTS (D). NS = NON-SIGNIFICANT ($P \geq 0.05$), * = $P < 0.05$, ** = $P \leq 0.01$, *** = $P \leq 0.001$, **** = $P \leq 0.0001$. ERROR BARS REPRESENT SD. N = 3 BIOLOGICAL REPLICATES. THE FULL DATA IS LOCATED IN FIGURE 8.9, APPENDIX 8.5. 147

FIGURE 3.26 - GRAPHS AND STATISTICAL ANALYSIS COMPARING THE MEAN P-546 FLUORESCENCE (P3HB) OF *C. NECATOR* CULTURES GROWN IN 0.08% (W/V) ME AND SUPPLEMENTED WITH 0%, 0.5%, 1% AND 1.5% (W/V) FRUCTOSE. MEAN P-546 FLUORESCENCE AT 4 (A), 24 (B) AND 48 HOURS (C) IS ANALYSED STATISTICALLY USING UNPAIRED T-TESTS TO COMPARE CONDITIONS AT THE SAME TIME POINT (D), AND PAIRED T-TESTS TO COMPARE CONDITIONS AT DIFFERENT TIME POINTS (E). NS = NON-SIGNIFICANT ($P \geq 0.05$), * = $P < 0.05$, ** = $P \leq 0.01$, *** = $P \leq 0.001$. ERROR BARS REPRESENT SD. N = 3 BIOLOGICAL REPLICATES. THE FULL DATA CAN BE FOUND IN FIGURE 8.10 (A) AND (B), APPENDIX 8.5. 149

FIGURE 3.27 - GRAPHS AND STATISTICAL ANALYSIS COMPARING THE MEAN PERCENTAGE OF P3HB^{++} CELLS IN *C. NECATOR* CULTURES GROWN IN 0.08% (W/V) ME AND SUPPLEMENTED WITH 0%, 0.5%, 1% AND 1.5% (W/V) FRUCTOSE. THE MEAN PROPORTION OF P3HB^{++} CELLS AT 4 (A), 24 (B) AND 48 HOURS (C) IS ANALYSED STATISTICALLY USING UNPAIRED T-TESTS TO COMPARE CONDITIONS AT THE SAME TIME POINT (D), AND PAIRED T-TESTS TO COMPARE CONDITIONS AT DIFFERENT TIME POINTS (E). NS = NON-SIGNIFICANT ($P \geq 0.05$), * = $P < 0.05$. ERROR BARS REPRESENT SD. N = 3 BIOLOGICAL REPLICATES. THE FULL DATA CAN BE FOUND IN FIGURE 8.10 (A) AND (B), APPENDIX 8.5. 151

FIGURE 3.28 - GRAPHS AND STATISTICAL ANALYSIS OF THE MEAN P-546 FLUORESCENCE (P3HB) OF THE P3HB^{+} AND P3HB^{++} *C. NECATOR* POPULATIONS WHEN GROWN IN 0.08% (W/V) ME AND SUPPLEMENTED WITH 0%, 0.5%, 1% AND 1.5% (W/V) FRUCTOSE. THE MEAN P-546 FLUORESCENCE OF CELLS IN THE P3HB^{+} AND P3HB^{++} POPULATIONS AT 4 (A), 24 (B) AND 48 HOURS (C) IS ANALYSED STATISTICALLY USING UNPAIRED T-TESTS TO COMPARE CONDITIONS AT THE SAME TIME POINT (D). ADDITIONAL STATISTICAL ANALYSIS WAS PERFORMED USING A PAIRED T-TEST TO COMPARE THE SAME CONDITION AT DIFFERENT TIME POINTS (E). NS = NON-SIGNIFICANT ($P \geq 0.05$), * = $P < 0.05$, ** = $P \leq 0.01$, *** = $P \leq 0.001$, **** = $P \leq 0.0001$, ***** = $P \leq 0.00001$. ERROR BARS REPRESENT SD. N = 3 BIOLOGICAL REPLICATES. THE FULL DATA CAN BE FOUND IN FIGURE 8.10 (E) AND (F), APPENDIX 8.5. 153

FIGURE 3.29 - GRAPHS AND STATISTICAL ANALYSIS COMPARING THE MEAN FSC OF *C. NECATOR* CULTURES GROWN IN 0.08% (W/V) ME AND SUPPLEMENTED WITH 0%, 0.5%, 1% AND 1.5% (W/V) FRUCTOSE. MEAN FSC AT 4 (A), 24 (B) AND 48 HOURS (C) IS ANALYSED STATISTICALLY USING UNPAIRED T-TESTS TO COMPARE CONDITIONS AT THE SAME TIME POINT (D). ADDITIONAL STATISTICAL ANALYSIS WAS PERFORMED USING A PAIRED T-TEST IN ORDER TO COMPARE THE SAME CONDITION AT DIFFERENT TIME POINTS (E). NS = NON-SIGNIFICANT ($P \geq 0.05$), * = $P < 0.05$, ** = $P \leq 0.01$, *** = $P \leq 0.001$. ERROR BARS REPRESENT SD. N = 3 BIOLOGICAL REPLICATES. THE FULL DATA CAN BE FOUND IN FIGURE 8.11 (A) AND (B), APPENDIX 8.5..... 155

FIGURE 3.30 - FLUORESCENT MICROSCOPY IMAGES OF CELLS AFTER 54 HOURS OF GROWTH IN 0.08% (W/V) ME SUPPLEMENTED WITH 0, 0.5, 1 AND 1.5% (W/V) FRUCTOSE. CELLS WERE STAINED WITH SYTO9 (1.33 MM). SCALE BARS REPRESENT 2 µM. 156

FIGURE 3.31 - GRAPHS AND STATISTICAL ANALYSIS SHOWING THE MEAN FSC OF THE P3HB^{+} AND P3HB^{++} *C. NECATOR* POPULATIONS WHEN GROWN IN 0.08% (W/V) ME AND SUPPLEMENTED WITH 0%, 0.5%, 1% AND 1.5% (W/V) FRUCTOSE. THE FSC OF CELLS IN THE P3HB^{+} AND P3HB^{++} POPULATIONS AT 4 (A), 24 (B) AND 48 HOURS (C) IS ANALYSED STATISTICALLY USING UNPAIRED T-TESTS TO COMPARE CONDITIONS AT THE SAME TIME POINT (D). ADDITIONAL STATISTICAL ANALYSIS WAS PERFORMED USING A PAIRED T-TEST TO COMPARE THE SAME CONDITION AT DIFFERENT TIME POINTS (E). NS = NON-SIGNIFICANT ($P \geq 0.05$), * = $P < 0.05$, ** = $P \leq 0.01$, *** = $P \leq 0.001$, **** = $P \leq 0.0001$. ERROR BARS REPRESENT SD. N = 3 BIOLOGICAL REPLICATES. THE FULL DATA CAN BE FOUND IN FIGURE 8.11(C) AND (D), APPENDIX 8.5. 158

FIGURE 3.32 - GRAPHS AND STATISTICAL ANALYSIS SHOWING THE OD_{600} OF 0.08% (W/V) ME *C. NECATOR* CULTURES SUPPLEMENTED WITH 0%, 0.6%, 1.1% OR 1.6% (W/V) SODIUM GLUCONATE. STATISTICAL ANALYSIS WAS PERFORMED USING UNPAIRED T-TESTS TO COMPARE INDIVIDUAL SODIUM GLUCONATE CONCENTRATIONS AT THE SAME TIME POINT (C) AND PAIRED T-TESTS TO COMPARE THE SAME CONDITION AT DIFFERENT TIME POINTS (D). NS = NON-SIGNIFICANT ($P \geq 0.05$), * = $P \leq 0.05$, ** = $P \leq 0.01$, *** = $P \leq 0.001$. ERROR BARS REPRESENT SD. N = 3 BIOLOGICAL REPLICATES. THE FULL DATA CAN BE FOUND IN FIGURE 8.12, APPENDIX 8.6. 162

FIGURE 3.33 - GRAPHS AND STATISTICAL ANALYSIS COMPARING THE OD_{600} AT 48 HOURS OF 0.08% (W/V) ME *C. NECATOR* CULTURES SUPPLEMENTED WITH EITHER 0%, 0.5%, 1% OR 1.5% (W/V) FRUCTOSE, OR 0%, 0.6%, 1.1% OR 1.6% (W/V) SODIUM GLUCONATE. PLOT (A) DISPLAYS THE OD_{600} OF FRUCTOSE-SUPPLEMENTED CULTURES AND PLOT (B) THAT OF SODIUM GLUCONATE. NON-PAIRED T-TESTS WERE USED TO COMPARE EACH FRUCTOSE AND SODIUM GLUCONATE SUPPLEMENTATION (C). NS = NON-SIGNIFICANT ($P \geq 0.05$), * = $P \leq 0.05$, ** = $P \leq 0.01$, *** = $P \leq 0.001$, **** = $P \leq 0.0001$. ERROR BARS REPRESENT SD. N = 3 BIOLOGICAL REPLICATES. THE FULL COMBINED DATA CAN BE VIEWED IN FIGURE 8.15, APPENDIX 8.7.. 163

FIGURE 3.34 - GRAPHS AND STATISTICAL ANALYSIS SUMMARISING THE MEAN P-546 FLUORESCENCE AS A MEASURE OF INTRACELLULAR P3HB OF 0.08% (W/V) ME *C. NECATOR* CULTURES SUPPLEMENTED WITH 0%, 0.6%, 1.1% OR 1.6% (W/V) SODIUM GLUCONATE. STATISTICAL ANALYSIS WAS PERFORMED USING UNPAIRED T-TESTS TO COMPARE INDIVIDUAL SODIUM GLUCONATE CONCENTRATIONS AT THE SAME TIME POINT (C) AND PAIRED T-TESTS TO COMPARE THE SAME CONDITION AT DIFFERENT TIME POINTS (D). NS = NON-SIGNIFICANT ($P \geq 0.05$), * = $P \leq 0.05$, ** = $P \leq 0.01$, *** = $P \leq 0.001$, **** = $P \leq 0.0001$, ***** = $P \leq 0.00001$. ERROR BARS REPRESENT SD. N = 3 BIOLOGICAL REPLICATES. THE FULL DATA CAN BE FOUND IN FIGURE 8.13, APPENDIX 8.6. 165

FIGURE 3.35 - GRAPHS AND STATISTICAL ANALYSIS COMPARING P-546 FLUORESCENCE AS A MEASURE OF INTRACELLULAR P3HB AT 48 HOURS FOR 0.08% (W/V) ME *C. NECATOR* CULTURES SUPPLEMENTED WITH EITHER 0%, 0.5%, 1% OR 1.5% (W/V) FRUCTOSE, OR 0%, 0.6%, 1.1% OR 1.6% (W/V) SODIUM GLUCONATE. PLOT (A) DISPLAYS THE DATA OF FRUCTOSE-SUPPLEMENTED CULTURES AND PLOT (B) THAT OF SODIUM GLUCONATE. NON-PAIRED T-TESTS WERE USED TO COMPARE EACH FRUCTOSE AND SODIUM GLUCONATE SUPPLEMENTATION (C). NS = NON-SIGNIFICANT ($P \geq 0.05$), * = $P \leq 0.05$, ** = $P \leq 0.01$. ERROR BARS REPRESENT SD. N = 3 BIOLOGICAL REPLICATES. THE FULL DATA CAN BE FOUND IN FIGURE 8.16, APPENDIX 8.7. 166

FIGURE 3.36 - GRAPHS AND STATISTICAL ANALYSIS SUMMARISING THE MEAN PERCENTAGE OF $P3HB^{++}$ CELLS IN 0.08% (W/V) ME *C. NECATOR* CULTURES SUPPLEMENTED WITH 0%, 0.6%, 1.1% OR 1.6% (W/V) SODIUM GLUCONATE. STATISTICAL ANALYSIS WAS PERFORMED USING UNPAIRED T-TESTS TO COMPARE INDIVIDUAL SODIUM GLUCONATE CONCENTRATIONS AT THE SAME TIME POINT (C) AND PAIRED T-TESTS TO COMPARE THE SAME CONDITION AT DIFFERENT TIME POINTS (D). NS = NON-SIGNIFICANT ($P \geq 0.05$), * = $P \leq 0.05$, ** = $P \leq 0.01$, *** = $P \leq 0.001$, **** = $P \leq 0.0001$, ***** = $P \leq 0.00001$. ERROR BARS REPRESENT SD. N = 3 BIOLOGICAL REPLICATES. 168

FIGURE 3.37 - GRAPHS AND STATISTICAL ANALYSIS COMPARING THE PERCENTAGE OF $P3HB^{++}$ CELLS AT 48 HOURS FOR 0.08% (W/V) ME *C. NECATOR* CULTURES SUPPLEMENTED WITH EITHER 0%, 0.5%, 1% OR 1.5% (W/V) FRUCTOSE, OR 0%, 0.6%, 1.1% OR 1.6% (W/V) SODIUM GLUCONATE. PLOT (A) DISPLAYS THE DATA OF FRUCTOSE-SUPPLEMENTED CULTURES AND PLOT (B) THAT OF SODIUM GLUCONATE. NON-PAIRED T-TESTS WERE USED TO COMPARE EACH FRUCTOSE AND SODIUM GLUCONATE

supplementation (c). NS = non-significant ($p \geq 0.05$), * = $p < 0.05$, ** = $p \leq 0.01$, *** = $p \leq 0.001$, **** = $p \leq 0.0001$. Error bars represent SD. n = 3 biological replicates. 169

Figure 3.38 - Graphs and statistical analysis summarising the mean P-546 fluorescence as a measure of intracellular P3HB for the $P3HB^{+}$ and $P3HB^{++}$ populations in 0.08% (w/v) ME *C. necator* cultures supplemented with 0%, 0.6%, 1.1% or 1.6% (w/v) sodium gluconate. Statistical analysis was performed using unpaired t-tests to compare individual sodium gluconate concentrations at the same time point (d) and paired t-tests to compare the same condition at different time points (e). NS = non-significant ($p \geq 0.05$), * = $p \leq 0.05$, ** = $p \leq 0.01$, *** = $p \leq 0.001$. Error bars represent SD. n = 3 biological replicates. 171

Figure 3.39 - Graphs and statistical analysis comparing P-546 fluorescence as a measure of intracellular P3HB for the $P3HB^{+}$ and $P3HB^{++}$ populations at 48 hours for 0.08% (w/v) ME *C. necator* cultures supplemented with either 0%, 0.5%, 1% or 1.5% (w/v) fructose, or 0%, 0.6%, 1.1% or 1.6% (w/v) sodium gluconate. Plot (a) displays the data of fructose-supplemented cultures and plot (b) that of sodium gluconate. Non-paired t-tests were used to compare each fructose and sodium gluconate supplementation (c). NS = non-significant ($p \geq 0.05$), * = $p \leq 0.05$, ** = $p \leq 0.01$, *** = $p \leq 0.001$. Error bars represent SD. n = 3 biological replicates. 172

Figure 3.40 - Graphs and statistical analysis summarising the mean FSC of 0.08% (w/v) ME *C. necator* cultures supplemented with 0%, 0.6%, 1.1% or 1.6% (w/v) sodium gluconate. Statistical analysis was performed using unpaired t-tests to compare individual sodium gluconate concentrations at the same time point (d) and paired t-tests to compare the same condition at different time points (e). NS = non-significant ($p \geq 0.05$), * = $p < 0.05$, ** = $p \leq 0.01$, *** = $p \leq 0.001$, **** = $p \leq 0.0001$, ***** = $p \leq 0.00001$. Error bars represent SD. n = 3 biological replicates. The full data can be found in Figure 8.14 (a) and (b), Appendix 8.6. 175

Figure 3.41 - Fluorescent microscopy images of *C. necator* grown in 0.08% (w/v) ME supplemented with (a) 0, (b)0.6, (c) 1.1 and (d) 1.6% sodium gluconate after 72 hours of growth. Scale bars represent 10 μm. 176

Figure 3.42 - Graphs and statistical analysis comparing the mean FSC at 48 hours for 0.08% (w/v) ME *C. necator* cultures supplemented with either 0%, 0.5%, 1% or 1.5% (w/v) fructose, or 0%, 0.6%, 1.1% or 1.6% (w/v) sodium gluconate. Plot (a) displays the data of fructose-supplemented cultures and plot (b) that of sodium gluconate. Non-paired t-tests were used to compare each fructose and sodium gluconate supplementation (c). NS = non-significant ($p \geq 0.05$), * = $p < 0.05$, ** = $p \leq 0.01$, *** = $p \leq 0.001$, **** = $p \leq 0.0001$, ***** = $p \leq 0.00001$, ****** = $p \leq 0.000001$. Error bars represent SD. n = 3 biological replicates. The full data can be found in Figure 8.18 (e) and (f), Appendix 8.7. 177

Figure 3.43 - Graphs and statistical analysis summarising the mean FSC of 0.08% (w/v) ME *C. necator* cultures supplemented with 0%, 0.6%, 1.1% or 1.6% (w/v) sodium gluconate. Statistical analysis was performed using unpaired t-tests to compare individual sodium gluconate concentrations at the same time point (d) and paired t-tests to compare the same condition at different time points (e). NS = non-significant ($p \geq 0.05$), * = $p \leq 0.05$, ** = $p \leq 0.01$, *** = $p \leq 0.001$, **** = $p \leq 0.0001$, ***** = $p \leq 0.00001$. Error bars represent SD. n = 3 biological replicates. The full data can be found in Figure 8.14 (c) and (d), section 8.6. 180

FIGURE 3.44 - GRAPHS AND STATISTICAL ANALYSIS COMPARING FSC FOR THE P3HB^{+} AND P3HB^{++} POPULATIONS AT 48 HOURS FOR 0.08% (W/V) ME *C. NECATOR* CULTURES SUPPLEMENTED WITH EITHER 0%, 0.5%, 1% OR 1.5% (W/V) FRUCTOSE, OR 0%, 0.6%, 1.1% OR 1.6% (W/V) SODIUM GLUCONATE. PLOT (A) DISPLAYS THE DATA OF FRUCTOSE-SUPPLEMENTED CULTURES AND PLOT (B) THAT OF SODIUM GLUCONATE. NON-PAIRED T-TESTS WERE USED TO COMPARE EACH FRUCTOSE AND SODIUM GLUCONATE CONDITION (C). NS = NON-SIGNIFICANT ($P \geq 0.05$), * = $P < 0.05$, ** = $P \leq 0.01$, *** = $P \leq 0.001$, **** = $P \leq 0.0001$, ***** = $P \leq 0.00001$, ****** = $P \leq 0.000001$. ERROR BARS REPRESENT SD. N = 3 BIOLOGICAL REPLICATES. THE FULL DATA CAN BE FOUND IN FIGURE 8.18, APPENDIX 8.7. 181

FIGURE 3.45 – GRAPHS DISPLAYING A SUMMARY OF FLOW CYTOMETRY EXPERIMENTS OPTIMISING THE STAINING OF *C. NECATOR* WITH P-546. PLOT (A) DEPICTS P-546 FLUORESCENCE FOR *C. NECATOR* CELLS STAINED WITH P-546 VARYING BETWEEN A CONCENTRATION OF 0 AND 1 μG/ML FOR 12 MINUTES. PLOT (B) SUMMARISES *C. NECATOR* P-546 STAINING AT A CONCENTRATION OF 0.2 μG/ML AT TEMPERATURES OF 24, 30 AND 37 °C WHEN STAINED FOR 12 MINUTES. PLOT (C) DEMONSTRATES THE P-546 FLUORESCENCE OF *C. NECATOR* CELLS AFTER 12 AND 60 MINUTES OF STAINING AT 30 °C. CULTURES CONTAINED 0.08% (W/V) ME WITH 0.6% (W/V) SODIUM GLUCONATE ADDED AT 0 HOURS. STATISTICAL ANALYSIS IS LOCATED EITHER BELOW THE CORRESPONDING PLOT OR INCLUDED AS A PLOT ANNOTATION. NS = NON-SIGNIFICANT ($P \geq 0.05$), * = $P < 0.05$, ** = $P \leq 0.01$, *** = $P \leq 0.001$, **** = $P \leq 0.0001$ NON-PAIRED T-TESTS WERE USED TO COMPARE DIFFERENT EXPERIMENTAL CONDITIONS. PAIRED T-TESTS WERE USED TO COMPARE THE SAME EXPERIMENTAL CONDITION OVER TIME. ERROR BARS REPRESENT SD. 185

FIGURE 3.46 – SUMMARISATION OF MEAN CELL COUNT DATA DETERMINED BY FLOW CYTOMETRY FOR *C. NECATOR* CULTURES GROWN IN 0.08% (W/V) ME SUPPLEMENTED WITH 0.6% (W/V) SODIUM GLUCONATE. ANNOTATIONS REPRESENT THE OUTCOME OF A PAIRED T-TEST COMPARING SAMPLES OVER TIME. NS = NON-SIGNIFICANT. ERROR BARS REPRESENT SD. N = 3 BIOLOGICAL REPLICATES. THE FULL DATA IS LOCATED IN FIGURE 8.20, APPENDIX 8.9. 188

FIGURE 3.47 – SUMMARISATION OF (A) MEAN P-546 FLUORESCENCE PER CELL, (B) MEAN PERCENTAGE OF P3HB^{++} CELLS AND THE MEAN P-546 PER ML (C) FOR *C. NECATOR* CULTURES GROWN IN 0.08% (W/V) ME SUPPLEMENTED WITH 0.6% (W/V) SODIUM GLUCONATE. ANNOTATIONS REPRESENT THE OUTCOME OF A PAIRED T-TEST COMPARING SAMPLES OVER TIME. NS = NON-SIGNIFICANT ($P \geq 0.05$), * = $P < 0.05$, ** = $P \leq 0.01$. ERROR BARS REPRESENT SD. N = 3 BIOLOGICAL REPLICATES. THE FULL DATA CAN BE FOUND IN FIGURE 8.21, APPENDIX 8.9. 190

FIGURE 3.48 - SUMMARISATION OF P3HB^{+} AND P3HB^{++} MEAN P-546 FLUORESCENCE PER CELL (A) , AND PER ML (B) FOR *C. NECATOR* CULTURES GROWN IN 0.08% (W/V) ME SUPPLEMENTED WITH 0.6% (W/V) SODIUM GLUCONATE. ANNOTATIONS REPRESENT THE OUTCOME OF A NON-PAIRED T-TEST COMPARING P3HB^{+} AND P3HB^{++} POPULATIONS. PAIRED T-TEST WERE USED TO COMPARE THE SAME CONDITION OVER TIME. NS = NON-SIGNIFICANT ($P \geq 0.05$), * = $P < 0.05$, ** = $P \leq 0.01$. ERROR BARS REPRESENT SD. N = 3 BIOLOGICAL REPLICATES. THE FULL DATA CAN BE FOUND IN FIGURE 8.22, APPENDIX 8.9. 191

FIGURE 3.49 - FLUORESCENT MICROSCOPE IMAGES SHOWING PHA^{++} AND PHA^{+} *C. NECATOR* CELLS AT 144 HOURS WHEN GROWN IN 0.08% (W/V) ME SUPPLEMENTED WITH 0.6% (W/V) SODIUM GLUCONATE. SAMPLES WERE PERMEABILISED WITH 35%

(v/v) ethanol and stained with 1 μM P-546 (green) and 2 μg mL^{-1} PI (red). The scale bar represents 10 μm. Labelled are possible $P3HB^{+}$ and $P3HB^{++}$ cells. 192

Figure 3.50 – Summarisation of (a) mean FSC and (b) mean $P3HB^{+}$ and $P3HB^{++}$ FSC for *C. necator* cultures grown in 0.08% (w/v) ME supplemented with 0.6% (w/v) sodium gluconate. Annotations represent the outcome of a paired t-test comparing samples over time. NS = non-significant ($p \geq 0.05$), * = $p < 0.05$, ** = $p \leq 0.01$, *** = $p \leq 0.001$, **** = $p \leq 0.0001$. Error bars represent SD. n = 3 biological replicates. Note the legend only applies to plot (b). The full raw data is located in Appendix 8.9, Figure 8.23. 194

Figure 3.51 – Summary of mean events per mL at 72 and 168-hour time points, for *C. necator* cultures containing either 0.08% and 0.2% (w/v) ME supplemented with 0.5%, 1% and 1.5% (w/v) fructose. Statistical significance was determined using paired t-tests to compare the same condition at different time points (displayed as figure annotations), and non-paired t-tests to compare different experimental conditions. NS = non-significant ($p \geq 0.05$), * = $p < 0.05$. Error bars represent SD. n = 2 biological replicates. The full data is located in Figure 8.24, Appendix 8.10. 198

Figure 3.52 – Comparison of flow cytometry events per mL at 24 hours for 0.08% (w/v) *C. necator* supplemented with 0.5%, 1% and 1.5% (w/v) fructose or 0.6% (w/v) sodium gluconate. Statistical significance was determined using non-paired t-tests to compare different experimental conditions. NS = non-significant ($p \geq 0.05$), * = $p < 0.05$. Error bars represent SD. Error bars represent SD. n = 2 biological replicates for fructose supplemented cultures and n = 3 for sodium gluconate supplemented cultures. The full data can be found in Figure 8.29, Appendix 8.11. 199

Figure 3.53 – Summary of mean P-546 fluorescence per cell at 72 and 168 hour time points, for *C. necator* cultures containing either 0.08% and 0.2% (w/v) ME supplemented with 0.5%, 1% and 1.5% (w/v) fructose. Statistical significance was determined using paired t-tests to compare the same condition at different time points (displayed as figure annotations), and non-paired t-tests to compare different experimental conditions. NS = non-significant ($p \geq 0.05$), * = $p < 0.05$, ** = $p \leq 0.01$. Error bars represent SD. n = 2 biological replicates. The full data is located in Figure 8.25 (a) and (b), Appendix 8.10. 201

Figure 3.54 - Summary of mean P-546 fluorescence per mL at 72 and 168 hour time points, for *C. necator* cultures containing either 0.08% and 0.2% (w/v) ME supplemented with 0.5%, 1% and 1.5% (w/v) fructose. Statistical significance was determined using paired t-tests to compare the same condition at different time points (displayed as figure annotations), and non-paired t-tests to compare different experimental conditions. NS = non-significant ($p \geq 0.05$), * = $p < 0.05$. Error bars represent SD. n = 2 biological replicates. The full data is located in Figure 8.25 (c) and (d), Appendix 8.10. 202

Figure 3.55 - Comparison of mean P-546 fluorescence per cell (a) and per mL (b) at 168 hours for 0.08% (w/v) *C. necator* supplemented with 0.5%, 1% and 1.5% (w/v) fructose or 0.6% (w/v) sodium gluconate. Statistical significance was determined using non-paired t-tests to compare different experimental conditions (c). NS = non-significant ($p \geq 0.05$), * = $p < 0.05$, ** = $p \leq 0.01$, *** = $p \leq 0.001$. Error bars represent SD. Error bars

REPRESENT SD. N = 2 BIOLOGICAL REPLICATES FOR FRUCTOSE-SUPPLEMENTED CULTURES AND N = 3 FOR SODIUM GLUCONATE-SUPPLEMENTED CULTURES. THE FULL DATA CAN BE FOUND IN FIGURE 8.30, APPENDIX 8.11. 203

FIGURE 3.56 - SUMMARY OF THE MEAN PERCENTAGE P3HB^{++} CELLS AT 72 AND 168 HOUR TIME POINTS, FOR *C. NECATOR* CULTURES CONTAINING EITHER 0.08% AND 0.2% (W/V) ME SUPPLEMENTED WITH 0.5%, 1% AND 1.5% (W/V) FRUCTOSE. STATISTICAL SIGNIFICANCE WAS DETERMINED USING PAIRED T-TESTS TO COMPARE THE SAME CONDITION AT DIFFERENT TIME POINTS (DISPLAYED AS FIGURE ANNOTATIONS), AND NON-PAIRED T-TESTS TO COMPARE DIFFERENT EXPERIMENTAL CONDITIONS. NS = NON-SIGNIFICANT ($P \geq 0.05$), * = $P < 0.05$, ** = $P \leq 0.01$. ERROR BARS REPRESENT SD. N = 2 BIOLOGICAL REPLICATES. ((C) THE RAW DATA IS LOCATED IN FIGURE 8.25 (E) AND (F), APPENDIX 8.10. 205

FIGURE 3.57 - SUMMARY OF MEAN P3HB^{+} AND P3HB^{++} P-546 FLUORESCENCE PER CELL AT 72 AND 168 HOUR TIME POINTS, FOR *C. NECATOR* CULTURES CONTAINING EITHER 0.08% AND 0.2% (W/V) ME SUPPLEMENTED WITH 0.5%, 1% AND 1.5% (W/V) FRUCTOSE. STATISTICAL SIGNIFICANCE WAS DETERMINED USING PAIRED T-TESTS TO COMPARE THE SAME CONDITION AT DIFFERENT TIME POINTS (DISPLAYED AS FIGURE ANNOTATIONS), AND NON-PAIRED T-TESTS TO COMPARE DIFFERENT EXPERIMENTAL CONDITIONS. NS = NON-SIGNIFICANT ($P \geq 0.05$), * = $P < 0.05$, ** = $P \leq 0.01$, *** = $P \leq 0.001$. ERROR BARS REPRESENT SD. N = 2 BIOLOGICAL REPLICATES. THE FULL DATA IS LOCATED IN FIGURE 8.26 (A) AND (B), APPENDIX 8.10.... 206

FIGURE 3.58 - SUMMARY OF MEAN P3HB^{+} AND P3HB^{++} P-546 FLUORESCENCE PER ML AT 72 AND 168 HOUR TIME POINTS, FOR *C. NECATOR* CULTURES CONTAINING EITHER 0.08% AND 0.2% (W/V) ME SUPPLEMENTED WITH 0.5, 1 AND 1.5% (W/V) FRUCTOSE. STATISTICAL SIGNIFICANCE WAS DETERMINED USING PAIRED T-TESTS TO COMPARE THE SAME CONDITION AT DIFFERENT TIME POINTS (DISPLAYED AS FIGURE ANNOTATIONS), AND NON-PAIRED T-TESTS TO COMPARE DIFFERENT EXPERIMENTAL CONDITIONS. NS = NON-SIGNIFICANT ($P \geq 0.05$), * = $P < 0.05$, ** = $P \leq 0.01$. ERROR BARS REPRESENT SD. N = 2 BIOLOGICAL REPLICATES. THE FULL DATA IS LOCATED IN FIGURE 8.26 (C) AND (D), APPENDIX 8.10..... 207

FIGURE 3.59 - SUMMARY OF FSC AT 72 AND 168 HOUR TIME POINTS, FOR *C. NECATOR* CULTURES CONTAINING EITHER 0.08% AND 0.2% (W/V) ME SUPPLEMENTED WITH 0.5%, 1% AND 1.5% (W/V) FRUCTOSE. STATISTICAL SIGNIFICANCE WAS DETERMINED USING PAIRED T-TESTS TO COMPARE THE SAME CONDITION AT DIFFERENT TIME POINTS (DISPLAYED AS FIGURE ANNOTATIONS), AND NON-PAIRED T-TESTS TO COMPARE DIFFERENT EXPERIMENTAL CONDITIONS. NS = NON-SIGNIFICANT ($P \geq 0.05$), * = $P < 0.05$, ** = $P \leq 0.01$. ERROR BARS REPRESENT SD. N = 2 BIOLOGICAL REPLICATES. 209

FIGURE 3.60 - SUMMARY OF MEAN P3HB^{+} AND P3HB^{++} FSC AT 72 AND 168 HOUR TIME POINTS, FOR *C. NECATOR* CULTURES CONTAINING EITHER 0.08% AND 0.2% (W/V) ME SUPPLEMENTED WITH 0.5%, 1% AND 1.5% (W/V) FRUCTOSE. STATISTICAL SIGNIFICANCE WAS DETERMINED USING PAIRED T-TESTS TO COMPARE THE SAME CONDITION AT DIFFERENT TIME POINTS (DISPLAYED AS FIGURE ANNOTATIONS), AND NON-PAIRED T-TESTS TO COMPARE DIFFERENT EXPERIMENTAL CONDITIONS. NS = NON-SIGNIFICANT ($P \geq 0.05$), * = $P < 0.05$, ** = $P \leq 0.01$. ERROR BARS REPRESENT SD. N = 2 BIOLOGICAL REPLICATES. 210

FIGURE 4.1 – GRAPH DISPLAYING THE MEAN EVENTS PER ML FOR *C. NECATOR* CULTURE CONTAINING 0.08%, 0.2% OR 0.4% (W/V) ME SUPPLEMENTED WITH 0.5% (W/V) FRUCTOSE AT 0 HOURS, WITH EITHER 0.6% OR 1.1% (W//V) SODIUM GLUCONATE ADDED AFTER 24 HOURS. STATISTICAL SIGNIFICANCE WAS DETERMINED USING PAIRED T-TESTS TO COMPARE THE SAME CONDITION AT DIFFERENT TIME POINTS (DISPLAYED AS FIGURE ANNOTATIONS). NS = NON-SIGNIFICANT ($P \geq 0.05$). ERROR BARS REPRESENT SD. N = 2 BIOLOGICAL REPLICATES. THE FULL DATA CAN BE FOUND IN FIGURE 9.1, APPENDIX 9.1. 216

FIGURE 4.2 – GRAPH DISPLAYING THE MEAN P-546 FLUORESCENCE (P3HB) PER CELL FOR *C. NECATOR* CULTURES CONTAINING 0.08%, 0.2% OR 0.4% (W/V) ME SUPPLEMENTED WITH 0.5% (W/V) FRUCTOSE AT 0 HOURS, WITH EITHER 0.6% OR 1.1% (W//V) SODIUM GLUCONATE ADDED AFTER 24 HOURS. STATISTICAL SIGNIFICANCE WAS DETERMINED USING PAIRED T-TESTS TO COMPARE THE SAME CONDITION AT DIFFERENT TIME POINTS (DISPLAYED AS FIGURE ANNOTATIONS). NS = NON-SIGNIFICANT ($P \geq 0.05$), * = $P < 0.05$, ** = $P \leq 0.01$. ERROR BARS REPRESENT SD. N = 2 BIOLOGICAL REPLICATES. THE FULL DATA CAN BE FOUND EXPRESSED PER CELL IN FIGURE 9.2, APPENDIX 9.1. 218

FIGURE 4.3 - GRAPH DISPLAYING THE MEAN P-546 FLUORESCENCE (P3HB) PER ML FOR *C. NECATOR* CULTURES CONTAINING 0.08%, 0.2% OR 0.4% (W/V) ME SUPPLEMENTED WITH 0.5% (W/V) FRUCTOSE AT 0 HOURS, WITH EITHER 0.6% OR 1.1% (W//V) SODIUM GLUCONATE ADDED AFTER 24 HOURS. STATISTICAL SIGNIFICANCE WAS DETERMINED USING PAIRED T-TESTS TO COMPARE THE SAME CONDITION AT DIFFERENT TIME POINTS (DISPLAYED AS FIGURE ANNOTATIONS). NS = NON-SIGNIFICANT ($P \geq 0.05$), * = $P < 0.05$, ** = $P \leq 0.01$. ERROR BARS REPRESENT SD. N = 2 BIOLOGICAL REPLICATES. THE FULL DATA CAN BE FOUND IN FIGURE 9.2, APPENDIX 9.1. 219

FIGURE 4.4 - GRAPH DISPLAYING THE MEAN PERCENTAGE OF $P3HB^{++}$ CELLS FOR *C. NECATOR* CULTURES CONTAINING 0.08%, 0.2% OR 0.4% (W/V) ME SUPPLEMENTED WITH 0.5% (W/V) FRUCTOSE AT 0 HOURS, WITH EITHER 0.6% OR 1.1% (W//V) SODIUM GLUCONATE ADDED AFTER 24 HOURS. STATISTICAL SIGNIFICANCE WAS DETERMINED USING PAIRED T-TESTS TO COMPARE THE SAME CONDITION AT DIFFERENT TIME POINTS (DISPLAYED AS FIGURE ANNOTATIONS). NS = NON-SIGNIFICANT ($P \geq 0.05$), * = $P < 0.05$, ** = $P \leq 0.01$. ERROR BARS REPRESENT SD. N = 2 BIOLOGICAL REPLICATES. 220

FIGURE 4.5 - GRAPH DISPLAYING THE MEAN $P3HB^{+}$ AND $P3HB^{++}$ P-546 FLUORESCENCE (P3HB) PER CELL FOR *C. NECATOR* CULTURES CONTAINING 0.08%, 0.2% OR 0.4% (W/V) ME SUPPLEMENTED WITH 0.5% (W/V) FRUCTOSE AT 0 HOURS, WITH EITHER 0.6% OR 1.1% (W//V) SODIUM GLUCONATE ADDED AFTER 24 HOURS. STATISTICAL SIGNIFICANCE WAS DETERMINED USING PAIRED T-TESTS TO COMPARE THE SAME CONDITION AT DIFFERENT TIME POINTS (DISPLAYED AS FIGURE ANNOTATIONS). NS = NON-SIGNIFICANT ($P \geq 0.05$), * = $P < 0.05$, ** = $P \leq 0.01$, *** = $P \leq 0.001$. ERROR BARS REPRESENT SD. N = 2 BIOLOGICAL REPLICATES. THE FULL DATA IS LOCATED IN FIGURE 9.3, APPENDIX 9.1. 221

FIGURE 4.6 - GRAPH DISPLAYING THE MEAN $P3HB^{+}$ AND $P3HB^{++}$ P-546 FLUORESCENCE (P3HB) PER ML FOR *C. NECATOR* CULTURES CONTAINING 0.08%, 0.2% OR 0.4% (W/V) ME SUPPLEMENTED WITH 0.5% (W/V) FRUCTOSE AT 0 HOURS, WITH EITHER 0.6% OR 1.1% (W//V) SODIUM GLUCONATE ADDED AFTER 24 HOURS. STATISTICAL SIGNIFICANCE WAS DETERMINED USING PAIRED T-TESTS TO COMPARE THE SAME CONDITION AT DIFFERENT TIME POINTS (DISPLAYED AS FIGURE ANNOTATIONS). NS = NON-SIGNIFICANT ($P \geq 0.05$), * = $P < 0.05$, ** = $P \leq 0.01$. ERROR BARS REPRESENT SD. N = 2 BIOLOGICAL REPLICATES. THE FULL DATA IS LOCATED IN FIGURE 9.4, APPENDIX 9.1. 222

FIGURE 4.7 - GRAPH DISPLAYING THE MEAN FSC FOR *C. NECATOR* CULTURES CONTAINING 0.08%, 0.2% OR 0.4% (W/V) ME SUPPLEMENTED WITH 0.5% (W/V) FRUCTOSE AT 0 HOURS, WITH EITHER 0.6% OR 1.1% (W//V) SODIUM GLUCONATE ADDED AFTER 24 HOURS. STATISTICAL SIGNIFICANCE WAS DETERMINED USING PAIRED T-TESTS TO COMPARE THE SAME CONDITION AT DIFFERENT TIME POINTS (DISPLAYED AS FIGURE ANNOTATIONS). NS = NON-SIGNIFICANT ($P \geq 0.05$), * = $P < 0.05$, ** = $P \leq 0.01$. ERROR BARS REPRESENT SD. N = 2 BIOLOGICAL REPLICATES. 224

FIGURE 4.8 - GRAPH DISPLAYING THE MEAN $P3HB^{+}$ AND $P3HB^{++}$ FSC FOR *C. NECATOR* CULTURES CONTAINING 0.08%, 0.2% OR 0.4% (W/V) ME SUPPLEMENTED WITH 0.5% (W/V) FRUCTOSE AT 0 HOURS, WITH EITHER 0.6% OR 1.1% (W//V) SODIUM

GLUCONATE ADDED AFTER 24 HOURS. STATISTICAL SIGNIFICANCE WAS DETERMINED USING PAIRED T-TESTS TO COMPARE THE SAME CONDITION AT DIFFERENT TIME POINTS (DISPLAYED AS FIGURE ANNOTATIONS). NS = NON-SIGNIFICANT ($P \geq 0.05$), * = $P < 0.05$, ** = $P \leq 0.01$. ERROR BARS REPRESENT SD. N = 2 BIOLOGICAL REPLICATES. 225

FIGURE 4.9 - MEAN EVENTS PER ML DETERMINED BY FLOW CYTOMETRY FOR 0.08% AND 0.2% (W/V) ME *C. NECATOR* CULTURES CONTAINING 0, 3, 6, 9, 12 OR 15 G/L AND SUPPLEMENTED WITH 0.5% (W/V) FRUCTOSE AT 0 HOURS AND 0.6% (W/V) SODIUM GLUCONATE AT 24 HOURS. STATISTICAL SIGNIFICANCE WAS DETERMINED USING PAIRED T-TESTS TO COMPARE THE SAME CONDITION AT DIFFERENT TIME POINTS (DISPLAYED AS FIGURE ANNOTATIONS). NS = NON-SIGNIFICANT ($P \geq 0.05$), * = $P < 0.05$, ** = $P \leq 0.01$, *** = $P \leq 0.001$. MISSING STATISTIC DUE TO REPLICATES HAVING THE SAME VALUES. ERROR BARS REPRESENT SD. N = 3 BIOLOGICAL REPLICATES. THE FULL DATA CAN BE FOUND IN FIGURE 9.6, APPENDIX 9.2. 228

FIGURE 4.10 – MEAN P-546 FLUORESCENCE (P3HB) PER CELL (PLOTS (A) AND (B)) AND PER ML (PLOTS (C) AND (D)) FOR 0.08% AND 0.2% (W/V) ME *C. NECATOR* CULTURES CONTAINING 0, 3, 6, 9, 12 OR 15 G/L AND SUPPLEMENTED WITH 0.5% (W/V) FRUCTOSE AT 0 HOURS AND 0.6% (W/V) SODIUM GLUCONATE AT 24 HOURS. STATISTICAL SIGNIFICANCE WAS DETERMINED USING PAIRED T-TESTS TO COMPARE THE SAME CONDITION AT DIFFERENT TIME POINTS (DISPLAYED AS FIGURE ANNOTATIONS). NS = NON-SIGNIFICANT ($P \geq 0.05$), * = $P < 0.05$, ** = $P \leq 0.01$. ERROR BARS REPRESENT SD. N = 3 BIOLOGICAL REPLICATES. THE FULL DATA CAN BE FOUND IN FIGURE 9.7 (A)-(D), APPENDIX 9.2. 231

FIGURE 4.11 – MEAN PERCENTAGE OF $P3HB^{++}$ CELLS FOR 0.08% AND 0.2% (W/V) ME *C. NECATOR* CULTURES CONTAINING 0, 3, 6, 9, 12 OR 15 G/L AND SUPPLEMENTED WITH 0.5% (W/V) FRUCTOSE AT 0 HOURS AND 0.6% (W/V) SODIUM GLUCONATE AT 24 HOURS. STATISTICAL SIGNIFICANCE WAS DETERMINED USING PAIRED T-TESTS TO COMPARE THE SAME CONDITION AT DIFFERENT TIME POINTS (DISPLAYED AS FIGURE ANNOTATIONS). NS = NON-SIGNIFICANT ($P \geq 0.05$), * = $P < 0.05$, ** = $P \leq 0.01$. MISSING STATISTIC DUE TO REPLICATES HAVING THE SAME VALUES. ERROR BARS REPRESENT SD. N = 3 BIOLOGICAL REPLICATES. 232

FIGURE 4.12 - MEAN $P3HB^{+}$ AND $P3HB^{++}$ P-546 FLUORESCENCE (P3HB) PER CELL FOR 0.08% AND 0.2% (W/V) ME *C. NECATOR* CULTURES CONTAINING 0, 3, 6, 9, 12 OR 15 G/L SODIUM CHLORIDE, AND SUPPLEMENTED WITH 0.5% (W/V) FRUCTOSE AT 0 HOURS AND 0.6% (W/V) SODIUM GLUCONATE AT 24 HOURS. STATISTICAL SIGNIFICANCE WAS DETERMINED USING PAIRED T-TESTS TO COMPARE THE SAME CONDITION AT DIFFERENT TIME POINTS (DISPLAYED AS FIGURE ANNOTATIONS). NS = NON-SIGNIFICANT ($P \geq 0.05$), * = $P < 0.05$, ** = $P \leq 0.01$, *** = $P \leq 0.001$. ERROR BARS REPRESENT SD. N = 3 BIOLOGICAL REPLICATES. THE FULL DATA IS LOCATED IN FIGURE 9.8, APPENDIX 9.2. 233

FIGURE 4.13 - MEAN $P3HB^{+}$ AND $P3HB^{++}$ P-546 FLUORESCENCE PER ML FOR 0.08% AND 0.2% (W/V) ME *C. NECATOR* CULTURES CONTAINING 0, 3, 6, 9, 12 OR 15 G/L SODIUM CHLORIDE AND SUPPLEMENTED WITH 0.5% (W/V) FRUCTOSE AT 0 HOURS AND 0.6% (W/V) SODIUM GLUCONATE AT 24 HOURS. STATISTICAL SIGNIFICANCE WAS DETERMINED USING PAIRED T-TESTS TO COMPARE THE SAME CONDITION AT DIFFERENT TIME POINTS (DISPLAYED AS FIGURE ANNOTATIONS). NS = NON-SIGNIFICANT ($P \geq 0.05$), * = $P < 0.05$, ** = $P \leq 0.01$, *** = $P \leq 0.001$. ERROR BARS REPRESENT SD. N = 3 BIOLOGICAL REPLICATES. THE FULL DATA IS LOCATED IN FIGURE 9.9, APPENDIX 9.2. 234

FIGURE 4.14 - MEAN FSC FOR 0.08% AND 0.2% (W/V) ME *C. NECATOR* CULTURES CONTAINING 0, 3, 6, 9, 12 OR 15 G/L AND SUPPLEMENTED WITH 0.5% (W/V) FRUCTOSE AT 0 HOURS AND 0.6% (W/V) SODIUM GLUCONATE AT 24 HOURS. STATISTICAL SIGNIFICANCE WAS DETERMINED USING PAIRED T-TESTS TO COMPARE THE SAME CONDITION AT DIFFERENT TIME POINTS

(displayed as figure annotations). NS = non-significant ($p \geq 0.05$), * = $p < 0.05$, ** = $p \leq 0.01$. Error bars represent SD. n = 3 biological replicates. The full data can be found in Figure 9.10 (a) and (b), Appendix 9.2. 236

Figure 4.15 - Mean P3HB^{+} and P3HB^{++} FSC for 0.08% and 0.2% (w/v) ME *C. necator* cultures containing 0, 3, 6, 9, 12 or 15 g/L and supplemented with 0.5% (w/v) fructose at 0 hours and 0.6% (w/v) sodium gluconate at 24 hours. Statistical significance was determined using paired t-tests to compare the same condition at different time points (displayed as figure annotations). NS = non-significant ($p \geq 0.05$)., * = $p < 0.05$, ** = $p \leq 0.01$. Error bars represent SD. n = 3 biological replicates. The full data is located in Figure 9.5 (c)-(f), Appendix 9.2. 237

Figure 4.16 - Mean pH of *C. necator* cultures grown initially in either 0.08% (a) or 0.2% (w/v) ME (b) up to 24 hours until the growth media was hanged to either 0.008% or 0.04% (w/v) ME. Media before and after 24 hours was supplemented with either 0.5% (w/v) fructose or 0.6% (w/v) sodium gluconate. Statistical significance was determined using paired t-tests to compare the same condition at different time points (displayed as figure annotations). NS = non-significant ($p \geq 0.05$), * = $p < 0.05$, ** = $p \leq 0.01$. Error bars represent SD. n = 6 biological replicates. 240

Figure 4.17 – Mean events per mL of *C. necator* cultures grown initially in either 0.08% (a) or 0.2% (w/v) ME (b) up to 24 hours until the growth media was hanged to either 0.008% or 0.04% (w/v) ME. Media before and after 24 hours was supplemented with either 0.5% (w/v) fructose or 0.6% (w/v) sodium gluconate. Statistical significance was determined using paired t-tests to compare the same condition at different time points (displayed as figure annotations). NS = non-significant ($p \geq 0.05$), * = $p < 0.05$, ** = $p \leq 0.01$. Error bars represent SD. n = 3 biological replicates. The full data can be found in Figure 9.11, Appendix 9.3. 242

Figure 4.18 - Mean P-546 fluorescence per cell (a) and per mL (b) for *C. necator* cultures grown initially in either 0.08% or 0.2% (w/v) ME up to 24 hours until the growth media was changed to either 0.008% or 0.04% (w/v) ME. Media before and after 24 hours was supplemented with either 0.5% (w/v) fructose or 0.6% (w/v) sodium gluconate. Statistical significance was determined using paired t-tests to compare the same condition at different time points (displayed as figure annotations). NS = non-significant ($p \geq 0.05$), * = $p < 0.05$, ** = $p \leq 0.01$, *** = $p \leq 0.001$. Error bars represent SD. n = 3 biological replicates. The full data can be found in Figure 9.12 (a)-(d), Appendix 9.3..... 245

Figure 4.19 - Mean percentage of P3HB^{++} cells in *C. necator* cultures grown initially in either 0.08% (a) or 0.2% (w/v) ME (b) up to 24 hours until the growth media was changed to either 0.008% or 0.04% (w/v) ME. Media before and after 24 hours was supplemented with either 0.5% (w/v) fructose or 0.6% (w/v) sodium gluconate. Statistical significance was determined using paired t-tests to compare the same condition at different time points (displayed as figure annotations). NS = non-significant ($p \geq 0.05$), * = $p < 0.05$, ** = $p \leq 0.01$, *** = $p \leq 0.001$, **** = $p \leq 0.0001$. Error bars represent SD. n = 3 biological replicates. The full data can be found in Figure 9.12 (e) and (f), Appendix 9.3..... 246

Figure 4.20 - Mean P3HB^{+} and P3HB^{++} P-546 fluorescence per cell for *C. necator* cultures grown initially in either 0.08% (a) or 0.2% (w/v) ME (b) up to 24 hours until the growth media was changed to either 0.008% or 0.04% (w/v) ME. Media before and after 24 hours was supplemented with either 0.5% (w/v) fructose or 0.6%

(w/v) sodium gluconate. Statistical significance was determined using paired t-tests to compare the same condition at different time points (displayed as figure annotations). NS = non-significant ($p \geq 0.05$), * = $p < 0.05$, ** = $p \leq 0.01$, *** = $p \leq 0.001$, **** = $p \leq 0.0001$, ***** = $p \leq 0.00001$. Error bars represent SD. n = 3 biological replicates. The full data can be found in Figure 9.13, Appendix 9.3. 247

Figure 4.21 - Mean $P3HB^{+}$ and $P3HB^{++}$ P-546 fluorescence per mL for *C. necator* cultures grown initially in either 0.08% (a) or 0.2% (w/v) ME (b) up to 24 hours until the growth media was changed to either 0.008% or 0.04% (w/v) ME. Media before and after 24 hours was supplemented with either 0.5% (w/v) fructose or 0.6% (w/v) sodium gluconate. Statistical significance was determined using paired t-tests to compare the same condition at different time points (displayed as figure annotations). NS = non-significant ($p \geq 0.05$), * = $p < 0.05$, ** = $p \leq 0.01$, *** = $p \leq 0.001$. Error bars represent SD. n = 3 biological replicates. The full data can be found in Figure 9.14, Appendix 9.3. 248

Figure 4.22 – Mean FSC for *C. necator* cultures grown initially in either 0.08% or 0.2% (w/v) ME up to 24 hours until the growth media was changed to either 0.008% or 0.04% (w/v) ME. Media before and after 24 hours was supplemented with either 0.5% (w/v) fructose or 0.6% (w/v) sodium gluconate. Statistical significance was determined using paired t-tests to compare the same condition at different time points (displayed as figure annotations). NS = non-significant ($p \geq 0.05$), * = $p < 0.05$, ** = $p \leq 0.01$, *** = $p \leq 0.001$, **** = $p \leq 0.0001$, ***** = $p \leq 0.00001$. Error bars represent SD. n = 3 biological replicates. The full data can be found in Figure 9.15 (a), Appendix 9.3. 250

Figure 4.23 - Mean FSC for *C. necator* cultures grown initially in either 0.08% or 0.2% (w/v) ME up to 24 hours until the growth media was changed to either 0.008% or 0.04% (w/v) ME. Media before and after 24 hours was supplemented with either 0.5% (w/v) fructose or 0.6% (w/v) sodium gluconate. Statistical significance was determined using paired t-tests to compare the same condition at different time points (displayed as figure annotations). NS = non-significant ($p \geq 0.05$), * = $p < 0.05$, ** = $p \leq 0.01$, *** = $p \leq 0.001$. Error bars represent SD. n = 3 biological replicates. The full data can be found in Figure 9.15 (b) and (c), Appendix 9.3. 251

Figure 4.24 - Mean events per mL for *C. necator* cultures initially containing 0.08% or 0.2% (w/v) ME and supplemented with 0.5% (w/v) fructose, 0.6% (w/v) sodium gluconate or both. At 24 hours growth media was either not changed or replaced with 0.04% (w/v) ME and supplemented with both 0.5% (w/v) fructose and 0.6% (w/v) sodium gluconate. Statistical significance was determined using paired t-tests to compare the same condition between 24 and 48, and 48 and 72 hours (see corresponding tables). NS = non-significant ($p \geq 0.05$), * = $p < 0.05$, ** = $p \leq 0.01$, *** = $p \leq 0.001$. Error bars represent SD. n = 3 biological replicates. The full data can be found in Appendix 2 (section 9.4), Figure 9.16. 256

Figure 4.25 - Mean pH of *C. necator* cultures initially containing 0.08% or 0.2% (w/v) ME and supplemented with 0.5% (w/v) fructose, 0.6% (w/v) sodium gluconate or both. The pH of cultures was taken from replaced media and therefore conditions 0.08% ME 3 and 0.2% ME 3 are missing due their media not being replaced at 24 hours. Statistical significance was determined using paired t-tests to compare the same condition at 72 and

168 hours (see annotations) . NS = non-significant ($P \geq 0.05$), * = $P < 0.05$, ** = $P \leq 0.01$, *** = $P \leq 0.001$, **** = $P \leq 0.0001$, ***** = $P \leq 0.00001$. Error bars represent SD. n = 3 biological replicates. 257

Figure 4.26 – Mean events per mL for *C. necator* cultures initially containing 0.08% or 0.2% (w/v) ME and supplemented with 0.5% (w/v) fructose, 0.6% (w/v) sodium gluconate or both. At 24 hours growth media was either not changed or replaced with 0.04% (w/v) ME and supplemented with both 0.5% (w/v) fructose and 0.6% (w/v) sodium gluconate. Statistical significance was determined using paired t-tests to compare the same condition at 72 and 168 hours (see annotations). NS = non-significant ($P \geq 0.05$), * = $P < 0.05$, ** = $P \leq 0.01$. Error bars represent SD. n = 3 biological replicates. The full data can be found in Appendix 2 (section 9.4), Figure 9.16. 257

Figure 4.27 - Mean P-546 fluorescence per cell (plots (a) and (b)) and per mL (plots (c) and (d)) for *C. necator* cultures initially containing 0.08% or 0.2% (w/v) ME and supplemented with 0.5% (w/v) fructose, 0.6% (w/v) sodium gluconate or both. At 24 hours growth media was either not changed or replaced with 0.04% (w/v) ME and supplemented with both 0.5% (w/v) fructose and 0.6% (w/v) sodium gluconate. Statistical significance was determined using paired t-tests to compare the same condition at 72 and 168 hours (see annotations). NS = non-significant ($P \geq 0.05$), * = $P < 0.05$, ** = $P \leq 0.01$, *** = $P \leq 0.001$. Error bars represent SD. n = 3 biological replicates. The full data for P-546 fluorescence per cell and per mL can be found in Figure 9.17 (a) and (b), Appendix 9.4. 259

Figure 4.28 - Mean percentage of P3HB^{++} cells for *C. necator* cultures initially containing 0.08% or 0.2% (w/v) ME and supplemented with 0.5% (w/v) fructose, 0.6% (w/v) sodium gluconate or both. At 24 hours growth media was either not changed or replaced with 0.04% (w/v) ME and supplemented with both 0.5% (w/v) fructose and 0.6% (w/v) sodium gluconate. Statistical significance was determined using paired t-tests to compare the same condition at 72 and 168 hours (see annotations). NS = non-significant ($P \geq 0.05$), * = $P < 0.05$, ** = $P \leq 0.01$, *** = $P \leq 0.001$. Error bars represent SD. n = 3 biological replicates. The full data can be found in Figure 9.17 (c), Appendix 9.4. 260

Figure 4.29 - Mean P-546 fluorescence per cell for P3HB^{+} and P3HB^{++} cells for *C. necator* cultures initially containing 0.08% or 0.2% (w/v) ME and supplemented with 0.5% (w/v) fructose, 0.6% (w/v) sodium gluconate or both. At 24 hours growth media was either not changed or replaced with 0.04% (w/v) ME and supplemented with both 0.5% (w/v) fructose and 0.6% (w/v) sodium gluconate. Statistical significance was determined using paired t-tests to compare the same condition at 72 and 168 hours (see annotations). NS = non-significant ($P \geq 0.05$), * = $P < 0.05$. Error bars represent SD. n = 3 biological replicates. The full data can be found in Figure 9.18, Appendix 9.4. 261

Figure 4.30 - Mean P-546 fluorescence per mL for P3HB^{+} and P3HB^{++} cells for *C. necator* cultures initially containing 0.08% or 0.2% (w/v) ME and supplemented with 0.5% (w/v) fructose, 0.6% (w/v) sodium gluconate or both. At 24 hours growth media was either not changed or replaced with 0.04% (w/v) ME and supplemented with both 0.5% (w/v) fructose and 0.6% (w/v) sodium gluconate. Statistical significance was determined using paired t-tests to compare the same condition at 72 and 168 hours (see annotations). NS =

non-significant ($P \geq 0.05$), * = $P < 0.05$, ** = $P \leq 0.01$, *** = $P \leq 0.001$. Error bars represent SD. n = 3 biological replicates. The full data can be found in Figure 9.19, Appendix 9.4. 262

Figure 4.31 - Mean FSC for *C. necator* cultures initially containing 0.08% or 0.2% (w/v) ME and supplemented with 0.5% (w/v) fructose, 0.6% (w/v) sodium gluconate or both. At 24 hours growth media was either not changed or replaced with 0.04% (w/v) ME and supplemented with both 0.5% (w/v) fructose and 0.6% (w/v) sodium gluconate. Statistical significance was determined using paired t-tests to compare the same condition at 72 and 168 hours (see annotations). NS = non-significant ($P \geq 0.05$), * = $P < 0.05$, ** = $P \leq 0.01$, *** = $P \leq 0.001$. Error bars represent SD. n = 3 biological replicates. The full data can be found in Figure 9.2 (a), Appendix 9.4. 264

Figure 4.32 - Mean $P3HB^{+}$ and $P3HB^{++}$ FSC for *C. necator* cultures initially containing 0.08% or 0.2% (w/v) ME and supplemented with 0.5% (w/v) fructose, 0.6% (w/v) sodium gluconate or both. At 24 hours growth media was either not changed or replaced with 0.04% (w/v) ME and supplemented with both 0.5% (w/v) fructose and 0.6% (w/v) sodium gluconate. Statistical significance was determined using paired t-tests to compare the same condition at 72 and 168 hours (see annotations). NS = non-significant ($P \geq 0.05$), * = $P < 0.05$, ** = $P \leq 0.01$. Error bars represent SD. n = 3 biological replicates. 265

Figure 8.1 - The mean OD_{600}, mean P-546 fluorescence (Intracellular PHB) and mean FSC (cell size) determined by flow cytometry for *C. necator* grown in 0.8% (w/v) ME seed cultures. The experiment was conducted in two independent experiments covering Cells were stained with SYTO62 (1 μM) and P-546 (1μM). Error bars represent SD. n=4. 314

Figure 8.2 - Graphs displaying the (a) mean OD_{600}, (b) mean P-546 fluorescence (Intracellular PHB) content and (c) mean FSC (cell size) of *C. necator* cultures grown in 0.2, 0.4, 0.6 and 0.8% (w/v) ME. Error bars represent SD. n=3. 315

Figure 8.3 - Graphs displaying the mean OD_{600} of *C. necator* cultures grown in 0.2%, 0.4%, 0.6% and 0.8% (w/v) ME with and without 0.5% (w/v) fructose supplementation. Error bars represent SD. n=3 biological replicates. 316

Figure 8.4 - Graphs displaying data for *C. necator* cultures grown in 0.2%, 0.4%, 0.6% and 0.8% (w/v) ME with (a) mean $P3HB^{++}$ P-546 fluorescence (P3HB) and (b) mean percentage of $P3HB^{++}$ cells comparing cultures with and without fructose supplementation and (c) mean $P3HB^{+}/P3HB^{++}$ fluorescence which displays data for cultures only with 0.5% (w/v) fructose. Error bars represent SD. n=3 biological replicates. 317

Figure 8.5 - Graphs displaying data for *C. necator* cultures grown in 0.2%, 0.4%, 0.6% and 0.8% (w/v) ME displaying (a) mean overall FSC comparing cultures with and without 0.5% (w/v) fructose supplementation and (b) mean $P3HB^{+}/P3HB^{++}$ FSC for cultures supplemented with 0.5% (w/v) fructose only. Error bars represent SD. n=3 biological replicates. 318

Figure 8.6 – Full OD_{600} data for *C. necator* cultures grown in 0.08% and 0.2% (w/v) ME with and without 0.5% (w/v) fructose supplementation. Error bars represent SD. n = 3 biological replicates. 319

Figure 8.7 – Full data representing mean P-546 (P3HB) per cell (A), mean percentage of $P3HB^{++}$ cells (B) and mean $P3HB^{+}$ and $P3HB^{++}$ P-546 fluorescence (P3HB) (C), for *C. necator* cultures grown in 0.08% and 0.2% (w/v) ME with and without 0.5% (w/v) fructose supplementation. Error bars represent SD. n = 3 biological replicates. 320

Figure 8.8 – Full data for mean overall (A) and $P3HB^{+}/P3HB^{++}$ (B) FSC (cell size) data for *C. necator* cultures grown in 0.08% and 0.2% (w/v) ME with and without 0.5% (w/v) fructose supplementation. Error bars represent SD. n = 3 biological replicates. 321

Figure 8.9 – Full OD_{600} data for *C. necator* cultures containing 0.08% (w/v) and supplemented with 0%, 0.5%, 1%, 1.5% (w/v) fructose. Error bars represent SD. n = 3 biological replicates. 322

Figure 8.10 - Full data representing mean P-546 (P3HB) per cell (A), mean percentage of $P3HB^{++}$ cells (B) and mean $P3HB^{+}$ and $P3HB^{++}$ P-546 fluorescence (P3HB) (C) for *C. necator* cultures containing 0.08% (w/v) and supplemented with 0%, 0.5%, 1%, 1.5% (w/v) fructose. Error bars represent SD. n = 3 biological replicates. 323

Figure 8.11 - Full data for mean overall (A) and $P3HB^{+}/P3HB^{++}$ (B) FSC (cell size) for *C. necator* cultures containing 0.08% (w/v) and supplemented with 0%, 0.5%, 1%, 1.5% (w/v) fructose. Error bars represent SD. n = 3 biological replicates. 324

Figure 8.12 – Full OD_{600} data for *C. necator* cultures containing 0.08% (w/v) ME and supplemented with 0%, 0.6%, 1.1% and 1.6% (w/v) sodium gluconate. Error bars represent SD. n = 3 biological replicates. 325

Figure 8.13 - Full data representing mean P-546 (P3HB) per cell ((A) and (B)), mean percentage of $P3HB^{++}$ cells ((C) and (D)) and mean $P3HB^{+}$ and $P3HB^{++}$ P-546 fluorescence (P3HB) ((E) and (F)) for *C. necator* cultures containing 0.08% (w/v) ME and supplemented with 0%, 0.6%, 1.1% and 1.6% (w/v) sodium gluconate. Error bars represent SD. n = 3 biological replicates. 326

Figure 8.14 - Full data for mean overall (A) and $P3HB^{+}/P3HB^{++}$ (B) FSC (cell size) for *C. necator* cultures containing 0.08% (w/v) ME and supplemented with 0%, 0.6%, 1.1% and 1.6% (w/v) sodium gluconate. Error bars represent SD. n = 3 biological replicates. 327

Figure 8.15 - Full OD_{600} data for *C. necator* cultures containing 0.08% (w/v) ME and supplemented with 0%, 0.6%, 1.1% and 1.6% (w/v) sodium gluconate or 0%, 0.5%, 1% and 1.5% (w/v) fructose. Error bars represent SD. n = 3 biological replicates 328

Figure 8.16 – Full data representing mean P-546 (P3HB) per cell ((A) and (B)), mean percentage of $P3HB^{++}$ cells ((C) and (D)) for *C. necator* cultures containing 0.08% (w/v) ME and supplemented with 0%, 0.6%, 1.1% and 1.6% (w/v) sodium gluconate or 0%, 0.5%, 1% and 1.5% (w/v) fructose. Error bars represent SD. n = 3 biological replicates. 329

Figure 8.17 - Full data representing mean $P3HB^{+}/P3HB^{++}$ P-546 (P3HB) per cell ((A) and (B)), mean percentage of $P3HB^{++}$ cells ((C) and (D)) for *C. necator* cultures containing 0.08% (w/v) ME and supplemented with 0%, 0.6%, 1.1% and 1.6% (w/v) sodium gluconate. Error bars represent SD. n = 3 biological replicates. 330

Figure 8.18 - Full data for mean overall FSC (cell size) ((a) and (b)) and mean P3HB^{+}/P3HB^{++} FSC (cell size) for *C. necator* cultures containing 0.08% (w/v) ME and supplemented with 0%, 0.6%, 1.1% and 1.6% (w/v) sodium gluconate ((c) and (d)) or 0%, 0.5%, 1% and 1.5% (w/v) fructose ((e) and (f)). Error bars represent SD. n = 3 biological replicates. 331

Figure 8.19 – Graphs displaying full data for SYTO62 and P-546 staining optimisations. Cultures used contained *C. necator* grown for 72 hours in 0.08% (w/v) ME supplemented with 0.6% (w/v) sodium gluconate. 332

Figure 8.20 – Full data showing mean events per mL for *C. necator* cultures grown in 0.08% (w/v) ME and supplemented with 0.6% (w/v) sodium gluconate. Error bars represent SD. n = 3 biological replicates. 333

Figure 8.21 – Full data showing mean P-546 fluorescence per cell ((a) and (b)) and per mL ((c) and (d)) in addition to the mean percentage of P3HB^{++} cells for *C. necator* cultures grown in 0.08% (w/v) ME and supplemented with 0.6% (w/v) sodium gluconate. Error bars represent SD. n = 3 biological replicates. 334

Figure 8.22 – Full data showing the mean P-546 fluorescence (P3HB) per cell ((a and (b)) and per mL ((c) and (d)) for *C. necator* cultures grown in 0.08% (w/v) ME and supplemented with 0.6% (w/v) sodium gluconate. Error bars represent SD. n = 3 biological replicates. 335

Figure 8.23 – Full data showing mean overall FSC (cell size) and P3HB^{+}/P3HB^{++} FSC (cell size) for *C. necator* cultures grown in 0.08% (w/v) ME and supplemented with 0.6% (w/v) sodium gluconate. Error bars represent SD. n = 3 biological replicates. 336

Figure 8.24 – Full mean events per mL for *C. necator* cultures containing either 0.08% or 0.2% (w/v) ME and supplemented with 0.5%, 1% and 1.5% (w/v) fructose. Error bars represent SD. n = 2 biological replicates. 337

Figure 8.25 – Full data showing mean P-546 fluorescence per cell ((a) and (b)) and per mL ((c) and (d)) and the mean percentage of P3HB^{++} cells for *C. necator* cultures containing either 0.08% or 0.2% (w/v) ME and supplemented with 0.5%, 1% and 1.5% (w/v) fructose. Error bars represent SD. n = 2 biological replicates. 338

Figure 8.26 – Full data showing mean P3HB^{+} ((a) and (b)) P3HB^{++} ((c) and (d)) P-546 fluorescence per cell for *C. necator* cultures containing either 0.08% or 0.2% (w/v) ME and supplemented with 0.5%, 1% and 1.5% (w/v) fructose. Error bars represent SD. n = 2 biological replicates. 339

Figure 8.27 – Full data showing mean P3HB^{+} ((a) and (b)) P3HB^{++} ((c) and (d)) P-546 fluorescence per mL for *C. necator* cultures containing either 0.08% or 0.2% (w/v) ME and supplemented with 0.5%, 1% and 1.5% (w/v) fructose. Error bars represent SD. n = 2 biological replicates. 340

Figure 8.28 – Full data showing mean FSC (cell size) for the overall population ((a) and (b)) and the P3HB^{+} ((c) and (d)) and P3HB^{++} ((e) and (f)) populations for *C. necator* cultures containing either 0.08% or 0.2% (w/v) ME and supplemented with 0.5%, 1% and 1.5% (w/v) fructose. Error bars represent SD. n = 2 biological replicates. 341

Figure 8.29 - Full data showing comparisons of flow cytometry events per mL at 24 hours for 0.08% (w/v) *C. necator* supplemented with 0.5%, 1% and 1.5% (w/v) fructose or 0.6% (w/v) sodium gluconate. Error bars

REPRESENT SD. N = 2 BIOLOGICAL REPLICATES FOR FRUCTOSE SUPPLEMENTED CULTURES AND N = 3 FOR SODIUM GLUCONATE SUPPLEMENTED CULTURES. 342

FIGURE 8.30 - FULL DATA SHOWING COMPARISONS OF MEAN P-546 FLUORESCENCE PER CELL ((A) AND (B)) AND PER ML ((C) AND (D)) AT 168 HOURS FOR 0.08% (W/V) *C. NECATOR* SUPPLEMENTED WITH 0.5%, 1% AND 1.5% (W/V) FRUCTOSE OR 0.6% (W/V) SODIUM GLUCONATE. ERROR BARS REPRESENT SD. N = 2 BIOLOGICAL REPLICATES FOR FRUCTOSE SUPPLEMENTED CULTURES AND N = 3 FOR SODIUM GLUCONATE SUPPLEMENTED CULTURES. 343

FIGURE 9.1 – FULL MEAN EVENTS PER ML DATA FOR *C. NECATOR* CULTURES CONTAINING 0.08%, 0.2% OR 0.4% (W/V) AND SUPPLEMENTED WITH 0.5% (W/V) FRUCTOSE AT 0 HOURS AND EITHER 0.6% OR 1.2% (W/V) SODIUM GLUCONATE AT 24 HOURS. ERROR BARS REPRESENT SD. N = 2 BIOLOGICAL REPLICATES. 344

FIGURE 9.2 – FULL DATA FOR P-546 FLUORESCENCE (P3HB) PER CELL ((A) AND (B)) AND PER ML ((C) AND (D)) IN ADDITION TO THE PERCENTAGE OF $P3HB^{++}$ CELLS ((E) AND (F)) FOR *C. NECATOR* CULTURES CONTAINING 0.08%, 0.2% OR 0.4% (W/V) AND SUPPLEMENTED WITH 0.5% (W/V) FRUCTOSE AT 0 HOURS AND EITHER 0.6% OR 1.2% (W/V) SODIUM GLUCONATE AT 24 HOURS. ERROR BARS REPRESENT SD. N = 2 BIOLOGICAL REPLICATES. 345

FIGURE 9.3 – FULL DATA DISPLAYING P-546 FLUORESCENCE (P3HB) PER CELL FOR THE $P3HB^{+}$ AND $P3HB^{++}$ POPULATIONS FOR *C. NECATOR* CULTURES CONTAINING 0.08%, 0.2% OR 0.4% (W/V) AND SUPPLEMENTED WITH 0.5% (W/V) FRUCTOSE AT 0 HOURS AND EITHER 0.6% OR 1.2% (W/V) SODIUM GLUCONATE AT 24 HOURS. ERROR BARS REPRESENT SD. N = 2 BIOLOGICAL REPLICATES. 346

FIGURE 9.4 - FULL DATA DISPLAYING P-546 FLUORESCENCE (P3HB) PER ML FOR THE $P3HB^{+}$ AND $P3HB^{++}$ POPULATIONS FOR *C. NECATOR* CULTURES CONTAINING 0.08%, 0.2% OR 0.4% (W/V) AND SUPPLEMENTED WITH 0.5% (W/V) FRUCTOSE AT 0 HOURS AND EITHER 0.6% OR 1.2% (W/V) SODIUM GLUCONATE AT 24 HOURS. ERROR BARS REPRESENT SD. N = 2 BIOLOGICAL REPLICATES. 347

FIGURE 9.5 - FULL DATA SHOWING MEAN FSC (CELL SIZE) FOR THE OVERALL POPULATION ((A) AND (B)) AND THE $P3HB^{+}$ ((C) AND (D)) AND $P3HB^{++}$ ((E) AND (F)) POPULATIONS FOR *C. NECATOR* CULTURES CONTAINING 0.08%, 0.2% OR 0.4% (W/V) ME AND SUPPLEMENTED WITH 0.5% (W/V) FRUCTOSE AT 0 HOURS AND EITHER 0.6% OR 1.2% (W/V) SODIUM GLUCONATE AT 24 HOURS. ERROR BARS REPRESENT SD. N = 2 BIOLOGICAL REPLICATES. 348

FIGURE 9.6 - FULL MEAN EVENTS DATA FOR *C. NECATOR* CULTURES GROWN IN MEDIA CONTAINING EITHER 0.08% OR 0.2% (W/V) ME, 0, 3, 6, 9, 12 OR 15 G/L SODIUM CHLORIDE AND SUPPLEMENTED WITH 0.5% (W/V) FRUCTOSE AT 0 HOURS AND 0.6% (W/V) SODIUM GLUCONATE AT 24 HOURS. ERROR BARS REPRESENT SD. N = 3 BIOLOGICAL REPLICATES. 349

FIGURE 9.7 - FULL DATA FOR P-546 FLUORESCENCE (P3HB) PER CELL ((A) AND (B)) AND PER ML ((C) AND (D)) IN ADDITION TO THE PERCENTAGE OF $P3HB^{++}$ CELLS ((E) AND (F)) FOR *C. NECATOR* CULTURES GROWN IN MEDIA CONTAINING EITHER 0.08% OR 0.2% (W/V) ME, 0, 3, 6, 9, 12 OR 15 G/L SODIUM CHLORIDE AND SUPPLEMENTED WITH 0.5% (W/V) FRUCTOSE AT 0 HOURS AND 0.6% (W/V) SODIUM GLUCONATE AT 24 HOURS. ERROR BARS REPRESENT SD. N = 3 BIOLOGICAL REPLICATES. 350

FIGURE 9.8 – FULL DATA DISPLAYING P-546 FLUORESCENCE (P3HB) PER CELL FOR THE $P3HB^{+}$ AND $P3HB^{++}$ POPULATIONS FOR *C. NECATOR* CULTURES CONTAINING EITHER 0.08% OR 0.2% (W/V) ME, 0, 3, 6, 9, 12 OR 15 G/L SODIUM CHLORIDE AND SUPPLEMENTED WITH 0.5% (W/V) FRUCTOSE AT 0 HOURS AND 0.6% (W/V) SODIUM GLUCONATE AT 24 HOURS. ERROR BARS REPRESENT SD. N = 3 BIOLOGICAL REPLICATES. 351

Figure 9.9 - Full data displaying P-546 fluorescence (P3HB) per cell for the P3HB^{+} and P3HB^{++} populations for *C. necator* cultures containing either 0.08% or 0.2% (w/v) ME, 0, 3, 6, 9, 12 or 15 g/L sodium chloride and supplemented with 0.5% (w/v) fructose at 0 hours and 0.6% (w/v) sodium gluconate at 24 hours. Error bars represent SD. n = 3 biological replicates. 352

Figure 9.10 - Full data showing mean FSC (cell size) for the overall population ((a) and (b)) and the P3HB^{+} ((c) and (d)) and P3HB^{++} ((e) and (f)) populations for *C. necator* cultures containing either 0.08% or 0.2% (w/v) ME, 0, 3, 6, 9, 12 or 15 g/L sodium chloride and supplemented with 0.5% (w/v) fructose at 0 hours and 0.6% (w/v) sodium gluconate at 24 hours. Error bars represent SD. n = 3 biological replicates. 353

Figure 9.11 – Full mean events per mL data for *C. necator* cultures grown initially in either 0.08% or 0.2% (w/v) ME up to 24 hours when the growth media was changed to either 0.008% or 0.04% (w/v) ME. Media before and after 24 hours was supplemented with either 0.5% (w/v) fructose or 0.6% (w/v) sodium gluconate. Error bars represent SD. n = 3 biological replicates. 354

Figure 9.12 - Full data for P-546 fluorescence (P3HB) per cell ((a) and (b)) and per mL ((c) and (d)) in addition to the percentage of P3HB^{++} cells ((e) and (f)) for *C. necator* cultures grown initially in either 0.08% or 0.2% (w/v) ME up to 24 hours when the growth media was changed to either 0.008% or 0.04% (w/v) ME. Media before and after 24 hours was supplemented with either 0.5% (w/v) fructose or 0.6% (w/v) sodium gluconate. Error bars represent SD. n = 3 biological replicates. 355

Figure 9.13 - Full data displaying P-546 fluorescence (P3HB) per cell for the P3HB^{+} and P3HB^{++} populations for *C. necator* cultures grown initially in either 0.08% or 0.2% (w/v) ME up to 24 hours when the growth media was changed to either 0.008% or 0.04% (w/v) ME. Media before and after 24 hours was supplemented with either 0.5% (w/v) fructose or 0.6% (w/v) sodium gluconate. Error bars represent SD. n = 3 biological replicates. 356

Figure 9.14 - Full data displaying P-546 fluorescence (P3HB) per mL for the P3HB^{+} and P3HB^{++} populations for *C. necator* cultures grown initially in either 0.08% or 0.2% (w/v) ME up to 24 hours when the growth media was changed to either 0.008% or 0.04% (w/v) ME. Media before and after 24 hours was supplemented with either 0.5% (w/v) fructose or 0.6% (w/v) sodium gluconate. Error bars represent SD. n = 3 biological replicates. 357

Figure 9.15 - Full data showing mean FSC (cell size) for the overall population ((a) and (b)) and the P3HB^{+} ((c) and (d)) and P3HB^{++} ((e) and (f)) populations for *C. necator* cultures grown initially in either 0.08% or 0.2% (w/v) ME up to 24 hours when the growth media was changed to either 0.008% or 0.04% (w/v) ME. Media before and after 24 hours was supplemented with either 0.5% (w/v) fructose or 0.6% (w/v) sodium gluconate. Error bars represent SD. n = 3 biological replicates. 358

Figure 9.16 – Full mean events data for *C. necator* cultures initially containing 0.08% or 0.2% (w/v) ME and supplemented with 0.5% (w/v) fructose, 0.6% (w/v) sodium gluconate or both. Media was either changed or not changed or replaced with 0.04% (w/v) ME and supplemented with both 0.5% (w/v) fructose and 0.6% (w/v) sodium gluconate. Error bars represent SD. n = 3 biological replicates. 359

Figure 9.17 - Full data for P-546 fluorescence (P3HB) per cell ((a) and (b)) and per mL ((c) and (d)) in addition to the percentage of $P3HB^{++}$ cells ((e) and (f)) for *C. necator* cultures initially containing 0.08% or 0.2% (w/v) ME and supplemented with 0.5% (w/v) fructose, 0.6% (w/v) sodium gluconate or both. Media was either changed or not changed or replaced with 0.04% (w/v) ME and supplemented with both 0.5% (w/v) fructose and 0.6% (w/v) sodium gluconate. Error bars represent SD. n = 3 biological replicates. 360

Figure 9.18 - Full data displaying P-546 fluorescence (P3HB) per cell for the $P3HB^{+}$ and $P3HB^{++}$ populations for *C. necator* cultures initially containing 0.08% or 0.2% (w/v) ME and supplemented with 0.5% (w/v) fructose, 0.6% (w/v) sodium gluconate or both. Media was either changed or not changed or replaced with 0.04% (w/v) ME and supplemented with both 0.5% (w/v) fructose and 0.6% (w/v) sodium gluconate. Error bars represent SD. n = 3 biological replicates. 361

Figure 9.19 - Full data displaying P-546 fluorescence (P3HB) per mL for the $P3HB^{+}$ and $P3HB^{++}$ populations for *C. necator* cultures initially containing 0.08% or 0.2% (w/v) ME and supplemented with 0.5% (w/v) fructose, 0.6% (w/v) sodium gluconate or both. Media was either changed or not changed or replaced with 0.04% (w/v) ME and supplemented with both 0.5% (w/v) fructose and 0.6% (w/v) sodium gluconate. Error bars represent SD. n = 3 biological replicates. 362

Figure 9.20 - Full data showing mean FSC (cell size) for the overall population ((a) and (b)) and the $P3HB^{+}$ ((c) and (d)) and $P3HB^{++}$ ((e) and (f)) populations for *C. necator* cultures initially containing 0.08% or 0.2% (w/v) ME and supplemented with 0.5% (w/v) fructose, 0.6% (w/v) sodium gluconate or both. Media was either changed or not changed or replaced with 0.04% (w/v) ME and supplemented with both 0.5% (w/v) fructose and 0.6% (w/v) sodium gluconate. Error bars represent SD. n = 3 biological replicates. 363

List of tables

TABLE 1 - CHEMICAL STRUCTURE OF SELECT SHORT AND MEDIUM-CHAIN LENGTH PHAS, PHB, PHV, PHHX, PHO, P(4HB) AND PMP. 49

TABLE 2 - COMPARISONS OF MECHANICAL AND THERMAL PROPERTIES OF P3HB IN COMPARISON TO PP, PE, AND PET. 61

TABLE 3 - SUMMARY OF P3HB CONTAINING CO-POLYMER PRODUCTION BY *C. NECATOR* DETAILING THE GROWTH CONDITIONS, MECHANICAL PROPERTIES AND THERMAL PROPERTIES. 63

TABLE 4 - A SUMMARY OF PUBLICATIONS DETAILING THE PRODUCTION OF P3HB CONTAINING CO-POLYMERS IN *E. COLI* STRAINS USING GENES ORIGINALLY FROM *C. NECATOR*. 67

TABLE 5 - A SUMMARY OF PUBLICATIONS DETAILING THE PRODUCTION OF P3HB CO-POLYMERS USING GENETICALLY MODIFIED *C. NECATOR*. 68

List of abbreviations

3D - 3 dimensional
ABS - Acrylonitrile butadiene styrene
ACP - Acyl carrier protein
C. necator - *Cupriavidus necator*
CA - Cellulose acetate
CAB - *phaC*, *phaA*, *phaA*
CoA - Coenzyme A
DCW - Dry cell weight
DMSO - Dimethyl sulfoxide
DNA - Deoxyribonucleic acid
E. coli - *Escherichia coli*
EDS - Energy dispersive x-ray spectroscopy
FSC - Forward scatter
GC - Gas chromatography
GPa - Gigapascal
H_2O - Water
HDPE - High density polyethylene
LCL - Long chain length
LDPE - Low density polyethylene
LLDPE - Linear low density poly ethylene
m - metres
MCL - Medium chain length
mL - Millilitre
MM - Mineral medium
MSM - Mineral salts medium
OD_{600} - Optical density at 600 nm
P-546 - Pyrromethene-546
P3HB - 3-hydroxybutyrate
P4HB - 4-hydroxybutyrate
PBS - Phosphate buffered saline
PBT - Polybutylene terephthalate
PCL - Polycaprolactone
PE - Polyethylene
PEG - Polyethylene glycol
PET - Polyethylene terephalate
PGAP - PHA granule associated protein
PHA - Polyhydroxyalkanoate
$P3HB^+$ - Low P3HB population
$P3HB^{++}$ - High P3HB population
PhaA - 3-ketothiolase
PhaB - Acetoacetyl-CoA reductase
PhaC - P3HB synthase
PhaG - Transacylase
PhaJ - (R)-specific enoyl-CoA hydratase
PHO - 3-hydroxyoctanoate
PHV - 3- hydroxyvalerate
PI - Propidium iodide
PLA - Polylactic acid
PMMA - polymethyl methacrylate
PMP - 3-mercaptopropionate
PMT - Photomultiplier tube
PP - Polypropylene
PTFE - Polytetrafluoroethylene
PUR - Polyurethane
PVA - Polyvinyl acetate
PVC - Polyvinyl chloride
SCL - Short chain length
SD - Standard deviation from the mean
SDS - Sodium dodecyl sulphate
SEM - Scanning electron microscopy
SSC - Side scatter
TCA - Tricarboxylic acid cycle
TEM - Transmission electron microscopy
TPS - Thermoplastic starch
UV - Ultra violet

Chapter 1 Introduction

1.1 The life cycle of plastics

Since the discovery of the first synthetic plastic Bakelite in 1906 by Belgian chemist Leo Baekeland (Baekeland, 1909), plastics have become increasingly preferred to conventional materials such as wood, metal and paper in the 20th and 21st centuries. Synthetic plastics are high molecular-weight organic polymers which consist of individual hydrocarbon monomer units originating chiefly from crude oil. To date, a wide variety of different hydrocarbon monomers have been discovered which when polymerised form plastic materials which have their own unique mechanical properties. The diversity of material properties that result from mixing and matching monomers means plastics are cheap, pliable, robust and lightweight materials with a multitude of applications (Claudio, 2012; Needhidasan *et al.*, 2014).

In everyday life, plastics have applications in the food packaging, automotive, construction and electronic industries to name but a few. However, while the societal and economic impact of plastic was predicted in the mid-20th century, the environmental impact of disposal and future sustainability of crude oil was not (Thompson *et al.*, 2009). Without consideration for waste and disposal, too often the life of plastic products has developed into a linear economy in which disposal represents an endpoint. Because of this, there is a great concern for the environmental impact of inappropriate waste plastic disposal in the ocean (Lebreton *et al.*, 2018), rivers (Lebreton *et al.*, 2017) and urban areas (Jambeck *et al.*, 2015), the issues of which are receiving global media attention to campaigns such as Sky Ocean Rescue (Sky, 2021). Of particular concern is the accumulation of particular microplastics resulting from the fragmentation of waste plastic and the subsequent lack of biodegradation in aquatic environments. Due to the persistent, non-biodegradable nature of plastic pollution, there is now a consensus that in addition to being more sustainably sourced plastic products should, where possible, move towards biodegradable alternatives. The following sections of this introductory chapter cover in more detail the life cycle of plastics and a group of biodegradable alternatives to synthetic plastics called PHAs will be introduced.

1.1.1 Crude oil distillation

Crude oil is one of the most relied-upon commodities on earth providing fuels, lubricants, road materials and the precursors of plastic production. The life cycle of synthetic plastics begins with the refinement of crude oil in which the hydrocarbon molecules contained in crude oil are separated based on molecular weight. This process is illustrated in Figure 1.1 and is known as crude oil distillation. The two most common hydrocarbon monomers used in plastic production are the alkanes ethane and propane, which can either be directly extracted near the top of the distillation column or produced by the cracking of the naphtha fraction. Some example chemical reactions which describe the cracking process are displayed in Figure 1.2. Cracking involves the rapid heating up of hydrocarbons which causes larger fractions such as naphtha to be broken down into a mixture of smaller alkanes and alkenes such as ethylene and propane. A zeolite catalyst is usually used which consists of solids such as aluminium or silicon which contain pores in which the reaction can take place (Ball, 2002). Ethylene and propane are used to make polypropylene (PP), polyethylene (PE) and PE terephthalate (PET) which in 2020 represented 57.1% of plastics used in Europe (Plastics Europe, 2020).

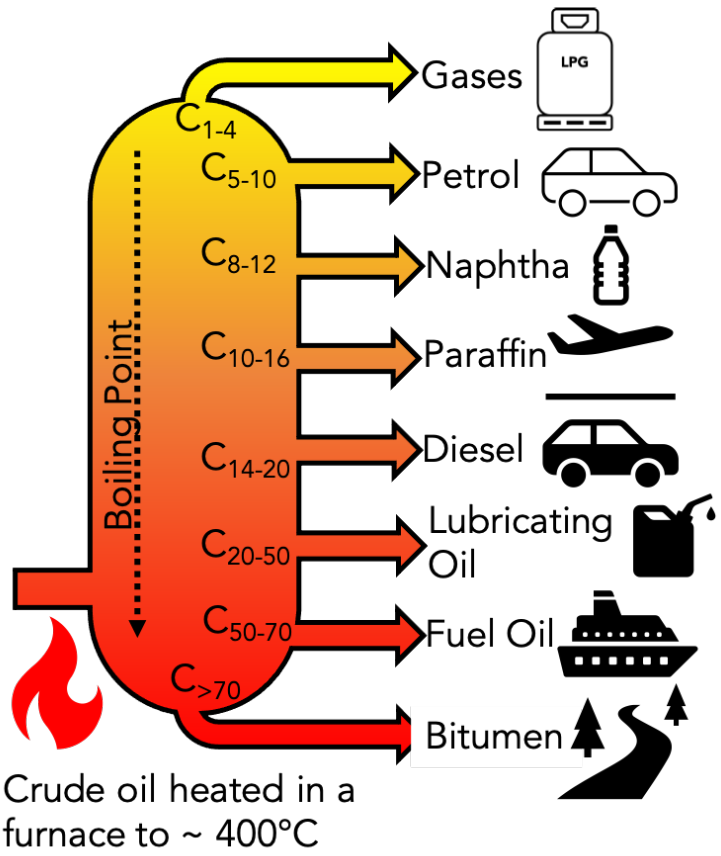


Figure 1.1 - The distillation and application of crude oil fractions illustrate the relationship between hydrocarbon boiling point, chain length and application. Adapted from (PSAC, 2021).

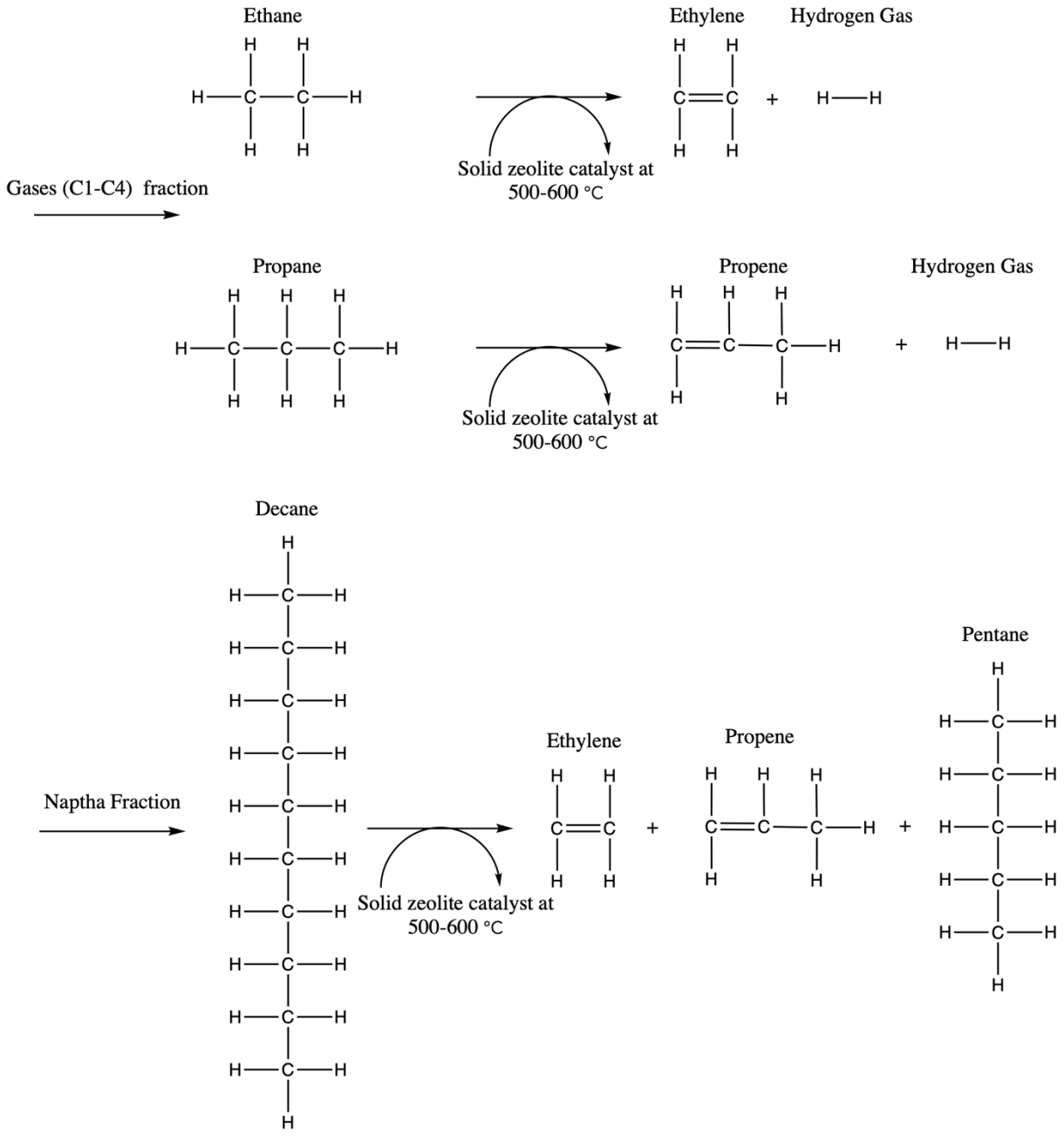


Figure 1.2 - Example steam cracking reactions which produce by far the most common precursors for plastic production, ethylene and propene.

1.1.2 Petrochemically derived plastics

The big 5 plastics in Europe, PE, PP, PVC, PUR and PS are all derived from petrochemical sources which when combined in 2019 represented 81% of the European plastic market. The common theme that connects all of the plastics covered in this section is not just that they are sourced from crude oil derivatives but also their resistance to biodegradation.

The most common plastic in Europe PE accounts for 29.7% of the European market share and is classed as either LLDPE, LDPE (both 0.91-0.94 g/cm^3) or HDPE (0.93-0.97 g/cm^3). Although the density of HDPE is only marginally higher than that of LDPE, it contains a much lower degree of branching resulting in a more crystalline structure that is stronger with a higher tensile strength (Plastics Europe, 2021). As a result, HDPE is used to make products such as pipes, shampoo bottles and toys whereas LLDPE and LDPE are used to make reusable bags, agricultural film and food packaging for example (Plastics Europe, 2020). While PE is thought to be non-toxic to humans it has been shown to interfere with Zebrafish gene expression when ingested as microplastics (McLain, 2007; Mak *et al.*, 2019).

With a market share of 19.3% (Plastics Europe, 2020), PP has vast applications including food packaging, hinged containers and piping (Plastics Europe, 2020). Studies have generally shown that when treated with soil, fungi or bacterial-based methods, PP only displays a reduction in material properties rather than complete biodegradation (Arutchelvi, 2008).

Next on the list representing 10% of the European market share is PVC which is used to make items such as window frames, doors, flooring and pipes. Formed from the combination of ethylene and chlorine gas (Petrović and Hamer, 2018), the production of PVC is the world's greatest consumer of chlorine (Lakshmanan and Murugesan, 2013). The production of chlorine gas is a controversial process which releases chloride and chlorate into the environment and depending on the process used can release mercury into the soil, or utilise asbestos (Lakshmanan and Murugesan, 2013; Petrović and Hamer, 2018). While more modern methods of production are thought to be less environmentally damaging, they have not proven to be non-toxic (Petrović and Hamer, 2018).

Fourth on the list representing 7.9% of the European market is PUR, an extremely versatile material made from polyols and diisocyanates, which has desirable thermal, mechanical and chemical properties suiting it to application in either foam form such as wall insulation and upholstered furniture; or in the thermoplastic form, it can be used as a sealant or elastomer (Zia *et al.*, 2007).

Closely behind PUR with 7.7% of the market share is PET, a polyester produced from the polymerisation of ethylene terephthalate and can be produced in two ways (Dutt and Soni, 2013). The first reaction involves the reaction of terephthalic acid with ethylene glycol. The second method of production is the

transesterification method in which dimethyl terephthalate is reacted with ethylene glycol. Primarily PET is used as a packaging material most notably for plastic bottles (Plastics Europe, 2020).

The last major contributor to the European plastic market is PS, a plastic made from the alkylation of benzene with ethylene which is then dehydrogenated to form styrene (Plastics Europe, 2018). Generally, PS is manufactured into 4 different types all of which have different applications: general purpose PS, used for disposable cutlery and bowls; high impact PS, used for yoghurt containers and cold drink cups; PS foam, used for cold/hot drinks cups and meat/poultry trays; and expanded PS foam, used for cavity wall insulation and electronic goods packaging (Plastics Europe, 2020). Polystyrene is non-biodegradable and microplastics of PS have been shown to have toxic effects on marine microorganisms (Sendra *et al.*, 2019).

Other notable plastics with much smaller market shares include PTFE used for cable coatings, ABS used for car wheel trims, PMMA used for touch screens and PBT used to make optical fibres (Plastics Europe, 2020).

1.1.3 Routes of plastic disposal

Following use, plastic can be disposed of in various ways which are broadly covered by recycling, landfill, litter and reuse and biodegradation. The following section on plastic disposal will predominantly focus on commodity plastic which are the most likely plastics to be disposed of after a single use and subsequently contribute significantly more to environmental pollution in comparison to higher-grade plastics. However, that said, this should not downplay the impact that engineering or high-performance plastics can have on the environment, one example being professional fishing equipment littered in the ocean (Smith *et al.*, 2018).

1.1.3.1 Recycling

Recycling is often thought of as a way for the plastic cycle to be completed in an environmentally friendly and sustainable manner. In reality, plastic recycling is a complicated and challenging procedure which contains controversial elements. There are 4 main types of recycling: primary, re-processing products into a similar product; secondary, re-processing into a material with lesser properties; tertiary, depolymerisation into chemical constituents; and quaternary, the recovery of energy (Hopewell *et al.*, 2009).

Primary recycling also referred to as re-extrusion, reprocesses plastics into a material of equal properties (Al-Salem *et al.*, 2009; Hopewell *et al.*, 2009). The advantage of primary recycling is that it

reintroduces scrap plastics into the plastic cycle by producing products made from the same material. However, this is often difficult in practice due to products being made of more than one type of plastic. Repeated re-extrusion has additionally been found to negatively affect material properties by increasing crystallisation rate, overall crystallinity, higher melting temperature, and a decrease in percentage elongation (Aurrekoetxea *et al.*, 2001). Even though primary recycling is often referred to as a closed-loop system, the evidence suggests there are a limited number of times a material can be reprocessed before material properties deteriorate too far.

Secondary recycling reprocesses plastics into materials of lesser quality and is also referred to as downgrading. The advantage of secondary recycling is that it's a relatively cheap method that enables plastic products to be repurposed when primary recycling is not an option (Hopewell *et al.*, 2009). A disadvantage of secondary recycling is that products generally have limited usage before material properties reduce too far for further downgrading.

Tertiary recycling refers to the depolymerisation of polymers into their chemical constituents and can be split into chemical and biological categories. Considering the problems already discussed with primary and secondary recycling, tertiary recycling may seem like a feasible way to complete the plastic cycle. The biodegradation of plastics is favourable as it prevents plastics from persisting in biological environments. However, as already discussed, the vast majority of the world's most popular plastics are not biodegradable, rendering chemical recycling the only viable method for recycling synthetic plastics.

Chemical recycling methods such as pyrolysis heat plastic in a non-reactive atmosphere to release the chemical constituents. The recovery of plastic chemical constituents can be advantageous as the recovered chemicals can be used to produce new plastics or other synthetic materials (Hopewell *et al.*, 2009). Chemical recycling is not commonly used as the costs associated with re-processing are often greater than the price of new raw materials (Hopewell *et al.*, 2009) and there is still a lack of clarity on the economic viability of this method in the future (Solis and Silveira, 2020).

Quaternary recycling involves the recovery of energy from waste plastic by incineration to produce steam for electricity production (Al-Salem and Baeyens, 2009). The advantages of quaternary recycling are that it reduces the amount plastic waste in the environment while also producing energy at relatively low cost (Gazzoti *et al.*, 2022). There are concerns that incineration releases dangerous levels of toxic compounds such as nitrogen oxides, sulphur oxides, smoke, heavy metals and carcinogenic compounds such as dioxins, polychlorinated dibenzofurans and polycyclic aromatic hydrocarbons (Al-Salem *et al.*, 2009). Generally, recycling symbols are viewed as confusing because symbols such as the Mobius Loop can indicate materials that are recyclable or non-recyclable with the same symbol. This

can be seen to occur for PVC, PS and other plastics which are non-recyclable materials labelled with the same symbol as PET, HDPE, LDPE and PS which are recyclable in the UK. In addition, the Green Dot which is a widespread recycling symbol used by the European Union is often thought to indicate that a material can or has been recycled but only means that the company has donated to the European Union to be able to use the symbol.

1.1.3.2 Disposal to Landfill

Another route for plastic waste to take is disposal to landfill which compartmentalises plastic waste reducing wider environmental impact, while also providing energy in the form of gasses such as methane (Ramprasad *et al.*, 2022). This not only prevents the completion of the plastic cycle but also poses a risk to human health as gradually plastics break down into persistent organic pollutants including endocrine-disrupting chemicals such as bisphenol A which leach into soil and groundwater in the local environment (Xu *et al.*, 2011). As a result, modern landfill sites are designed to contain their contents using an array of linings made from clay, PP and PET in addition to leachate systems and other geomembrane lining systems (Ikehata and Liu, 2011).

1.1.3.3 Disposal as litter

When not disposed of correctly, non-biodegradable plastics accumulate in the environment where they are degraded by a combination of oxidative, hydrolytic, thermal, photo and mechanical stress (Arutchelvi *et al.*, 2008). When non-biodegradable plastics enter an aquatic environment they embrittle exposed to chemical/physical factors and are then broken into micro-plastic particles. Based on size, aquatic litter can be divided into four categories: micro (< 5 mm), meso (< 2.5 cm), macro (< 1 m) and mega (> 1 m) (Smith *et al.*, 2018). In aquatic environments, microplastics can be described as either primary or secondary microplastics (Smith *et al.*, 2018). Primary microplastics are intentionally manufactured to be < 5 mm in size with examples including microbeads contained in cosmetic products (Guerranti *et al.*, 2019) and pellets used to construct larger products. Secondary microplastics originate from larger plastic fragments which degrade into smaller pieces. The contamination of marine environments with microplastics is particularly concerning as marine wildlife can ingest microplastics either directly by feeding strategies such as filter feeding or indirectly as a result of predators consuming prey (Germanov *et al.*, 2018). Another issue aside from microplastics is the release of chemical additives that are known to disrupt the endocrine system of aquatic organisms and affect their breeding capabilities (Chen *et al.*, 2019). Microplastics are also a problem in wastewater which is

contaminated by items such as wet wipes and fibres from clothing materials such as nylon and polyester. In just one wash polyester material can produce 7360 fibres m^2 L^{-1}. Clothing fibres are of particular concern in cities as they have also been detected in the air and can be easily inhaled into the respiratory system (Prata, 2018). Fibres have also been found as far afield as the arctic ocean (Lusher, *et al.*, 2015) and in some artic regions, plastic litter has been reported as hundreds of thousands of pieces per square kilometre (Cózar *et al.*, 2017).

Unfortunately, as the vast majority of plastics released into the environment are of petrochemical origin, biodegradation is not possible and the polymers can take hundreds of years to fully degrade.

1.1.3.4 Reuse

In recent years, the reuse of waste plastic in the construction industry as additives for concrete and asphalt has become more popular (Gu and Ozbakkaloglu, 2016). In addition, plastics have also been reused as equestrian surfaces, providing cheap cushioned all weather indoor, outdoor and gallop surfaces (Universal Recycling, 2021). Efforts in the UK are now being made to ensure engineering and high-performance plastics are recycled or reused at the end of their lifetimes in the UK by directives such as the Waste Electrical and Electronic Equipment (WEEE) Regulations (GOV.UK, 2010) to avoid waste going to landfill.

1.1.3.5 Biodegradation

Biodegradable plastics are defined as materials that are capable of decomposing into H_2O, methane, CO_2, inorganic compounds or biomass within a specific period of time (Song *et al.*, 2009). In aerobic conditions, biodegradable plastics degrade to CO_2 and H_2O, and in anaerobic conditions degrade to CO_2 and methane (Bátori *et al.*, 2018; Basak *et al.*, 2022). It is considered that biodegradable plastics are the most promising method of avoiding the problems associated with plastic pollution such as the formation of microplastics. As a result, the Plastics Microbial Biodegradation Database has been started to gather information regarding the microbes capable of biodegrading plastics, the genes involved and the enzymes responsible (Gan and Zhang, 2019). The following section introduces plastics that are considered greener than those covered in section 1.1.2 some of which are sustainably sourced, biodegradable or in some cases both.

1.1.4 Green alternatives to conventional plastic

1.1.4.1 Sustainably sourced non-biodegradable plastics

To improve the sustainability of plastic a number of plastics derived from green sources have been developed. Plastics referred to as "green" can mistakenly be thought of as biodegradable, but while they offer much-improved sourcing for raw materials green plastics are not always biodegradable.

For example, Nylon 11, also known as polyamide 11, is an engineering plastic belonging to the diverse nylon group of polymers that is produced from the polymerisation of 11-aminoundecanoic acid which is made from ricinoleic acid derived from castor (*Ricinus communis*) oil (Brown *et al.*, 2011). Due to its excellent cryogenic, saltwater resistance, oil resistance and piezoelectric properties, Nylon 11 is used in numerous offshore and automotive applications (Mancic *et al.*, 2016; Di Lorenzo *et al.*, 2019). However while Nylon 11 originates from a sustainable source, it is not biodegradable.

The same applies to green PE which is a biogenic recyclable alternative to conventional PE produced using ethanol derived from sugar cane (Braskem, 2018). The application of green PE includes plastic bags, food packaging and plastic bottles.

Another green-sourced plastic is acetyl cellulose, also known as CA, which is a plastic produced via the acetylation of one of the most abundant natural polymers cellulose (Puls *et al.*, 2011). Cellulose acetates with a low level of acetylation are biodegradable (Tokiwa *et al.*, 2009) but are generally considered non-biodegradable as they need to undergo significant de-acetylation before becoming biodegradable (Puls *et al.*, 2010). The most common application of CA is in clothing fibres but it also has applications in other products such as photographic film.

1.1.4.2 Biodegradable plastics derived from petrochemical sources

Another category that green plastics can fall under is those that are biodegradable but sourced from petrochemical sources.

One example is polybutylene succinate, an aliphatic polyester produced from succinic acid and 1,4-butanediol derived from petrochemical precursors (Puchalski *et al.*, 2018). Due to the biodegradable properties of polybutylene succinate, it is used extensively in agriculture as a means to slowly release compounds such as pesticides (Han *et al.*, 2019) and fertilisers into the soil (Hongsriphan and Pinpueng, 2019). Polybutylene succinate is also considered a promising candidate to replace non-biodegradable food packaging (Siracusa *et al.*, 2017).

Another plastic in this category is PCL, an aliphatic polyester that is made up of repeating hexanoate units (Labet and Thielemans, 2009) which can be made either by the ring-opening polymerisation of ε-

caprolactone using various catalysts or by the radical ring-opening polymerisation of 2-methylene-1-3-dioxepane (Chen *et al.*, 2015). Polycaprolactone is extremely miscible with other polymers and can be mixed with polymers such as PVC as a plasticising agent (Deanin and Bai, 1984). Due to a slow biodegradation rate of 2 to 4 years in comparison to other drug-delivery polymers, PCL has been applied in medicine as a drug-delivery device (Labet and Thielemans, 2009). As a result, PCL has been used under the trade name Maxon™ and used for slow-degrading sutures and drug-delivery systems that stay active for over a year (Woodruff and Hutmacher, 2010).

1.1.4.3 Biodegradable plastics derived from green sources

The final category of green plastics is those that originate from green sources that have the additional advantage of being biodegradable.

The first example is TPS, formed when starch granules extracted from plants are combined with H_2O using heat and shear (Nafchi *et al.*, 2013). Starch in its native form comprises anhydroglucose units which are joined by α-1,4 glycosidic bonds (Ogunsona *et al.*, 2018). Thermoplastic starch is held back by poor mechanical properties most notably progressive crystallisation and brittleness (Ogunsona *et al.*, 2018). As a result, TPS is often modified at its -OH group (Ogunsona *et al.*, 2018) with plasticisers such as water, glycerine and sorbitol to improve material properties (Nafchi *et al.*, 2013).

A second example is PLA which can be produced chemically by reacting acetaldehyde derived from the oxidation of ethylene with hydrogen cyanide to form lactonitrile which can then be hydrolysed by sulfuric acid into an equal mixture of D and L-lactic acid (Singhvi *et al.*, 2019). However, as hydrogen cyanide and sulfuric acid are both extremely toxic to humans the more sustainable and environmentally friendly microbial fermentation method is preferred. This involves polylactic acid being formed by the polymerisation of lactic acid which is sourced from the fermentation of sugar derived from renewable sources such as sugar cane or corn starch (Singhvi *et al.*, 2019). Polylactic acid is both biodegradable and non-toxic to the human body and as such has been used for many pharmaceutical and medical purposes such as slow-release drug coatings and biodegradable implants (Gupta *et al.*, 2007). Additionally, PLA is one of the main filaments used in 3D printing which is becoming increasingly popular (Chen *et al.*, 2020). A problem with PLA is that it is uses biomass that can also be used for food creating ethical issues regarding its sourcing (Tachibana *et al.*, 2010). The focus of the remainder of this thesis however is on the production of P3HB, a member of the PHA class of biodegradable polyesters produced by the intracellular polymerisation of 3HB. The following sections will explore the biosynthesis and industrial production of PHAs in particular P3HB in more depth.

1.2 Polyhydroxyalkanoates

1.2.1 Intracellular PHA granule structure and function

During conditions of nutrient limitation when the ratio of available C to key nutrients is high, certain bacteria can store carbon as an energy source in the form of cytoplasmic PHA granules. This is a defence mechanism which primarily provides resistance to nutrient stress but additionally provides resistance to other physical, chemical and biological stresses (Wang *et al.*, 2009) such as freezing temperatures (Obruca *et al.*, 2016). The polymer granules consist of a PHA polymer core and a stabilising outer layer of PGAPs which compartmentalise the PHA to prevent an osmotic change that would cause detrimental nutrient leakage out of the cell (Verlinden *et al.*, 2007). Typically, PHA granules are 0.2-0.5 μm in diameter (Hermawan and Jendrossek, 2007) and can contribute up to 85% of the DCW (Wang *et al.*, 2009). Consisting of between 600 and 35,000 R-hydroxy fatty acid monomers (Anjum *et al.*, 2016), PHAs are natural biodegradable polyesters the general structure of which is displayed in Figure 1.3. If the PHA monomer consists of 5 or fewer carbon atoms, then it is referred to as a short chain length (SCL) PHA, for example, poly-3-hydroxybutyrate (P3HB) and poly-3-hydroxyvalerate (P3HV). If a PHA monomer contains 6 to 16 carbon atoms they are referred to as medium chain length (MCL) PHAs an example of which is poly-3-hydroxyhexanoate (P3HHx). If a PHA consists of more than 16 C atoms then it is known as a long chain length (LCL) PHA. The structure of some PHA monomers reported in literature are displayed in Figure 1.3. In SCL PHAs, crystals are densely packed creating a rigid structure with low flexibility and tensile strength (Nakajima *et al.*, 2017). With increasing chain length, the crystals are unable to pack as densely thus increasing flexibility (Nakajima *et al.*, 2017). In biologically active environments such as soil, PHAs completely degrade into H2O and CO_2 in aerobic conditions and methane CO_2 in anaerobic conditions (Bátori *et al.*, 2018; Basak *et al.*, 2022). This has made PHAs an attractive alternative to conventional plastics with potential applications as food packaging, slow-release agricultural compounds and various medical devices. The most commonly produced PHA is PH3B which is most widely studied in the bacterium *C. necator*. The following sections will explore the biosynthesis, production and extraction of P3HB in *C. necator* and other PHA-producing bacteria in more detail.

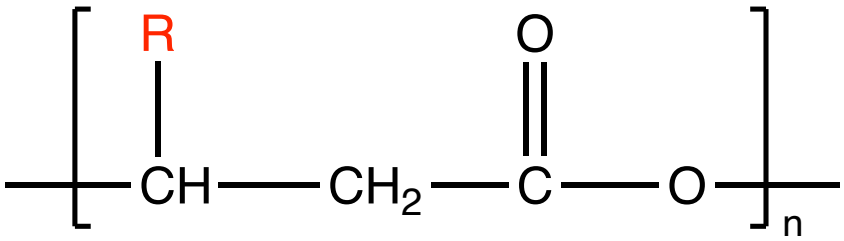
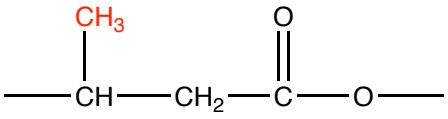
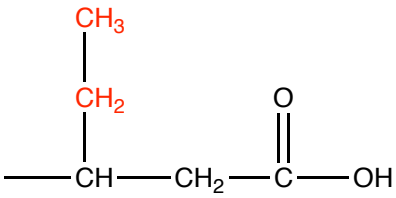
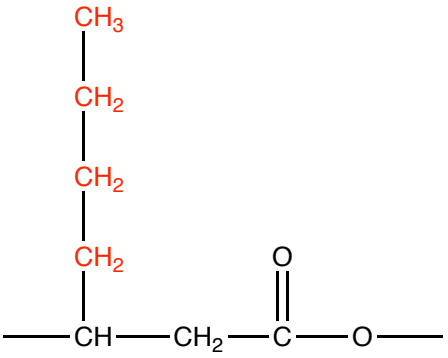
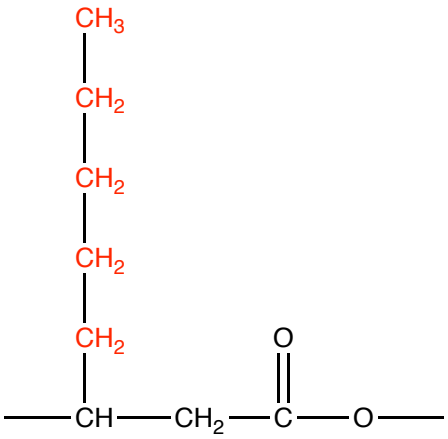
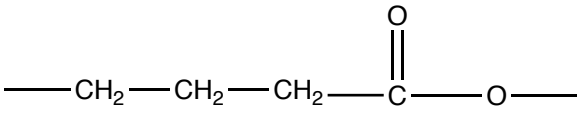
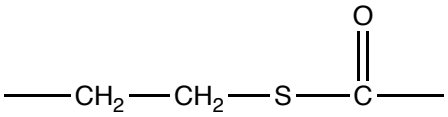


Figure 1.3 - General chemical structure of PHA monomer units where n is the number of repeating units.

Table 1 - Chemical structure of select short and medium-chain length PHAs, PHB, PHV, PHHx, PHO, P(4HB) and PMP.

Monomer	Polymer Abbreviation	Chemical Structure
3-hydroxybutyrate	P3HB	
3-hydroxyvalerate	P3HV	
3-hydroxyhexanoate	P3HHx	
3-hydroxyoctanoate	P3HO	

4-hydroxybutyrate	P4HB	
3-mercaptopropionate	PMP	

1.2.2 The biosynthesis of P3HB in *C. necator*

The biosynthesis of P3HB in *C. necator* is controlled by the *phaCAB* operon which consists of the *phaA*, *phaB* and *phaC* genes, the relative size and direction of transcription of which are illustrated in Figure 1.4, and the illustrated metabolic pathway is illustrated in Figure 1.5. The first gene in the operon *phaA* acts effectively as a molecular switch that communicates the metabolic state of the cell. During normal growth-promoting conditions acetyl-CoA is consumed by the Krebs cycle to produce energy for the cell and the resulting free CoA is thought to inhibit the PhaA enzyme (Mansfield *et al.*, 1995). However, when key nutrients particularly nitrogen and phosphorous-containing compounds or oxygen are depleted, cell proliferation stops and free CoA reduces in concentration and the transcription of the PhaA enzyme is no longer inhibited. This allows for the PhaA enzyme to become active and convert acetyl-CoA to acetoacetyl-CoA in a thiolase reaction (Verlinden *et al.*, 2007). The enzyme PhaB then creates the monomer 3-hydroxybutyryl-CoA via a reductase reaction which is then polymerised by the PhaC1. The resulting polyesters comprise between 600-35,000 R-hydroxy fatty acid monomers (Anjum *et al.*, 2016) which are polymerised via an ester linkage between the hydroxyl and carboxyl groups (Madison and Huisman, 1999).

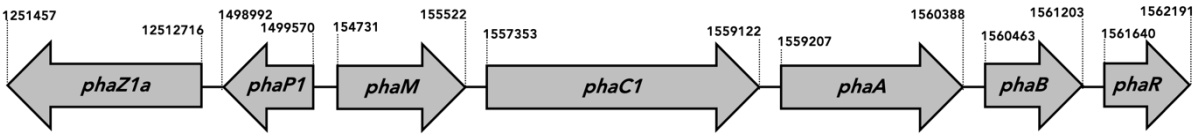


Figure 1.4 - A diagram illustrating the gene positions and direction of transcription of the *C. necator phaCAB* operon responsible for the intracellular production of P3HB in addition to the genes responsible for the transcription of other key PGAPs in *C. necator*.

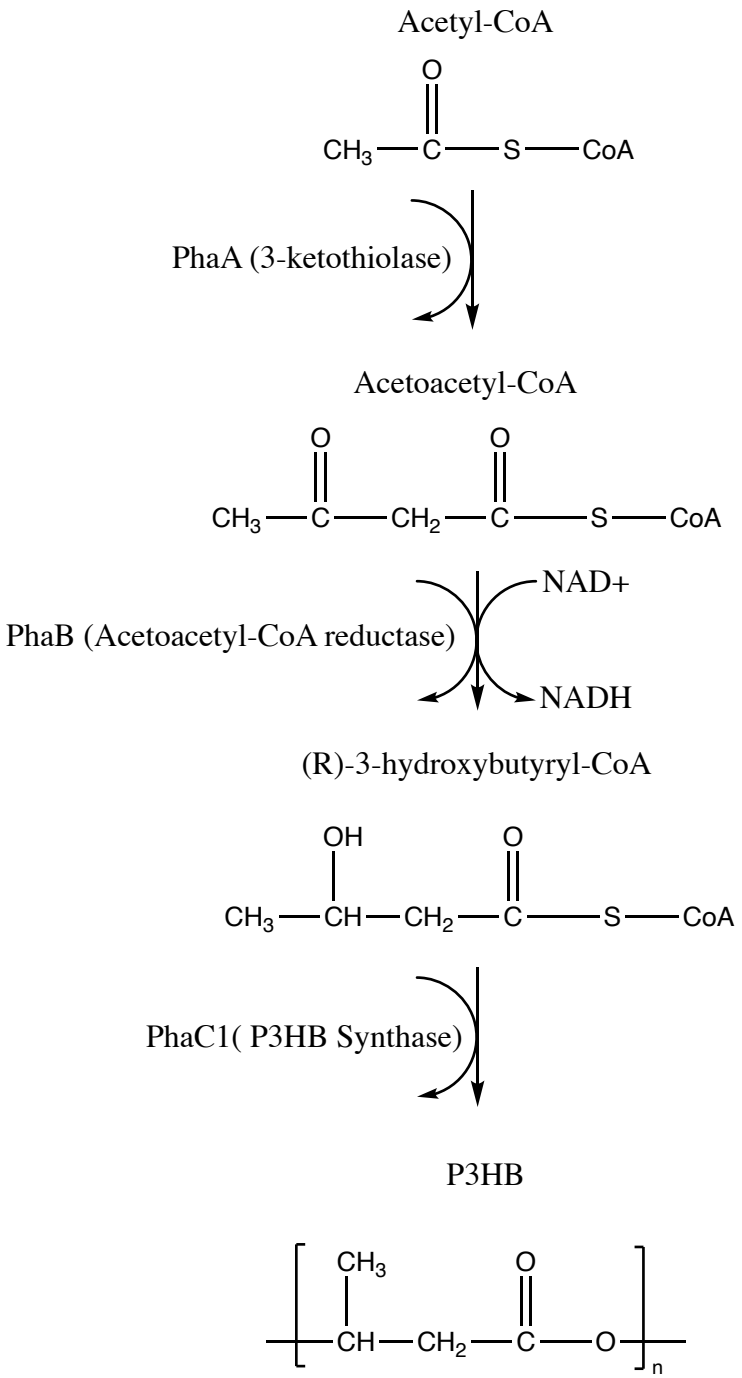


Figure 1.5 - The biosynthetic pathway of the *phaCAB* operon in *C. necator* responsible for the production of intracellular PH3B. n represents the number of repeating units. Adapted from Verlinden *et al*. (2007).

1.2.3 Polyhydroxyalkanoate-associated proteins

1.2.3.1 Phasins - PhaP1 and its regulation by PhaR in *C. necator*

Encapsulating PHA granules is a multi-functional protein scaffold which has various architectural, regulatory and metabolic functions (Maestro and Sanz, 2017). The most abundant group of PGAPs present in this layer are called phasins (Jendrossek, 2009). Phasins are amphiphilic proteins that prevent the non-specific binding of cellular components to the hydrophobic PHA and are phylogenetically comparable between PHA-producing bacteria (Maestro and Sanz, 2017).

In *C. necator* the most common Phasin protein is PhaP1 which interacts with the granule to determine polymer length, surface area and size (York *et al.*, 2001). Phasin proteins PhaP2 (Schwartz *et al.*, 2003), PhaP3, PhaP4 (Pötter *et* al., 2004), PhaP5 (Pfeiffer *et al.*, 2011) PhaP6 and PhaP7 (Pfeiffer and Jendrossek, 2012) are much less abundant in comparison to PhaP1 and their exact function is largely unknown. Mutants deficient in PhaP1 lose the ability to form P3HB inclusions and are more rapidly degraded. However, the deletion of the other phasins does not appear to alter wild-type P3HB accumulation and usage by bacteria (Maestro and Sanz, 2017). The transcription of PhaP is regulated by the DNA-binding protein PhaR (Figure 1.6) which in non-P3HB promoting conditions binds to the PhaP promotor preventing transcription (Maehara *et al.*, 2001; (Maehara *et al.*, 2002). When P3HB begins to be formed, PhaR instead binds to the P3HB granule thus activating the transcription of PhaP. As this regulation system is well understood, Fukui *et al.* (2011) have developed a reporter plasmid which produces green fluorescent protein at the same time as PhaP, allowing PhaP to be quantified. Unlike PhaP, PhaM has been shown to interact with the nucleoid, PhaC1 and PhaP5 (Pfeiffer *et al.*, 2011).

1.2.3.2 PhaM in *C. necator*

The PhaM protein has been shown to exhibit similar control over P3HB granule size as that displayed by PhaP1, but additionally has a key role in the equal segregation of P3HB granules during cell division (Pfeiffer *et al.*, 2011; Bresan and Jendrossek, 2017). The PhaP5 protein appears to play a key role in granule segregation during cell division, interacting with the PhaM protein (Pfeiffer *et al.*, 2011). For many years it was unclear if phospholipids were additionally found on the granule surface (Griebel *et al.*, 1968). However, more recent studies have provided more substantial evidence ruling out the presence of phospholipids (Bresnan *et al.*, 2016).

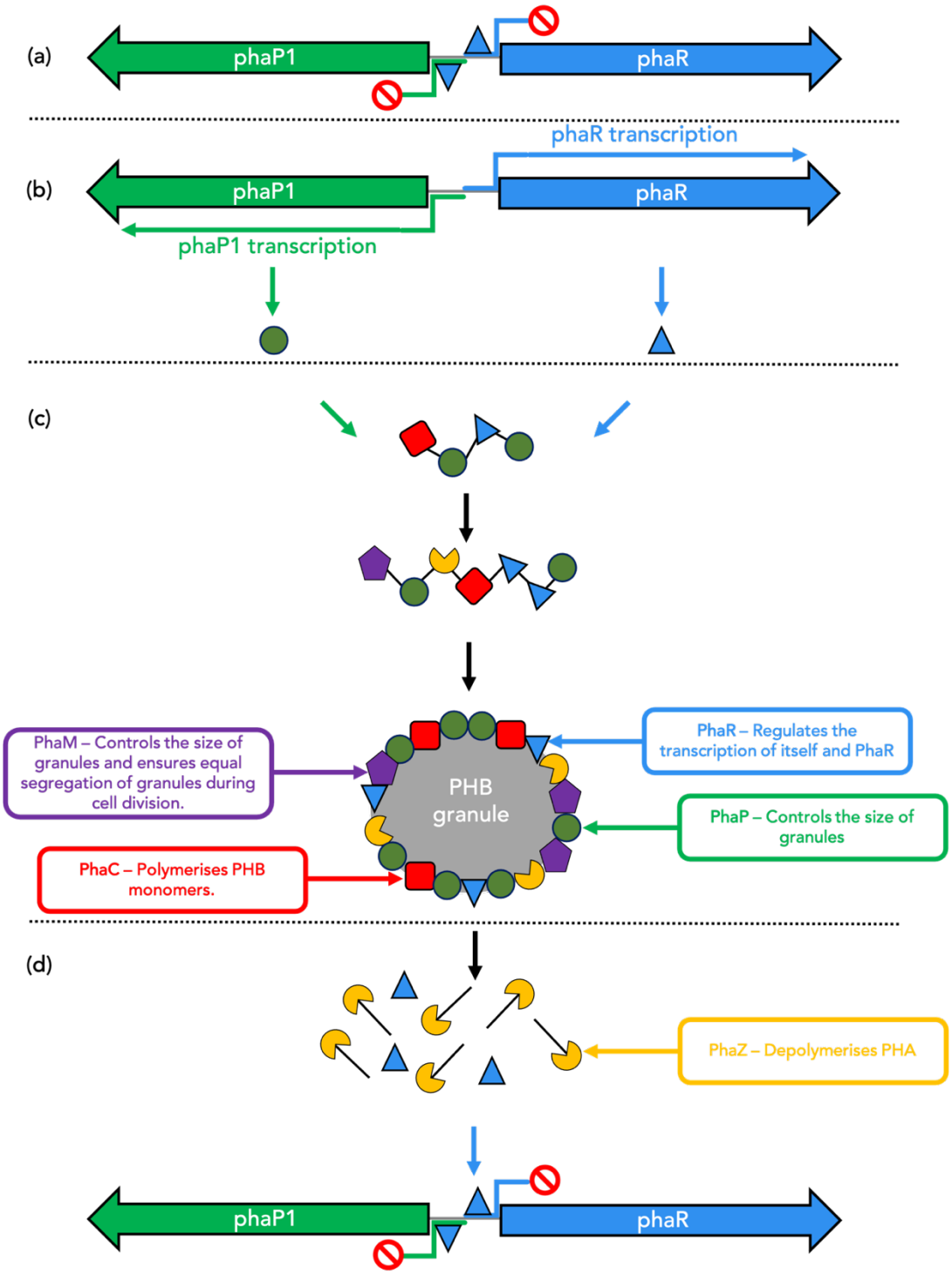


Figure 1.6 - The transcriptional regulation of PhaP1 in *C. necator* by PhaR during P3HB-promoting and non-P3HB-promoting conditions. (a) When growth-promoting levels of key nutrients are available PhaR binds to the promotor region of *phaP* and *phaR*. (b) During growth-limiting nutrient conditions, PhaR detaches from the *phaP* and *phaR* promotors migrate to the newly forming P3HB granules allowing transcription to proceed. (c) Granule formation with PGAP matrix dictating granule formation. (d) When nutrient-promoting conditions return P3HB granules are depolymerisation by PhaZ which releases bound PhaR which binds to the *phaP* and *phaR* promotors once again inhibiting transcription.

1.2.3.3 Poly-3-hydroxybutyrate synthase in *C. necator*

In *C. necator* the enzyme responsible for catalysing the polymerisation of 3-hydroxybutyrate-CoA monomers into P3HB is PhaC1 (Zhang *et al.*, 2015). The PhaC enzymes are divided into 4 groups based on their structure and substrate specificity with classes I, III and IV producing short-chain length PHAs and class II producing medium-chain length PHAs (Mezzolla *et al.*, 2018). In *C. necator*, type I PhaC1 is present and able to catalyse the polymerisation of 3HB, 3HV and 3HHx (Dennis *et al.*, 1998). Studies have shown that PhaC1 is activated upon the binding of PhaM, the binding of which both decreases the lag time for PhaC1 to start polymerising PHA and (Uchino *et al.*, 2008) increases the specific activity of the enzyme (Pfeiffer and Jendrossek, 2014). Additionally, PhaC1 has been linked with the depolymerisation of P3HB, with Uchino and Saito (2006) showing that when P3HB granules and PhaC1 are incubated with CoASH, 3HB-CoA produced via a thiolysis reaction.

1.2.3.4 Poly-3-hydroxybutyrate depolymerase

The depolymerisation of PH3B is less well understood in comparison to that of PH3B biosynthesis. As a result, the PHA Depolymerase Engineering Database has been used to keep track of developments and to allow for systemic analysis (Knoll *et al.*, 2009). Currently, *C. necator* has been found to have 7 intracellular and 2 extracellular PHA depolymerase enzymes (University of Stuttgart, 2009). The two most studied P3HB depolymerase are PhaZ1a, which depolymerises P3HB via thiolysis; and PhaZ2 which depolymerises PH3B via hydrolysis (Kobayashi *et al.*, 2003). *In vitro*, PhaZa1 has been shown to depolymerise P3HB to 3HB and acetyl-CoA via a thiolysis reaction when incubated with CoA (Uchino *et al.*, 2007). On the other hand, PhaZa1 when expressed in *E. coli* with *C. necator* genes *phaCAB* and *phaP* phasin proteins resulted in the formation of 3HB and crotonyl-CoA during *in vitro* incubation (Eggers and Steinbüchel, 2013). Interestingly, the absence of phasin genes in the study by Eggers and Steinbüchel (2013) almost completely prevented the degradation of P3HB by PhaZa1. On the other hand, PhaZ2 appears to play a role in P3HB granule architecture and has been shown to play a role in the regulation of granule density (Brigham *et al.*, 2012). The specific capacity of *in vivo* PH3B depolymerase enzymes is 200-400 fold less than measured *in vitro*, which raises concerns that the use of non-granule bound recombinant depolymerase results in inferior catalysis due to a lack of interfacial catalysis. Additionally, artificial granules created in hosts such as *E. coli* using genes from *C. necator*, do not have the complex PGAP architecture surrounding them which could be vital for the function and specific activity of depolymerases (Stubbe *et al.*, 2005). The PGAP layer is vital to the production and breakdown of P3HB granules. However, more research is required before the exact mechanisms

governing when and how granules are synthesised or metabolised, and additionally how bacteria avoid futile cycling of P3HB are fully understood.

1.2.3.5 Medium chain length PHA biosynthesis in *Pseudomonas putida*

In MCL-PHA-producing bacteria such as *Pseudomonas* species, the production of PHAs can originate from 4 different sources: the catabolism of compounds indirectly linked to PHA production that originates from cycles such as the pentose phosphate and the Entner Doudoroff cycles; β-oxidation of fatty acids; biosynthesis of fatty acids; and direct PHA production using the *phaCIZC2*D and *phaFI* operons (Prieto *et al*., 2016) displayed in Figure 1.7 both of which are transcriptionally activated by the PhaD in response to the β-oxidation cycle (de Eugenio *et al*., 2010). The production of MCL-PHAs in *Pseudomonas* has been extensively studied generally using the strain *Pseudomonas putida* K12440. Figure 1.8 summarises the key molecular pathways involved in the production of MCL-PHAs in *P. putida*.

In *P. putida*, compounds non-structurally related to PHAs such as glucose, fructose, glycerol and gluconate are oxidised to acetyl-CoA. Acetyl-CoA can either be converted to acyl-ACP and enter the *de novo* fatty acid synthesis cycle or can be directed into the β-oxidation cycle to elongate the molecule by 2 carbon atoms.

On the other hand, compounds related structurally to PHAs such as fatty acids are processed via the β-oxidation cycle in which fatty acid molecules are first converted to acyl-CoA by thiokinase CoA-transferase. Acyl-CoA is then oxidised to enoyl-CoA by acyl-CoA dehydrogenase. From this point enoyl-CoA can take 4 possible routes: exit the β-oxidation cycle and be converted to (R)-3-hydroxyacyl-CoA by PhaJ; be further oxidised to (S)-3-hydoxyacyl-CoA and then undergo a stereochemical inversion to (R)-3-hydroxyacyl-CoA by an epimerase enzyme; or β-oxidation can continue further and convert (S)-3-hydroxyacyl-CoA to 3-keto-acyl CoA via the PhaB enzyme which can be converted to (R)-3-hydroxyacyl-CoA by ketoacyl-CoA reductase; or another round of the β-oxidation cycle can be completed using acetyl-CoA to extend the carbon chain by 2 carbon atoms. In each circumstance, once (R)-3-hydroxyacyl-CoA is produced it can then be converted to PHA via the PhaC enzyme. From *de novo* fatty acid synthesis the intermediate compound that can be converted to PHA is (S)-hydroxyacyl-ACP which can be converted to (R)-3-hydroxyacyl-CoA by the PhaG enzyme. Both acetyl-CoA and malonyl-CoA can be activated by transacylation to ACP. Malonyl-ACP and acetyl-ACP can then be condensed to 3-ketoacetyl-ACP by 3-ketoacetyl-ACP synthase. Subsequently, 3-keto-acetyl-ACP can then be either reduced to (S)-3-hydroxyacyl-ACP and converted by transacylase and PhaG to (R)-3-

hydroxyacyl-CoA, or converted to 3-ketoacetyl-CoA by PhaG and then to R)-3-hydroxyacyl-CoA. Once (R)-3-hydroxyacyl-CoA is formed it can be converted into PHA by either PhaC1 or PhaC2.

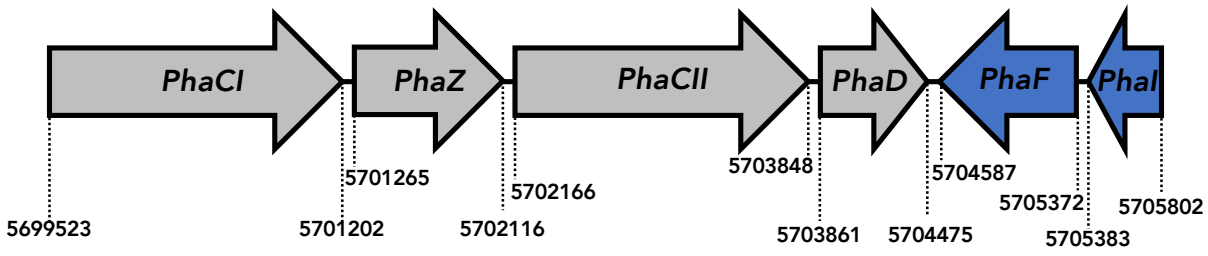


Figure 1.7 - Diagram illustrating the genomic positions and direction of translation of the genes involved in the *phaCIZC2D* (grey) and *phaFI* (blue) operons in *P. putida*.

1.2.3.6 Polyhydroxyalkanoate granule associated proteins in *P. putida*

The production of MCL-PHA in *Pseudomonas* appears to be regulated by the transcriptional regulator PhaD (de Euginio *et al.*, 2010), which is the only protein involved in MCL-PHA synthesis that does not bind to the PHA granule (Mozejko-Ciesielska *et al.*, 2019). In addition, PhaD is able to activate the *phaFI* locus as well as the *phaC1* gene (de Euginio *et al.*, 2010). *Pseudomonas putida* produces MCL-PHAs using class II PHA synthases which are similar to class I PHA synthases by having only one subunit, but differing by being able to incorporate MCL monomers into the PHA chain (Mezzolla *et al.*, 2018). The *phaFI* locus of *P. putida* encodes 2 phasin proteins PhaI and PhaF. The PhaF phasin has been demonstrated to distribute granules into a linear axis along the cell, organise the equal distribution of PHA granules during cell division (Prieto *et al.*, 2016), and also control cell shape and size (Obeso *et al.*, 2015). The role of the PhaI protein is less well understood, but it is thought to have a similar role to PhaF and possibly interact with PhaF (Klinke *et al.*, 2000).

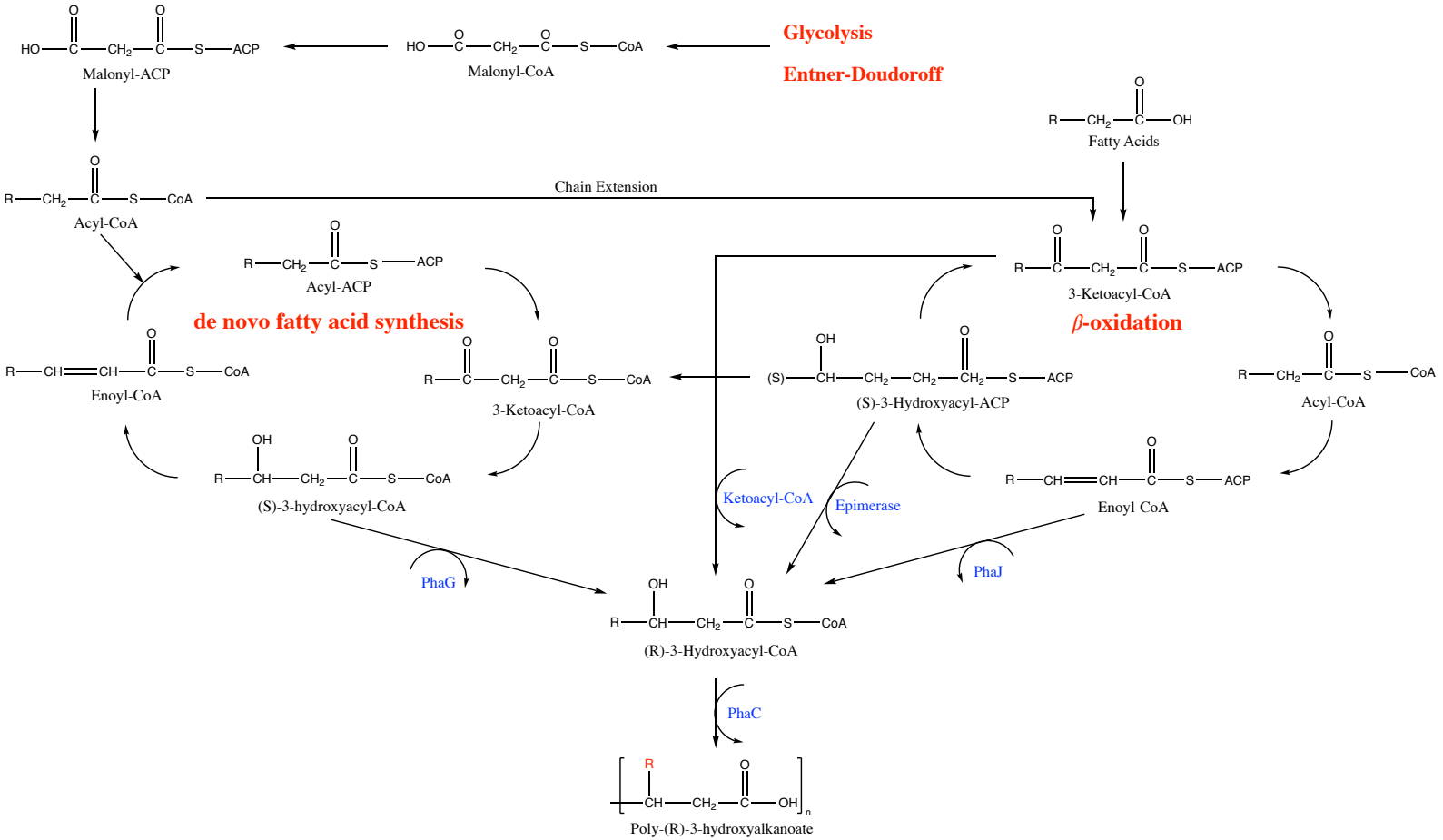


Figure 1.8 - A summary of the molecular pathways linked to MCL-PHA production in *P. putida* K12440. PhaJ = (R)-specific enoyl-CoA hydratase. PhaG = transacylase. PhaC = PHA synthase I and II. Adapted from Magdouli *et al.* (2015) and Mozejko-Ciesielska *et al.*, (2019). n represents the number of repeating units.

1.2.4 Strategies for producing PHAs

1.2.4.1 Growth Media

For the production of P3HB in *C. necator* the growth medium used is of utmost importance for maximising yield. Media must contain a nitrogen source for protein synthesis, phosphorus for nucleic acid production and carbon sources to act both as an energy source and also a source of P3HB production.

In addition, trace elements such as magnesium are required for functions such as enzyme co-factors (Westerholm *et al.*, 2015). Often, particularly at laboratory scale, chemically defined media is used to precisely control N:C ratios. The most common chemically defined media are MSM (González-Villanueva *et al.*, 2019) and MM (Budde *et al.*, 2010). However, the use of purified chemicals to produce chemically defined media is expensive and not economically viable for industrial scale-up. As an alternative, complex media can be used which contains ingredients such as peptone, tryptone, yeast extract and ME to create media-rich in amino acids, proteins, carbohydrates and vitamins. Generally, complex media is used for seed culture cultivation or as a biomass-producing step before media is changed to one of low nitrogen. The most commonly used complex media are ME (Fukui and Doi, 1997), LB, TSB (York *et al.*, 2001) and NB (Sznajder and Jendrossek, 2014).

Carbon sources aimed towards both culture growth and PHA production can be supplied in the form of TCA cycle intermediates such as sodium gluconate (Bresnan *et al.*, 2016), fructose (Budde *et al.* 2011), N-acetylglucosamine (González-Villanueva *et al.*, 2019) and glycerol (Tanadchangsaeng and Yu, 2012). In addition, a variety of waste products (Marciniak and Możejko-Ciesielska, 2021) such as cooking oil (Martino *et al.*, 2014) and crude glycerol byproduct from biodiesel production (Sharma *et al.*, 2016) can be used as a green option.

1.2.4.2 Fermentation Strategy

Combined with the choice of growth media, the type of fermentation strategy used is crucial for maximising PHA yields. The main 5 types of fermentation strategies employed to produce PHA are batch, fed-batch, cell recycling, repeated cell batch and continuous fed-batch; all of which are reviewed in detail by (Koller, 2018).

Batch fermentation is the simplest form of production used to make P3HB in which all ingredients are added to a closed system at the start (Koller, 2018). This method is usually used in smaller-scale laboratory experiments such as Pfeiffer *et al.* (2011) who grew *C. necator* in 0.5% (w/v) NB 0.8% (w/v) sodium gluconate in 10 mL Erlenmeyer flasks or Ng *et al.* (2011) who used 100 mL of MM supplemented with jatropha oil.

On the other hand, in fed-batch fermentations, particular substrates can be added to the growth medium when the concentration decreases below a set concentration (Koller, 2018). For example, Pradella *et al*. (2012) maintained a soybean oil concentration of 20 or 40 gL^{-1} in a 10 L bioreactor containing mineral medium by using a pulse of oil when the concentration dropped to 5 g L^{-1}.

One of the drawbacks of fed-batch fermentation is that the feeding solution increases the media volume, especially for dilute feeding solutions. As a result, cell-recycling fermentations utilise a membrane attached to the bioreactor to keep the media volume constant while retaining all biomass (Koller, 2018). Ienczak *et al*. (2016) used a fed-batch cell recycling method to retain *C. necator* biomass in a 5 L reactor while maintaining concentrations of fructose, glucose, urea and dipotassium phosphate.

Repeated fed-batch fermentation alternatively partially replaces growth media to avoid an increase in toxic byproducts (Koller, 2018). For example, Ibrahim and Steinbüchel (2010) produced P3HB using the bacterium *Chelatococcus sp*. Strain MW10 in a 42 L bioreactor by withdrawing 23 L^{-1} of the total 25 L^{-1} MSM and replacing it with an equal volume.

Continuous-fed-batch systems instead see substrates supplied to a bioreactor permanently to account for substrate usage (Koller, 2018). For example, Du and Yu (2002) utilised a secondary anaerobic bioreactor that produced acetate, propionate and lactate from waste foods using a mixed microbial consortium. The products of the anaerobic bioreactor were fed into the PHA-producing bioreactor through a silicone dialysis membrane to prevent microbial contamination of the *C. necator* fermentation.

Currently, the production of PHAs by fermentation is a costly process, around 4 times higher than that of PP and PE, that prevents PHA-containing products from being competitive on a large scale with conventional synthetic plastics (Kourmentza *et al.*, 2017).

1.2.4.3 Mechanical and thermal properties of P3HB

This section will provide an overview of the material properties that P3HB has in comparison to conventional petrochemically derived plastics PP, PE and PET, using the data presented in Table 2 as a reference.

Depending on how crystalline their structure is, polymers can be classified as either crystalline or amorphous materials. In a crystalline polymer, atoms are arranged into well-ordered structures which have a low degree of branching from pendant groups, resulting in a compact, rigid and brittle material. On the other hand, if a polymer is amorphous, atoms are disordered and the polymer contains a greater number of side chains, creating a material with more flexible elastic material properties. In reality, polymers are a mixture of crystalline and amorphous regions which are known as semi-crystalline polymers and can be described by their degree of crystallinity (Bugnicourt *et al.*, 2014).

Homopolymers of P3HB are classified as crystalline materials with a percentage crystallinity exceeding 50%. This makes P3HB more brittle than PP which generally has a degree of crystallinity of around 50% or below. . In addition, P3HB is known to be limited by progressive embrittlement in which the polymer becomes more crystalline and thus more brittle over time (Biddlestone *et al.*, 1996).

Another key property of polymers is Young's modulus, defined as a measure of how a polymer can withstand a change in length when under tension or compression. The elongation percentage on the other hand describes the change in length required for a polymer to break. Both the Youngs modulus and the elongation percentage of polymers are known to be dependent on molecular weight (Ogawa, 1992).

Another branch of plastic material properties relates to the thermal properties of plastics which are governed by two key parameters, the glass transition temperature (T_g) and the melting temperature (T_m). The T_m occurs when a polymer is heated enough for the covalent bonds between the crystal layers to be overcome. As such, the polymer reaches its melting point and becomes more amorphous and less crystalline in structure. The T_g refers to the point at which a polymer reaches its glass state, becoming brittle and hard rather than having a degree of flexibility (Roos, 2009; Pye and Roth, 2011). An understanding of the T_g and T_m is vital for choosing the correct plastic for a particular job. If this is ignored a plastic used for packaging may, for example, seem perfectly fine at room temperature but when exposed to temperatures in a freezer fail structurally.

From this brief overview and the values displayed in Table 2, it is noted that some of P3HBs material properties are far from ideal particularly if progressive crystallisation has occurred (Biddlestone *et al.*, 1996). As a result, to improve material properties, P3HB is often produced as a co-polymer. In the following two sections, methods for creating P3HB co-polymers are established along with the resulting material properties.

Mechanical/thermal property	P3HB	P3HB	P3HB	P3HB	PP	PP	PP	PP	PP
Molecular weight (g/mol)	$2.2x10^5$	$1.005x10^6$	$5.06x10^5$	$5x10^4$	$7.2x10^5$	$3.1x10^5$	$1.6x10^6$	$1.1x10^6$	$4.15.x10^5$
T_m °C	173	172	176	172	163	161	164.7	162.5	164
T_g °C	-	-	-	-	-	-	-	-	-
Elongation %	10	-	-	-	-	-	44	11	798
Youngs Modulus (GPa)	1.7	-	-	2.45	-	-	2.33	1.27	-
% crystallinity	55	50	58	-	-	-	41	50	50
Reference	El-Haddi *et al.*, 2002	Horng *et al.*, 2011	Horng *et al.*, 2011	Pachekoski, 2009	Kida *et al.*, 2021	Kida *et al.*, 2021	Stern *et al.*, 2007	Stern *et al.*, 2007	Qi *et al.*, 2019

Mechanical/thermal property	PE	PE	PE	PE	PE	PET
Molecular weight (g/mol)	$9.1855x10^4$	$9.9941x10^4$	$5.9x10^4$	$1.47\ 10^5$	$1.224x10^5$	$1.41x10^4$
T_m °C	111.8	114.04	-	-	130	250.5
T_g °C	-	-	-	-	-	-
Elongation %	-	-	-	-	-	-
Youngs Modulus (GPa)	-	-	$7.01x10^{-7}$	$6.59x10^{-7}$	-	-
% crystallinity	48.88	50.92	-	-	66	34.9
Reference	Poh *et al.*, 2022	Poh *et al.*, 2022	Perkins *et al.*, 1976	Perkins *et al.*, 1976	Picard *et al.*, 2015	Wang *et al.*, 2017

Table 2 - Comparisons of mechanical and thermal properties of P3HB in comparison to PP, PE, and PET.

1.2.4.4 Co-Polymers containing P3HB

One way of overcoming the poor thermal and mechanical properties associated with P3HB is the incorporation of other monomers into the polymer chain. The resulting polymers are called co-polymers, the first of which was produced in the 1980s and was called Biopol©. Biopol consists of P(3HB-co-3HV) which like P3HB is non-toxic, highly biocompatible and fully biodegradable (Pederson *et a*l., 2006). Co-polymers produced using periodic feeding with different substrates are known as block co-polymers (Tripathi *et al.*, 2012) and those produced using a mixed substrate feed are referred to as random co-polymers (Matsumoto *et al.*, 2001). Since the 1980s, a wide variety of P3HB co-polymers have been produced a summary of which is provided in Table 3.

Table 3 - Summary of P3HB containing co-polymer production by *C. necator* detailing the growth conditions, mechanical properties and thermal properties.

Polymer	Media	C Source	Biomass (g/L)	PHA Weight (g/L)	PHA % of biomass	Monomer content (%)	% crystallinity	M_w	Tm (°C)	Tg (°C)	Reference
3HB-co-3HV	Mineral salts	Fructose, Valeric acid	-	PHB-co-PHV=0.03g/L/hour PHB=0.033g/L/hour	66	PHB-co-PHV = 59 PHB = 41	-	-	-	PHB-co-PHV = -5 PHB = 5	Kelley and Srienc, 1999
3HB-co-3MP	Mineral Salts	Sodium gluconate, DTDP	5.09-7.45	0.2-1.24	2.9-20.2	3MP = 3.6-70	-	2.51-6.06 x10^5	55.1-153	-10.7 - 2	Isemori *et al.*, 2006
3HB-co-3MB	Mineral Salts	3-mecaptobutyric acid, gluconate	-	-	21.9-31.3	3MB = 33.2-72.2%		5.6-7.9x10^5	-	-	Lütke-Eversloh, 2001
3HB-co-3HV	Mineral Salts	Levulinic acid, glucose	15.53	12.61 (3HV)	81.2	3HV = 53.9	51.92	-	101.93	-	Wang *et al.*, 2013
3HB-3HV	Medium E + modified MT	Butyric acid, valeric acid	-	-	40	3HV = 0-62		0.9568-1.2286 x10^6	76.8 - 178.2	-4.1 - 5.9	Zinn *et al.*, 2003
3HB-co-3HV	Nutrient Rich	Fructose, sodium propionate	-	-	-	PHB = 78.2	-	1.36x10^6	164.7	-3.87	Zhao *et al.*, 2015

3HB-co-3HV	Mineral Salts	Fructose, propionic acid	-	0.18	-	3HV = 24	35	-	154	-10	Pereira *et al.*, 2008
3HB-co-3HV-co-3HHx	TSB	Oxidised polyethylene wax	3.66	1.24	33.8	-	-	-	-	-	Radecka *et al.*, 2016
3HB-co-3HV	MSM or DSM81	Pure glycerol, glycerol + biodiesel, udder, enzyme digested oil.	-	-	55-90	97.52-99.01	-	-	-	-	Favaro *et al.*, 2018
3HB-co-3MP	MSM	Dithiodipropinoic acid	-	-	-	-	-	-	161-170	-17-3	Huang *et al.*, 2019
3HB-co 3HHx-co-3HO	MSM and/or LB	Sodium Octanoate			32-80	3HB = 94.3-99.92, 3HHx = 0.08-5.68, 3HO = trace-$0.02x10^{-3}$					Green *et al.*, 2002

1.2.4.5 Co-polymers of P3HB genetically engineered *C. necator* and *E. coli*

To increase P3HB yields and have more control over polymer composition, various genetic modification strategies have been used. Bacterial strains used for recombinant PHA production must be non-pathogens, have a well-studied genome, be easy to genetically modify and have a fast growth rate (Wang *et al.*, 2014). The bacteria that fits the criteria best is *E. coli* which is widely employed in molecular biology as a model system (Blount, 2015) and is industrially used for protein production. Various studies in which *E. coli* has had P3HB-producing genes such as the *C. necator phaCAB* operon inserted to genetically modify *E. coli* are summarised in Table 4. As *E. coli* is not a natural producer of P3HB it does not degrade accumulated P3HB, can have P3HB production induced at an optimised time point and is additionally much faster growing than natural P3HB producers such as *C. necator* (Aldor and Keasling, 2013). In addition, *E. coli* is not able to organise P3HB into discrete granules using PGAPs resulting in granules with a low surface area to volume ratio, which when coupled with the weak cell membrane of *E. coli* makes extraction easier (Aldor and Keasling, 2013).

Genetic modification using P3HB-related genes has not just been limited to producing P3HB in *E. coli* though. Using *C. necator*, Wu *et al*. (2016) produced 80% more P3HB by promoting multiple cell division by removing binary cell division-related genes *minL* and *minD*. In addition, the molecular evolution of enzymes such as PhaC1 using random mutagenesis is also a method used to increase the specificity and speed of P3HB production in *C. necator* (Kichise *et al.*, 2002). Gene copy number and gene position are also thought to be key to increasing P3HB production in *C. necator* (Yin *et al.*, 2015). In addition to these genetic modifications to *C. necator*, a summary of the genetic modification of *C. necator* using genes from other PHA-producing bacteria is presented in Table 5.

1.2.4.6 Metabolic engineering approaches to *C. necator*

A problem that limits the production of SCL-PHAs is that excluding 3HB, SCL-PHAs require structurally related substrates such as valerate, propionate, hexanoate and 1,4-butane diol which are expensive and can be toxic (Chen *et al.*, 2015). Research has therefore been directed towards the metabolic engineering of pathways which can provide PHA synthesis with precursors from different sources such as low-cost sugars (Chen *et al.*, 2015). For example, the extracellular β-fructofuranosidase enzyme encoded by the *Mannheimia succiniciproducens* gene *SacC* has been successfully instated into *C. necator* allowing sucrose to be broken down into glucose and fructose, both of which can be used for PHA production (Park *et al.*, 2015). Metabolic engineers can also use the heterologous expression of enzymes to enhance the metabolism of metabolites or to produce different PHAs. Fukui *et al.* (2014) modified *C. necator* with the *E. coli* genes aquaglyceroporin and glycerol kinase to enhance the metabolism of glycerol.

Other efforts have attempted to use metabolic engineering to prioritise PHA production over fatty acid synthesis. There are 3 main ways in which fatty acid metabolism can be engineered: directing the common intermediate (R)-3-hydroxyacyl-CoA to PHA biosynthesis (Magdouli *et al.*, 2015); controlling C flux from fatty acid biosynthesis and β-oxidation; and engineering the production of PHAs from fatty acid metabolism intermediate compounds (Riedel *et al.*, 2014). Inhibitor compounds can also be used to prioritise PHA biosynthesis over pathways that prevent PHA production or limit PHA chain length (Aldor and Keasling, 2003). This was demonstrated by Green *et al*. (2002) who inhibited β-oxidation with sodium acrylate leading to the production of MCL-PHAs PHHx and PHO in addition to SCL-PHAs P3HB and poly-3-hydroxypropionate in wild-type *C. necator* (Riedel *et al.*, 2014).

Table 4 - A summary of publications detailing the production of P3HB containing co-polymers in *E. coli* strains using genes originally from *C. necator*.

Host *E. coli* Strain	Strain	Key Gene Changes	Gene Source	Polymer	Media	C Source	Biomass (g/L)	PHA % of biomass	Monomer content (%)	Reference
XL1-Blue	pPs619C1-CpPCT, pMCS104CnAB	pPs619C1-CpPCT= *Pct* (Propionate CoA transferase) *phaC1* pMCS104CnAB= *phaA* *phaB*	*Clostridium propionicum* *Pseudomonas* sp. MBEL 6-19 *C. necator* *C. necator*	3HB-co-LA	MR	Glucose	-	-	LA = 9-64	Yang *et al.*, 2010
BL21	$ABC_{Ah}J_{Ah}$	pETDuet-ABC_{Ah} = *phaA* *phaB* *phaC* pCDFDuet-J_{Ah} = phaJ	*C. necator* *C. necator* *Aeromonas hydrophilia* *A. hydrophilia*	3HB-co-3HHx	M9	Glycerol	-	1.7	3HB = 96, 3HHx = 4	Prithakrotc-hanakoon *et al.*, 2013
	$ABC_{Ah}J4_{Pp}$	pETDuet-ABC_{Ah} = see above pCDFDuet-$J4_{Pp}$ = *phaJ*	*P. putida*	3HB-co-3HHx-co-3HO-co 3HD			-	0.1	3HB = 65, 3HHx = 6, 3HO = 16, 3HD =13	
BL21	$ABC_{Ah}J_{Ah}$	See above	See above	3HB-co-3HHx	M9	Crude glycerol, pure glycerol, sodium dodecanoate	0.9-2.8	2.9-4.3	3HB = 97-99, 3HHx = 1-3	Prithakrotc-hanakoon *et al.*, 2015

Table 5 - A summary of publications detailing the production of P3HB co-polymers using genetically modified *C. necator*.

Host	Strain	Key Gene Changes	Gene Source	Polymer	Media	C Source	Biomass (g/L)	PHA concentration (g/L)	PHA % of biomass	Monomer content (%)	Reference
H16	Re2058/ pCB113	ΔphaC1 ΔproC	*C. necator* *C. necator*	3HB-co-3HHx	Minimal	Palm Oil	3.6	-	73.1	HHx = 12.7	Budde *et al.*, 2011
		pCB110= *phaC2* *phaA* *phaJ*, *proC*	 *R. aetherivorans* *R. aetherivorans* *P. aeruginosa* *C. necator*								
H16	Re2160/ pCB113	ΔphaB ΔphaB2 ΔphaB3 ΔphaC1	*C. necator* *C. necator* *C. necator* *C. necator*	3HB-co-3HHx	Minimal	Palm Oil	2.74	-	63.99	HHx = 24.13	Budde *et al.*, 2011
		pCB110	See above								
H16	Re2001	ΔphaC1	*C. necator*	3HB-co-3HHx	Minimal	Palm oil	2.19	-	50	HHx = 1.5	Budde *et al.*, 2011
		phaC2	*R. aetherivorans*								
DSM-541	Cn-Kad1	ΔPHB isolate		3HB-co-4HB	Nutrient rich	Sodium 4-hydroxybutyrate, γ-butyrolactone	1.7-2.6	0.01-0.5	0.5-20	3HB = 49-97, 4HB = 3-51	Al-Kaddo *et al.*, 2020
		phaC	*B. contaminans*								
H16	Re2058/ pCB113	See above	See above	3HB-co-3HHx	Mineral	African elemi oil, Amygdalus pedunculata oil, bitter apple oil, desert date oil.	4.2-8.8	2.2-5.3	50-69	HB = 69-80, HHx = 20-30	Zainab-L *et al.*, 2018
H16	Re2058/ pCB113	See above	See above	3HB-co-3HHx	Mineral	Crude palm kernel oil, oil palm tree sap.	3.95-6.58	1.4-4.5	13-68	HB = 73-86, HHx = 14-27	Murugan *et al.*, 2016
DSM-545	Glucose utilising isolate	N/A	N/A	3HB-co-3HV	Mineral salts	Crude glycerol, valeric acid	-	-	-	-	Gahlawat and Soni, 2017

H16	H16 (pZL-dhaT-aldD)	pZL-dhaT-aldD = dhaT (1,3-propanediol dehydrogenase) aldD (aldehyde dehydrogenase)	*P. putida* *P. putida*	3HB-co-4HV	Mineral salts or LB	Fructose, 1,4-butanediol, 4HB	5.5-10.4	-	49-61	3HB = 0.3-13.1, 4HB = 1.3-13.1.	Zhang *et al.*, 2009
DSM-541	PHB-4 PsF2	ΔPHB isolate PsF2 = *phaC1*	*P. aeruginosa*	3HHx-co-3HOx-co-3HD	NB + acrylic acid inhibitor	Decanoate	-	-	3.2-4.5	3HHx = 6-7, 3HO = 50-55, 3HD = 39-43	Green *et al.*, 2002
H16	Re2058/ pCB113	See above	See above	3HB-co-3HHx	Minimal	Palm oil	24.7	-	70.9-73.5	HHx = 17.3-23.9	Riedel *et al.*, 2012
DSM-541	PHB-4/pJRDBB39d3	PJRDBB39d3= phaC ORF1	*A. caviae* *A. caviae*	3HB-co-3HHx	Mineral Salt	Fructose, octanoate	-	-	35-46	3HB-53-100, 3HHx = 0-47	Kichise *et al.*, 1999
H16	Re2133/pCB81	ΔphaC ΔphaB1	*C. necator* *C. necator*	3HB-co-3HHx	Minimal	Coffee oil	-	-	69	3HB = 78, 3HHx = 22	Bhatia *et al.*, 2017
		pCB81= *phaC2* *phaA* *phaJ*	*R. aetherivorans* *R. aetherivorans* *P. aeruginosa*								
DSM-545	Glucose utilising isolate	N/A	N/A	3HB-co-4HB	Basal medium	Waste glycerol, γ-butyrolactone	-	4-9.7	14.8-25.9	4HB =17-21.5, 3HV = 0	Cavalheiro *et al.*, 2012
				3HB-co-4HB-co-3HV		Waste glycerol, γ-butyrolactone, propionic acid	-	10.8-11	25-29.5	4HB = 26.2-30.3, 3HV = 6.7-9.8	
H16	Re2160/ pCB113	See above	See above	3HB-co-3HHx	Mineral	Crude palm kernel oil	2.73-6.73	1.3-5.1	45-88	3HB = 32-45, 3HHx = 55-68	Wong *et al.*, 2012

						Coconut oil	2.61-4.49	1.3-3.4	48-79	3HB=30-44, 3HHx = 56-70	
DSM-541	PHB-4 (pCV8)	phaC phaA	*C. violaceum* *C. violaceum*	3HB-co-3HC	Mineral salts	Butyric acid, hexanoic acid, octanoic acid, decanoic acid	-	-	68-83	3HB= 88-98, 3HC = 2-11	Kolibachuk *et al.*, 1999
				3HB-co-3HV		Valeric acid	-	-	31	3HB = 19, 3HV = 81	
				3HB-co-3HV-co-3HHx		Heptanoic acid, nonanoic acid	-	-	55-59	3HB = 68-87, 3HV = 10-27, 3HHx = 3-5	
				3HB-co-3HV-co-3HC-co-3HO		Myristic acid, palmitic acid, stearic acid.	-	-	31-41	3HB = 85-89, 3HV = 2-10, 3HC = 4-10, 3HO = 1-2	
H16	Re2133/ pCB81	ΔphaC ΔphaB1	*C. necator* *C. necator*	3HB-co-3HV-co-3HHx	Minimal	Butyrate	-	-	31-83	3HB = 82.5, 3HV = 11, 3HHx = 6.5	Jeon *et al.*, 2014
		pCB81= *phaC2* *phaA* *phaJ*	*R. aetherivorans* *R. aetherivorans* *P. aeruginosa*								

1.2.5 Applications of 3HB containing polymers

1.2.5.1 Medical Applications

Biomaterials play an important role in medicine by providing structural means for promoting healing from injuries and biochemical methods for the treatment of disease (NIBIB, 2017). In this sub-chapter, examples will be given from literature of the current medical applications of P3HB and 3HB containing copolymers covering areas of medicine including discussions of biocompatibility, medical scaffolds, wound healing and controlled drug release.

1.2.5.1.1 Biocompatibility

For a biomaterial to be used for medical purposes it must meet strict criteria that ensure patient safety and the delivery of effective treatment. Depending on the specific application the material must have high strength, flexibility hydrophobicity and specific diffusion rates (Bonartsev *et al.*, 2019). In addition, a biomaterial must not promote an immune response and be compatible with human soft tissue, organs and bone (Brigham and Sinskey, 2012). Found naturally in the human body, 3HB is a ketone body resulting from the metabolism of fatty acids in the liver during periods of low blood glucose concentration (Newman and Verdin, 2019). As a result, the breakdown of P3HB in the human body is a non-toxic process. A study has found that P3HB is biocompatible in mouse muscle when implanted as P3HB microspheres (Shishatskaya *et al.*, 2008). Additionally, a study into the hemocompatibility of PHBV sheets found the material to have good blood compatibility (Mohandas, 2021). Furthermore, Reis *et al*. (2010) conducted a study into the osteoconductivity of P3HB-hydroxyapatite composites and found the material to be biocompatible with rabbit bone.

1.2.5.1.2 Medical Scaffolds

Medical scaffolds are materials key in the field of tissue engineering, providing structural support that allows for tissue regeneration via cell attachment (Chan and Leong, 2008). In sheep, P3HB combined with polyglycolic acid has been used to construct *in vitro* pulmonary artery valves which were inserted *in vivo* to replace existing valves (Sodian *et al.*, 1999). The same polymer combination has additionally been used to produce autologous aortic grafts *in vitro* (Shum-Tim *et al.*, 1999). When combined with hydroxyapatite, P3HB has been shown to facilitate healing between broken bones and orthopaedic implants (Doyle *et al.*, 1991; Knowles, *et al*. 1992; Luklinska and Bonfield 1997). In addition, P3HB exhibits piezoelectric properties that have been shown to enhance osteoblastic cell growth (Chernozem *et al.*, 2020). Co-polymers of poly(3HB-co-3HHx) (Wang *et al.*, 2008) and poly(3HB-co-3HV) (Köse *et*

al., 2005) have been used for the in vitro regeneration of cartilage tissue taken from rabbits. A study by Wang *et al*. (2005) also found that fibroblast and osteoblast cells both grown on P(3HB-co-PHV) polymers with fibroblast cells most compatible with P(3HB-co-20%-HHx) and osteoblasts more compatible with P(3HB-co-12%-3HHx). Fibres of P3HB have also been used to treat spinal cord injury in rats acting as a matrix that supports neuronal survival and regeneration following injury (Novikov *et al.*, 2002). In addition, P3HB, P(3HB-co-4HB) and poly(3HB-co-3HHx) have been shown to support the growth of neural stem cells furth paving the way for use as central nervous system repairing implants (Xu *et al.*, 2010).

1.2.5.1.3 Wound Healing

Polymer based sutures are used in medicine as biodegradable alternatives to conventional materials such as silk. Sutures are used to close open wounds that result from either injury or surgery and must have a high level of tensile strength in order to keep the wound closed. Biodegradable sutures are a vital part of surgery, preventing the need for secondary procedures thus decreasing patient recovery time and risk involved with surgery (Maitz, 2015). Sutures made of P3HB and PHV have been shown to be suitable for use in the healing of muscle-facial wounds (Shishatskaya *et al*. 2002; Shishatskaya *et al*. 2004). Bio-polymers consisting of P4HB are thought to be the most promising PHA composition suitable for sutures due to a higher tensile strength, elongation at break and more rapid biodegradation rate in comparison to P3HB polymers (Martin and Williams, 2003).

1.2.5.1.4 Controlled Drug Release

Polymers containing P3HB have also been applied to numerous types of controlled drug release treatments in which a drug is inserted into the polymer matrix from which it is gradually released. Replacement joints and other surgical implants are subject to a high degree of infection compared to other operations. One reason for this is the reduced degree of vasculature around an implant which can prevent both the immune system and conventional methods of administering antibiotics from reaching infection at the implant surface (Gurselt *et al.*, 2002). Rossii *et al*. (2004) applied poly(3HB-co-3HV) films containing gentamycin to the surface of femoral hip implants and found that increasing the 3HV content from 8 to 12% increased the speed of gentamycin release. In a similar study, Gurselt *et al*. (2002) showed that poly(3HB-co-3HV) containing sulbactam, cefoperazone and gentamycin could be applied to the surface of implantable rods. This study in contrast found that changing the 3HV content of the polymer did not influence drug release although changes in antibiotic to polymer ratio

did. However, PH3B drug delivery systems are not limited to antibiotics, anti-inflammatory ketoprofen, hypertension-reducing clonidine and enlarged prostate treatment tamsulosin have all been introduced into P3HB-containing patches (Wang *et al.*, 2003). This study found that when implanted into a P3HB-containing film the drugs could easily disperse into the skin but when applied without the film in liquid form displayed very poor skin penetration. Nano-spheres of PEG-coated P3HB containing chemotherapy drug doxorubicin and kidney/liver cancer-treating drug sorafenib could be liberated quicker in acidic tumour-specific environments (Babos *et al.*, 2020).

1.2.5.2 Food Packaging Applications

Biopolymers consisting of P3HB are a strong candidate for replacing the current petrochemically derived packaging materials such as PP and PE (Boey *et al.*, 2021). To be used as food packaging, plastics are required to protect against microbial or chemical contamination, mechanical damage, changes in humidity, UV light and desiccation (Koller, 2014). In order to satisfy such criteria, packaging must be stable at low temperatures, not chemically migrate to the food and in some cases be able to maintain a modified atmosphere (Koller, 2014). Miguel and Iruin (1999) reported that P3HB and poly(3HB-co-3HV) with a low 3HV content had similar CO_2 and, H_2O vapour permeation to PET and PVC, but were more permeable to organic compounds. Bucci *et al*. (2005) performed dimensional tests on dimensions, weight thickness and volumetric capacity and mechanical tests on compression and mechanical resistance. This study found that compared to PP, P3HB was less flexible and more rigid, performing worse than PP at low temperatures but better at higher temperatures. Additionally, the same research group compared the chemical migration and UV resistance of P3HB to PP with great success (Bucci *et al.*, 2007). In addition, the study recommended that pigmented P3HB was suitable for use as food packaging. Dagnon *et al*. (2010) coated biodegradable Kraft paper with P(3HB-co-4HB) which fills the surface and internal pores reducing the rate of paper weight loss and improving stiffness to a level suitable for food packaging. The addition of P(3HB-co-4HB) also improved the rate of biodegradation in soil by forming surface microbial communities. Merklein and Hagenah (2012) created a material highly suited to the wrapping of food by blending P(3HB-co-3-HV) with PLA which was superior to current 3-layer PLA P(3HB-co-3-HV) films. To improve the barrier properties of P(3HB-co-3HV) films Fabra *et al*. (2013) incorporated zein protein derived from corn kernels into the polymer which improved barrier properties to CO_2, O_2 and limonene. Similarly, Koller *et al*. (2007) incorporated whey retentate into P3HB films which resulted in an easily recyclable material with O_2 barriers. Vandewijngaarden *et al*. (2016) mixed organomodified montmorillonite clay nanocomposites with

P(3HB-co-3HHx) which resulted in lower O_2, CO_2 and H_2O vapour permeability. Sabharwal *et al*. (2018) increased the anti-microbial activities of P(3HB-co-3-HV) films by adding triclosan which was effective at killing *E. coli* and *Staphylococcus aureus*. Danimer Scientific (2021) have produced drinking straws that biodegrade in marine environments using their Nodax™ PHA technology.

1.2.5.3 Cosmetic Applications

Micro Powders, Inc. (2015) has developed a product called BIOSCRUB® which is an exfoliant based on PHB particles that range from 150 to 840 μm in diameter. This product is a pioneer in the commercial use of biodegradable microplastics in the cosmetics industry.

1.2.5.4 Agricultural Applications

Kampeerapappun and Phanomkate (2013) developed slow-release fertiliser consisting of a P3HB shell encapsulating a PLA/fertiliser core which releases fertiliser gradually over 1 month. Similarly, Grillo *et al*. (2011) used P3HB and PHBV microparticles to encapsulate ametryn herbicide. This method of slow release was also successful with the amount of herbicide realised upon application from 75% for PHB and 81% for PHBV. Savenkova *et al*. (2002) incorporated the antifungal compounds Ranilan and Sumilex into films made of P3HB which decreased the count of spoilage bacteria *Botrytis cinerea* and biodegraded by 92-96% in 4 weeks. Mirel™ (2021) additionally sell biodegradable PHA-based sheets that can be used for agricultural mulch film. Havens *et al*. (2014) filed a patent for biodegradable PHA fishing gear which loses its ability to retain fish over time reducing the environmental impact of ocean-dwelling creatures becoming entangled in the waste line.

1.2.6 Extraction of PHAs

The extraction of intracellular PHAs is a fundamental part of production at both laboratory and industrial scales, with an aim to extract as much PHA as possible from each cell while maintaining high levels of purity. While conventional solvent extraction of PHA results in highly pure polymers with excellent recovery, the downside is that halogenated solvents are highly toxic which makes scaling up difficult as the release of such chemicals causes significant problems for wastewater treatment (Kurian and Das, 2021; Pagliano *et al*., 2021). Additionally, conventional PHA extraction is expensive, with downstream processing representing around 30% of total production costs (Sun *et al*., 2007). The extraction of PHA is a broad topic and is reviewed in depth by Koller *et al*. (2013), Madkour *et al*. (2013), Pagliano *et al*.

(2021) and Boey *et al*. (2021). In the following sections, the main types of PHA extraction will be covered with some examples from literature.

1.2.6.1 Pre-treatments

The purpose of pre-treating PHA-containing biomass is to assist the progress of the extraction process by disrupting non-PHA cellular material (Kourmentza *et al.*, 2017). Lyophilisation, thermal drying, enzymatic, chemical and biological methods have all been used to pre-treat harvested biomass. Lyophilisation, also known as freeze drying, is a method originally utilised for the long-term preservation of bacterial cells. The general process consists of freezing bacteria and then applying a vacuum before a drying phase removes any water present. Lyophilisation renders the bacteria biologically inactive preventing any mechanisms within the cell that could degrade P3HB and allowing the samples to be stored for long periods. Freeze-dried bacteria can be revived in a suitable medium, but when treated with solvents or other chemicals non-P3HB containing biomass is much more readily digested in comparison to non-pre-treated cells (Jacquel *et al.*, 2008).

Heat pre-treatment on the other hand denatures the cell membrane of bacteria and additionally degrades proteins and genetic material, preventing the degradation of P3HB depolymerase enzymes. The freezing pre-treatment of biomass aims to rupture or weaken the cell membrane by forming sharp ice crystals. Other pre-treatment methods that compromise the cell membrane are pH treatments using chemicals such as ammonium hydroxide (Fiorese *et al.*, 2009) and acidic-alcohol treatments using alcohols such as methanol combined with an acid such as sulfuric acid method (Lau *et al.*, 2011). Organic solvents can be used to remove residual extracellular lipids from biomass in a process called degreasing (Koller *et al.*, 2013).

1.2.6.2 Solvent Extraction

The use of halogenated solvents such as chloroform and dichloromethane represents the benchmark method of PHA extraction as the purity of extracted polymers typically exceeds 90% (Pagliano *et al.*, 2021). Typically solvent extraction consists of pre-treatment, solvent extraction and alcohol precipitation (Madkour *et al.*, 2013) and unlike other extraction methods aims to cause PHA leakage by solubilising intracellular PHA rather than by disrupting the cell membrane (Madkour *et al.*, 2013). Santhanam and Sasidharan (2010) extracted PHA from types of various bacteria including *C. necator* by rinsing cells with methanol to remove residual lipids before drying at 60°C. The cells were then heated to 95 °C in chloroform, cooled, and left overnight before PHA was precipitated with 70% (v/v)

methanol. Fiorese *et al*. (2009) extracted PHA from *C. necator* using 1,2-propylene carbonate to disrupt cells achiving a total PHA recovery of 95% and a purity of 84%. Unlike most solvent extractions which use alcohol, this study utilised acetone to precipitate PHA. Another study by Fiorese *et al*. (2009) found that pH and heat pre-treatments did not affect polymer yields but did increase polymer molecular weight from $7.4x10^5$ to $1.3x10^6$ g/mol. As chloroform is such a toxic chemical efforts have been made to try and find alternatives that are more environmentally friendly and safer to use. Aramvash *et al*. (2018) compared the performance of propanol, methanol, acetic acid, hexane, dimethyl formamide, dimethyl sulfoxide and ethylene carbonate. Their study found that pre-treating *C. necator* with sodium hypochlorite followed by extraction with ethylene carbonate and precipitation with ethanol led to a very high PHA recovery of 98.6% and purity of 98%.

1.2.6.3 Chemical Digestion

The extraction of PHAs by chemical digestion works by disrupting the cell membrane, thus releasing the cell contents from the cell, rather than solubilising the polymer as was the case for solvent extraction. The two main chemical extraction methods to be covered in this introduction are extractions utilising sodium hypochlorite and different types of surfactants.

Sodium hypochlorite extraction works by disrupting all non-PHA cellular material due to its strong oxidisation properties. At large scale, disruption by sodium hypochlorite should be treated very carefully as the reaction is exothermic and releases a large amount of heat (Madkour *et al.*, 2013). In addition, sodium hypochlorite can lead to a reduction in polymer purity and molecular weight in comparison to solvent extractions (Pagliano *et al.*, 2021). Heinrich *et al*. (2012) reported the extraction of PHA from *C. necator* cells using lyophilisation as a pre-treatment, disrupting cells using sodium hypochlorite, and achieving a recovery of 91% and a 96% purity. López-Abelairas *et al*. (2015) obtained a purity of 98% and found that sulfuric acid pre-treatment led to the highest purity for sodium hypochlorite extraction.

Surfactants on the other hand extract PHA by incorporating into the bacterial cell lipid bilayer, producing micelles consisting of phospholipids and sufactants, thus solubilising non-PHA cellular material (Pagliano *et al.*, 2021). The most common surfactant used in PHA extraction is an anionic surfactant SDS. Arikawa *et al*. (2017) combined SDS treatment with sonication to recover PHA and then rinsed the extracted PHA with water and ethanol achieving a purity of ≥ 96%. Yang *et al*. (2011) also investigated an ionic surfactant called alkylbenzene sulfonic acid (LAS-99) and found that less detergent was required for extraction than with SDS. Although, in comparison to SDS yields in terms of PHA

recovery and purity were lower at 87% and 86%, respectively. Irdahayu *et al*. (2017) found that a combination of sodium hydroxide and Lysol detergent was more effective than Triton X-100 and cetyltrimethylammonium bromide (CTAB) recovering 97% of total PHA with a purity of 98%.

A combination of surfactants and sodium hypochlorite can also be used as was demonstrated by Ramsay *et al*. (1990) and Dong and Sun (2000), both of whom reported PHA extracted from *C. necator* with a purity of 97-98%.

1.2.6.4 Supercritical Fluids

A supercritical fluid is a pressurised fluid with properties of both a gas and fluid, compressing in a container like a gas while having a liquid-like density (Hitchen and Dean, 1993). Supercritical CO_2 is the most commonly used supercritical fluid used to extract PHA as it evaporates leaving no residue and requires little drying time (Koller *et al*., 2013). Hampson and Ashby (1999) extracted PHA from *Pseudomonas resinovorans* using supercritical CO_2 as a pre-treatment and residual lipid removal. However, the recovery of this method was very poor with just 42.4% of the total PHA extracted. Khosravi-Darani *et al*., (2004) used supercritical CO_2 combined with a NaOH pre-treatment and two pressure releases to extract 89% of total PHA from *C. necator* cells. Hejaz *et al*., (2003) instead of CO_2 used supercritical methanol to extract PHA from *C. necator* after a NaOH pre-treatment resulting in a recovery efficiency of 89%. Generally, the use of supercritical fluids has been criticised for low rates of total PHA recovery and for requiring further chemical treatments to sufficiently extract polymer from cells (Madkour *et al*., 2013).

1.2.6.5 Enzymatic Digestion

Enzymes can be used for the recovery of PHA by degrading bacterial proteins with enzymes such as proteases and/or carbohydrates with glycosidase enzymes (Pagliano *et al*., 2021). A study by Lakshman and Shamala (2006) evaluated the performance of CelluMax ®, an enzyme commercially used to degrade polysaccharides such as cellulose in animal feed (Bio-Cat, 2021). Neves and Müller, (2012) trialled a wide range of proteases and glycosidase enzymes but also found that CelluMax ® was the best achieving a 93.2% recovery of P(3HB-3HV) with a 94% purity. The study found that when tested on PHA accumulating *Sinorhizobium meliloti*, a PHA recovery efficiency of 94% and a purity of 92% were achieved. Alternatively, Kapritchkoff *et al*. (2006) compared the effectiveness of trypsin, bromelain, lysozyme and pancreatin to extract PHA from *C. necator* DSM545. Bromelain and pancreatin were found to be the most effective achieving 88.8% and 90% purity, respectively.

Investigating the use of alcalase and lysozyme enzymes combined with SDS and EDTA to recover PHA from *P. putida*, Yasotha *et al.*, (2006) found that this method was able to extract 90% PHA with a purity of 92.6% from *P. putida*. Using a different approach, Divyashree *et al*. (2009) used protease produced by a *Microbispora sp.* culture to lyse PHA-producing *Bacillus flexus* cells however when the extracted PHA was recovered by phase separation only a maximum of 52% PHA was recovered. Kachrimanidou *et al*. (2016) used enzymes produced by the fungus *Aspergillus oryzae* to extract PHA from *C. necator* with a recovery efficiency of 98% and a purity of 96.7%. Generally, the high PHA recovery and purity come at a high cost as the enzymes are extremely expensive (Madkour *et al.*, 2013).

1.2.6.6 Mechanical Disruption

The mechanical disruption of PHA-containing bacteria aims to release PHA granules from cells without the need for chemicals, using only external forces to disrupt the cells. This is a desirable method as it is cheap and doesn't require toxic chemicals but the drawback is secondary purification is often required with additional chemicals (Madkour *et al*. 2013). One method of mechanical disruption is bead milling which for Tamer *et al*. (1998) involved combining *Alcaligenus latus* cells with 512 µm beads at 2800 rpm for 90 mins. When combined with SDS treatment this released 90% of cellular protein. Gutt *et al*. (2016) used a bead mill along with SDS treatment to achieve a 100% polymer recovery and 94% purity. The disadvantage of using a bead mill is that a high level of cooling is required making it difficult to scale up to industrial volumes (Madkour *et al.*, 2013). Another method is high-pressure homogenisation which involves forcing bacterial cells under pressure through small apertures which disrupt the cell membrane. Koller *et al*. (2013) used this method to extract PHA from *Methylobacterium sp*. V49, reporting an extraction efficiency of 98% and a purity of 95% when processed in an SDS solution. Generally, high-pressure homogenisation works well for high-density industrial-size fermentations but a reduction in extraction efficiency is observed at low cell densities (Madkour *et al.*, 2013). Another method is the use of ultrasonic waves which Murugesan and Iyyaswami (2017) used coupled with Triton X-100 to extract PHA from *C. necator*, achieving a purity of 94.34%.

1.2.7 Methods of PHA analysis

1.2.7.1 Dry weight

The DCW of a sample refers to the weight of a biological sample after drying has removed sufficient moisture to a point where further drying maintains a constant weight. A DCW measurement is used principally due to the lack of consistency achieved by analysing wet samples. For the quantification of

PHA DCW is often compared to the corresponding dry weight of extracted PHA in order to calculate the percentage of dry cell weight. Alternatively, either DCW or the weight of extracted are reported on their own usually expressed per litre.

1.2.7.2 Flow Cytometry

Flow cytometry is a high throughput technology capable of recording multiple parameters based on fluorescence and light scattering when a laser is incident on a cell. In this thesis, a BD Accuri™ C6 flow cytometer will be the primary tool used for analysis, a simplified diagram of which is displayed in Figure 1.9.

The process starts off with a bacterial sample which is diluted to an appropriate cell density and taken up into the machine in a tube known as the sip. Once in the machine, sheath fluid is used to hydrodynamically focus the sample of cells into a single file ensuring that only one cell passes through the lasers at a time. When the light from the lasers hits a cell, one way it can scatter is forward 0°, this is known as forward scatter (FSC). Values of FSC are proportional to cell size and can be used to track changes in cell size during experiments. Light can also be scattered to the side 90° which is called side scatter (SSC). Values of SSC are proportional to the internal complexity of cells. In addition to scattered light, cells can also fluoresce different colours when stained with fluorophores. For the analysis of PHA by flow cytometry, Nile Red or P-546 (also known as BODIPY™ 493/503) have been used in literature as either a single stain or as a double stain with a nucleic acid stain in order to allow for the differentiation of cells from noise. Nile red is generally used as a single stain (Tyo *et al.*, 2006; Saranya *et al.*, 2012; Alves *et al.*, 2017) during flow cytometry but has also been double stained with the green nucleic acid stain SYTO™ 13 (Vidal-Mas *et al.*, 2001). Alternatively, P-546 is often counter-stained SYTO™ 62 (Karmann *et al.*, 2016; Vizcaino-Caston, *et al.*, 2016; Fernández-Castané, *et al.*, 2018). Staining with P-546 is versatile and can be used to stain SCL-PHAs and MCL-PHAs (Karmann *et al.*, 2016) in addition to lipid droplets in microalgae (Cooper *et al.*, 2010). Thus, P-546 is not specific to P3HB but to 3-hydroxyacids. For this reason, studies have been conducted to ensure the specificity of P-546 in bacteria. Staining with P-546 compared to Nile Red has been found to be more specific to PHA (Brown *et al.*, 2020) and P-546 fluorescence has been found to strongly correlate with GC analysis of extracted PHA (Karmann *et al.*, 2016).

The emitted light from stained bacteria travels through a series of dichroic mirrors which are selectively transparent or reflective to light of specific wavelengths. The dichroic mirrors ensure any residual light from the lasers is removed and guide the emitted light to the correct PMT. The PMT multiplies the signal of the incident light and sends the data to a computer. The subsequent plotting of thousands of

data points can be used to quantify levels of stain and also as a method to identify sub-populations based. The main drawbacks of flow cytometry are the high cost of machinery and the level of maintenance required to keep machines in full working order (Cassarizza *et al.*, 2019). In addition, there is a requirement for cells to enter machines as individual cells and not as aggregates due to the risk of microfluidics blockages and the risk of data distortion caused by multiple cells being recorded as a single event (Ou *et al.*, 2017). Another limitation of flow cytometry is caused by the spectral overlap of fluorophores which limits the number of fluorophores that can be used, and prevents fluorophores with similar emission spectra from being used together (Cassarizza *et al.*, 2019). Crucial to any flow cytometry experiments is the use of control samples. In the context of P3HB accumulation, seed cultures should be grown such that cells at the start of an experiment contain negligible P3HB, thus providing a controlled starting point consistent between experiments. In addition, control samples containing cells only, stains only and buffer only should be run in order to check the machine is in full working order and that gating strategies are working as expected.

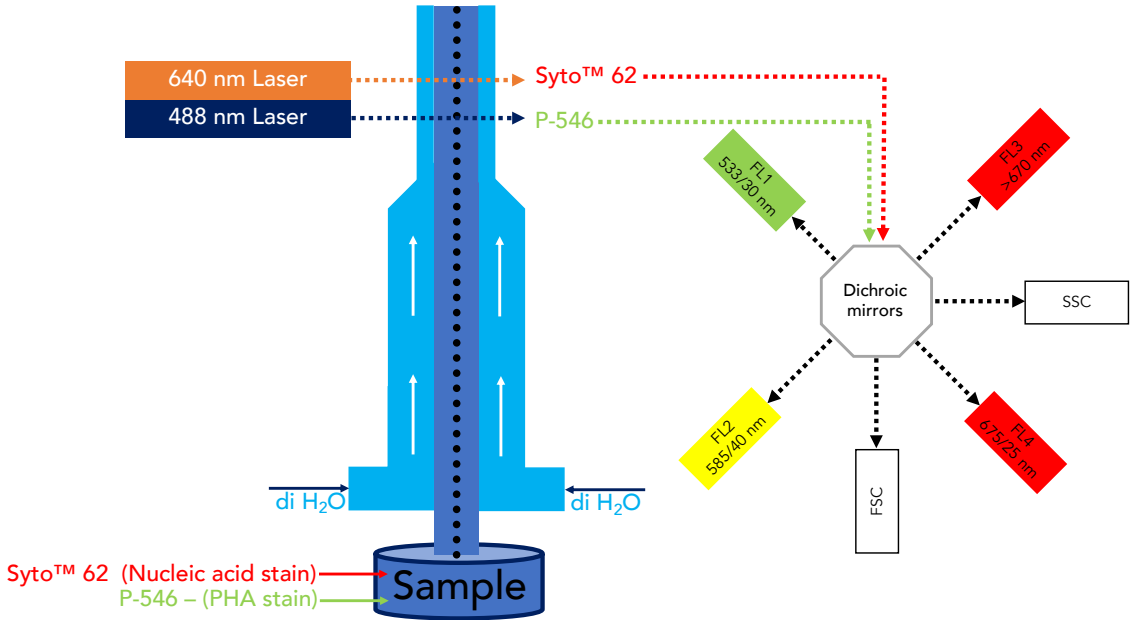


Figure 1.9 - A simplified illustration of the BD Accuri™ C6 flow cytometer used in this study.

1.2.7.3 Agar Plate Colony Screening

The screening of PHA-producing colonies does not quantify the amount of intracellular PHA but can be used to screen bacterial populations for PHA-producing isolates. Generally, due to the large quantities of stain required per agar plate, less expensive dyes such as Nile Red and Sudan Black are used instead of P-546. Goh and Tan (2021) used sodium octanoate and glucose-containing agar to grow bacteria from Antarctic soil from which they isolated PHA-producing strains by staining with Nile Red and identifying stained colonies with UV light. Shrivastav *et al*. (2010) similarly used Nile red and UV light to screen for PHA-producing bacteria in soil and marine environments. Alias and Tan (2005) on the other hand used Sudan Black B to isolate PHA-producing bacteria from palm oil mill effluent. The advantage of using Sudan Black B is that colonies can easily be distinguished by eye without the requirement of UV illumination. This approach was also used by Bhuwal *et al*. (2013) who used Sudan Black B to screen wastewater from pulp, paper and cardboard industries.

1.2.7.4 Microscopy

Different types of microscopy are able to offer scientists a range of approaches to both screen populations for PHA-producing bacteria and also track PHA production and cell physiology. Fluorescent microscopy uses cell fluorescence originating from targeted staining with fluorophores or intracellular fluorescent reporter proteins to produce an image. One way in which this can be used is to screen for PHA-producing bacteria, a technique that Castro *et al*. (2021) used to isolate PHA accumulators from Amazonia Blackwater by staining with BODIPY™ 505/515. Using optical filters to select only the light from certain fluorophores, fluorescent microscopy can also be used to overlay images of the same cell with different dyes. For example, Cánovas *et al*. (2021) double-stained *Haloferax mediterranei* with Nile Red and SYBR™ Green and then overlayed the images to show the cell as a whole and the position of PHA within the cell. Additionally, this study combined the double overlay with phase contrast images to create even more detailed images.

Fluorescent microscopy can also be used to observe protein-DNA and protein-protein interactions. Pfeiffer *et al*. (2011) used a two-hybrid approach to investigate the interactions of PhaC1 and PhaP1 in *C. necator*. Additionally, this study also fused PhaM with the fluorescent protein eYgfp in order to assess the cellular location of PhaM. Bresnan *et al*., (2016) used fusion proteins such as DsRed2EC, LactC2, sfGFP in fluorescent microscopy experiments in order to prove that PHA granules do not have a phospholipid bilayer.

Phase contrast microscopy on the other hand is used to produce a more 3-dimensional appearance than conventional microscopy by creating light and dark regions based on light phase shift patterns. Phase contrast images can also be enhanced by staining with dyes such as Sudan Black B, Sudan Blue A and Nile Red as was shown by Legat *et al*. (2010) who used the technique to evaluate if 20 different *Halococcus* species were PHA producers.

Electron microscopes, on the other hand, use a beam of electrons to illuminate a sample, with SEM building a 3-dimensional image based on reflected electrons and TEM relies on electrons passing through the sample to create a thin 2-dimensional image. Tian *et al*. (2020) used crossectional TEM images of PHA accumulation *C. necator* to study the kinetics of PHA granule formation by calculating the mean cell volume and also the total surface area of granules in cells. In contrast, SEM is more typically used to investigate the microstructure of extracted PHA by allowing the visualisation of features such as pore sizes resulting from blending PHA with plasticisers such as glycerol, PEG and PVA (Shamala *et al*., 2009). Nwinyi and Owolabi (2019) used SEM to analyse the microstructure of extracted PHA and also used the accompanying EDS spectra to analyse the chemical composition of the PHA.

1.2.7.5 Fourier-transform infrared spectroscopy (FTIR)

Fourier-transform infrared spectroscopy is an analytical technique used to collect an infrared absorption or emission spectrum of a solid, liquid or gas. The quantity of PHA in a sample can be determined based on a peak at 1728-1738 cm^{-1} which results from a carbonyl bond stretching (Isak *et al*., 2016). The advantage of FTIR is that it does not require any solvents, requires minimum preparation and works with small samples. Xu *et al*. (2002) used FTIR to identify peaks related to amorphous and crystalline polymer regions to calculate the T_m and T_g of P3HB. Ranriamahefa *et al*. (2003) used the absorbance of PHA ester bonds to calculate the content of PHO and P3HB contained within *Pseudomonas* cultures. A big advantage of FTIR is that it can be incorporated into bioprocesses to provide online monitoring of solids, liquids and gases and was used by Jarute *et al*. (2004) to detect P3HB and glucose simultaneously.

1.2.7.6 Gas chromatography and GCMS

Gas chromatography is an analytical method used to determine the composition of samples by analysing vaporised samples by separation when combined with mass spectrometry which ionises and fragments the components further before analysing the chemical components in a mass analyser. Because GC requires volatile sample samples of lyophilised cells or extracted polymer must first be

derivatised by hydrolysis and methylation/propylation (Bassas, 2010), with processes such as methanolysis using sulfuric acid and methanol which hydrolyses and methylates the sample (Brandl *et al.*, 1988) or by propanolysis with hydrochloric acid and isopropyl alcohol which hydrolyses and propylates the sample (Riis and Mai, 1988). Furrer *et al*. (2007) have developed an improved method of methanolysis which uses boron trifluoride in order to improve the analysis of MCL PHAs. Generally, GCMS is considered the gold standard of PHA quantification and is often used as a comparison in experiments evaluating PHA extraction efficiencies (Karmann *et al.*, 2016).

1.2.7.7 Nuclear magnetic resonance

Nuclear magnetic resonance is an analytical spectroscopic technique based on the atomic nuclei magnetic properties which are able to reveal details of a polymer's molecular structure (Lens and Hemminga, 1998). One of the advantages of NMR analysis of PHA is that the is no need for hydrolysis to occur before analysis (Bassas Galià, 2010). In addition, NMR can determine both the content of individual monomers within PHA but also determine if the polymer is a random or block co-polymer. This was demonstrated by Hu *et al*. (2011) who used NMR to show PHA produced by recombinant *P. putita* consisted of P(3HB-co-4HB) in blocks of 20% P3HB (mol %) and 80% (mol %) P4HB.

1.2.7.8 Differential scanning caliometry

In order to calculate the Tm and Tg of PHAs, DCS can be used to assess thermal properties by measuring the heat flow in and out of a sample (Chiu and Prenner, 2011). In literature, DCS has been used to calculate the T_m and T_g of P3HB (Vizcaino-Caston *et al.*, 2016) in addition to the individual T_m and T_g of polymer blocks in P(3HB-co-4HB) block co-polymers (Hu *et al.*, 2011).

1.3 Aims and objectives

The overall aim of this study was to use flow cytometry to investigate if it is possible to use cost-effective, nutrient-rich ME media to produce maximum P3HB within a 72-hour timeframe using fructose and sodium gluconate as supplements. The use of ME supplemented with acetic acid as a media for P3HB production has been used previously by (Passanha *et al*. 2014) as a cost-effective alternative to expensive chemically defined media. The individual objectives of the study are as follows:

1. To evaluate intracellular P3HB accumulation of individual *C. necator* cells using P-546 fluorescence determined by flow cytometry, and use this to compare media strategies. Media strategies included batch, fed-batch and repeated-batch all of which tested a range of ME, fructose and sodium gluconate concentrations. Fructose (Budde *et al.*, 2011) and sodium gluconate (Henrich *et al.*, 2012) are known to be metabolised by *C. necator* and have been demonstrated to induce P3HB production in *C. necator*. Thus, the objective of adding fructose and sodium gluconate to cultures is to increase P3HB production by increasing the C to ME ratio.
2. To produce maximum P3HB in a realistic timeframe of 72 hours. This timeframe has been decided as suitable based on the findings of previous research (Budde *et al.*, 2011; Pradella *et al.*, 2012; Ienczak *et al.*, 2016).
3. To study changes occurring in cell morphology using FSC determined by flow cytometry and fluorescent microscopy, and assess potential impacts on P3HB production. This is key as aggregate morphologies are known to produce extracellular components which compete with precursors of P3HB production (Zhu and Rock, 2008). Additionally, cell morphology can indicate if media conditions are growth-promoting or suitable for P3HB accumulation.
4. To use OD_{600} determined by UV-visible spectroscopy and cell counts determined by flow cytometry to infer if media conditions promote cell proliferation or P3HB production, and in the case of cell counts to enable the calculation of P3HB per mL of culture.

1.4 Outline of thesis

This thesis is arranged into 8 chapters the first of which is an introductory chapter covering key concepts of the environmental impact of a plastics life cycle, the biosynthesis of P3HB, strategies for producing P3HB-containing polymers, the applications of P3HB-containing polymers, the extraction of PHAs and methods for analysing PHAs. Chapter 2 details the materials and methods used in the experiments presented in this thesis. Chapter 3 presents the results and discussion related to batch culture strategies in which concentrations of ME, fructose and sodium gluconate are tested in efforts to increase P3HB production. Chapter 4 presents the results of fed-batch and repeated-batch strategies in which experiments aimed to reduce a lag-time in P3HB production. Chapter 5 discusses overall results and finishes with a conclusion bringing the results of the thesis together. Chapter 6 provides details of future research which could build on the results of this thesis. Chapter 7 and 8 contain the full data which corresponds to summarised data in Chapter 3 and Chapter 4, respectively. Finally, Chapter 9 lists references used in this thesis.

Chapter 2 Materials and Methods

2.1 Microbiological culture

2.1.1 General laboratory practice

All work involving the preparation and sampling of microbiological culture was conducted in sterile conditions either close to a Bunsen flame, or in a sterile cabinet. Routinely hands were washed, and laboratory surfaces were wiped with either 70% (v/v) ethanol (Thermo Fisher, UK) or 1% (w/v) Virkon (Lanxess, Germany) prior to usage. Pipettes were washed with copious 70% (v/v) ethanol before use and pipette tips were autoclaved at 121 °C for 15 minutes and dried at 60 degrees in a static Memmert IPP110 (Memmert GmbH and Co., Germany) incubator. Before and after sampling, the openings of culture flasks were passed through a Bunsen flame to maintain sterility. Sterile gaseous exchange in Erlenmeyer flasks was maintained using a foam bung (Thermo Fisher, UK) which was inserted into the flask stem prior to autoclaving and the flask opening covered with foil to prevent evaporation and to maintain media sterility. All media unless otherwise stated was made using deionised water (Sartorius, UK) and autoclaved (Astell Scientific, UK) was sterilised at 121 °C for 15 minutes. The pH of all media was checked to be 7 using an accumet XL200 pH metre (FisherScientific, UK) and did not require adjustment in any experiments.

2.1.2 Bacterial strains

The work presented in this thesis used *C. necator* H16, the model organism for P3HB production, and was kindly provided by Professor Izabela Radecka from the University of Wolverhampton, UK.

2.1.3 General growth media and culture conditions

Nutrient-rich ME was selected for the growth of *C. necator* based on the recommended media for *C. necator* by DSMZ (DSMZ, 2007). Standard 0.8% (w/v) ME media contained 5g L^{-1} peptone from soybean (Fluka Analytical, USA) and 3g L^{-1} ME powder (Sigma-Aldrich, Germany) dissolved in deionised water. All *C. necator* cultures were grown at 30 °C and rotated at 150 rpm in a MaxQ 6000 (Thermo Scientific, UK) shaker.

2.1.4 Long-term glycerol storage of *C. necator*

In order to preserve *C. necator* over a long period of time, glycerol stocks were prepared as follows. A solution of 50% (v/v) glycerol (Thermo Scientific, UK) was prepared. A culture of *C. necator* was grown for 24 hours in 0.8% (w/v) ME and the culture was then mixed with the cooled sterile glycerol solution to a final glycerol concentration of 25% (v/v) before being stored at -80 °C. Before each experiment, to ensure cells were freshly grown, *C. necator* cells were taken from glycerol stocks and streaked onto 0.8% (w/v) ME agar (see section 2.1.5).

2.1.5 Short-term ME agar storage of *C. necator*

For the short-term storage of *C. necator*, 0.8% (w/v) ME was prepared with the addition of 1.5% (w/v) bacteriological agar (Sigma-Aldrich, Germany). The ME agar solution was then poured into sterile Petri dishes around a Bunsen flame and left at room temperature for 15 minutes. Using a flame-sterilised loop, *C. necator* cells were scraped from the surface of glycerol stocks and streaked onto the agar. Agar plates were incubated at 30 °C for around 48 hours before use.

2.1.6 Growth of *C. necator* seed cultures

Seed cultures were used in this study to provide sufficient biomass for experimental cultures and were grown in 500 mL Erlenmeyer flasks containing 50 mL of 0.8% (w/v) ME. Cultures were inoculated using a loopful of *C. necator* taken from a fresh agar plate prepared 2 days prior. Seed cultures were routinely grown for 24 hours before being used to inoculate experimental cultures unless otherwise stated.

2.1.7 Experimental cultures

All experimental cultures were grown in 100 mL Erlenmeyer flasks containing 10 mL of ME of varying concentration and were inoculated to an OD_{600} of 0.1 using a seed culture (Vizcaino-Caston *et al.*, 2016). Dilutions of ME were performed prior to autoclaving using deionised water. Diluted media was routinely checked to be pH 7 and did not require adjustment in any experiments.

2.1.7.1 Experimental culture supplements

Some experimental cultures were supplemented with either fructose (Sigma-Aldrich, Germany) or sodium gluconate (Sigma-Aldrich, Germany). Fructose was added from a stock solution of 50% (w/v) and sodium gluconate from a stock solution of 30% (w/v). Both stock solutions were filter sterilised

using a 0.22 μm syringe filter into sterile falcon tubes and added to growth media after autoclaving. Sodium chloride (Sigma-Aldrich, Germany) was prepared as a 150 g/L stock and added to media prior to autoclaving at concentrations of 3, 6, 9, 12 and 15 g/L.

2.1.7.2 Batch cultures

Batch cultures contained 10mL of between 0.08% to 0.8% (w/v) ME, and either contained only ME or fructose ranging in concentration from 0.5% to 1.5% (w/v) and/or sodium gluconate ranging in concentration from 0.6% to 1.6% (w/v). In batch culture, the media was not changed or supplemented after 0 hours.

2.1.7.3 Fed-batch cultures

Fed-batch cultures contained 10 mL of between 0.08% to 0.8% (w/v) ME. In fed-batch cultures, supplements of either fructose or sodium gluconate were added to the media after culture inoculation at 0 hours, and at 24 hours. The concentration of supplements was calculated to account for any volume change due to sample withdrawal. Supplementation of media always occurred after a sample had been taken when both events occurred at the same time point.

2.1.7.4 Repeated-batch cultures

In repeated-batch cultures, initial media consisted of 10 mL of between 0.08% and 0.8% (w/v) ME supplemented with 0.5% (w/v) fructose and/or 0.6% (w/v) sodium gluconate. After 24 hours of growth, *C. necator* was separated from the media by centrifugation at 1811 RCF for 3 minutes using an Eppendorf 5810 centrifuge (Eppendorf, Germany). Cells were then resuspended in 10 mL of either 0.04% or 0.008% (w/v) ME media which was supplemented with 0.5% (w/v) fructose and/or 0.6% (w/v) sodium gluconate.

2.2 Analytical techniques

2.2.1 Measurements of OD_{600}

The OD_{600} of cultures was measured using an Evolution™ UV-Vis spectrophotometer (ThermoFisher Scientific) at a wavelength of 600 nm. Samples with an OD_{600} of more than 0.9 were diluted with PBS (Dulbecco A) (Oxoid, UK) to ensure a linear trend between biomass and OD_{600}.

2.2.2 Flow cytometry

Flow cytometry experiments were conducted using a BD Accuri™ C6 flow cytometer (BD, UK) equipped with 488 and 640 nm lasers. The fluidics flow rate was set to medium (35 μL/min) (16 μm core). A threshold of 8000 units was set on the FSC-A channel to remove noise smaller than that of *C. necator* cells. The green fluorescence of P-546 (Photonic Solutions, USA), used to detect intracellular P3HB, was detected using the FL1 filter (533/30 nm). The far-red fluorescence of SYTO62 (ThermoFisher Scientific, UK) using the FL4 filter (675/25 nm) was used to separate cells from noise. Flow cytometry data was recorded using BD Accuri™ C6 software (BD, UK). Data was collected until 25,000 SYTO62 positive events had been recorded. Cleaning of the flow cytometer was performed according to the manufactures instructions. Samples were diluted using PBS such that the flow cytometer recorded between 1000 and 4000 events per second. Culture cell counts were calculated as events per mL of culture, a value calculated using the volume (μL) of sample used to record 25,000 events, and the dilution factor. Mean P-546 fluorescence per cell was used to quantify intracellular P3HB on a cell-by-cell basis. Mean P-546 fluorescence per mL culture was used to assess overall culture P3HB and was calculated by multiplying values for mean events per mL and mean P-546 fluorescence per cell. The stock solution of P-546 was prepared in DMSO (FisherScientific, UK) at a concentration of 1 mg/mL and stored at -20 °C (Vizcaino-Caston *et al.*, 2016). Long-term stocks of SYTO62 were stored as supplied by the manufacturer at a concentration of 5mM in DMSO. Short-term stocks were prepared by diluting to a concentration of 0.2 mM in 0.22 μm deionised water.

2.2.2.1 Flow cytometry staining protocol 1

Culture diluted with PBS was stained with 5 μM SYTO62 for 30 minutes, and after 18 minutes 1 μg/mL P-546 (Vizcaino-Caston *et al.*, 2016) was added and incubated for a further 12 minutes. Staining was conducted at room temperature (24 °C). Samples were mixed well following stain addition.

2.2.2.2 Staining optimisation conditions

For the staining optimisation (section 3.7) batch *C. necator* experimental cultures containing 0.08% (w/v) ME and 0.6% (w/v) sodium gluconate were grown for 72 hours. The culture was then diluted in PBS and stained with 0, 1, 2, 3, 4 or 5 μM SYTO62. Separately, the culture was also stained with 0, 0.25, 0.5, 0.75, 1 or 1.25 μg/mL. Each dye concentration was tested at room temperature (24), 30 and 37 °C. Samples tested at 30 and 37 °C were incubated in a Memmert IPP110 (Memmert GmbH and Co., Germany) and was PBS preheated to ensure samples were at the correct temperature.

2.2.2.3 Flow cytometry staining protocol 2

Culture diluted with PBS was stained with 1 μM SYTO62 and 0.2 μg/mL P-546 was added and incubated at 30 °C for 12 minutes. Samples were mixed well following stain addition.

2.2.3 Fluorescent Microscopy

2.2.3.1 Method 1

Long-term stocks of SYTO62 were stored as supplied by the manufacturer at a concentration of 5mM in DMSO. Short-term stocks were prepared by diluting to a concentration of 0.2 mM in 0.22 μm deionised water. Cells were stained with 1.33 μM SYTO9 for 5 minutes at room temperature and viewed using a Zeiss Axiolab (Carl Zeiss Ltd, UK) fitted with Zeiss filter 9 (Excitation: BP 450-490, Beamsplitter: FT 510, Emission: LP 515) (Carl Zeiss Ltd, UK). Images were taken using a ZeissAxioCam Icm1 camera (Carl Zeiss Ltd, UK) using Zeiss ZenLite 2012 software (Carl Zeiss Ltd, UK). Images were monochrome and artificially coloured green using ImageJ (NIH, USA).

2.2.3.2 Method 2

Media was separated from *C. necator* cells by centrifugation at 2236 RCF for 5 minutes in an Eppendorf 5418 centrifuge (Eppendorf, Germany). Cells were then resuspended in a permeabilisation solution consisting of 35% (v/v) ethanol (FisherScientific, UK) for 10 minutes. Centrifugation was again used to separate cells from the permeabilisation solution before cells were finally resuspended in PBS. A stock solution of PI was stored as supplied by the manufacturer at a temperature of 4 °C with a concentration of 1 mg/mL in water. For experimental work, another stock was prepared by diluting to a concentration of 0.2 mg/mL in deionised water and storing at 4 °C. Cells were stained in PBS with 2 μg/mL PI and 1 μM P-546 for 10 minutes. Stained cells were then viewed with a Zeiss AX10 microscope (Carl Zeiss Ltd, UK) fitted with Zeiss filter 10 (Excitation: BP 546/12, Beamsplitter: FT 510, Emission: LP 515-565 (Carl Zeiss Ltd, UK) and a Zeiss filter 20 (Excitation: BP 450-490, Beamsplitter: FT 510, Emission: LP 515-565 (Carl Zeiss Ltd, UK).

2.3 Statistical Analysis

Values for mean and standard deviation (SD) were calculated using Microsoft Excel (Microsoft, USA). Comparisons between different experimental conditions at the same, or different time points were made non-paired t-tests of unequal variance using Microsoft Excel. Comparisons between the same

conditions over time were made using paired t-tests, also in Microsoft Excel. For t-tests a threshold of $p \geq 0.05$ was used to determine statistical significance. In bar graphs where the results of 2 adjacent were statistically compared, the significance of the comparison is displayed centrally, above the pair of results. Linear regression was used to plot a line of best fit, and the coefficient of determination (R^2) was used to assess the ability of linear regression to predict a linear relationship between variables and is expressed as a value between 0 and 1. Linear regression and the calculation of R^2 values was performed using the ggpubr package of RStudio (R Studio Team, USA).

Chapter 3 Results and Discussion

3.1 Why does inoculation using a 12-hour seed culture produce multi-cell aggregates?

Bacterial cultures used for scientific study are typically divided into experimental and seed cultures. Experimental cultures are used as a means to make observations and generate quantitative data. On the other hand, seed cultures are used to provide multiple experimental cultures with sufficient and constant starting biomass. Seed cultures are normally inoculated from long-term stock by loop and experimental cultures by liquid pipetting. Liquid by pipette is the preferred method of inoculation for experimental cultures as inoculation by loop has been shown to have up to a 12-fold variation in the number of cells added to growth media (Webb and Kamat, 1993). For the reasons explained, experimental cultures in the current study were inoculated to an OD_{600} of 0.1 using a pre-grown seed culture.

Pilot experiments initially tested the growth of *C. necator* in 0.8% (w/v) ME experimental cultures which were inoculated from a 0.8% (w/v) ME seed culture grown for 12 hours. Culturing *C. necator* in this way led to the formation of large cell aggregates, which persisted and prevented the growth of platonic culture. The persistent aggregation of *C. necator* cells was not observed in experimental cultures when a 24-hour-old seed culture was used for inoculation. A study by Kragh *et al*. (2018) found the inoculation method of experimental bacterial cultures can influence the outcome of microbiological experiments. It was found that by varying the source of cells used to initiate seed cultures (frozen stocks, agar grown or liquid grown) the phenotype of cells in experimental cultures can be altered, creating cultures varying from platonic cells to multi-cell aggregates. Cell aggregates form due to the interactions of cell surface molecules which self-associate and are thought to be expressed in response to environmental stress as a defence mechanism (Nwoko and Okeke, 2021). The formation of large cell aggregates should be avoided during flow cytometry to reduce the risk of blockages and to prevent data distortion caused by the machine recognising multi-cell aggregates as a single cell (Ou *et al.*, 2017).

Based on observations of cell aggregation in the pilot experiments, and the information provided by Ou *et al*. (2017) and Kragh *et al*. (2018), the following section compares *C. necator* seed cultures at 12 and 24-hour time points, to identify possible causes for persistent cell aggregation in experimental cultures.

3.1.1 Initial studies use OD_{600} rather than flow cytometry cell counting

In the current study up to section 3.8, OD_{600} was used as a means to monitor the cell density of *C. necator* cultures instead of using flow cytometry events per mL. This was due to a fault with the BD C6™ Accuri flow cytometer used in this study, with BD advising that the flow cytometer was not in good enough working order for cell counting. The use of OD_{600} was chosen instead of agar plate colony counting due to the number of agar plates required to cover a wide range of dilutions with replicates of each. The large number of plates required stems from the need for replicates to calculate a mean value, and also the wide range of dilutions that need to be tested in order to get the optimal amount of colonies on each plate. The subsequent time required to process such a large amount of plates and count the colonies would result in a trade-off, either acquiring more agar plate count data or more flow cytometry data. The drawback of using OD_{600} to monitor the cell density of P3HB-producing bacteria such as *C. necator* is that P3HB also absorbs light at 600 nm making OD_{600} measurements unreliable especially when the intracellular levels of P3HB are high (Martinez and Déziel, 2020). Therefore up to section 3.8, OD_{600} results are used as a guide rather than a definitive result, and the reliability of particular time points can be judged according to the corresponding time points P-546 fluorescence.

3.1.2 Seed culture cell density does not influence cell aggregation in experimental cultures.

Figure 3.1 provides a summary of the OD_{600} of *C. necator* seed cultures at 12 and 24 hours when grown in 0.8% (w/v) ME. Figure 8.1 (a) in Appendix 8.1 presents the data in full.

Measurements of OD_{600} quantify bacterial cell density which is known to have an important role in bacterial aggregation and biofilm formation, principally because bacteria communicate cell density within a population by quorum sensing (Waters and Bassler, 2005). Quorum sensing allows bacteria to monitor cell density and other external factors by altering the expression of multiple genes (Papenfort and Bassler, 2016). Garg *et al*. (2000) demonstrated *C. necator* has a functional homologue of Phc cell density sensing system found in the plant pathogen *Ralstonia solanacearum*, that is known to control cell aggregation activity (Senuma *et al*., 2020).

In the current study, the OD_{600} of cultures at 12 and 24 hours was found not to be significantly different when statistically compared. This suggests that the cell density of seed cultures at the time of inoculation does not influence aggregate formation in experimental cultures. Futher to this, as experimental cultures are always inoculated to an OD_{600} of 0.1, this rules out the possibility that the starting cell density of experimental cultures causes persistent clumping.

The OD_{600} of cultures at both 12 and 24 hours was found to be suitable to innoculate experimental cultures. For instance, a 50 mL seed culture with an OD_{600} of 3 contains enough biomass to innoculate over 150 10 mL experimental cultures to a starting OD_{600} of 0.1.

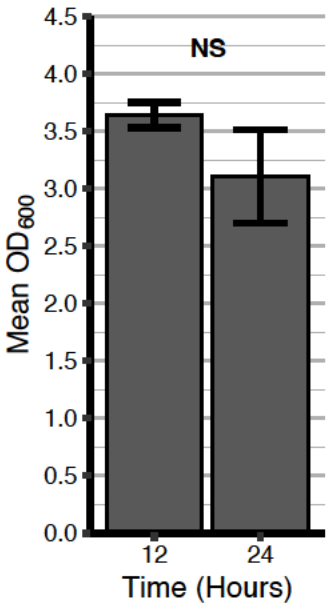


Figure 3.1 – Summary of mean OD_{600} for 0.8% (w/v) ME *C. necator* seed cultures, compared at 12 and 24-hour time points. Statistical significance was determined using a paired t-test to compare the same condition at different time points. NS = non-significant ($p \geq 0.05$). Error bars represent SD. n = 4 biological replicates. The full data can be found in Figure 8.1 (a) in Appendix 8.1.

3.1.3 Intracellular P3HB in seed cultures is not linked to persistent clumping in experimental cultures.

Figure 3.2 presents a summary of the P3HB per cell for 0.8% (w/v) ME *C. necator* seed cultures at 12 and 24-hour time points. The full data can be found in Figure 8.1 (b), Appendix 8.1.

Statistical analysis in Figure 3.2 shows that when comparing the 12 and 24-hour seed culture time points, there was no significant difference in P-546 fluorescence. Thus inferring that the P3HB content of *C. necator* seed cultures did not cause persistent clumping in experimental cultures.

Components of the bacterial extracellular matrix are known to have an important role in the process of cell aggregation (Voloshin and Kaprelyants, 2004). A study by Wang *et al*. (2021) demonstrated that in *E. coli* overexpressing the *C. necator phaCAB* operon, the disruption of lipopolysaccharide, colonic acid, flagella and fimbria gene clusters increases P3HB production by making acetyl-CoA more readily available for to P3HB biosynthesis. The results of Wang *et al*. (2021) suggested P3HB biosynthesis competes for acetyl-CoA with the biosynthesis of outer membrane components involved in cell aggregation and biofilm production. This was also found to be the case in studies by Zhu and Rock (2008) in *Pseudomonas aeruginosa* and Irorere *et al*. (2018) in *Burkholderia thailandensis* E264 during rhamnolipid biosynthesis. The biosynthesis of rhamnolipid utilises malonyl-CoA via the fatty acid *de novo* biosynthesis pathway which is formed from the carboxylation of acetyl-CoA (Gutierrez *et al*., 2013). Abdel-Mawgoud *et al*. (2014) also found by inhibiting the β-oxidation pathway that rhamnolipids and P3HB share the same 3-hydroxyalkanoate intracellular pool. Such competition could be problematic in media containing fatty acids such as biodiesel waste, as *C. necator* cleaves fatty acid chains from glycerol before entering the β-oxidation pathway (Sharma *et al*., 2016). The avoidance of cell aggregation before P3HB has reached a desired level should be avoided to ensure acetyl-CoA is utilised for P3HB productions and not by extracellular components or the Krebs cycle. Furthermore, while flocculation can be advantageous towards the end of P3HB accumulation to aid cell separation prior to P3HB extraction, aggregation at an early stage puts cells on the inside of the aggregate at a disadvantage by receiving less nutrition that can be used to produce P3HB (Kragh *et al*., 2016).

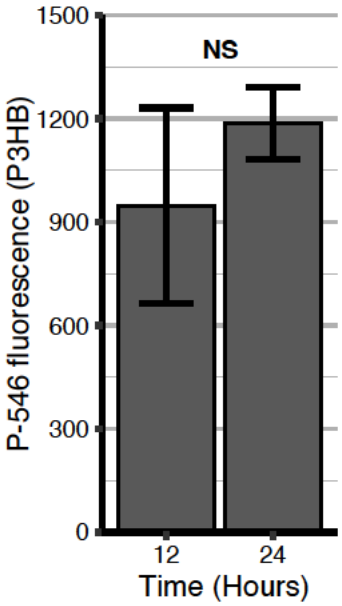


Figure 3.2 – Summary of mean P-546 fluorescence (P3HB) of 0.8% (w/v) ME *C. necator* seed cultures compared at 12 and 24-hour time points. Statistical significance was determined using a paired t-test to compare the same condition at different time points. NS = non-significant ($p \geq 0.05$). Error bars represent SD. n = 4 biological replicates. The full data can be found in Figure 8.1 (b), Appendix 8.1.

3.1.4 Seed culture cell size and aggregation are not linked

Figure 3.3 compares the mean FSC of 0.8% (w/v) ME *C. necator* seed cultures at 12 and 24 hour time points. The full data can be found in Figure 8.1 (c), Appendix 8.1.

Statistical analysis could not link cell size to persistent experimental culture clumping as there was no significant difference between mean seed culture FSC at 12 and 24 hours. The influence of cell size on aggregation appears to be absent from relevant literature, with the consensus instead being that cell density (Waters and Bassler, 2005) and extracellular matrix composition (Voloshin and Kaprelyants, 2004) are chiefly responsible.

Autoaggregation occurs usually during periods of cell stress and the process is mediated by self-recognising components of the extracellular matrix (Trunk *et al.*, 2018). Various components of the extracellular matrix such as lipopolysaccharides, colonic acid, flagellar, fimbria (Wang *et al.*, 2021) and type-IV pili (Kang *et al.*, 2002) are likely the components responsible in *C. necator* extracellular matrix that enable aggregates to form and persist.

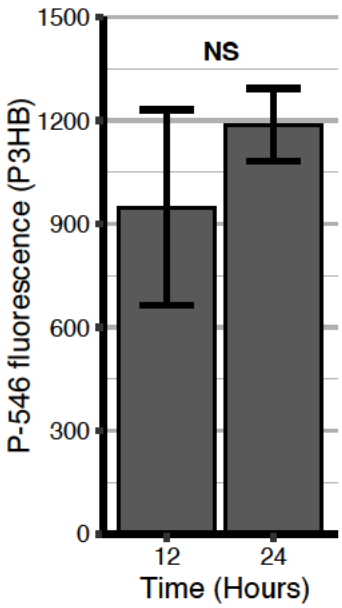


Figure 3.3 – Summary of mean FSC of 0.8% (w/v) ME *C. necator* seed cultures compared at 12 and 24 hour time points. Statistical significance was determined using a paired t-test to compare the same condition at different time points. NS = non-significant ($p \geq 0.05$). Error bars represent SD. n = 4 biological replicates. The full data can be found in Figure 8.1 (c), Appendix 8.1.

3.1.5 Various *C. necator* morphologies are observed during seed culture growth

Figure 3.4 displays fluorescent microscope images of *C. necator* morphologies observed during 0.8% (w/v) ME seed culture growth. Accompanying each microscope image in Figure 3.4 are FSC histograms which provide further context of cell size distribution for the overall cell population.

The first morphology observed is displayed in Figure 3.4 (a), and shows a doublet cell most likely in the process of cell division. The model system for studying cell division in gram-negative bacteria is based on that of *E. coli* (Jacobs and Shapiro, 1999), which is controlled, in part, by three key genes *minC*, *minD* and *minE*, referred to as the mini-cell locus (de Boer *et al.*, 1989). Homologues of mini cell locus genes can be found in the *C. necator* genome (KEGG, 2021).

At the 4-hour time point, *C. necator* cells formed small aggregates an example of which is displayed in Figure 3.4 (b). The maximum size of an object that can pass through a flow cytometer is governed by the diameter of a sample core, a tube in which cells pass through laser beams. For the BD C6 Accuri™ flow cytometer, the core can be adjusted between diameters of 5 and 40 μm and was set to 16 μm for this study meaning objects as large as 16 μm could pass freely through the core. In addition, larger objects can also protrude into the surrounding sheath fluid or be compressed to a smaller size, although the extent to which this occurs is unclear. The clump pictured in Figure 3.4 (b) is below 16 μm and would have passed through the flow cytometer. However, if the clumps passed through the instrument a second larger sized population would be expected. It is therefore likely that aggregates were broken up by shear forces during hydrodynamic focusing, before entering the flow cytometer core. The appearance of *C. necator* aggregates comprising cells positioned adjacent to each other in Figure 3.4 (b) resembles the appearance of *Bacillus subtilis* cells which were demonstrated to be undergoing horizontal gene transfer via conjugation by Babic *et al*. (2011). Unlike the persistent aggregates observed in experimental cultures, the aggregates in seed cultures were transient and by 8 hours had disappeared.

At 8 (Figure 3.4 (c)) and 12-hour time points (Figure 3.4 (d)) the morphology of some *C. necator* cells had changed to elongated cells connected by SYTO9 negative regions (Figure 3.4 (c)), which appear to be Z-rings. Occurring at the division site, Z-rings are ubiquitous to bacteria that divide by binary fission and consist of the tubulin homologue FtsZ and function to recruit division proteins to the divisome and also direct the formation of septal peptidoglycan (Du and Lutkenhaus, 2019). The over-expression of MinCD proteins prevents the formation of a Z-ring at the mid-cell point (Jacobs and Shapiro, 1999). MinD also ensures that the FtsZ ring forms in the middle of the dividing cell and not between the centre and poles of the cell (Raskin and de Boer, 1999). In rod-shaped bacteria, the

elongation of cells is controlled by the highly conserved rod system, which involves the polymerisation of peptidoglycan with the glycan polymerase RodA and the PBP2 crosslinking enzymes (Rohs *et al.*, 2018). In *Streptococcus* species, which form similar chains to that of *C. necator* observed in this study, chain formation is thought to increase the chances of cell aggregation (Evans *et al.*, 2014). In addition, chains of cells are thought to make the horizontal transfer of genes more efficient by acquiring DNA at the cell poles and then sharing the acquired genetic material with other cells in the chain by intra-chain conjugation (Babic *et al.*, 2011). Elongated cells can be split into chains of cells which can then separate into daughter cells by the action of peptidoglycan hydrolases (Arrigucci and Pozzi, 2017). Cell elongation has also been observed to occur when *minE* is deleted which causes the formation of long filamentous cells (de Boer *et al.*, 1989).

At 24 hours, *C. necator* cells were very small and spherical (Figure 3.4 (e)) and appear to be in a dormant or persister state (Miyaue *et al.*, 2018), which *C. necator* appears to enter when nutrients are limited and C is not sufficiently available to store as P3HB.

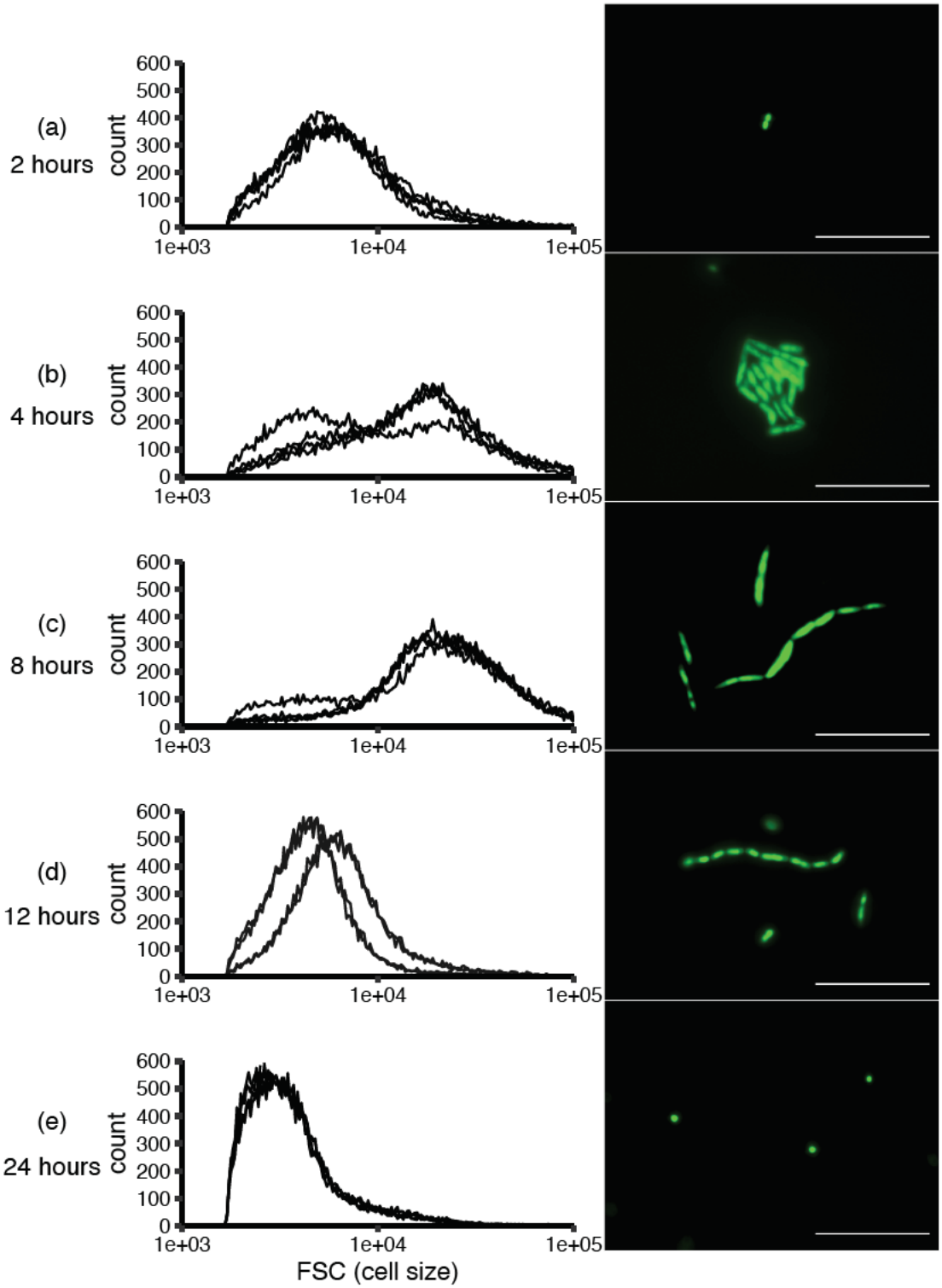


Figure 3.4 - Fluorescent microscopy images and the corresponding FSC histograms depicting different *C. necator* morphologies observed in 0.8% (w/v) ME seed cultures. On the left of the figure are histograms showing the FSC of each individual replicate. On the right are the corresponding fluorescent microscope images of *C. necator* cells at various time points. Cells were stained with 1.33 mM SYTO9 for microscopy and separately stained with SYTO62 (5 µM) and P-546 (1 µM) for flow cytometry. Scale bars represent 10 µm. For FSC histograms n=4 biological replicates.

3.1.6 The impact of cell morphology and nucleic acid staining on the flow cytometry threshold

In flow cytometry when a stained cell passes through a laser it either fluoresces or scatters light. The resulting light is collected by a PMT which converts the light into a signal based on light intensity. A threshold is set providing a cut-off value that represents the lowest signal intensity at which the flow cytometer will count an event. In this study, FSC is used as a threshold but in other studies, SYTO62 fluorescence has been the preferred method of setting a threshold (Karmann *et al.*, 2016).

Figure 3.5 contains a microscope image enlarged from Figure 3.4 (d) in section 3.1.5, which is stained green with SYTO9 to allow for visualisation by fluorescent microscopy. This image in particular consisted of chains of cells appearing to be in a state of division and the multiple Z-rings did not stain with SYTO9. For flow cytometry experiments, SYTO9's red equivalent SYTO62 was used as an alternative to avoid spectral clashes with the green fluorescence of P-546. In Figure 3.5, a theoretical PMT signal trace for SYTO62 is drawn as a red line against the *C. necator* cell displayed. As the dark, Z-ring, regions in the image contain little or no stain at all, they would likely register well below any threshold set on the far-red PMT used to collect SYTO62 fluorescence. This would lead to the flow cytometer registering several small cells instead of a single large structure. For this reason, using FSC as a primary threshold is more appropriate to use for *C. necator* than SYTO62 fluorescence.

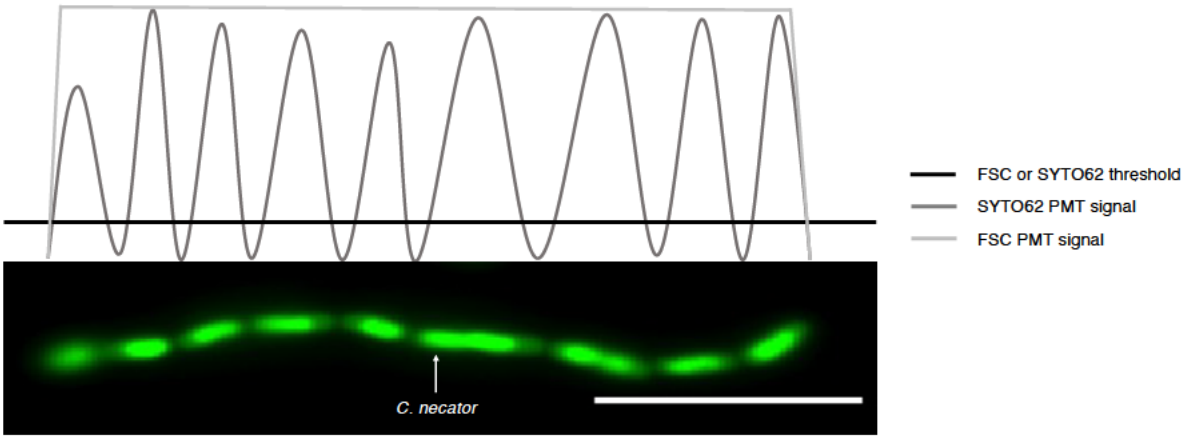


Figure 3.5 - Visualising the theoretical implications on flow cytometry results using the SYTO62 fluorescence as a threshold compared to FSC. Scale bar represents 5 µm. Cells were stained with 1.33 mM SYTO9.

3.1.7 Discussion

Experimental cultures of *C. necator* formed persistent cell aggregates when inoculated with a seed culture grown for 12 hours, a problem which was rectified by growing seed cultures for 24 hours instead. When statistically compared at 12 and 24 hours, there was found to be no significant difference in seed culture OD_{600} thus indicating that cell density-dependant quorum sensing did not induce persistent clumping (Waters and Bassler, 2005). Likewise, there was also found to be no significant difference in intracellular P3HB between 12 and 24-hour-old seed cultures. Components of the bacterial cell membrane key to cell aggregation such as rhamnolipids may compete with intracellular pools of common intermediate molecules such as acetyl-CoA (Zhu and Rock, 2008). As a result, cell aggregation should be avoided in order for P3HB biosynthesis to be prioritised (Wang *et al.*, 2021). Cell size was also found to be indifferent in 12 and 24-hour seed cultures. Therefore it is likely that in 12-hour seed cultures cells are equipped with self-recognising extra-cellular matrix components such as type-IV pili which mediate cell auto aggregation (Wang *et al.*, 2021). During growth *C. necator* was observed to change morphology, starting off as doublet cells resembling binary fission observed in *E. coli* (Jacobs and Shapiro, 1999). Aggregates formed at 4 hours resembled *Bacillus subtilis* cells found by Babic *et al*. (2011) to be undergoing horizontal gene transfer via conjugation. Elongated cells were divided by Z-rings (Jacobs and Shapiro, 1999) which means they were likely in the process of dividing into multiple cells. The final morphology observed was small cells which resembled the morphology of cells in a persister state (Miyaue *et al.*, 2018), presumably formed due to limited key nutrients and limited C.

3.2 Initial *C. necator* ME experimental cultures

Seed cultures typically consist of non-chemically defined, nutrient-rich media, which is used to produce biomass in a short period of time. At laboratory scale, experimental P3HB accumulating cultures often consist of precisely defined media, prepared using analytical grade chemicals. However, while this strategy allows for control over the chemical constituents of the media, the use of media with a defined chemical composition is not economically viable for many scaled-up fermentations. As a result, non-chemically defined ME media was used in this study for both seed and experimental cultures. In section 3.2, data is presented based on standard 0.8% (w/v) ME, which was diluted to 0.6%, 0.4% and 0.2% (w/v) in order to reduce the nutrient content of the media and evaluate if ME alone was able to induce P3HB accumulation in *C. necator* cultures.

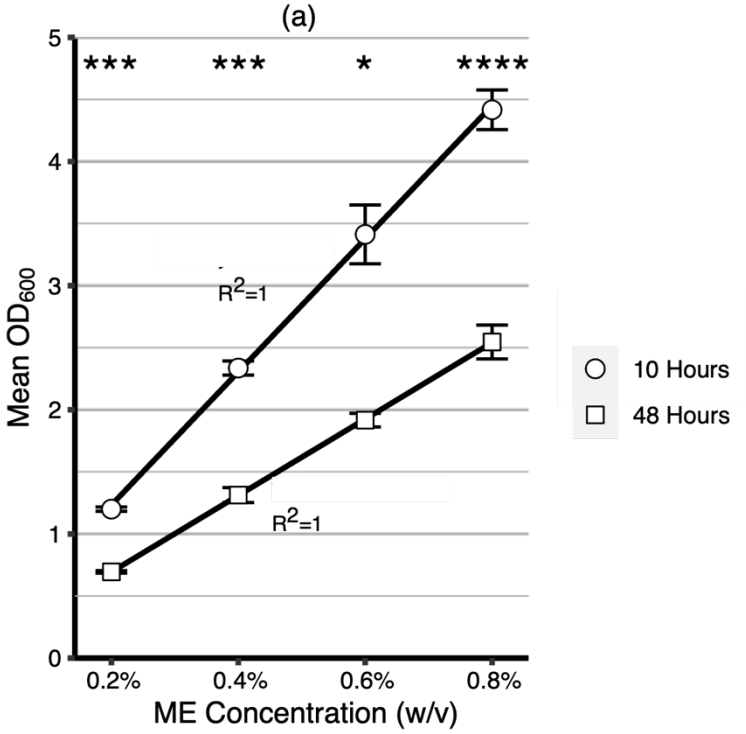
3.2.1 Increasing ME concentration correlates with increasing OD_{600}

Figure 3.6 displays a summary of OD_{600} at 10 and 48-hour time points for *C. necator* cultures containing 0.2%, 0.4%, 0.6% and 0.8% (w/v) ME. The full data is displayed in Figure 8.2 (a), Appendix 8.2.

Statistical comparisons between 10 and 48 hours, annotated in Figure 3.6 (a), show that for each ME concentration tested, OD_{600} was greater at 10 hours and had significantly decreased by 48 hours. Also presented in Figure 3.6 (a) is a positive correlation between increasing ME and OD_{600} at 10 and 48 hours. Figure 3.6 (b) provides further statistical comparison showing that at both time points summarised, all ME concentrations tested produced cultures with significantly different OD_{600}.

A strong correlation between ME concentration and OD_{600} is indicative of nutrient-rich conditions, in which C-containing compounds are metabolised by the citric acid and Entner-Doudoroff cycles as a source of energy (Ienczak *et al.*, 2011). Also essential for bacterial growth are nitrogen-containing compounds for protein synthesis, phosphorous-containing compounds for nucleic acid synthesis and vitamins for use as enzyme co-factors (Bonnet *et al.*, 2020). Culture growth observed and analysed in Figure 3.6 matches the growth expected of *C. necator* in ME media which contains soybean extract peptone which provides nitrogen-containing compounds and a high concentration of carbohydrates (Merck KGaA, 2022(b)), and ME which provides bacteria also with nitrogen-containing compounds, minerals and phosphates (Merck KGaA, 2022(a)).

(a)



(b)

Non-paired t-test comparing OD_{600} for each condition at 10 and 48 hours.			
Media comparison (w/v)		10 hours	48 hours
0.2%	0.4%	***	**
0.2%	0.6%	**	***
0.2%	0.8%	***	**
0.4%	0.6%	*	***
0.4%	0.8%	***	***
0.6%	0.8%	**	***

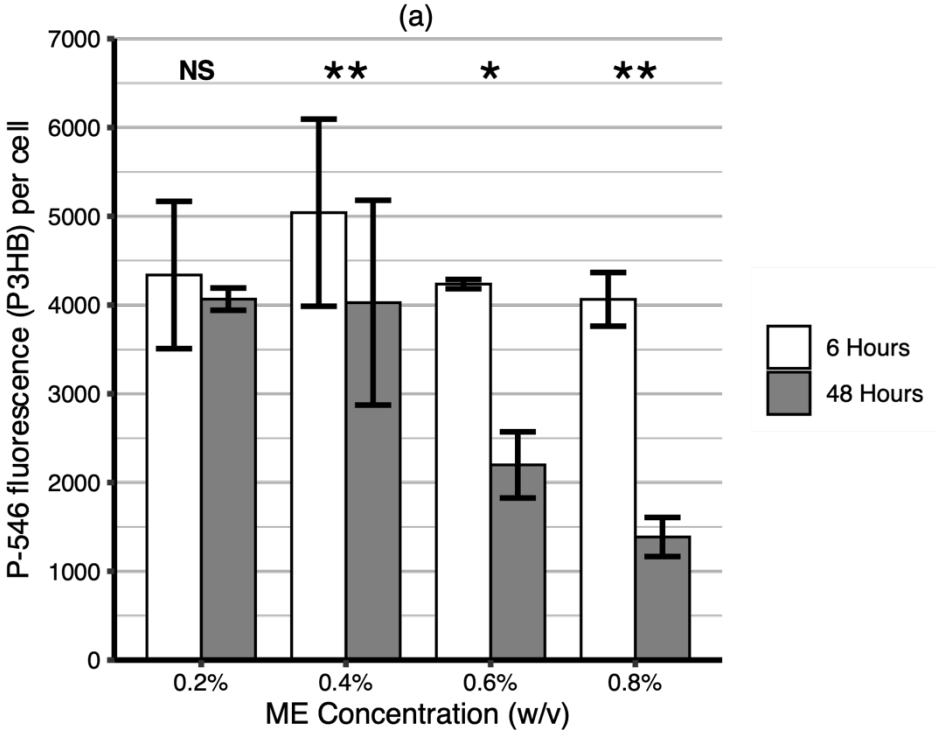
Figure 3.6 - Comparison of mean OD_{600} of *C. necator* cultures grown in 0.2%, 0.4%, 0.6% and 0.8% (w/v) ME at 10 and 48-hour time points. Plot (a) compares OD_{600} at 10 and 48 hours and includes annotations representing statistical significance determined by paired t-tests. Table (b) contains statistical comparisons between each ME condition at 10 and 48 hours, determined by non-paired t-tests. NS = non-significant ($p \geq 0.05$), * = $p < 0.05$, ** = $p \leq 0.01$, *** = $p \leq 0.001$, **** = $p \leq 0.0001$. Trend lines were calculated using linear regression. R^2 represents the coefficient of determination. Error bars represent SD. n = 3 biological replicates. The full data is displayed in Figure 8.2 (a), Appendix 8.2.

3.2.2 More P3HB is produced by *C. necator* in 0.2% (w/v) ME that 0.6% and 0.8% after 48 hours.

A summary analysing the mean intracellular P3HB per cell of *C. necator* cells grown in 0.2%, 0.4%, 0.6% and 0.8% (w/v) ME is presented in Figure 3.7. The full data is located in Figure 8.2 (b), Appendix 8.2. Statistical analysis comparing 6 and 48-hour time points (annotated in Figure 3.7 (a)) found 0.2% (w/v) ME was the only condition tested not to significantly decrease in P3HB content, instead remaining indifferent between time points. Further statistical analysis presented in (Figure 3.7 (b)) determined there to be no significant difference between each culture condition at 6 hours. However, at 48 hours, 0.6% and 0.8% (w/v) ME cultures were found to contain *C. necator* cells with less mean P3HB per cell than 0.2% cultures. Although, both 0.6% and 0.8% (w/v) ME cultures were not significantly different from that of 0.6%.

Results, therefore, suggest that at 48 hours a lower concentration of ME results in more intracellular P3HB accumulation on average per cell. Although literature generally suggests the C to key nutrient ratio is fundamental to the induction of P3HB biosynthesis, the statistical analysis presented in Figure 3.7 (b) suggests that the same C to ME ratio, but at lower concentrations, can also induce P3HB biosynthesis. However, it should not be discounted that other factors such as differing rates of nutrient depletion and lower cell density in 0.2% and 0.4% (w/v) cultures could also influence levels of P3HB at 48 hours. An initial spike in mean P3HB per cell at 6 hours for *C. necator* cells in all conditions tested goes against the general theory of P3HB accumulation in which growth-limiting, nutrient deficient but C-rich conditions are required to initiate P3HB production. In fact, P3HB production during the exponential phase of growth has previously been reported by Dey and Rangarajan (2017) and Nygaard *et al*. (2019) who observed increases in biomass and P3HB simultaneously. Increased P3HB production during the *C. necator* exponential growth phase has also been achieved by genetic modification in *Azotobacter vinelandii* (Page and Knosp, 1989; Segura *et al.*, 2003; Segura and Espín, 2004).

(a)



(b)

Non-paired t-test comparing P-546 fluorescence (P3HB) per cell for each condition at 6 and 48 hours.			
Media comparison (w/v)		6 hours	48 hours
0.2%	0.4%	NS	NS
0.2%	0.6%	NS	*
0.2%	0.8%	NS	***
0.4%	0.6%	NS	NS
0.4%	0.8%	NS	NS
0.6%	0.8%	NS	*

Figure 3.7 - Comparison of mean P-546 fluorescence (P3HB) per cell of *C. necator* cultures grown in 0.2%, 0.4%, 0.6% and 0.8% (w/v) ME at 10 and 48-hour time points. Plot (a) compares P-546 fluorescence (P3HB) per cell at 6 and 48 hours and includes annotations representing statistical significance determined by paired t-tests. Table (b) contains statistical comparisons between each ME condition at each time point determined by non-paired t-tests. NS = non-significant ($p \geq 0.05$), * = $p < 0.05$, ** = $p \leq 0.01$, *** = $p \leq 0.001$. Error bars represent SD. n = 3 biological replicates. The full data is located in Figure 8.2 (b), Appendix 8.2.

3.2.3 Cultures of *C. necator* in 0.2% (w/v) ME do not form aggregates

Figure 3.8 provides a summary of *C. necator* cell size in cultures containing 0.2%, 0.4%, 0.6% and 0.8% (w/v) ME after 6 and 24 hours of growth. The full data can be found in Figure 8.2 (c), Appendix 8.2. Paired statistical analysis, annotated in Figure 3.8 (a), found that *C. necator* cells were significantly larger at 6 hours when compared to 48 hours. Comparing ME concentration at each time point (Figure 3.8 (b)) found that at 6 hours cell size significantly increased with increasing ME concentration except for when comparing 0.6% and 0.8% (w/v) ME cultures.

It's likely that a larger cell size at 6 hours is the result of cell elongation during proliferation. Cell elongation in bacteria is primarily associated with the actin-resembling protein MreB and is thought to function similarly to the FtsZ protein, which forms Z-rings during cell division, by directing the synthesis of peptidoglycan (Egan *et al.*, 2017; Sperber and Herman, 2017). A study by Sharpe *et al.* (1998) found that growth rate in *Bacillus subtilis* influenced cell length but not width as in *E. coli*, while Pierucci (1978) found that envelope synthesis during *E. coli* cell division remains constant, irrespective of growth rate. On the other hand, Sperber and Herman (2017) suggest that key nutrient and C concentrations rather than growth rate determine cell size in bacteria. In the current study, it would appear that changes in cell size during proliferation are linked to nutrient concentration and thus likely growth rate. However, due to the presence of P3HB at differing levels, OD_{600} could not be reliably used to calculate specific growth rates.

Figure 3.9 displays fluorescent microscope images of *C. necator* cells at 6 hours, demonstrating a lack of cell aggregation in 0.2% (w/v) ME cultures (Figure 3.9 (a)), in comparison to 0.4%, 0.6% and 0.8% ME containing cultures (Figure 3.9 (b-d)). As discussed in section 3.1, bacterial aggregates can form due to multiple reasons, including changes in cell density and extra-cellular matrix ultrastructure. It is possible that the lower cell density of 0.2% (w/v) ME cultures causes the Phc cell density sensing system not to be sufficiently stimulated via quorum sensing to activate the signal transduction pathway responsible for cell aggregation (Garg *et al.*, 2000). However, other factors such as key nutrient and carbon concentration, cell size and changes in extra-cellular matrix ultrastructure should not be ruled out without sufficient evidence.

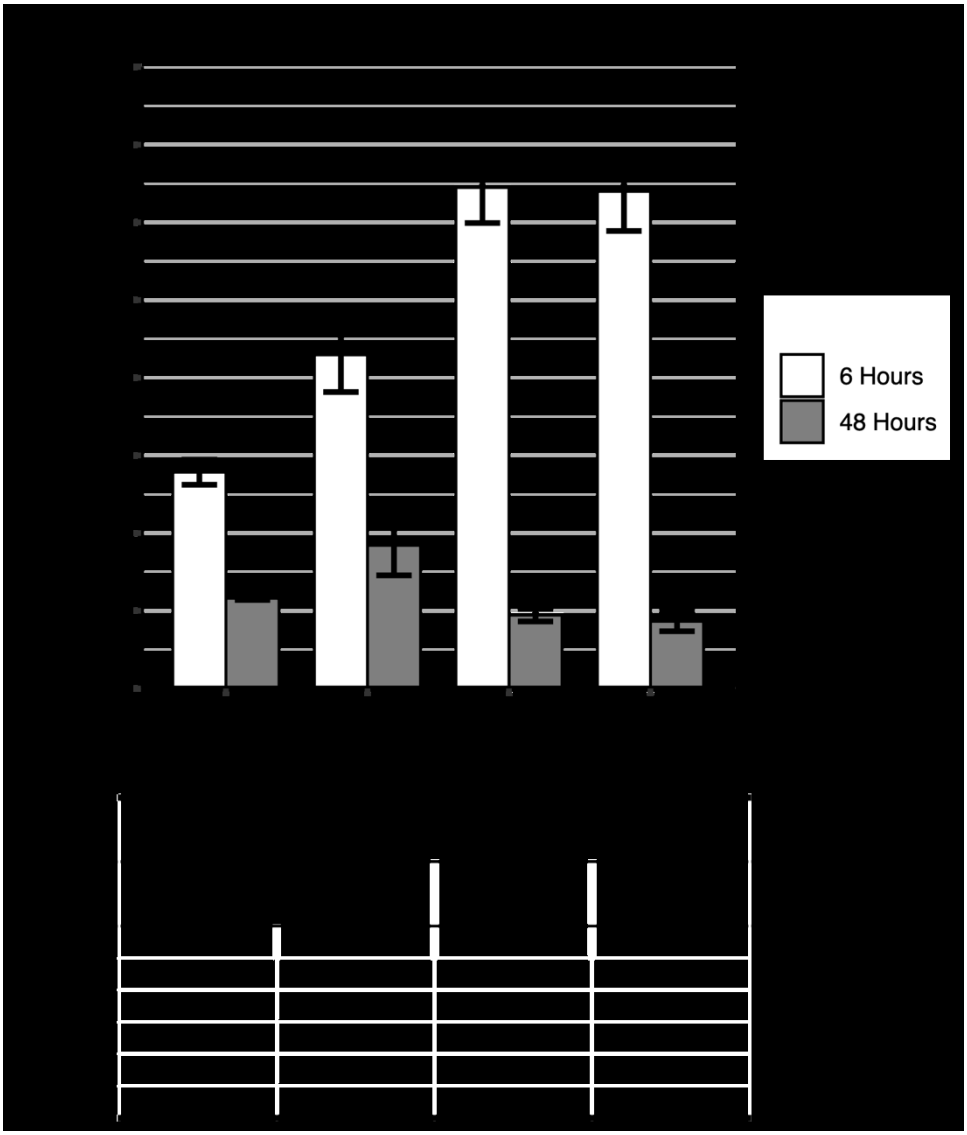


Figure 3.8 - Comparison of mean FSC (cell size) of *C. necator* cultures grown in 0.2%, 0.4%, 0.6% and 0.8% (w/v) ME at 6 and 48-hour time points. Plot (a) compares FSC at 6 and 48 hours and includes annotations representing statistical significance determined by paired t-tests. Table (b) contains statistical comparisons between each ME condition at each time point determined by non-paired t-tests. NS = non-significant ($p \geq 0.05$), * = $p < 0.05$, ** = $p \leq 0.01$. Error bars represent SD. n = 3 biological replicates. The full data can be found in Figure 8.2 (c), Appendix 8.2.

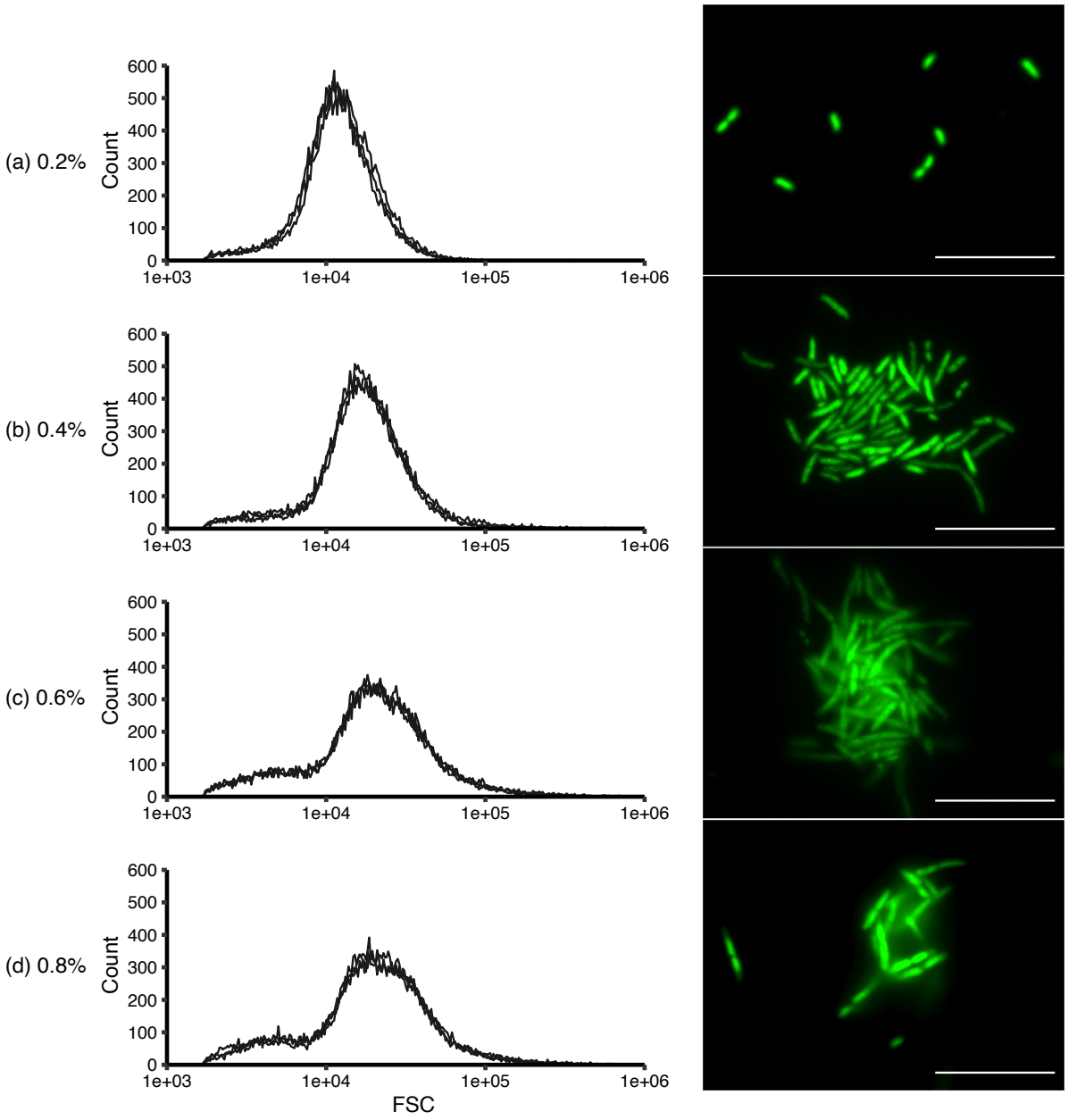


Figure 3.9 - Fluorescent microscope images showing variable *C. necator* aggregation after 6 hours of growth in 0.2%, 0.4%, 0.6% and 0.8% (w/v) ME accompanied by corresponding FSC histograms. Cells were stained with 1.33 mM SYTO9. Scale bars represent 10 µm. n=3 biological replicates for histograms.

3.2.4 Discussion

Experiments evaluating the growth of *C. necator* in 0.2%, 0.4%, 0.6% and 0.8% (w/v) ME found that at 6 and 48 hours a positive relationship exists between ME concentration and OD_{600}. This indicates that media conditions were growth-promoting, and C compounds were metabolised by the Entner-Doudoroff pathway and citric acid cycle rather than entering the P3HB biosynthetic pathway (Ienczak *et al.*, 2011). There is evidence that P3HB is produced during exponential growth at around 6 hours, a feature also reported by Dey and Rangarajan (2017) and Nygaard *et al*. (2019). The production of P3HB during exponential growth-promoting conditions is a desirable characteristic of PHA-producing bacteria and has been achieved by genetic modification in *Azotobacter vinelandii* (Page and Knosp, 1989; Segura et al., 2003; Segura and Espín, 2004). Overall P3HB per cell did not show significant signs of increasing between 6 and 48 hours. Thus, ME media likely requires the supplementation of a C source for *C. necator* to accumulate more P3HB as increasing the C to key nutrient ratio has been demonstrated to increase PHA production (Passanha *et al.*, 2014). Cell size was greater at 6 hours, a trait attributed to either cell aggregation or cell elongation during division which has been linked to bacterial growth rate (Sharpe *et al*. 1998) or possibly key nutrient or C concentration (Sperber and Herman, 2017).

3.3 Growing *C. necator* in ME supplemented with fructose

In the previous section 3.2, *C. necator* cultures of varying ME concentrations were tested to evaluate *C. necator* growth and P3HB accumulation without the addition of a C source. The dilution of 0.8% (w/v) ME to 0.6%, 0.4% and 0.2% resulted in a linear trend between OD_{600} and ME concentration. Additionally, while there was no significant difference in culture P3HB at 4 hours, by 48 hours 0.2% (w/v) cultures had produced significantly more P3HB than 0.6% and 0.8%, and 0.6% produced significantly more P3HB than 0.8%. Following on from the experimental work in section 3.2, section 3.3 analyses the effect of 0.5% (w/v) fructose addition to the same ME concentrations. Fructose is preferred to glucose in the wild-type *C. necator* H16 strain for heterotrophic growth exclusively via the Entner-Doudoroff pathway (Fleige *et al.*, 2011), and research has found that fructose-supplemented cultures can reach a P3HB content of around 80% DCW when fructose is used as a sole carbon source (Budde *et al.*, 2011).

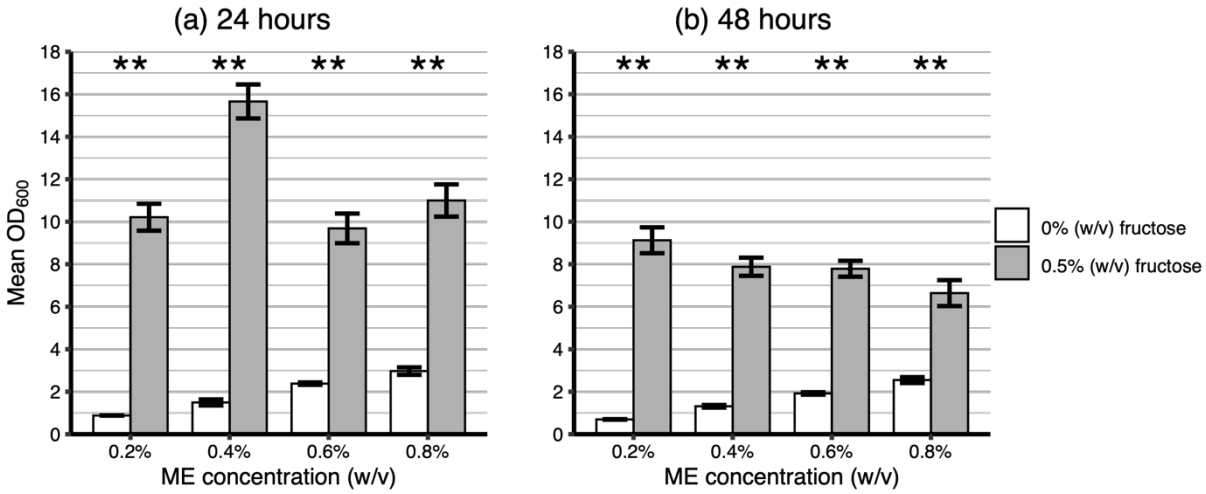
3.3.1 Fructose supplementation significantly increases OD_{600} by a factor of 5 to 15

Figure 3.10 contains a summary of OD_{600} data comparing the growth of *C. necator* in 0.2%, 0.4%, 0.6% and 0.8% (w/v) ME with and without 0.5% (w/v) fructose. The full data can be found in Figure 8.3, Appendix 8.3.

The mean OD_{600} data displayed in Figure 3.10 (a) and (b) is annotated with the statistical significance of comparisons between cultures with and without 0.5% (w/v) fructose. Analysis at both 24 and 48 hours found that for all ME concentrations tested the addition of 0.5% (w/v) fructose to the media significantly increased OD_{600}. A high degree of error prevented this trend from continuing at 48 hours, the source of which was the varying presence of a high P3HB *C. necator* population ($P3HB^{++}$) that will be discussed in the next section. Statistical analysis comparing individual media conditions at each time point (Figure 3.10 (c)) demonstrated that at 24 hours, cultures containing 0.4% (w/v) ME and 0.5% (w/v) fructose were more optically dense than all other fructose-supplemented media conditions. At 48 hours though, cultures containing fructose and 0.2% and (w/v) ME had significantly greater OD_{600} than the other conditions tested. Statistical analysis over time (Figure 3.10 (d)) showed that between 24 and 48 hours all fructose-supplemented cultures decreased in OD_{600} except for 0.2% (w/v) ME samples which did not significantly change between 24 and 48 hours.

A significant increase in OD_{600} is indicative of fructose being converted to pyruvate by the Entner-Doudoroff which is then fed into the citric acid cycle (Ienczak *et al.*, 2011). Without fructose addition,

it's likely the nutrients contained in ME media are not fully utilised as the amount of fructose appears to represent a limiting factor. This may explain why the linear correlation between ME concentration and OD_{600} disappears once fructose is added.



(c)

Non-paired t-test comparing mean OD_{600} at 24 and 48 hours for fructose supplemented samples only.			
ME concentration (w/v) comparison		24 hours	48 hours
0.2%	0.4%	***	*
0.2%	0.6%	NS	*
0.2%	0.8%	NS	**
0.4%	0.6%	***	NS
0.4%	0.8%	**	*
0.6%	0.8%	NS	NS

(d)

Paired t-test comparing OD_{600} between 24 and 48 hours for fructose supplemented samples only.	
ME concentration (w/v)	Significance
0.2%	NS
0.4%	**
0.6%	**
0.8%	*

Figure 3.10 - Graphs and statistical analysis comparing the OD_{600} of *C. necator* cultures grown in 0.2%, 0.4%, 0.6% and 0.8% (w/v) ME with and without 0.5% (w/v) fructose. Statistical analysis was performed using unpaired t-tests to evaluate the same ME concentration with and without fructose supplementation at 24 hours (annotations in plot (a)) and 48 hours (annotations in plot (b)), and also to compare each fructose-supplemented condition at each time point (c). Additional statistical analysis was performed using paired t-tests in order to compare the same condition at different time points (d). NS = non-significant ($p \geq 0.05$), * = $p < 0.05$, ** = $p \leq 0.01$, *** = $p \leq 0.001$. Error bars represent SD. n = 3 biological replicates. The full data can be found in Figure 8.3, Appendix 8.3.

3.3.2 Supplementing with 0.5% (w/v) fructose increases P3HB production most for 0.2% (w/v) ME cultures

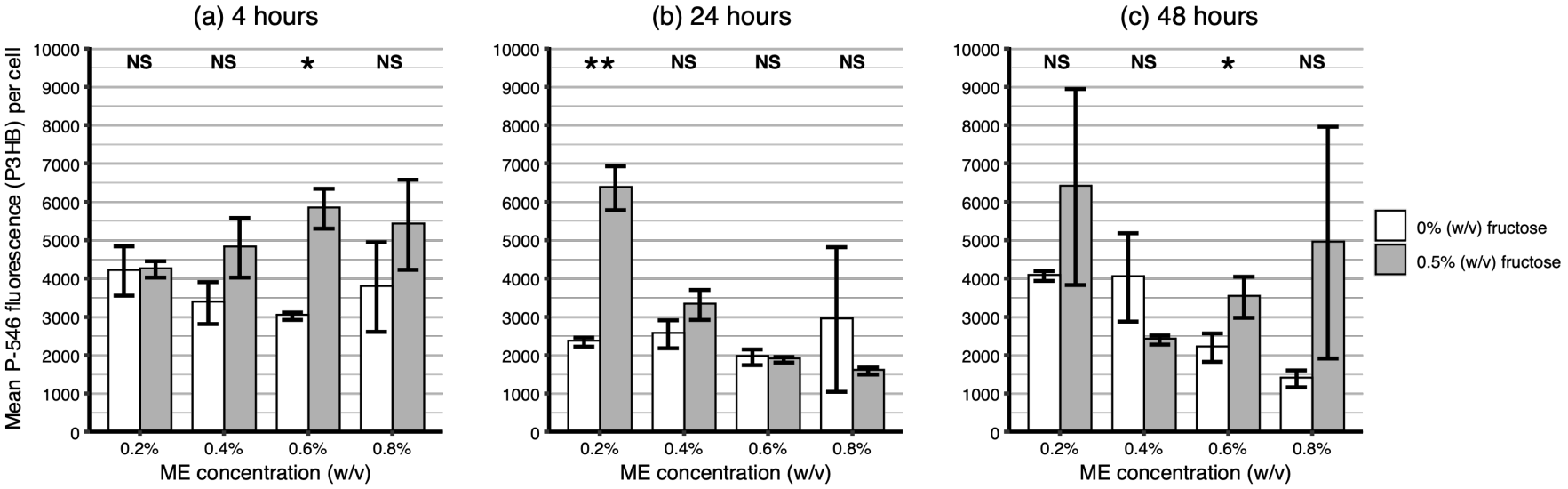
Figure 3.11 provides a summary of intracellular P3HB per cell for *C. necator* cultures grown in 0.2%, 0.4%, 0.6% and 0.8% (w/v) ME with and without 0.5% (w/v) fructose supplementation. The full data can be found in Figure 8.4 (a), Appendix 8.3.

Statistical comparisons analysing *C. necator* P3HB production in ME media with and without fructose supplementation at 4 (Figure 3.11 (a)), 24 (Figure 3.11 (b)) and 48 hours (Figure 3.11 (c)) revealed that generally the was no significant difference in P3HB per cell when fructose was added ME. Although, media containing 0.6% (w/v) ME at 4 hours, 0.2% (w/v) ME at 24 hours and 0.6% (w/v) ME at 48 hours all produced significantly more P3HB when fructose was included in starting media. Statistically comparing each fructose-supplemented condition at each time point (Figure 3.11(d)) showed that most notably, at 24 hours there was a significant difference between all fructose-supplemented conditions, with P-546 fluorescence increasing with decreasing ME concentration. Cultures containing 0.2% (w/v) ME supplemented and 0.5% (w/v) fructose produced *C. necator* cells with considerably more P3HB than other fructose-containing cultures. Statistical comparisons over time for fructose supplemented cultures (Figure 3.11(e)) found that between 4 and 24 hours only cultures containing 0.2% (w/v) ME supplemented with 0.5% (w/v) fructose significantly increased in P3HB. Between 24 and 48 hours, in contrast, there was no significant change in intracellular P3HB for all conditions except for fructose-supplemented 0.6% (w/v) ME which significantly increased.

Aramvash *et al*. (2015) observed a linear increase in P3HB as fructose concentration increased for *C. necator* cells grown in basal mineral salt medium. The data presented in the current section shows that at 24 hours (Figure 3.11 (b)), decreasing ME concentration, while fructose remains at a concentration of 0.5% (w/v), increases the average P3HB per cell. Both the observations presented in the current study and Aramvash *et al*. (2015) suggest that increasing the fructose to key nutrient ratio increases intracellular P3HB production. However, plotting FSC against P-546 fluorescence for the 24-hour time point (Figure 3.12) found there to be a strong linear correlation between cell size and intracellular P3HB. In literature, no direct link between intracellular P3HB levels and cell size has been established (Mravec *et al.*, 2016), instead, it is thought that any link that develops is due to P3HB biosynthesis and biofilm production being instigated by similar stress. Fluorescent microscopy (Figure 3.13) demonstrated that cells grown in fructose-supplemented 0.2% (w/v) ME (Figure 3.13 (a)) formed longer chains than the other higher conditions containing more concentrated ME. The chains observed appeared to be C. necator in the process of division with the dark unstained regions being Z-rings, a key division site at

which cell septation occurs (Du and Lutkenhaus, 2019). The evidence suggests that the increase in P3HB production observed in Figure 3.11 for fructose-supplemented 0.2% (w/v) ME resulted from the combined P3HB of cell chains rather than a decreased ME to fructose ratio. The findings presented in this section do not align with the results of Aramvash *et al*. (2015), instead suggesting that the media conditions tested do not provide *C. necator* with conditions suitable for P3HB production. Additionally, decreasing the ME to fructose ratio does not increase P3HB production in contrast to the findings of Passanha *et al*. (2014). It is possible that reducing the ME concentration to 0.2% (w/v) provides *C. necator* still with too much ME, and a surplus remains once fructose and other carbohydrates in the media are exhausted.

Fluorescent microscope images for each condition, presented in Figure 3.13, do not show evidence of intracellular P3HB granules. This does not mean that P3HB granules were not present as small inclusions beyond the resolution of the imaging but does rule out the presence of multiple granules that make up the majority of the volume of a cell such as that reported previously in literature (Hermawan and Jendrossek, 2007; Beeby *et al.*, 2011; Kawashima *et al.*, 2015).



(d)

Non-paired t-test comparing P-546 fluorescence (P3HB) per cell at 4, 24 and 48 hours for fructose supplemented samples only.				
ME concentration (w/v) comparison		4 hours	24 hours	48 hours
0.2%	0.4%	NS	**	NS
0.2%	0.6%	*	**	NS
0.2%	0.8%	NS	**	NS
0.4%	0.6%	NS	*	NS
0.4%	0.8%	NS	*	NS
0.6%	0.8%	NS	*	NS

(e)

Paired t-test comparing P-546 fluorescence (P3HB) per cell at 24 and 48 hours for fructose supplemented samples only.		
ME concentration (w/v)	4-24 hours	24-48 hours
0.2%	**	NS
0.4%	NS	NS
0.6%	**	*
0.8%	*	NS

Figure 3.11- Graphs and statistical analysis comparing the P-546 fluorescence (P3HB) per cell of *C. necator* cultures grown in 0.2%, 0.4%, 0.6% and 0.8% (w/v) ME and with and without 0.5% (w/v) fructose. Statistical analysis was performed using unpaired t-tests to evaluate the same ME concentration with and without fructose supplementation at 4, 24 and 48 hours (annotations in plots (a), (b) and (c) respectively) and also to compare each fructose-supplemented condition (d). Additional statistical analysis was performed using a paired t-test in order to compare the same fructose-supplemented condition at different time points (e). NS = non-significant ($p \geq 0.05$), * = $p < 0.05$, ** = $p \leq 0.01$, *** = $p \leq 0.001$. Error bars represent SD. n = 3 biological replicates. The full data can be found in Figure 8.4 (a) Appendix 8.3.

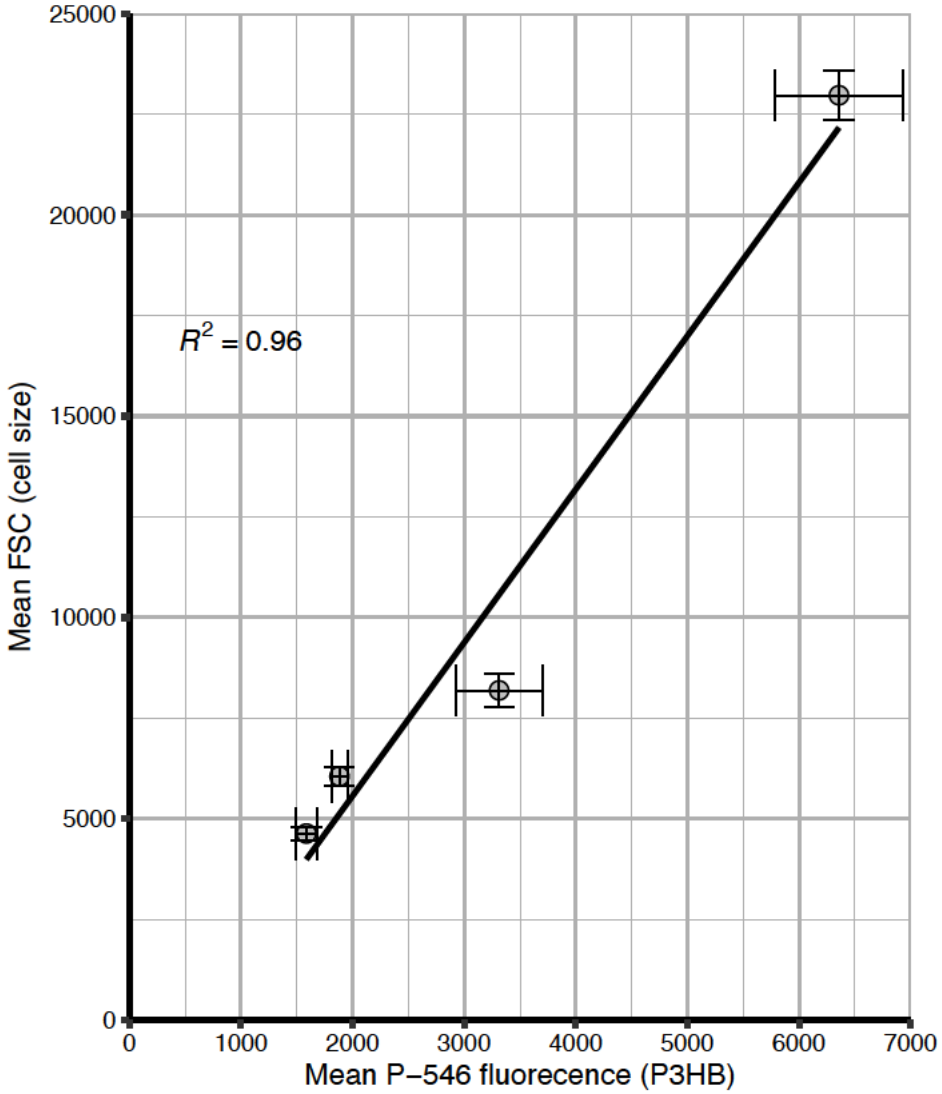


Figure 3.12 – Graph displaying the mean FSC and mean P-546 fluorescence (P3HB) at 24 hours for C. necator cultures containing 0.2%, 0.4%, 0.6% and 0.8% (w/v) ME and supplemented with 0.5% fructose. R^2 represents the coefficient of determination. Error bars represent SD. n = 3 biological replicates. The full data for mean P-546 fluorescence can be found in Figure 8.4 (a), Appendix 8.3. The full mean FSC data can be found in Figure 8.5 (a), Appendix 8.3.

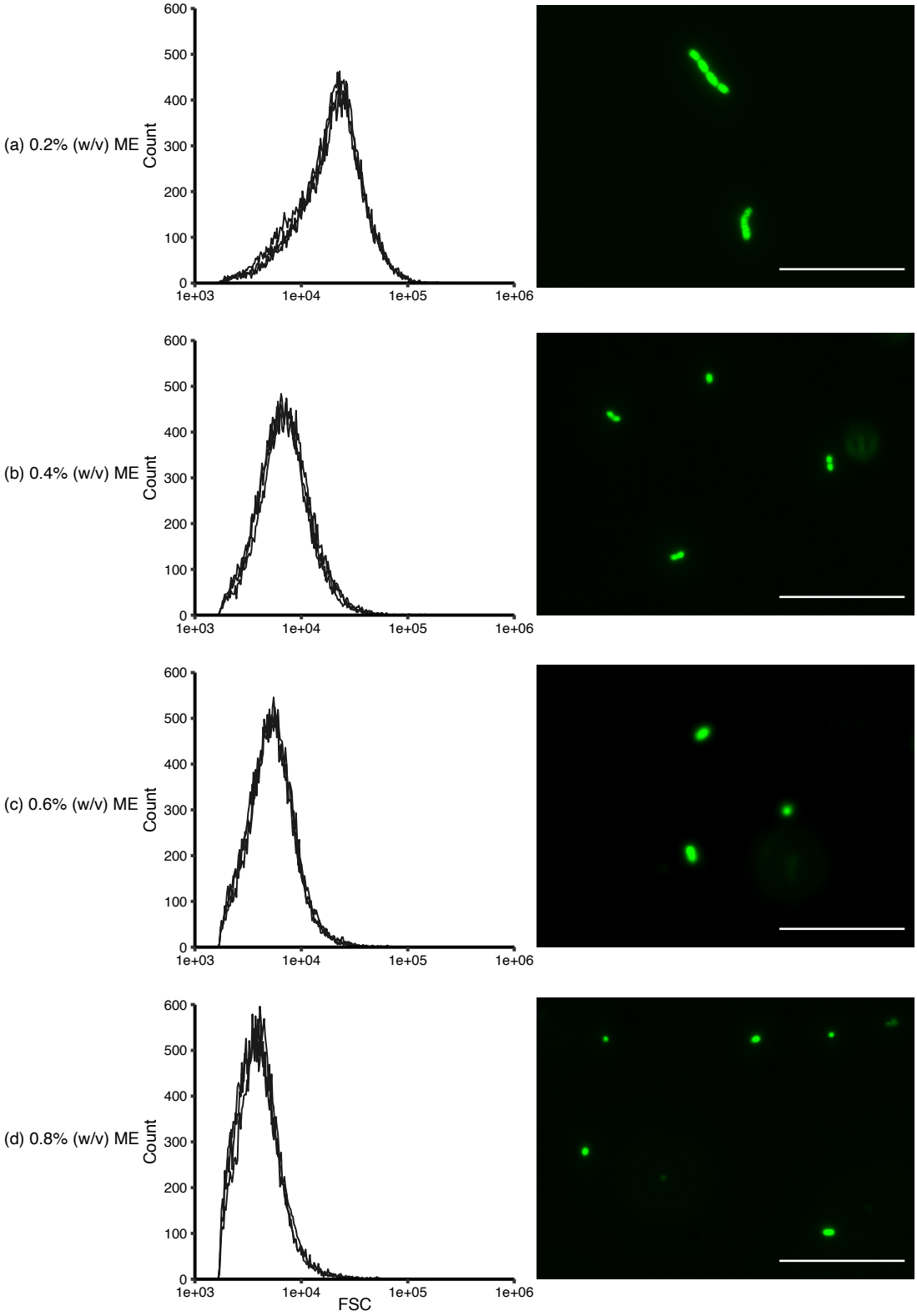


Figure 3.13 – Fluorescent microscope images and corresponding FSC histograms showing *C. necator* cells after 24 hours of growth in 0.2%, 0.4%, 0.6% and 0.8% (w/v) ME and supplemented with 0.5% fructose. Cells in microscope images were stained with 1.33 mM SYTO9. Scale bars represent 10 µm. n=3 biological replicates for FSC histograms.

3.3.3 Cultures of *C. necator* contain a P3HB^{++} super-producing population

In *C. necator* cultures supplemented with 0.5% (w/v) fructose, flow cytometry experiments revealed the presence of a high P3HB-producing *C. necator* population when plotting FSC against P-546 fluorescence (Figure 3.14). This population was termed P3HB^{++}, and the remaining data points P3HB^{+}. Comparisons between the proportion of P3HB^{++} cells produced in ME media with and without 0.5% (w/v) fructose at 4, 24 and 48 hours are displayed in Figure 3.15 and the full data can be found in Figure 8.4 (b), Appendix 8.3.

At the 4-hour time point (Figure 3.15 (a)), for cultures not supplemented with fructose, the mean percentage of P3HB^{++} cells did not exceed 0.035% and at 24 and 48 hours did not exceed 0.1% of the total population. Despite there being such a low proportion of P3HB^{++} cells in non-fructose supplemented cultures, at 4 hours due to a high level of variation between the amount of P3HB^{++} cells only 0.2% (w/v) ME cultures contained significantly more P3HB^{++} cells. In contrast, at 24 (Figure 3.15 (b)) and 48 hour time points (Figure 3.15 (c)), all cultures contained significantly more P3HB^{++} cells when fructose was added to the starting media, except for 0.4% (w/v) ME cultures at 48 hours.

Statistical comparisons between fructose-supplemented conditions at each time point ((Figure 3.15 (d)) showed that at 4 hours and 48 hours, there was no significant difference between any of the conditions tested, partially due to a high-level variability between replicates. At 24 hours, the was no significant difference between cultures containing 0.2% and 0.4% (w/v) ME and also 0.6% (w/v) and 0.8% (w/v) but all other condition combinations were found to be significantly different.

Comparing changes in the mean percentage of P3HB^{++} cells between time points (Figure 3.16 (e)) (the full data can be found in Figure 8.4 (c), Appendix 8.3) found that between 4 and 24 hours, only fructose-supplemented samples containing 0.2% (w/v) ME significantly increased. Between 24 and 48 hours on the other hand, there was no significant change, except for samples except for cultures containing 0.6% (w/v) ME supplemented with 0.5% (w/v) fructose which significantly increased.

Further analysis of the mean P-546 fluorescence per cell of the P3HB^{+} and P3HB^{++} populations is summarised in Figure 3.16. The full data is displayed in Figure 8.4 (c), Appendix 8.3. At 4 (Figure 3.16 (a)), 24 (Figure 3.16 (b)) and 48 hour (Figure 3.16 (c)) timepoints, non-paired t-tests determined the P3HB^{++} population to contain significantly more P3HB than cells in the P3HB^{+} population. Comparisons between conditions (Figure 3.16 (d)) revealed there was generally little difference between cultures except for the P3HB^{+} population at 4 hours, at which point intracellular P3HB decreased with increasing ME concentration. Analysis over time (Figure 3.16 (e)) revealed that only the P3HB^{++} population significantly increased intracellular P3HB between time points.

The formation of a P3HB^{++} *C. necator* population appears to be an example of phenotypic heterogeneity, which in bacterial populations can result from either genetic (Arber, 2000) or non-genetic (van Boxtel *et al*., 2017) factors. Stochastic events are known to influence the response of bacteria to changes in nutrient concentrations, for example, Choi *et al*. (2008) found that *E. coli* cells either had low or high lactose metabolising phenotypes arising from common partial dissosociation or vary rare complete dissociation of the lactose repressor protein from DNA. As a result, in the case of the *E. coli lac* operon, the stochastic nature of repressor DNA binding means positive feedback regulation does not ensure multistability (Ozbudak *et al*., 2004). In fact, gene expression as a whole is a stochastic process, not only because gene expression is influenced by random protein associations and dissassociations, but also because transcription is a rare process and proteins are typically at low concentrations in a bacterial cell (Paulsson, 2005). Additionally, the level of transcription for a particular gene can vary due to regulatory interactions with gene networks. This is known as the gene regulation function, a factor which fluctuates over time, meaning there are times when a bacterium will be more prepared to undergo phenotypic adaptation due to having a higher gene regulation function and thus more transcription factors (Hillenbrand *et al.*, 2016).

A similar scenario has been observed in *C. necator* cultures by Franz *et al.*, (2011) who observed a small population of glucose-utilising colonies, and by picking colonies and growing in glucose-rich agar repeatedly was able to evolve a glucose-utilising stain. Similarly, González-Villanueva *et al*. (2019) grew *C. necator* colonies repeatedly in multi-well plates in order to direct the evolution of a variant capable of rapid glycerol utilisation. In both cases, variants were subjected to several rounds of successful directed evolution raising the prospect that the high P3HB-producing population in the current study could be used to enhance P3HB production without the need for application-limiting genetic modification.

Bacterial phenotypic heterogeneity can be viewed as a bet-hedging strategy in an attempt to survive and reproduce in diverse environmental conditions (de Jong *et al.*, 2011). This is observed in *E. coli* cells, which when transitioning from glucose depletion to gluconeogenic growth, the vast majority of cells (>99%) enter a dormant persistor state while the remaining cells proliferate (Kotte *et al.*, 2014). Solopova *et al*. (2014) also found that proliferating and persister populations form similarly in cultures of *Lactococcus lactis*. Once *L. lactis* has used up glucose in the media there is a reduction in growth rate known as a diauxic lag phase after which *L. lactis* utilises cellobiose as a C source. However, only the population that proliferated first using glucose continues to grow using cellobiose, while the persister population remains in a dormant state. Persistor cells are dormant phenotypic variants that are stress resistant and cause particular problems when produced by bacterial species such as

Pseudomonas aeruginosa in cystic fibrosis patients due to high tolerance to antibiotics (Lewis, 2010). Formed predominantly during nutrient-rich phases of exponential growth (Norman *et al.*, 2015), persistor cell production is reduced 1000-fold when respiration is inhibited (Orman and Brynildsen, 2015). The persistor cell state however is temporary, and when re-grown cells lose their antibiotic resistance (Balaban *et al.*, 2004). Stochastic phenotype changes can also occur due to the random distribution of RNAs and proteins within a bacterium, which lacks a sophisticated mechanism, like that of genomic DNA, to equally partition into daughter cells (Toro and Shapiro, 2010; Huh and Paulsson, 2011).

Genetic factors on the other hand typically result in more permanent changes, especially when DNA sequence changes occur in genomic DNA. Single nucleotide polymorphisms, in which one base pair in a DNA sequence is altered, can result in genetic variation. Such changes can either be classed as synonymous mutations in which the codon still codes for the same amino acid or non-synonymous in which a different amino acid is coded for which can cause an alteration in protein function (Bryant *et al.*, 2012). Single nucleotide insertions or deletions cause frameshifts which change all downstream codons including stop codons. While insertions or deletions are more likely to result in truncated proteins, they can still be a source of genetic variation. The rate of single nucleotide polymorphisms is in part governed by DNA repair mechanisms which exist principally due to the inherent instability of nucleotides and aim to provide a degree of genetic stability (Arber, 2000). Another source of genetic variation results from the changing of gene position and genome frequency by the action of transposons, also known as jumping genes (Ladd and Bordoni, 2021). Transposons are known to be responsible for a large proportion of mutations which increase genetic diversity (Kawakami *et al.*, 2017). Bacteria are known to horizontally transfer plasmid DNA between individual cells as a mechanism to provide bacterial populations with advantageous genes such as antibiotic resistance (Virolle *et al.*, 2020). While plasmid DNA can be lost as conditions change, some plasmids contain plasmid addiction elements which use toxin anti-toxin systems to ensure the post-segregational death of cells that have not received the plasmid (Tsang, 2017). Restiction-modification systems, on the other hand, act as a kind of primitive immune system by cutting up foreign DNA, thus reducing the uptake of DNA but at the same time digesting the DNA into smaller fragments making it more recombinogenic (Arber, 2000). In the current study, it is difficult without further investigation to state the exact reason that causes the $P3HB^{++}$ population. However, given that intracellular P3HB confers stress resistance (Wang *et al.*, 2009; Obruca *et al.*, 2016), persistor cell populations generally make up a small proportion of the cell population, $P3HB^{++}$ cells form mostly during growth-promoting nutrient-rich conditions and are smaller

than proliferating cells, it is plausible that the P3HB^{++} phenotype is a *C. necator* persister state aimed at increasing survival during harsh conditions.

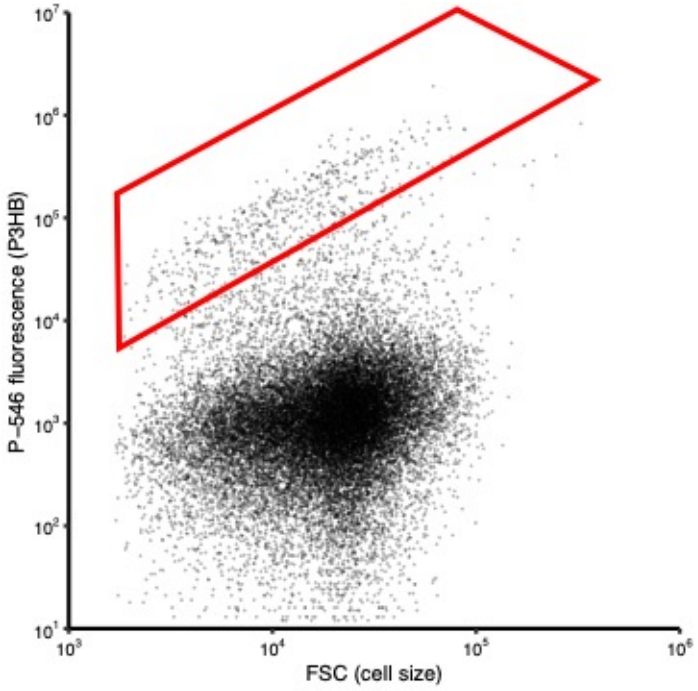
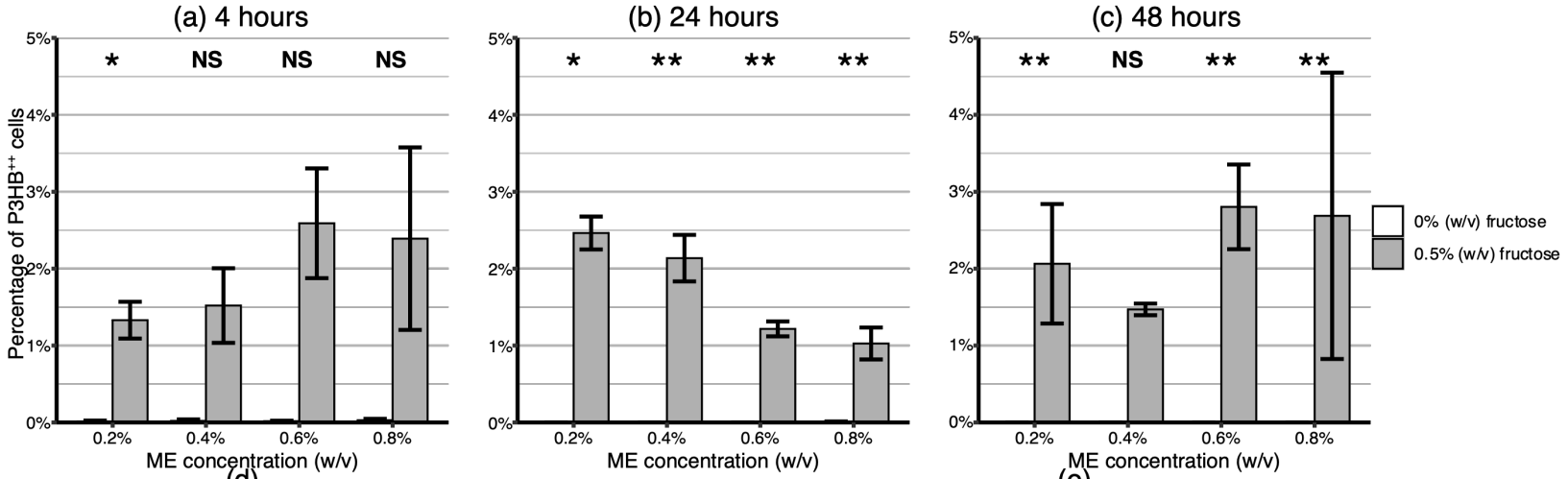


Figure 3.14 - Flow cytometry gating strategy used to monitor the P3HB^{++} population. This example plot represents the first replicate of the 0.2% (w/v) ME supplemented with 0.5% (w/v) fructose condition summarised in Figure 3.11 (b).



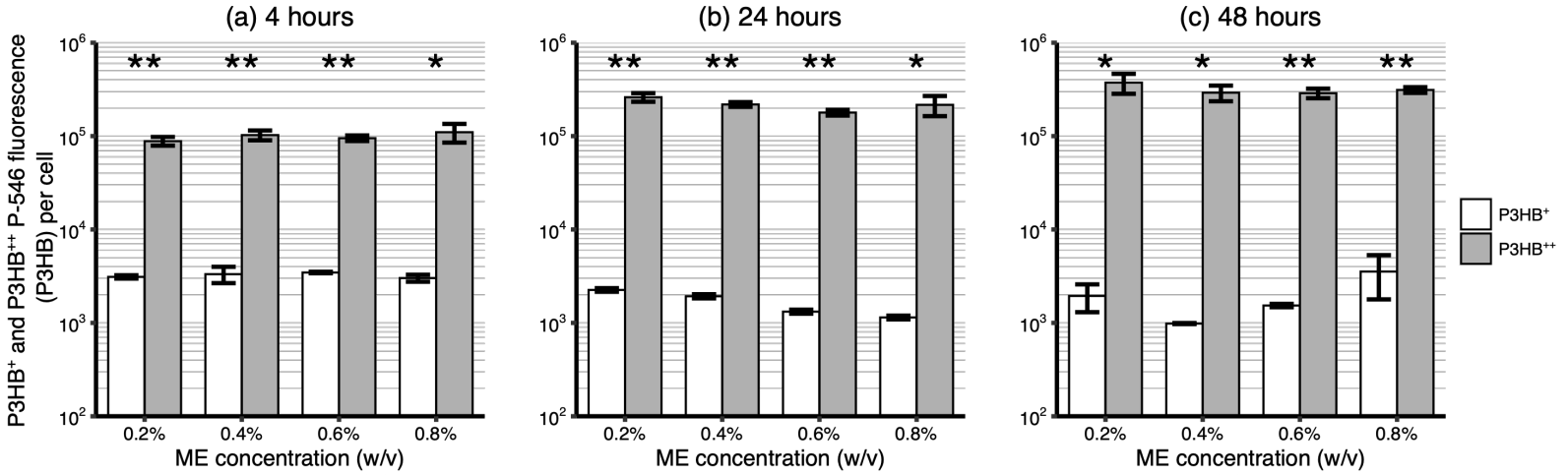
(d)

Non-paired t-test comparing the percentage of P3HB++ cells at 4, 24 and 48 hours for fructose supplemented samples only.				
ME concentration (w/v) comparison		4 hours	24 hours	48 hours
0.2%	0.4%	NS	NS	NS
0.2%	0.6%	NS	**	NS
0.2%	0.8%	NS	**	NS
0.4%	0.6%	NS	*	NS
0.4%	0.8%	NS	**	NS
0.6%	0.8%	NS	NS	NS

(e)

Non-paired t-test comparing the percentage of P3HB++ cells between 4 and 24 hours, and 24 and 48 hours for fructose supplemented samples only.		
ME concentration (w/v)	4-24 hours	24-48 hours
0.2%	*	NS
0.4%	NS	NS
0.6%	NS	*
0.8%	NS	NS

Figure 3.15 - Graphs and statistical analysis comparing the proportion of P3HB++ cells of *C. necator* cells cultured in 0.2%, 0.4%, 0.6% and 0.8% (w/v) ME and supplemented with 0.5% (w/v) fructose with comparison to cultures without fructose supplementation. Statistical analysis was performed using unpaired t-tests. In plots (a), (b) and (c), annotations show the statistical comparisons between samples with and without 0.5% (w/v) fructose addition. Table (d) contains statistical comparisons of each fructose-supplemented condition. Table (e) statistically compares samples at different time points for fructose-supplemented samples only. NS = non-significant ($p \geq 0.05$), * = $p < 0.05$, ** = $p \leq 0.01$. Error bars represent SD. n = 3 biological replicates. the full data can be found in Figure 8.4 (c), Appendix 8.3



(d)

Non-paired t-test comparing P-546 fluorescence (P3HB) per cell at 4, 24 and 48 hours for fructose supplemented samples only							
		P3HB+			P3HB++		
ME concentration (w/v) comparison		4 hours	24 hours	48 hours	4 hours	24 hours	48 hours
0.2%	0.4%	NS	*	NS	NS	NS	NS
0.2%	0.6%	*	***	NS	NS	*	NS
0.2%	0.8%	NS	***	NS	NS	NS	NS
0.4%	0.6%	NS	**	**	NS	*	NS
0.4%	0.8%	NS	**	NS	NS	NS	NS
0.6%	0.8%	NS	*	NS	NS	NS	NS

(e)

Paired t-test comparing P-546 fluorescence (P3HB) per cell at 24 and 48 hours for fructose supplemented samples only				
ME concentration (w/v)	P3HB+		P3HB++	
	4-24 hours	24-48 hours	4-24 hours	24-48 hours
0.2%	**	NS	**	NS
0.4%	NS	**	*	NS
0.6%	***	NS	*	*
0.8%	**	NS	NS	NS

Figure 3.16 - Graphs and statistical analysis comparing the mean P-546 fluorescence (P3HB) of the P3HB^{+} and P3HB^{++} populations for *C. necator* cells cultured in 0.2%, 0.4%, 0.6% and 0.8% (w/v) ME and supplemented with 0.5% fructose. Statistical analysis was performed using unpaired t-tests to evaluate the same ME concentration with and without fructose supplementation (annotations in plots (a), (b) and (c)) and also to compare each fructose-supplemented condition (d). Additional statistical analysis was performed using a paired t-test in order to compare the same condition at different time points (e). NS = non-significant ($p \geq 0.05$), * = $p < 0.05$, ** = $p \leq 0.01$, *** = $p \leq 0.001$. Error bars represent SD. n = 3 biological replicates. The full data is displayed in Figure 8.4 (c), Appendix 8.3.

3.3.4 Increasing the fructose to ME ratio leads to sustained larger cells

Figure 3.17 contains a summary of cell size for *C. necator* cultures grown in 0.2%, 0.4%, 0.6% and 0.8% (w/v) ME with and without 0.5% (w/v) fructose. The full data can be found in Figure 8.5 (a), Appendix 8.3.

Statistical tests comparing cultures with and without the addition of 0.5% (w/v) fructose supplemented at 4 hours (Figure 3.17 (a)) determined that FSC was significantly greater in cultures to which 0.5% (w/v) fructose was added. At the 24-hour time point (Figure 3.17 (b)), this was only the case for 0.2%, 0.4% and 0.6% (w/v) ME samples. The 0.8% (w/v) ME analysis was affected by air bubbles in the flow cytometer, which resulted in a high degree of error in non-fructose-supplemented data. Notably, the addition of fructose to 0.2% (w/v) ME cultures resulted in a considerable increase in cell size, and also in comparison to that of the other fructose-supplemented conditions.

Comparisons between fructose-supplemented cultures (Figure 3.17 (d)) at 4 hours showed 0.2% (w/v) ME fructose-supplemented cultures produced significantly larger cells than 0.6% and 0.8% cultures but not 0.4%. At both 24 and 48 hours 0.2% (w/v) ME cultures supplemented with 0.5% (w/v) fructose contained considerably larger *C. necator* cells than higher ME concentrations.

Statistical comparisons between time points for fructose-supplemented cultures (Figure 3.17 (e)) showed that between 4 and 24, and 24 and 48 hours, mean FSC significantly decreased for all conditions at both sets of time points, except for 0.8% (w/v) ME samples which did not significantly change between 24 and 48 hours.

Cell size in *E. coli* has been reported to be primarily determined by nutrient concentration and growth rate (Hill *et al*. 2013) In fact, the findings of Hill *et al*. (2013) have linked the enzyme glucosyltransferase OpgH, which is involved in fructose metabolism in *C. necator*, to cell size by demonstrating that it antagonises FtsZ to prevent Z-ring formation. However, while this would suggest that cell division is inhibited to some degree while fructose is metabolised, it does not explain why in the current study cell chains were only observed in cultures containing 0.2% (w/v) ME supplemented with 0.5% (w/v) fructose. Cell chains are typically formed from an elongated cell which divides into multiple cells at the cell division site perpendicular to the long axis of the cell (Arrigucci and Pozzi, 2017). Cell chains similar to that observed in Figure 3.13 (a) are also a feature of gram-positive *Streptococcus* cultures and in which longer chain length has been associated with increased cell adhesion and aggregation, thus increasing the likelihood of biofilm formation (Murchison *et al.*, 1982). Bacteria are also known to form chains in order to facilitate the horizontal transfer of DNA, as intrachain conjugation is considerably more efficient than relying on random cell encounters (Babic *et al.*, 2011).

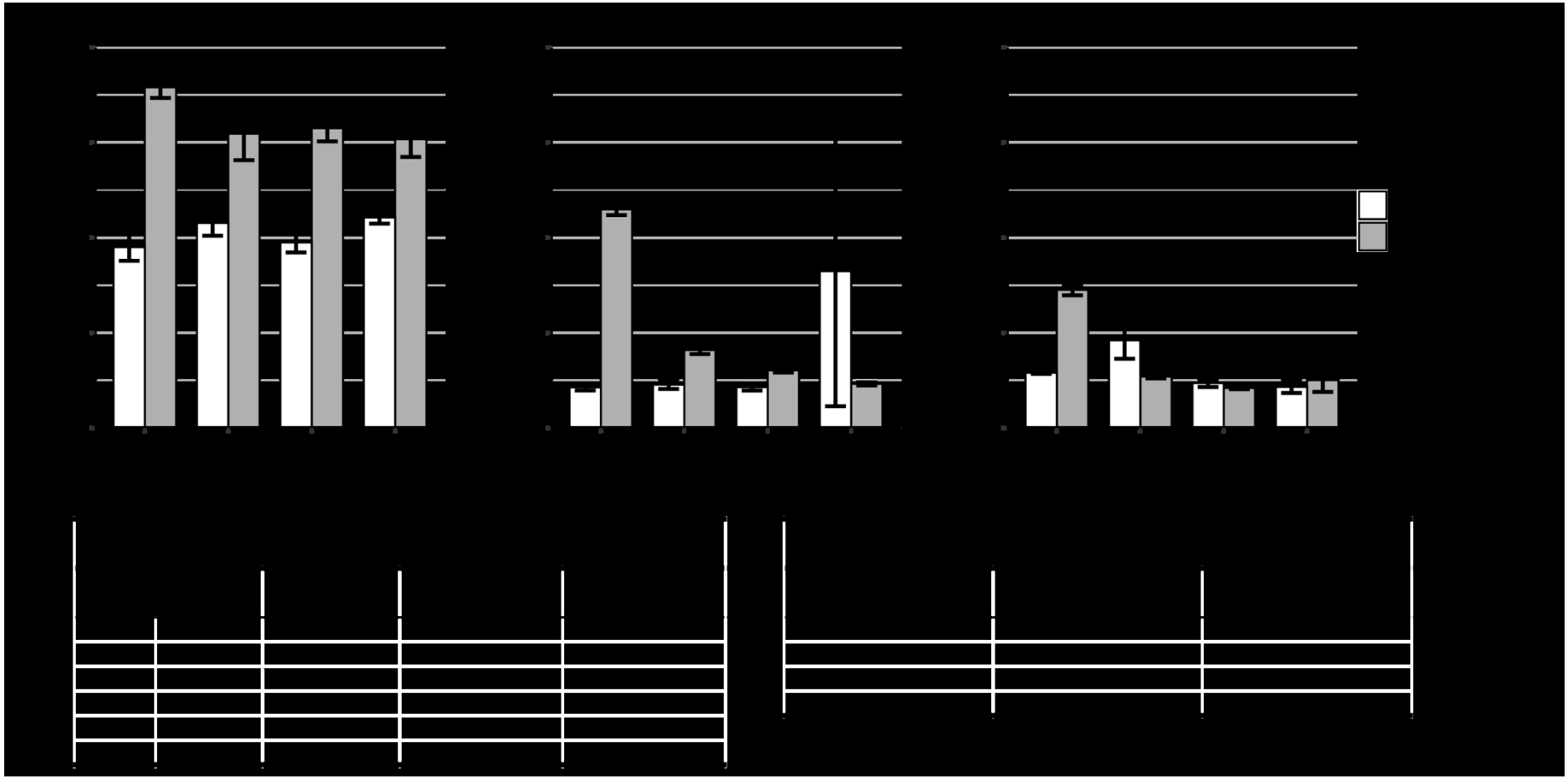


Figure 3.17 - Graphs and statistical analysis comparing the mean FSC (cell size) of *C. necator* cells cultured in 0.2%, 0.4%, 0.6% and 0.8% (w/v) ME and supplemented with 0.5% fructose with comparison to cultures without fructose supplementation. Statistical analysis was performed using unpaired t-tests to evaluate the same ME concentration with and without fructose supplementation (annotations in plots (a), (b) and (c)) and also to compare each fructose-supplemented condition (d). Additional statistical analysis was performed using a paired t-test in order to compare the same condition at different time points (e). NS = non-significant ($p \geq 0.05$), * = $p < 0.05$, ** = $p \leq 0.01$, *** = $p \leq 0.001$, **** = $p \leq 0.0001$, ***** = $p \leq 0.00001$. Error bars represent SD. n = 3 biological replicates. Large error bar in plot (b) for 0.8% (w/v) ME samples due to air in the flow cytometry system. The full data can be found in Figure 8.5 (a), Appendix 8.3.

3.3.5 Cells in the P3HB^{++} population are smaller than P3HB^{+} cells

A summary of mean P3HB^{+} and P3HB^{++} FSC for *C. necator* cultures grown in 0.2%, 0.4%, 0.6% and 0.8% (w/v) ME with and without the addition of 0.5% (w/v) fructose can be found in Figure 3.18. The full data collected can be found in Figure 8.5 (b), Appendix 8.3.

In Figure 3.18 (a), comparisons of mean cell size at 4 hours indicate cells in the P3HB^{+} population were significantly larger than cells in the P3HB^{++} population. However, by the 24-hour timepoint (Figure 3.18 (b)), only 0.2% (w/v) fructose-supplemented cultures produced P3HB^{+} cells that were significantly larger than P3HB^{++}. This was also true at 48 hours Figure 3.18 (c), but the difference in size between the P3HB^{+} and P3HB^{++} populations was much closer.

Non-paired t-tests comparing individual conditions at each time point Figure 3.18 (d), found that at 4 hours cultures containing 0.6% and 0.8% (w/v) ME produced significantly larger P3HB^{+} cells than 0.2% cultures. By 24 hours, mean cell size in the P3HB^{+} population significantly decreased with increasing ME concentration. This was also the case at 48 hours, except for when comparing 0.8% (w/v) ME cultures to that of 0.4% and 0.6%, between which there was no significant difference.

For the P3HB^{++} population, comparisons between conditions at 4 hours showed that cell size was largely non-significantly different, with only 0.4% (w/v) ME and 0.6% cultures significantly different. At 24 hours, 0.2% (w/v) ME cultures produced P3HB^{++} cells that were significantly larger than that found in other conditions tested, whereas there was no significant difference in P3HB^{++} cell size between 0.2%, 0.4% and 0.6% cultures. The same was also true at 48 hours, the only difference being the P3HB^{++} population 0.2% (w/v) ME cultures could not be statistically separated in terms of FSC from that of 0.4% cultures.

Paired t-tests comparing cultures between time points found that for all growth conditions tested, the P3HB^{+} population significantly decreased in mean cell size between 4 and 24 hours. Between 24 and 48 hours, the mean cell size of the P3HB^{+} population decreased again for all conditions tested except for cultures containing 0.2% (w/v) ME for which there was no significant change. The cell size of the P3HB^{++} population decreased in all conditions tested between 4 and 24 hours except for 0.2% (w/v) ME for which no significant change was recorded. In contrast, the P3HB^{++} population in all conditions tested did not significantly change in mean cell size between 24 and 48 hours.

Lower levels of cell expansion during cell division have been linked to a lower growth rate in bacteria (Sharpe *et al*. 1998). In *E. coli*, cell size during cell proliferation is linked to growth rate and nutrient concentration (Hill *et al*. (2013)). A smaller cell phenotype for *C. necator* P3HB^{++} cells at 4 hours is indicative of a lower growth rate in relation to P3HB^{+} cells. The data shown in Figure 3.18 (a) fits with the theory that persister cells remain in a small, dormant state, increasing in number relatively slowly while the other cells proliferate and are responsible for culture growth (Kotte *et al.*, 2014).

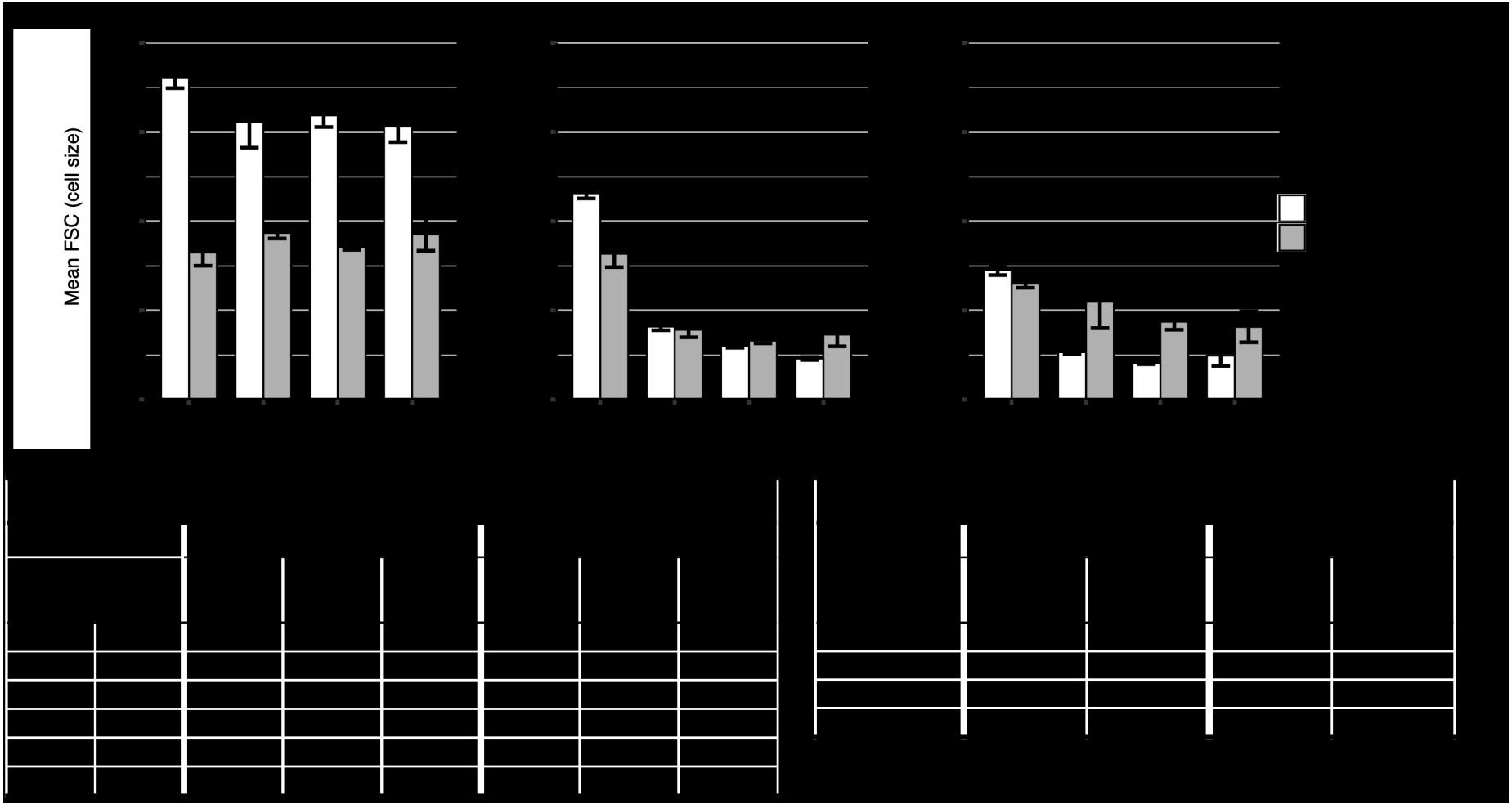


Figure 3.18 - Graphs and statistical analysis comparing the mean FSC (cell size) of the P3HB^{+} and P3HB^{++} populations for *C. necator* cells cultured in 0.2%, 0.4%, 0.6% and 0.8% (w/v) ME and supplemented with 0.5% (w/v) fructose. Statistical analysis was performed using unpaired t-tests to evaluate the same ME concentration with and without fructose supplementation (annotations in plots (a), (b) and (c)) and also to compare each fructose-supplemented condition (d). Additional statistical analysis was performed using a paired t-test in order to compare the same condition at different time points (e). NS = non-significant ($p \geq 0.05$), * = $p < 0.05$, ** = $p \leq 0.01$, *** = $p \leq 0.001$, **** = $p \leq 0.0001$, ***** = $p \leq 0.00001$. Error bars represent SD. n = 3 biological replicates. The full data collected can be found in Figure 8.5 (a), Appendix 8.3.

3.3.6 Discussion

The addition of 0.5% (w/v) fructose to 0.2%, 0.4%, 0.6% and 0.8% (w/v) ME cultures significantly increased OD_{600} for all conditions tested. This is indicative of fructose being metabolised by the Entner-Doudoroff pathway (Fleige *et al.*, 2011) and acetyl-CoA being channelled into the citric acid cycle rather than P3HB biosynthesis (Ienczak *et al.*, 2011). Cultures containing 0.2% (w/v) ME and supplemented with 0.5% (w/v) fructose produced considerably more P3HB than cultures with more concentrated ME. While this finding appears to concur with the findings of Passanha *et al*. (2014), who found that increasing the C to key nutrient ratio increased PHA production, this was in fact due to the formation of cell chains. In fructose-supplemented cultures, *C. necator* forms a $P3HB^{++}$ population which produces up to 100 times more P3HB per cell than $P3HB^{+}$ *C. necator*. Similar findings have been reported describing small *C. necator* populations able to utilise glucose effectively (Franz *et al.*, 2011) and use glycerol more readily (González-Villanueva *et al*. 2019). Populations such as $P3HB^{++}$ can arise due to a variety of genetic (Arber, 2000) or non-genetic (van Boxtel *et al.*, 2017) factors which can result from stochastic events (Choi *et al.*, 2008). It is possible the $P3HB^{++}$ population consists of persistor cells which represent an insurance policy for *C. necator* in case the main population is eradicated (Kotte *et al.*, 2014).

3.4 Growth of *C. necator* in 0.08% and 0.2% (w/v) ME supplemented with 0.5% (w/v) fructose.

In the previous section 3.3, supplementing ME cultures with 0.5% (w/v) fructose was found to increase the mean OD_{600} by between 5 and 15 times. In addition, the supplementation of ME with fructose led to the formation of a $P3HB^{++}$ population. An increase in intracellular P3HB for cultures containing 0.2% (w/v) ME and 0.5% (w/v) fructose was found to be due to the formation of cell chains, rather than due to an increased fructose to ME ratio. In this section, a lower ME concentration of 0.08% (w/v) is compared to that of 0.2% (w/v) ME to assess if a further reduction in ME concentration will induce higher levels of intracellular P3HB accumulation.

3.4.1 Supplementing 0.08% (w/v) ME with fructose increases OD_{600}

A summary of OD_{600} at 24 and 48 hours for *C. necator* cultures grown in 0.08% (w/v) ME with and without fructose supplementation is presented in Figure 3.19. The full data is located in Figure 8.6, Appendix 8.4.

In Figure 3.19 (a) and (b), 0.08% and 0.2% (w/v) ME cultures are shown to significantly increase in OD_{600} when supplemented with 0.5% (w/v) fructose. Statistical comparisons between each condition in Figure 3.19 (c) show that at 24 hours, OD_{600} was greater in fructose-supplemented 0.2% (w/v) ME cultures. However, at 48 hours, there was no significant difference in OD_{600} between 0.08% and 0.2% (w/v) ME fructose-supplemented cultures.

Paired comparisons between time points (Figure 3.19 (d)) found fructose-supplemented 0.08% (w/v) ME samples significantly increased between 24 and 48-hour time points whereas, 0.2% (w/v) ME fructose-supplemented cultures did not significantly change.

As expected based on the findings of experiments in section 3.3.1, the addition of fructose increases the OD_{600} of 0.08% (w/v) ME cultures, in similarity to that of 0.2% (w/v) ME cultures, when 0.5% (w/v) fructose is supplemented. This is due to fructose being utilised by the Entner-Doudoroff pathway and acetyl-CoA entering into the citric acid cycle (Ienczak *et al.*, 2011). However, while the results presented in Figure 3.19 (a) were consistent with previous results in section 3.2.1, in which decreasing ME correlated with decreasing OD_{600}, the results displayed in Figure 3.19 (a) at 48 hours found that there was no significant difference between the OD_{600} of fructose-supplemented 0.08% and 0.2% (w/v) ME cultures. It should be noted that culture OD_{600}, in addition to cell number, can be influenced by factors such as cell size (Stevenson *et al.*, 2016). It may be possible that different cell size is causing fructose-supplemented 0.08% and 0.2% (w/v) ME cultures to have similar OD_{600} readings at 48 hours, and this will be discussed further in section 3.4.5.

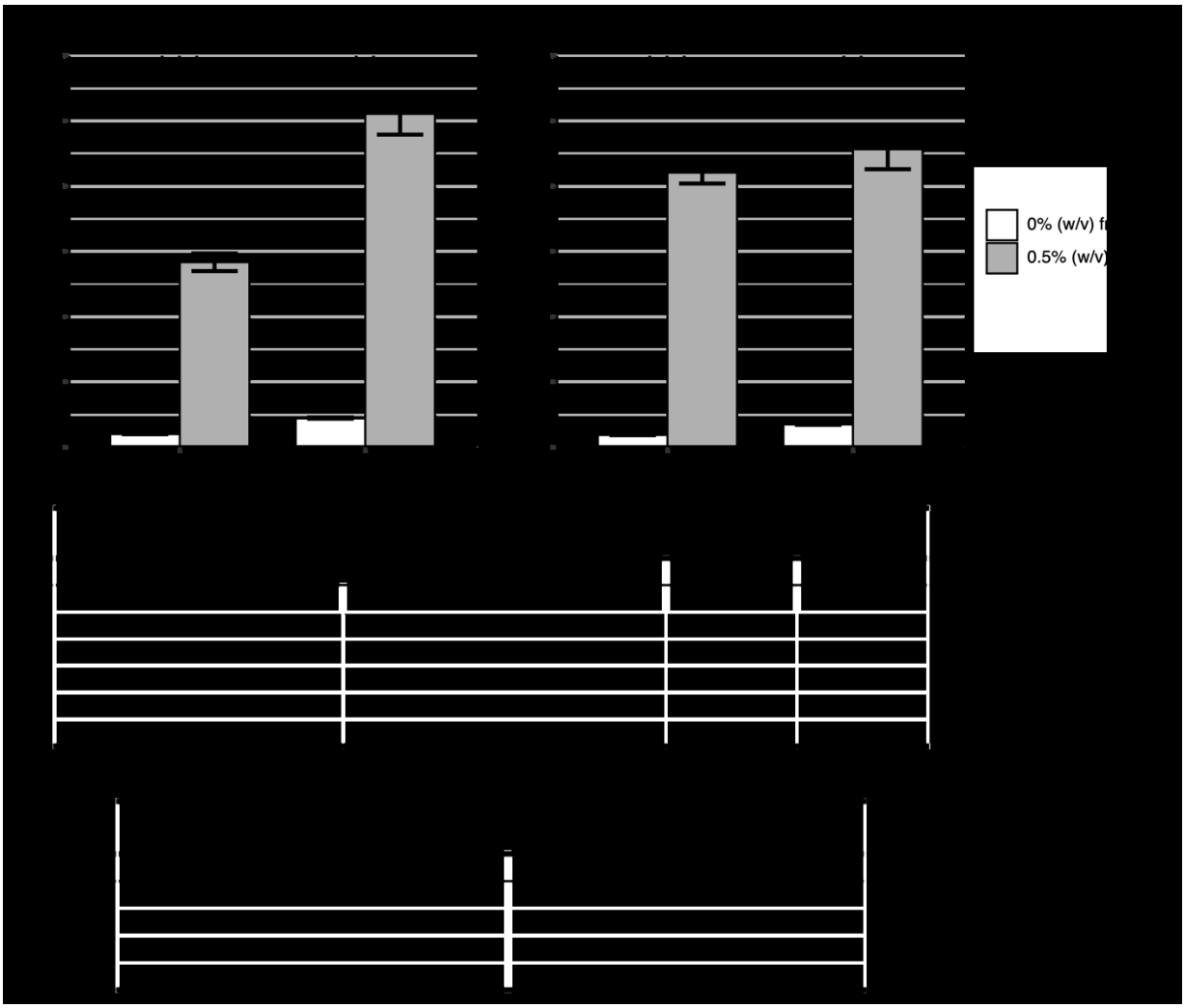


Figure 3.19 - Graphs and statistical analysis comparing the mean OD_{600} of *C. necator* cultures grown in 0.08% and 0.2% (w/v) ME with and without 0.5% (w/v) fructose supplementation. Statistical analysis was performed using unpaired t-tests to evaluate the same ME concentration with and without fructose supplementation (indicated by) annotations in plots (a) and (b)) and also to compare conditions at each time point (d). Additional statistical analysis was performed using paired t-tests in order to compare the same condition at different time points (d). NS = non-significant ($p \geq 0.05$), * = $p < 0.05$, ** = $p \leq 0.01$, *** = $p \leq 0.001$, **** = $p \leq 0.0001$, ***** = $p \leq 0.00001$. Error bars represent SD. n = 3 biological replicates. The full data is located in Figure 8.6, Appendix 8.4.

3.4.2 Reducing the ME concentration to 0.08% (w/v) does not increase P3HB

Figure 3.20 contains a summary of *C. necator* intracellular P3HB for cultures containing 0.08% and 0.2% (w/v) ME with and without 0.5% (w/v) fructose. The full data can be found in Figure 8.7 (a) and (b), Appendix 8.4.

Statistical analysis after 4 hours of growth (Figure 3.20 (a)) shows the addition of 0.5% (w/v) fructose to 0.08% (w/v) ME resulted in significantly less intracellular P3HB, but when added to 0.2% (w/v) ME cultures, no significant difference was observed. In contrast, at 24 hours (Figure 3.20 (b)) fructose supplementation significantly increased P3HB levels for both 0.08% and 0.2% (w/v) cultures. At 48 hours (Figure 3.20 (c)), a significant increase in P3HB occurred when 0.08% (w/v) ME cultures were supplemented with fructose, but 0.2% (w/v) ME cultures could not be statistically distinguished due to variable amounts of $P3HB^{++}$ cells creating a high degree sample variation.

Further comparisons between conditions at the same time point (Figure 3.20 (d)) showed at 4 hours, 0.08% (w/v) ME without fructose produced more P3HB than the other conditions tested. In fact, this result was significantly greater than all other conditions tested at 4, 24 and 48 hours (statistics not summarised in Figure 3.20). Statistical analysis over time (Figure 3.20 (e)), on the other hand, showed that only cultures containing 0.2% (w/v) ME were observed to accumulate P3HB between the time points summarised.

Overall evidence presented in Figure 3.20 suggests that increasing the key nutrient to ME ratio by keeping fructose concentration at 0.5% (w/v) while decreasing ME concentration from 0.2% to 0.08% (w/v) does not increase mean P3HB per *C. necator* cell. Once again, in line with the findings of Dey and Rangarajan (2017) and Nygaard *et al*. (2019) there was evidence of P3HB production during a phase of exponential growth at 4 hours. However, the raw data in Figure 8.6 (Appendix 8.4), shows that the OD_{600} of cultures is very low meaning the overall amount of P3HB in the culture as a whole would be negligible. Literature on the production of P3HB in *C. necator* states that increasing the C to key nutrient ratio is vital to stimulating P3HB accumulation (Passanha *et al.*, 2014). However, the results in this section suggest that increasing the fructose to ME ratio, particularly after 24 hours of growth, does not increase the mean intracellular P3HB per cell. This may be due to there being insufficient fructose remaining in the media once fructose is utilised for cell proliferation and conversely there may be too much ME remaining due to insufficient fructose availability.

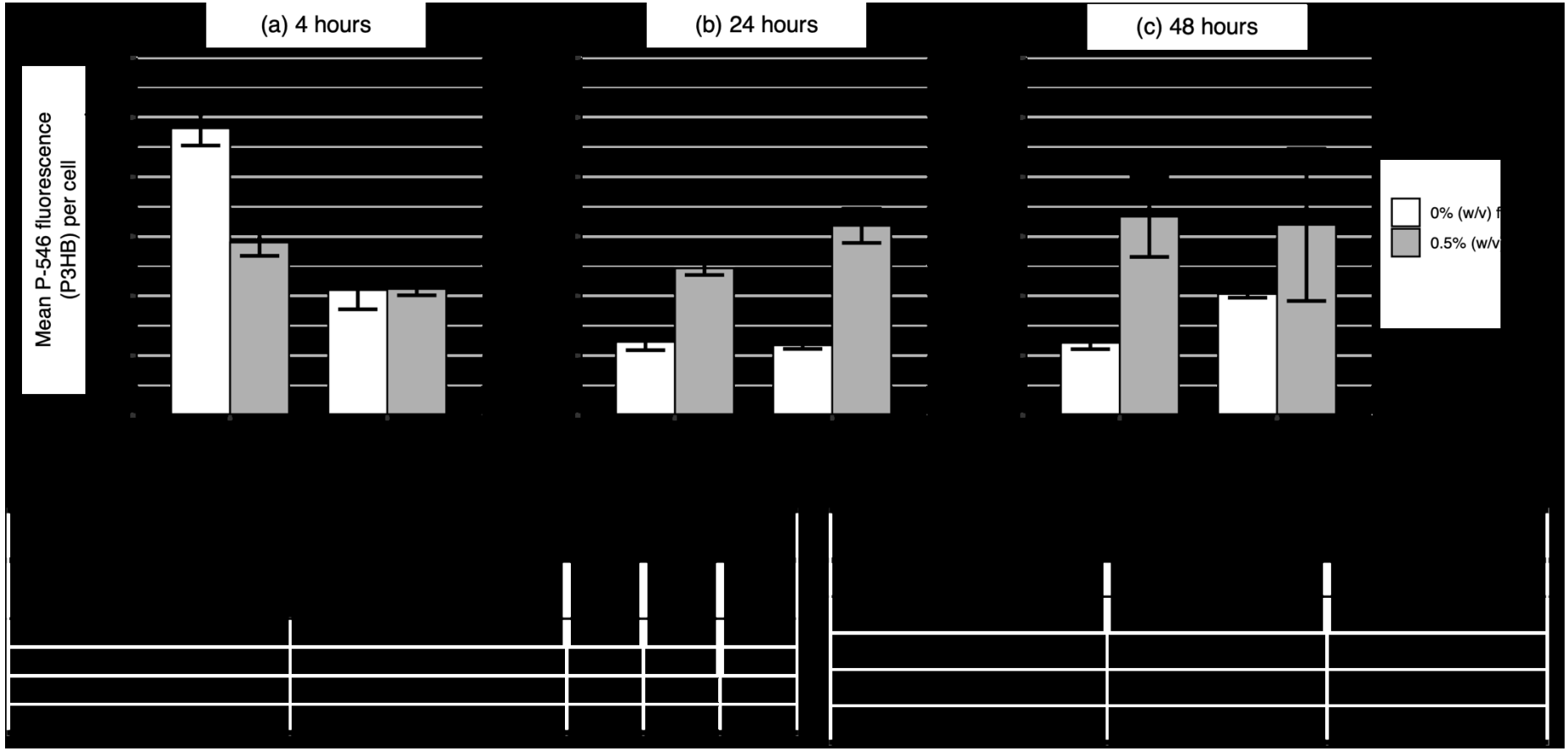


Figure 3.20 - Graphs and statistical analysis comparing the mean P-546 fluorescence (P3HB) of *C. necator* cultures grown in 0.08% and 0.2% (w/v) ME with and without 0.5% (w/v) fructose supplementation. Statistical analysis was performed using unpaired t-tests to evaluate the same ME concentration with and without fructose supplementation (annotations in plots (a), (b) and (c)) and also to compare conditions at each time point (d). Additional statistical analysis was performed using a paired t-test in order to compare the same condition at different time points (e). NS = non-significant ($p \geq 0.05$), * = $p < 0.05$, ** = $p \leq 0.01$, *** = $p \leq 0.001$. Error bars represent SD. n = 3 biological replicates. The full data can be found in Figure 8.7 (a) and (b), Appendix 8.4.

3.4.3 The P3HB^{++} phenotype is influenced by the ME-to-fructose ratio

Figure 3.21 contains a summary of the percentage of P3HB^{++} cells produced in media containing 0.08% (w/v) ME with and without the addition of 0.5% (w/v) fructose. The full data can be found in Figure 8.7 (c) and (d), Appendix 8.4.

Statistical comparisons evaluating the effect of fructose supplementation (Figure 3.21 (a)) showed that while there was no significant difference between fructose supplemented and non-supplemented 0.08% (w/v) ME cultures, there was a statistical difference for 0.2% (w/v) samples with fructose addition increasing the mean percentage of P3HB^{++} cells. In fact, non-fructose supplemented 0.2% (w/v) ME cultures only registered 5 events in the P3HB^{++} flow cytometry gate out of a total 25,000 events. Further to this, at 24 and 48 hours, non-fructose supplemented 0.2% (w/v) ME cultures did not register any events in the P3HB^{++} gate at either 24 (Figure 3.21 (b)) or 48 hours (Figure 3.21 (c)). Analysis between the same time points presented in Figure 3.21 (d)) determined the only time that 0.08% (w/v) with or without fructose had significantly fewer P3HB^{++} cells was at 24 hours.

Further statistical analysis presented in Figure 3.21 (e)) showed that non-fructose supplemented 0.08% and 0.2% (w/v) samples were not significantly different between either 4 and 24 or 24 and 48 hours. Fructose-supplemented samples, on the other hand, were significantly different between each time point with 0.08 (w/v) fructose-containing samples increasing between 4 and 24 hours before decreasing between 24 and 48 hours. Fructose-supplemented 0.2% (w/v) samples on the other hand increased between 4 and 24 hours before decreasing between 24 and 48 hours. As in previous sections in which intracellular P3HB levels for 0.08% (w/v) at 4 hours were not surpassed for the remainder of the experiment, 0.08% (w/v) was found to be not significantly different from 0.2% (w/v) fructose supplemented samples at 24 hours and 48-hours, and was significantly greater than all other results at 24 and 48 hour time points.

Overall, results in this section show that the development of a P3HB^{++} subpopulation is influenced by both ME concentration and fructose. In cultures containing only ME, a reduction in ME concentration from 0.2% to 0.08% (w/v) induces the formation of P3HB^{++} cells. On the other hand, the addition of fructose to 0.2% (w/v) ME can also induce the development of a P3HB^{++} population. Thus, while results presented in section 3.4.2 suggest the *C. necator* population as a whole does not respond to increased fructose to ME ratio by increasing P3HB production, the P3HB^{++} phenotype appears to be initiated by an increased fructose to ME ratio.

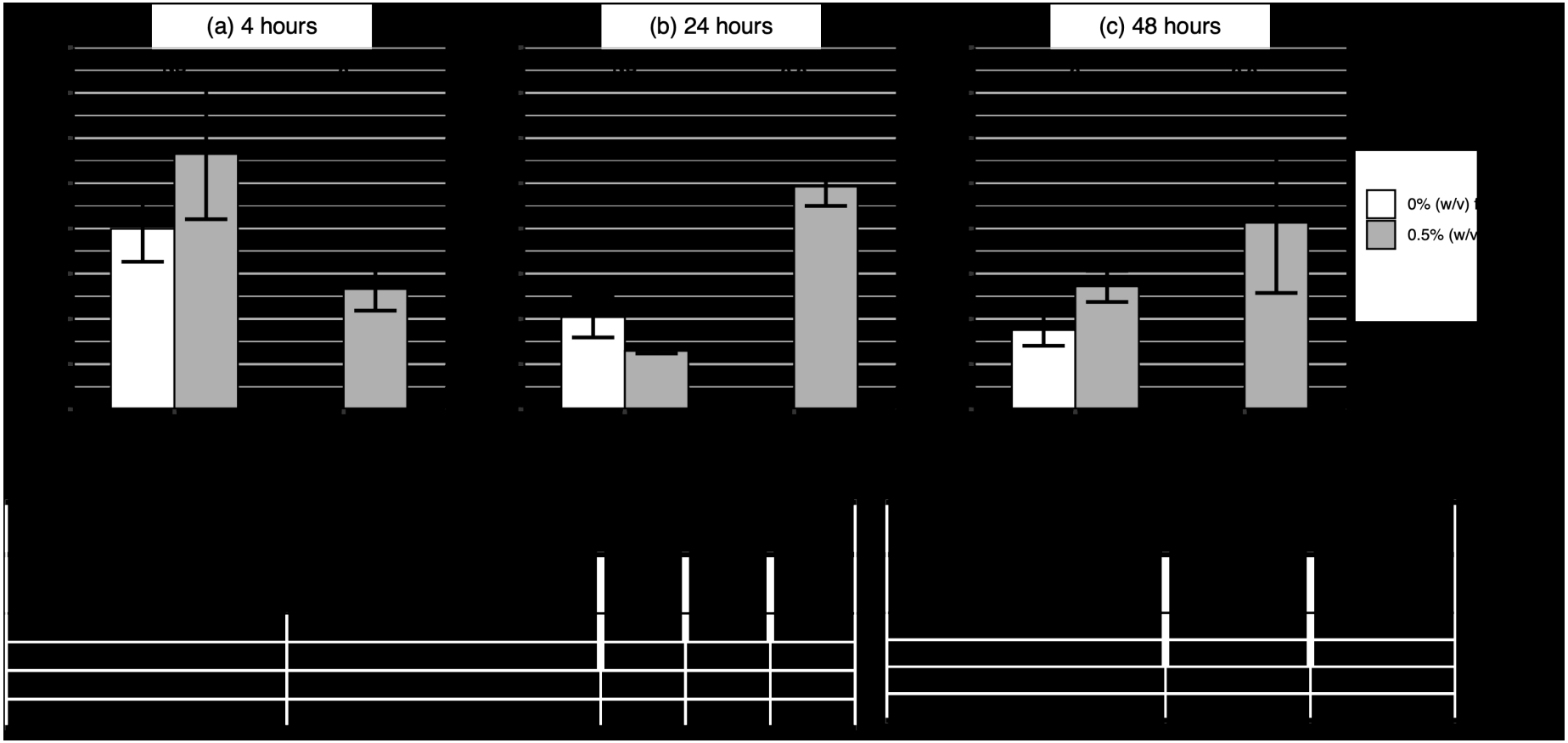


Figure 3.21 - Graphs and statistical analysis comparing the mean percentage of P3HB^{++} cells in *C. necator* cultures grown in 0.08% and 0.2% (w/v) ME with and without 0.5% (w/v) fructose supplementation. Statistical analysis was performed using unpaired t-tests to evaluate the same ME concentration with and without fructose supplementation (annotations in plots (a), (b) and (c)) and also to compare samples containing non-supplemented 0.08% ME cultures to other conditions (d). Additional statistical analysis was performed using a paired t-test in order to compare conditions at each time point (e). NS = non-significant ($p \geq 0.05$), * = $p < 0.05$, ** = $p \leq 0.01$, *** = $p \leq 0.001$. Error bars represent SD. n = 3 biological replicates. The full data can be found in Figure 8.4 (b) and (c), Appendix 8.4.

3.4.4 Fructose addition increases intracellular P3HB for the P3HB^{++} population

Figure 3.22 provides a summary of mean intracellular P3HB for P3HB^{+} and P3HB^{++} *C. necator* populations, in cultures containing 0.08% (w/v) ME with and without the addition of 0.5% (w/v) fructose. The full data can be found in Figure 8.7 (e) and (f), Appendix 8.4.

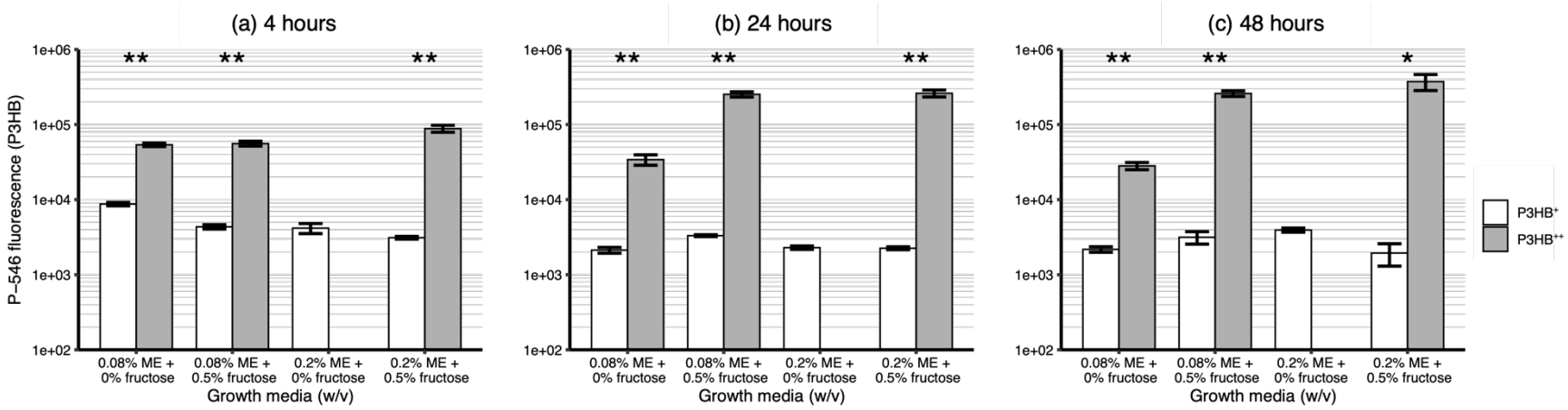
In accordance with previous results, statistical analysis showed that the P3HB^{++} population contained significantly more P3HB than the P3HB^{+} population at 4 (Figure 3.22 (a)), 24 (Figure 3.22 (b)) and 48-hour (Figure 3.22 (c)) time points for all conditions except for cultures containing 0.2% (w/v) ME without fructose added. For 0.2% (w/v) ME cultures not supplemented with fructose, the P3HB^{++} population was not included in Figure 3.22 as there were either too few flow cytometry events, or none at all, in the P3HB^{++} gate.

Figure 3.22 (d) provides non-paired statistical comparisons of individual conditions, for the P3HB^{+} and P3HB^{++} populations, at 4, 24 and 48 hours. For the P3HB^{+} population, at 4 hours 0.08% (w/v) ME cultures without fructose contained significantly more P3HB than the remaining conditions. In contrast, at 24 hours 0.08% (w/v) ME cultures supplemented with 0.5% (w/v) fructose produced P3HB^{+} cells with the most P3HB. At 48 hours, only non-fructose supplemented 0.08% and 0.2% (w/v) ME and 0.2% (w/v) ME samples with and without fructose were found to be significantly different. For the P3HB^{++} population at 4 hours, 0.2% (w/v) cultures with fructose contained significantly more P3HB than 0.08% (w/v) ME cultures, both with and without fructose. At 24 and 48 hours, fructose-supplemented 0.08% and 0.2% (w/v) ME cultures were not significantly different but contained significantly more P3HB than 0.08% (w/v) samples without fructose.

Statistical analysis comparing the same media conditions over time, presented in Figure 3.22 (e), found that for the P3HB^{+} population, between 4 and 24 hours 0.2% (w/v) ME cultures without fructose were the only condition to significantly increase. For the P3HB^{++} population, on the other hand, fructose-supplemented 0.08% and 0.2% (w/v) ME cultures both significantly increased intracellular P3HB per cell between 4 and 24 hours, and then did not statistically change between 24 and 48 hours. Cultures containing 0.08% (w/v) ME without fructose on contrast did not significantly change between 4 and 24, or 24 and 48 hours.

In addition to the findings of section 3.4.3, the data summarised in Figure 3.22 demonstrates that the addition of fructose to ME media induces more P3HB production in P3HB^{++} cells in comparison to P3HB^{+}. It is likely that P3HB^{+} cells metabolise fructose in a conventional manner via the Entner-Doudoroff pathway, producing pyruvate in the process (Fleige *et al.*, 2011). Pyruvate is converted into acetyl-CoA, which is then fed into the citric acid cycle. Free CoA released from the introduction of acetyl-CoA to the Krebs cycle inhibits the PhaA enzyme, preventing the initiation of the P3HB biosynthetic pathway (Mansfield *et al.*, 1995). In P3HB^{++} cells, this regulatory process appears to be

limited allowing P3HB^{++} cells to accumulate intracellular P3HB in a period of growth-promoting conditions. Cells in the P3HB^{++} population resemble metabolically inactive persister cells reported in literature (Kotte *et al.*, 2014; Solopova *et al.*, 2014). However, the results in this section P3HB^{++} demonstrate that P3HB^{++} *C. necator* cells differ from previously reported persister cells by maintaining some metabolic activity between 4 and 24 hours to produce P3HB during growth promoting conditions.



(d)

Non-paired t-tests comparing P3HB+ and P3HB++ P-546 fluorescence (P3HB) at 4, 24 and 48 hours.

Growth media comparison		P3HB+			P3HB++		
		4 hours	24 hours	48 hours	4 hours	24 hours	48 hours
0.08% ME + 0% fructose	0.08% ME + 0.5% fructose	***	**	NS	NS	**	**
0.08% ME + 0% fructose	0.2% ME + 0% fructose	***	NS	***	-	-	-
0.08% ME + 0% fructose	0.2% ME + 0.5% fructose	**	NS	NS	*	**	*
0.08% ME + 0.5% fructose	0.2% ME + 0% fructose	NS	**	NS	-	-	-
0.08% ME + 0.5% fructose	0.2% ME + 0.5% fructose	**	***	NS	*	NS	NS
0.2% ME + 0% fructose	0.2% ME + 0.5% fructose	NS	NS	*	-	-	-

(e)

Paired t-tests comparing P3HB+ and P3HB++ FSC between 4 and 24, and 24 and 48 hours.

Growth media (w/v)	P3HB+		P3HB++	
	4-24 hours	24-48 hours	4-24 hours	24-48 hours
0.08% ME	**	NS	NS	NS
0.08% ME + 0.5% fructose	*	NS	**	NS
0.2% ME	NS	*	-	-
0.2% ME + 0.5% fructose	**	NS	**	NS

Figure 3.22 - Graphs and statistical analysis comparing the mean P-546 fluorescence (P3HB) of the P3HB+ and P3HB++ *C. necator* populations when grown in 0.08% and 0.2% (w/v) ME with and without 0.5% (w/v) fructose supplementation. Statistical analysis was performed using unpaired t-tests to evaluate the same ME concentration with and without fructose supplementation (annotations in plots (a), (b) and (c)) and also to compare each condition (d). Additional statistical analysis was performed using a paired t-test in order to compare the same conditions at each time point (e). NS = non-significant ($p \geq 0.05$), * = $p < 0.05$, ** = $p \leq 0.01$, *** = $p \leq 0.001$.The full data can be found in Figure 8.7 (e) and (f), Appendix 8.4.

3.4.5 Fructose supplemented 0.08% (w/v) ME cultures produce smaller cells at 4 hours, but larger cells after 24 hours

Figure 3.23 presents a summary of mean cell size for *C. necator* cultures containing 0.08% or 0.2% (w/v) ME with and without the addition of 0.5% (w/v) fructose. The full data can be found in Figure 8.8 (a) and (b), Appendix 8.4.

Comparing media with and without fructose revealed that at 4 (Figure 3.23 (a)), 24 (Figure 3.23 (b)) and 48 hours (Figure 3.23 (c)) *C. necator* cultures supplemented with 0.5% (w/v) fructose contained significantly larger cells than media without.

Comparisons between media conditions at each time point (Figure 3.23 (d)) showed that at 4 hours, 0.2% (w/v) ME cultures contained larger cells than 0.08% (w/v) cultures. At 24 hours, fructose-supplemented 0.08% (w/v) ME cultures contained significantly larger cells than 0.2% (w/v) ME cultures. This was also the case at 48 hours, at which point 0.08% (w/v) ME fructose-supplemented cultures were almost 4 times larger than fructose-supplemented 0.2% (w/v). Further statistical analysis over time revealed that between 4 and 24 hours, fructose-supplemented cultures significantly increased in size whereas non-supplemented samples decreased in cell size. Between 24 and 48 hours, 0.08% (w/v) ME fructose-supplemented cultures almost doubled in cell size while 0.2% (w/v) ME cultures decreased in size.

Results overall in this section show that when 0.5% (w/v) fructose is added to 0.08% and 0.2% (w/v) ME, an increase in cell size is observed. This corroborates the results of section 3.3.4 in which similar cell size increases were observed when fructose was supplemented particularly at 4 and 24-hour time points. Bacterial cell size during cell proliferation has been linked with growth rate in literature (Sharpe *et al.*, 1998; Sperber and Herman, 2017; Zhang *et al.*, 2020). When fructose is supplemented, 0.2% (w/v) ME cultures may produce larger cells due to an increased growth rate in comparison to that of the less nutritious 0.08% (w/v) ME cultures. This would appear to align results with literature suggesting that the metabolism of key nutrients (Sperber and Herman, 2017) and C (Hill *et al.*, 2013) have regulatory roles in bacterial cell size. However, at 24 and 48-hour time points, fructose-supplemented 0.08% (w/v) cultures contained larger cells than that of 0.2% (w/v) ME cultures containing fructose. It's likely that by 24 hours growth rate had slowed down, meaning cell size was less dependent on growth rate. Thus, fructose-supplemented 0.08% (w/v) ME media may produce larger cells at 24 hours due to a decreased osmolarity caused by there being less surplus ME. Changes in osmolarity can influence cell size by altering turgor pressure which causes either an influx or efflux of water in the cell (Oldewurtel *et al.*, 2021). Although studies by Rojas *et al.* (2014) have suggested that bacterial cell expansion occurs independent of turgor pressure. Larger cells in 0.08% (w/v) fructose-supplemented

cultures may be the reason for an increase in OD_{600} between 24 and 48 hours (Figure 3.19), as cell size is known to influence measurements of OD_{600} (Stevenson *et al.*, 2016).

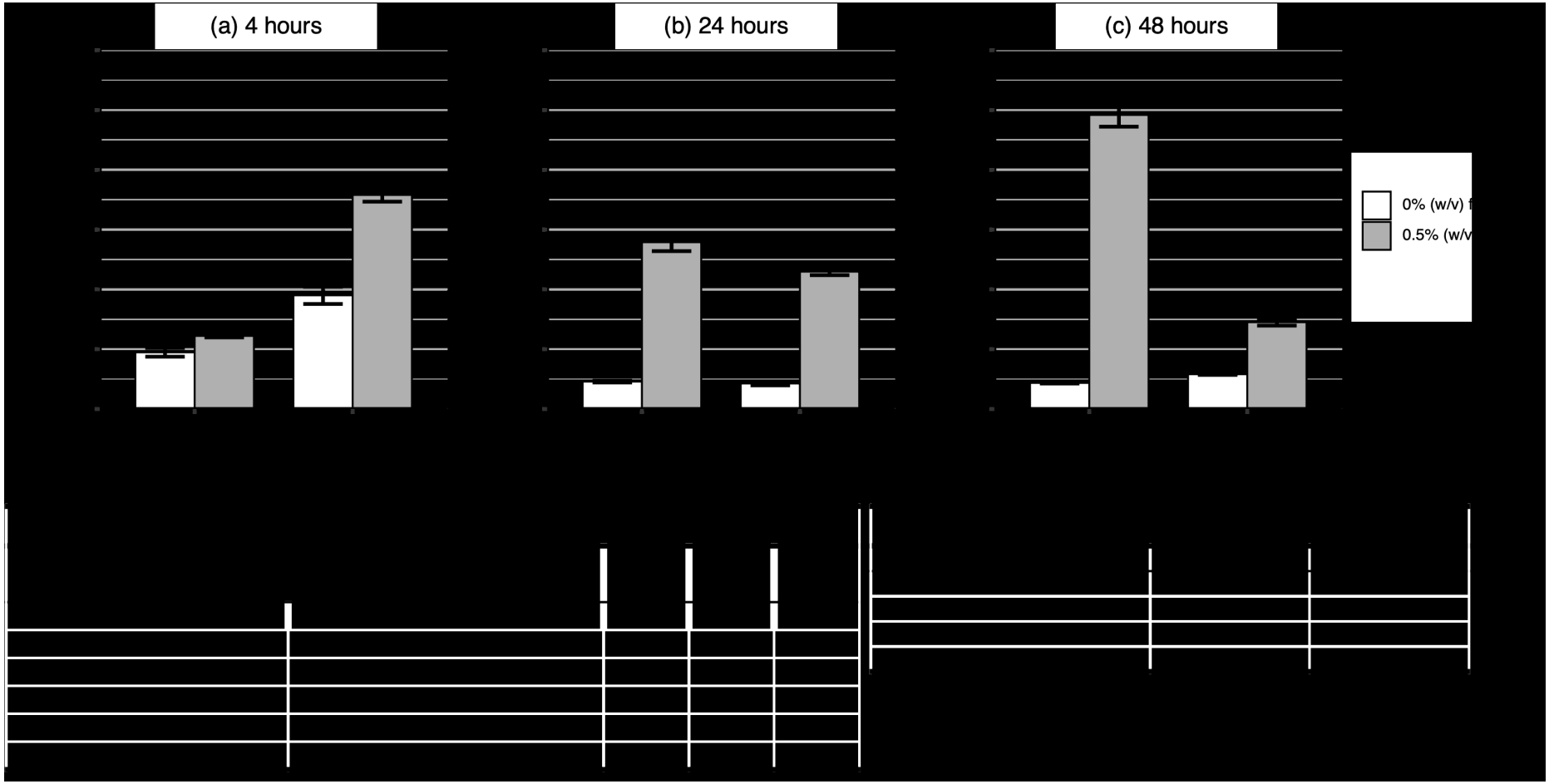


Figure 3.23 - Graphs and statistical analysis comparing the mean FSC of *C. necator* cultures grown in 0.08% and 0.2% (w/v) ME with and without 0.5% (w/v) fructose supplementation. Statistical analysis was performed using unpaired t-tests to evaluate the same ME concentration with and without fructose supplementation (annotations in plots (a), (b) and (c)) and also to compare each condition (d). Additional statistical analysis was performed using a paired t-test in order to compare the same compare conditions at each time point (e). NS = non-significant ($p \geq 0.05$), * = $p < 0.05$, ** = $p \leq 0.01$, *** = $p \leq 0.001$, **** = $p \leq 0.0001$. Error bars represent SD. n = 3 biological replicates. The full data can be found in Figure 8.8 (a) and (b), Appendix 8.4.

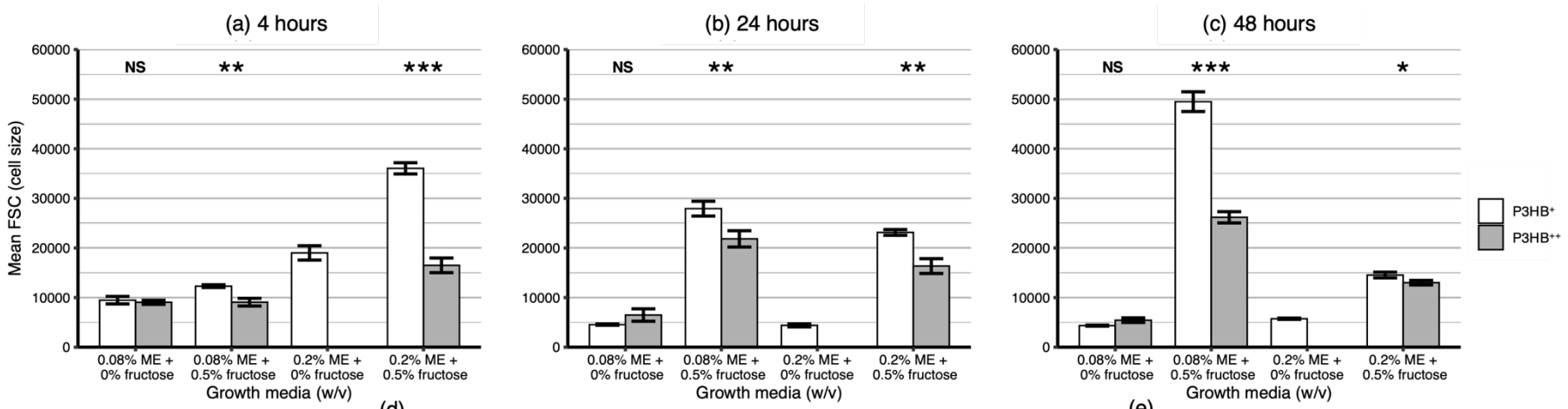
3.4.6 PH3B^{++} cells are also smaller than P3HB^{+} in fructose supplemented 0.08% (w/v) ME

Figure 3.24 contains a summary of P3HB^{+} and P3HB^{++} FSC for *C. necator* cultured in 0.08% or 0.2% (w/v) ME with and without the addition of 0.5% (w/v) fructose. The full data can be found in Figure 8.8 (c) and (d), Appendix 8.4.

Statistical comparisons between P3HB^{+} and P3HB^{++} populations at 4 (Figure 3.24 (a)), 24 (Figure 3.24 (b)) and 48 hours (Figure 3.24 (c)) showed that for fructose-supplemented conditions P3HB^{+} cells were significantly larger in size than cells in the P3HB^{++} population. For 0.08% (w/v) ME without fructose supplemented there was no significant difference between the two populations, whereas a comparison for non-supplemented 0.2% (w/v) ME cultures was not possible as the P3HB population registered negligible flow cytometry events.

Comparisons between each individual condition at the same time point (Figure 3.24 (d)) showed that at 4 hours the P3HB^{+} population showed that 0.2% (w/v) ME-containing cultures produced larger P3HB^{+} cells than 0.08% (w/v) ME media, and 0.5% (w/v) fructose-supplementation produced larger P3HB^{+} cells. At 24 hours, P3HB^{+} cells were largest in fructose-supplemented media and 0.08% (w/v) ME fructose-supplemented media produced significantly larger cells than that of 0.2% (w/v) ME with fructose. At 48 hours, fructose-supplemented media once again produced the largest P3HB^{+} cells with those cultured in 0.08% (w/v) ME supplemented with 0.5% (w/v) fructose considerably larger than any other condition tested. Statistical analysis between time points in Figure 3.24 (e) showed that P3HB^{+} cells in 0.08% (w/v) ME with fructose increased in size consecutively between time points and almost doubled in size between 24 and 48 hours. On the other hand, P3HB^{+} cells in 0.2% (w/v) ME media supplemented with fructose consecutively decreased in size. Changes in the cell size of P3HB^{+} cells in non-fructose supplemented media were non-significant for 0.2% (w/v) ME cultures and for 0.08% (w/v) media P3HB^{+} cells slightly decreased between 4 and 24 hours and slightly increased between 24 and 48 hours. For the P3HB^{++} population at 4 hours, individual comparisons at each time point revealed that P3HB^{++} cells in 0.2% (w/v) ME media supplemented with fructose were significantly larger in cell size than both 0.08% (w/v) ME cultures with and without fructose. At 24 hours, fructose-supplemented 0.08% (w/v) ME media produced significantly larger cells than 0.08% (w/v) media without fructose and were also slightly larger than 0.2% (w/v) with fructose added. At the 48-hour time point, P3HB^{++} were significantly larger in the 0.08% (w/v) ME with fructose added. Statistical analysis over time for the P3HB^{++} population showed that only P3HB^{++} cells in 0.08% (w/v) media supplemented with 0.5% (w/v) fructose significantly increased between both 4 and 24, and 24 and 48 hours.

In this section both 0.08% and 0.2% (w/v) ME cultures supplemented with 0.5% (w/v) fructose were found to have larger $P3HB^{+}$ cells compared to $P3HB^{++}$ at 4, 24 and 48 hours. It was suggested in section 3.3.5 that the small $P3HB^{++}$ cell phenotype provides evidence that the population may comprise of persister cells similar to that observed in *E. coli* by Khlebodarova and Likoshvai (2018). Results in this section corroborate the findings of section 3.3.5.



(d)

Non-paired t-tests comparing P3HB⁺ and P3HB⁺⁺ FSC at 4, 24 and 48 hours.

Growth media comparison		P3HB⁺			P3HB⁺⁺		
		4 hours	24 hours	48 hours	4 hours	24 hours	48 hours
0.08% ME + 0% fructose	0.08% ME + 0.5% fructose	**	**	***	NS	***	****
0.08% ME + 0% fructose	0.2% ME + 0% fructose	**	NS	***	-	-	-
0.08% ME + 0% fructose	0.2% ME + 0.5% fructose	****	***	**	*	***	****
0.08% ME + 0.5% fructose	0.2% ME + 0% fructose	*	**	***	-	-	-
0.08% ME + 0.5% fructose	0.2% ME + 0.5% fructose	***	*	**	**	*	***
0.2% ME + 0% fructose	0.2% ME + 0.5% fructose	****	****	**	-	-	-

(e)

Paired t-tests comparing P3HB⁺ and P3HB⁺⁺ FSC between 4 and 24, and 24 and 48 hours.

Growth media (w/v)	P3HB⁺		P3HB⁺⁺	
	4-24 hours	24-48 hours	4-24 hours	24-48 hours
0.08% ME + 0% fructose	**	*	NS	NS
0.08% ME + 0.5% fructose	**	***	**	**
0.2% ME + 0% fructose	NS	NS	-	-
0.2% ME + 0.5% fructose	***	****	NS	NS

Figure 3.24 - Graphs and statistical analysis comparing the mean FSC of the P3HB⁺ and P3HB⁺⁺ *C. necator* populations when grown in 0.08% and 0.2% (w/v) ME with and without 0.5% (w/v) fructose supplementation. Statistical analysis was performed using unpaired t-tests to evaluate the same ME concentration with and without fructose supplementation (annotations in plots (a), (b) and (c)) and also to compare each condition (d). Additional statistical analysis was performed using a paired t-test in order to compare the same condition at different time points (e). NS = non-significant ($p \geq 0.05$), * = $p < 0.05$, ** = $p \leq 0.01$, *** = $p \leq 0.001$, **** = $p \leq 0.0001$ Error bars represent SD. n = 3 biological replicates. The full data can be found in Figure 7.8 (c) and (d), Appendix 8.4.

3.4.7 Discussion

When supplementing cultures with 0.5% (w/v) fructose, decreasing ME concentration from 0.2% to 0.08% (w/v) does not decrease OD_{600} as would be expected based on the findings of section 3.2.1. This may be due to the presence of larger cells in 0.08% (w/v) ME cultures, with a larger cell size known to influence measurements of OD_{600} (Stevenson *et al.*, 2016). Fructose supplementation does not increase P3HB per cell, an observation which goes against literature which states increasing the key nutrient to C ratio increases P3HB accumulation (Passanha *et al.*, 2014). Once again there is evidence to suggest P3HB production is occurring during exponential growth, observations which are in line with the findings of Dey and Rangarajan (2017) and Nygaard *et al.* (2019).

Without fructose supplementation, decreasing the ME concentration to 0.08% (w/v) induces the formation of a $P3HB^{++}$ population. In cultures containing 0.2% (w/v) ME only, a $P3HB^{++}$ population is not observed. However, when 0.5% (w/v) fructose is added to 0.08% and 0.2% (w/v) a $P3HB^{++}$ population is observed. The $P3HB^{++}$ population may resemble persistor cells reported in literature (Kotte *et al.*, 2014; Solopova *et al.*, 2014) in terms of cell size and culture proportion, but the one key difference is that $P3HB^{++}$ *C. necator* are not totally dormant and remain capable of producing P3HB at least between 4 and 24 hours. In fructose-supplemented cultures at 4 hours, cultures containing the more nutritious 0.2% (w/v) ME produce larger cells, a result which corroborates with previous research connecting cell size with growth rate. However, fructose-supplemented 0.08% (w/v) ME cultures produce larger cells at 24 and 48 hours when the growth rate is less likely to influence cell size. Instead, at 24 and 48 hours, cell size may be more influenced by osmotic pressure caused by the media composition which may indicate surplus ME was present in 0.2% (w/v) ME cultures (Oldewurtel *et al.*, 2021).

3.5 Increasing fructose concentration in 0.08% (w/v) ME

Results in section 3.4.4 found that fructose-supplemented 0.08% (w/v) ME *C. necator* cultures do not produce more P3HB than that of 0.2% (w/v) ME fructose containing cultures despite the increased fructose to ME ratio. In section 3.5, fructose at concentrations of 0%, 0.5%, 1% and 1.5% (w/v) were added to 0.08% (w/v) ME, to test if further increasing the fructose to ME ratio is able to increase P3HB production.

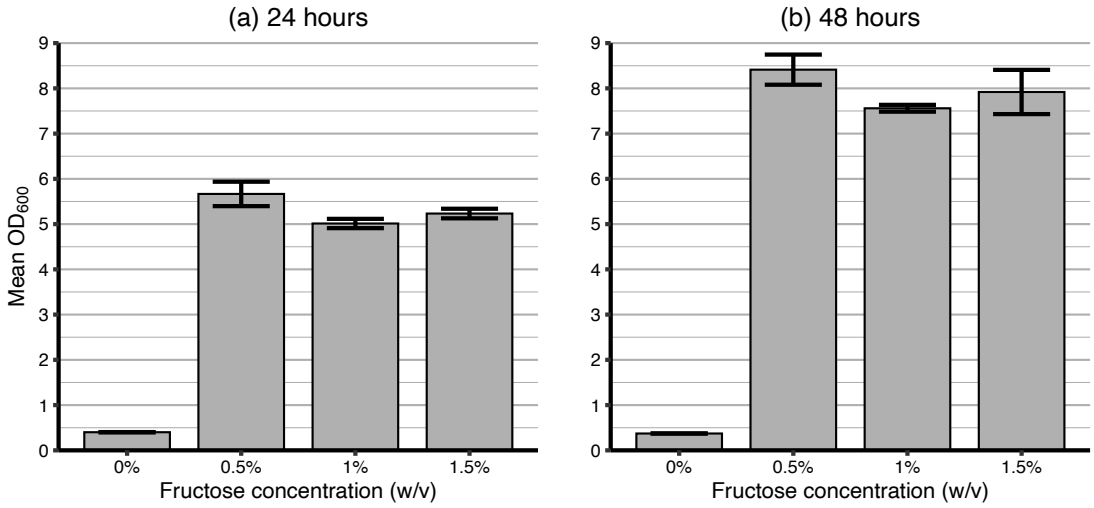
3.5.1 Increasing fructose concentration does not increase OD_{600}

Figure 3.25 contains a summary of OD_{600} for *C. necator* cultures grown in 0.08% (w/v) ME, with comparisons made between the supplementation of fructose at concentrations of 0%, 0.5%, 1% and 1.5% (w/v). The full data is located in Figure 8.9, Appendix 8.5.

At both 24 (Figure 3.25 (a)) and 48-hour (Figure 3.2 (b)) time points, comparisons between each condition, presented in Figure 3.25 (c), increasing the fructose concentration above 0.5% (w/v) does not significantly change culture OD_{600}.

Paired comparisons between corresponding 24 and 48-hour samples (Figure 3.2 (d)), showed that for all conditions tested a significant increase in OD_{600} was observed.

No increase in OD_{600} with increasing fructose concentration above 0.5% (w/v) demonstrates that increasing fructose concentration in 0.08% (w/v) ME media does not increase culture growth in the time scale tested. However, as cultures containing 0.5%, 1% and 1.5% (w/v) fructose all significantly increased in OD_{600} between 24 and 48 hours, it is possible that acetyl-CoA was still being directed into the citric acid cycle (Ienczak *et al.*, 2011) rather than the P3HB biosynthesis pathway. A lack of additional growth above a fructose concentration of 0.5% (w/v) is unlikely to be due to the inhibitory effects of fructose on growth, as fructose has been demonstrated to support high levels of *C. necator* growth at a concentration of 4% (w/v) (Azubuike *et al.*, 2020).



(c)

Non-paired t-tests comparing OD_{600} between 24 and 48 hours.			
Fructose concentration (w/v) comparison		24 hours	48 hours
0%	0.5%	***	***
0%	1%	***	****
0%	1.5%	***	**
0.5%	1%	*	*
0.5%	1.5%	NS	NS
1%	1.5%	NS	NS

(d)

Paired t-tests comparing OD_{600} between 4 and 24, and 24 and 48 hours.	
Fructose concentration (w/v)	24-48 hours
0%	**
0.5%	**
1%	***
1.5%	*

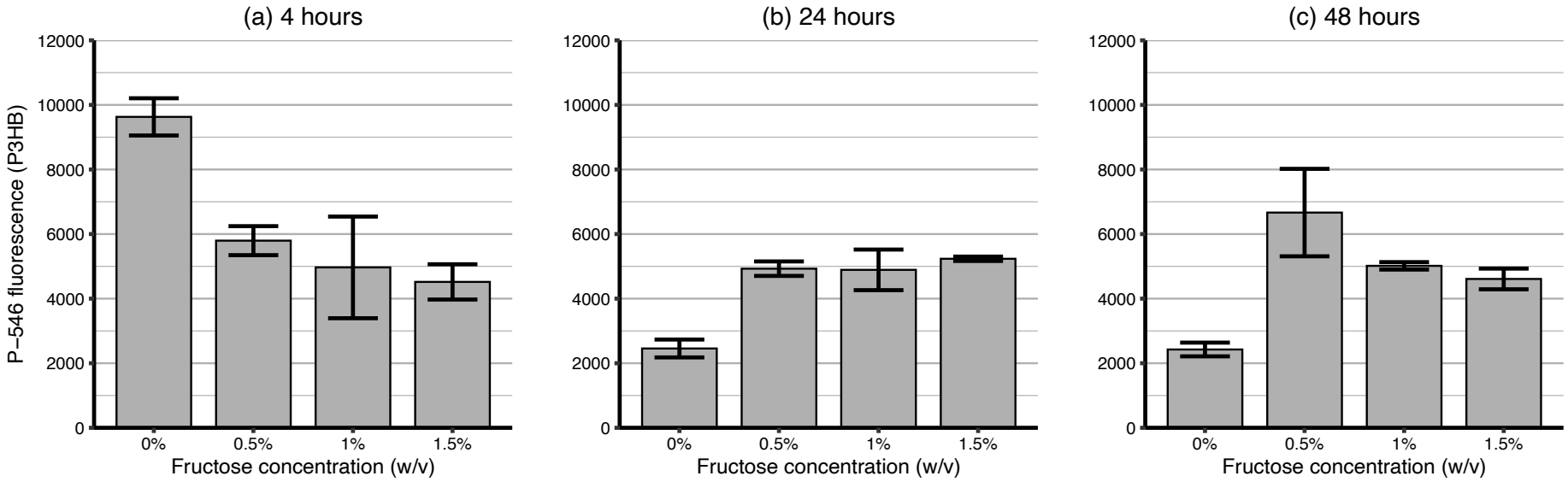
Figure 3.25 - Graphs and statistical analysis comparing the mean OD_{600} of *C. necator* cultures grown in 0.08% (w/v) ME and supplemented with 0%, 0.5%, 1% and 1.5% (w/v) fructose. Mean OD_{600} at 24 (a) and 48 hours (b) is analysed statistically using unpaired t-tests to compare conditions at the same time point (c), and paired t-tests to compare conditions at different time points (d). NS = non-significant ($p \geq 0.05$), * = $p < 0.05$, ** = $p \leq 0.01$, *** = $p \leq 0.001$, **** = $p \leq 0.0001$. Error bars represent SD. n = 3 biological replicates. The full data is located in Figure 8.9, Appendix 8.5.

3.5.2 Increasing fructose concentration does not increase intracellular P3HB

Figure 3.26 provides a summary of intracellular P3HB per cell at 4 (Figure 3.26 (a)), 24 (Figure 3.26 (b)) and 48-hour (Figure 3.26 (c)) time points for 0.08% (w/v) ME *C. necator* cultures supplemented with 0%, 0.5%, 1% or 1.5% (w/v) fructose. The full data can be found in Figure 8.10 (a) and (b), Appendix 8.5.

At 4 hours, the statistical analysis presented in Figure 3.26 (d) found that non-fructose supplemented cultures produced significantly more P3HB per cell than 0.5%, 1% and 1.5% (w/v) fructose supplementation. Further analysis comparing the result at 4 hours for 0% (w/v) fructose supplementation to that of 0.5%, 1% and 1.5% (w/v) fructose at 24 and 48 hours (statistics not summarised in Figure 3.26) showed that P-546 fluorescence at 4 hours was significantly greater than that of 0.5%, 1% and 1.5% (w/v) fructose supplemented cultures at 24 and 48-hour time points. Additionally, statistical comparisons over time (Figure 3.26 (e)) showed a decrease in intracellular P3HB occurs between 4 and 24 hours and there is then no significant difference between 24 and 48 hours. The analysis in Figure 3.26 (d) also revealed that at 24 and 48 hours, fructose supplemented *C. necator* had significantly more intracellular P3HB per cell than non-fructose-supplemented. However, increasing the fructose concentration above 0.5% (w/v) fructose did not increase P3HB levels at either 24 or 48 hour time points.

Increasing the fructose concentration above 0.5% (w/v) in 0.08% (w/v) ME cultures without an observed increase in intracellular P3HB suggests that acetyl-CoA is still being directed into the citric acid cycle due to the continued presence of growth-promoting nutrients (Ienczak *et al.*, 2011). This result is in agreement with the observations of OD_{600} in section 3.5.1.



(d)

Non-paired t-tests comparing P-546 fluorescence (P3HB) for each condition at 4, 24 and 48 hours.				
Fructose concentration (w/v) comparison		4 hours	24 hours	48 hours
0%	0.5%	***	***	*
0%	1%	*	**	***
0%	1.5%	***	**	**
0.5%	1%	NS	NS	NS
0.5%	1.5%	*	NS	NS
1%	1.5%	NS	NS	NS

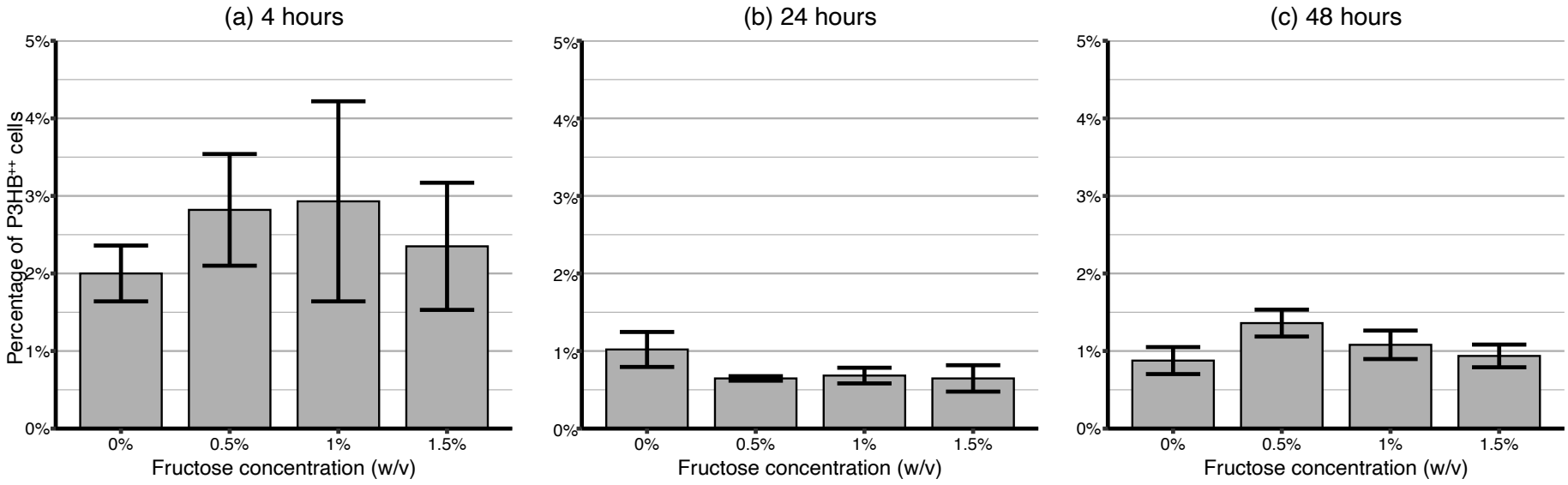
(e)

Paired t-tests comparing P-546 fluorescence (P3HB) between 4 and 24, and 24 and 48 hours.		
Fructose concentration (w/v)	4-24 hours	24-48 hours
0%	**	NS
0.5%	*	NS
1%	NS	NS
1.5%	NS	NS

Figure 3.26 - Graphs and statistical analysis comparing the mean P-546 fluorescence (P3HB) of *C. necator* cultures grown in 0.08% (w/v) ME and supplemented with 0%, 0.5%, 1% and 1.5% (w/v) fructose. Mean P-546 fluorescence at 4 (a), 24 (b) and 48 hours (c) is analysed statistically using unpaired t-tests to compare conditions at the same time point (d), and paired t-tests to compare conditions at different time points (e). NS = non-significant ($p \geq 0.05$), * = $p < 0.05$, ** = $p \leq 0.01$, *** = $p \leq 0.001$. Error bars represent SD. n = 3 biological replicates. The full data can be found in Figure 8.10 (a) and (b), Appendix 8.5.

3.5.3 Increasing fructose concentration does not increase the proportion of P3HB^{++} cells

Figure 3.27 contains a summary of the percentage of P3HB^{++} cells in 0.08% (w/v) ME containing 0%, 0.5%, 1% and 1.5% (w/v) fructose. The full data can be found in Figure 8.10 (a) and (b), Appendix 8.5. At 4 hours (Figure 3.27 (a)), samples were subject to a relatively high degree of error whereas at 24 (Figure 3.27 (b)), and 48 hours (Figure 3.27 (c)) error was reduced for all samples. The large degree of error at 4 hours was due to a high level of variance between culture replicates. Statistical analysis presented in Figure 3.27 (d), found that at 24 and 48 hours there was no significant difference between any of the conditions tested. At 48 hours, the only significantly different comparisons were cultures containing 0.5% (w/v) fructose which contained significantly more P3HB^{++} cells than both 0% and 1.5% (w/v) fructose containing samples. Results were either not significantly different, or were statistically greater at 4 hours when compared over time at 24 and 48 hours (Figure 3.27 (e)). Between 24 and 48 hours, only media containing 0.5% (w/v) fructose significantly increased the proportion of P3HB^{++} cells. Results up to this section have provided evidence to suggest that the P3HB^{++} population may be a type of persister cell population (Kotte *et al.*, 2014; Solopova *et al.*, 2014), previously unreported in *C. necator*. In the current section, increasing fructose concentration above 0.5% (w/v) in cultures has been found not increase the proportion of P3HB^{++} cells. While this suggests there is no link between P3HB^{++} cell production and fructose concentration, this was not the case in 0.2% (w/v) ME cultures which only produced P3HB^{++} cells when 0.5% (w/v) fructose was added (Figure 3.22 section 3.4.4).



(d)

Non-paired t-test comparing P-546 fluorescence (P3HB) for each condition at 4, 24 and 48 hours.				
Fructose concentration (w/v) comparison		4 hours	24 hours	48 hours
0%	0.5%	NS	NS	*
0%	1%	NS	NS	NS
0%	1.5%	NS	NS	NS
0.5%	1%	NS	NS	NS
0.5%	1.5%	NS	NS	*
1%	1.5%	NS	NS	NS

(e)

Paired t-test comparing P-546 fluorescence (P3HB) between 4 and 24, and 24 and 48 hours.		
Fructose concentration (w/v)	4-24 hours	24-48 hours
0%	NS	NS
0.5%	*	*
1%	NS	NS
1.5%	*	NS

Figure 3.27 - Graphs and statistical analysis comparing the mean percentage of P3HB^{++} cells in *C. necator* cultures grown in 0.08% (w/v) ME and supplemented with 0%, 0.5%, 1% and 1.5% (w/v) fructose. The mean proportion of P3HB^{++} cells at 4 (a), 24 (b) and 48 hours (c) is analysed statistically using unpaired t-tests to compare conditions at the same time point (d), and paired t-tests to compare conditions at different time points (e). NS = non-significant ($p \geq 0.05$), * = $p < 0.05$. Error bars represent SD. n = 3 biological replicates. The full data can be found in Figure 8.10 (a) and (b), Appendix 8.5.

3.5.4 Increasing fructose concentration has little impact on intracellular P3HB levels in P3HB^{+} and P3HB^{++} populations.

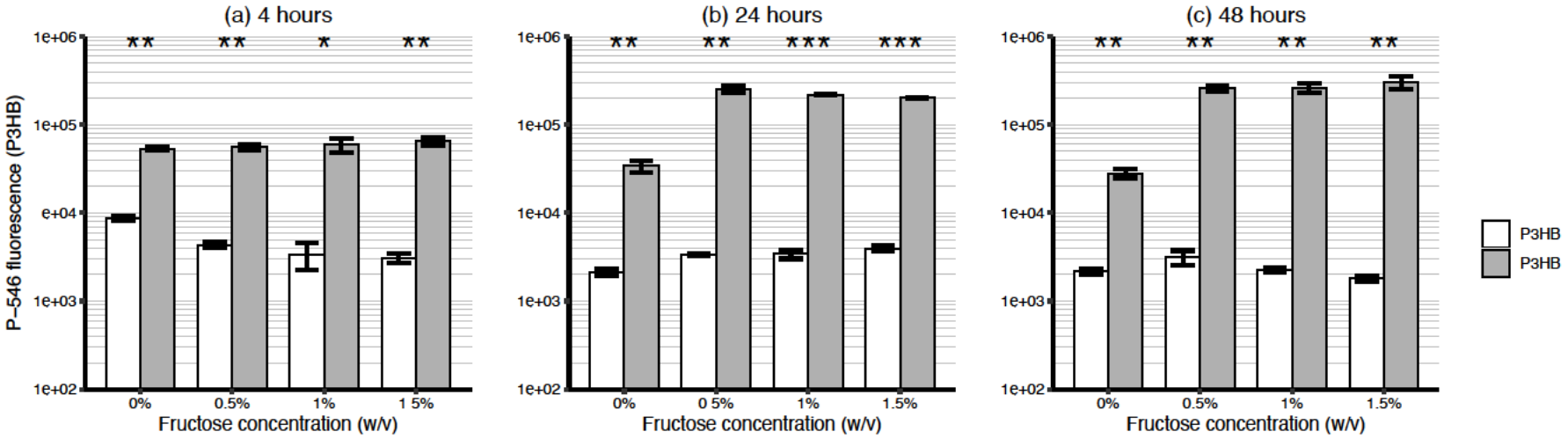
Figure 3.28 presents a summary of intracellular P3HB per cell for the PH3B^{+} and P3HB^{++} *C. necator* populations when cultured in 0.08% (w/v) ME supplemented with 0%, 0.5%, 1% and 1.5% (w/v) fructose. The full data can be found in Figure 8.10 (e) and (f), Appendix 8.5.

For all fructose concentrations added to 0.08% (w/v) ME, at 4 (Figure 3.28 (a)), 24 (Figure 3.28 (b)) and 48 hours (Figure 3.28 (c)) cells in the P3HB^{++} population contained significantly more intracellular P3HB than cells in the P3HB^{+} population.

Statistical comparisons between conditions at the same time point (Figure 3.28 (d)) found that at 4 hours for the P3HB^{+} population, cultures without fructose supplementation contained significantly more P3HB than cultures supplemented with fructose. Cultures without fructose at 24 hours, on the other hand, produced significantly less P3HB than 0.5%, 1% and 1.5% (w/v) fructose cultures. The fructose-containing cultures though could not be statistically separated. At 48 hours only 0% and 1.5% (w/v) fructose cultures and 1 and 1.5% (w/v) cultures were found to be significantly different. For the P3HB^{++} population, statistical analysis at the same point between conditions (Figure 3.28 (d)) revealed that at 4 hours, there was no significant difference between any of the fructose concentrations tested. At 24 hours, the P3HB^{++} population produced more P3HB in fructose-supplemented 0.08% (w/v) fructose-supplemented samples. In addition, 0.5% (w/v) fructose cultures contained significantly more P3HB that 1% and 1.5% (w/v) samples. At 48 hours, cultures without fructose still contained significantly less P3HB than fructose supplemented-samples for the P3HB^{++} population but unlike at 24 hours, there was no statistical difference between 0.5%, 1% and 1.5% (w/v) fructose samples.

Statistical analysis comparing the P3HB^{+} population over time (Figure 3.28 (e)) showed that for all conditions tested, there was either no significant difference or significant decreases between time points, with no conditions significantly increasing for the P3HB^{+} population. Statistical analysis over time showed that for the P3HB^{++} population between 4 and 24 hours, 0.5%, 1% and 1.5% (w/v) fructose cultures all significantly increased in P3HB whereas cultures without fructose did not significantly change. Between 24 and 48 hours there was no significant difference between any of the conditions tested for the P3HB^{++} population.

Previous results presented in section 3.4.4 showed that P3HB^{++} cells differ from reports of persister cells in literature (Kotte *et al.*, 2014; Solopova *et al.*, 2014) by producing P3HB. Results in this section align with those of section 3.4.4 in demonstrating that fructose addition to cultures increases P3HB^{++} P3HB per cell between 4 and 24 hours. However, results also showed that increasing fructose concentration above 0.5% (w/v) does not increase P3HB per cell in the P3HB^{++} population.



(d)

Non-paired t-test comparing the P-546 fluorescence (P3HB) of the P3HB⁺ and P3HB⁺⁺ populations at 4, 24 and 48 hours.

Fructose concentration (w/v) comparison		P3HB⁺			P3HB⁺⁺		
		4 hours	24 hours	48 hours	4 hours	24 hours	48 hours
0%	0.5%	***	**	NS	NS	**	**
0%	1%	**	*	NS	NS	*****	**
0%	1.5%	****	***	*	NS	*****	*
0.5%	1%	NS	NS	NS	NS	NS	NS
0.5%	1.5%	**	NS	NS	NS	NS	NS
1%	1.5%	NS	NS	*	NS	**	NS

(e)

Paired t-test comparing mean P-546 fluorescence (P3HB) of the P3HB⁺ and P3HB⁺⁺ populations between 4 and 24, and 24 and 48 hours.

Media (w/v)	P3HB⁺		P3HB⁺⁺	
	4-24 hours	24-48 hours	4-24 hours	24-48 hours
0%	**	NS	NS	NS
0.5%	*	NS	**	NS
1%	NS	*	**	NS
1.5%	NS	**	**	NS

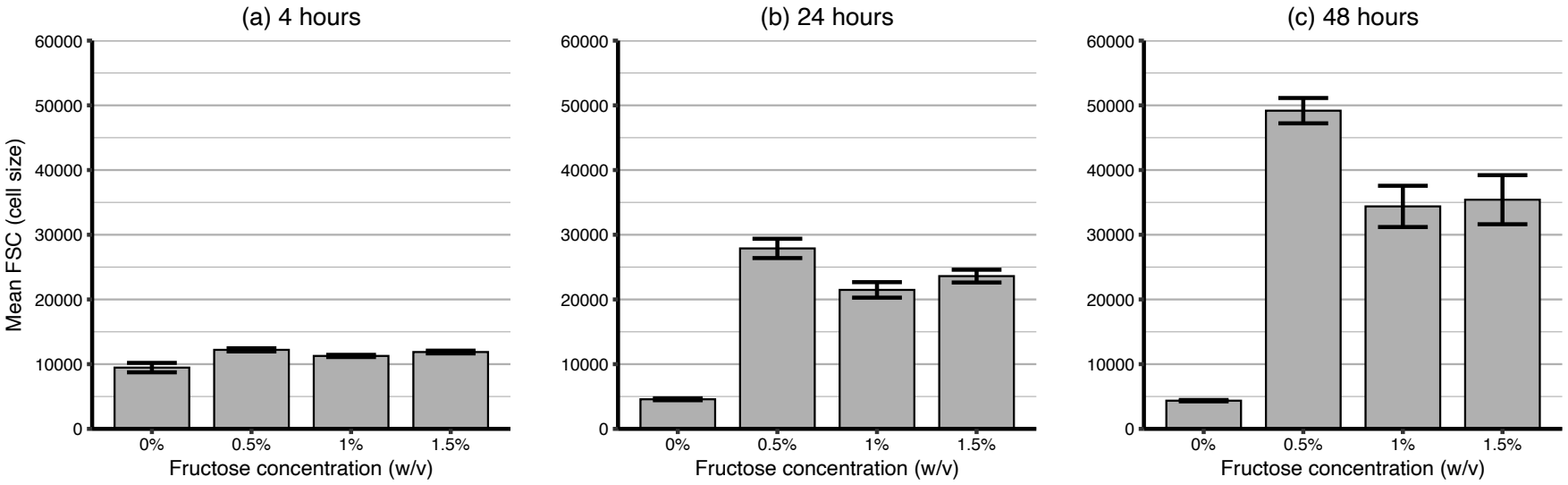
Figure 3.28 - Graphs and statistical analysis of the mean P-546 fluorescence (P3HB) of the P3HB⁺ and P3HB⁺⁺ *C. necator* populations when grown in 0.08% (w/v) ME and supplemented with 0%, 0.5%, 1% and 1.5% (w/v) fructose. The mean P-546 fluorescence of cells in the P3HB⁺ and P3HB⁺⁺ populations at 4 (a), 24 (b) and 48 hours (c) is analysed statistically using unpaired t-tests to compare conditions at the same time point (d). Additional statistical analysis was performed using a paired t-test to compare the same condition at different time points (e). NS = non-significant ($p \geq 0.05$), * = $p < 0.05$, ** = $p \leq 0.01$, *** = $p \leq 0.001$, **** = $p \leq 0.0001$, ***** = $p \leq 0.00001$. Error bars represent SD. n = 3 biological replicates. The full data can be found in Figure 8.10 (e) and (f), Appendix 8.5.

3.5.5 Increasing fructose concentration has little impact on cell size

Figure 3.29 contains a summary of mean FSC for 0.08% (w/v) ME cultures supplemented with either 0%, 0.5%, 1% or 1.5% (w/v) fructose at 4 (Figure 3.29 (a)), 24 (Figure 3.29 (b)) and 48 hours (Figure 3.29 (c)) timepoints. The full data can be found in Figure 8.11(a) and (b), Appendix 8.5.

Comparisons between media conditions at each time point in Figure 3.29 (d) showed that at 4, 24 and 48 hours, *C. necator* cells in cultures supplemented with 0.5%, 1% and 1.5% (w/v) fructose were significantly larger than cultures containing only ME. At 24 and 48 hours the difference between fructose-supplemented samples and non-supplemented was much greater. In addition, at each time point 1% and 1.5% (w/v) fructose cultures contained significantly smaller cells in comparison to cultures with 0.5% (w/v) fructose. Statistical comparisons between time points showed that only 0.5% (w/v) samples significantly increased between 4 and 24 hours whereas all conditions were non-significantly different between 24 and 48 hours.

Figure 3.30 contains a fluorescent microscope image for each condition at 54 hours. In the cells of cultures that were fructose-supplemented, P3HB granules are visible along with Z-ring structures indicating the cells are in the process of division (Du and Lutkenhaus, 2019). This is in contrast to Figure 3.13 in which no dark regions resembling P3HB granules were observed. The dark globular regions are a typical hallmark of bacteria accumulating intracellular P3HB and have been observed in previous research (Hermawan and Jendrossek, 2007; Beeby *et al.*, 2011; Kawashima *et al.*, 2015). Previous research has suggested that an increased bacterial growth rate can lead to a larger cell size during cell proliferation (Sharpe *et al.*, 1998; Sperber and Herman, 2017; Zhang *et al.*, 2020) and that the metabolism of key nutrients (Sperber and Herman, 2017) and C (Hill *et al.*, 2013) have regulatory roles in bacterial cell size. Results in this section at 4 hours show that mean FSC changed very little when fructose concentration increases. This is indicative of the growth rate being similar despite the fructose concentration increasing. In section 3.4.5 it was suggested that at 24 and 48 hours the increased osmolarity of fructose supplemented 0.2% (w/v) ME media in relation to fructose supplemented 0.08% (w/v) ME may be due to residual nutrients left over from the more nutritious 0.2% (w/v) ME. In the current section, no significant difference in cell size was recorded suggesting that the osmolarity may have been similar in each fructose supplement culture.



(d)

Non-paired t-test comparing P-546 fluorescence (P3HB) for each condition at 4, 24 and 48 hours.				
Fructose concentration (w/v) comparison		4 hours	24 hours	48 hours
0%	0.5%	***	***	*
0%	1%	*	**	***
0%	1.5%	***	**	**
0.5%	1%	NS	NS	NS
0.5%	1.5%	*	NS	NS
1%	1.5%	NS	NS	NS

(e)

Paired t-test comparing P-546 fluorescence (P3HB) between 4 and 24, and 24 and 48 hours.		
Fructose concentration (w/v)	4-24 hours	24-48 hours
0%	**	NS
0.5%	*	NS
1%	NS	NS
1.5%	NS	NS

Figure 3.29 - Graphs and statistical analysis comparing the mean FSC of *C. necator* cultures grown in 0.08% (w/v) ME and supplemented with 0%, 0.5%, 1% and 1.5% (w/v) fructose. Mean FSC at 4 (a), 24 (b) and 48 hours (c) is analysed statistically using unpaired t-tests to compare conditions at the same time point (d). Additional statistical analysis was performed using a paired t-test in order to compare the same condition at different time points (e). NS = non-significant ($p \geq 0.05$), * = $p < 0.05$, ** = $p \leq 0.01$, *** = $p \leq 0.001$. Error bars represent SD. n = 3 biological replicates. The full data can be found in Figure 8.11 (a) and (b), Appendix 8.5.

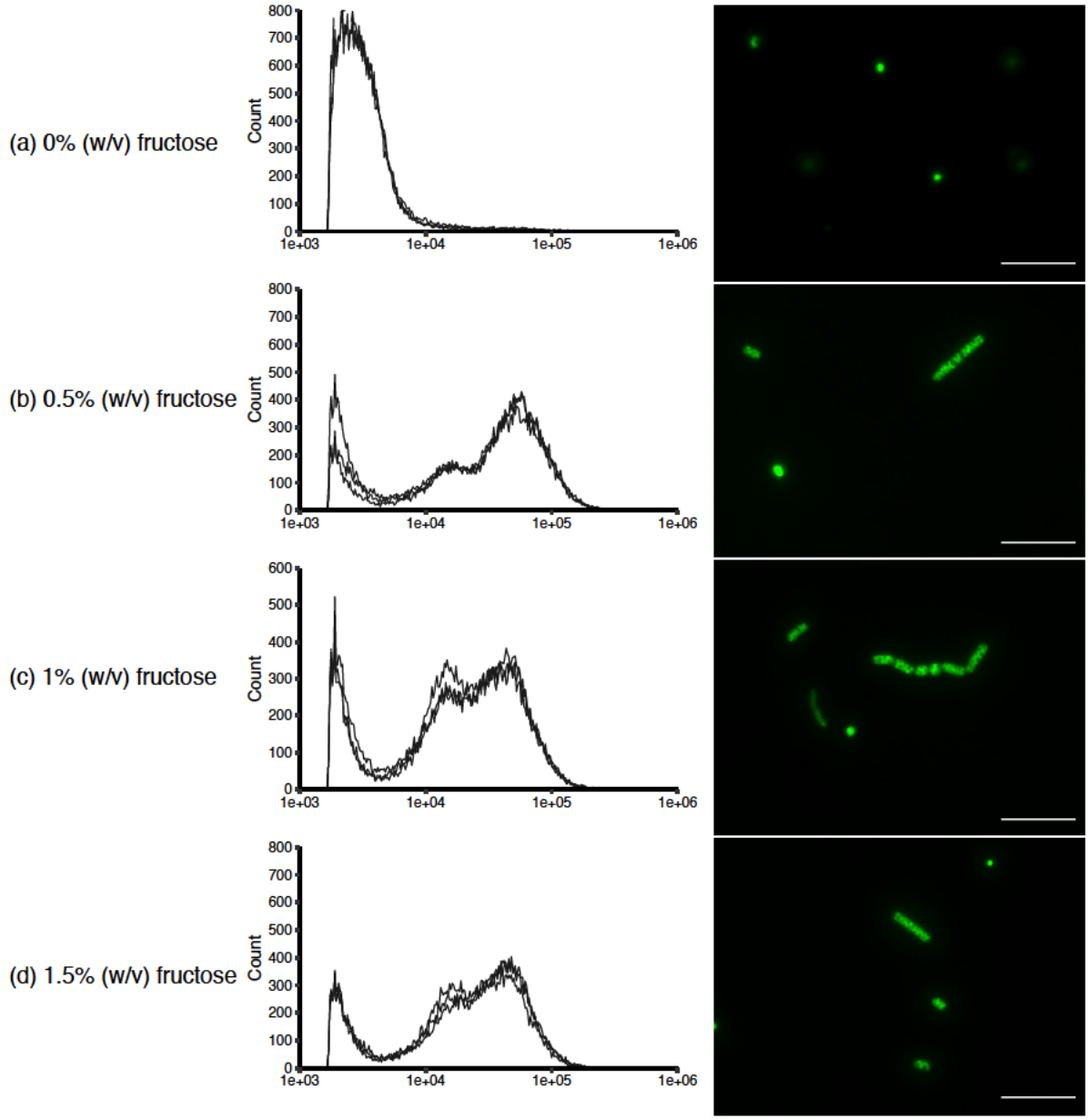


Figure 3.30 - Fluorescent microscopy images of cells after 54 hours of growth in 0.08% (w/v) ME supplemented with 0, 0.5, 1 and 1.5% (w/v) fructose. Cells were stained with SYTO9 (1.33 mM). Scale bars represent 2 μm.

3.5.6 Increasing fructose concentration above 0.5% (w/v) has little effect on cell size FSC

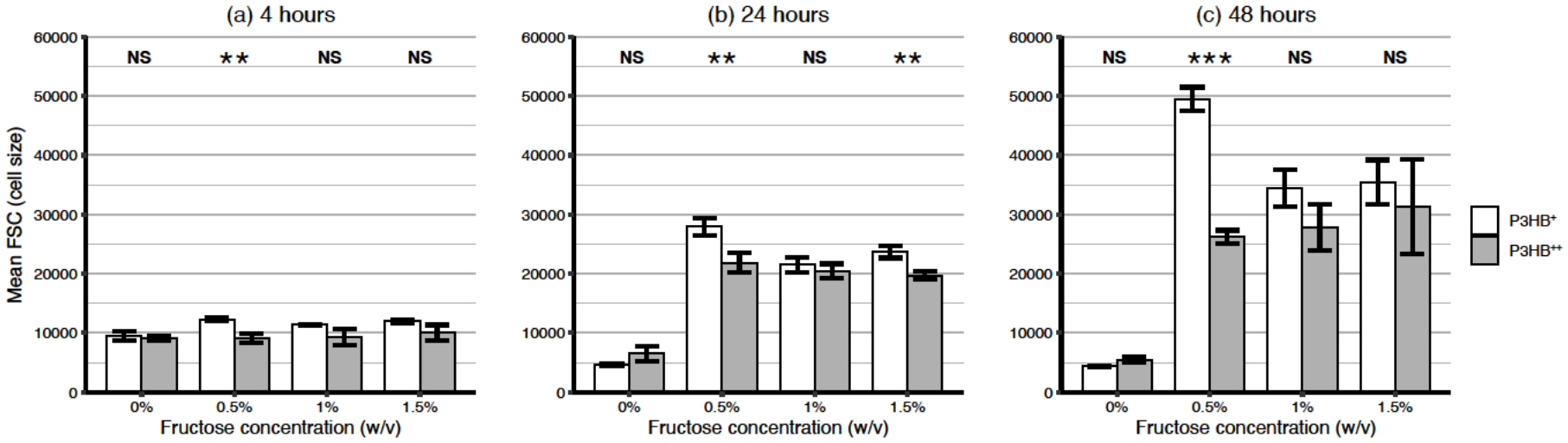
Figure 3.31 presents a summary of $PH3B^{+}$ and $PH3B^{++}$ FSC for *C. necator* cultures in which media contained 0.08% (w/v) ME supplemented with either 0%, 0.5%, 1% or 1.5% (w/v) fructose. The full data can be found in Figure 8.11(c) and (d), Appendix 8.5.

Statistical analysis comparing cell size at 4 (Figure 3.31 (a)), 24 (Figure 3.31 (b)) and 48 hours (Figure 3.31 (c)) revealed that 0.5% (w/v) fructose addition was the only condition tested in which $P3HB^{+}$ cells were significantly larger than that of the $P3HB^{++}$ population at 4, 24 and 48 hours. For all other conditions tested at each time point the difference between $P3HB^{+}$ and $P3HB^{++}$ populations was not significant except for 1.5% (w/v) fructose-supplementation at 24 hours at which point $P3HB^{+}$ cells were also larger than $P3HB^{++}$ cells.

For the $P3HB^{+}$ population, statistical comparisons between conditions at the same time point (Figure 3.31 (d)) showed that 0.5% (w/v) fructose supplemented media produced the largest or joint largest $P3HB^{+}$ cells. Analysis over time presented in (Figure 3.31 (e)) showed that $P3HB^{+}$ cells progressively increased in cell size between 4 and 24, and 24 and 48 hours.

Statistical analysis comparing experimental conditions at each time point for the $P3HB^{++}$ population (Figure 3.31 (d)) showed that at 4 hours there was no significant difference between any of the conditions tested. At both 24 and 48 hours, 0.5%, 1% and 1.5 (w/v) fructose supplementations could not be separated based on $P3HB^{++}$ cells size but could be significantly separated for samples not containing fructose. Comparisons between time points (Figure 3.31 (e)) showed that for the 0.08% (w/v) ME without fructose addition, $P3HB^{++}$ cell size did not significantly change between time points. Cultures supplemented with 1% or 1.5% (w/v) fructose significantly increased $P3HB^{++}$ cell size between 4 and 24 hours although there was no significant difference between 24 and 48 hours. Samples supplemented with 0.5% (w/v) fructose were the only cultures to produce $P3HB^{++}$ cells that increased successively between 4 and 24, and 24 and 48 hours.

Previous results in this thesis have found $P3HB^{+}$ cells to commonly be larger than $P3HB^{++}$ cells or at least not significantly different. This trait has been aligned with the results of previous research *E. coli* by (Khlebodarova and Likoshvai, 2018) who report persister sub-populations to be smaller than that of the dominant phenotype. Generally, apart from cultures supplemented with 0.5% (w/v) fructose, there was little size difference between cells in the $P3HB^{+}$ and $P3HB^{++}$ populations. The reason for this is unclear but could be due to reasons such the formation of more cell chains in 0.5% (w/v) fructose-supplemented cultures, particularly at 48 hours.



(d)

Non-paired t-test comparing the FSC of the P3HB+ and P3HB++ populations at 4, 24 and 48 hours.

Fructose concentration (w/v) comparison		P3HB+			P3HB++		
		4 hours	24 hours	48 hours	4 hours	24 hours	48 hours
0%	0.5%	**	**	***	NS	***	****
0%	1%	NS	**	**	NS	***	*
0%	1.5%	*	***	**	NS	***	*
0.5%	1%	*	**	**	NS	NS	NS
0.5%	1.5%	NS	*	*	NS	NS	NS
1%	1.5%	*	NS	NS	NS	NS	NS

(e)

Paired t-test comparing the FSC of the P3HB+ and P3HB++ populations between 4 and 24, and 24 and 48 hours.

Media (w/v)	P3HB+		P3HB++	
	4-24 hours	24-48 hours	4-24 hours	24-48 hours
0%	**	*	NS	NS
0.5%	**	***	**	**
1%	**	*	*	NS
1.5%	**	*	**	NS

Figure 3.31 - Graphs and statistical analysis showing the mean FSC of the P3HB$^+$ and P3HB^{++} *C. necator* populations when grown in 0.08% (w/v) ME and supplemented with 0%, 0.5%, 1% and 1.5% (w/v) fructose. The FSC of cells in the P3HB$^+$ and P3HB^{++} populations at 4 (a), 24 (b) and 48 hours (c) is analysed statistically using unpaired t-tests to compare conditions at the same time point (d). Additional statistical analysis was performed using a paired t-test to compare the same condition at different time points (e). NS = non-significant ($p \geq 0.05$), * = $p < 0.05$, ** = $p \leq 0.01$, *** = $p \leq 0.001$, **** = $p \leq 0.0001$. Error bars represent SD. n = 3 biological replicates. The full data can be found in Figure 8.11(c) and (d), Appendix 8.5.

3.5.7 Discussion

Increasing fructose concentration above a concentration of 0.5% (w/v) does not increase OD_{600}. However, as OD_{600} increased for all conditions between 24 and 48 hours, and P3HB per cell did not increase, it's likely that fructose was still being directed into the Entner-Doudoroff pathway (Fleige *et al.*, 2011), and acetyl-CoA was still being directed into the citric acid cycle rather than P3HB biosynthesis (Ienczak *et al.*, 2011). Concentrations of fructose above 0.5% (w/v) are unlikely to result in inhibitory effects as fructose has been demonstrated to support high levels of *C. necator* growth at a concentration of 4% (w/v) (Azubuike *et al.*, 2020). Increasing fructose concentration also didn't increase the proportion of $P3HB^{++}$ cells in cultures. Results have so far demonstrated that the $P3HB^{++}$ population may be a persister cell population due to its low proportion in cultures and that $P3HB^{++}$ are typically smaller than the dominant $P3HB^{+}$ phenotype (Khlebodarova and Likoshvai, 2018). In this section, apart from cultures supplemented with 0.5% (w/v) fructose, there was little size difference between cells in the $P3HB^{+}$ and $P3HB^{++}$ populations. The reason for this is unclear but could be due to reasons such as the formation of more cell chains in 0.5% (w/v) fructose or differences in media osmolarity. Generally, there was no significant difference in cell size when increasing fructose concentration. Based on previous research, this may suggest that increasing fructose concentration does not increase the growth rate of *C. necator* in the current study (Sharpe *et al.*, 1998; Sperber and Herman, 2017; Zhang *et al.*, 2020).

3.6 *Cupriavidus necator* grown in 0.08% (w/v) ME with 0%, 0.6,% 1.2% and 1.6% (w/v) sodium gluconate.

In sections 3.4 and 3.5 fructose and ME were tested at varying concentrations in order to test the effects of reducing the ME to fructose ratio. The reduction in this ratio led to an increase in mean FSC which was sustained until the end of the experiment but was unable to induce a high level of P3HB production exceeding a value of 10,000 for mean P-546 fluorescence per cell. In this section, a different C source sodium gluconate is used as a media supplement. The supplementation of sodium gluconate has been shown to induce up to 70% of DCW P3HB when used at concentrations as high as 3% (w/v) (Henrich *et al.*, 2012). In the current study initial sodium gluconate concentrations of 0.6%, 1.1% and 1.6% (w/v) were used which equates to the same number of C atoms contained in 0.5%, 1% and 1.5% (w/v) fructose, respectively.

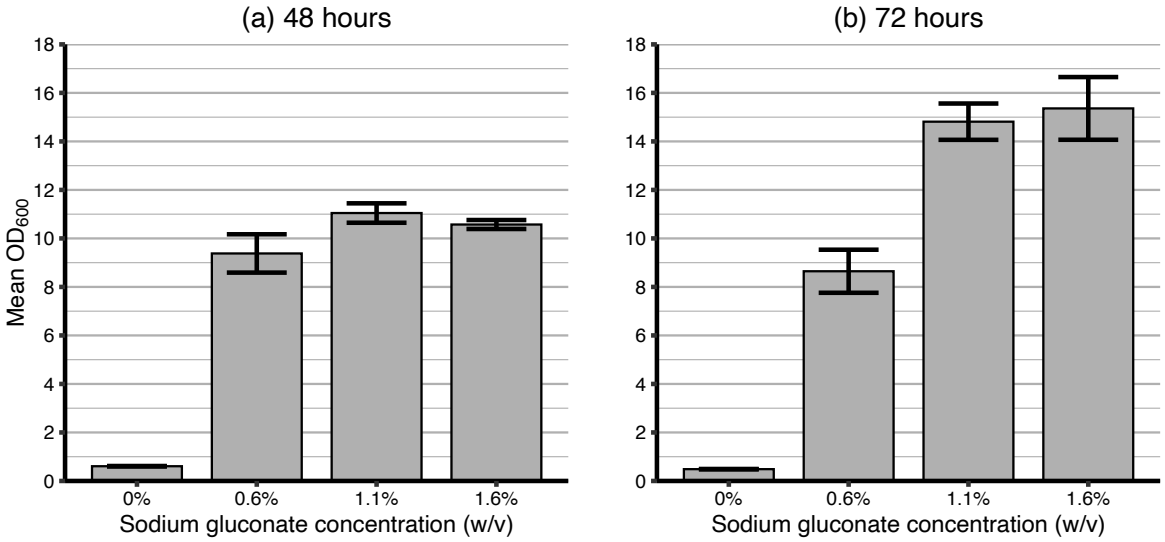
3.6.1 At 48 hours,1.1 and 1.6% (w/v) sodium gluconate supplementation leads to higher OD_{600} values than fructose-supplemented cultures

Figure 3.32 presents a summary of OD_{600} data for *C. necator* cultures containing 0.08% (w/v) supplemented with 0%, 0.6%, 1.1% or 1.6% (w/v) sodium gluconate at 48 (Figure 3.32 (a)) and 72 hours (Figure 3.32 (b)). The full data can be found in Figure 8.12, Appendix 8.6.

Statistical comparisons between conditions at each time point (Figure 3.32 (c)) showed that media supplemented with sodium gluconate increased OD_{600} at both 48 and 72 hours. At 48 hours, measurements of OD_{600} for cultures containing 0.6%, 1.1% and 1.6% (w/v) sodium gluconate were similar with the only statistical difference occurring between cultures supplemented with 1.1% and 0.6% (w/v) sodium gluconate. At 72 hours, cultures containing 1.1% and 1.6% (w/v) sodium gluconate were significantly more optically dense than 0.6% cultures. Statistical analysis over time (Figure 3.32 (d)) showed that between 48 and 72 hours, 0.6% cultures did not significantly increase in OD_{600} whereas 1.1% and 1.6% cultures did increase.

Figure 3.33 compares fructose supplementation (Figure 3.33 (a)) in 0.08% (w/v) ME to that of sodium gluconate (Figure 3.33 (b)). The full combined data can be viewed in Figure 8.15, Appendix 8.7. Statistical comparisons between each fructose or sodium gluconate condition in Figure 3.33 (c) showed that non-supplemented media, which are the same, in the sodium gluconate experiment was slightly greater than that of the fructose experiment. The reason for this difference is unfortunately unclear and raises concerns that a batch effect could be influencing data. Analysis between conditions also found that 1.1% and 1.6% (w/v) sodium gluconate supplementation significantly increased OD_{600} in comparison to fructose-containing cultures while 0.6% supplementation could not be statistically distinguished from any of the fructose-containing cultures.

In similarity to fructose-supplemented cultures presented in section 3.5.1, cultures containing 1.1% and 1.6% (w/v) sodium gluconate were observed to increase in OD_{600} suggesting that gluconate was still being processed by the Entner-Doudoroff pathway and that acetyl-CoA was still entering the citric acid cycle. Thus, only 0.6% (w/v) sodium gluconate showed evidence of P3HB accumulating conditions by not increasing in OD_{600} between 48 and 72 hours. Comparisons between fructose and sodium gluconate-supplemented cultures show that similar OD_{600} results were observed, although results are discussed further in this section due to P3HB and cell size possibly influencing the OD_{600} of sodium gluconate-supplemented cultures.



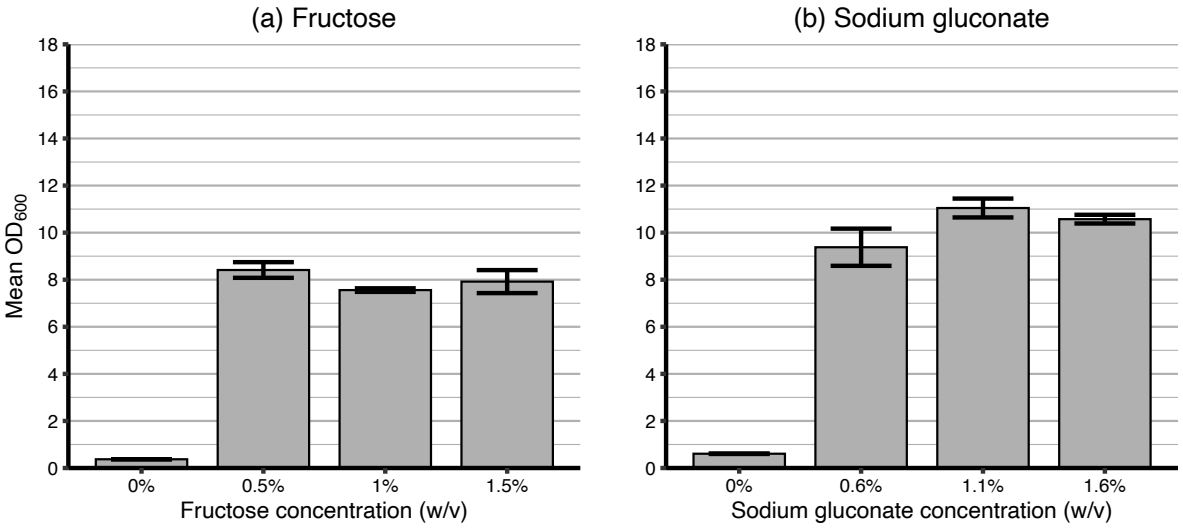
(c)

Non-paired t-test comparing the mean OD_{600} for each condition at 4, 48 and 72 hours.			
Sodium gluconate concentration (w/v) comparison		48 hours	72 hours
0%	0.6%	**	**
0%	1.1%	***	***
0%	1.6%	***	**
0.6%	1.1%	*	***
0.6%	1.6%	NS	**
1.1%	1.6%	NS	NS

(d)

Paired t-test comparing the mean OD_{600} between 4 and 48 hours, and 48 and 72 hours.	
Sodium gluconate concentration (w/v)	48-72 hours
0%	**
0.6%	NS
1.1%	*
1.6%	*

Figure 3.32 - Graphs and statistical analysis showing the OD_{600} of 0.08% (w/v) ME *C. necator* cultures supplemented with 0%, 0.6%, 1.1% or 1.6% (w/v) sodium gluconate. Statistical analysis was performed using unpaired t-tests to compare individual sodium gluconate concentrations at the same time point (c) and paired t-tests to compare the same condition at different time points (d). NS = non-significant ($p \geq 0.05$), * = $p \leq 0.05$, ** = $p \leq 0.01$, *** = $p \leq 0.001$. Error bars represent SD. n = 3 biological replicates. The full data can be found in Figure 8.12, Appendix 8.6.



(c)

Non-paired t-test comparing OD_{600} for fructose and sodium gluconate supplementation at 48 hours.

Fructose/sodium gluconate comparison (w/v)		48 hours	Fructose/sodium gluconate comparison (w/v)		48 hours
0%	0%	***	1%	0%	****
0%	0.6%	**	1%	0.6%	NS
0%	1.1%	***	1%	1.1%	**
0%	1.6%	***	1%	1.6%	***
0.5%	0%	***	1.5%	0%	**
0.5%	0.6%	NS	1.5%	0.6%	NS
0.5%	1.1%	***	1.5%	1.1%	**
0.5%	1.6%	**	1.5%	1.6%	***

Figure 3.33 - Graphs and statistical analysis comparing the OD_{600} at 48 hours of 0.08% (w/v) ME *C. necator* cultures supplemented with either 0%, 0.5%, 1% or 1.5% (w/v) fructose, or 0%, 0.6%, 1.1% or 1.6% (w/v) sodium gluconate. Plot (a) displays the OD_{600} of fructose-supplemented cultures and plot (b) that of sodium gluconate. Non-paired t-tests were used to compare each fructose and sodium gluconate supplementation (c). NS = non-significant ($p \geq 0.05$), * = $p \leq 0.05$, ** = $p \leq 0.01$, *** = $p \leq 0.001$, **** = $p \leq 0.0001$. Error bars represent SD. n = 3 biological replicates. The full combined data can be viewed in Figure 8.15, Appendix 8.7.

3.6.2 Sodium gluconate media supplementation leads to significantly more P3HB than fructose at 48 hours

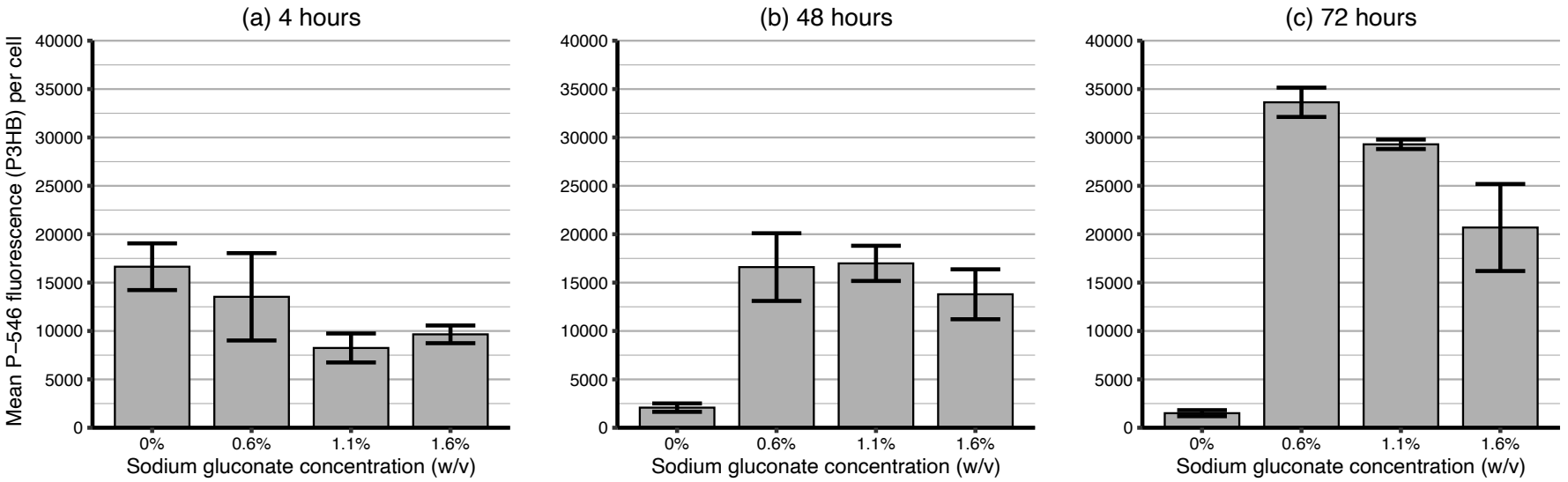
A summary of P-546 fluorescence per cell (P3HB) for 0.08% (w/v) ME *C. necator* cultures supplemented with 0%, 0.6%, 1.1% or 1.6% (w/v) sodium gluconate can be found in Figure 3.34. The full data can be found in Figure 8.13 (a) and (b), Appendix 8.6. Figure 3.34 (a) shows P-546 fluorescence at 4 hours, Figure 3.34 (b) at 48 hours and Figure 3.34 (c) at 72 hours. Figure 3.34 (d) contains statistical comparisons between conditions at each time point.

At 4 hours, intracellular P3HB did not significantly increase when sodium gluconate was added to 0.08% (w/v) ME. In contrast, at 48 hours, all sodium gluconate-supplemented cultures contained significantly more P3HB than non-supplemented media. However, there was no significant difference in P3HB between 0.6%, 1.1% and 1.6% (w/v) sodium gluconate-containing cultures. By 72 hours, sodium gluconate supplementation still significantly increased P3HB in relation to cultures without, but 0.6% (w/v) sodium gluconate produced more P3HB than both 1.1% and 1.6% cultures.

Analysis over time (Figure 3.34 (e)) showed that cultures containing 0.08% (w/v) ME only decreased in P3HB between 4 and 48 and did not significantly change between 48 and 72 hours. Conversely, 0.6% (w/v) sodium gluconate cultures significantly increased only between 48 and 72 hours, whereas 1.1% cultures increased between both sets of time points. No statistical difference was found between either 4 and 48, or 48 and 72 hours, for cultures with 1.6% (w/v) sodium gluconate added.

Figure 3.35 compares the mean P-546 fluorescence at 48 hours of cultures supplemented with fructose (Figure 3.35 (a)) and that of sodium gluconate (Figure 3.35 (b)). The full data can be found in Figure 8.16 (a) and (b), Appendix 8.7.

Statistical comparisons in Figure 3.35 (c) show that at 48 hours, all sodium gluconate cultures produced more intracellular P3HB in *C. necator* than fructose. The reason for this may be due to the presence of sodium ions in sodium gluconate. In bacteria, sodium ions are known to provide an important link across the cell membrane (Dimroth, 1990). The transport of solutes and sugars can be facilitated using sodium ions to move against a concentration gradient via secondary membrane transporters (Henriquez *et al.*, 2021). It's possible that gluconate is transported more easily in comparison to fructose due to the presence of sodium ions in the media.



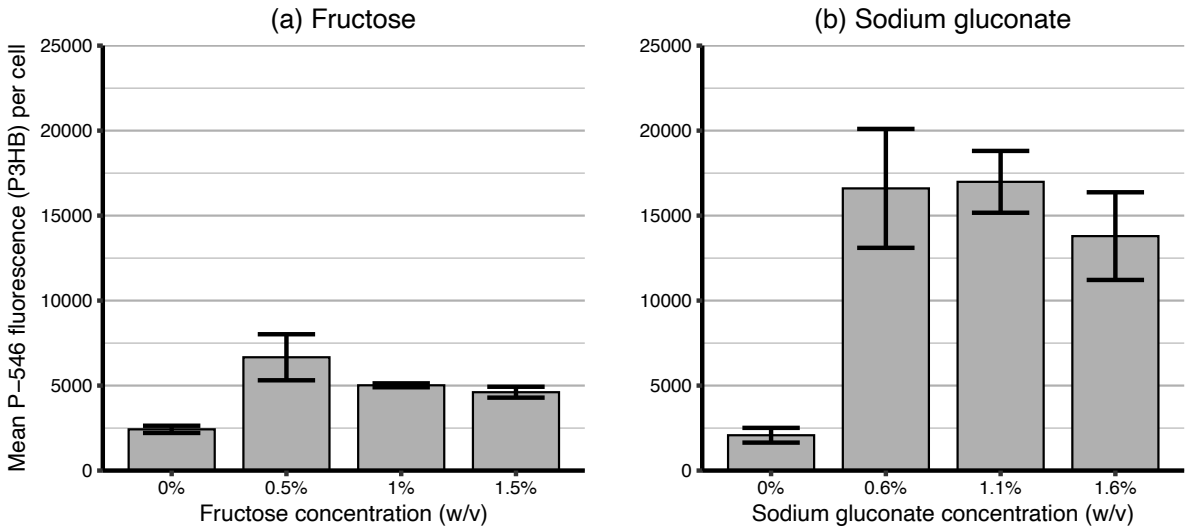
(d)

Non-paired t-test comparing the mean P-546 fluorescence per cell for each condition at 4, 48 and 72 hours.				
Sodium gluconate concentration (w/v) comparison		4 hours	48 hours	72 hours
0%	0.6%	NS	*	***
0%	1.1%	*	**	*****
0%	1.6%	*	*	*
0.6%	1.1%	NS	NS	*
0.6%	1.6%	NS	NS	*
1.1%	1.6%	NS	NS	NS

(e)

Paired t-test comparing the mean P-546 fluorescence per cell between 4 and 48 hours, and 48 and 72 hours.		
Sodium gluconate concentration (w/v)	4-48 hours	48-72 hours
0%	**	NS
0.6%	NS	*
1.1%	*	**
1.6%	NS	NS

Figure 3.34 - Graphs and statistical analysis summarising the mean P-546 fluorescence as a measure of intracellular P3HB of 0.08% (w/v) ME *C. necator* cultures supplemented with 0%, 0.6%, 1.1% or 1.6% (w/v) sodium gluconate. Statistical analysis was performed using unpaired t-tests to compare individual sodium gluconate concentrations at the same time point (c) and paired t-tests to compare the same condition at different time points (d). NS = non-significant ($p \geq 0.05$), * = $p \leq 0.05$, ** = $p \leq 0.01$, *** = $p \leq 0.001$, **** = $p \leq 0.0001$, ***** = $p \leq 0.00001$. Error bars represent SD. n = 3 biological replicates. The full data can be found in Figure 8.13, Appendix 8.6.



(c)

Non-paired t-test comparing P-546 fluorescence (P3HB) per cell for fructose and sodium gluconate supplementation at 48 hours.

Fructose/sodium gluconate comparison (w/v)		48 hours	Fructose/sodium gluconate comparison (w/v)		48 hours
0%	0%	NS	1%	0%	**
0%	0.6%	*	1%	0.6%	*
0%	1.1%	**	1%	1.1%	**
0%	1.6%	*	1%	1.6%	*
0.5%	0%	*	1.5%	0%	**
0.5%	0.6%	*	1.5%	0.6%	*
0.5%	1.1%	**	1.5%	1.1%	**
0.5%	1.6%	*	1.5%	1.6%	*

Figure 3.35 - Graphs and statistical analysis comparing P-546 fluorescence as a measure of intracellular P3HB at 48 hours for 0.08% (w/v) ME *C. necator* cultures supplemented with either 0%, 0.5%, 1% or 1.5% (w/v) fructose, or 0%, 0.6%, 1.1% or 1.6% (w/v) sodium gluconate. Plot (a) displays the data of fructose-supplemented cultures and plot (b) that of sodium gluconate. Non-paired t-tests were used to compare each fructose and sodium gluconate supplementation (c). NS = non-significant ($p \geq 0.05$), * = $p \leq 0.05$, ** = $p \leq 0.01$. Error bars represent SD. n = 3 biological replicates. The full data can be found in Figure 8.16, Appendix 8.7.

3.6.3 Cultures containing sodium gluconate produce more P3HB^{++} cells

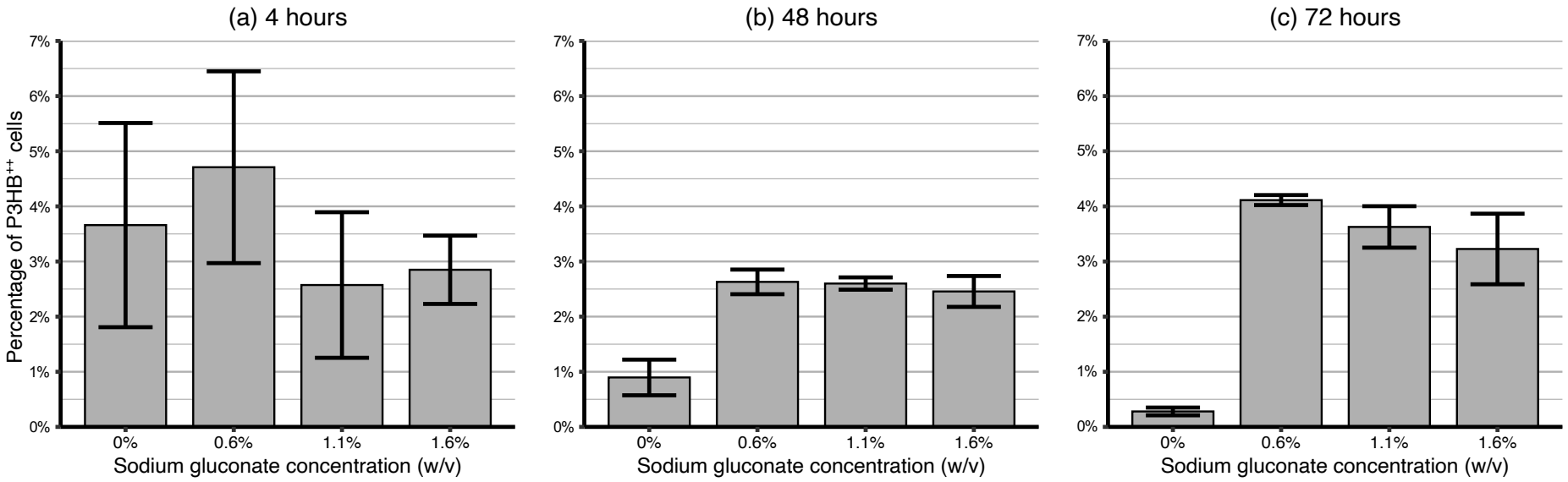
Figure 3.36 presents a summary of the percentage of P3HB^{++} cells at 4 (Figure 3.36 (a)), 48 (Figure 3.36 (b)), and 72 hours (Figure 3.36 (c)), in 0.08% (w/v) ME supplemented with 0%, 0.6%, 1.1% or 1.6% (w/v) sodium gluconate. The full data can be found in Figure 8.13 (c) and (d), Appendix 8.6.

Statistical analysis comparing conditions at each time point (Figure 3.36 (d)), showed that at 4 hours there was no significant difference between any of the conditions tested, with inconsistent P3HB^{++} populations once again causing a high degree of error. In contrast, at both 48 and 72 hours, the was a significant difference between supplemented and non-supplemented cultures, but no statistical difference between individually tested sodium gluconate concentrations.

Statistical analysis over time (Figure 3.36 (e)) found for all cultures there was no significant difference in the percentage of P3HB^{++} cells between 4 and 48 hours. The only cultures to significantly change were those containing 0.6% and 1.1% (w/v) sodium gluconate which increased the proportion of P3HB^{++} cells between 48 and 72 hours.

Figure 3.37 compares fructose addition (Figure 3.37(a)) (first presented in Figure 3.27(c)) to that of sodium gluconate (Figure 3.37(a)) at 48 hours. Statistical analysis (Figure 3.37(c)) showed that at 48 hours, cultures containing sodium gluconate produced significantly more P3HB^{++} cells than fructose supplemented 0.08% (w/v) ME cultures.

In the previous section, it was suggested that a higher amount of P3HB per cell produced when *C. necator* cultures were supplemented with sodium gluconate may have been due to sodium ions acting as a secondary transporter to facilitate the uptake of gluconate. Evidence in this section shows that a higher proportion of P3HB^{++} cells are produced when sodium gluconate is supplemented rather than fructose. While this would corroborate the theory that sodium ions increase the uptake of gluconate, an increase in the proportion of P3HB^{++} could be due to other factors such as lower cell division and more cell expansion in the P3HB^{+} population, for example.



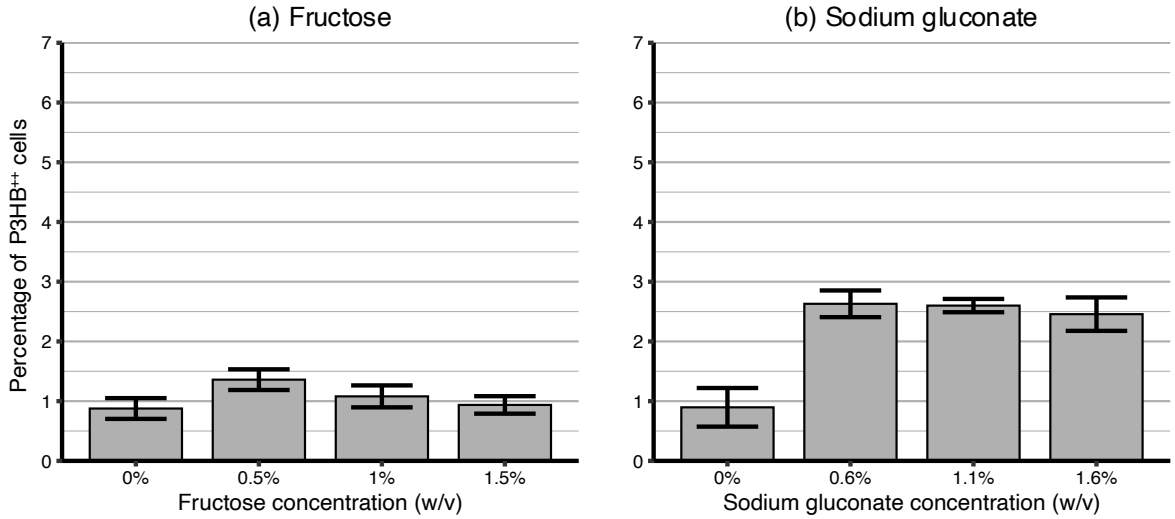
(d)

Non-paired t-test comparing the percentage of P3HB^{++} cells for each condition at 4, 48 and 72 hours.				
Sodium gluconate concentration (w/v) comparison		4 hours	48 hours	72 hours
0%	0.6%	NS	**	*****
0%	1.1%	NS	*	**
0%	1.6%	NS	**	*
0.6%	1.1%	NS	NS	NS
0.6%	1.6%	NS	NS	NS
1.1%	1.6%	NS	NS	NS

(e)

Paired t-test comparing the percentage of P3HB^{++} cells between 4 and 48 hours, and 48 and 72 hours.		
Sodium gluconate concentration (w/v)	4-24 hours	48-72 hours
0%	NS	NS
0.6%	NS	*
1.1%	NS	*
1.6%	NS	NS

Figure 3.36 - Graphs and statistical analysis summarising the mean percentage of P3HB^{++} cells in 0.08% (w/v) ME *C. necator* cultures supplemented with 0%, 0.6%, 1.1% or 1.6% (w/v) sodium gluconate. Statistical analysis was performed using unpaired t-tests to compare individual sodium gluconate concentrations at the same time point (c) and paired t-tests to compare the same condition at different time points (d). NS = non-significant ($p \geq 0.05$), * = $p \leq 0.05$, ** = $p \leq 0.01$, *** = $p \leq 0.001$, **** = $p \leq 0.0001$, ***** = $p \leq 0.00001$. Error bars represent SD. n = 3 biological replicates.



(c)

Non-paired t-test comparing the percentage of P3HB^{++} cells for fructose and sodium gluconate supplemented cultures at the 48 hour time point.

Fructose/sodium gluconate comparison (w/v)		48 hours	Fructose/sodium gluconate comparison (w/v)		48 hours
0%	0%	NS	1%	0%	NS
0%	0.6%	***	1%	0.6%	***
0%	1.1%	***	1%	1.1%	**
0%	1.6%	**	1%	1.6%	**
0.5%	0%	NS	1.5%	0%	NS
0.5%	0.6%	**	1.5%	0.6%	**
0.5%	1.1%	**	1.5%	1.1%	****
0.5%	1.6%	*	1.5%	1.6%	**

Figure 3.37 - Graphs and statistical analysis comparing the percentage of P3HB^{++} cells at 48 hours for 0.08% (w/v) ME *C. necator* cultures supplemented with either 0%, 0.5%, 1% or 1.5% (w/v) fructose, or 0%, 0.6%, 1.1% or 1.6% (w/v) sodium gluconate. Plot (a) displays the data of fructose-supplemented cultures and plot (b) that of sodium gluconate. Non-paired t-tests were used to compare each fructose and sodium gluconate supplementation (c). NS = non-significant ($p \geq 0.05$), * = $p < 0.05$, ** = $p \leq 0.01$, *** = $p \leq 0.001$, **** = $p \leq 0.0001$. Error bars represent SD. n = 3 biological replicates.

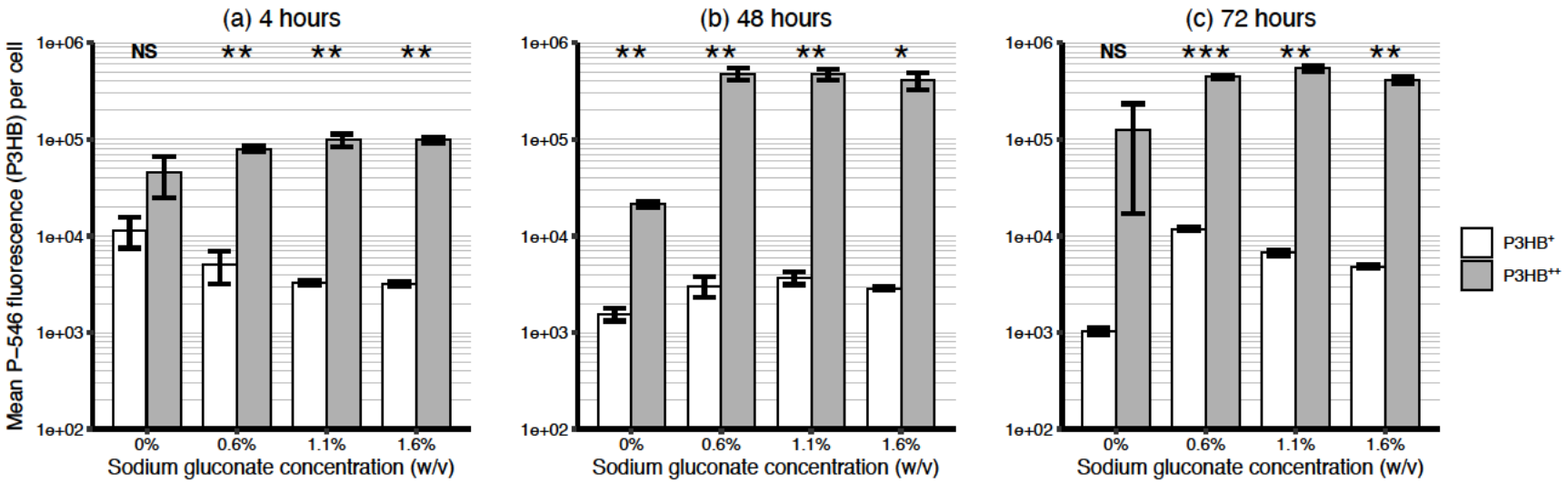
3.6.4 Concentration of 0.6% and 1.1% (w/v) sodium gluconate produce increase P3HB per cell in the P3HB^{++} population

Figure 3.38 contains a summary of P-546 fluorescence (P3HB) at 4 (Figure 3.38 (a)), 48 (Figure 3.38 (b)), and 72 hours (Figure 3.38 (c)), for P3HB^{+} and P3HB^{++} cell populations for 0.08% (w/v) ME *C. necator* cultures supplemented with 0%, 0.6%, 1.1% or 1.6% (w/v) sodium gluconate. The full data can be found in Figure 8.13 (e) and (f), Appendix 8.6.

Statistical analysis between conditions at each time point (Figure 3.38 (d)) showed that at 4 hours there was no significant difference between any of the conditions tested for the P3HB^{+} population. At 48 hours 1.1% and 1.6% (w/v) sodium gluconate addition significantly increased P3HB in the P3HB^{+} population in comparison to non-supplemented cultures. At 48 hours, the P3HB^{+} population of sodium gluconate-supplemented cultures was significantly greater in P3HB than non-supplemented cultures and 0.6% cultures contained more P3HB than both 1.1% and 1.6% cultures. Comparisons between time points (Figure 3.38 (e)) showed that for all sodium gluconate supplemented cultures there was no significant difference in P3HB^{+} P3HB between 4 and 48 hours, but between 48 and 72 hours the P3HB^{+} population in all supplemented cultures increased in P3HB.

For the P3HB^{++} population comparisons between experimental conditions (Figure 3.38 (d)) showed that at 4 hours only 0% and 1%, and 0.6% and 1.6% (w/v) sodium gluconate comparisons were significantly different. At 48 hours, sodium gluconate supplementation significantly increased intracellular P3HB in the P3HB^{++} population in relation to media without. This was also the case at 48 hours although 1.1% (w/v) sodium gluconate produced significantly more P3HB in the P3HB^{++} population in comparison to 0.6% cultures but not 1.6% cultures. Analysis between time points (Figure 3.38 (e)) for the P3HB^{++} population showed that while 0.6% and 1.6% (w/v) sodium gluconate supplementation increased P3HB in the P3HB^{++} population between 4 and 48 hours but not between 48 and 72 hours, 1.1% cultures increased between both sets of time points.

Figure 3.39 compares fructose (Figure 3.39 (a)) and sodium gluconate (Figure 3.39 (b)) supplementation at the 48-hour time point. The full data can be found in Figure 8.17, Appendix 8.7. Comparisons for the P3HB^{+} population (Figure 3.39 (c)) show that results, in this case, were mixed in terms of statistically significant differences. In contrast, sodium gluconate-supplemented cultures contained P3HB^{++} cells with more intracellular P3HB than those supplemented with fructose, except for 1.6% (w/v) sodium gluconate addition which was not significantly different to all fructose concentrations tested.



(d)

Non-paired t-test comparing mean P-546 fluorescence of the P3HB+ and P3HB++ populations at 4, 48 and 72 hours.

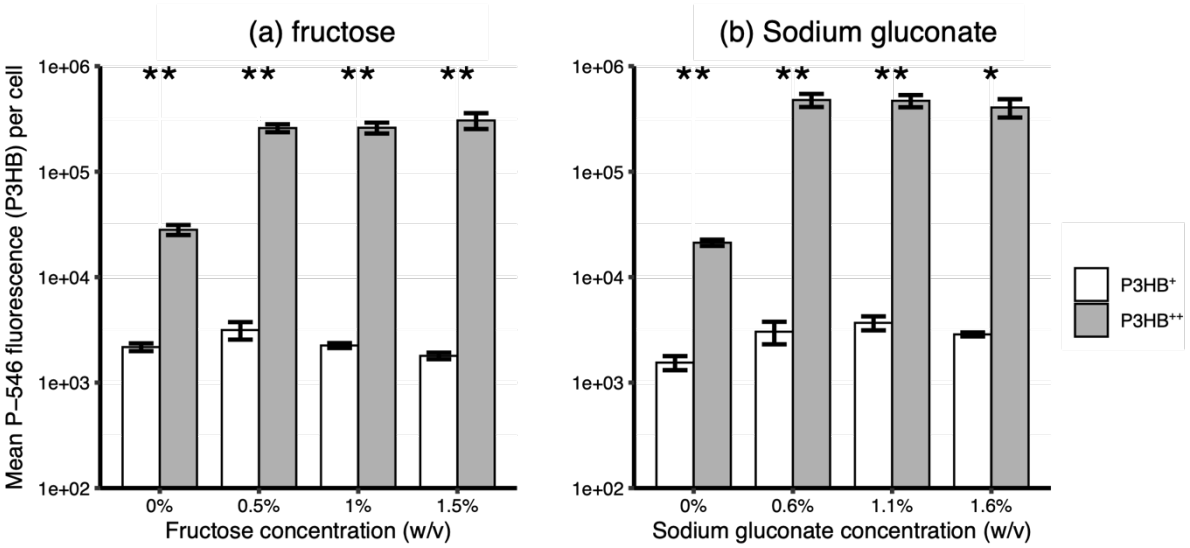
Sodium gluconate concentration (w/v) comparison		P3HB+			P3HB++		
		4 hours	48 hours	72 hours	4 hours	48 hours	72 hours
0%	0.6%	NS	NS	***	NS	**	*
0%	1.1%	NS	**	**	*	**	*
0%	1.6%	NS	**	***	NS	*	*
0.6%	1.1%	NS	NS	***	NS	NS	*
0.6%	1.6%	NS	NS	***	*	NS	NS
1.1%	1.6%	NS	NS	**	NS	NS	NS

(e)

Paired t-test comparing mean P-546 fluorescence (P3HB) of the P3HB+ and P3HB++ populations between 4 and 24, and 24 and 72 hours.

Sodium gluconate concentration (w/v)	P3HB+		P3HB++	
	4-48 hours	48-72 hours	4-48 hours	48-72 hours
0%	*	*	NS	NS
0.6%	NS	**	**	NS
1.1%	NS	*	**	*
1.6%	NS	**	*	NS

Figure 3.38 - Graphs and statistical analysis summarising the mean P-546 fluorescence as a measure of intracellular P3HB for the P3HB+ and P3HB++ populations in 0.08% (w/v) ME *C. necator* cultures supplemented with 0%, 0.6%, 1.1% or 1.6% (w/v) sodium gluconate. Statistical analysis was performed using unpaired t-tests to compare individual sodium gluconate concentrations at the same time point (d) and paired t-tests to compare the same condition at different time points (e). NS = non-significant ($p \geq 0.05$), * = $p \leq 0.05$, ** = $p \leq 0.01$, *** = $p \leq 0.001$. Error bars represent SD. n = 3 biological replicates.



(c)

Non-paired t-test comparing the P-546 fluorescence of the P3HB+ population for fructose and sodium gluconate supplemented cultures at the 4 8hour time point.					
Fructose/sodium gluconate comparison (w/v)		48 hours	Fructose/sodium gluconate comparison (w/v)		48 hours
0%	0%	*	1%	0%	*
0%	0.6%	NS	1%	0.6%	NS
0%	1.1%	*	1%	1.1%	*
0%	1.6%	**	1%	1.6%	**
0.5%	0%	*	1.5%	0%	NS
0.5%	0.6%	NS	1.5%	0.6%	NS
0.5%	1.1%	NS	1.5%	1.1%	*
0.5%	1.6%	NS	1.5%	1.6%	***

(d)

Non-paired t-test comparing the P-546 fluorescence of the P3HB++ population for fructose and sodium gluconate supplemented cultures at the 4 8hour time point.					
Fructose/sodium gluconate comparison (w/v)		48 hours	Fructose/sodium gluconate comparison (w/v)		48 hours
0%	0%	NS	1%	0%	**
0%	0.6%	**	1%	0.6%	*
0%	1.1%	**	1%	1.1%	*
0%	1.6%	*	1%	1.6%	NS
0.5%	0%	**	1.5%	0%	*
0.5%	0.6%	*	1.5%	0.6%	*
0.5%	1.1%	*	1.5%	1.1%	*
0.5%	1.6%	NS	1.5%	1.6%	NS

Figure 3.39 - Graphs and statistical analysis comparing P-546 fluorescence as a measure of intracellular P3HB for the P3HB+ and P3HB++ populations at 48 hours for 0.08% (w/v) ME *C. necator* cultures supplemented with either 0%, 0.5%, 1% or 1.5% (w/v) fructose, or 0%, 0.6%, 1.1% or 1.6% (w/v) sodium gluconate. Plot (a) displays the data of fructose-supplemented cultures and plot (b) that of sodium gluconate. Non-paired t-tests were used to compare each fructose and sodium gluconate supplementation (c). NS = non-significant ($p \geq 0.05$), * = $p \leq 0.05$, ** = $p \leq 0.01$, *** = $p \leq 0.001$. Error bars represent SD. n = 3 biological replicates.

3.6.5 Sodium gluconate-supplemented cultures produce larger cells than fructose supplemented

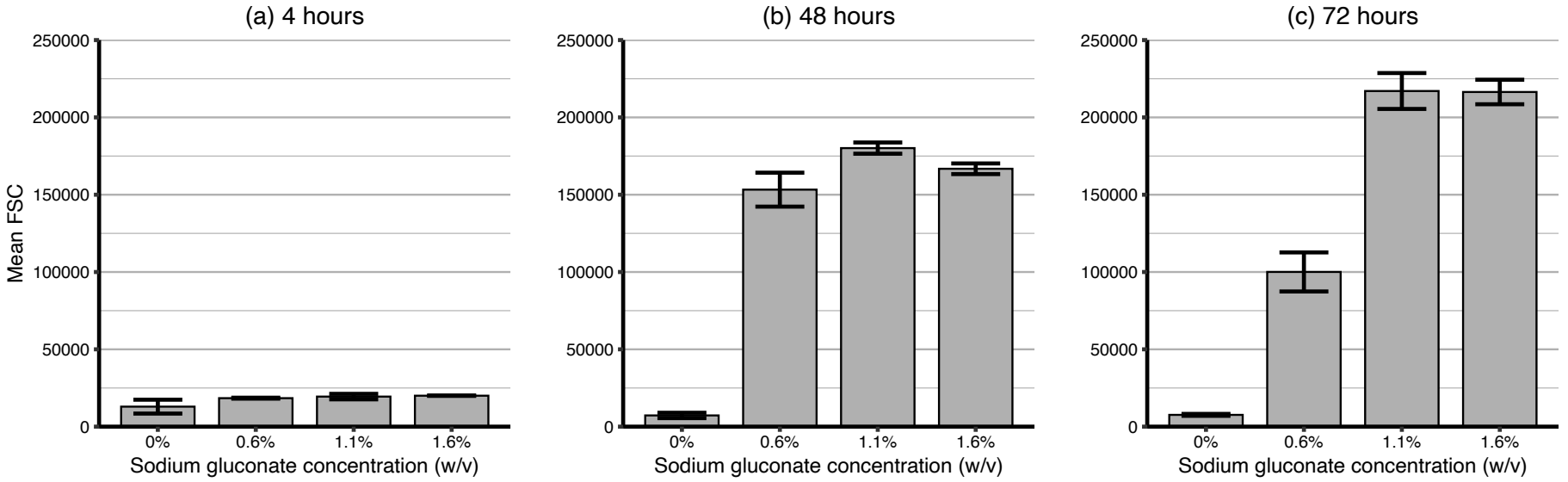
Figure 3.40 contains summaries at 4 (Figure 3.40 (a)), 48 (Figure 3.40 (b)) and 72 hours (Figure 3.40 (c)) of FSC as a gauge of cell size for 0.08% (w/v) ME *C. necator* cultures supplemented with 0%, 0.6%, 1.1% or 1.6% (w/v) sodium gluconate. The full data can be found in Figure 8.14 (a) and (b), Appendix 8.6.

Statistical analysis between conditions at the same time point (Figure 3.40 (d)) showed that at 4 hours cultures were largely non-significantly different in terms of cell size, except for 0.6% and 1.6% (w/v) sodium gluconate comparisons. At 48 hours supplemented cultures contained considerably larger cells than media that contained only ME. A slight decrease in cell size was observed in cultures containing 1.6% (w/v) sodium gluconate compared to 1.1%. At 72 hours supplemented cultures were still significantly larger than non-supplemented, but cultures which initially contained 0.6% (w/v) sodium gluconate were considerably smaller than that of 1.1% and 1.6%. Analysis over time (Figure 3.40 (e)) showed that cultures containing 0.6% (w/v) sodium gluconate increased in mean cell size between 4 and 48 hours but decreased between 48 and 72 hours. Cultures containing 1.1% (w/v) sodium gluconate increased only between 4 and 48 hours while 1.6% (w/v) cultures increased in mean cell size between both sets of time points.

In Figure 3.41, fluorescent microscope images show examples of the much-enlarged cells containing P3HB granules, both in terms of length and width of *C. necator* cells produced when cultures were supplemented with sodium gluconate. Additionally shown in Figure 3.41 (a), is a new *C. necator* phenotype previously not observed in this study, consisting of long thin cells aggregated together. Previous literature Hermawan and Jendrossek, 2007; Beeby *et al.*, 2011; Kawashima *et al.*, 2015) have demonstrated that PHA granules appear as dark globular structures which do not stain with nucleic acid stains. These cells could also be seen to contain non-stained P3HB inclusions which appeared to be larger than that previously observed in Figure 3.13, which had no visible granules, and Figure 3.30 in which small granules were observed. While the results for P3HB per cell (Figure 3.35) demonstrate that sodium gluconate supplementation results in greater P3HB per cell than fructose supplementation, there was concern that the results for sodium gluconate supplementation in Figure 3.35 did not represent what was observed to be a considerable increase in P3HB observed microscopically. Previous research indicated that temperature staining time and P-546 concentration can affect P-546 fluorescence during flow cytometry experiments. (Karmann *et al*. (2016). It is therefore possible that, in the current study using flow cytometry method 1, P-546 was not penetrating effectively into P3HB granules. This possibility is explored in section Figure 3.7.

Figure 3.42 compares at 48-hour time points, the mean FSC of *C. necator* cultures supplemented either with fructose (Figure 3.42 (a)) or sodium gluconate (Figure 3.42 (b)). The full data can be found in Figure 4.10 (a) and (b), Appendix 8.7. Statistical analysis summarised in Figure 3.42 (c) showed that at 48 hours *C. necator* cultures supplemented with sodium gluconate were considerably larger than cells produced when 0.08% (w/v) ME was supplemented with fructose.

In section 3.6.2, it was suggested that in comparison to that of fructose, sodium gluconate supplementation may produce more P3HB per cell due to sodium ions facilitating the movement of gluconate across the cell membrane via secondary transport proteins (Henriquez *et al.*, 2021). This is a theory which also provides an indication of which sodium gluconate supplementation increases *C. necator* cell size. The addition of sodium chloride to bacterial cultures has been reported in literature to stop cell proliferation and induce an increase in cell volume (Vijaranakul *et al.*, 1995; Piuri *et al.*, 2012). Organic acid ions are known to influence bacterial cell growth (Warnecke and Gill, 2005) and there is an established link between bacterial cell size, membrane potential and the intracellular concentration of monovalent ions such as sodium ions (Kay, 2017). The regulation of bacterial cell volume by altering intracellular ion concentration is a known mechanism for offsetting osmotic stress conditions (Björklund and Marguerat, 2017). Increases in cell volume, such as that observed in the current study when sodium gluconate is supplemented, are generally due to the effects of turgor pressure and the concentration of peptidoglycan precursors (Harris and Theriot, 2018). A key protein involved in cell elongation is the MreB protein which organises the elongosome complex responsible for cell membrane expansion (Plaitakis *et al.*, 2017) by organising enzymes responsible for peptidoglycan and teichoic acid synthesis (Szatmári *et al.*, 2020). In fact, the rate at which MreB polymerises in the cell membrane has been found to be increased in the presence of sodium ions (Szatmári *et al.*, 2020).



(d)

Non-paired t-test comparing the mean FSC for each condition at 4, 48 and 72 hours.				
Sodium gluconate concentration (w/v) comparison		4 hours	48 hours	72 hours
0%	0.6%	NS	**	**
0%	1.1%	NS	*****	**
0%	1.6%	NS	*****	***
0.6%	1.1%	NS	NS	***
0.6%	1.6%	*	NS	***
1.1%	1.6%	NS	**	NS

(e)

Paired t-test comparing the mean FSC between 4 and 48 hours, and 48 and 72 hours.		
Sodium gluconate concentration (w/v)	4-48 hours	48-72 hours
0%	NS	NS
0.6%	**	**
1.1%	****	NS
1.6%	***	**

Figure 3.40 - Graphs and statistical analysis summarising the mean FSC of 0.08% (w/v) ME *C. necator* cultures supplemented with 0%, 0.6%, 1.1% or 1.6% (w/v) sodium gluconate. Statistical analysis was performed using unpaired t-tests to compare individual sodium gluconate concentrations at the same time point (d) and paired t-tests to compare the same condition at different time points (e). NS = non-significant ($p \geq 0.05$), * = $p < 0.05$, ** = $p \leq 0.01$, *** = $p \leq 0.001$, **** = $p \leq 0.0001$, ***** = $p \leq 0.00001$. Error bars represent SD. n = 3 biological replicates. The full data can be found in Figure 8.14 (a) and (b), Appendix 8.6.

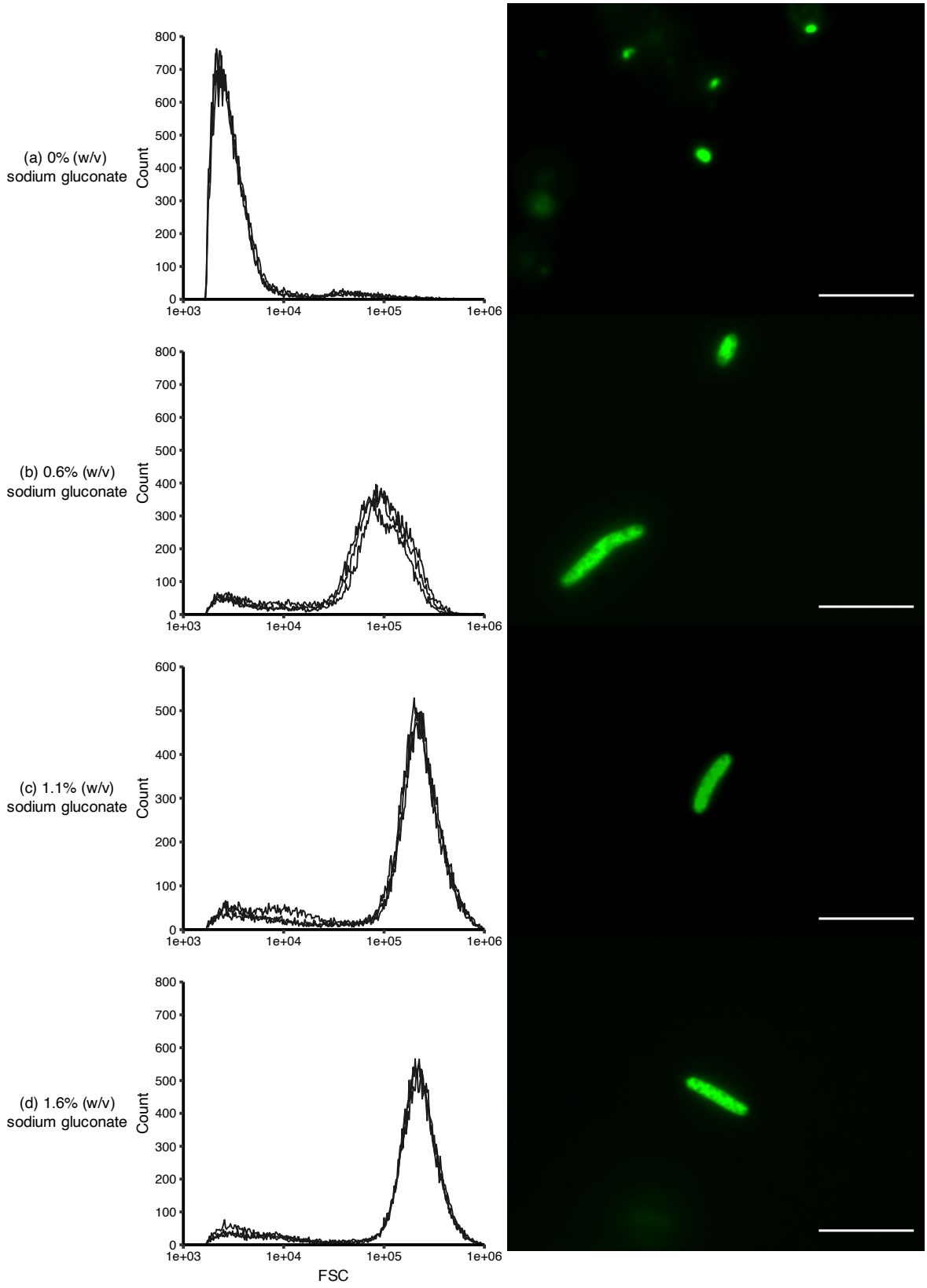
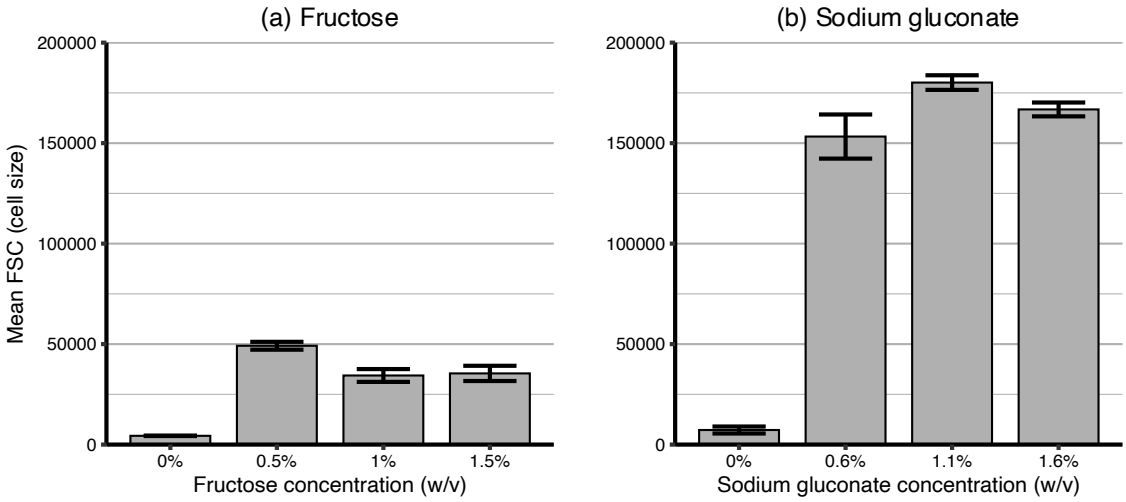


Figure 3.41 - Fluorescent microscopy images of *C. necator* grown in 0.08% (w/v) ME supplemented with (a) 0, (b)0.6, (c) 1.1 and (d) 1.6% sodium gluconate after 72 hours of growth. Scale bars represent 10 µm.



(c)

Non-paired t-test comparing the FSC of fructose and sodium gluconate supplemented cultures at the 48 hour time point.

Fructose/sodium gluconate comparison (w/v)		48 hours	Fructose/sodium gluconate comparison (w/v)		48 hours
0%	0%	NS	1%	0%	***
0%	0.6%	**	1%	0.6%	**
0%	1.1%	***	1%	1.1%	******
0%	1.6%	***	1%	1.6%	*****
0.5%	0%	*****	1.5%	0%	**
0.5%	0.6%	**	1.5%	0.6%	**
0.5%	1.1%	****	1.5%	1.1%	*****
0.5%	1.6%	****	1.5%	1.6%	*****

Figure 3.42 - Graphs and statistical analysis comparing the mean FSC at 48 hours for 0.08% (w/v) ME *C. necator* cultures supplemented with either 0%, 0.5%, 1% or 1.5% (w/v) fructose, or 0%, 0.6%, 1.1% or 1.6% (w/v) sodium gluconate. Plot (a) displays the data of fructose-supplemented cultures and plot (b) that of sodium gluconate. Non-paired t-tests were used to compare each fructose and sodium gluconate supplementation (c). NS = non-significant ($p \geq 0.05$), * = $p < 0.05$, ** = $p \leq 0.01$, *** = $p \leq 0.001$, **** = $p \leq 0.0001$, ***** = $p \leq 0.00001$, ****** = $p \leq 0.000001$. Error bars represent SD. n = 3 biological replicates. The full data can be found in Figure 8.18 (e) and (f), Appendix 8.7.

3.6.6 Sodium gluconate supplementation increases P3HB^{+} cell size considerably

Figure 3.43 contains summaries of mean FSC for P3HB^{+} and P3HB^{++} *C. necator* populations from 0.08% (w/v) ME cultures supplemented with either 0%, 0.6%, 1.1% and 1.6% (w/v) sodium gluconate. The full data can be found in Figure 8.14 (c) and (d), section 8.6.

At 4 hours (Figure 3.43 (a)) statistical comparisons between PH3B^{+} and P3HB^{++} populations showed that P3HB^{+} cells were marginally larger than P3HB^{++} cells for 0.6% and 1.6% (w/v) sodium gluconate supplemented cultures. At 48 (Figure 3.43 (b)) and 72 hours (Figure 3.43 (c)) though, P3HB^{+} cells were considerably larger than that of P3HB^{++}.

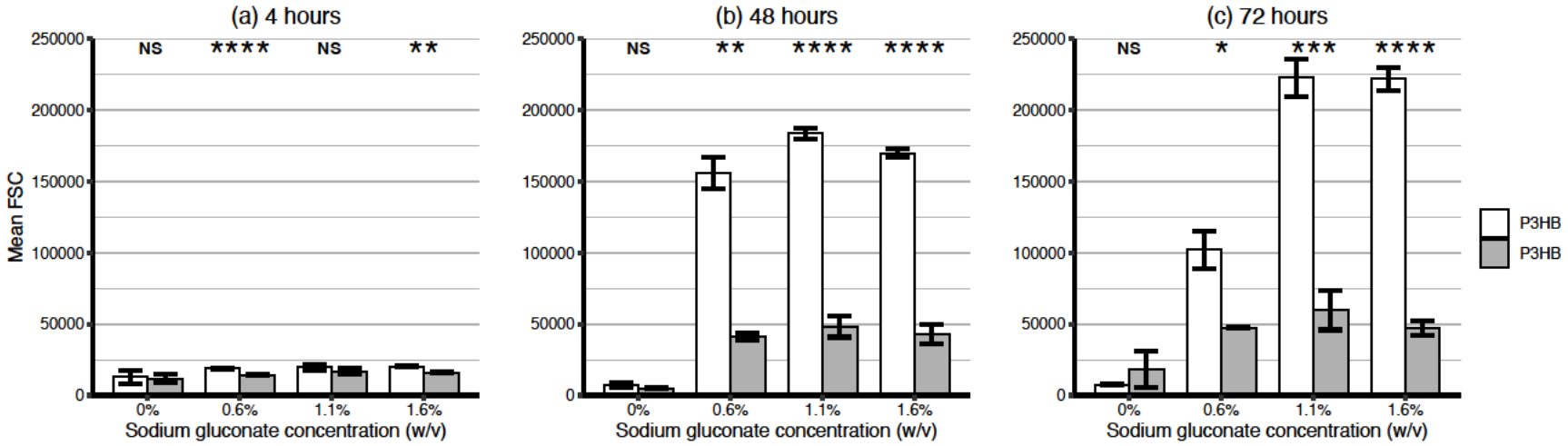
Statistical analysis comparing experimental conditions at the same time point (Figure 3.43 (d)) shows that at 4 hours for the P3HB^{+} population, there was no significant difference between conditions except for 0.6% and 1.6% (w/v) sodium gluconate. At 48 hours, P3HB^{+} *C. necator* cells in cultures supplemented with sodium gluconate were considerably larger than those in media containing only ME. This was also true at 72 hours, but cultures with 0.6% (w/v) sodium gluconate contained significantly smaller cells than that of 1.1% and 1.6%. Comparisons between time points (Figure 3.43 (e)) showed that P3HB^{+} cells in 0.6%, 1.1% and 1.6% (w/v) sodium gluconate-supplemented cultures significantly increased between 4 and 48 hours. However, between 48 and 72 hours 0.6% samples decreased, 1.1% didn't significantly change and 1.6% (w/v) sodium gluconate-containing cultures significantly increased.

For the P3HB^{++} population comparisons between conditions (Figure 3.43 (d)) at 4 hours also showed that all conditions tested could not be significantly separated except for 0.6% and 1.6% (w/v) sodium gluconate. At 48 hours, sodium gluconate-supplemented cultures contained significantly larger P3HB^{++} cells than non-supplemented cultures. This was also the case at 72 hours although 0.6% (w/v) sodium gluconate samples could not be separated from samples without. Statistical analysis over time showed that P3HB^{++} cells in sodium gluconate-supplemented cultures all increased in mean FSC between 4 and 48 hours but did not significantly change between 48 and 72 hours.

Figure 3.44 presents a comparison of FSC at 48 hours for P3HB^{+} and P3HB^{++} populations grown in media supplemented with either fructose (Figure 3.44 (a)) or sodium gluconate (Figure 3.44 (b)). The full data can be found in Figure 8.18, Appendix 8.7.

Statistical comparisons for P3HB^{+} cells at (Figure 3.44 (c)) 48 hours showed that cultures supplemented with sodium gluconate produced significantly larger P3HB^{+} cells than when supplemented with fructose. For P3HB^{++} cells (Figure 3.44 (d)) 1% (w/v) sodium gluconate produced significantly larger P3HB^{++} cells than any fructose concentration tested. However, sodium gluconate did not significantly change P3HB^{++} cell size in relation to 1.5% (w/v) fructose-containing cultures.

In line with previous results in this thesis, a smaller cell phenotype for $P3HB^{++}$ cells is indicative of a persister cell population. Interestingly, only $P3HB^{+}$ cells are observed to undergo cell expansion as outlined in the previous section. Persister cells are known to depolarise their cell membrane in order to enter a period of dormancy (Benarroch and Asally, 2020). Cell elongation has been found to be stopped in cells in which the membrane is depolarised (Stratford *et al.*, 2019).



(d)

Non-paired t-test comparing mean FSC of the P3HB⁺ and P3HB⁺⁺ populations at 4, 24 and 48 hours.

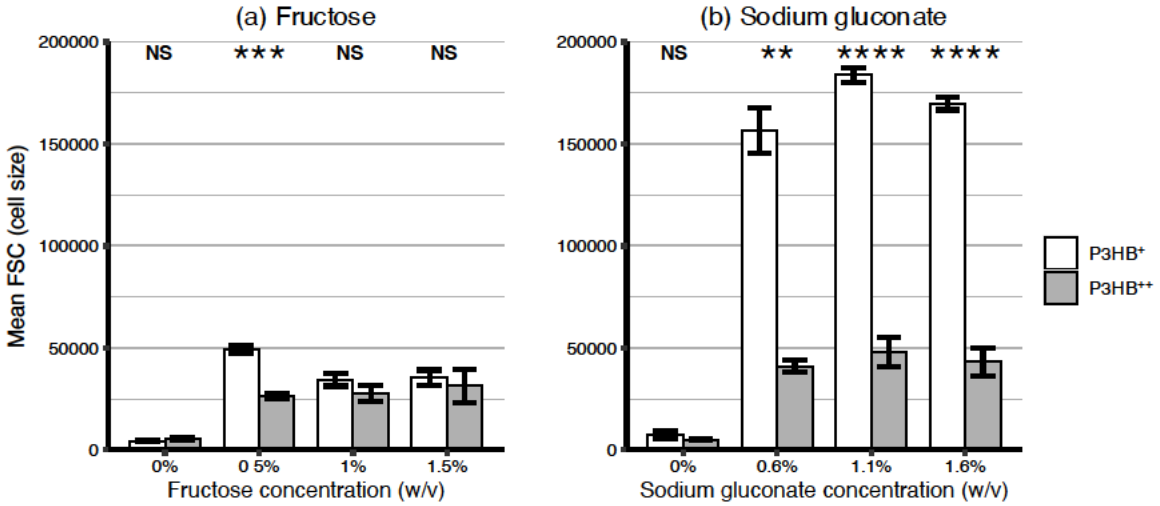
Sodium gluconate concentration (w/v) comparison		P3HB⁺			P3HB⁺⁺		
		4 hours	48 hours	72 hours	4 hours	48 hours	72 hours
0%	0.6%	NS	**	**	NS	**	NS
0%	1.1%	NS	*****	**	NS	**	*
0%	1.6%	NS	*****	***	NS	*	*
0.6%	1.1%	NS	NS	***	NS	NS	NS
0.6%	1.6%	**	NS	***	*	NS	NS
1.1%	1.6%	NS	**	NS	NS	NS	NS

(e)

Paired t-test comparing mean FSC of the P3HB⁺ and P3HB⁺⁺ populations between 4 and 24, and 48 and 72 hours.

Sodium gluconate concentration (w/v)	P3HB⁺		P3HB⁺⁺	
	4-48 hours	48-72 hours	4-48 hours	48-72 hours
0%	NS	NS	NS	NS
0.6%	**	**	**	NS
1.1%	****	NS	*	NS
1.6%	***	**	*	NS

Figure 3.43 - Graphs and statistical analysis summarising the mean FSC of 0.08% (w/v) ME *C. necator* cultures supplemented with 0%, 0.6%, 1.1% or 1.6% (w/v) sodium gluconate. Statistical analysis was performed using unpaired t-tests to compare individual sodium gluconate concentrations at the same time point (d) and paired t-tests to compare the same condition at different time points (e). NS = non-significant ($p \geq 0.05$), * = $p \leq 0.05$, ** = $p \leq 0.01$, *** = $p \leq 0.001$, **** = $p \leq 0.0001$, ***** = $p \leq 0.00001$. Error bars represent SD. n = 3 biological replicates. The full data can be found in Figure 8.14 (c) and (d), section 8.6.



(c)

Non-paired t-test comparing the FSC the P3HB+ population for fructose and sodium gluconate supplemented cultures at the 48 hour time point.

Fructose/sodium gluconate comparison (w/v)		48 hours	Fructose/sodium gluconate comparison (w/v)		48 hours
0%	0%	NS	1%	0%	***
0%	0.6%	**	1%	0.6%	**
0%	1.1%	***	1%	1.1%	******
0%	1.6%	***	1%	1.6%	******
0.5%	0%	****	1.5%	0%	**
0.5%	0.6%	**	1.5%	0.6%	**
0.5%	1.1%	******	1.5%	1.1%	*****
0.5%	1.6%	******	1.5%	1.6%	******

(d)

Non-paired t-test comparing the FSC of the P3HB++ population for fructose and sodium gluconate supplemented cultures at the 48 hour time point.

Fructose/sodium gluconate comparison (w/v)		48 hours	Fructose/sodium gluconate comparison (w/v)		48 hours
0%	0%	NS	1%	0%	**
0%	0.6%	**	1%	0.6%	**
0%	1.1%	**	1%	1.1%	*
0%	1.6%	*	1%	1.6%	*
0.5%	0%	**	1.5%	0%	*
0.5%	0.6%	**	1.5%	0.6%	NS
0.5%	1.1%	*	1.5%	1.1%	NS
0.5%	1.6%	NS	1.5%	1.6%	NS

Figure 3.44 - Graphs and statistical analysis comparing FSC for the P3HB+ and P3HB++ populations at 48 hours for 0.08% (w/v) ME *C. necator* cultures supplemented with either 0%, 0.5%, 1% or 1.5% (w/v) fructose, or 0%, 0.6%, 1.1% or 1.6% (w/v) sodium gluconate. Plot (a) displays the data of fructose-supplemented cultures and plot (b) that of sodium gluconate. Non-paired t-tests were used to compare each fructose and sodium gluconate condition (c). NS = non-significant ($p \geq 0.05$), * = $p < 0.05$, ** = $p \leq 0.01$, *** = $p \leq 0.001$, **** = $p \leq 0.0001$, ***** = $p \leq 0.00001$, ****** = $p \leq 0.000001$. Error bars represent SD. n = 3 biological replicates. The full data can be found in Figure 8.18, Appendix 8.7.

3.6.7 Discussion

Cultures containing 0.08% (w/v) ME were supplemented with 0%, 0.6%, 1.1% or 1.6% (w/v) sodium gluconate. Like fructose, gluconate is also metabolised by the Entner-Doudoroff pathway and has been observed to induce up to 70% of DCW P3HB in *C. necator* (Heinrich *et al.*, 2021). After 48 hours, sodium gluconate-supplemented cultures had a comparable OD_{600} to cultures containing fructose. Cultures supplemented with sodium gluconate did however produce significantly more P3HB per cell, and a higher proportion of $P3HB^{++}$ cells. In bacteria, sodium ions are known to provide an important link across the cell membrane (Dimroth, 1990). The transport of various solutes and sugars can be facilitated using sodium ions to move against a concentration gradient via secondary membrane transporter proteins (Henriquez *et al.*, 2021). It's possible that sodium ions aid the transport of gluconate into the cell, particularly when the gluconate concentration is lower outside the cell. An influx of sodium ions into the cell may also be the reason for *C. necator* cells being considerably larger when sodium gluconate is supplemented. The regulation of bacterial cell volume by altering intracellular ion concentration is a known mechanism for offsetting osmotic stress (Björklund and Marguerat, 2017). Generally increases in bacterial cell volume are due to the combined effects of turgor pressure and the intracellular concentration of peptidoglycan precursors (Harris and Theriot, 2018). A key protein involved in bacterial cell expansion is MreB (Plaitakis *et al.*, 2017) which organises enzymes which synthesise peptidoglycan and teichoic acid (Szatmári et al., 2020) and the rate at which this occurs has been demonstrated to increase in the presence of sodium ions (Szatmári *et al.*, 2020).

3.7 Optimisation of SYTO62 and P-546 staining for flow cytometry experiments

A feature of the fluorescent microscopy images presented in section 3.5.5, Figure 3.30 (b-d), and section 3.6.5, Figure 3.41, was the presence of dark intracellular regions lacking in green SYTO9 staining. While such dark unstained regions could be other intracellular structures such as polyphosphates or Z-rings, given the increases in P-546 fluorescence particularly for *C. necator* cells in sodium gluconate-supplemented cultures, a globular morphology and irregular positioning, it seems most the unstained regions are intracellular P3HB granules.

When observing SYTO9 stained *C. necator* cells during fluorescent microscopy, it was noted that increases in the number of dark regions resembling P3HB granules were not perceived to match the corresponding results for P-546 fluorescence determined by flow cytometry. This was particularly evident during the imaging of the samples presented in Figure 3.30 (b-d), which only produced marginally more intracellular P3HB than previous experiments, and didn't exceed a value of 10,000 units of mean P-546 fluorescence per cell (Figure 3.26). As a result, there was concern the current flow cytometry staining procedure was not effectively reflecting possible increases in P3HB observed microscopically. It was noted that fluorescent microscopy does not offer anything close to the same sample size as flow cytometry, and the observations made microscopically may not be representative of the full *C. necator* population. That said, it was decided that the flow cytometry staining procedure is possibly the most important part of the current study, and should be optimised to ensure the procedure was effectively staining cells.

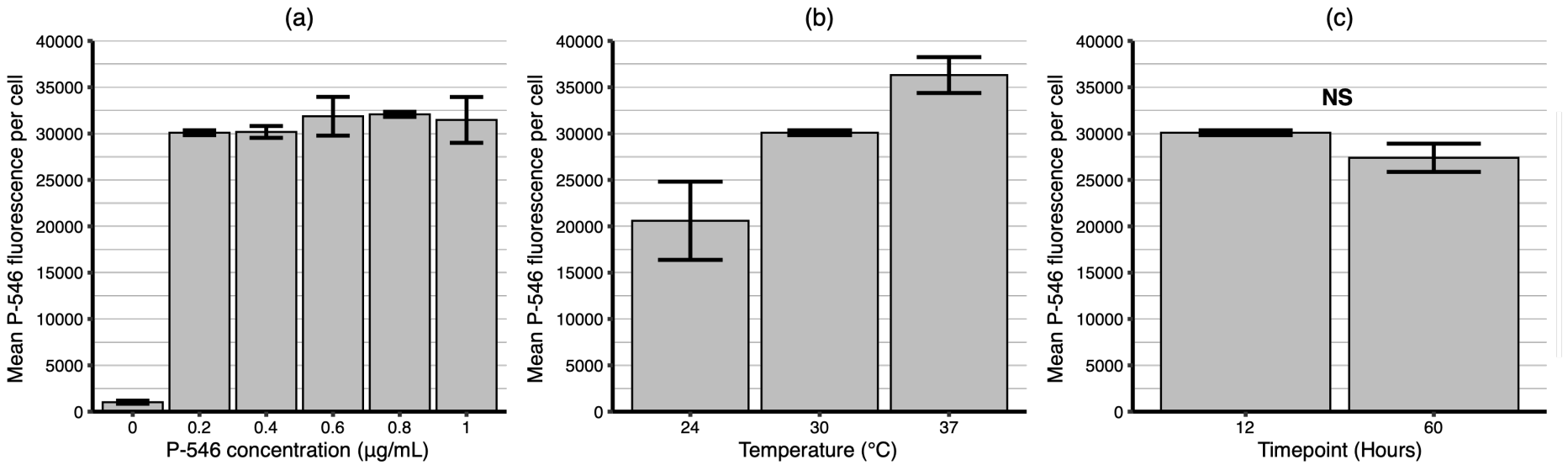
For the optimisation experiments, *C. necator* batch cultures were produced which contained 0.08% (w/v) ME media supplemented with 0.6% (w/v) sodium gluconate. Cultures were grown for 72 hours. Staining conditions were based on the P-546 and SYTO62 concentrations and temperatures used in various studies (Karmann *et al.*, 2016; Vizcaino-Caston *et al.*, 2016; Fernández-Castané *et al.*, 2017). For P-546, concentrations of 0, 0.25, 0.5, 0.75, 1 and 1.25 μg mL^{-1} were tested, and for SYTO62, concentrations of, 0, 1, 2, 3, 4 and 5 μM were used. Each of these conditions were tested at room temperature (maintained at 24 °C), 30 °C and 37 °C at intervals of 6 minutes up to 1 hour. Staining with P-546 and SYTO62 was done separately and PBS was pre-heated in order to ensure staining occurred at the correct temperature.

3.7.1 Outcomes of flow cytometry staining optimisation

Counter-staining with green P-546 and red SYTO62 has been used previously been used by Karmann *et al*. (2016), Vizcaino-Caston *et al*. (2016), Fernández-Castané *et al*. (2017) in conjunction with a BD Accuri™ C6 flow cytometer in order to quantify intracellular P3HB in a variety of bacterium. While other studies such as Kacmar *et al*. (2005) wash cells to remove cell debris and permeabilise with solutions such as 35% (v/v) ethanol in order to increase the speed of dye uptake. Counterstaining with P-546 and SYTO62 streamlines this process by removing the need for time-intensive washing and permeabilisation procedures (Karmann *et al*. 2016). The role of P-546 in the counterstaining procedue is to quantify intracellular P3HB, and the role of SYTO62 is to provide sufficient staining to bacterial cells such that a cell and noise population can be distinguished using flow cytometry software. Temperature is known to affect bacterial membrane fluidity, and thus the diffusion of molecules into the cell (Mansilla *et al.*, 2004). In addition, P3HB by definition as a polymer is known to be brittle at lower temperatures and more soft and flexible at higher temperatures (Keskin *et al.*, 2017). Because of the effects of temperature discussed in this section, different temperatures of 24, 30 and 37 °C were tested and to ensure sufficient dye was present to stain cells P-546 was varied between 0 and 1 μg/mL and SYTO62 was varied between 1 and 5 μM.

The raw data for this section can be found in Appendix 8.8, Figure 8.19. Summarised data is located in Figure 3.45. Overall, *C. necator* cells were found to stain more completely when incubated at 30 °C than 24 °C and with less error than 37 °C. In Figure 3.45 (a), staining *C. necator* with above 0.2 μg/mL did not significantly increase P-546 fluorescence except for 0.8 μg/mL which was marginally higher in P-546 fluorescence. Figure 3.45 (b) demonstrates that there was no significant difference between the temperatures tested and P-546 fluorescence after 12 minutes of staining. Figure 3.45 (c) on the other hand demonstrates that P-456 fluorescence remains stable between 12 and 60 minutes.

The results of this experiment were encouraging as there was no evidence that the previous staining protocol of 5 μM SYTO62 (30 minutes staining time) and 1 μg mL^{-1} P-546 (10 minutes staining time) at room temperature was not causing any problems was insufficient in terms of time, dye concentration temperature. While the method could have been left as it was, the new optimised method (flow cytometry staining method 2) was chosen for future experiments as it saves significant quantities of expensive dyes and is a more time efficient method.



Non-paired t-tests comparing 0.2 µg/L P-546 to other conditions at 12 minutes, at 30 °C	
P-546 concentration (µg/L)	Significance
0	****
0.4	NS
0.6	NS
0.8	*
1	NS

Non-paired t-tests comparing 0.2 µg/L P-546 staining at 12 minutes at 24, 30 and 37 °C	
Temperature (°C) comparison	Significance
24	NS
30	NS
37	NS

Figure 3.45 – Graphs displaying a summary of flow cytometry experiments optimising the staining of *C. necator* with P-546. Plot (a) depicts P-546 fluorescence for *C. necator* cells stained with P-546 varying between a concentration of 0 and 1 µg/mL for 12 minutes. Plot (b) summarises *C. necator* P-546 staining at a concentration of 0.2 µg/mL at temperatures of 24, 30 and 37 °C when stained for 12 minutes. Plot (c) demonstrates the P-546 fluorescence of *C. necator* cells after 12 and 60 minutes of staining at 30 °C. Cultures contained 0.08% (w/v) ME with 0.6% (w/v) sodium gluconate added at 0 hours. Statistical analysis is located either below the corresponding plot or included as a plot annotation. NS = non-significant ($p \geq 0.05$), * = $p < 0.05$, ** = $p \leq 0.01$, *** = $p \leq 0.001$, **** = $p \leq 0.0001$ Non-paired t-tests were used to compare different experimental conditions. Paired t-tests were used to compare the same experimental condition over time. Error bars represent SD.

3.7.2 Discussion

In the previous sections presented in the current study, C. necator cells were stained with 5 μM SYTO62 (30 minutes staining time) and 1 μg/mL P-546 (10 minutes staining time) at room temperature (Vizcaino-Caston *et al.*, 2016). While this procedure was time efficient, avoiding time-consuming alcohol permeabilisation and washing procedures (Karmann *et al.*, 2016), there was concern that the increases in intracellular P3HB observed microscopically were not being observed in P-546 fluorescence. Based on the conditions of previous studies (Karmann *et al.*, 2016; Vizcaino-Caston *et al.*, 2016; Fernández-Castané *et al.*, 2017) P-546 concentrations of 0, 0.25, 0.5, 0.75, 1 and 1.25 μg/mL were tested, and for SYTO62, concentrations of, 0, 1, 2, 3, 4 and 5 μM were used, and temperatures of 24 °C, 30 °C and 37 °C over the course of an hour were tested. The temperature was found not to significantly increase P-546 staining, as was P-546 fluorescence on the whole. The evidence presented therefore gave confidence that P-546 was staining P3HB granules effectively without impairment due to P-546 concentration or temperature. A revised staining strategy which uses expensive stains more sparingly, consisting of 1 μM SYTO62 and 0.2 μg mL-1 P-546 incubated at 30 °C for 12 minutes, is used for the following results sections in this thesis. A limitation of this new method is that a linear trend between P-546 fluorescence and extracted P3HB was not established, as demonstrated by (Karmann *et al.*, 2016). In section 6.2, future work is recommended to rectify this problem.

3.8 Growing *C. necator* cultures for a longer period of time

From the staining optimisation in section 3.7, it was clear that the original flow cytometry staining protocol could not be improved by increasing incubation temperature or by increasing incubation time. This alleviated concerns that P-546 fluorescence may not have been reflecting the level of intracellular P3HB observed microscopically. Attention, therefore, reverted to increasing the amount of P3HB being produced in experiments albeit with a revised flow cytometry staining procedure.

It was noted that statistical evaluations over time in Figure 3.34 (section 3.6.2) and also in the corresponding raw data in Figure 8.13 (b) (Appendix 8.6), in which 0.08% (w/v) ME *C. necator* cultures were supplemented with 0.6%, 1.1% and 1.6% (w/v) sodium gluconate, that mean P-546 per cell increased during the last two to three time points.

While the aim of this study was to produce maximum P3HB within a realistic 72-hour timeframe in line with the timescales of P3HB production in previous studies (Budde *et al.*, 2011; Pradella *et al.*, 2012; Ienczak *et al.*, 2016), it was decided that *C. necator* should be grown for a longer period of time in order to determine how much P3HB production occurs beyond 72 hours. As such, if a large increase in P3HB was found to occur after 72 hours in the current study, this would represent a target level of P-546 fluorescence to try and achieve within 24 hours.

Unfortunately, due to time limitations, the experiments presented in this section only consist of one concentration of sodium gluconate (0.6% (w/v)) in comparison to the 3 concentrations tested in section 3.6. As there was no evidence to suggest higher sodium gluconate concentrations would lead to more P3HB in Figure 8.13 (a), 0.6% (w/v) sodium gluconate was chosen as the condition to be tested.

Additionally in this sub-chapter, changes were also made to the fluorescent microscopy protocol. Unfortunately, the microscope used up to this point (microscope method 1) was broken and a new microscope had to be assembled, which in part is the reason for the lack of conditions tested. As the new microscope had different filters that were more suited to different stains a new protocol was put together which involved permeabilising *C. necator* cells with 35% (v/v) ethanol (Kacmar *et al.*, 2005) before staining with PI and P-546 (microscope method 2). It should be noted that the ethanol permeabilisation step allows PI to enter both live and dead cells meaning PI in this context is not being used to distinguish between live and dead cells.

3.8.1 Cell count determined by flow cytometry

This experiment presented in section 3.8 represents the first point in the current study at which BD certified the Accuri™ C6 flow cytometer calibrated for accurate cell counting. Before this point, BD had advised the flow cytometer was not working sufficiently to be used for accurate cell counting. In the sections previous, OD_{600} was used as a method of tracking the cell density of cultures.

A summarisation of cell count data can be found in Figure 3.46, and the full raw data is located in Figure 8.20, Appendix 8.9. Comparing the 72 and 168-hour time points found there to be no significant difference in mean events per mL. This is indicative of cell proliferation ceasing due to a lack of remaining growth-promoting nutrients, conditions which could promote P3HB production. The full data in Figure 8.20 shows an increase in mean events of less than 10 fold occurs during growth. In contrast, raw OD_{600} data in Figure 8.12, Appendix 8.6, testing the same growth condition showed an increase in OD_{600} of around 160 fold. While OD_{600} has previously been used to monitor cell density in P3HB-producing bacterial cultures (Ahn *et al.*, 2000), it is generally viewed as unreliable due to P3HB absorbing light at similar wavelengths to that of non-P3HB cell biomass (Martinez and Déziel, 2020). For that reason, and due to the cell counting and OD_{600} observations made in sodium gluconate-supplemented cultures, the use of OD_{600} was discontinued in this study.

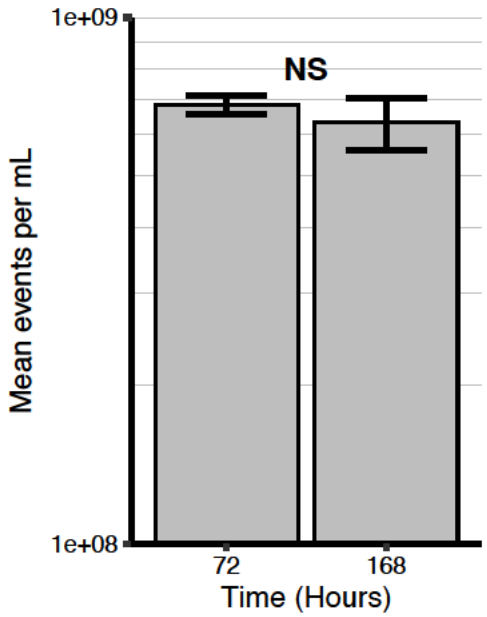


Figure 3.46 – Summarisation of mean cell count data determined by flow cytometry for *C. necator* cultures grown in 0.08% (w/v) ME supplemented with 0.6% (w/v) sodium gluconate. Annotations represent the outcome of a paired t-test comparing samples over time. NS = Non-significant. Error bars represent SD. n = 3 biological replicates. The full data is located in Figure 8.20, Appendix 8.9.

3.8.2 Cultures supplemented with sodium gluconate produce more P3HB

The growth of *C. necator* in 0.08% (w/v) ME supplemented with 0.6% (w/v) sodium gluconate for 6 days revealed that mean P3HB per cell (Figure 3.47(a)) significantly increased between 72 and 168 hours. This was also the case for P3HB per mL of culture (Figure 3.47(b)) and the percentage of $P3HB^{++}$ cells (Figure 3.47(c)). The results of Figure 3.47 are concurrent with that of the cell count data presented in Figure 3.46, providing more evidence to suggest that media conditions beyond 72 hours are more suited to P3HB accumulation. The full data can be found in Figure 8.21, Appendix 8.9.

The results presented in Figure 3.47 show that a lag in P3HB production is occurring which shifts major P3HB accumulation beyond 72 hours. This could suggest that the ME to gluconate concentration is not at a ratio that promotes P3HB biosynthesis. However, this seems unlikely as Passanha *et al*. (2014) found that peak P3HB accumulation in 0.8% (w/v) ME occurred after just 28 hours and *C. necator* after this point metabolised P3HB. The concentration of ME used by Passanha *et al*. (2014) is 10 times greater than the 0.08% (w/v) ME used for culture growth in this section. The main difference between the results presented in Figure 3.47 and the results of Passanha *et al*. (2014) is the carbon source added to ME media, with experiments in the current section using sodium gluconate and Passanha *et al*. (2014) using acetic acid. Henrich *et al*., (2012) also demonstrated that sodium gluconate can produce maximum P3HB in 68 hours. The PhaC1 enzyme, used by *C. necator* to polymerise 3HB, is known to have an initial lag phase before reaching peak P3HB polymerisation, although, this is only around 6 hours (Juengert *et al*., 2018). However, Juengert *et al*. (2018) found that mutating key amino-acid residues in PhaC1 could significantly increase the lag time in 3HB polymerisation. However, the presence of PhaM restored PhaC1 to normal function. It should be noted that in the study by Juengert *et al*. (2018), the lag in 3HB polymerisation was only observed in vitro and not in vivo even when PhaM was absent. The reason for the lag phase in P3HB production in this section is unclear.

Figure 3.48 contains summaries of mean P-546 fluorescence per cell and per mL for the $P3HB^{+}$ and $P3HB^{++}$ populations. The full data can be found in Figure 8.22, Appendix 8.9. Figure 3.48 (a) shows that between 72 and 168 hours, P3HB per cell for both the $P3HB^{+}$ and $P3HB^{++}$ populations remained similar. Expressing P-546-fluorescence per mL though found that at 168 hours, the $P3HB^{++}$ contributed considerably more P3HB per mL of culture at 168 hours than at 72 hours. This is likely due to $P3HB^{+}$ cells gradually accumulating P3HB in a more conventional manner, rather than the rapid accumulation of $P3HB^{++}$ cells observed in this study as early as 4 hours.

Figure 3.49 presents a fluorescent microscope image and is annotated with potential $P3HB^{+}$ and $P3HB^{++}$ labels. The figure shows the presence of mainly large elongated cells with high levels of P3HB and little DNA visibly stained. The large elongated cells most likely represent a different kind of $P3HB^{++}$ cell to that reported to be small persistor cells that rapidly produce P3HB in as little as 4 hours. These

cells are likely cells which originally started off as P3HB^{+} cells and that have accumulated P3HB by more conventional means.

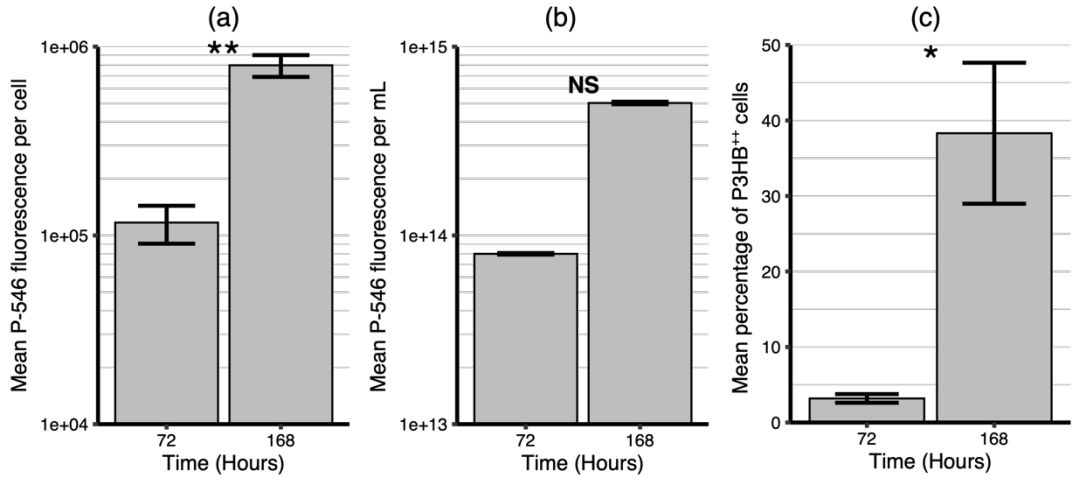
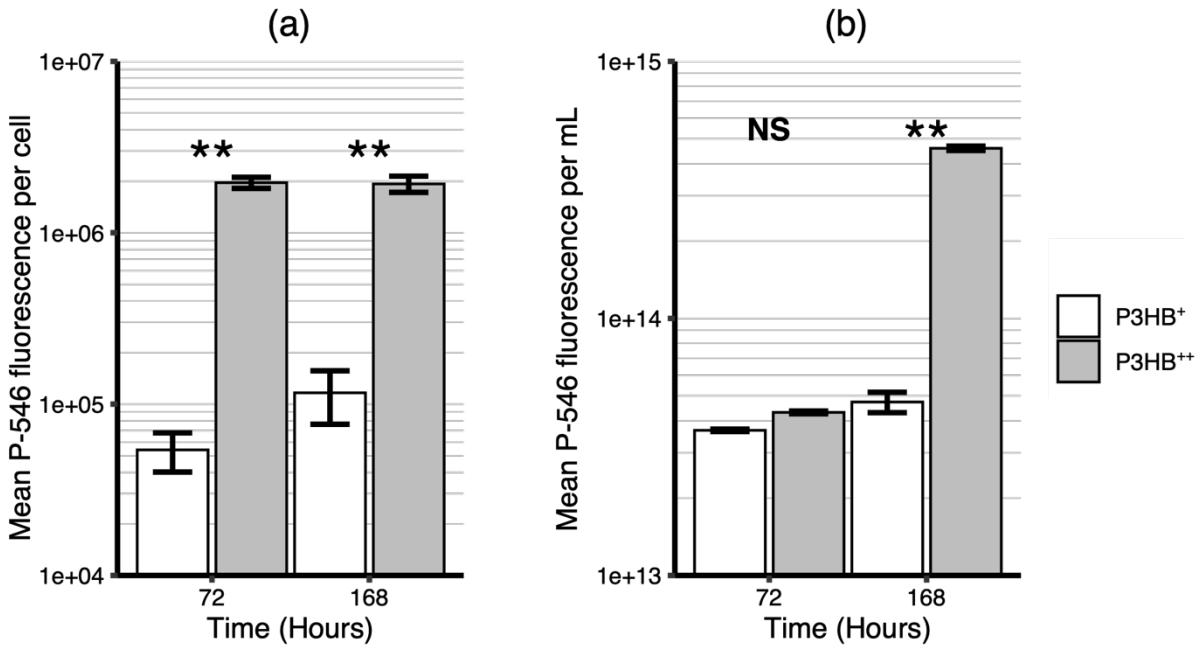


Figure 3.47 – Summarisation of (a) mean P-546 fluorescence per cell, (b) mean percentage of P3HB^{++} cells and the mean P-546 per mL (c) for *C. necator* cultures grown in 0.08% (w/v) ME supplemented with 0.6% (w/v) sodium gluconate. Annotations represent the outcome of a paired t-test comparing samples over time. NS = non-significant ($p \geq 0.05$), * = $p < 0.05$, ** = $p \leq 0.01$. Error bars represent SD. n = 3 biological replicates. The full data can be found in Figure 8.21, Appendix 8.9.



Paired t-test comparing individual *C. necator* populations over time.	
P3HB+	NS
P3HB++	NS

Paired t-test comparing individual *C. necator* populations over time.	
P3HB+	NS
P3HB++	**

Figure 3.48 - Summarisation of P3HB^{+} and P3HB^{++} mean P-546 fluorescence per cell (a) , and per mL (b) for *C. necator* cultures grown in 0.08% (w/v) ME supplemented with 0.6% (w/v) sodium gluconate. Annotations represent the outcome of a non-paired t-test comparing P3HB^{+} and P3HB^{++} populations. Paired t-test were used to compare the same condition over time. NS = non-significant ($p \geq 0.05$), * = $p < 0.05$, ** = $p \leq 0.01$. Error bars represent SD. n = 3 biological replicates. The full data can be found in Figure 8.22, Appendix 8.9.

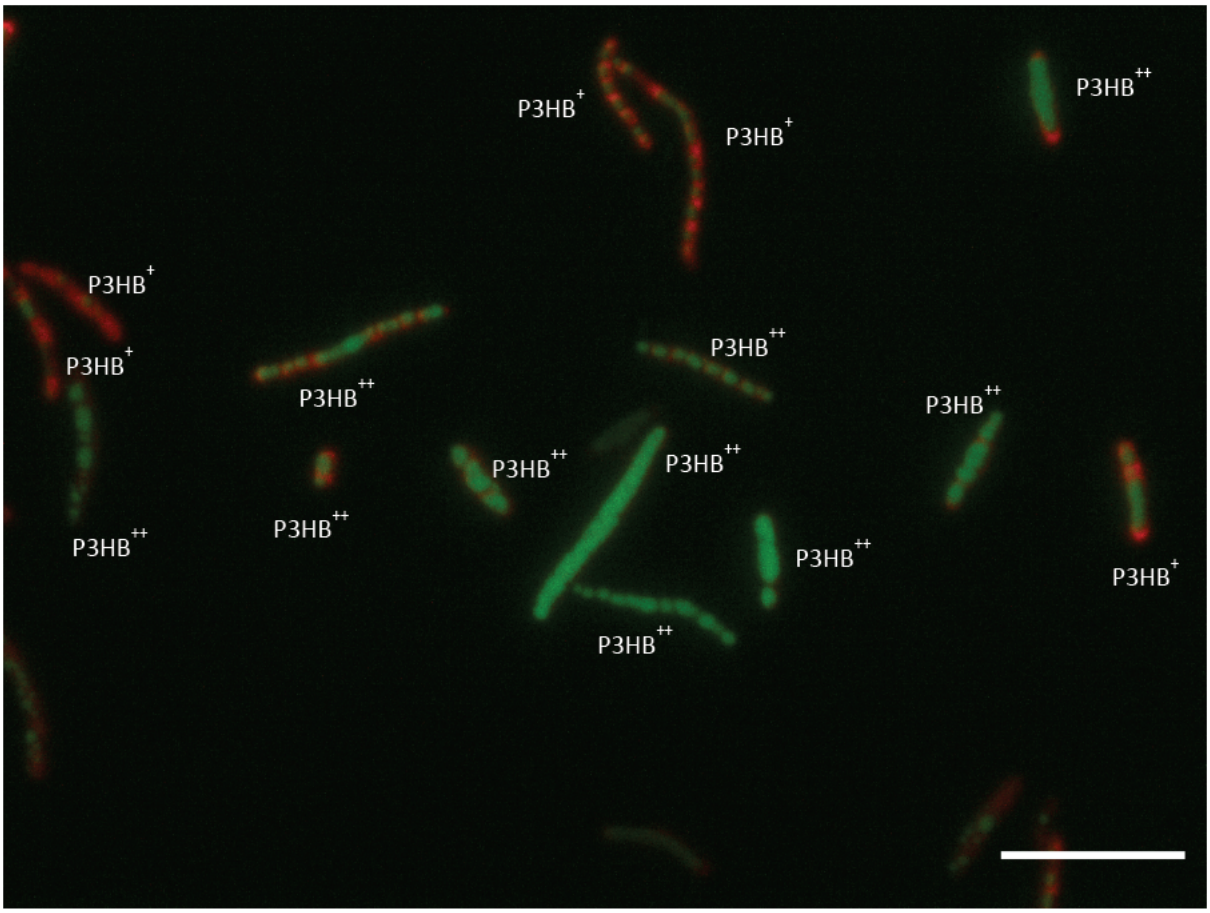


Figure 3.49 - Fluorescent microscope images showing PHA^{++} and PHA^{+} *C. necator* cells at 144 hours when grown in 0.08% (w/v) ME supplemented with 0.6% (w/v) sodium gluconate. Samples were permeabilised with 35% (v/v) ethanol and stained with 1 µM P-546 (green) and 2 µg mL^{-1} PI (red). The scale bar represents 10 µm. Labelled are possible P3HB^{+} and P3HB^{++} cells.

3.8.3 Overall cell size decreases after 72 hours

Figure 3.50 contains a summary of the overall mean FSC (Figure 3.50 (a)) and mean $P3HB^{+}$/$P3HB^{++}$ FSC (Figure 3.50 (b)). The full raw data is located in Appendix 8.9, Figure 8.23. Overall mean FSC significantly decreased between 72 and 168 hours. However, while the same was true for the $P3HB^{+}$ and $P3HB^{++}$ populations over time, at 72 hours $P3HB^{+}$ cells were larger than $P3HB^{++}$, and at 168 $P3HB^{++}$ cells were larger than $P3HB^{+}$.

The overall decrease observed in cell size is likely due to a reduction in cell volume resulting from osmotic changes in the growth media. Cell chains, which can divide into multiple cells thus reducing mean cell size, were not observed in sodium gluconate-supplemented cultures. Additionally given the increase in P3HB between 72 and 168 hours it is highly unlikely that media composition was suitable for cell proliferation. Results up to this section have suggested that the often smaller phenotype of $P3HB^{++}$ cells is due to $P3HB^{++}$ cells being persister cells. While this is the case at 72 hours, at 168 hours $P3HB^{+}$ cells were larger than $P3HB^{++}$ cells. This is likely due to the high levels of intracellular P3HB in $P3HB^{++}$providing resistance to osmotic stress. Osmotic stress is known to cause bacterial cell shrinkage (Oldewurtel *et al.*, 2021) and P3HB granules are known to provide resistance to a variety of environmental stress conditions (Obruca *et al.*, 2016). In this case, P3HB likely provides mechanical support to the cell membrane of $P3HB^{++}$ cells preventing further shrinkage, and additionally occupies intracellular space that would otherwise contain H_20 which could leave the cell during osmotic imbalance.

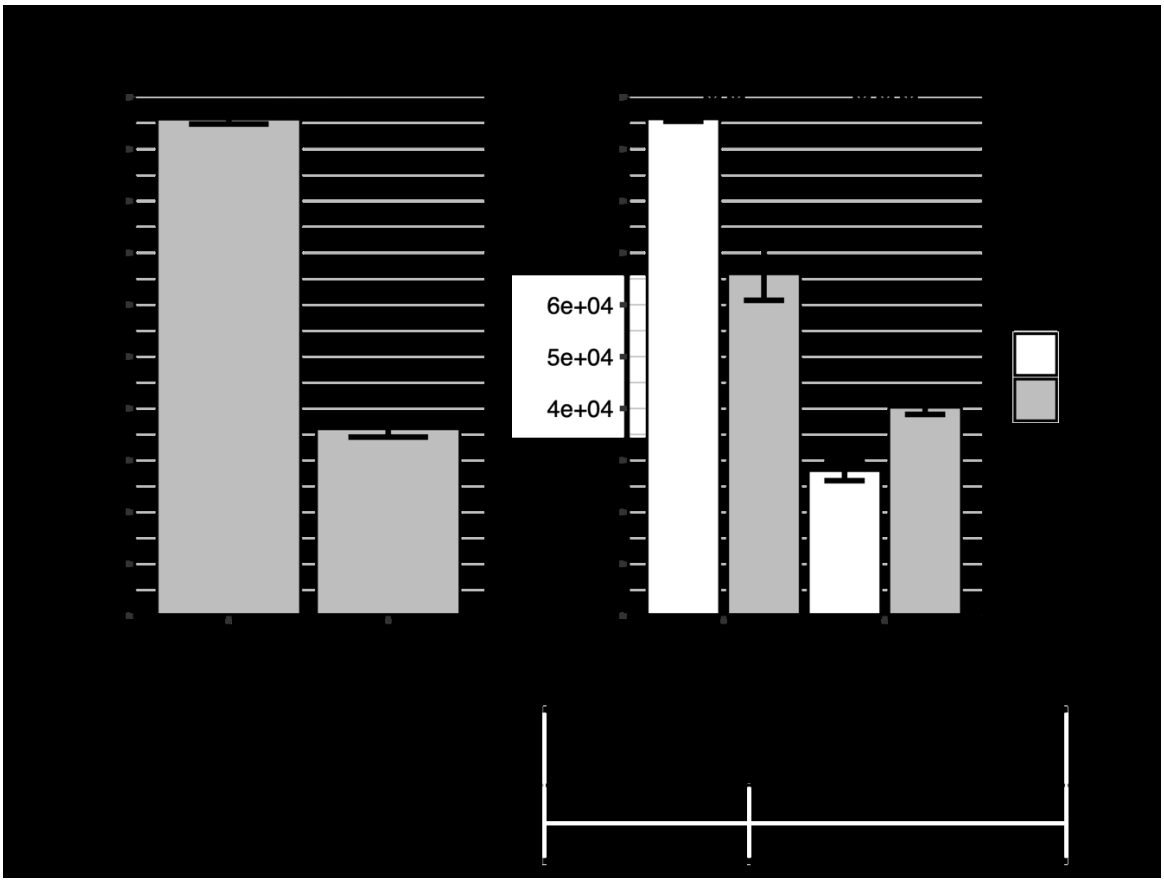


Figure 3.50 – Summarisation of (a) mean FSC and (b) mean P3HB^{+} and P3HB^{++} FSC for *C. necator* cultures grown in 0.08% (w/v) ME supplemented with 0.6% (w/v) sodium gluconate. Annotations represent the outcome of a paired t-test comparing samples over time. NS = non-significant ($p \geq 0.05$), * = $p < 0.05$, ** = $p \leq 0.01$, *** = $p \leq 0.001$, **** = $p \leq 0.0001$. Error bars represent SD. n = 3 biological replicates. Note the legend only applies to plot (b). The full raw data is located in Appendix 8.9, Figure 8.23.

3.8.4 Discussion

Monitoring growth for a longer period for 0.6% (w/v) sodium gluconate supplemented 0.08% (w/v) ME cultures, using flow cytometry cell counting, revealed that no significant culture growth occurred between 72 and 168 hours. Comparing the corresponding raw data of flow cytometry cell counts (Figure 8.20, Appendix 8.9) to that of the OD_{600} (Figure 8.12, Appendix 8.6) found that cell count determined by flow cytometry increased by a smaller proportion that of OD_{600}. This is possibly due to P3HB absorbing light at OD_{600} (Martinez Déziel, 2020) and thus causing an overestimation of culture cell density. Additionally, an increase in cell size may lead to OD_{600} increasing (Stevenson *et al.*, 2016), a factor which would not affect flow cytometry cell counting.

Data presented for P3HB per cell and per mL demonstrates a significant increase in P3HB between 72 and 168 hours, providing evidence to suggest a lag phase in P3HB is occurring, causing production to continue increasing after 72 hours. A lag phase is known to exist for 3HB polymerisation due to the enzyme PhaC1 taking around 6 hours to reach peak polymerisation (Juengert *et al.*, 2018). Although this is not long enough to cause the P3HB production lag in this section. The cause of the lag phase is unlikely to be due to the insufficient consumption of key nutrients, as Passanha *et al.* (2014) found that peak intracellular PHA could be achieved in just 28 hours using 10 times more concentrated 0.8% (w/v) ME.

Overall cell size decreased between 72 and 168 hours possibly due to osmotic stress (Oldewurtel *et al.*, 2021). However, in contrast to previous results in which $P3HB^{++}$ cells were smaller than $P3HB^{+}$ cells, at 168 hours $P3HB^{+}$ cells were significantly smaller than $P3HB^{++}$ cells. The reason for this may be due to the resistance high levels of intracellular P3HB give *C. necator* against osmotic stress. Thus, while $P3HB^{+}$ contain more H_20 that moves out of the cell down the osmotic gradient, $P3HB^{++}$ cells contain less water and are able to use P3HB granules to structurally reinforce the cell membrane preventing the need for such drastic adjustment of cell volume.

3.9 Growing *C. necator* in cultures supplemented with fructose for 10 days

In Figure 3.35, section 3.6.2, statistical analysis found supplementing 0.08% (w/v) ME cultures with sodium gluconate resulted in *C. necator* accumulating more P3HB per cell in comparison to cultures fructose supplemented when experiments were concluded in under 72 hours. Increasing the growth time of sodium gluconate supplemented 0.08% (w/v) ME cultures, and comparing 72 and 168-hour time points (Figure 3.47, section 3.8.2) found that *C. necator* carried on accumulating intracellular P3HB beyond 72 hours. Further to this, the availability of flow cytometry cell counting in section 3.8.1 showed that sodium gluconate-supplemented cultures increased cell number by less than a factor of 10 (Figure 3.46). This result coincided with observations made during previous flow cytometry experiments in which fructose-supplemented cultures generally needed greater dilution than sodium gluconate-supplemented cultures to achieve suitable events per second on the flow cytometer. Unfortunately prior to section 3.8, dilutions were not recorded and this could not be proven with data, only observations. If sodium gluconate-supplemented cultures produce more P3HB and fewer cells than fructose-supplemented cultures, this would suggest fructose would be better added at the start to increase biomass levels and then sodium gluconate added later to produce P3HB. Experiments in this section will therefore focus on the supplementation of *C. necator* grown in 0.08% (w/v) ME with fructose. The aim of this experiment will be: firstly, does fructose supplementation produce more cells per mL of culture than that of sodium gluconate; and secondly, does fructose supplementation produce significantly more P3HB after 72 hours? While more studies on the effects of sodium gluconate concentration would have been useful, in terms of the time scale available and the overall thesis objectives it was deemed more appropriate to proceed with assessing fructose supplementation.

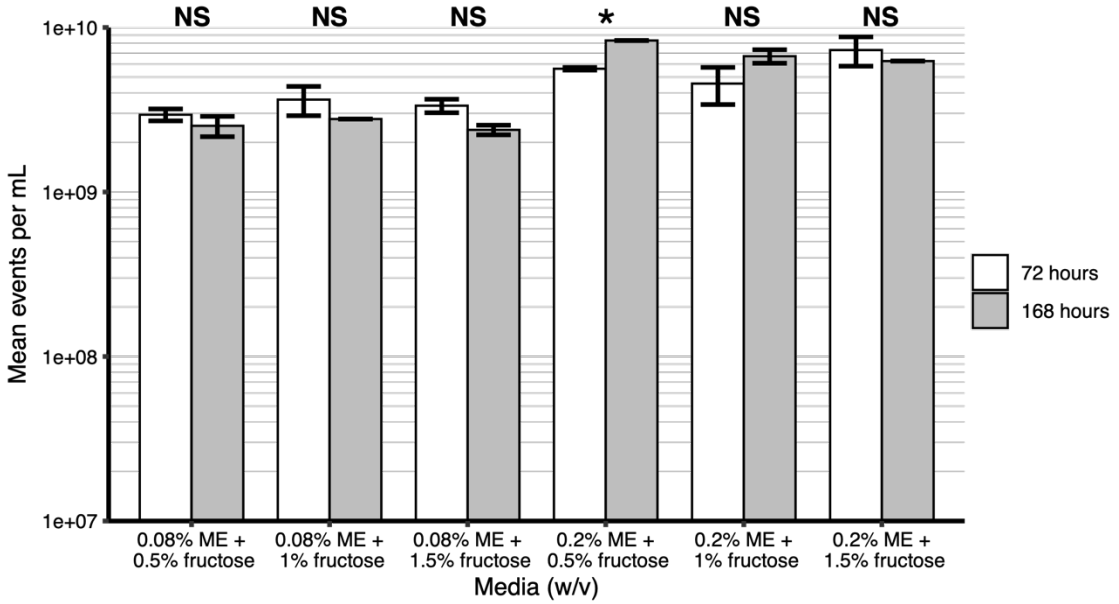
3.9.1 Fructose-supplemented *C. necator* proliferates whereas sodium gluconate-supplemented *C. necator* elongates

Figure 3.51 contains a summary of *C. necator* cell counts at 72 and 168-hour time points for cultures containing either 0.08% or 0.2% (w/v) ME and supplemented with either 0.5, 1 or 1.5% (w/v) fructose. The full data is located in Figure 8.24, Appendix 8.10.

Generally, there was no significant difference between culture cell counts at 72 hours and 168 hours, although cultures containing 0.2% (w/v) ME and 0.5% (w/v) fructose did significantly increase slightly. Non-paired statistical analysis (Figure 3.51 (b)) analysing the effect of increasing ME concentration found that, unlike previous sections, increasing ME concentration did not always increase cell density. While this suggests that for cultures containing more than 0.5% (w/v) fructose, an increase ME concentration does not increase cell density, this is likely to be due to the reduced sample size of 2 biological replicates, as opposed to 3, weakening the outcome of the statistical comparisons.

Figure 3.52 compares the mean cell counts of 0.08% (w/v) ME cultures supplemented with fructose with sodium gluconate-supplemented cultures at 24 hours after which growth appears to enter a stationary phase. The full data can be found in Figure 8.29, Appendix 8.11. Statistical comparisons presented in Figure 3.52 found fructose supplementations of 0.5% and 1% to produce significantly more cells in 0.08% (w/v) ME cultures than 0.6% (w/v) sodium gluconate.

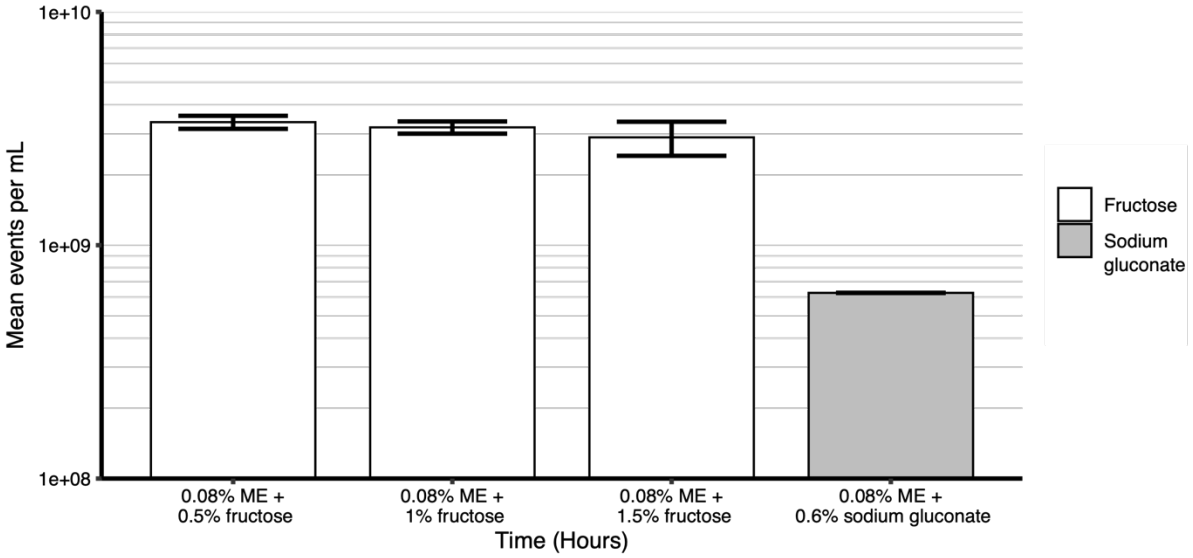
The decreased cell counts of sodium gluconate-containing cultures, in relation to that of fructose, is linked to the increased cell size of *C. necator* cells when grown in media supplemented with sodium gluconate. While *C. necator* cells in sodium gluconate cultures expand, possibly due to the effects of sodium ions increasing turgor pressure (Björklund and Marguerat, 2017) or increasing the rate at which expansion-related proteins such as MreB aid expansion (Szatmári *et al.*, 2020), fructose supplemented *C. necator* cells favour cell division. The overall process which decides if a cell elongates or proliferates can be explained by the two-competing-sites model in which Z-ring septation sites competed with cell elongation machinery (Lleo *et al.*, 1990). Bacterial cell division is thought to be dependent on the intracellular concentration of the FtsZ protein which during the division process form Z-rings which function to recruit division proteins to the divisome and also direct the formation of septal peptidoglycan (Du and Lutkenhaus, 2019). The MinCD protein complex prevents the formation of a Z-ring at the mid-cell point (Jacobs and Shapiro, 1999). The elongation of cells is controlled by the highly conserved rod system, which involves the polymerisation of peptidoglycan with the glycan polymerase RodA and the PBP2 crosslinking enzymes (Rohs *et al.*, 2018).



Non-paired t-test comparing different ME concentrations		
Fructose concentration (w/v)	72 hours	168 hours
0.5%	*	*
1%	NS	NS
1.5%	NS	*

Non-paired t-test comparing different ME concentrations			
ME concentration (w/v)	Fructose concentration comparison (w/v)	72 hours	168 hours
0.08%	0.5% 1%	NS	NS
	0.5% 1.5%	NS	NS
	1% 1.5%	NS	NS
0.2%	0.5% 1%	NS	NS
	0.5% 1.5%	NS	NS
	1% 1.5%	NS	NS

Figure 3.51 – Summary of mean events per mL at 72 and 168-hour time points, for *C. necator* cultures containing either 0.08% and 0.2% (w/v) ME supplemented with 0.5%, 1% and 1.5% (w/v) fructose. Statistical significance was determined using paired t-tests to compare the same condition at different time points (displayed as figure annotations), and non-paired t-tests to compare different experimental conditions. NS = non-significant ($p \geq 0.05$), * = $p < 0.05$. Error bars represent SD. n = 2 biological replicates. The full data is located in Figure 8.24, Appendix 8.10.



Non-paired t-test comparing sodium gluconate supplemented cultures to those fructose supplemented	
Fructose concentration (w/v)	Significance
0.5%	*
1%	*
1.5%	NS

Figure 3.52 – Comparison of flow cytometry events per mL at 24 hours for 0.08% (w/v) *C. necator* supplemented with 0.5%, 1% and 1.5% (w/v) fructose or 0.6% (w/v) sodium gluconate. Statistical significance was determined using non-paired t-tests to compare different experimental conditions. NS = non-significant ($p \geq 0.05$), * = $p < 0.05$. Error bars represent SD. Error bars represent SD. n = 2 biological replicates for fructose supplemented cultures and n = 3 for sodium gluconate supplemented cultures. The full data can be found in Figure 8.29, Appendix 8.11.

3.9.2 After 168 hours sodium gluconate-supplemented cultures produce more P3HB per cell and per mL

A summary of *C. necator* intracellular P3HB per cell and per mL, at 72 and 168 hour time points for cultures containing either 0.08% or 0.2% (w/v) ME and supplemented with either 0.5, 1 or 1.5% (w/v) fructose can be found in Figure 3.53 and Figure 3.54, respectively. The full data is located in Figure 8.25 (a)-(d), Appendix 8.10.

Given that cell counts generally did not significantly increase in Figure 3.51 (a), it would be expected that *C. necator* has used the key nutrients in the media, creating a key nutrient-to-C ratio suitable for P3HB accumulation. However, statistical annotations in Figure 3.53 (a) show that only cultures containing 0.08% (w/v) ME and 0.5% (w/v) fructose significantly increased P3HB per cell between the 72 and 168-hour time points. Statistical comparisons presented in Figure 3.53 (b) found that increasing ME concentration from 0.08% to 0.2% (w/v) ME only decreased P3HB per cell for cultures supplemented with 0.5% (w/v) fructose, while increased fructose supplementation led to increased ME concentration having no significant effect on P3HB per cell. Comparing different fructose concentrations within the same ME condition found that only cultures supplemented with 0.5% and 1.5% (w/v) significantly changed P3HB levels per cell, decreased fructose concentration increasing P3HB for 0.08% (w/v) ME cultures, and decreasing P3HB for 0.2% (w/v) cultures.

Comparing mean P3HB per mL between 72 and 168 hours (Figure 3.54 (a)) found that all conditions tested could not be statistically separated. This was also largely true when comparing increasing ME concentration (Figure 3.54 (b)) and comparing increasing fructose concentration (Figure 3.54 (c)).

Figure 3.55 contains summaries comparing the mean P-546 fluorescence per cell (Figure 3.55 (a)) and per mL (Figure 3.55 (b)) of 0.08% (w/v) ME *C. necator* cultures supplemented with either fructose or sodium gluconate. The full data can be found in Figure 8.30, Appendix 8.11. Statistical analysis of each plot presented in Figure 3.55 (c), shows that cultures supplemented with sodium gluconate produced significantly more P3HB per cell and per mL than cultures containing fructose.

Overall, results in this section show that sodium gluconate supplementation leads to more intracellular P3HB production on average per cell and per mL of culture in comparison to fructose after 168 hours of growth. This is further to results presented in section 3.6.2 which found that after 48 hours, sodium gluconate supplementation led to more P3HB per cell than fructose. In section 3.6.2 a possible reason for more P3HB production in cultures containing sodium gluconate that was due to the movement of gluconate against the concentration gradient using sodium ions to facilitate movement via secondary transport proteins (Henriquez *et al.*, 2021). It's possible that a lag phase in P3HB production, like that observed for sodium gluconate-supplemented cultures in section 3.8.2, was also observed in cultures

containing fructose. However, statistical comparisons appeared to be weakened by a reduced culture replicate number of 2.

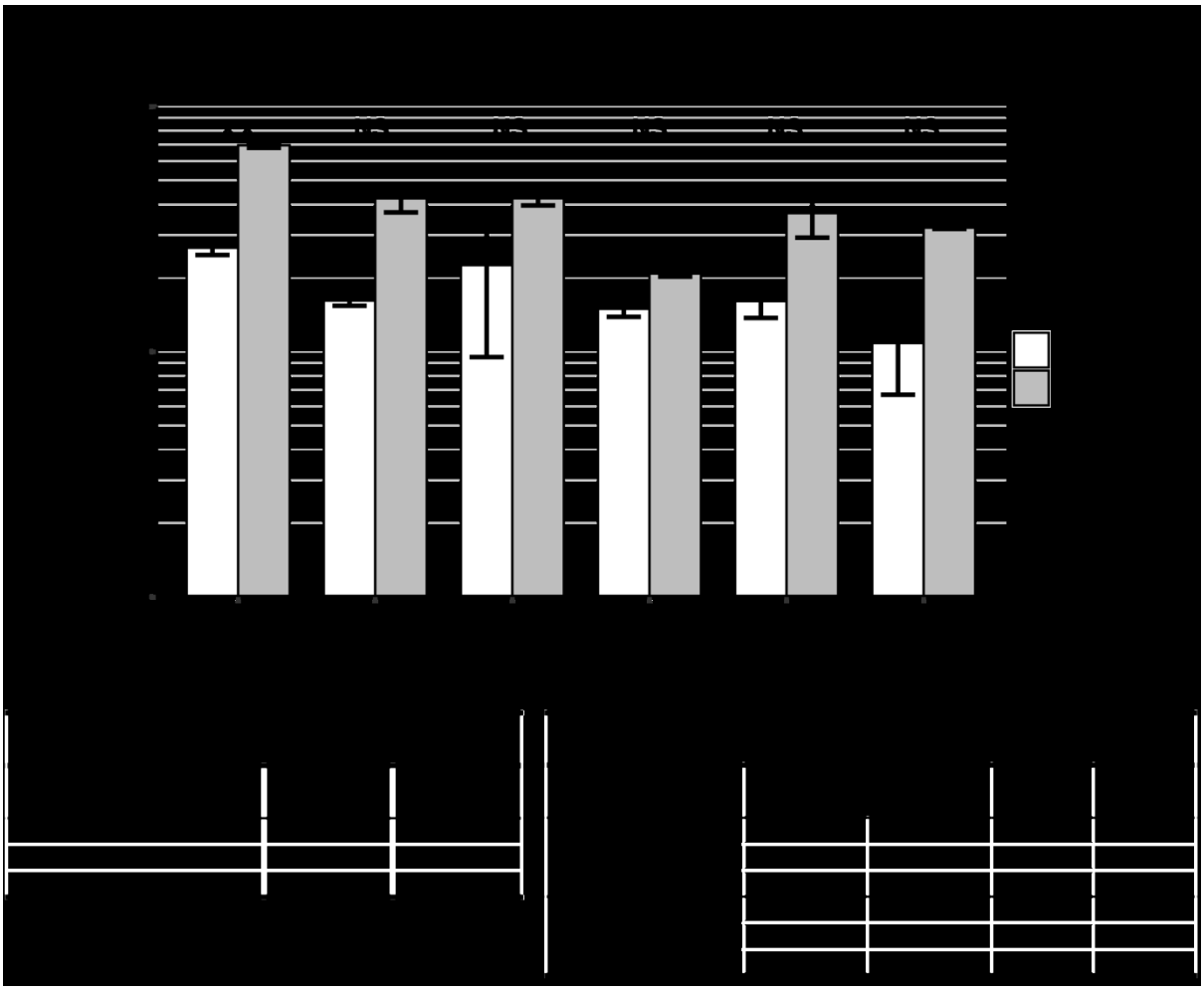
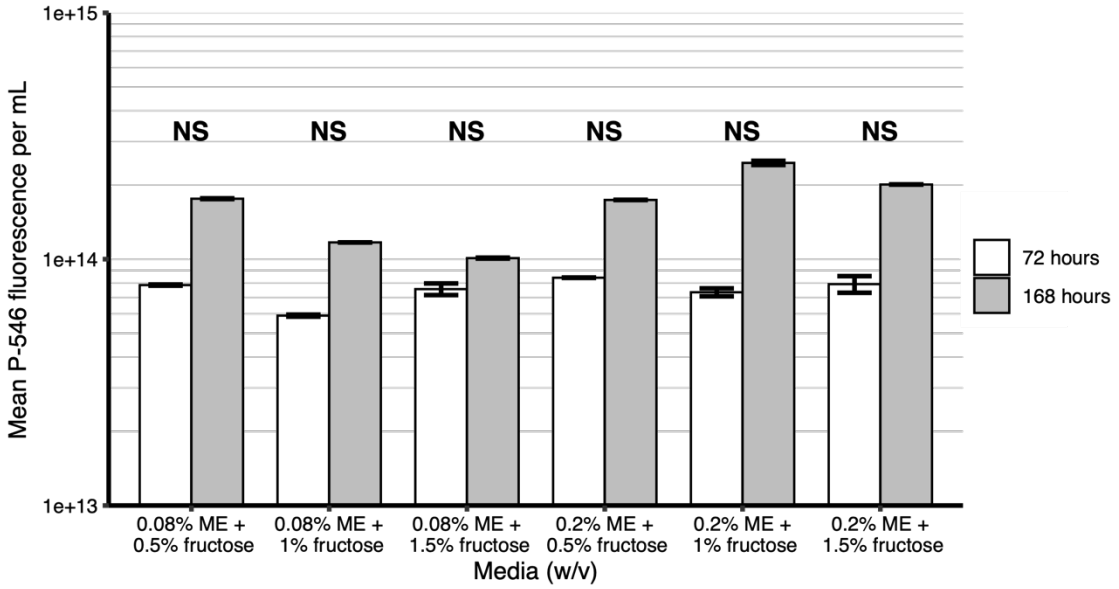


Figure 3.53 – Summary of mean P-546 fluorescence per cell at 72 and 168 hour time points, for *C. necator* cultures containing either 0.08% and 0.2% (w/v) ME supplemented with 0.5%, 1% and 1.5% (w/v) fructose. Statistical significance was determined using paired t-tests to compare the same condition at different time points (displayed as figure annotations), and non-paired t-tests to compare different experimental conditions. NS = non-significant ($p \geq 0.05$), * = $p < 0.05$, ** = $p \leq 0.01$. Error bars represent SD. n = 2 biological replicates. The full data is located in Figure 8.25 (a) and (b), Appendix 8.10.

(a)



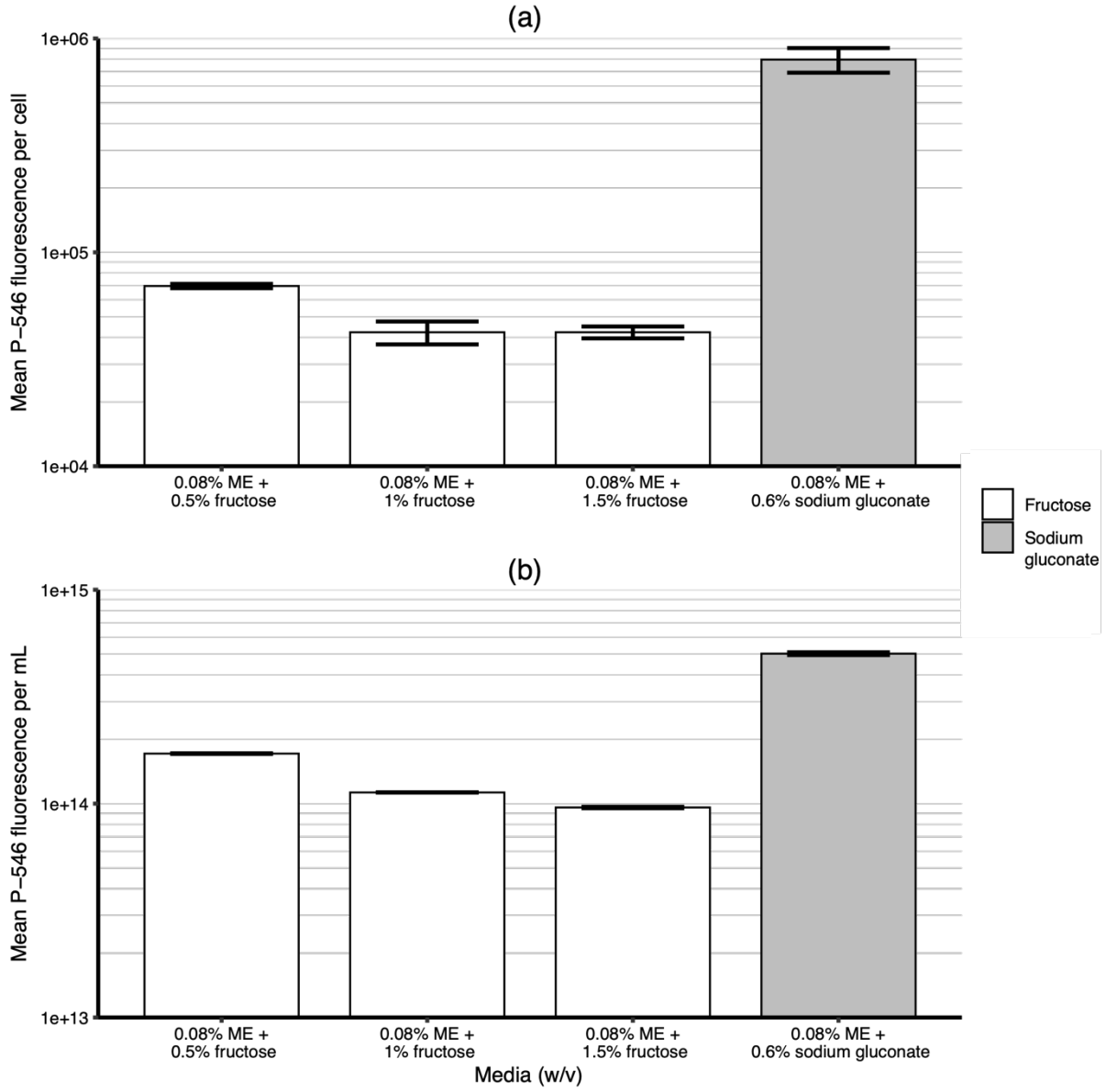
(b)

Non-paired t-test comparing different ME concentrations		
Fructose concentration (w/v)	72 hours	168 hours
0.5%	NS	NS
1%	NS	*
1.5%	NS	NS

(c)

Non-paired t-test comparing different ME concentrations				
ME concentration (w/v)	Fructose concentration comparison (w/v)		72 hours	168 hours
0.08%	0.5%	1%	NS	NS
	0.5%	1.5%	NS	NS
	1%	1.5%	NS	NS
0.2%	0.5%	1%	NS	NS
	0.5%	1.5%	NS	NS
	1%	1.5%	NS	NS

Figure 3.54 - Summary of mean P-546 fluorescence per mL at 72 and 168 hour time points, for *C. necator* cultures containing either 0.08% and 0.2% (w/v) ME supplemented with 0.5%, 1% and 1.5% (w/v) fructose. Statistical significance was determined using paired t-tests to compare the same condition at different time points (displayed as figure annotations), and non-paired t-tests to compare different experimental conditions. NS = non-significant ($p \geq 0.05$), * = $p < 0.05$. Error bars represent SD. n = 2 biological replicates. The full data is located in Figure 8.25 (c) and (d), Appendix 8.10.



(c)

Non-paired t-test comparing sodium gluconate supplemented cultures to those fructose supplemented		
Fructose concentration (w/v)	P-546 fluorescence per cell significance	P-546 fluorescence per mL significance
0.5%	**	**
1%	**	***
1.5%	**	**

Figure 3.55 - Comparison of mean P-546 fluorescence per cell (a) and per mL (b) at 168 hours for 0.08% (w/v) *C. necator* supplemented with 0.5%, 1% and 1.5% (w/v) fructose or 0.6% (w/v) sodium gluconate. Statistical significance was determined using non-paired t-tests to compare different experimental conditions (c). NS = non-significant ($p \geq 0.05$), * = $p < 0.05$, ** = $p \leq 0.01$, *** = $p \leq 0.001$. Error bars represent SD. Error bars represent SD. n = 2 biological replicates for fructose-supplemented cultures and n = 3 for sodium gluconate-supplemented cultures. The full data can be found in Figure 8.30, Appendix 8.11.

3.9.3 The P3HB^{++} population likely produces more P3HB per mL but sample size restricts statistical outcomes

Figure 3.56 contains a summary detailing the mean percentage of P3HB^{++} cells at 72 and 168-hour time points, for *C. necator* cultures containing either 0.08% or 0.2% (w/v) ME and supplemented with either 0.5%, 1% or 1.5% (w/v) fructose. The raw data is located in Figure 8.25 (e) and (f), Appendix 8.10.

For all conditions tested the mean percentage of P3HB^{++} cells increased between 72 and 168 hours. However, the increases were found to be not significant when statistically comparing the same cultures at different time points (Figure 3.56 (a)), comparing different ME concentrations (Figure 3.56 (b)) and different fructose concentrations (Figure 3.56 (c)).

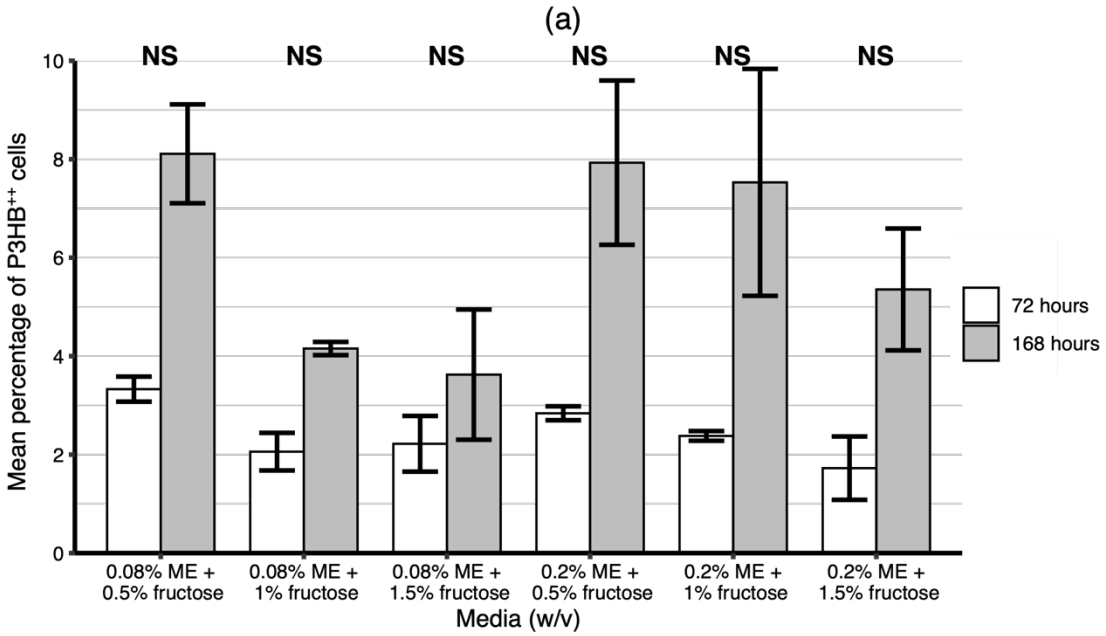
Summaries of mean P-546 fluorescence for the P3HB^{+} and P3HB^{++} *C. necator* populations can be found expressed as per cell in Figure 3.57, and per mL in Figure 3.58. The full data is located in Figure 8.26, Appendix 8.10.

Unlike in previous sections, statistical comparisons comparing the mean P3HB per cell (Figure 3.57 (a)), and per mL of culture (Figure 3.58 (a)) did not find cells in the P3HB^{++} population to have significantly more P3HB than P3HB^{+} cells. Although in all samples the P3HB^{++} population contained more P3HB per cell and per mL than P3HB and based on previous results, it's likely with further replicates a significant difference would be determined. Statistical comparisons analysing the effect of increasing ME concentration on P3HB per cell (Figure 3.57 (b)) found that when supplementing cultures with 0.5% (w/v) fructose, increasing the ME concentration to 0.2% (w/v) decreased the mean P3HB per cell. However, identical analysis analysing P3HB per mL of culture (Figure 3.58 (b)) showed that the P3HB^{+} population actually decreased its overall P3HB contribution, although this result was not significantly different. Further statistical analysis analysing the significance of fructose concentration on P3HB levels per cell (Figure 3.57 (c)) and per mL, (Figure 3.58 (c)) found all conditions tested to be not significantly different.

In previous sections, *C. necator* cells in the P3HB^{++} population have been found to contain significantly more P3HB than P3HB^{+} cells. The production of P3HB^{++} cells by *C. necator* appears to be a survival strategy, comparably to persister cell formation in *E. coli*, as an insurance policy in case the main proliferating population is eradicated (Kotte *et al.*, 2014; Solopova *et al.*, 2014). The main difference between the *C. necator* P3HB^{++} population and *E. coli* persister cells is that P3HB^{++} cells rapidly produce P3HB. In the current section, the statistical analysis appears to have been weakened by a reduced sample size of 2 replicates. However, results infer, albeit not statistically, that the proportion

of P3HB^{++} cells increases slightly between 72 and 168 hours, and the P3HB^{++} population accounts for more P3HB per mL at 168 hours.

(a)



(b)

Non-paired t-test comparing different ME concentrations		
Fructose concentration (w/v)	72 hours	168 hours
0.5%	NS	NS
1%	NS	NS
1.5%	NS	NS

(c)

Non-paired t-test comparing different ME concentrations				
ME concentration (w/v)	Fructose concentration comparison (w/v)		72 hours	168 hours
0.08%	0.5%	1%	NS	NS
	0.5%	1.5%	NS	NS
	1%	1.5%	NS	NS
0.2%	0.5%	1%	NS	NS
	0.5%	1.5%	NS	NS
	1%	1.5%	NS	NS

Figure 3.56 - Summary of the mean percentage P3HB^{++} cells at 72 and 168 hour time points, for *C. necator* cultures containing either 0.08% and 0.2% (w/v) ME supplemented with 0.5%, 1% and 1.5% (w/v) fructose. Statistical significance was determined using paired t-tests to compare the same condition at different time points (displayed as figure annotations), and non-paired t-tests to compare different experimental conditions. NS = non-significant ($p \geq 0.05$), * = $p < 0.05$, ** = $p \leq 0.01$. Error bars represent SD. n = 2 biological replicates. ((c) The raw data is located in Figure 8.25 (e) and (f), Appendix 8.10.

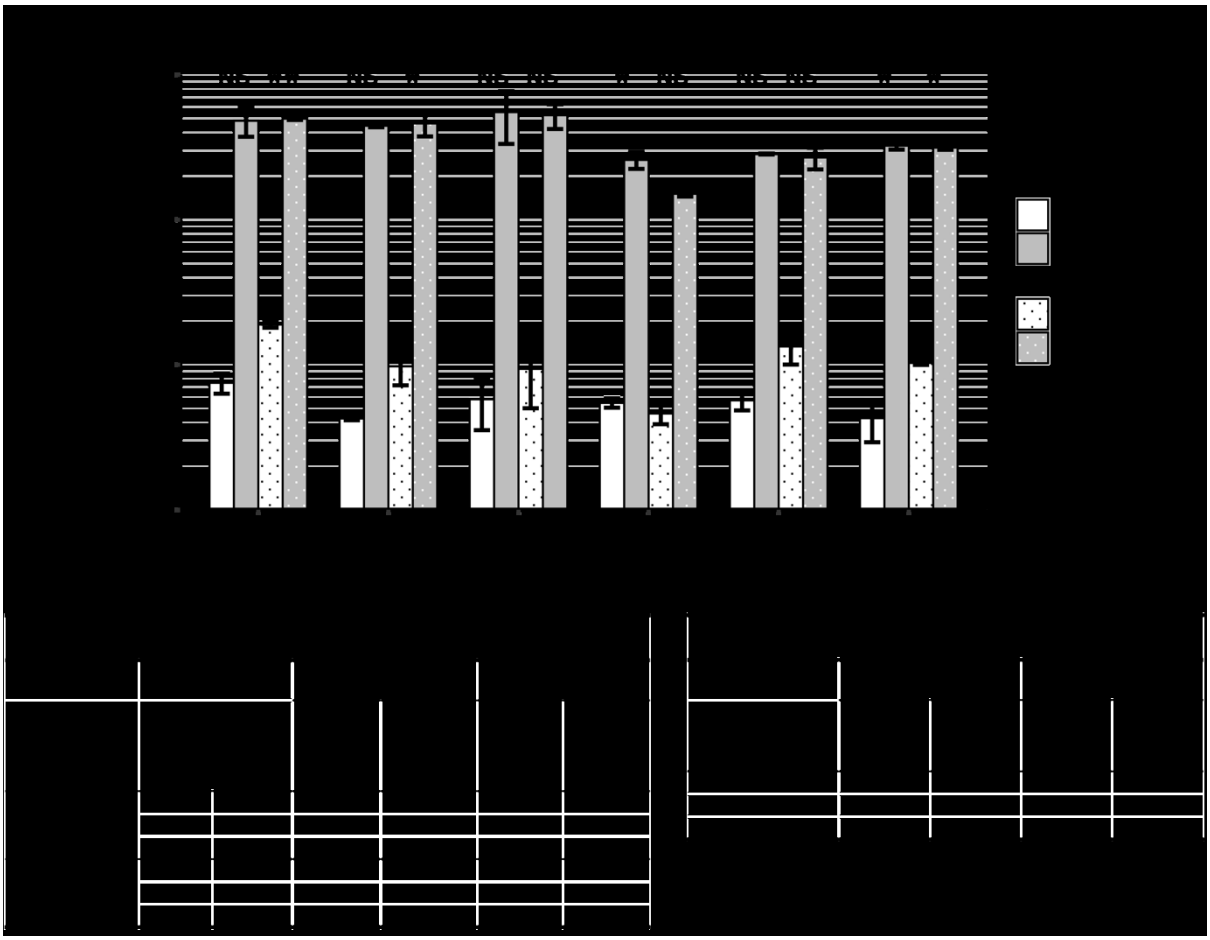


Figure 3.57 - Summary of mean P3HB^{+} and P3HB^{++} P-546 fluorescence per cell at 72 and 168 hour time points, for *C. necator* cultures containing either 0.08% and 0.2% (w/v) ME supplemented with 0.5%, 1% and 1.5% (w/v) fructose. Statistical significance was determined using paired t-tests to compare the same condition at different time points (displayed as figure annotations), and non-paired t-tests to compare different experimental conditions. NS = non-significant ($p \geq 0.05$), * = $p < 0.05$, ** = $p \leq 0.01$, *** = $p \leq 0.001$. Error bars represent SD. n = 2 biological replicates. The full data is located in Figure 8.26 (a) and (b), Appendix 8.10.

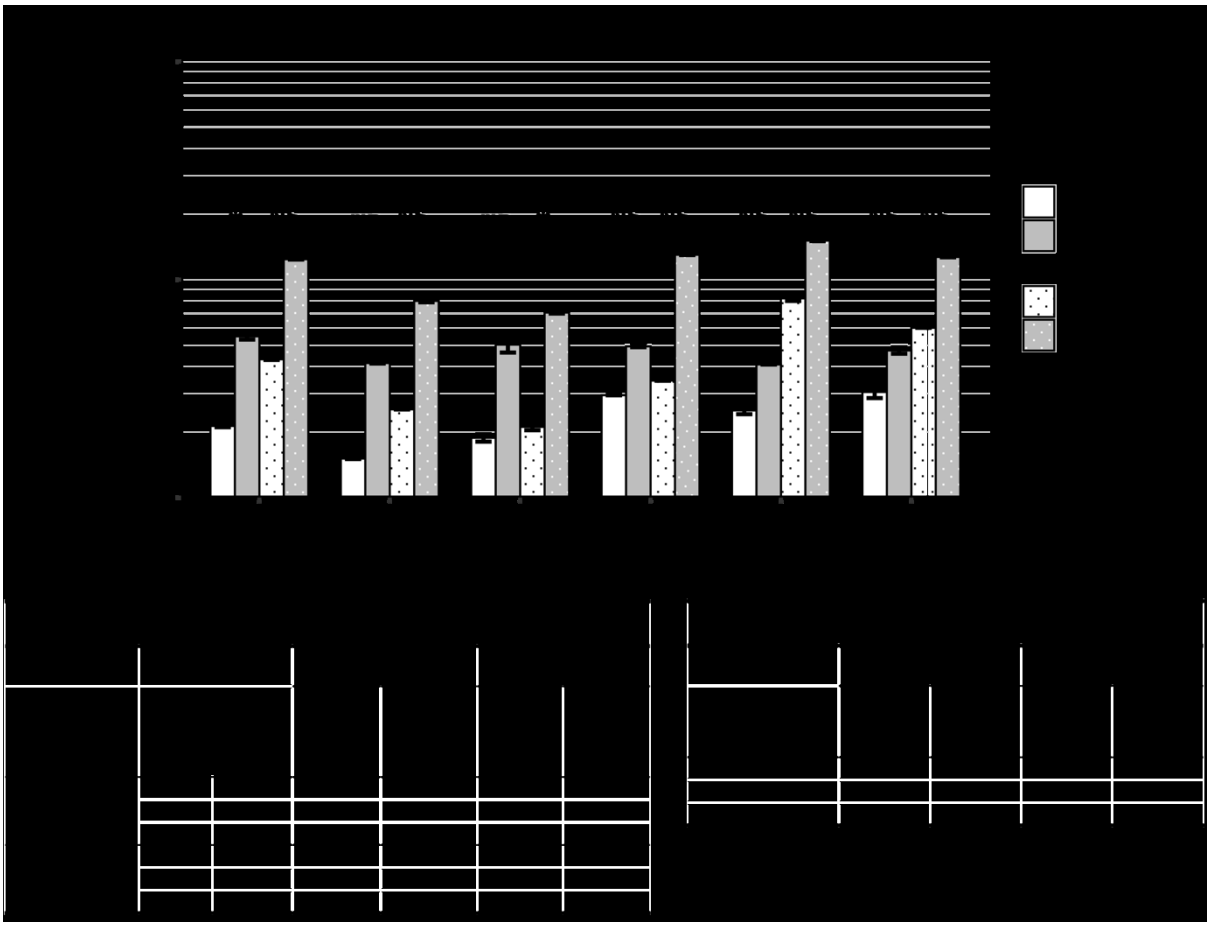


Figure 3.58 - Summary of mean P3HB^{+} and P3HB^{++} P-546 fluorescence per mL at 72 and 168 hour time points, for *C. necator* cultures containing either 0.08% and 0.2% (w/v) ME supplemented with 0.5, 1 and 1.5% (w/v) fructose. Statistical significance was determined using paired t-tests to compare the same condition at different time points (displayed as figure annotations), and non-paired t-tests to compare different experimental conditions. NS = non-significant ($p \geq 0.05$), * = $p < 0.05$, ** = $p \leq 0.01$. Error bars represent SD. n = 2 biological replicates. The full data is located in Figure 8.26 (c) and (d), Appendix 8.10.

3.9.4 Cells in the P3HB^{++} population once again have a significantly smaller phenotype in most instances

Figure 3.59 contains a summary of mean FSC at 72 and 168-hour time points, for *C. necator* cultures containing either 0.08% or 0.2% (w/v) ME and supplemented with either 0.5%, 1% or 1.5% (w/v) fructose. The raw data is located in Figure 8.28 (a) and (b), Appendix 8.10.

Statistical comparisons between 72 and 168 hours (Figure 3.59 (a)) For 0.08% (w/v) ME cultures there was no significant difference in cell size between any of the fructose concentrations tested. For 0.2% (w/v) ME cultures on the other hand, 0.5% (w/v) fructose significantly decreased FSC between 72 and 168 hours, whereas 1% and 1.6% (w/v) fructose decreased cell size.

Non-paired statistical comparisons between the same fructose concentration at either 0.08% or 0.2% (w/v) ME found that only 0.5% (w/v) fructose-supplemented cultures decreased in cell size with increasing ME concentration.

Further non-paired t-tests comparing different fructose concentrations at each ME concentration found that generally there was no significant difference between fructose concentrations, except for 0.5% (w/v) fructose supplemented 0.08% (w/v) ME cultures which were found to contain significantly smaller in size than 0.08% (w/v) ME with 1% and 1.5% (w/v) fructose supplementations.

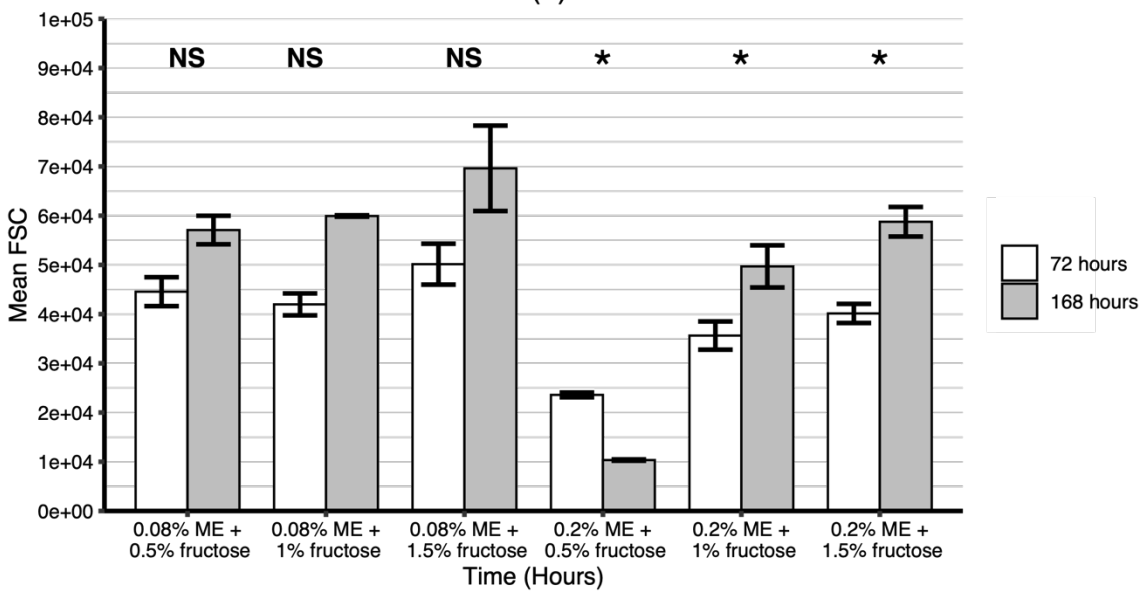
Figure 3.60 contains a summary of mean P3HB^{+} and P3HB^{++} at 72 and 168-hour time points, for *C. necator* cultures containing either 0.08% or 0.2% (w/v) ME and supplemented with either 0.5%, 1% or 1.5% (w/v) fructose. The raw data is located in Figure 8.28 (c)- (f).

Comparisons between the P3HB^{+} and P3HB^{++} populations at 72 and 168 hours (Figure 3.60 (a)) found that for all conditions, at each time point, P3HB^{++} cells were smaller than P3HB^{+} cells. Although, the differences in cell size were not always statistically significant.

Further comparisons between different fructose concentrations at 0.08% and 0.2% (w/v) ME (Figure 3.60 (b)) and the same fructose concentration at different ME concentrations, found that generally there was little statistical variability in the data.

Once again, a significantly smaller phenotype for P3HB^{++} cells, in most instances, provides evidence consistent with the small cell phenotype observed for *E. coli* persister cells Kotte *et al.*, 2014; Solopova *et al.*, 2014). In addition, in the more nutritious 0.2% (w/v) ME cultures changes, in overall cell size were observed between 72 and 168 hours. This appears to again be indicative of cell volume changes due to media osmolarity which seems to be influenced by both starting ME and fructose concentration in this case (Oldewurtel *et al.*, 2021).

(a)



(b)

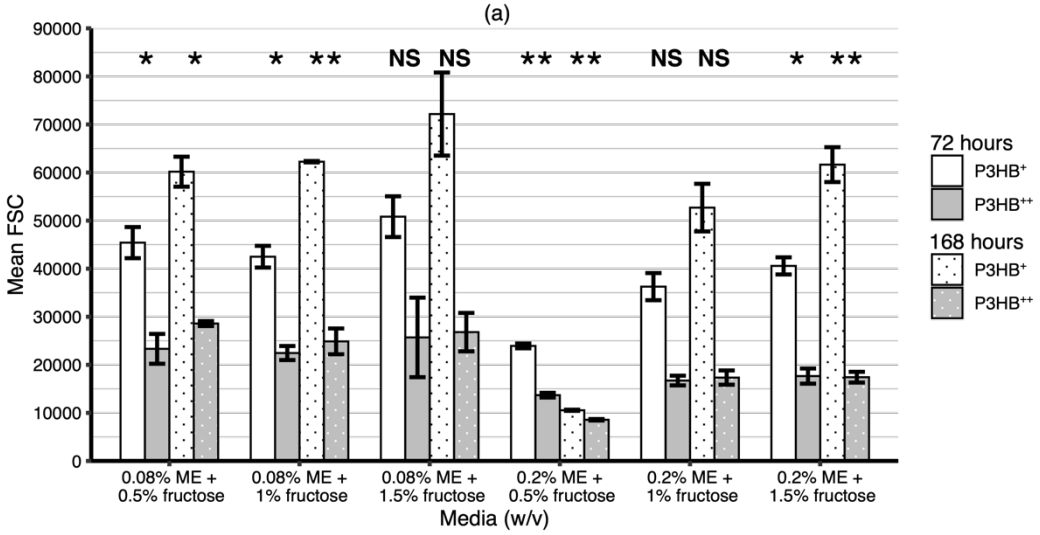
Non-paired t-test comparing different ME concentrations		
Fructose concentration (w/v)	72 hours	168 hours
0.5%	NS	*
1%	NS	NS
1.5%	NS	NS

(c)

Non-paired t-test comparing different ME concentrations				
ME concentration (w/v)	Fructose concentration comparison (w/v)		72 hours	168 hours
0.08%	0.5%	1%	NS	*
	0.5%	1.5%	NS	*
	1%	1.5%	NS	NS
0.2%	0.5%	1%	NS	NS
	0.5%	1.5%	NS	NS
	1%	1.5%	NS	NS

Figure 3.59 - Summary of FSC at 72 and 168 hour time points, for *C. necator* cultures containing either 0.08% and 0.2% (w/v) ME supplemented with 0.5%, 1% and 1.5% (w/v) fructose. Statistical significance was determined using paired t-tests to compare the same condition at different time points (displayed as figure annotations), and non-paired t-tests to compare different experimental conditions. NS = non-significant ($p \geq 0.05$), * = $p < 0.05$, ** = $p \leq 0.01$. Error bars represent SD. n = 2 biological replicates.

(a)



(b)

Non-paired t-test comparing different ME concentrations						
			P3HB+		P3HB++	
ME concentration (w/v)	Fructose concentration comparison (w/v)		72 hours	168 hours	72 hours	168 hours
0.08%	0.5%	1%	NS	NS	NS	NS
	0.5%	1.5%	NS	NS	NS	NS
	1%	1.5%	NS	NS	NS	NS
0.2%	0.5%	1%	NS	NS	NS	NS
	0.5%	1.5%	*	*	NS	NS
	1%	1.5%	NS	NS	NS	NS

(c)

Non-paired t-test comparing different ME concentrations				
	P3HB+		P3HB++	
Fructose concentration (w/v)	72 hours	168 hours	72 hours	168 hours
0.5%	NS	*	NS	NS
1%	NS	NS	*	NS
1.5%	NS	NS	NS	NS

Figure 3.60 - Summary of mean P3HB^{+} and P3HB^{++} FSC at 72 and 168 hour time points, for *C. necator* cultures containing either 0.08% and 0.2% (w/v) ME supplemented with 0.5%, 1% and 1.5% (w/v) fructose. Statistical significance was determined using paired t-tests to compare the same condition at different time points (displayed as figure annotations), and non-paired t-tests to compare different experimental conditions. NS = non-significant ($p \geq 0.05$), * = $p < 0.05$, ** = $p \leq 0.01$. Error bars represent SD. n = 2 biological replicates.

3.9.5 Discussion

Comparisons after 24 hours of growth, between cultures supplemented with fructose or sodium gluconate, found few cells were produced in cultures supplemented with sodium gluconate. This likely occurs due to sodium gluconate-supplemented *C. necator* cells expanding and those supplemented with fructose proliferating. Sodium ions may facilitate cell expansion in cultures supplemented with sodium gluconate, by causing turgor pressure-induced expansion (Björklund and Marguerat, 2017) or due to increasing the rate at which expansion-related proteins such as MreB aid expansion (Szatmári et al., 2020).

Summarised data compared 72 and 168-hour time points for cultures containing either 0.08% or 0.2% (w/v) ME and supplemented with either 0.5, 1 or 1.5% (w/v) fructose. Cell count data found that fructose-supplemented cultures produce around 10 times the amount of cells than sodium gluconate-supplemented at 24 hours. In addition, after 168 hours, fructose-supplemented cultures produced less P3HB per cell and per mL of culture. It was therefore concluded that a fed-batch system in which ME media was supplemented with fructose at 0 hours for an initial growth period of 24 hours (phase 1). Then at 24 hours, once a high cell count has been established, sodium gluconate should be added in order to induce P3HB formation up to 72 hours (phase 2). Phase 2 represents the desired period in which P3HB is produced. Phase 3 would then represent a period in which sampling occurs to observe if P3HB keeps increasing after 72 hours, or if indeed maximum P3HB production has been achieved in phase 2.

3.10 Conclusions

In Chapter 3 the growth of *C. necator* in ME of varying concentrations supplemented with either fructose or sodium gluconate has been studied using flow cytometry, UV-visible spectroscopy and fluorescent microscopy.

Increasing the ME to C ratio has generally failed to increase P3HB per *C. necator* cell and a lag phase in P3HB production is observed in which the majority of P3HB production continues beyond 72 hours. However, sodium gluconate supplementation increases P3HB per cell in relation to fructose. It's possible this is because sodium ions facilitate the uptake of gluconate via secondary transport proteins, particularly when the gluconate concentration is lower in the growth media than in *C. necator* cells. The addition of fructose to ME media produces more cells per mL of culture than sodium gluconate. In fact, C. necator responds to fructose supplementation by proliferating and to sodium gluconate by expanding cell volume. The increased cell size observed for sodium gluconate supplemented *C. necator* may also be due to the presence of sodium ions, which influence changes in cell volume by causing cell turgor pressure to rise, and also by increasing the rate at which peptidoglycan precursors are able to influence cell expansion.

A proportionally small population of $P3HB^{++}$ C. necator cells are able to produce up to 1000 times more P3HB per cell than the dominant $P3HB^{+}$ phenotype. Such cells not only accumulate superior intracellular P3HB but also accumulate P3HB in as little as 4 hours. It's possible the $P3HB^{++}$ population is a type of persister cell which act as a survival strategy in case the main population is eradicated.

Multiple morphologies of *C. necator* were observed, including chains of elongated cells separated by Z-rings, cell aggregates and large expanded cells when sodium gluconate was supplemented. Cell aggregates should be avoided during cultures which aim to produce P3HB, as extracellular membrane components key to aggregate formation such as rhamnolipids may compete with intracellular pools of common intermediate molecules such as acetyl-CoA.

Overall, the results in Chapter 3 have demonstrated that a 2 stage fed-batch strategy may be able to increase culture P3HB production, and reduce the lag-phase in P3HB production, by utilising the strengths of fructose and sodium gluconate supplementation. The strategy therefore consists of utilising fructose initially to increase culture cell density in which key nutrients a utilised (phase 1), and then adding sodium gluconate at 24 hours once culture growth is completed at 24 hours with a view to producing maximum P3HB by 72 hours (phase 2)

Chapter 4 Fed-batch *C. necator* cultures using fructose to increase cell number and sodium gluconate to produce P3HB

4.1 Introduction

In Chapter 3, results found in comparison that that of fructose, sodium gluconate supplemented *C. necator* cultures produced more P3HB per cell and also per mL of culture. Fructose, on the other hand, produced more cells per mL of culture than that of sodium gluconate. The cells in fructose-supplemented cultures were smaller and appeared to favour cell division, whereas *C. necator* cells in sodium gluconate-supplemented cultures favoured less division and more cell expansion. The main drawback of the results was the inability of cultures to produce P3HB in a reasonable timeframe of 72 hours. This appeared to be due to a lag phase in P3HB production occurring prior to 72 hours.

Therefore, in Chapter 4 experiments are split into 3 phases. Phase 1 serves as an initial period, between 0 and 24 hours, in which biomass accumulation takes place. Phase 2 occurs between 24 and 72 hours and is the period in which the study aims to produce maximum P3HB. Because P3HB accumulation has been shown to increase more after 72 hours in Chapter 3, Phase 3 is investigated after 72 hours to show how much P3HB *C. necator* is capable of producing. As such, when P3HB production keeps increasing into phase 3, the aim is then to achieve the amount observed in phase 3 in phase 2 of future cultures.

Experiments in sections 4.2 and 4.3 aim to utilise the strengths of fructose and sodium gluconate in fed-batch strategies, by using fructose to produce biomass in phase 1, and sodium gluconate to produce P3HB in phase 2. In sections 4.4 and 4.5, the results of repeated-batch experiments are presented in which media is changed to more dilute ME at the end of phase 1. In these sections, fructose and sodium gluconate are used as in sections 4.2 and 4.3, but additionally in section 4.4 in which sodium gluconate is trailed as a supplement in phase one, and in section 4.5 both fructose and sodium gluconate are trialled together in phase 1.

4.2 Does the addition of fructose at 0 hours and sodium gluconate to ME media at 24 hours increase P3HB production?

In section 4.2, a fed-batch method of cultivation was used in which 0.5% (w/v) fructose was added to 0.08%, 0.2% or 0.4% (w/v) ME at the start of phase 1 at 0 hours, before the addition of either 0.6% or 1.2% (w/v) sodium gluconate at the start of phase 2 at 24 hours. The addition of fructose aims to increase biomass up to 24 hours and utilise key nutrients provided by ME to create media conditions suitable for the initiation of P3HB production in *C. necator*. At the start of phase 2, at 24 hours, sodium gluconate was supplemented with the aim of producing maximum P3HB up to in 72 hours.

4.2.1 Cell proliferation does not occur in phase 3

Figure 4.1 contains a summary of mean events per mL for *C. necator* cultures containing 0.08%, 0.2% or 0.4% (w/v) ME supplemented with 0.5% (w/v) fructose at 0 hours, with either 0.6% or 1.1% (w//v) sodium gluconate added after 24 hours. The full data can be found in Figure 9.1, Appendix 9.1.

For all culture conditions tested the mean events per mL did not significantly change between 72 and 288 hours. The evidence presented in Figure 4.1 shows that cell proliferation was not occurring beyond the end of phase 2 at 72 hours up to phase 3 at 288 hours. This is indicative of P3HB-promoting conditions as acetyl-CoA is not being used by the citric acid cycle for cell proliferation.

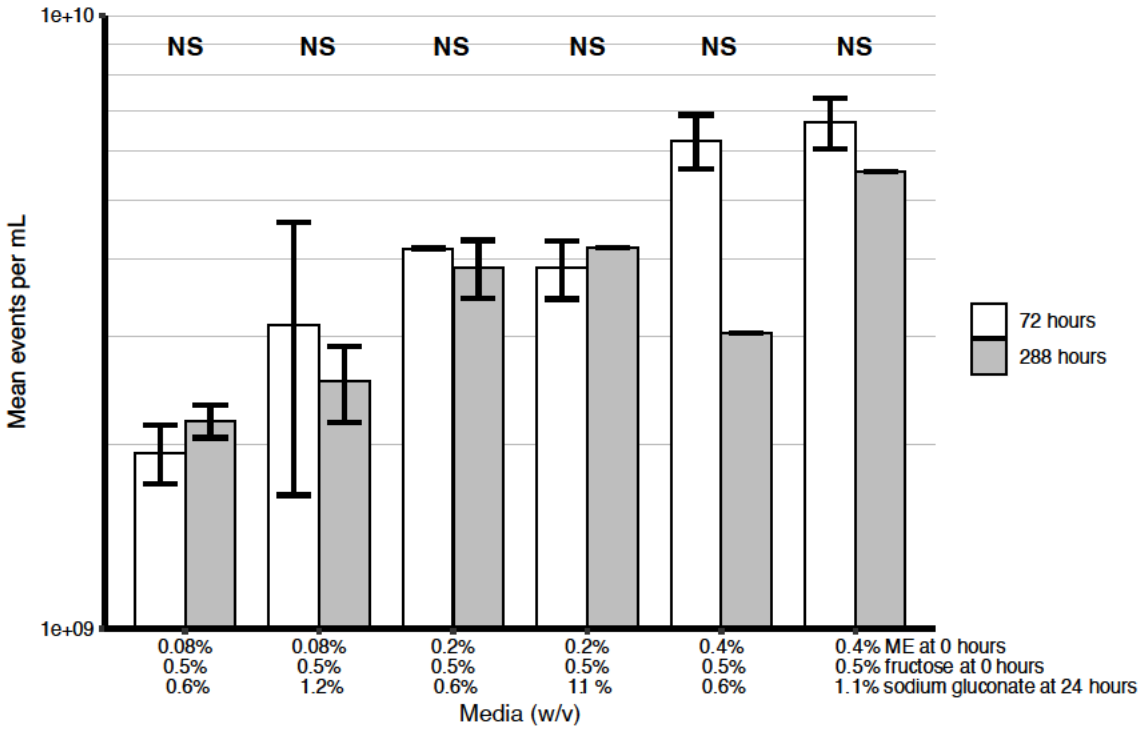


Figure 4.1 – Graph displaying the mean events per mL for *C. necator* culture containing 0.08%, 0.2% or 0.4% (w/v) ME supplemented with 0.5% (w/v) fructose at 0 hours, with either 0.6% or 1.1% (w//v) sodium gluconate added after 24 hours. Statistical significance was determined using paired t-tests to compare the same condition at different time points (displayed as figure annotations). NS = non-significant ($p \geq 0.05$). Error bars represent SD. n = 2 biological replicates. The full data can be found in Figure 9.1, Appendix 9.1.

4.2.2 Greater P-546 fluorescence is recorded in phase 3

Figure 4.2 contains a summary of P-546 fluorescence (P3HB) per cell, and Figure 4.3 a summary of mean P-546 fluorescence (P3HB) per mL, for *C. necator* culture containing 0.08%, 0.2% or 0.4% (w/v) ME supplemented with 0.5% (w/v) fructose at 0 hours, and either 0.6% or 112% (w//v) sodium gluconate added after 24 hours. The full data can be found expressed per cell in Figure 9.2 (a) and (b), and per mL in Figure 9.2 (c) and (d), Appendix 9.1.

For all conditions tested, except for 0.4% (w/v) ME supplemented with 0.5% (w/v) fructose at 0 hours and 0.6% (w/v) sodium gluconate at 24 hours, a significant increase in P3HB per cell was observed between the end of phase 2 at 72 hours and phase 3 at 288 hours (Figure 4.2). Mean P3HB per mL (Figure 4.3) also increased between 72 and 288 hours for all conditions tested, however, the increase was not statistically significant for cultures containing 0.08% (w/v) ME.

Figure 4.4 contains a summary of the mean percentage of $P3HB^{++}$ cells for *C. necator* cultures containing 0.08%, 0.2% or 0.4% (w/v) ME supplemented with 0.5% (w/v) fructose at 0 hours, with either 0.6% or 1.1% (w//v) sodium gluconate added after 24 hours. The full data can be found in Figure 9.2 (e) and (f), Appendix 9.1.

For all conditions tested except for 0.4% (w/v) ME supplemented with 0.5% (w/v) fructose at 0 hours and 0.6% (w/v) sodium gluconate at 24 hours, a significant increase in the amount of $P3HB^{++}$ cells was observed at the end of phase 2 at 72 hours and during phase 3 at 288 hours was observed.

Figure 4.5 contains a summary of $P3HB^{+}$ and $P3HB^{++}$ P-546 fluorescence (P3HB) per cell, and Figure 4.6 a summary of mean P-546 fluorescence (P3HB) per mL, for *C. necator* culture containing 0.08%, 0.2% or 0.4% (w/v) ME supplemented with 0.5% (w/v) fructose at 0 hours, with either 0.6% or 1.1% (w//v) sodium gluconate added after 24 hours. The full data for P3HB per cell is located in Figure 9.3 and per mL in Figure 9.4, Appendix 9.1.

Overall data in this section suggests that the fed-batch strategy of feeding initially with fructose before adding sodium gluconate to accumulate P3HB has not stopped a lag in P3HB production, and as a result, P3HB per cell and per mL increase greatly in phase 3. In an ideal scenario, P3HB would increase during phases 1 and 2, before peaking and degrading during phase 3. Indeed, this scenario was reported in acetic acid supplemented 0.8% (w/v) ME by Passanha *et al*. (2014) in which *C. necator* reached peak PHA after 26 hours after which point a decline was observed. Once again, a significantly higher proportion $P3HB^{++}$ cells in culture at 288 hours demonstrates the less rapid production of $P3HB^{++}$ cells which likely results from $P3HB^{+}$ cells increasing intracellular P3HB, rather than the rapid production of $P3HB^{++}$ cells which accumulate P3HB in as little as 4 hours. It should be noted that once again, a reduced replicate number of 2 likely weakened statistical significance and this can be seen

most in Figure 4.5 and Figure 4.6 in which it was difficult in some instances to compare data due to a lack of statistical significance.

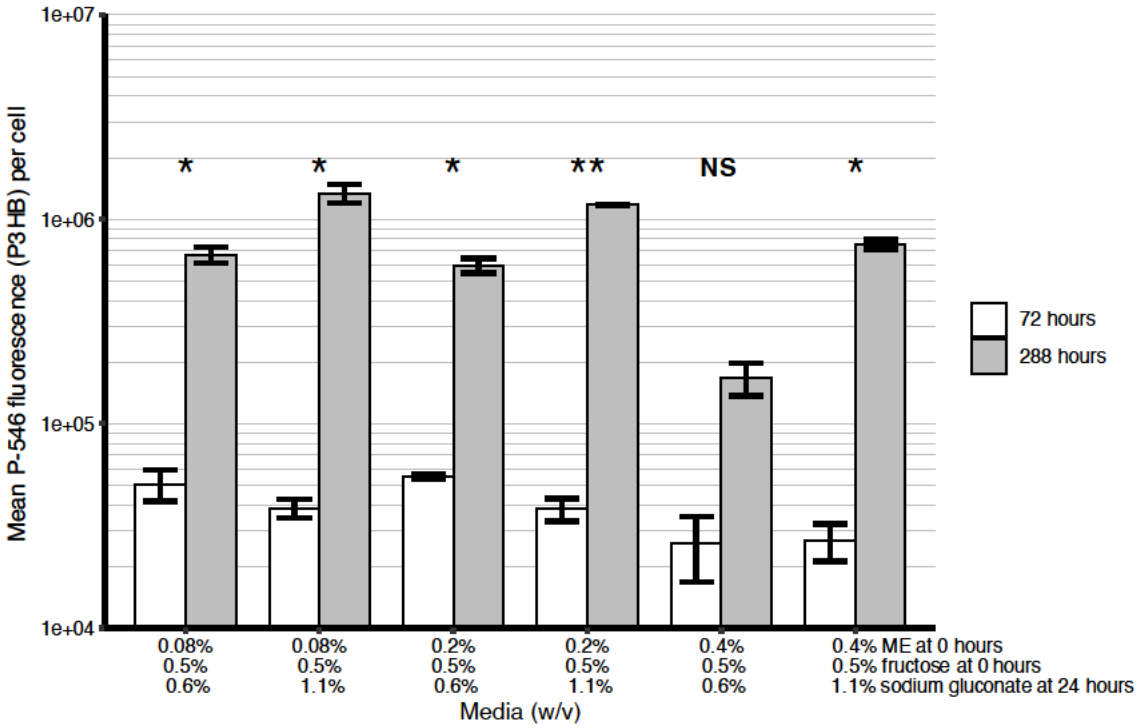


Figure 4.2 – Graph displaying the mean P-546 fluorescence (P3HB) per cell for *C. necator* cultures containing 0.08%, 0.2% or 0.4% (w/v) ME supplemented with 0.5% (w/v) fructose at 0 hours, with either 0.6% or 1.1% (w//v) sodium gluconate added after 24 hours. Statistical significance was determined using paired t-tests to compare the same condition at different time points (displayed as figure annotations). NS = non-significant ($p \geq 0.05$), * = $p < 0.05$, ** = $p \leq 0.01$. Error bars represent SD. n = 2 biological replicates. The full data can be found expressed per cell in Figure 9.2, Appendix 9.1.

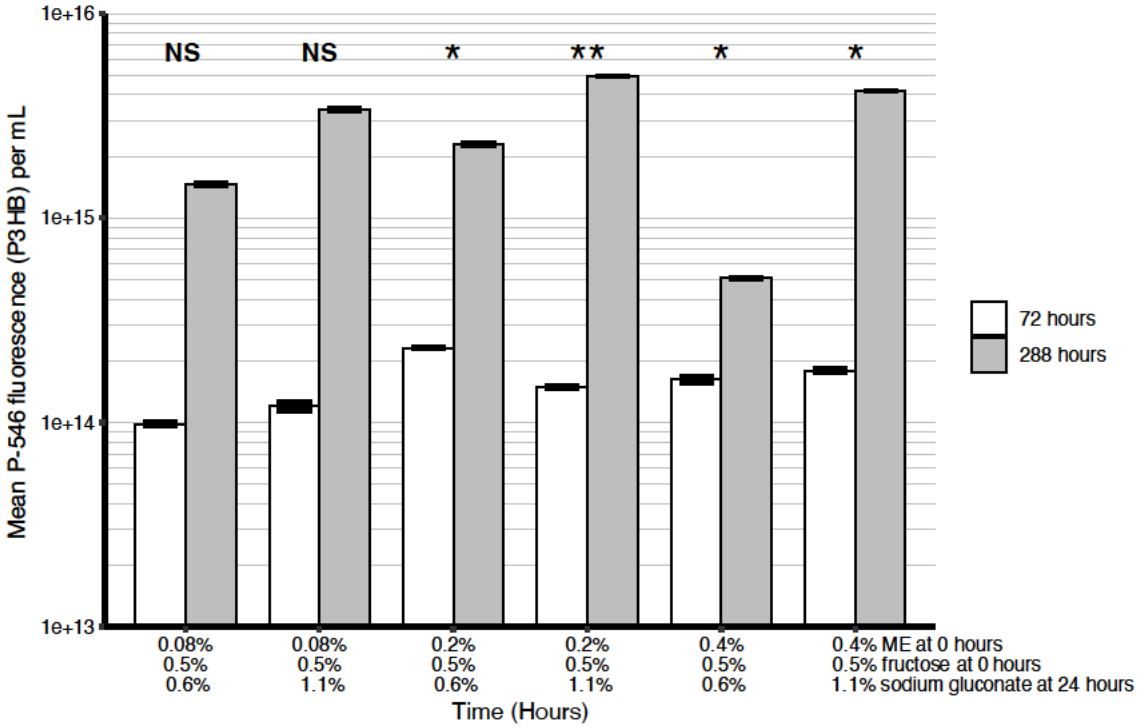


Figure 4.3 - Graph displaying the mean P-546 fluorescence (P3HB) per mL for *C. necator* cultures containing 0.08%, 0.2% or 0.4% (w/v) ME supplemented with 0.5% (w/v) fructose at 0 hours, with either 0.6% or 1.1% (w//v) sodium gluconate added after 24 hours. Statistical significance was determined using paired t-tests to compare the same condition at different time points (displayed as figure annotations). NS = non-significant ($p \geq 0.05$), * = $p < 0.05$, ** = $p \leq 0.01$. Error bars represent SD. n = 2 biological replicates. The full data can be found in Figure 9.2, Appendix 9.1.

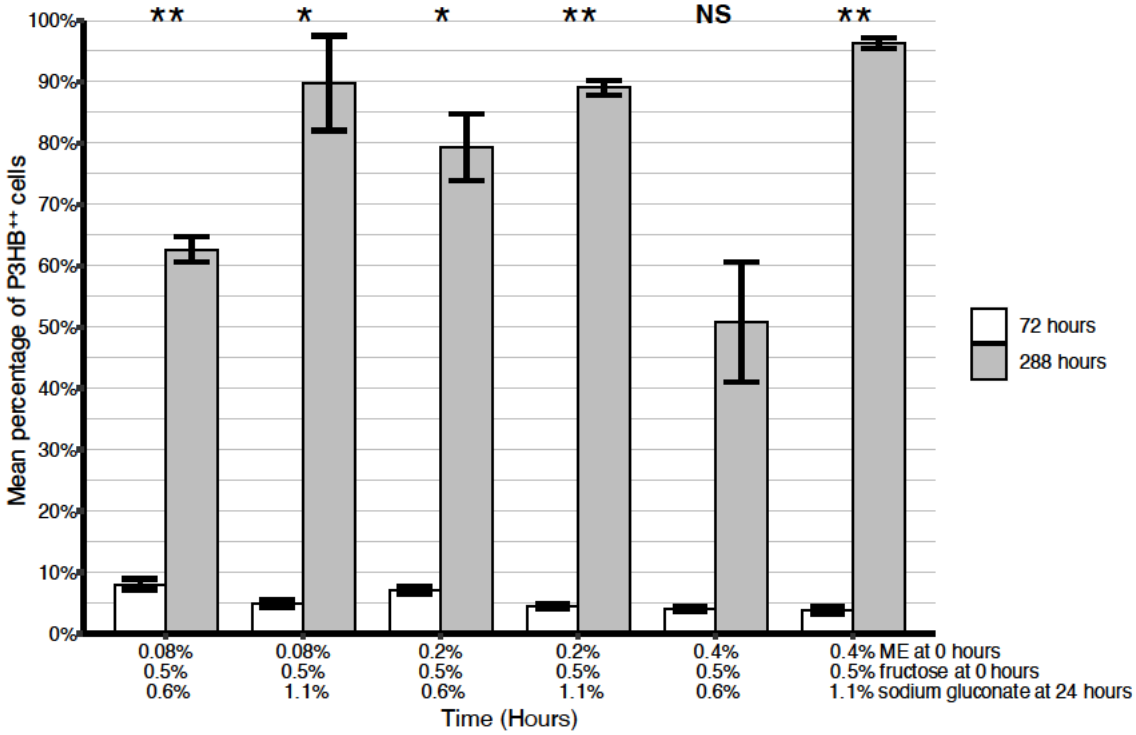


Figure 4.4 - Graph displaying the mean percentage of P3HB^{++} cells for *C. necator* cultures containing 0.08%, 0.2% or 0.4% (w/v) ME supplemented with 0.5% (w/v) fructose at 0 hours, with either 0.6% or 1.1% (w//v) sodium gluconate added after 24 hours. Statistical significance was determined using paired t-tests to compare the same condition at different time points (displayed as figure annotations). NS = non-significant ($p \geq 0.05$), * = $p < 0.05$, ** = $p \leq 0.01$. Error bars represent SD. n = 2 biological replicates.

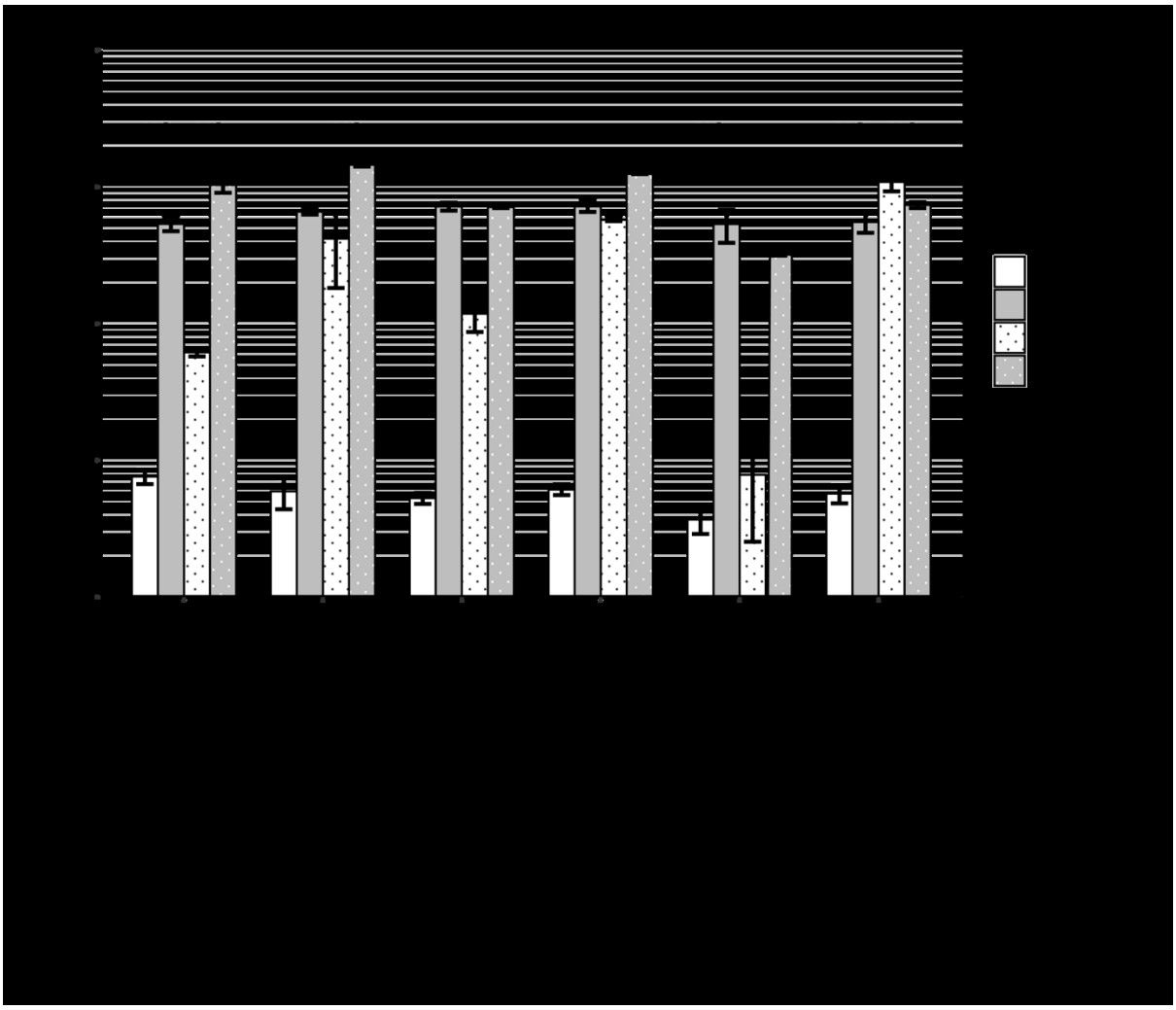


Figure 4.5 - Graph displaying the mean P3HB^{+} and P3HB^{++} P-546 fluorescence (P3HB) per cell for *C. necator* cultures containing 0.08%, 0.2% or 0.4% (w/v) ME supplemented with 0.5% (w/v) fructose at 0 hours, with either 0.6% or 1.1% (w//v) sodium gluconate added after 24 hours. Statistical significance was determined using paired t-tests to compare the same condition at different time points (displayed as figure annotations). NS = non-significant ($p \geq 0.05$), * = $p < 0.05$, ** = $p \leq 0.01$, *** = $p \leq 0.001$. Error bars represent SD. n = 2 biological replicates. The full data is located in Figure 9.3, Appendix 9.1.

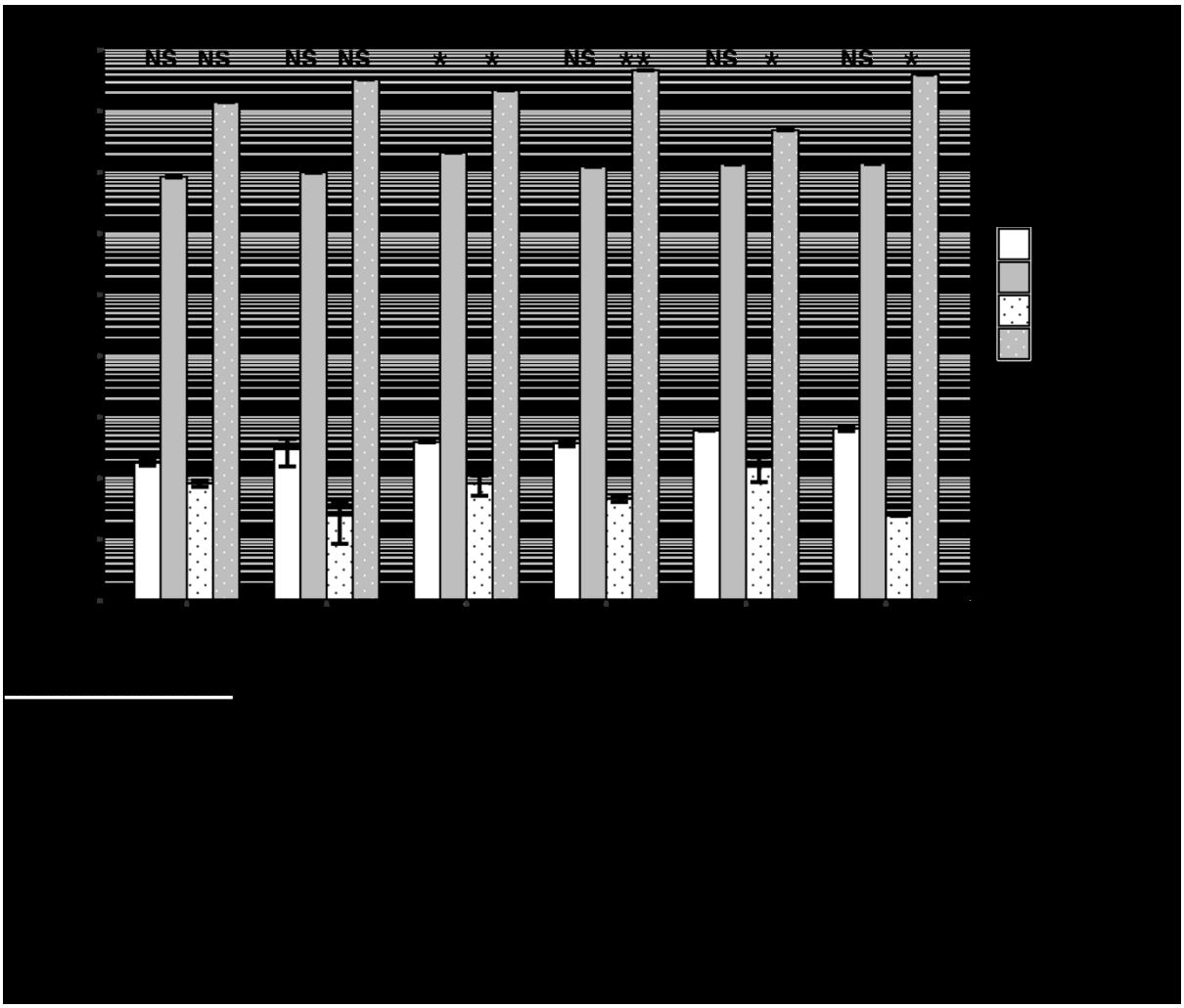


Figure 4.6 - Graph displaying the mean P3HB^{+} and P3HB^{++} P-546 fluorescence (P3HB) per mL for *C. necator* cultures containing 0.08%, 0.2% or 0.4% (w/v) ME supplemented with 0.5% (w/v) fructose at 0 hours, with either 0.6% or 1.1% (w//v) sodium gluconate added after 24 hours. Statistical significance was determined using paired t-tests to compare the same condition at different time points (displayed as figure annotations). NS = non-significant ($p \geq 0.05$), * = $p < 0.05$, ** = $p \leq 0.01$. Error bars represent SD. n = 2 biological replicates. The full data is located in Figure 9.4, Appendix 9.1.

4.2.3 Cells in 0.4% (w/v) ME cultures decrease in cell size in phase 3

Figure 4.7 contains a summary of mean cell size for *C. necator* cultures containing 0.08%, 0.2% or 0.4% (w/v) ME supplemented with 0.5% (w/v) fructose at 0 hours, and either 0.6% or 1.1% (w//v) sodium gluconate added after 24 hours. The full data can be found in Figure 9.5 (a) and (b), Appendix 9.1.

For 0.08% (w/v) ME cultures supplemented with 0.5% (w/v) fructose and 0.6% (w/v) sodium gluconate, and 0.4% (w/v) ME cultures supplemented with 0.5% (w/v) fructose and 0.6% or 1.1 (w/v) sodium gluconate, a decrease in cell size was observed between the end of phase 2 at 72 hours and phase 3 at 288 hours. For all other media conditions tested, results at each time point could not be separated statistically.

Figure 4.8 contains a summary of mean cell size for P3HB^{+} and P3HB^{++} *C. necator* in cultures containing 0.08%, 0.2% or 0.4% (w/v) ME supplemented with 0.5% (w/v) fructose at 0 hours, and either 0.6% or 1.1% (w//v) sodium gluconate added after 24 hours. The full data can be found in Figure 9.5 (c)-(f), Appendix 9.1.

In Chapter 4, P3HB^{++} cells were often smaller than P3HB^{+} cells, an observation that linked P3HB^{++} cells to persister cell populations observed in literature (Khlebodarova and Likoshvai, 2018). However, in the current section, the majority of results could not be statistically separated, once again demonstrating the weakness of 2, rather than 3, biological replicates. The reason for overall cell size in 0.4% (w/v) decreasing by a large proportion is likely down to the osmolarity of the growth media (Oldewurtel *et al.*, 2021) changing for unknown reasons but could also be due to the separation of cell chains into individual cells as previously observed in section 3.3.4.

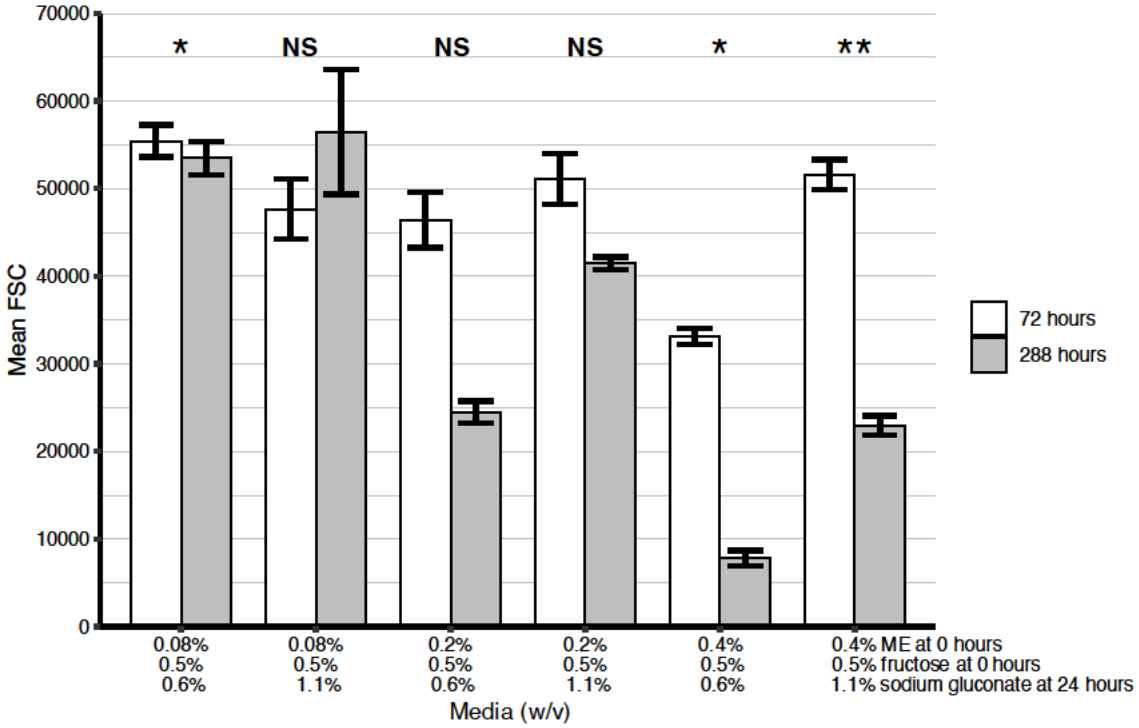
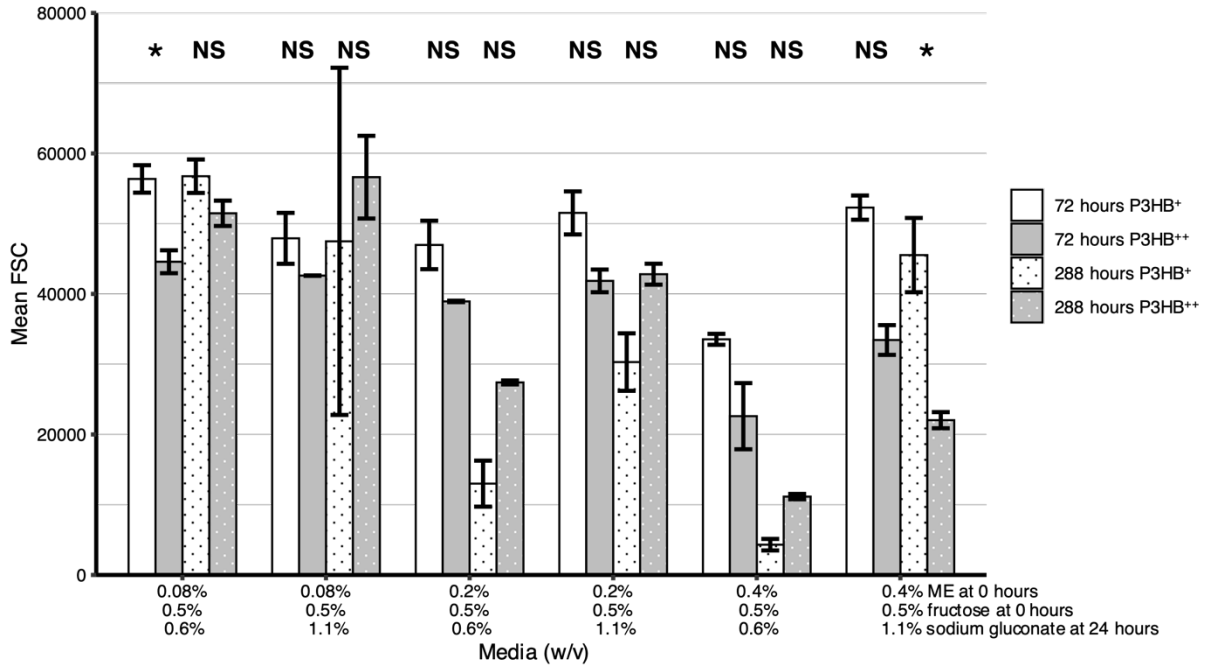


Figure 4.7 - Graph displaying the mean FSC for *C. necator* cultures containing 0.08%, 0.2% or 0.4% (w/v) ME supplemented with 0.5% (w/v) fructose at 0 hours, with either 0.6% or 1.1% (w//v) sodium gluconate added after 24 hours. Statistical significance was determined using paired t-tests to compare the same condition at different time points (displayed as figure annotations). NS = non-significant ($p \geq 0.05$), * = $p < 0.05$, ** = $p \leq 0.01$. Error bars represent SD. n = 2 biological replicates.



Paired t-test comparing the FSC of the P3HB+ and P3HB++ populations between 72 and 288 hours.

Media composition (w/v)			Statistical significance	
ME	Fructose	Sodium gluconate	P3HB+	P3HB++
0.08%	0.5%	0.6%	NS	*
0.08%	0.5%	1.1%	NS	NS
0.2%	0.5%	0.6%	NS	**
0.2%	0.5%	1.1%	*	NS
0.4%	0.5%	0.6%	*	NS
0.4%	0.5%	1.1%	NS	NS

Figure 4.8 - Graph displaying the mean P3HB+ and P3HB++ FSC for *C. necator* cultures containing 0.08%, 0.2% or 0.4% (w/v) ME supplemented with 0.5% (w/v) fructose at 0 hours, with either 0.6% or 1.1% (w//v) sodium gluconate added after 24 hours. Statistical significance was determined using paired t-tests to compare the same condition at different time points (displayed as figure annotations). NS = non-significant ($p \geq 0.05$), * = $p < 0.05$, ** = $p \leq 0.01$. Error bars represent SD. n = 2 biological replicates.

4.2.4 Discussion

Cultures of *C. necator* were grown using a fed-batch strategy in which 0.08% and 0.2% (w/v) ME was supplemented with 0.5% (w/v) fructose at 0 hours in order to increase cell density in phase 1 (0-24 hours), and either 0.6% or 1.1% sodium gluconate at 24 hours to increase intracellular P3HB during phase 2 (24-72 hours).

There was found to be no significant difference in culture cell number between 72 and 168 hours. This suggests growth-promoting nutrients were used before the end of phase 2 at 72 hours and P3HB-promoting conditions, as described by Ienczak *et al*. (2011), were likely to be present. Results are presented as comparisons between the end of phase 2 at 72 hours and phase 3 at 168 because a delay in P3HB production was observed. This meant, once again, that maximum P3HB production did not occur as desired in phase 2 but in phase 3. It would be expected that during phase 3, P3HB would be depolymerised due to the exhaustion of key nutrients and C. In fact, this is what was observed for 0.8% (w/v) ME cultures in a study by Passanha *et al*. (2014) who observed a peak in P3HB after just 26 hours and a decline phase thereafter. Multiple other studies have observed peak P3HB or PHA production to occur within 72 hours (Budde *et al.*, 2011; Pradella *et al.*, 2012; Ienczak *et al.*, 2016). As with previous results, the reason for the lag time in this section is unknown but is unlikely to be due to the natural delay observed for PhaC1 to reach maximum 3HB polymerisation as this has been reported to be only 6 hours (Juengert *et al.*, 2018).

Evidence once again suggested that cultures which had higher initial ME concentration (0.4% (w/v)) had a decreased mean cell size. As cells are not proliferating in between 72 and 168 hours, changes in cell size are more likely linked to media osmolarity (Oldewurtel *et al.*, 2021) rather than growth rate (Sharpe *et al.*, 1998; Sperber and Herman, 2017; Zhang *et al.*, 2020). The exact reason cultures with higher ME concentrations tend to decrease in cell size during phase 3 is unclear but one possibility is that residual nutrients and/or fructose or sodium gluconate remain in the media.

4.3 Attempting to reduce the P3HB production lag time by adding sodium chloride to growth media

A continuing problem in the current study is the time taken for *C. necator* cells to reach their highest levels of P3HB. The aim of this study is to produce P3HB in 72 hours and therefore the objective at this stage of this thesis is to try and reduce the lag time in which P3HB production reaches its maximum level, such that it occurs within 72 hours and not considerably longer as has been the case so far. Wen *et al*. (2018) after testing sodium chloride concentrations of between 0 and 15g/L found that 5g/L of sodium chloride increases PHA production in a mixed microbial community grown in food waste fermentation leachate. In addition, Passanha *et al*. (2014) reported that 9g/L of sodium chloride increased the production of PHA in *C. necator* by 30% and was also found to reduce the time required for PHA production. As a result, this section attempts to reduce the lag time in P3HB production in the current study by testing sodium chloride at concentrations ranging from 0 to 15g/L.

4.3.1 No significant changes in cell counts are observed as sodium chloride concentration increases between 3 and 15g/L

Figure 4.9 contains a summary of mean events per mL for *C. necator* cultures containing 0.08% or 0.2% (w/v) ME, 0, 3, 6, 9, 12 or 15 g/L sodium chloride and supplemented with 0.5% (w/v) fructose at 0 hours and 0.6% (w/v) sodium gluconate at 24 hours. The full data can be found in Figure 9.6, Appendix 9.2.

For 0.08% (Figure 4.9 (a)) and 0.2% (w/v) ME (Figure 4.9 (b)) cultures, the addition of 3 g/L or more sodium chloride resulted in a non-significant increase in mean culture events. In contrast, cultures without sodium chloride did significantly increase in mean events between 72 and 240 hours.

An increase in mean events is indicative of growth-promoting nutrient conditions, in which fructose and gluconate are directed into energy metabolism via the Entner-Doudoroff pathway rather than into the P3HB biosynthetic pathway. While in Figure 4.1 0.08% and 0.2% (w/v) ME cultures were found to not significantly increase a later time point of 288 hours was used for comparison to the 72-hour result. Thus the cultures may be in a state of decline by 288 hours. Its therefore possible that the lag phase in P3HB production observed between the end of phase 2 at 72 hours, and post-72 hour phase 3 may result from the incomplete usage of growth-promoting nutrients in the growth medium, even at the lowest ME concentration tested of 0.08% (w/v).

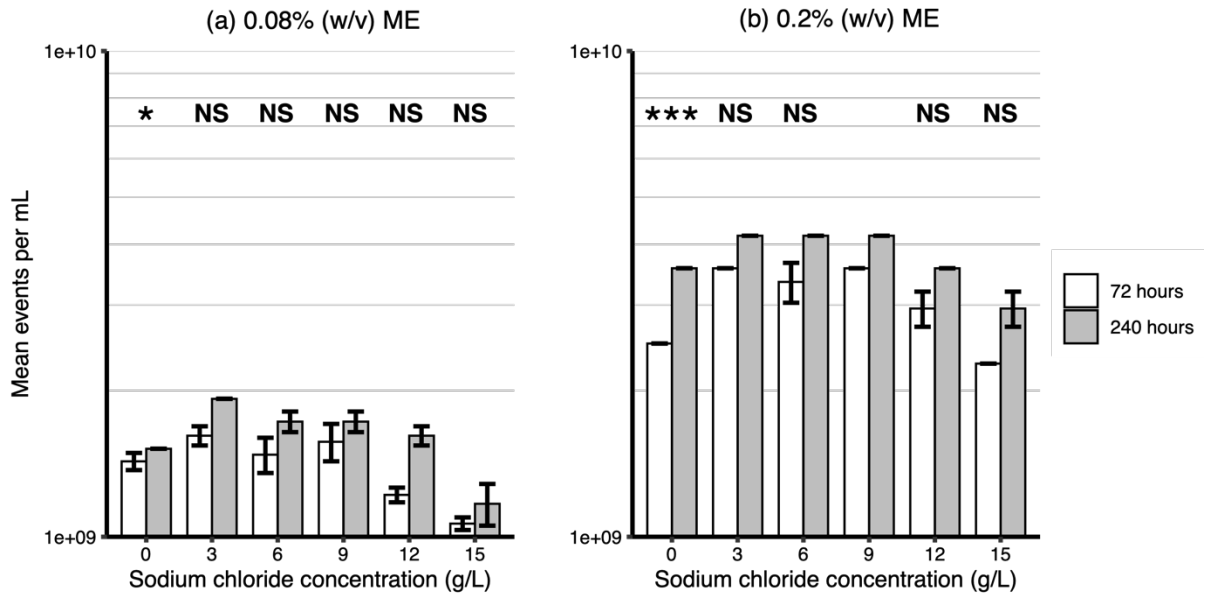


Figure 4.9 - Mean events per mL determined by flow cytometry for 0.08% and 0.2% (w/v) ME *C. necator* cultures containing 0, 3, 6, 9, 12 or 15 g/L and supplemented with 0.5% (w/v) fructose at 0 hours and 0.6% (w/v) sodium gluconate at 24 hours. Statistical significance was determined using paired t-tests to compare the same condition at different time points (displayed as figure annotations). NS = non-significant ($p \geq 0.05$), * = $p < 0.05$, ** = $p \leq 0.01$, *** = $p \leq 0.001$. Missing statistic due to replicates having the same values. Error bars represent SD. n = 3 biological replicates. The full data can be found in Figure 9.6, Appendix 9.2.

4.3.2 The addition of sodium chloride to media does not prevent the lag time in P3HB production

Figure 4.10 contains a summary of mean P-546 fluorescence per cell (plots (a) and (b)) and per mL (plots (c) and (d)) for *C. necator* cultures containing 0.08% or 0.2% (w/v) ME, 0, 3, 6, 9, 12 or 15 g/L sodium chloride and supplemented with 0.5% (w/v) fructose at 0 hours and 0.6% (w/v) sodium gluconate at 24 hours. The full data can be found in Figure 9.7 (a)-(d), Appendix 9.2.

Quantifying P3HB in terms of P3HB per cell (Figure 4.10 (a) and (b)) and per mL (Figure 4.10 (b) and (c)) found that between 72 and 240 hours, in the majority of cultures P3HB significantly increased.

Figure 4.11 contains a summary detailing the mean percentage of $P3HB^{++}$ cells when varying sodium chloride concentration in 0.08% (Figure 4.11 (a)) and 0.2% (w/v) (Figure 4.11 (b)) cultures supplemented as described above. In similarity to mean P3HB per cell and per mL, the mean proportion of $P3HB^{++}$ cells significantly increased between 72 and 240 hours for the majority of cultures tested.

Summaries of mean P-546 fluorescence for the $P3HB^{+}$ and $P3HB^{++}$ populations are located in Figure 4.12 (per cell) and in Figure 4.13 (per mL). The full data is located in Figure 9.8 (per cell) and Figure 9.9 (per mL), Appendix 9.2.

In the majority of conditions tested, both P3HB per cell and per mL increased between 72 and 240 hours for both the $P3HB^{+}$ and $P3HB^{++}$ populations. However, while for the $P3HB^{++}$ population the difference between 72 and 240 hours was generally significant, this was less often the case for the $P3HB^{+}$ population. Analysing the difference in P3HB content over time for the $P3HB^{+}$ and the $P3HB^{++}$ populations shows that the lag in P3HB production observed in the current study is represented by the slow development of $P3HB^{+}$ cells into $P3HB^{++}$. Once again this demonstrates the lag-time in P3HB production occurring between the end of phase 2 at 72 hours and phase 3, and that sodium chloride addition does not reduce the effects of the lag phase.

The addition of NaCl to growth media has been found to increase PHA production *in C. necator* by 30%, with cultures producing 5.33 g/L PHA in just 24 hours (Passanha *et al.*, 2014). The study by Passanha *et al*. (2014) used acetic acid supplemented 0.8% (w/v) ME. However, Passanha *et al*. (2014) did not observe a lag time in P3HB as in the current study, and in fact observed that the addition of 9 g/L NaCl decreased PHA production from 26 to 24 hours, and increased the peak weight of PHA produced from 4.08 to 5.33 g/L. Although Passanha *et al*. (2014) used the same nutrient-rich ME media as the current study, there were differences between the studies which may provide indications as to why the P3HB lag phase in the current study is observed. The current study used Erlenmyler flasks for growth which allowed little control over the culture other than the addition of supplements and the withdrawal of cells for analysis. Passanha *et al*. (2014) used a 5 L fermentor that allowed for the fed-

batch maintenance of pH 7 and for the control of mixing and airflow such that the dissolved O_2 was at 40%. Increasing pH has been shown to increase PHV content in mixed microbial cultures up to a pH of 9.5 (Villano *et al.*, 2010). Low-dissolved O_2 does not decrease the ability of microbes to produce P3HB (Wang *et al.*, 2019) but appears to be crucial during the stage of cell proliferation (Wang *et al.*, 2017). As factors such as dissolved O_2 and pH have not been measured up to this stage of the thesis it is possible that O_2 or pH during culture could be creating conditions unsuitable for the production of P3HB.

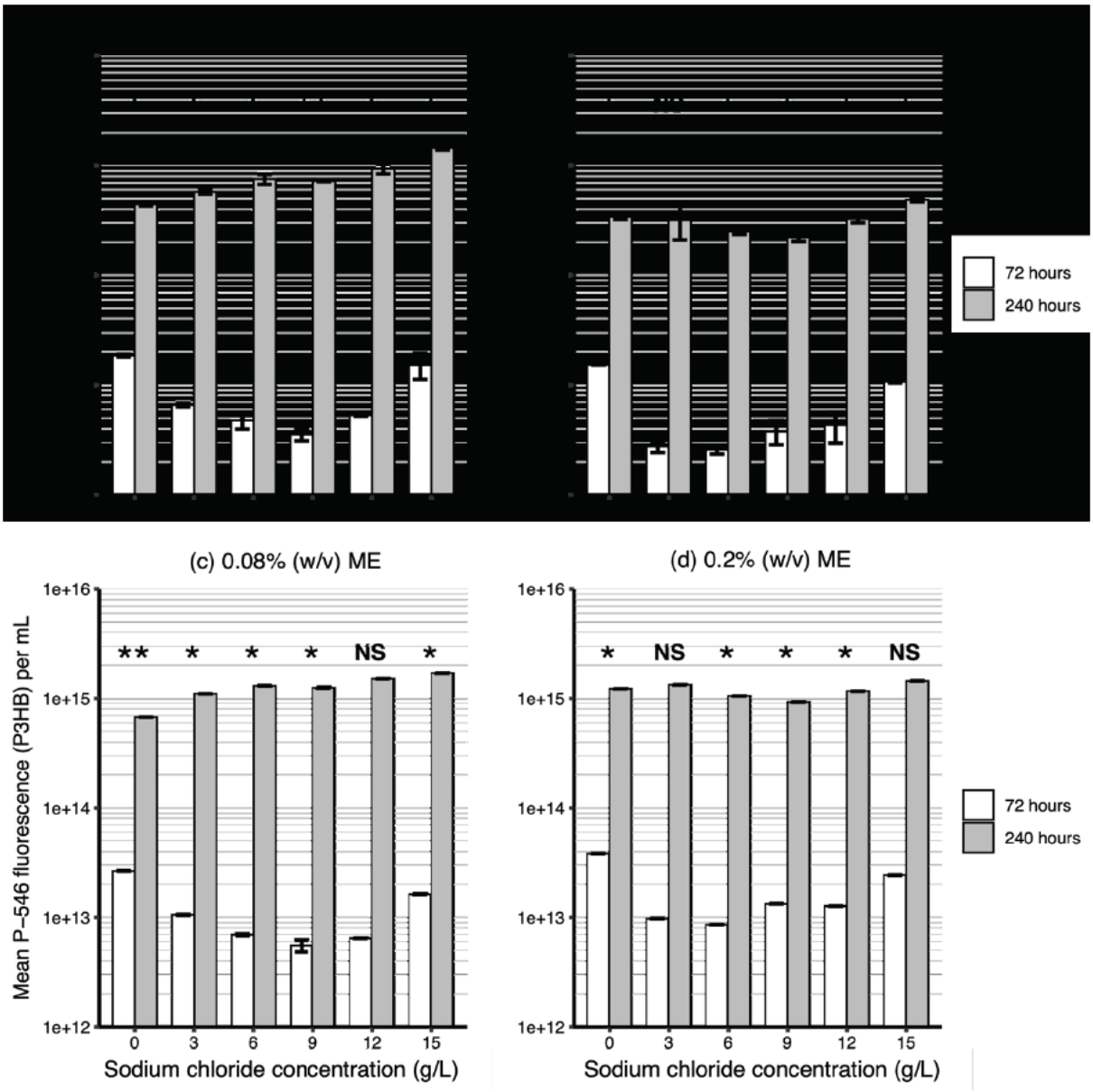


Figure 4.10 – Mean P-546 fluorescence (P3HB) per cell (plots (a) and (b)) and per mL (plots (c) and (d)) for 0.08% and 0.2% (w/v) ME *C. necator* cultures containing 0, 3, 6, 9, 12 or 15 g/L and supplemented with 0.5% (w/v) fructose at 0 hours and 0.6% (w/v) sodium gluconate at 24 hours. Statistical significance was determined using paired t-tests to compare the same condition at different time points (displayed as figure annotations). NS = non-significant ($p \geq 0.05$), * = $p < 0.05$, ** = $p \leq 0.01$. Error bars represent SD. n = 3 biological replicates. The full data can be found in Figure 9.7 (a)-(d), Appendix 9.2.

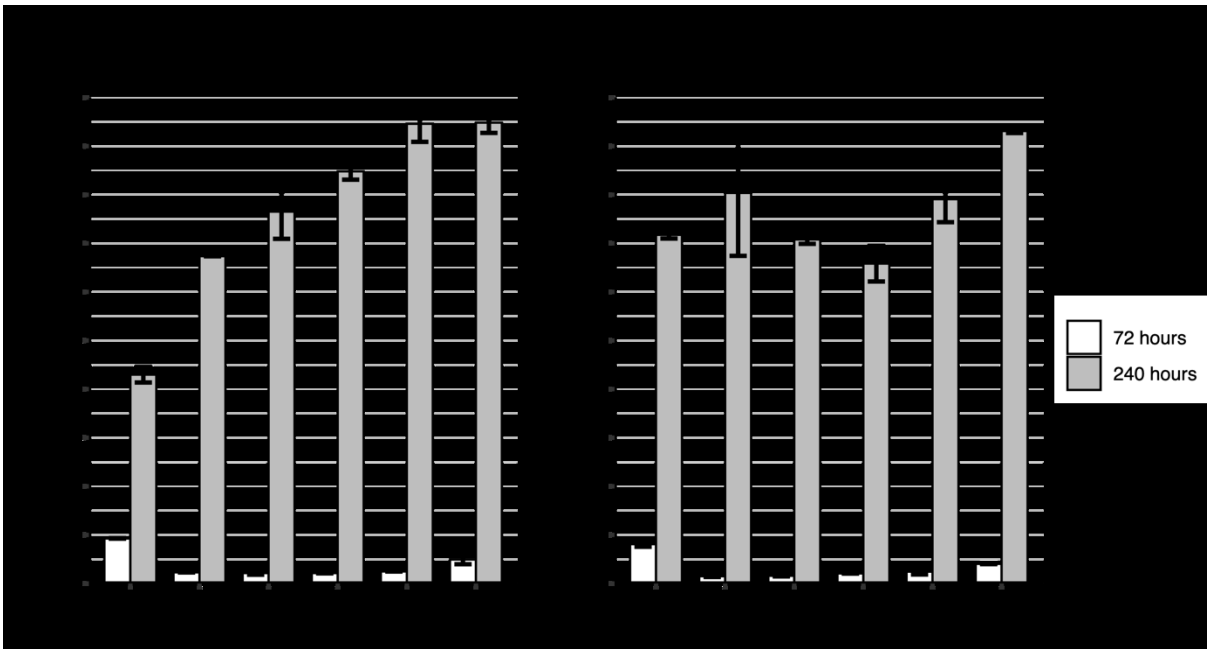


Figure 4.11 – Mean percentage of P3HB^{++} cells for 0.08% and 0.2% (w/v) ME *C. necator* cultures containing 0, 3, 6, 9, 12 or 15 g/L and supplemented with 0.5% (w/v) fructose at 0 hours and 0.6% (w/v) sodium gluconate at 24 hours. Statistical significance was determined using paired t-tests to compare the same condition at different time points (displayed as figure annotations). NS = non-significant ($p \geq 0.05$), * = $p < 0.05$, ** = $p \leq 0.01$. Missing statistic due to replicates having the same values. Error bars represent SD. n = 3 biological replicates.

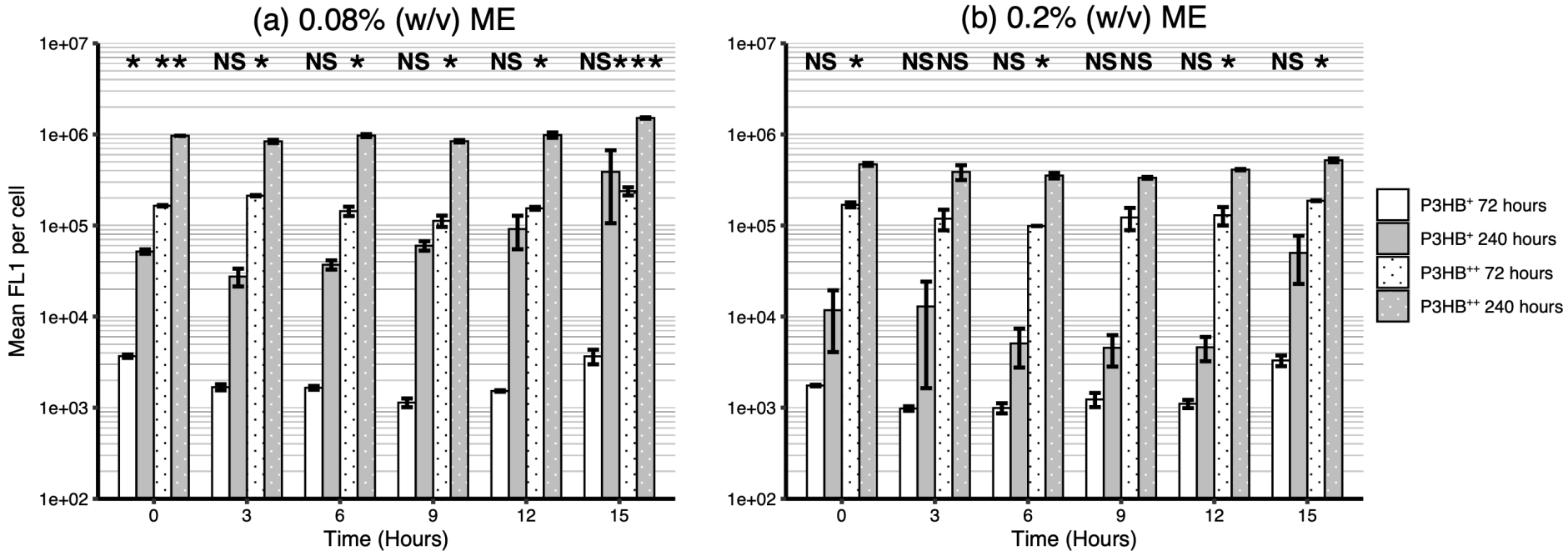


Figure 4.12 - Mean P3HB^{+} and P3HB^{++} P-546 fluorescence (P3HB) per cell for 0.08% and 0.2% (w/v) ME *C. necator* cultures containing 0, 3, 6, 9, 12 or 15 g/L sodium chloride, and supplemented with 0.5% (w/v) fructose at 0 hours and 0.6% (w/v) sodium gluconate at 24 hours. Statistical significance was determined using paired t-tests to compare the same condition at different time points (displayed as figure annotations). NS = non-significant ($p \geq 0.05$), * = $p < 0.05$, ** = $p \leq 0.01$, *** = $p \leq 0.001$. Error bars represent SD. n = 3 biological replicates. The full data is located in Figure 9.8, Appendix 9.2.

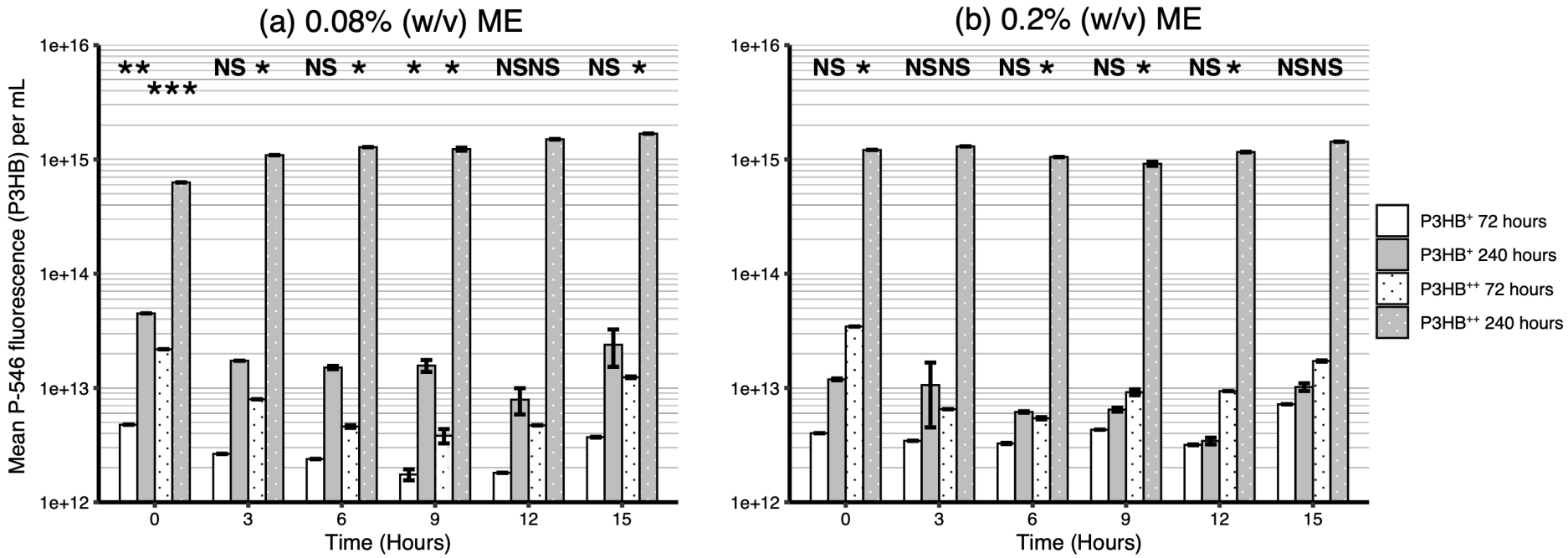


Figure 4.13 - Mean P3HB^{+} and P3HB^{++} P-546 fluorescence per mL for 0.08% and 0.2% (w/v) ME *C. necator* cultures containing 0, 3, 6, 9, 12 or 15 g/L sodium chloride and supplemented with 0.5% (w/v) fructose at 0 hours and 0.6% (w/v) sodium gluconate at 24 hours. Statistical significance was determined using paired t-tests to compare the same condition at different time points (displayed as figure annotations). NS = non-significant ($p \geq 0.05$), * = $p < 0.05$, ** = $p \leq 0.01$, *** = $p \leq 0.001$. Error bars represent SD. n = 3 biological replicates. The full data is located in Figure 9.9, Appendix 9.2.

4.3.3 Sodium chloride addition does not alter the influence of decreasing ME concentration on maintaining cell size

Figure 4.14 contains a summary of mean overall FSC for *C. necator* cultures containing 0.08% or 0.2% (w/v) ME, 0, 3, 6, 9, 12 or 15 g/L sodium chloride and supplemented with 0.5% (w/v) fructose at 0 hours and 0.6% (w/v) sodium gluconate at 24 hours. The full data can be found in Figure 9.10 (a) and (b), Appendix 9.2.

Overall mean FSC for 0.08% (w/v) ME cultures (Figure 4.14 (a)) did not significantly change but for 0.2% (w/v) ME cultures (Figure 4.14 (b)) a significant decrease in cell size was observed. For 0.08% (w/v) ME cultures when sodium chloride was added to the media a reduction in cell size was observed between 72 and 240 hours. However, this was only found to be a statistically significant decrease for 0.08% (w/v) ME cultures with 6, 12 and 15 g/L sodium chloride added. For 0.2% (w/v) ME cultures, with the exception of cultures with 3 g/L sodium chloride added, all cultures with sodium chloride added significantly reduced in terms of cell size.

A summary dividing FSC into $P3HB^{+}$ and $P3HB^{++}$ populations can be found in Figure 4.15. The full data is located in Figure 9.5 (c)-(f), Appendix 9.2.

Cells of the $P3HB^{+}$ population in 0.08% (w/v) ME cultures (Figure 4.15 (a)) without sodium chloride added did not significantly change in cell size between 72 and 240 hours, which is in contrast to that of 0.2% (w/v) ME cultures which significantly decreased in cell size. Cultures to which sodium chloride was added decreased cell size between 72 and 240 hours. This was found to be a significant decrease in cell size for all sodium chloride containing 0.2% (w/v) ME cultures, but was found to be not significant for 0.08% (w/v) ME cultures with either 3 or 15 g/L sodium chloride.

Cells of the $P3HB^{++}$ population in sodium chloride free 0.08% (w/v) ME cultures (Figure 4.15 (a)) did not significantly change in cell size between 72 and 240 hours. This was in contrast to that of 0.2% (w/v) ME cultures in which $P3HB^{++}$ cells significantly decreased in size. In 0.08% (w/v) ME cultures, $P3HB^{++}$ cells significantly increased in size between 72 and 240 hours, except for cultures containing 9 g/L sodium chloride was added a non-significant difference in cell size occurred. Cells in the $P3HB^{++}$ population in 0.2% (w/v) ME cultures, on the other hand, significantly decreased in cell size between 72 and 240 hours.

In part the findings in this section back up the results of Dai and Zhu (2018) who found that *E. coli* cell size reduces due to sodium chloride causing hyperosmotic stress. However, this does not provide an explanation of why in ME media with sodium chloride added, $P3HB^{++}$ cells increase for 0.08% (w//v) ME cultures and decrease in size for 0.2% (w//v) ME cultures. Results indicate that between the end of phase 2 at 72 hours and phase 3 at 240 hours, 0.2% (w/v) ME cultures decrease in overall mean cell

size by a greater proportion than that of 0.8% (w/v) ME cultures. This may be because in 0.2% (w/v) ME cultures residual ME increases media osmolarity thus increasing the osmotic stress on cells. One would expect cells in the P3HB^{++} population to be somewhat resistant to osmotic stress, as P3HB granules have been shown to confer resistance against osmotic stress (Sedlacek *et al.*, 2019). It's possible that in 0.08% (w/v) ME cultures there is less residual ME at 240 hours, and the cells are able to expand or possibly form chains or aggregates. On the other hand, residual ME in 0.2% (w/v) ME cultures creates greater osmotic stress to which cells respond by decreasing their volume.

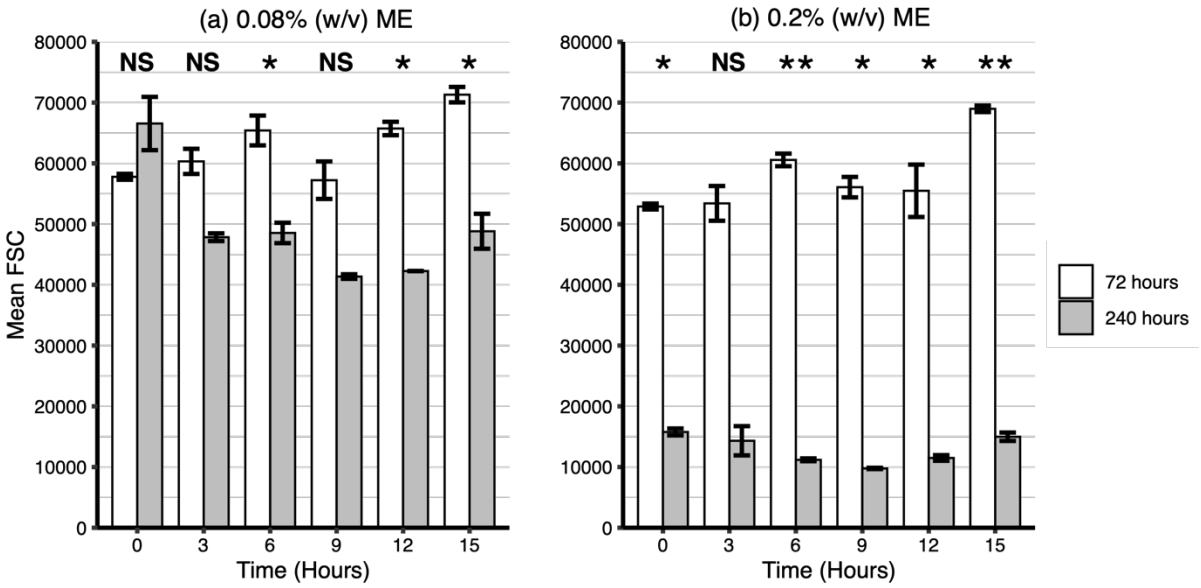


Figure 4.14 - Mean FSC for 0.08% and 0.2% (w/v) ME *C. necator* cultures containing 0, 3, 6, 9, 12 or 15 g/L and supplemented with 0.5% (w/v) fructose at 0 hours and 0.6% (w/v) sodium gluconate at 24 hours. Statistical significance was determined using paired t-tests to compare the same condition at different time points (displayed as figure annotations). NS = non-significant ($p \geq 0.05$), * = $p < 0.05$, ** = $p \leq 0.01$. Error bars represent SD. n = 3 biological replicates. The full data can be found in Figure 9.10 (a) and (b), Appendix 9.2.

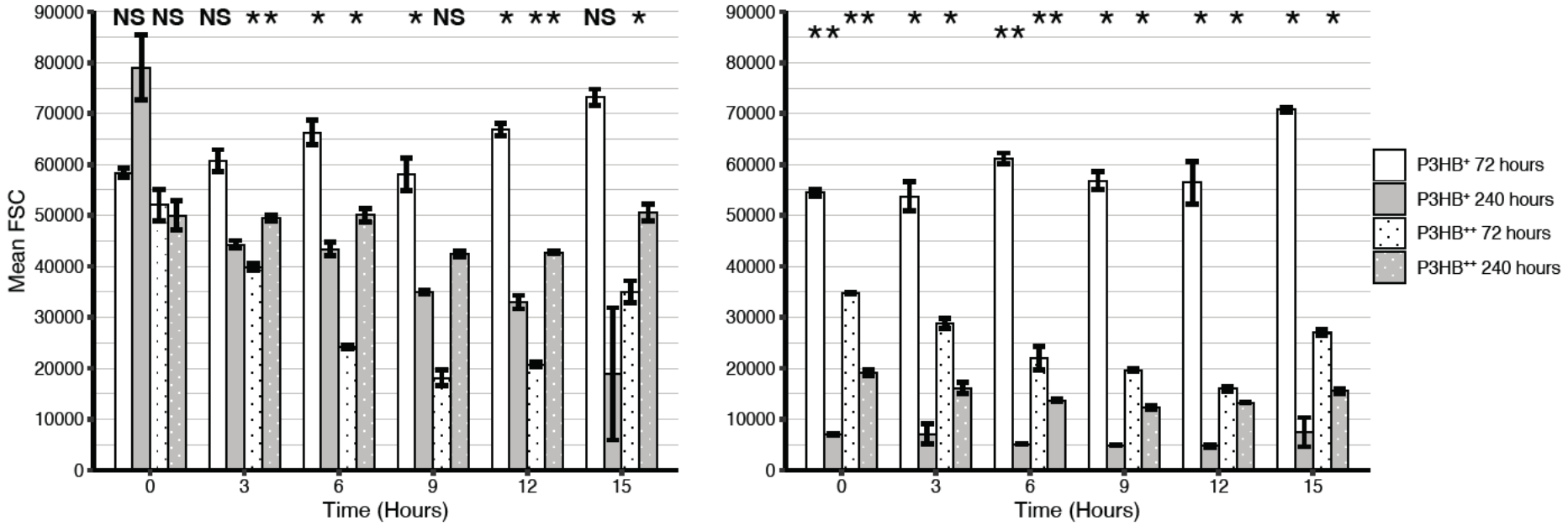


Figure 4.15 - Mean P3HB^{+} and P3HB^{++} FSC for 0.08% and 0.2% (w/v) ME *C. necator* cultures containing 0, 3, 6, 9, 12 or 15 g/L and supplemented with 0.5% (w/v) fructose at 0 hours and 0.6% (w/v) sodium gluconate at 24 hours. Statistical significance was determined using paired t-tests to compare the same condition at different time points (displayed as figure annotations). NS = non-significant ($p \geq 0.05$)., * = $p < 0.05$, ** = $p \leq 0.01$. Error bars represent SD. n = 3 biological replicates. The full data is located in Figure 9.5 (c)-(f), Appendix 9.2.

4.3.4 Discussion

In section 4.3, the same fed-batch feeding strategy as section 4.2 was used along with the addition of 0, 3, 6, 9, 12 or 15 g/L sodium chloride. In *C. necator* cultures the addition of sodium chloride (9 g/L) has been found to decrease the peak PHA time from 26 to 24 hours and increase PHA production by 30% (Passanha *et al.*, 2014). However, in the current study, the addition of sodium chloride to media did not prevent a P3HB producing lag-phase which extended into phase 3, beyond 72 hours. Research conducted by Passanha *et al.* (2014), to the best of knowledge, is the only other study which uses standard 0.8% ME media (DSMZ, 2007) which consists of 3 g/L ME and 5 g/L peptone. While the current study used a small-scale shake flask method to grow *C. necator*, Passanha *et al.* (2014) used a 5 L fermenter that allowed for the fed-batch maintenance of pH 7 and for the control of mixing and airflow such that the dissolved O_2 was at 40%. However, an increase in pH of 9.5 has been shown to increase the PHV content of mixed microbial cultures (Villano *et al.*, 2010) and low dissolved O_2 has been found not to alter bacterial ability to produce P3HB (Wang *et al.*, 2019), although dissolved O_2 is crucial for cell proliferation (Wang *et al.*, 2017). Passanha *et al.* (2014) also supplemented cultures with acetic acid rather than fructose or sodium gluconate in the current study. However, fructose (Budde *et al.*, 2011) and sodium gluconate (Heinrich *et al.*, 2021) have been also demonstrated to produce peak P3HB in *C. necator* within 72 hours. There is therefore insufficient evidence that any of the stated differences in culture conditions between this study and that of Passanha *et al.* (2014) are the cause of the lag phase observed in the current study.

In part the findings in this section back up the results of Dai and Zhu (2018) who found that *E. coli* cell size reduces due to sodium chloride causing hyperosmotic stress. However, this does not provide an explanation of why in ME media with sodium chloride added, $P3HB^{++}$ cells increase for 0.08% (w//v) ME cultures and decrease in size for 0.2% (w//v) ME cultures. One would expect cells in the $P3HB^{++}$ population to be somewhat resistant to osmotic stress to be resistant to osmotic stress, as P3HB granules have been shown to confer resistance against osmotic stress (Sedlacek *et al.*, 2019).

4.4 Does changing the growth media at 24 hours move peak P3HB production from phase 3 to phase 2?

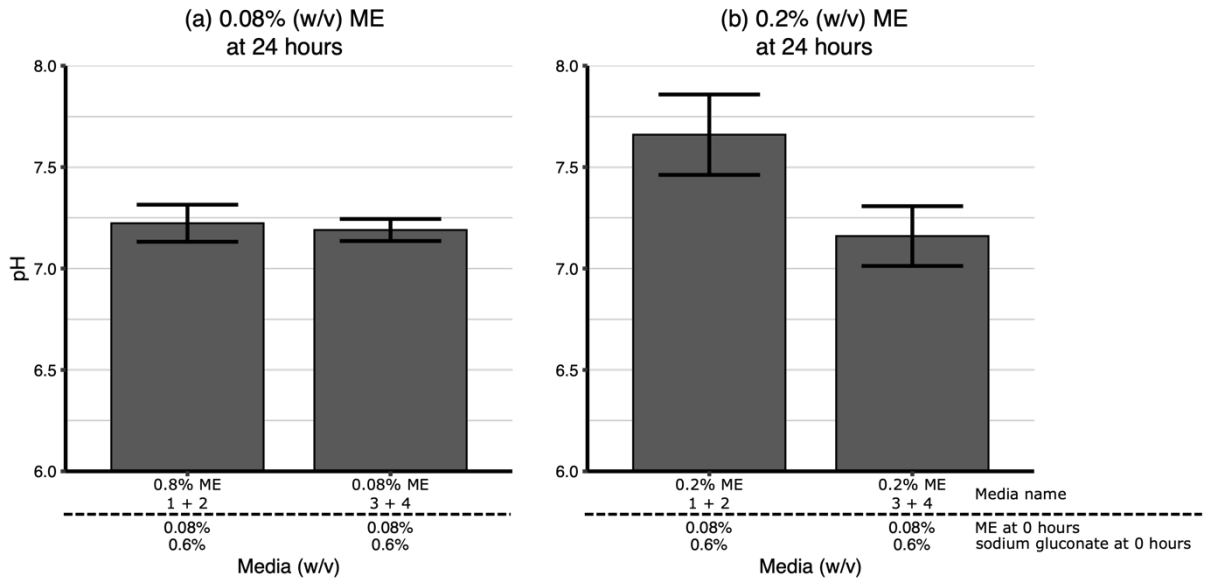
In sections 4.2 and 4.3, a fed-batch strategy aimed to use fructose in phase 1 to produce biomass and use sodium gluconate to produce P3HB in phase 2. In addition, in section 4.3 sodium chloride was added at varying concentrations. The strategies in both sections aimed to prevent a lag in P3HB production and move peak P3HB production into phase 2. In the current section, a repeated-batch method is instead tested in which growth media was replaced at the end of phase 1 at 24 hours, and replaced with new dilute 0.008% or 0.04% (w/v) ME. A similar strategy reported by Santolin *et al*. (2021) found following a biomass accumulation phase, a PHA content of around 80% could be achieved in 42 hours. A detailed summary of the media used can be viewed under each graph. Note that media names only apply to media used in this section 4.4.

4.4.1 Increased pH is indicative of amino-acid deamination

Figure 4.16 presents pH data collected when media was removed from cultures containing either 0.08% or 0.2% (w/v) ME and supplemented with either 0.5% (w/v) fructose or 0.6% (w/v) sodium gluconate at 24 hours. Note that Experimental conditions annotated on the x-axis of Figure 4.16 are combined, as up to 24 hours when the media was changed there were 4 experimental conditions. When the media was changed at 24 hours 8 different experimental conditions were created.

Increasing the initial ME concentration from 0.08% (Figure 4.16 (a)) to 0.2% (w/v) (Figure 4.16 (b)) resulted in a significant increase in pH for samples supplemented with sodium gluconate but not fructose.

An increase in pH during fermentation is indicative of a build-up of ammonia due to the deamination of amino acids (Krebs, 1935). During conditions of surplus C sources, which can be directly fed into the citric acid cycle, amino acids are used for protein synthesis (Neis *et al.*, 2015). However, during C-limiting conditions, amino acids are instead used as a C source in a process that begins with the transamination of amino acids which releases ammonia as a by-product. In the context of this study, the release of ammonia means that the citric acid cycle is not receiving a C source while amino acids are present in the media. Meat extract media is highly rich in nitrogen-containing compounds and it is likely to also be rich in amino acids. As 0.2% (w/v) ME likely contains more amino acids than 0.08% (w/v) ME cultures this may be why 0.2% (w/v) ME cultures have an elevated pH. Evidence in this section, therefore, suggests that in phase 1 (0-24 hours), in 0.2% ME 1 and 2 cultures, gluconate is exhausted before amino acids are exhausted.



Non-paired t-tests comparing culture pH in 0.08% and 0.2% ME.		
Media comparison		Significance level
0.08% 1 + 2	0.2% 1 + 2	**
0.08% 3 + 4	0.2% 3 + 4	NS

Figure 4.16 - Mean pH of *C. necator* cultures grown initially in either 0.08% (a) or 0.2% (w/v) ME (b) up to 24 hours until the growth media was hanged to either 0.008% or 0.04% (w/v) ME. Media before and after 24 hours was supplemented with either 0.5% (w/v) fructose or 0.6% (w/v) sodium gluconate. Statistical significance was determined using paired t-tests to compare the same condition at different time points (displayed as figure annotations). NS = non-significant ($p \geq 0.05$), * = $p < 0.05$, ** = $p \leq 0.01$. Error bars represent SD. n = 6 biological replicates.

4.4.2 Little cell proliferation occurs between 72 and 216 hours.

Figure 4.17 contains a summary of mean events per mL *for C. necator* cultures which initially comprised either 0.08% or 0.2% (w/v) ME before media was replaced with either 0.008% or 0.04% (w/v) ME at 24 hours. Both before and after 24 hours, media was supplemented with either 0.5% (w/v) fructose or 0.6% (w/v) sodium gluconate. The full data can be found in Figure 9.11, Appendix 9.3.

For cultures initially containing 0.08% (w/v) ME (Figure 4.17 (a)), when media was replaced and supplemented with 0.6% (w/v) sodium gluconate (0.08% ME 1 and 3), mean events significantly decreased between the end of phase 2 at 72 hours and phase 3 at 216 hours. In contrast, when media was replaced at 24 hours and contained 0.5% (w/v) fructose there was no significant difference between mean events per mL at 72 and 216 hours.

Cultures initially containing 0.2% (w/v) ME generally could not be statistically separated between 72 and 216 hours, except for condition 0.2% ME 1 which significantly increased.

Results indicate that, except for condition 0.2% ME 1, cultures did not proliferate between the end of phase 2 at 72 hours and phase 3 at 216 hours. This is indicative of conditions in which growth-promoting levels of nutrients were not available between the time points summarised, and gluconate and fructose are not being directed into the Entner-Doudoroff pathway, and acetyl-CoA is not being directed into the citric acid cycle (Ienczak *et al.*, 2011). The reason for the presence of sodium gluconate in cultures reducing events per mL for conditions 0.08% ME 1 and 3 is unclear, as is the reason why this is not observed when the initial ME concentration is increased to 0.2% (w/v).

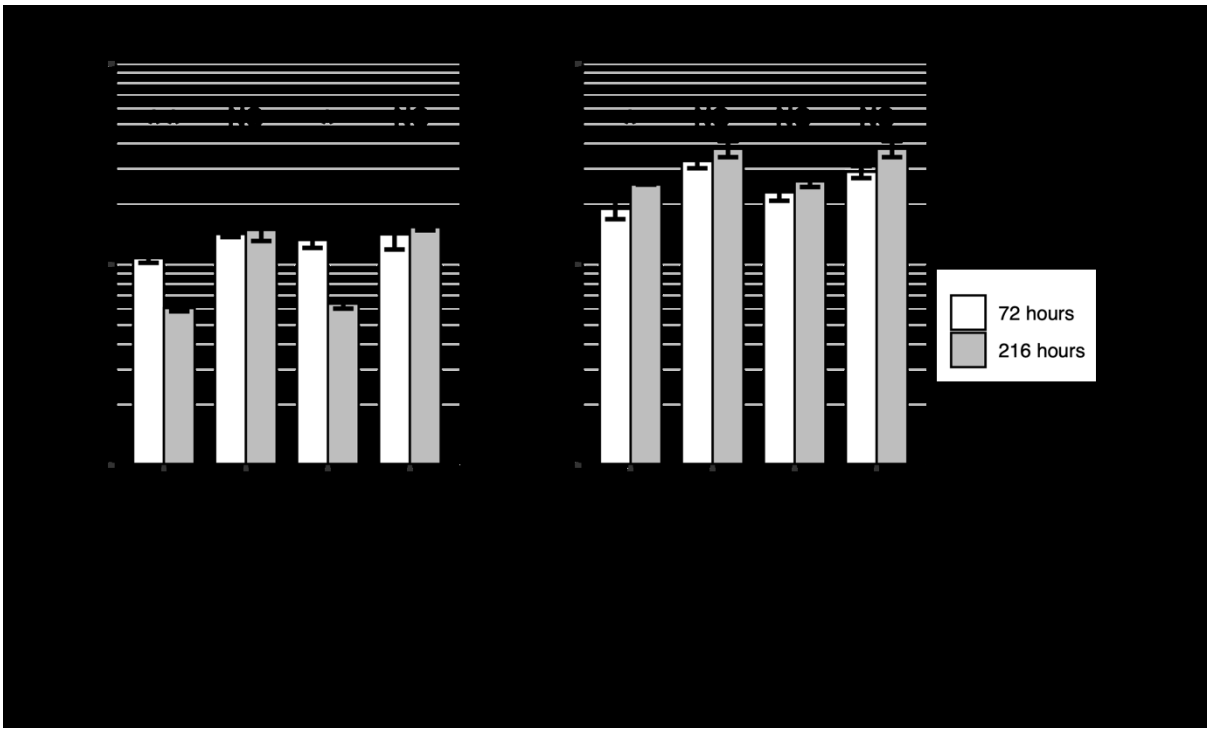


Figure 4.17 – Mean events per mL of *C. necator* cultures grown initially in either 0.08% (a) or 0.2% (w/v) ME (b) up to 24 hours until the growth media was hanged to either 0.008% or 0.04% (w/v) ME. Media before and after 24 hours was supplemented with either 0.5% (w/v) fructose or 0.6% (w/v) sodium gluconate. Statistical significance was determined using paired t-tests to compare the same condition at different time points (displayed as figure annotations). NS = non-significant ($p \geq 0.05$), * = $p < 0.05$, ** = $p \leq 0.01$. Error bars represent SD. n = 3 biological replicates. The full data can be found in Figure 9.11, Appendix 9.3.

4.4.3 Changing to dilute ME media after 24 hours does not produce more P3HB in comparison to batch cultures.

Figure 4.18 contains a summary of mean P-546 fluorescence per cell and per mL for *C. necator* cultures which initially comprised either 0.08% or 0.2% (w/v) ME before media was replaced with either 0.008% or 0.04% (w/v) ME at 24 hours. Both before and after 24 hours, media was supplemented with either 0.5% (w/v) fructose or 0.6% (w/v) sodium gluconate. The full data can be found in Figure 9.12 (a)-(d), Appendix 9.3.

Paired statistical analysis comparing mean P-546 fluorescence per cell for 0.08% (Figure 4.18 (a)) and 0.2% (w/v) ME cultures (Figure 4.18 (b)) found that all conditions increased between the end of phase 2 at 72 hours and phase 3 at 216 hours. The increase was significant for all conditions except 0.08% ME 4. Analysis of P-546 fluorescence per mL of culture for 0.08% (Figure 4.18 (c)) and 0.2% (w/v) ME cultures (Figure 4.18 (d)) also revealed that all conditions tested increased P3HB per mL between 72 and 216 hours. However, conditions 0.08% ME 3 and 4 were found not to significantly increase.

Figure 4.19 contains a summary of the mean percentage of $P3HB^{++}$ cells. The full data can be found in Figure 9.12 (e) and (f), Appendix 9.3

Comparing the percentage of $P3HB^{++}$ cells for 0.08% and 0.2% (w/v) cultures between 72 and 168 hours found that $P3HB^{++}$ increased in proportion for all conditions tested.

Summaries of P-546 fluorescence for the $P3HB^{+}$ and $P3HB^{++}$ populations are presented per cell in Figure 4.20 and per mL in Figure 4.21. The full data can be found in Figure 9.13 (per cell) and Figure 9.14 (per mL), Appendix 9.3.

Mean P-546 fluorescence in the $P3HB^{+}$ and $P3HB^{++}$ populations for 0.08% (Figure 4.20 (a)) and 0.2% (w/v) ME cultures (Figure 4.20 (b)) either significantly increased or did not significantly change, although, there was no pattern to the results. Comparing P3HB per mL in 0.08% (Figure 4.21 (a)) and 0.2% (w/v) ME cultures (Figure 4.21 (b)) found that the contribution of the $P3HB^{+}$ population to P3HB per mL diminished between 72 and 216 hours. However, some of the decreases observed were found to be non-statistically significant. On the other hand, the $P3HB^{++}$ population increased in terms of P-546 fluorescence per mL between 72 and 216 hours for all conditions tested. The increases were found to be significant except for media 0.08% ME 3 and 4.

Overall, changing the growth media at 24 hours did not prevent a lag in P3HB production into phase 3. It was expected that given the very low ME concentrations of 0.008% and 0.04% (w/v) used for media replacement at 24 hours, *C. necator* would have plenty of surplus fructose and gluconate to use for P3HB biosynthesis without significant delay. Given that 0.008% (w/v) ME is 100 times more dilute

than standard ME recommended for *C. necator* growth by DSMZ (DSMZ, 2007) and used by Passanha *et al*. (2014) to produce PHA in just 24 hours. Results therefore suggest that the delay in peak P3HB in the current study may not be due to the media conditions. The PhaC1 enzyme, used by *C. necator* to polymerise 3HB, is known to have an initial lag phase before reaching peak P3HB polymerisation, although, this is only around 6 hours (Juengert *et al.*, 2018). However, Juengert *et al*. (2018) found that mutating key amino-acid residues in PhaC1 could significantly increase the lag time in 3HB polymerisation. However, the presence of PhaM restored PhaC1 to normal function. It should be noted that in the study by Juengert *et al*. (2018), the lag in 3HB polymerisation was only observed in vitro and not in vivo even when PhaM was absent. The regulation of PhaC1 appears to be complex and not completely understood in literature. The cause of the lag phase in the current study could be due to a problem with PhaC1 or its associated regulation. However, this is purely hypothetical, and considerable further investigation would be required to establish such a link.

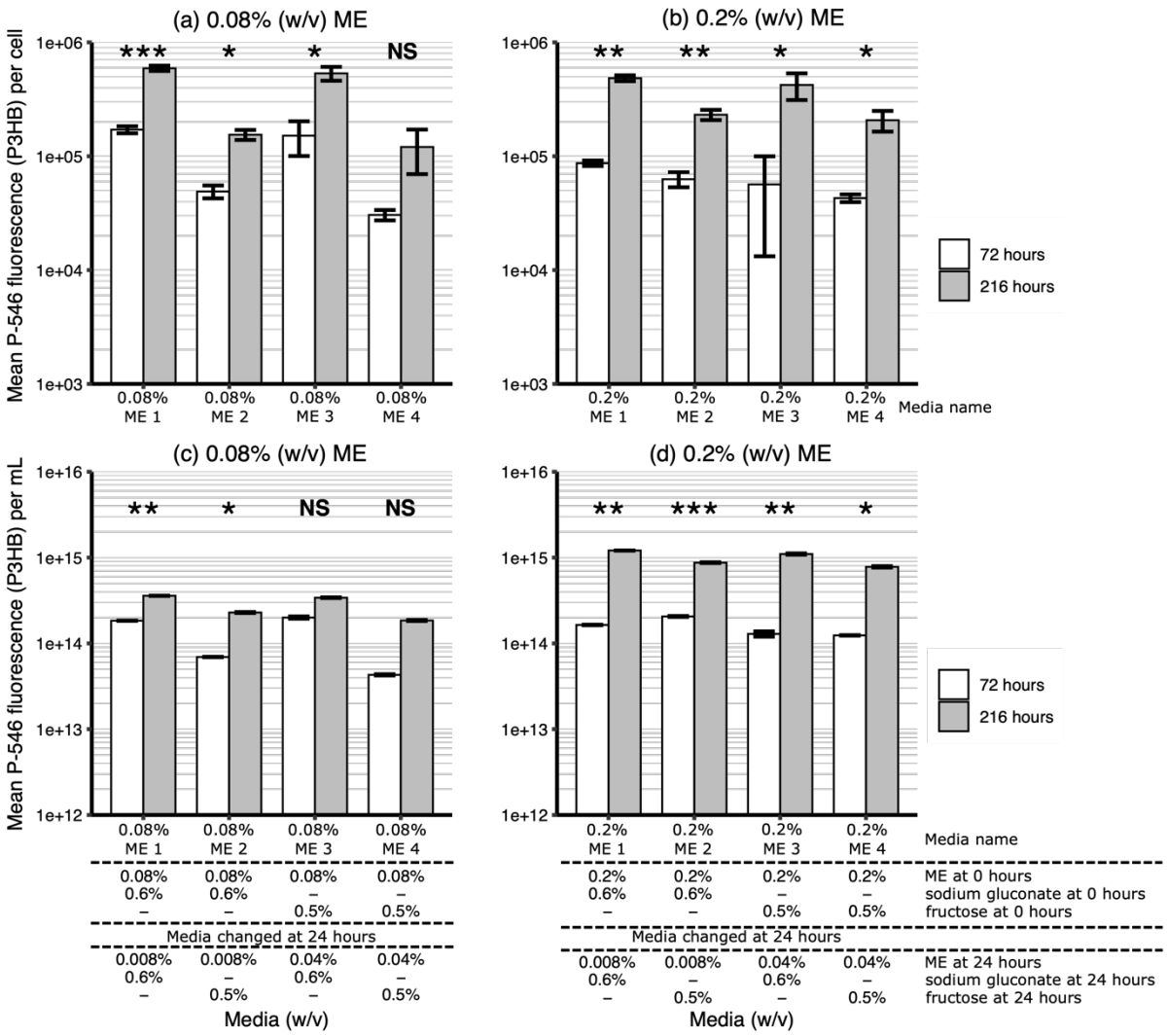


Figure 4.18 - Mean P-546 fluorescence per cell (a) and per mL (b) for *C. necator* cultures grown initially in either 0.08% or 0.2% (w/v) ME up to 24 hours until the growth media was changed to either 0.008% or 0.04% (w/v) ME. Media before and after 24 hours was supplemented with either 0.5% (w/v) fructose or 0.6% (w/v) sodium gluconate. Statistical significance was determined using paired t-tests to compare the same condition at different time points (displayed as figure annotations). NS = non-significant ($p \geq 0.05$), * = $p < 0.05$, ** = $p \leq 0.01$, *** = $p \leq 0.001$. Error bars represent SD. n = 3 biological replicates. The full data can be found in Figure 9.12 (a)-(d), Appendix 9.3.

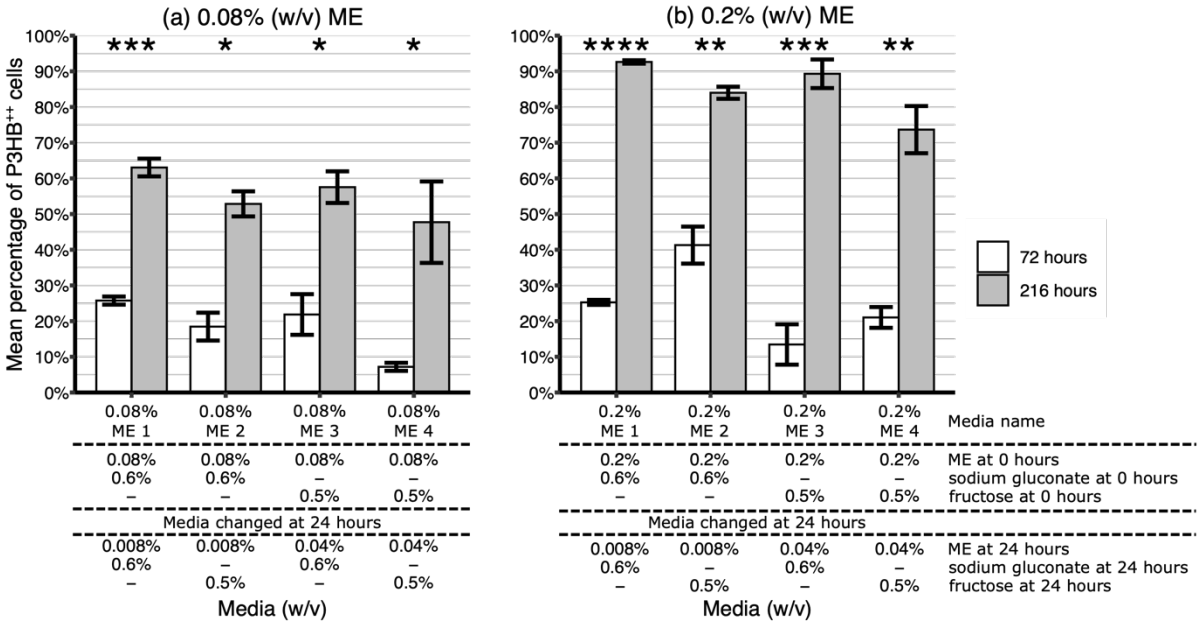


Figure 4.19 - Mean percentage of P3HB^{++} cells in *C. necator* cultures grown initially in either 0.08% (a) or 0.2% (w/v) ME (b) up to 24 hours until the growth media was changed to either 0.008% or 0.04% (w/v) ME. Media before and after 24 hours was supplemented with either 0.5% (w/v) fructose or 0.6% (w/v) sodium gluconate. Statistical significance was determined using paired t-tests to compare the same condition at different time points (displayed as figure annotations). NS = non-significant ($p \geq 0.05$), * = $p < 0.05$, ** = $p \leq 0.01$, *** = $p \leq 0.001$, **** = $p \leq 0.0001$. Error bars represent SD. n = 3 biological replicates. The full data can be found in Figure 9.12 (e) and (f), Appendix 9.3.

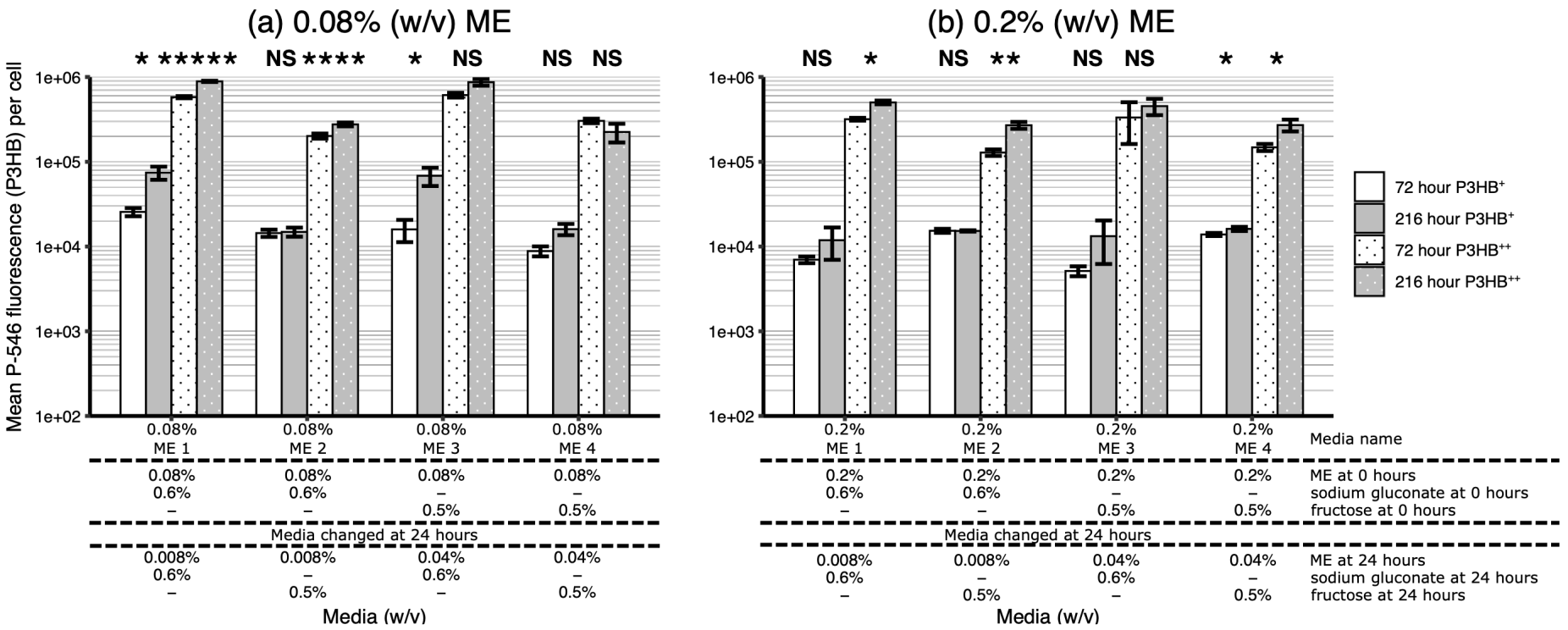


Figure 4.20 - Mean P3HB⁺ and P3HB⁺⁺ P-546 fluorescence per cell for *C. necator* cultures grown initially in either 0.08% (a) or 0.2% (w/v) ME (b) up to 24 hours until the growth media was changed to either 0.008% or 0.04% (w/v) ME. Media before and after 24 hours was supplemented with either 0.5% (w/v) fructose or 0.6% (w/v) sodium gluconate. Statistical significance was determined using paired t-tests to compare the same condition at different time points (displayed as figure annotations). NS = non-significant ($p \geq 0.05$), * = $p < 0.05$, ** = $p \leq 0.01$, *** = $p \leq 0.001$, **** = $p \leq 0.0001$, ***** = $p \leq 0.00001$. Error bars represent SD. n = 3 biological replicates. The full data can be found in Figure 9.13, Appendix 9.3.

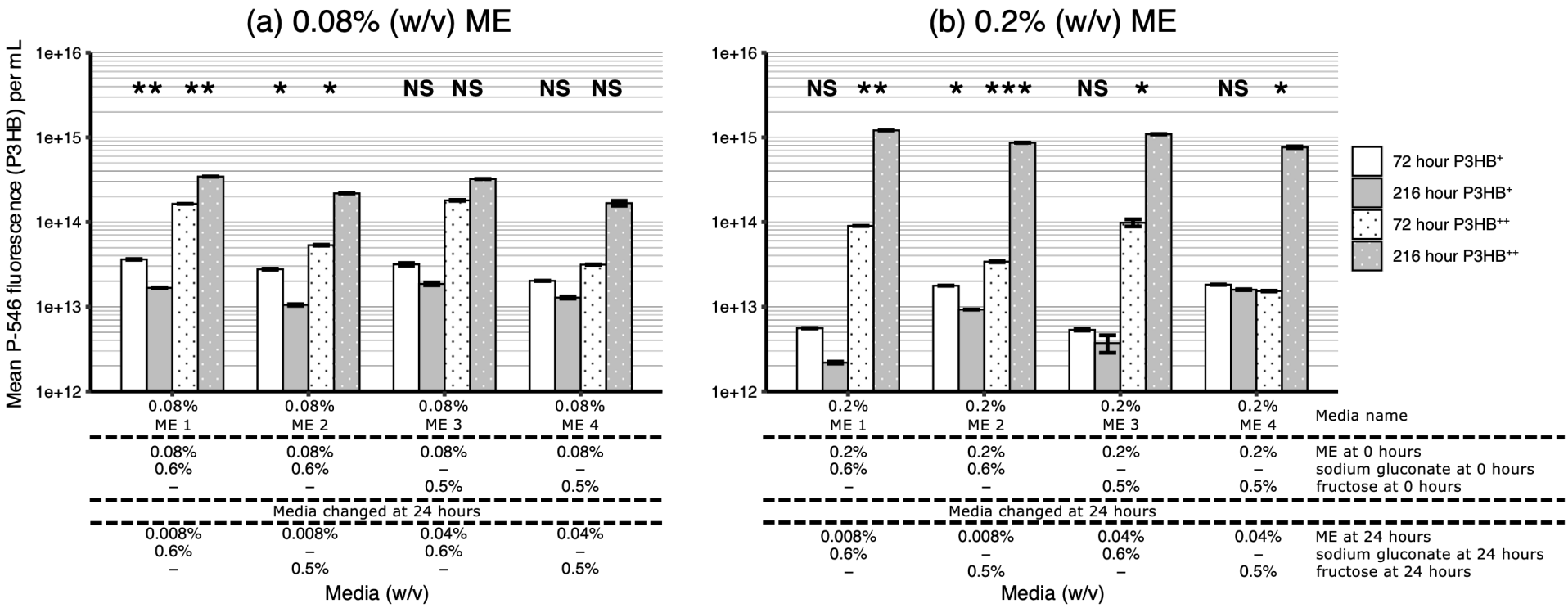


Figure 4.21 - Mean P3HB⁺ and P3HB⁺⁺ P-546 fluorescence per mL for *C. necator* cultures grown initially in either 0.08% (a) or 0.2% (w/v) ME (b) up to 24 hours until the growth media was changed to either 0.008% or 0.04% (w/v) ME. Media before and after 24 hours was supplemented with either 0.5% (w/v) fructose or 0.6% (w/v) sodium gluconate. Statistical significance was determined using paired t-tests to compare the same condition at different time points (displayed as figure annotations). NS = non-significant ($p \geq 0.05$), * = $p < 0.05$, ** = $p \leq 0.01$, *** = $p \leq 0.001$. Error bars represent SD. n = 3 biological replicates. The full data can be found in Figure 9.14, Appendix 9.3.

4.4.4 Cultures which initially contained 0.2% (w/v) ME and sodium gluconate in changed media decrease mean cell size

Figure 4.22 contains a summary of mean P-546 fluorescence per cell and per mL for *C. necator* cultures which initially comprised either 0.08% or 0.2% (w/v) ME before media was replaced with either 0.008% or 0.04% (w/v) ME at 24 hours. Both before and after 24 hours, media was supplemented with either 0.5% (w/v) fructose or 0.6% (w/v) sodium gluconate. The full data can be found in Figure 9.15 (a), Appendix 9.3.

Comparing the mean FSC of 0.08% (w/v) cultures (Figure 4.22 (a)) found that media 0.08% ME 1 and 4 significantly decreased and there was no significant difference between conditions 0.08% ME 2 and 3. In 0.2% (w/v) ME cultures, media supplemented with 0.6% (w/v) sodium gluconate (0.2% ME 1 and 3) resulted in a decreased cell size between 72 and 216 hours. Fructose-supplemented media (0.2% ME 2 and 4), on the other hand, slightly increased in cell size.

Figure 4.23 contains a summary of mean FSC for the $P3HB^{+}$ and $P3HB^{++}$ populations. The full data can be found in Figure 9.15 (b) and (c), Appendix 9.3.

For cultures initially containing 0.08% (w/v) ME (Figure 4.23 (a)), there was generally little difference in cell size between 72 and 216 hours. The same applies for cultures initially containing 0.2% (w/v) ME (Figure 4.23 (b)) to which fructose was supplemented in the changed media at 24 hours (0.2% ME 2 and 4). However when the media was changed and sodium gluconate supplemented at 24 hours a large and statistically significant decrease in cell size occurred in both the $P3HB^{+}$ and $P3HB^{++}$ populations.

Generally, little change in cell size of cultures occurs between 72 and 216 hours except for cultures which contained 0.6% (w/v) in the second media added at 24 hours. This only occurs for culture which initially contained 0.2% (w/v) ME in the initial growth media. It's possible that the observed decrease in cell size stems from cultures which initially contained 0.2% (w/v) ME producing more cells than cultures initially containing 0.08% (w/v), which meant that sodium ions were spread across more cells. Once media was changed at 24 hours, conditions 0.08% and 0.2% ME 1 and ME 3 contained the same sodium gluconate concentration of 0.6% (w/v). Between 72 and 216 hours, gluconate may have been depleted in these cultures, which due to the very dilute ME concentrations used in changed media may have resulted in a very low media osmolarity. As sodium ions are known to be used by bacteria as a method of osmotic adjustment to prevent the adverse effects of osmotic stress (Björklund and Marguerat, 2017), it's possible that in 0.2% ME 1 and ME 3 cultures that too few sodium ions were present per cell to prevent an efflux of water out of the cell down an osmotic gradient. However, it should be noted that without evidence such as gluconate concentration in media, this can be

considered no more than a theory, as it's unclear why a decrease in cell size is not observed in 0.08% and 0.2% ME 2 and 4 cultures which were supplemented with fructose after the media was changed at 24 hours.

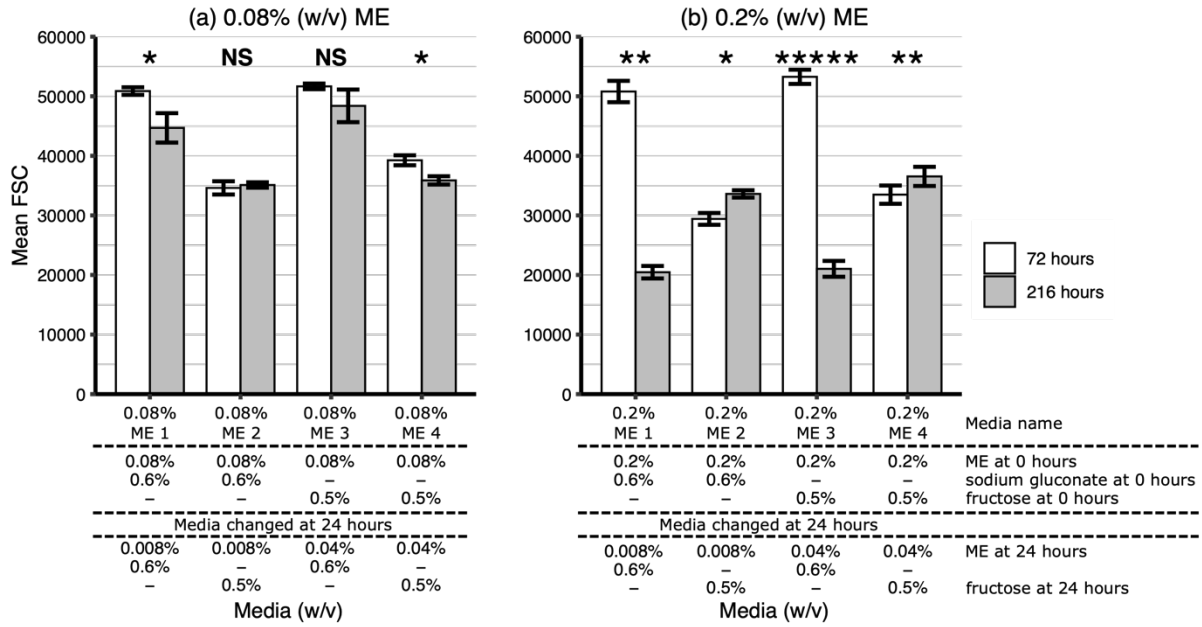


Figure 4.22 – Mean FSC for *C. necator* cultures grown initially in either 0.08% or 0.2% (w/v) ME up to 24 hours until the growth media was changed to either 0.008% or 0.04% (w/v) ME. Media before and after 24 hours was supplemented with either 0.5% (w/v) fructose or 0.6% (w/v) sodium gluconate. Statistical significance was determined using paired t-tests to compare the same condition at different time points (displayed as figure annotations). NS = non-significant ($p \geq 0.05$), * = $p < 0.05$, ** = $p \leq 0.01$, *** = $p \leq 0.001$, **** = $p \leq 0.0001$, ***** = $p \leq 0.00001$. Error bars represent SD. n = 3 biological replicates. The full data can be found in Figure 9.15 (a), Appendix 9.3.

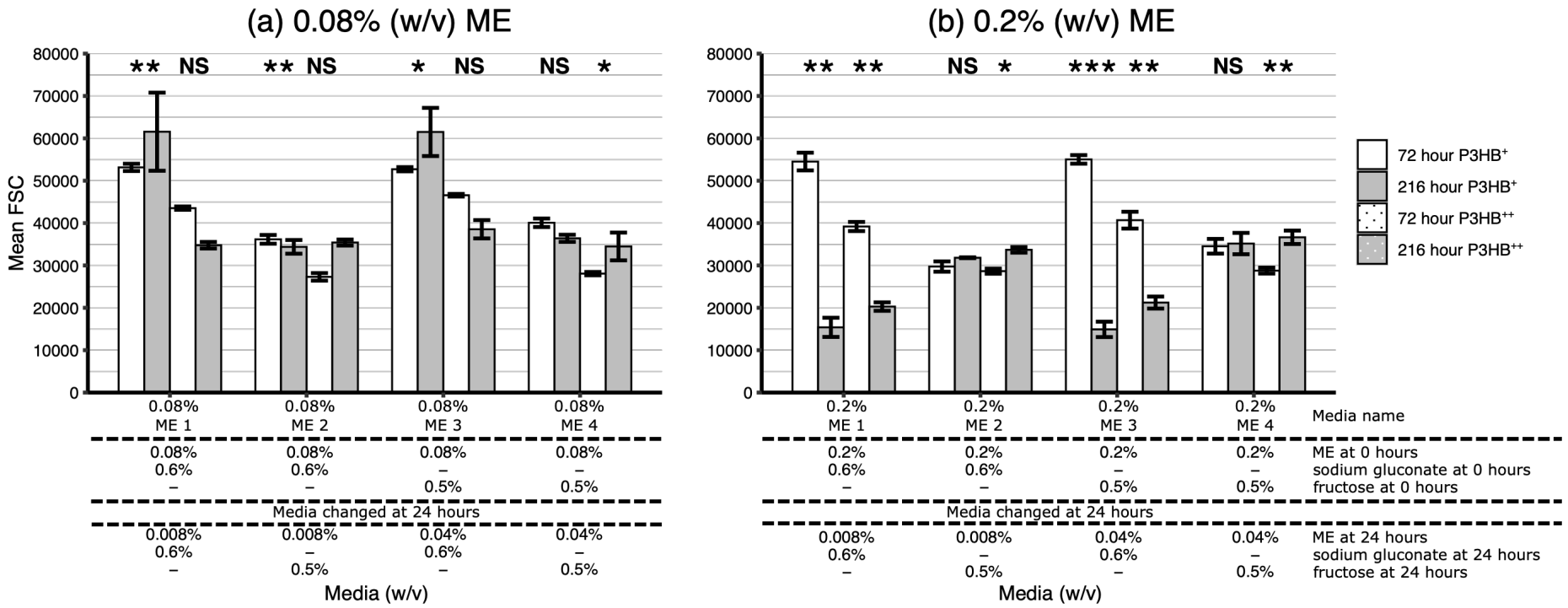


Figure 4.23 - Mean FSC for *C. necator* cultures grown initially in either 0.08% or 0.2% (w/v) ME up to 24 hours until the growth media was changed to either 0.008% or 0.04% (w/v) ME. Media before and after 24 hours was supplemented with either 0.5% (w/v) fructose or 0.6% (w/v) sodium gluconate. Statistical significance was determined using paired t-tests to compare the same condition at different time points (displayed as figure annotations). NS = non-significant ($p \geq 0.05$), * = $p < 0.05$, ** = $p \leq 0.01$, *** = $p \leq 0.001$. Error bars represent SD. n = 3 biological replicates. The full data can be found in Figure 9.15 (b) and (c), Appendix 9.3.

4.4.5 Discussion

In section 4.4 a change of strategy using repeated-batch culture initially consisting of 0.08% or 0.2% (w/v) ME before media was replaced with either 0.008% or 0.04% (w/v) ME at 24 hours. Both before and after 24 hours, media was supplemented with either 0.5% (w/v) fructose or 0.6% (w/v) sodium gluconate. Growth media removed at 24 hours was found to be elevated in pH for cultures containing 0.2% (w/v) ME and 0.6% (w/v) sodium gluconate in phase 1 (0.2% ME 1 and 3). An elevated pH was not observed in fructose-supplemented cultures and was not observed in sodium gluconate-supplemented cultures when the ME concentration was reduced to 0.08% (w/v) ME. An elevated pH is indicative of amino acid deamination (Krebs, 1935) which occurs when a C source is not sufficiently available and amino acids are instead fed into the citric acid cycle in a process which releases ammonia as a by-product (Neis *et al.*, 2015). This would appear to suggest that gluconate is used up in more nutritious 0.2% (w/v) ME cultures, and then surplus amino acids are instead utilised as a C source.

Moving forward in time from the 24-hour media change, between the end of phase 2 at 72 hours and phase 3 at 216 hours, cell size was relatively stable except for conditions 0.2% ME 1 and 3, which were supplemented with sodium gluconate after the media was changed at 24 hours and observed to decrease in size by more than 50%. The reason for this is unclear as fructose supplementation doesn't result in the same decrease in cell size. However, it is possible that in 0.2% ME 1 and 3 cultures, the increased cell number compared to conditions 0.08% ME 1 and 3, in which a decrease in cell size was not observed, may make it more difficult for cells to adjust to osmotic changes using sodium ions as there are fewer ions available per cell.

4.5 What effect on P3HB production does the simultaneous addition of fructose and sodium gluconate have?

In the current study experiments up to this point have explored the production of P3HB *in C. necator* cultures which have fructose and sodium gluconate added separately. In addition to this, experiments have also explored the addition of fructose at 0 hours and sodium gluconate at 24 hours as part of a two-stage feeding strategy. In this section, experiments additionally evaluate the P3HB production of *C. necator* cultures supplemented simultaneously with fructose and sodium gluconate. As in the previous section, this experiment contains a lot of conditions which change at 24 hours. A detailed summary of the media used can be viewed under each graph. Note that media names only apply to media used in this section 4.5.

4.5.1 Gluconate appears to prevent fructose usage through catabolite repression

Figures in the current section contain summaries of mean events per mL and mean pH for *C. necator* cultures initially containing 0.08% or 0.2% (w/v) ME and supplemented with 0.5% (w/v) fructose, 0.6% (w/v) sodium gluconate or both. At 24 hours, growth media was either not changed or replaced with 0.04% (w/v) ME and supplemented with both 0.5% (w/v) fructose and 0.6% (w/v) sodium gluconate. While section 4.5 as a whole focuses on comparing the end of phase 2 at 72 hours and phase 3 at 168 hours, section 4.5.1 additionally focuses on key results found during phases 1 and 2.

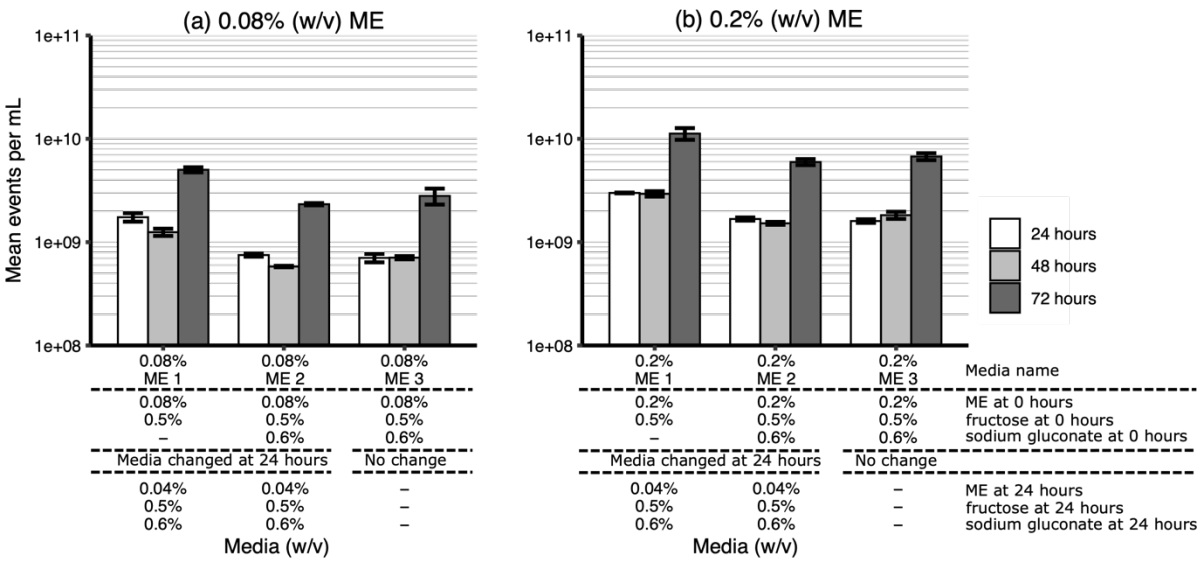
Figure 3.32 summarises mean events for cultures initially containing 0.08% (Figure 3.32 (a)) and 0.2% (w/v) ME (Figure 3.32 (b)). The full data for mean events per mL can be found in Appendix 2 (section 9.4), Figure 9.16. Between the end of phase 1 at 24 hours and the middle of phase 2 at 48 hours growth appeared to be slow, with most cultures either not significantly increasing in cell number or significantly decreasing. The only exception to this was condition 0.2% ME 3 which was observed to marginally increase significantly. On the other hand, between 48 hours and the end of phase 3 at 72 hours, the mean events per mL of all cultures significantly increased.

At 24 hours, for cultures 0.08% ME 1 and 2, and 0.2% ME 1 and 2, the growth media was replaced. The pH of the removed media was recorded and the full data of which is presented in Figure 4.25. For cultures initially containing both 0.08% (Figure 4.25 (a)) and 0.2% (w/v) ME (Figure 4.25 (b)) the pH at 24 hours was significantly higher in cultures supplemented with both 0.6% (w/v) sodium gluconate and 0.5% (w/v) fructose.

Further to the analysis of mean evens per mL and mean pH between the end of phase 1 and phase 2, Figure 4.26 summarises mean events between the end of phase 2 at 72 hours and during phase 3 at 168 hours. During this period, cultures with changed media slightly increased in cell number. This suggests that cell proliferation occurs after media change and that the nutrient content of the media is not P3HB-promoting. On the other hand, cultures which did not have the media replaced did not significantly change in terms of cell number between 72 and 168 hours.

These observations suggest that the presence of sodium gluconate in the growth media prevents *C. necator* from using fructose, instead using the transamination of amino acids as a C source. In *E. coil* gluconate is known to cause catabolite repression (Hogema *et al.*, 1997). In addition, a lack of growth between 24 and 48 hours, and an increase in mean events between 48 and 72 hours suggests that a diauxic lag phase occurs during the switch over from gluconate to fructose metabolism. Diauxic growth is a hallmark of bacteria growth influenced by catabolite repression, and it describes the lag phase that occurs as bacteria switch from one preferred C source to the next in the hierarchy (Chu and Barnes,

2016). This represents the first time that catabolite repression by gluconate has been reported in *C. necator*. As covered in the previous section, an increase in pH during fermentation is indicative of a build-up of ammonia due to the deamination of amino acids (Krebs, 1935). During conditions of surplus carbon sources, which can be directly fed into the citric acid cycle, amino acids are used for protein synthesis (Neis *et al.*, 2015). Results in this section suggest that there are 3 possible catabolite regulation scenarios occurring. First, when fructose only is supplemented there is no evidence of a pH increase suggesting that fructose is used preferentially as a C source. The second, when only gluconate is supplemented, pH rises indicating that in the first 24 hours of growth, amino acids have been metabolised. In this case, it is unclear if amino acids are preferred to gluconate by *C. necator*, or if amino acids are used after gluconate is exhausted. It is possible that certain amino acids are preferred to organic acids and sugars, as some bacteria utilise amino acids as a C source before organic acids or sugars (Moreno *et al.*, 2009). A third scenario in which media is supplemented with both gluconate and fructose also raises pH in phase 1, indicating that gluconate represses fructose.



Paired t-tests comparing events per mL over time.

Media	Significance level	
	24-48 hours	48-72 hours
0.08% 1	*	**
0.08% 2	**	***
0.08% 3	NS	*

Paired t-tests comparing events per mL over time.

Media	Significance level	
	24-48 hours	48-72 hours
0.2% 1	NS	*
0.2% 2	NS	**
0.2% 3	*	**

Figure 4.24 - Mean events per mL for *C. necator* cultures initially containing 0.08% or 0.2% (w/v) ME and supplemented with 0.5% (w/v) fructose, 0.6% (w/v) sodium gluconate or both. At 24 hours growth media was either not changed or replaced with 0.04% (w/v) ME and supplemented with both 0.5% (w/v) fructose and 0.6% (w/v) sodium gluconate. Statistical significance was determined using paired t-tests to compare the same condition between 24 and 48, and 48 and 72 hours (see corresponding tables). NS = non-significant ($p \geq 0.05$), * = $p < 0.05$, ** = $p \leq 0.01$, *** = $p \leq 0.001$. Error bars represent SD. n = 3 biological replicates. The full data can be found in Appendix 2 (section 9.4), Figure 9.16.

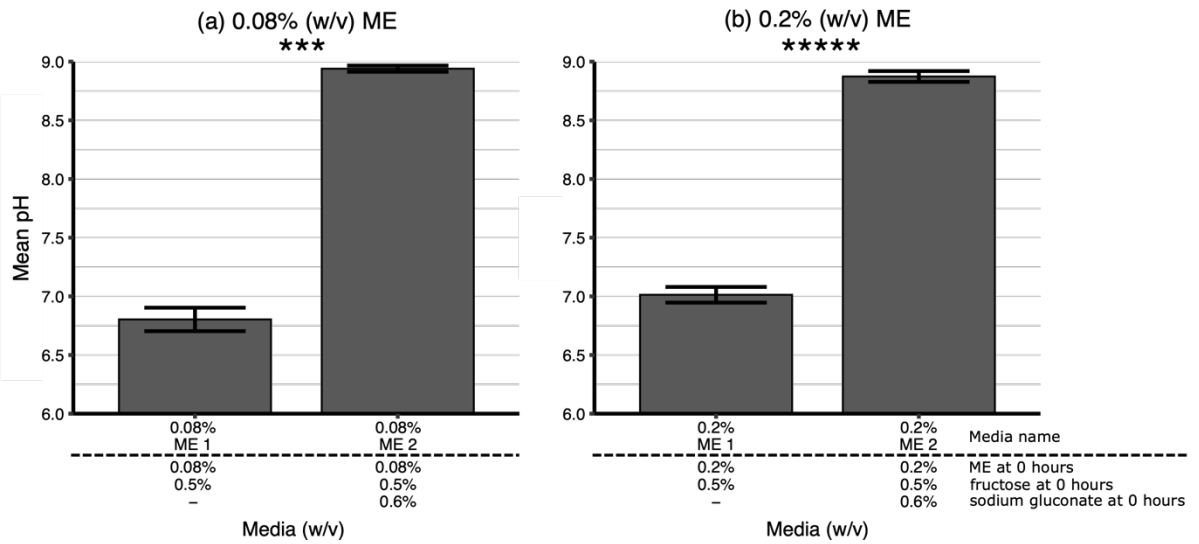


Figure 4.25 - Mean pH of *C. necator* cultures initially containing 0.08% or 0.2% (w/v) ME and supplemented with 0.5% (w/v) fructose, 0.6% (w/v) sodium gluconate or both. The pH of cultures was taken from replaced media and therefore conditions 0.08% ME 3 and 0.2% ME 3 are missing due their media not being replaced at 24 hours. Statistical significance was determined using paired t-tests to compare the same condition at 72 and 168 hours (see annotations) . NS = non-significant ($p \geq 0.05$), * = $p < 0.05$, ** = $p \leq 0.01$, *** = $p \leq 0.001$, **** = $p \leq 0.0001$, ***** = $p \leq 0.00001$. Error bars represent SD. n = 3 biological replicates.

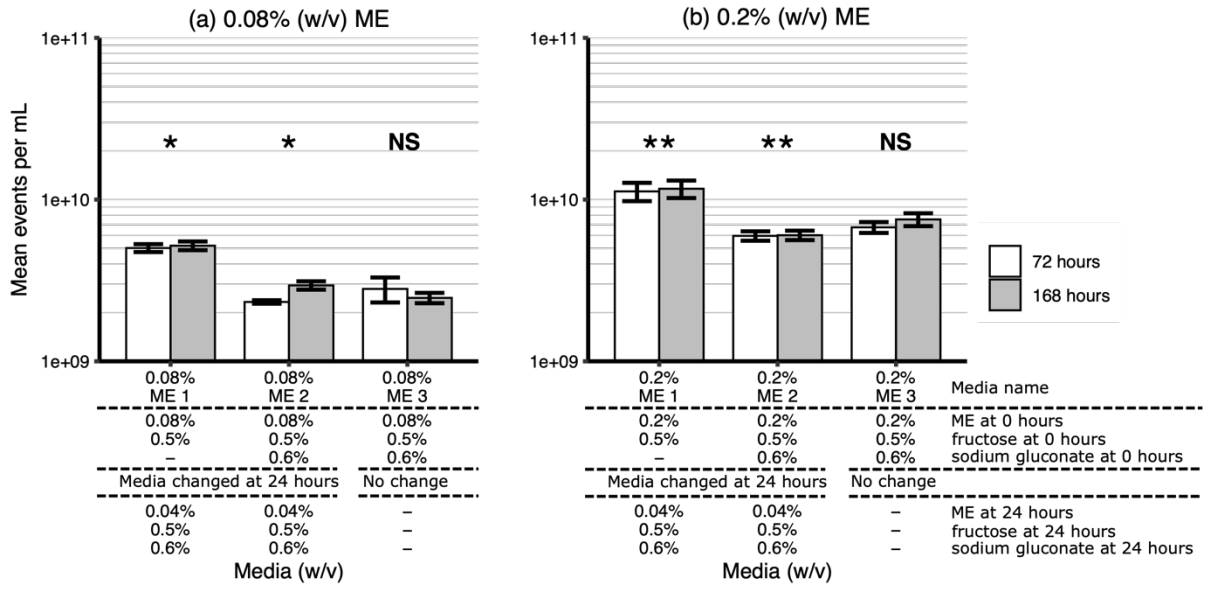


Figure 4.26 – Mean events per mL for *C. necator* cultures initially containing 0.08% or 0.2% (w/v) ME and supplemented with 0.5% (w/v) fructose, 0.6% (w/v) sodium gluconate or both. At 24 hours growth media was either not changed or replaced with 0.04% (w/v) ME and supplemented with both 0.5% (w/v) fructose and 0.6% (w/v) sodium gluconate. Statistical significance was determined using paired t-tests to compare the same condition at 72 and 168 hours (see annotations). NS = non-significant ($p \geq 0.05$), * = $p < 0.05$, ** = $p \leq 0.01$. Error bars represent SD. n = 3 biological replicates. The full data can be found in Appendix 2 (section 9.4), Figure 9.16.

4.5.2 Combining fructose and sodium gluconate addition leads to high P3HB production in phase 2.

Figure 4.27 contains summaries of P-546 fluorescence per cell and per mL for *C. necator* cultures initially containing 0.08% (Figure 4.27 (a) and (b)) or 0.2% (w/v) ME (Figure 4.27 (c) and (d)) and supplemented with 0.5% (w/v) fructose, 0.6% (w/v) sodium gluconate or both. At 24 hours growth media was either not changed or replaced with 0.04% (w/v) ME and supplemented with both 0.5% (w/v) fructose and 0.6% (w/v) sodium gluconate**.** The full data for P-546 fluorescence per cell and per mL can be found in Figure 9.17, Appendix 9.4. For all conditions tested, both P-546 fluorescence per cell and per mL increased between the end of phase 2 at 72 hours and during phase 3 at 168 hours. This increase was significant for all conditions except for 0.2% ME 1 (Figure 4.27 (d)).

Figure 4.28 contains a summary of the mean percentage of $P3HB^{++}$ cells. The full data can be found in Figure 9.17 (c), Appendix 9.4. In similarity to P-546 fluorescence, the mean percentage of $P3HB^{++}$ cells in all cultures significantly increased between 72 and 168 hours.

Figure 4.29 and Figure 4.30 contain a summaries of mean P-546 fluorescence per cell and per mL, respectively. The full data can be found expressed per cell in Figure 9.18 and per mL in Figure 9.19, Appendix 9.4. Generally, P-546 fluorescence per cell for both $P3HB^{+}$ and $P3HB^{++}$ changed little between 72 and 168 hours. On the other hand, P-546 fluorescence per mL significantly increased for the $P3HB^{++}$ population for all conditions.

In *Pseudomonads*, the model system used for the study of catabolite repression centres around the Crc protein (Rojo, 2010). The Crc protein controls the metabolism of C by post-transcriptionally regulating multiple genes simultaneously (La Rosa *et al.*, 2014). In fact, La Rosa *et al.* (2014) found that Crc binds to PhaC mRNA preventing transcription, although this was only observed to occur when a high C to nitrogen was present. There is no literature reporting a Crc protein in *C. necator*, however, the findings of Ampe *et al.* (1998) suggest that *C. necator* and *P. putida* have common C catabolite repression mechanisms in which C source utilisation is governed by a substrate hierarchy. It's possible that in the current study, the aim of producing maximum P3HB production in 72 hours is being hampered by catabolite repression inhibiting the transcription of PhaC1. Thus, P3HB production may only increase after catabolite repression has ceased due to gluconate depletion, and a diauxic lag phase has ended.

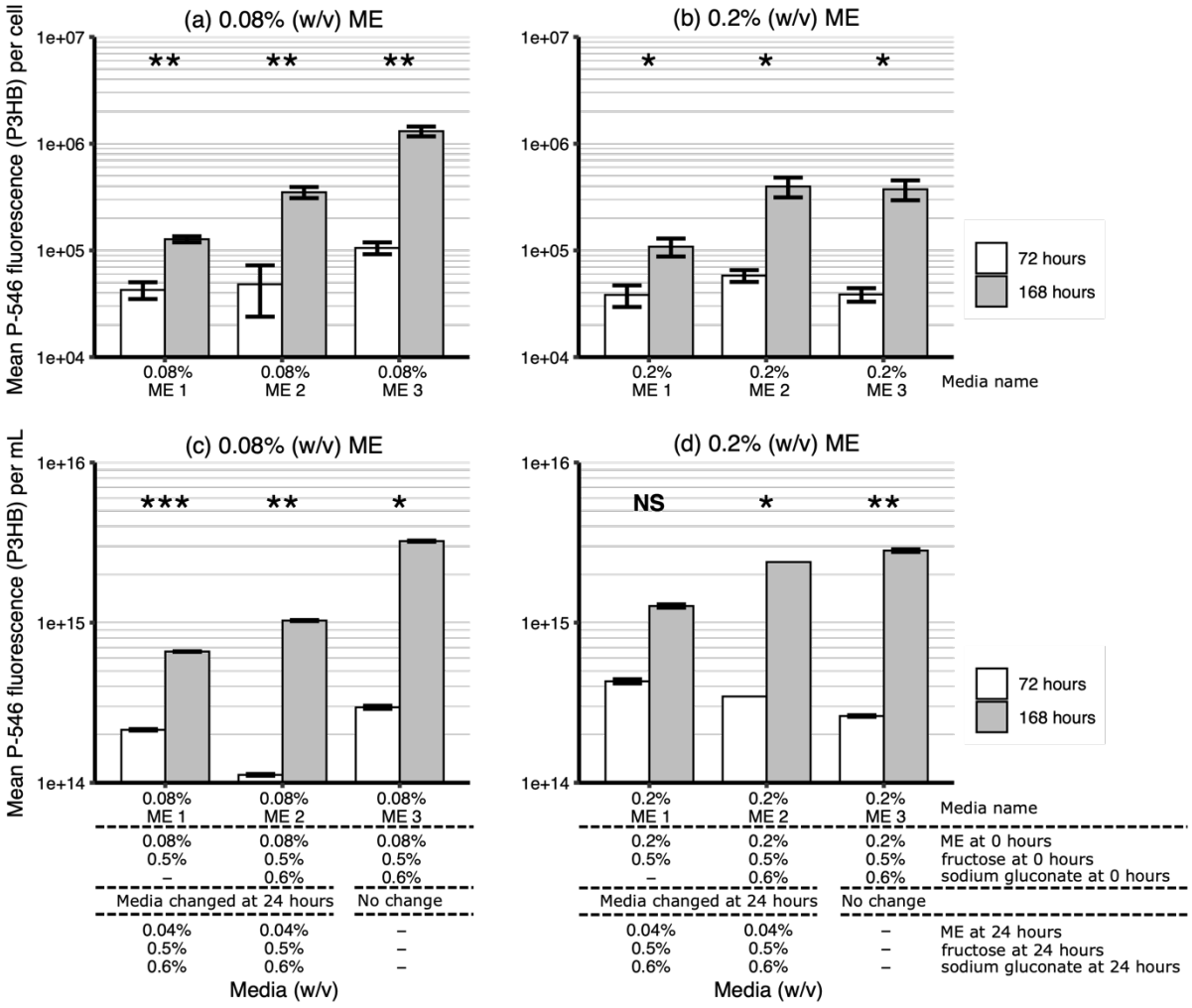


Figure 4.27 - Mean P-546 fluorescence per cell (plots (a) and (b)) and per mL (plots (c) and (d)) for *C. necator* cultures initially containing 0.08% or 0.2% (w/v) ME and supplemented with 0.5% (w/v) fructose, 0.6% (w/v) sodium gluconate or both. At 24 hours growth media was either not changed or replaced with 0.04% (w/v) ME and supplemented with both 0.5% (w/v) fructose and 0.6% (w/v) sodium gluconate. Statistical significance was determined using paired t-tests to compare the same condition at 72 and 168 hours (see annotations). NS = non-significant ($p \geq 0.05$), * = $p < 0.05$, ** = $p \leq 0.01$, *** = $p \leq 0.001$. Error bars represent SD. n = 3 biological replicates. The full data for P-546 fluorescence per cell and per mL can be found in Figure 9.17 (a) and (b), Appendix 9.4.

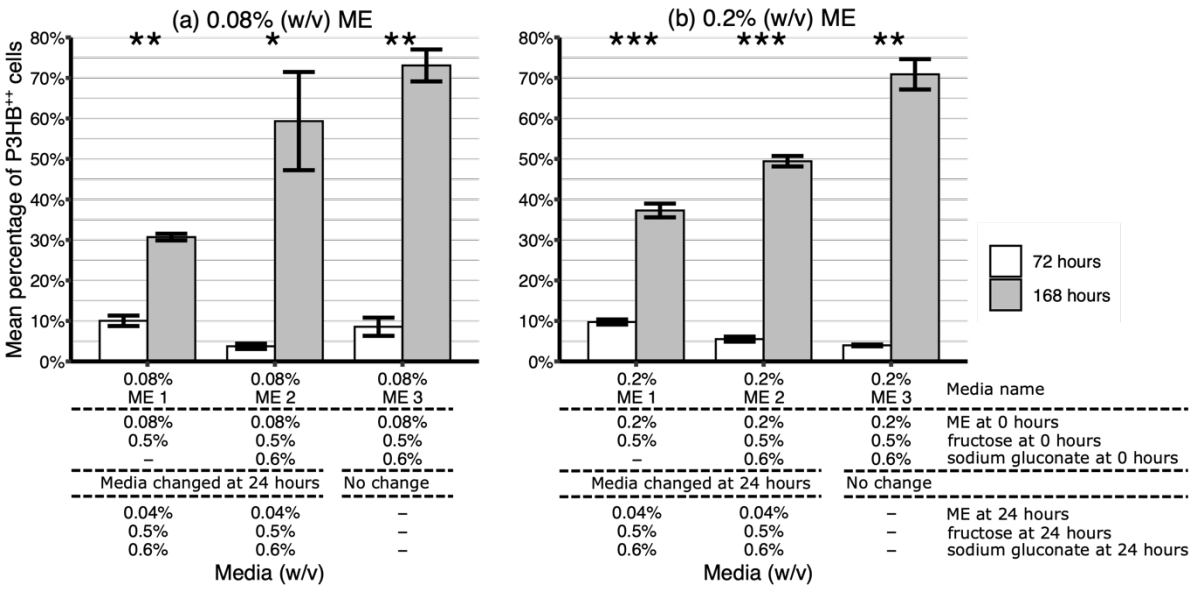


Figure 4.28 - Mean percentage of P3HB^{++} cells for *C. necator* cultures initially containing 0.08% or 0.2% (w/v) ME and supplemented with 0.5% (w/v) fructose, 0.6% (w/v) sodium gluconate or both. At 24 hours growth media was either not changed or replaced with 0.04% (w/v) ME and supplemented with both 0.5% (w/v) fructose and 0.6% (w/v) sodium gluconate. Statistical significance was determined using paired t-tests to compare the same condition at 72 and 168 hours (see annotations). NS = non-significant ($p \geq 0.05$), * = $p < 0.05$, ** = $p \leq 0.01$, *** = $p \leq 0.001$. Error bars represent SD. n = 3 biological replicates. The full data can be found in Figure 9.17 (c), Appendix 9.4.

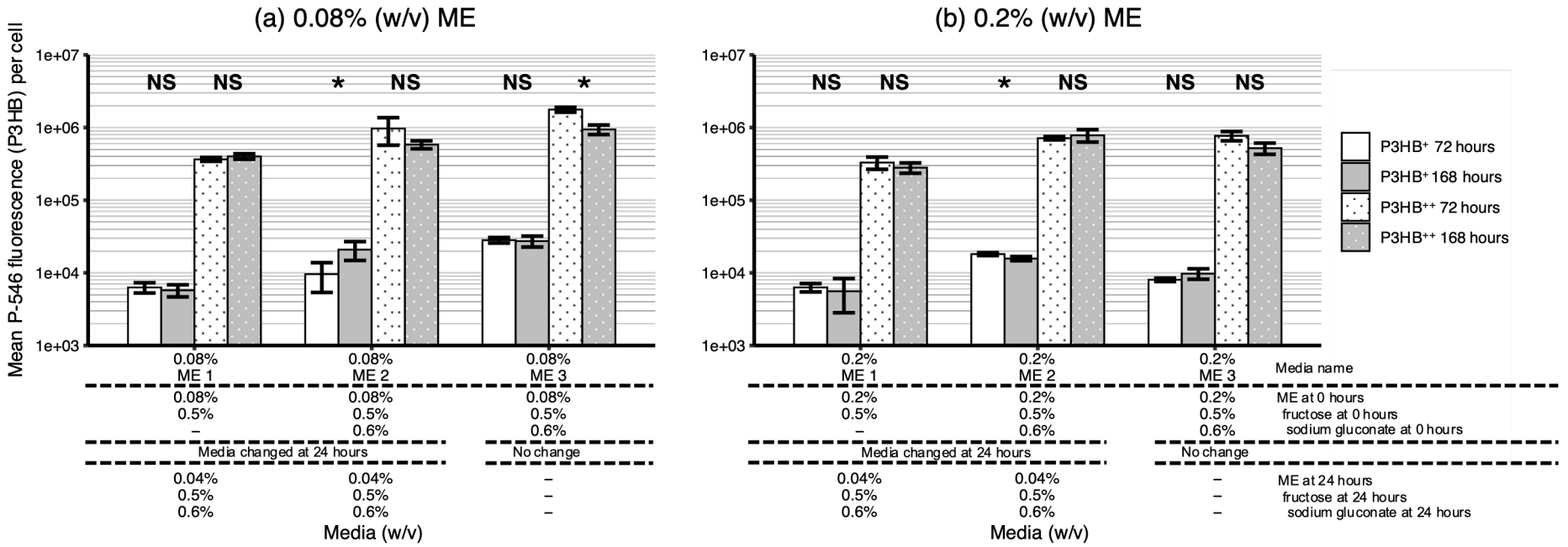


Figure 4.29 - Mean P-546 fluorescence per cell for P3HB^{+} and P3HB^{++} cells for *C. necator* cultures initially containing 0.08% or 0.2% (w/v) ME and supplemented with 0.5% (w/v) fructose, 0.6% (w/v) sodium gluconate or both. At 24 hours growth media was either not changed or replaced with 0.04% (w/v) ME and supplemented with both 0.5% (w/v) fructose and 0.6% (w/v) sodium gluconate. Statistical significance was determined using paired t-tests to compare the same condition at 72 and 168 hours (see annotations). NS = non-significant ($p \geq 0.05$), * = $p < 0.05$. Error bars represent SD. n = 3 biological replicates. The full data can be found in Figure 9.18, Appendix 9.4.

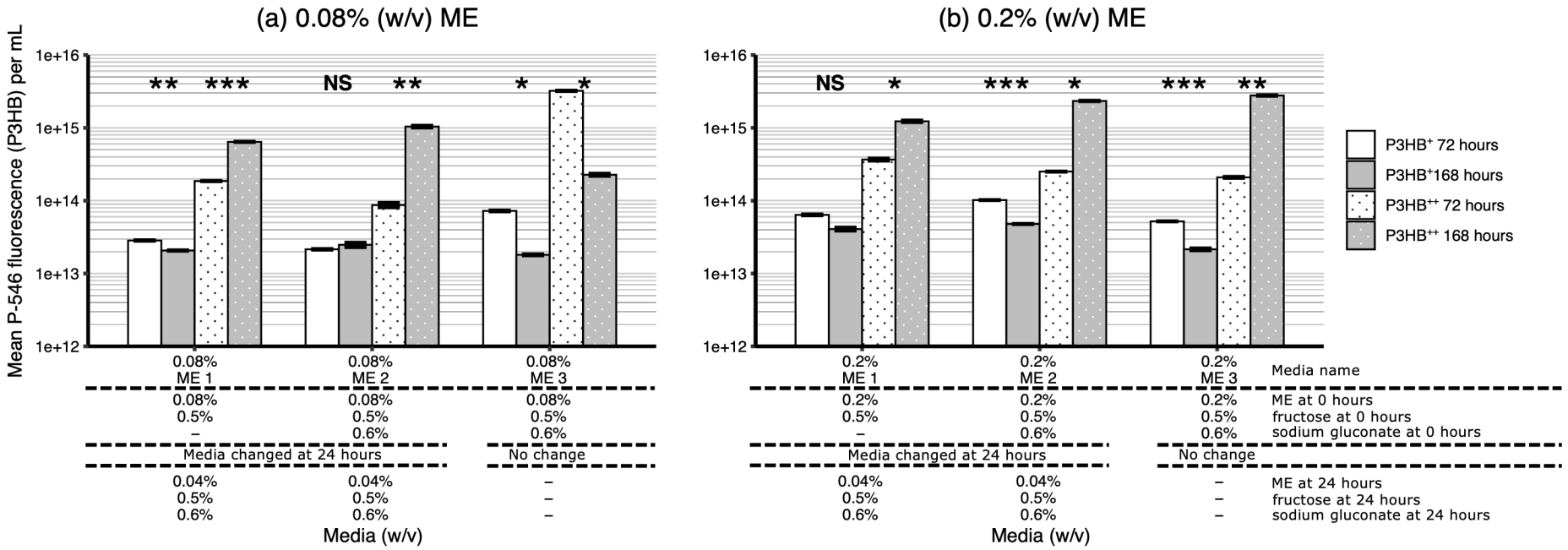


Figure 4.30 - Mean P-546 fluorescence per mL for P3HB^{+} and P3HB^{++} cells for *C. necator* cultures initially containing 0.08% or 0.2% (w/v) ME and supplemented with 0.5% (w/v) fructose, 0.6% (w/v) sodium gluconate or both. At 24 hours growth media was either not changed or replaced with 0.04% (w/v) ME and supplemented with both 0.5% (w/v) fructose and 0.6% (w/v) sodium gluconate. Statistical significance was determined using paired t-tests to compare the same condition at 72 and 168 hours (see annotations). NS = non-significant ($p \geq 0.05$), * = $p < 0.05$, ** = $p \leq 0.01$, *** = $p \leq 0.001$. Error bars represent SD. n = 3 biological replicates. The full data can be found in Figure 9.19, Appendix 9.4.

4.5.3 Cell size generally decreases between 72 and 168 hours

Figure 4.31 contains a summary of mean FSC for *C. necator* cultures initially containing 0.08% (Figure 4.31 (a)) or 0.2% (w/v) ME Figure 4.31 (b)) and supplemented with 0.5% (w/v) fructose, 0.6% (w/v) sodium gluconate or both. At 24 hours growth media was either not changed or replaced with 0.04% (w/v) ME and supplemented with both 0.5% (w/v) fructose and 0.6% (w/v) sodium gluconate. The full data can be found in Figure 9.2 (a), Appendix 9.4. Once again cell size significantly decreased for all conditions except for 0.2% ME 1. In fact, cell size changed by a much smaller proportion in 0.08% and 0.2% ME 1 cultures.

Figure 4.32 contains a summary of mean FSC for the $P3HB^{+}$ and $P3HB^{++}$ cell populations. The full data can be found in Figure 9.2 (b) and (c), Appendix 9.4. The data for $P3HB^{+}$ and $P3HB^{++}$ cell populations appears to add little to that summarised in Figure 4.31. Except when breaking down the data into individual populations, $P3HB^{++}$ *C. necator* cells grown in 0.08% and 0.2% ME 2 media significantly increased in size a feature which did not occur in other media conditions. While the reason for this occurrence is unclear, this once again provides evidence that both $P3HB^{+}$ and $P3HB^{++}$ populations react to varying conditions in different ways.

Cell size decreases in the current study are likely due to the presence of extracellular ammonia causing osmotic stress. In media conditions 0.08% and 0.2% ME 1 and 2, although media was changed to more dilute ME at 24 hours, it is likely ammonia was still produced due to further supplementation with fructose and sodium gluconate. It is possible that the smaller cells are able to mitigate for osmotic changes and resist cell size changes more than larger cells due to the structural support provided by intracellular P3HB.

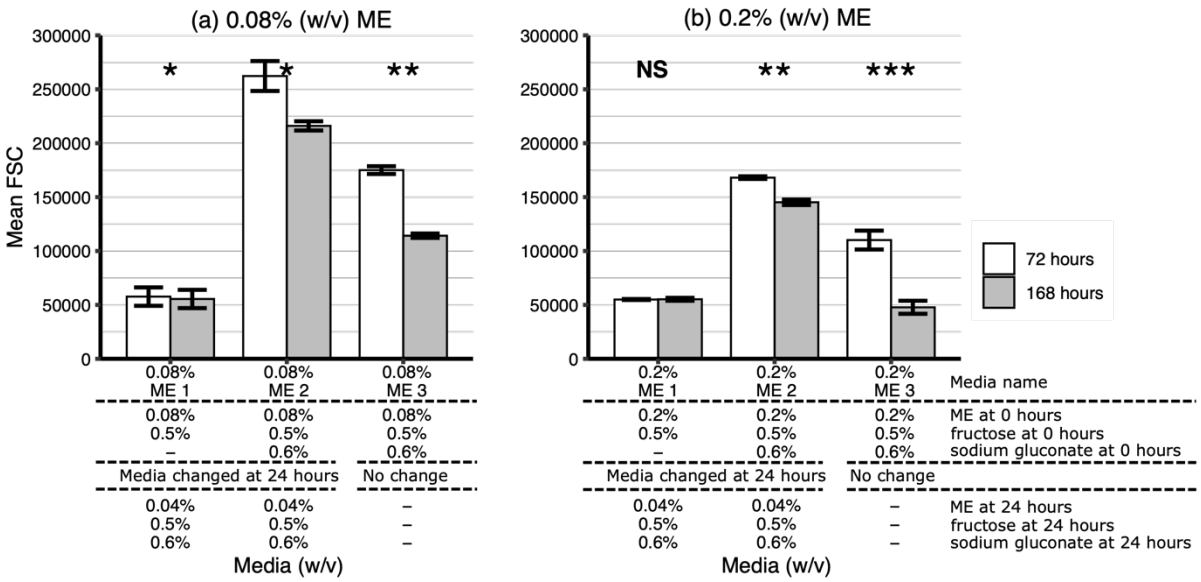


Figure 4.31 - Mean FSC for *C. necator* cultures initially containing 0.08% or 0.2% (w/v) ME and supplemented with 0.5% (w/v) fructose, 0.6% (w/v) sodium gluconate or both. At 24 hours growth media was either not changed or replaced with 0.04% (w/v) ME and supplemented with both 0.5% (w/v) fructose and 0.6% (w/v) sodium gluconate. Statistical significance was determined using paired t-tests to compare the same condition at 72 and 168 hours (see annotations). NS = non-significant ($p \geq 0.05$), * = $p < 0.05$, ** = $p \leq 0.01$, *** = $p \leq 0.001$. Error bars represent SD. n = 3 biological replicates. The full data can be found in Figure 9.2 (a), Appendix 9.4.

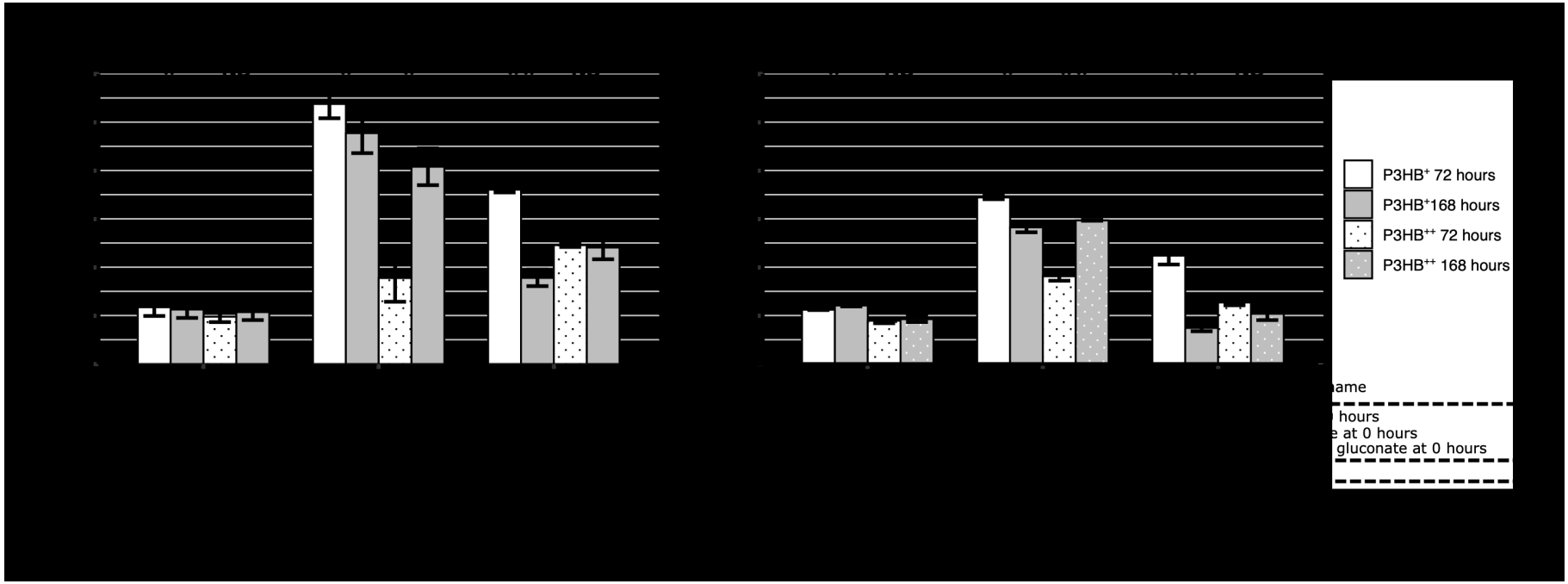


Figure 4.32 - Mean P3HB^{+} and P3HB^{++} FSC for *C. necator* cultures initially containing 0.08% or 0.2% (w/v) ME and supplemented with 0.5% (w/v) fructose, 0.6% (w/v) sodium gluconate or both. At 24 hours growth media was either not changed or replaced with 0.04% (w/v) ME and supplemented with both 0.5% (w/v) fructose and 0.6% (w/v) sodium gluconate. Statistical significance was determined using paired t-tests to compare the same condition at 72 and 168 hours (see annotations). NS = non-significant ($p \geq 0.05$), * = $p < 0.05$, ** = $p \leq 0.01$. Error bars represent SD. n = 3 biological replicates.

4.5.4 Discussion

In the final results section of this thesis, cultures of *C. necator* initially containing 0.08% or 0.2% (w/v) ME, supplemented with 0.5% (w/v) fructose, 0.6% (w/v) sodium gluconate or both were investigated. An elevated pH at 24 hours for culture supplemented with both fructose and sodium gluconate, gluconate appears to prevent the metabolism of fructose through catabolite repression. Gluconate is known to cause catabolite repression in *E. coli* (Hogema *et al.*, 1997). However, this represents the first report of gluconate-related catabolite repression in *C. necator*. Cell count data between 24 and 72 hours demonstrated that diauxic growth was occurring, which is a hallmark of catabolite repression and occurs due to a lag time in switching metabolism from a preferred C source to the next available in the hierarchy (Chu and Barnes, 2016). The strategy of feeding cultures with fructose and sodium gluconate did not prevent a lag time in P3HB production into phase 3. This may be due to the action of a protein in *C. necator* similar to the Crc protein present in *Pseudomonads* (Rojo, 2010). The Crc protein controls catabolite repression in *Pseudomonads* (Rojo, 2010) controlling the metabolism of C by post-transcriptionally regulating multiple genes simultaneously (La Rosa *et al.*, 2014). Ampe *et al.* (1998) suggests that *C. necator* and *P. putida* have common C catabolite repression mechanisms in which C metabolism is governed by a substrate hierarchy. Its therefore possible that catabolite regulation causes the lag phase in P3HB production observed in this study, by preventing the transcription of PhaC1. The P3HB producing lag-phase likely extends beyond 72 hours due to the slow changeover in C metabolism associated with catabolite regulation.

It's possible that ammonia reduces media osmolarity causing a reduction in cell volume due to an efflux of water out of cells. This appears to happen to a lesser degree in cells which start off smaller, most likely due to the structural support provided to the cell membrane by P3HB granules.

4.6 Conclusions

The experiments presented in Chapter 4 have aimed to reduce a lag time in P3HB production which extends production beyond the target period of 72 hours. Fed-batch and repeated-batch strategies were divided into 3 phases: phase 1, an initial biomass accumulation phase from 0 to 24 hours; phase 2, the period in which P3HB production is targeted to peak in; phase 3, a period after 72 hours evaluating if maximum P3HB production occurs after 72 hours or before. Initial experiments aiming to utilise the strengths of fructose supplementation for biomass accumulation in phase 1 and sodium gluconate for P3HB production in phase 2 failed to reduce the delay in P3HB production. The addition of between 3 and 15g/L of sodium chloride also did not reduce the lag time. Changing the strategy to a repeated-batch system in which media was changed and replaced with more dilute ME also failed to reduce the lag time in P3HB production. However, testing the pH of media removed at 24 hours from repeated batch cultures found that in cultures supplemented with sodium gluconate, or sodium gluconate and fructose together, pH was elevated. This was indicative of amino acid deamination, a process which occurs when more typical C sources are unavailable and amino acids are instead used as a C source. In cultures supplemented with both fructose and sodium gluconate together, an elevated pH and a staggered growth pattern presenting evidence of diauxic growth suggest that gluconate represses the metabolism of fructose in *C. necator* by C catabolite repression. It's possible that C catabolite repression in *C. necator* is the cause of the lag phase of P3HB production observed in the current study. In this scenario, the lengthy time delay which shifts P3HB production into phase 3 is likely the result of the slow speed of metabolic changeover from one C source to the next available in the hierarchy. Often between the end of phase 2 at 72 hours and phase 3, a decrease in cell size occurs in cultures with higher ME concentrations. This may be attributed to the release of ammonia due to the deamination of amino acids which are likely more residual in more nutritious ME cultures.

Chapter 5 Overall Discussion and conclusion

5.1 Initial studies varying the C to ME ratio and optimising cell staining for flow cytometry

Polyhydroxyalkanoates are a class of bio-polymer which naturally accumulate in some bacteria, and have the potential to provide sustainable, biodegradable plastic products suitable for medical and consumer markets. The overall aim of this study was to produce P3HB, the most commonly produced PHA (McAdam *et al.*, 2020), in a maximum P3HB in 72 hours, a timeframe that was consistent with the results of previous literature (Budde *et al.*, 2011; Pradella *et al.*, 2012; Ienczak *et al.*, 2016). The growth media used in this study was ME (DSMZ, 2007), an inexpensive, nutrient-rich media which has been used in literature in P3HB related studies for biomass accumulation (Fukui *et al.*, 1998) and also for both biomass and P3HB production (Passanha *et al.*, 2014). The organism chosen for P3HB accumulation in this study was *C. necator* H16, a bacterium established as the model system for biosynthesis of P3HB biosynthesis (Verlinden *et al.*, 2007). Carbon sources were added to ME media in the form of sodium gluconate (Wahl *et al.*, 2012) and fructose (Budde *et al.*, 2011), with both having been used in literature to create a C-to-nutrient ratio suitable for inducing P3HB biosynthesis. This study presents a unique cell by cell analysis of *C. necator* growth and P3HB accumulation, using flow cytometry to simultaneously count cells, quantify intracellular P3HB and monitor changes in cell size.

In sections 3.1 to 3.7 due to a problem preventing flow cytometry cell counting from being available, OD_{600} measured by UV-visible spectroscopy was used as a means to quantify culture cell density. Measurements of OD_{600} are considered to be proportional to dry weight and cell count (Myers *et al.*, 2013) and have previously been used to monitor culture biomass of P3HB-producing bacteria (Ahn *et al.*, 2000). However, OD_{600} measurements can become disproportional to cell counts when cell size changes (Stevenson *et al.*, 2016) and to both biomass and cell counts when intracellular components such as P3HB absorb at OD_{600} (Martinez and Déziel, 2020). Cell counting by flow cytometry, on the other hand, is not influenced by the accumulation of intracellular P3HB or by changes in cell size but can underestimate cell counts when cells aggregate, causing distortion to data due to multiple cells being recorded as a single cell (Ou *et al.*, 2017). Both measurements of OD_{600} and cell counts were found to be useful for evaluating *C. necator* metabolism and assessing if nutrient conditions were suitable for cell proliferation or possible P3HB accumulation.

In seed cultures and non-supplemented experimental cultures, in the early stages of growth, at around 4-6 hours, *C. necator* multicellular aggregates were observed. While cell aggregates are not suited to

flow cytometry analysis due to the risk of fluidics blockages and data distortion (Ou *et al.*, 2017), there are also implications for P3HB biosynthesis. Wang *et al.* (2021) suggested that aggregation-associated components of the extracellular matrix such as lipopolysaccharide, colonic acid, flagella and fimbria utilise cellular pools of acetyl-CoA, and in doing so compete with P3HB biosynthesis. Furthermore, this was also found to be the case in the biosynthesis of rhamnolipid (Zhu and Rock, 2008), which utilises malonyl-CoA via the fatty acid de novo biosynthesis pathway which is formed from the carboxylation of acetyl-CoA (Gutierrez *et al.*, 2013). Abdel-Mawgoud *et al.* (2014) also found, by inhibiting the β-oxidation pathway, rhamnolipids and P3HB share the same 3-hydroxyalkanoate intracellular pool. The avoidance of *C. necator* aggregates is therefore important to stop competition between metabolic pathways. Microscopic analysis in the current study showed that persistent cell aggregation could be prevented by inoculating with a seed culture grown for 24 hours rather than 12 hours. The supplementation of media with either fructose or sodium gluconate was also observed to help avoid aggregate formation.

Also observed in *C. necator* cultures grown in either ME only or with fructose supplemented were chains of cells seemingly consisting of individual cells joined at the cell poles. Such cells are likely to be in the process of cell division, and the regions joining cell poles which do not stain with nucleic acid stains such as SYTO9 are Z-rings. Consisting of the tubulin homologue FtsZ, a Z-ring is a key part of the cell division site and functions to recruit division proteins to the divisome and direct the formation of septal peptidoglycan (Du and Lutkenhaus, 2019). The observation of *C. necator* forming cell chains in the process of division is that it is likely growth-promoting nutrients are still present in the growth media. Thus, if *C. necator* is proliferating and has growth promoting nutrient levels available it is less likely that P3HB biosynthesis will be initiated.

Increasing the C to key nutrient ratio is established as a fundamental requirement for the initiation of P3HB biosynthesis. In fact, Ahn *et al.* (2015) found that by increasing the C to key nutrient ratio in *C. necator* cultures, both overall P3HB and the speed of production increased, with the most accumulation occurring in the first 12 hours. Initial experiments in the current study therefore investigated decreasing the ME concentration ranging from standard 0.8% (w/v) ME (DSMZ, 2007) to more dilute 0.08% ME. While decreasing the ME concentration did increase P3HB per cell in some circumstances, the increases were generally relatively small, and in some cases due to multiple cells joined in chains in the process of cell division due to the formation of Z-rings at cell poles (Du and Lutkenhaus, 2019). In a similar strategy, fructose and sodium gluconate concentrations were increased in order to further increase the C to ME ratio. Experiments in which ME media was supplemented found that by adding either fructose or sodium gluconate to cultures to ME cultures, P3HB per cell could be increased, but any further attempts to increase P3HB by increasing the C to ME ratio did not.

In section 3.7, a staining optimisation study was conducted due to concerns the amount of P3HB granules observed microscopically was not being reflected by the increase observed in P-546 fluorescence. Temperature, staining time and P-546 concentration are known to affect the staining of P3HB granules (Karmann *et al.*, 2016), and were therefore investigated. Optimisation found that current P-546 staining was adequate, with P-546 fluorescence remaining stable for up to one hour, and there was found to be no significant difference in P-546 fluorescence when concentrations of 0.2 or 1 µg/mL were used. Temperature was also found not to significantly change results. However, results did show that there was an opportunity to use less stain and thus make the staining procedure more economical. The final staining procedure after optimisation, and the procedure used beyond section 3.7 in the current study, was 12 minutes at 30 °C with 0.2 µg/mL of P-546 to stain P3HB, and 1 µM SYTO62, to distinguish cells from noise. A limitation of the staining optimisation was that P-546 fluorescence should have been correlated with extracted P3HB, as reported by Karmann *et al.* (2016), to ensure a linear trend was observed. A linear trend between extracted P3HB and P-546 fluorescence should have been established for both flow cytometry methods as this would have allowed for units of P-546 fluorescence to be related to a specific amount of P3HB.

5.2 Cultures of *C. necator* contain a population of P3HB^{++} cells which produce up to 1000 times more P3HB than the dominant P3HB^{+} phenotype

In this study, a P3HB^{++} sub-population of *C. necator* has been observed which typically represents less than 5% of the total population and produces considerably more P3HB in less time than the dominant P3HB^{+} phenotype. The production of P3HB^{++} cells appears to be sensitive to both key nutrients and the presence of fructose or sodium gluconate. For example, if *C. necator* cells are grown in 0.2% (w/v) ME without supplementation, the amount of P3HB^{++} cells produced is negligible. However, if 0.5% (w/v) fructose is supplemented to this media, a P3HB^{++} population is observed representing around 2.5% of the total *C. necator* population. On the other hand, 0.08% (w/v) ME cultures produce a P3HB^{++} population without the need for C supplementation. The production of P3HB^{++} cells occurs as early as 4 hours and appears to be due to phenotypic heterogeneity (Reyes Ruiz *et al.*, 2020). Bacterial sub-populations can arise from a variety of genetic (Arber, 2000) or non-genetic factors (van Boxtel *et al.*, 2017) which can be stochastic in nature (Choi *et al.*, 2008). Small variant populations of *C. necator* cells have previously been reported. For example, Franz *et al.*, (2011) observed a small population of glucose utilising colonies, and by picking colonies and growing in glucose-rich agar repeatedly was able to evolve a glucose utilising *C. necator* strain. Similarly, González-Villanueva *et al.* (2019) grew *C.*

necator colonies repeatedly in multi-well plates in order to direct the evolution of a variant capable of rapid glycerol utilisation. In both cases, variants were subjected to several rounds of successful directed evolution raising the prospect that the high P3HB-producing population in the current study could be used to enhance P3HB production without the need for application-limiting genetic modification. However, this would only likely be successful if more permanent changes, such as genomic DNA mutations (Arber, 2000), were the reason for P3HB^{++} cell production, rather than stochastic mechanisms such as transcription factor concentration (Hillenbrand *et al*., 2016).

It's possible that the P3HB^{++} cells are a type of persister cell, which are dormant phenotypic variants that are stress resistant, and cause particular problems when produced by bacterial species such as *Pseudomonas aeruginosa* in cystic fibrosis patients due to high tolerance to antibiotics (Lewis, 2010). Formed predominantly during nutrient-rich phases of exponential growth (Norman *et al*., 2015), persister cell production is reduced 1000-fold when respiration is inhibited (Orman and Brynildsen, 2015). In the current study, the proportion of P3HB^{++} *C. necator* cells remains relatively constant suggesting that P3HB^{++} cells are produced during periods of cell proliferation. In addition to representing a small proportion of the bacterial population, persister cells are reported to be smaller in size when compared to the dominant population (Kotte *et al*., 2014; Solopova *et al*., 2014), traits also often observed for P3HB^{++} cells in the current study. The main difference between persister cells such as those produced by *E. coli* and *C. necator* P3HB^{++} cells is that P3HB^{++} cells display evidence of not being strictly dormant by producing P3HB not just rapidly in 4 hours, but also over extended culture periods. However, it should be noted that *E. coli* are not a P3HB-producing bacteria. Producing persister cells which accumulate P3HB, fits with the principle that persister cells are produced in case the main population are unable to survive, as P3HB has been reported to offer considerable survival advantages to abiotic stresses such as freezing temperatures (Obruca *et al*., 2016).

5.3 Supplementing cultures with fructose or sodium gluconate has implications on P3HB production, cell proliferation and cell expansion.

In sections 3.8 and 3.9 flow cytometry cell counting became available, and allowed for the calculation of cell counts expressed as events per mL, and also P3HB per mL of culture in addition to the already available P3HB per cell. While expressing intracellular P3HB as P3HB per cell is informative, its weakness compared to P3HB per mL is that it doesn't show increases in overall culture P3HB that occur due to an increase in cell number. Once flow cytometry cell counting was available after section 3.8, it was established that there were key differences between cultures supplemented with fructose or

sodium gluconate. Sodium gluconate-supplemented cultures produced significantly more P3HB per cell and per mL compared to fructose. This may have been due to the presence of sodium ions which are known to provide an important link across the bacterial cell membrane (Dimroth, 1990). In fact, bacteria are able to transport an array of solutes and sugars across the cell membrane using secondary transport proteins, which use sodium ions to move molecules such as glucose across the cell membrane against a concentration gradient (Henriquez *et al.*, 2021). It's therefore possible the presence of sodium ions allowed gluconate to move across the cell membrane more effectively, particularly against the concentration gradient, in comparison to fructose. The movement of sodium ions into the cell also provides a possible explanation for why *C. necator* cells are considerably larger when sodium gluconate is supplemented. The addition of sodium chloride to bacterial cultures has been reported to stop cells proliferating and instead cause expansion (Vijaranakul *et al.*, 1995; Piuri *et al.*, 2012). Organic acid anions are also known to have an influence on bacterial cell growth (Warnecke and Gill, 2005) and there is an established link between the movement of monovalent ions, changes in membrane potential and bacterial cell size (Kay, 2017). As a mechanism against osmotic stress, bacteria alter intracellular ion concentrations in order to offset the effects by increasing or decreasing cell size (Björklund and Marguerat, 2017). Increases in cell size, such as that observed in *C. necator* cells in this study when sodium gluconate is supplemented, are due to the effects of turgor pressure, the concentration of peptidoglycan precursors, or both (Harris and Theriot, 2018). A key protein involved in cell elongation is the MreB protein which organises the elongosome complex responsible for cell membrane expansion (Plaitakis *et al.*, 2017) by directing enzymes responsible for peptidoglycan and teichoic acid synthesis (Szatmári *et al.*, 2020). In fact, the rate at which MreB polymerises in the cell membrane has been found to be increased in the presence of sodium ions (Szatmári *et al.*, 2020). While *C. necator* cells expand in cultures supplemented with sodium gluconate when fructose is supplemented cells proliferate. The process governing if a bacterial cell proliferates or expands can be explained by the two-competing-sites model, in which Z-ring sites of septation compete with cell elongation machinery (Lleo *et al.*, 1990). The division of bacterial cells is thought to be dependent on the concentration of the FtsZ protein which functions to recruit proteins key for the division process (Du and Lutkenhaus, 2019). On the other hand, the elongation of cells is controlled by the highly conserved rod system, which involves the polymerisation of peptidoglycan with the glycan polymerase RodA and the PBP2 crosslinking enzymes (Rohs *et al.*, 2018).

5.4 A delay causing P3HB production to extend beyond 72 hours may be due to catabolite regulation

From the results presented in Chapter 3 it was clear that fructose was more suited to producing *C. necator* cultures which proliferated, and sodium gluconate was more suited to preventing proliferation and producing more P3HB. These two observations set the precedent for a fed-batch strategy to start Chapter 4 in which fructose was added to cultures at 0 hours in order to accumulate a large amount of cells. Fed-batch fermentation strategies have been previously used to produce P3HB (Pradella *et al.*, 2012) and generally work by adding a substrate into the reactor during growth while the product formed remains in the reactor for the duration of the fermentation. This period, between 0 and 24 hours, was termed phase 1. Following phase 1 was then phase 2, which occurred between 24 and 72 hours and was defined as the period in which maximum P3HB production should occur. Phase 3, from 72 hours onwards then represented a period in which cultures are sampled to determine if maximum P3HB production did indeed occur during phase 2. Results for some batch experiments and this initial fed-batch strategy revealed there was a lag phase delaying P3HB production beyond phase 2. The PhaC enzyme is known to have a lag time of around 6 hours, a time which can be extended by mutating key residues, although the effects of mutations could be cancelled by the presence of PhaM (Juengert *et al.*, 2018). It's unlikely that the lag time, observed to last beyond 72 hours into phase 3, is due to a delay in the polymerisation of 3HB based on the findings of Juengert *et al.* (2018). In addition, *C. necator* H16 contains PhaM (Bresan and Jendrossek, 2017) and its expression may have mitigated any potential point mutations in the phaC gene (Juengert *et al.*, 2018).

Research by Passanha *et al.* (2014) found the addition of sodium chloride to ME media increased the rate of PHA production in the first 24 hours of growth. Based on the experiments of Passanha *et al.* (2014), results presented in section 4.4 tested the addition of between 3 and 15 g/L of sodium chloride to ME media. However, sodium chloride addition was found to not prevent a delay in P3HB production with a considerable amount of P3HB production still occurring in phase 3, rather than phase 2.

Another strategy tested was a repeated-batch method. In repeated batch fermentations, either part of (Khanna and Srivastava, 2005), or the whole media (Fukui *et al.*, 1998) are replaced with fresh media. This change of strategy aimed to remove media, after an initial fructose or sodium gluconate-supplemented phase 1, at 24 hours. Dilute media of either 0.008% or 0.04% (w/v) ME was then used to replace the phase 1 media and supplemented with either fructose or sodium gluconate. Once again, this didn't prevent a lag phase in P3HB production although it should be noted that some results were non-significant. However, a decrease in P3HB which would be expected to be observed once P3HB production had peaked did not occur. The removal of media provided the first opportunity in the study

to test media pH at the end of phase 1 at 24 hours. This revealed that 0.2% (w/v) ME cultures which were supplemented with sodium gluconate had a significantly elevated pH in relation to fructose supplemented 0.2% (w/v) ME. A similar increase in pH was not observed in cultures containing 0.08% (w/v) ME. A rise in pH during fermentation is indicative of a build-up of ammonia due to the deamination of amino acids (Krebs, 1935). Ammonia is released as a by-product of amino acid deamination, occurring when a C source is unavailable and instead amino acids are used as a source of energy to be fed into the citric acid cycle (Neis *et al.*, 2015). The fact that pH is only elevated in 0.2% (w/v) ME cultures suggests that the higher ME concentration meant that surplus amino acids were available.

In the final results section 4.5, repeated-batch was again chosen as a strategy but on this occasion, some cultures were supplemented with both fructose and sodium gluconate at the start of phase 1 at 0 hours. The pH of media removed at the end of phase 1 at 24 hours was significantly elevated for cultures containing both fructose and sodium gluconate, but not for cultures supplemented with fructose only. This suggests that gluconate prevents *C. necator* from metabolising fructose and instead uses amino acids as a C source for the citric acid cycle. Carbon catabolite regulation is not just limited to organic acids and sugars, but has also been demonstrated to also encompass some amino acids (Moreno *et al.*, 2009). Generally, literature regarding catabolite repression centres around *Pseudomonads* in which the Crc protein is responsible for the regulation of C catabolite repression (Rojo, 2010). The Crc protein is responsible for optimising the metabolism of C by post-transcriptionally regulating genes (La Rosa *et al.*, 2014). In fact, La Rosa *et al*. (2014) found that the Crc binds to PhaC mRNA preventing transcription, although this was only observed to occur when a high C to nitrogen was present. Even though there is no literature directly reporting a Crc protein in *C. necator*, the findings of Ampe *et al*. (1998) suggest that *C. necator* and *P. putida* have common C catabolite repression mechanisms in which carbon source utilisation is governed by a substrate hierarchy.

In the current study, 3 key scenarios have been observed which relate to C catabolite repression. The first, when fructose only is supplemented there is no evidence of a pH increase suggesting that fructose is used preferentially as a C source. The second, when only gluconate is supplemented, pH rises indicating that in the first 24 hours of growth amino acids have been metabolised. In this case, it is unclear if gluconate or amino acids are preferred by *C. necator*. A third scenario in which media is supplemented with both gluconate and fructose also raises pH in phase 1, indicating that gluconate represses fructose. It's possible that the lag time observed in P3HB production in the current study results from the hierarchal nature of C catabolite repression.

5.5 Overall conclusions

The experiments presented in this thesis have generally demonstrated that the production of P3HB in *C. necator* when supplemented with fructose or sodium gluconate increases, but increasing the concentration of each supplement does not lead to further P3HB synthesis. Fructose supplementation was found to be more suitable for inducing cell proliferation, whereas sodium gluconate-supplemented cultures produced more P3HB and induced cell expansion. It's possible *C. necator* accumulates more P3HB when sodium gluconate is present due to sodium ions facilitating gluconate transport into cells via secondary membrane transport proteins. An uptake of sodium ions may also influence cell expansion by altering turgor pressure, membrane potential and by interacting with peptidoglycan precursors.

A $P3HB^{++}$ *C. necator* population containing cells which produce up to 1000 times more P3HB than the dominant $P3HB^{+}$ is present in cultures as early as 4 hours into growth. As $P3HB^{++}$ cells are of low proportion before 72 hours, are generally smaller than the dominant $P3HB^{+}$ phenotype and appear to be produced during exponential growth, it's possible that $P3HB^{++}$ cells are a type of persister cell. The function of persister cells is to allow a bacterial community to survive if the main population is eradicated. This is a purpose which fits with P3HB production which is known to confer resistance to a variety of abiotic stress.

In order to try and reduce the lag in P3HB production the strengths of fructose and sodium gluconate supplementation were utilised in fed-batch cultures. Fructose supplementation was used to induce cell proliferation up to 24 hours (phase 1) when sodium gluconate was then added to try and induce P3HB production between 24 and 72 hours (phase 2). However, this strategy did not prevent the majority of P3HB production occurring after phase 2, in phase 3. Using the same fed-batch strategy with the addition of between 3 and 15 g\L sodium chloride also failed to reduce the delay. Repeated-fed-batch cultures, in which media was replaced at the end of phase 1 at 24 hours, also failed to reduce the lag-time. However, amino acid deamination occurred in some cultures, indicated by an elevated pH, suggesting that amino acids were being used by *C. necator* as a source of C. When fructose and sodium gluconate were supplemented together, an elevated pH was observed, but not when only fructose was supplemented. This suggested that gluconate represses the metabolism of fructose by catabolite repression a claim that was substantiated by evidence of diauxic growth occurring. Evidence in *Pseudomonas* species has found that a key protein governing C catabolite repression is able to bind to the mRNA of PhaC1. This raises the possibility that C catabolite repression in the current study could be the reason why a lag-time in P3HB production is observed.

Chapter 6 Future work

6.1 Scale-up experiments and different media supplementation

Studies presented in this thesis have only focused on laboratory-scale Erlenmeyer flask experiments. Future work could therefore involve scaling up experiments to fermentation vessels in which stirring speed, pH, dissolved oxygen and substrate addition can be more tightly monitored (Tikhomirova *et al.*, 2018). In particular, based on the findings presented in this study, control over pH is vital in order to offset increases due to ammonia release during periods of amino acid metabolism. Different C substrates such as sodium valerate could also be trailed as a means to produce copolymers such as P(3HB-co-3HV) (Rivera-Briso *et al.*, 2018). Different substrate addition strategies could also be employed in which substrates could be added gradually at a determined rate rather than added in single doses.

6.2 Biomass harvesting, P3HB separation, and P3HB characterisation

Biomass could be separated from growth media by centrifugation and washing and the separated biomass pre-treated using methods such as lyophilisation, thermal drying, freeze-thaw, or enzymatic treatment (Kourmentza *et al.*, 2017). To separate P3HB from biomass, solvent extraction using chloroform followed by polymer precipitation with methanol is the benchmark P3HB separation method. Although, safer more environmentally friendly extractions using solvents such as DMSO and ethanol for P3HB precipitation are available (Viscaino-caston *et al.*, 2016). To categorise the extracted and purified polymer a variety of methods could be used. In order to quantify extracted polymer and correlate with P-546 fluorescence, GCMS represents the gold standard (Karmann *et al.*, 2016). This is vital to establish if a linear trend exists between extracted P3HB and P-546 fluorescence when staining using the revised protocol in section 3.7. A calibration curve demonstrating the linear trend between extracted P3HB and P-546 fluorescence is important to allow units of P-546 fluorescence to be related to an amount of P3HB, a comparison which is missing in this study. To identify the type of PHA present in the extracted polymer NMR could be used (Hu *et al.*, 2011). To evaluate the T_m and T_g of the extracted polymer, thermal characterisation by DCS could be used (Chiu and Prenner, 2011).

6.3 Separation of P3HB^{++} cells and directed evolution

Based on the findings of Franz *et al*. (2011), and González-Villanueva *et al*. (2019), it's possible that the directed evolution of P3HB^{++} cells could produce C. necator cells able to produce superior amounts of P3HB more quickly. There are 3 main options that could be used to separate P3HB^{++} from P3HB^{+}

cells. The first is fluorescent-activated cell sorting (FACS) which utilises flow cytometry to isolate gated cell populations (Ambriz-Aviña *et al.*, 2014). The second option is to isolate agar plate colonies using a stain such as Sudan black to identify colonies rich in P3HB (Higuchi-Takeuchi *et al.*, 2016). A third option, based on the probability that the $P3HB^{++}$ population are persister cells, would be to eradicate $P3HB^{+}$ cells only using antibiotics. As persister cells are known to be more resistant to antibiotics than the dominant phenotype this may allow for efficient selection (Lewis, 2010). Research has shown that chloramphenicol, tetracycline and kanamycin are suitable for screening *C. necator* (Pan *et al.*, 2021).

6.4 Monitoring substrate usage

Future work should also monitor the concentration of fructose and gluconate in growth media. This would provide valuable information on substrate usage which would be particularly important to studying C catabolite repression occurring during experiments. Assay kits suitable for determining fructose (Megazyme Ltd, 2023a) and gluconate (Megazyme Ltd, 2023b) concentration are commercially available and would be suitable for future research.

Chapter 7 Bibliography

A. Rohs, P. D., Buss, J., Sim, S. I., Squyres, G. R., Srisuknimit, V., Smith, M., Cho, H., Sjodt, M., Kruse, A. C., Garner, E. C., Walker, S., Kahne, D. E., & Bernhardt, T. G. (2018). A central role for PBP2 in the activation of peptidoglycan polymerization by the bacterial cell elongation machinery. PLoS Genetics. 14(10). DOI: 10.1371/journal.pgen.1007726

Abdel-Mawgoud, A. M., Lépine, F. and Déziel, E., 2014. A Stereospecific Pathway Diverts β-Oxidation Intermediates to the Biosynthesis of Rhamnolipid Biosurfactants. Chemistry and Biology, 21(1), 156-164. DOI: 10.1016/j.chembiol.2013.11.010

Ahn, J., Jho, E. H. and Nam, K., 2015. Effect of C/N ratio on polyhydroxyalkanoates (PHA) accumulation by Cupriavidus necator and its implication on the use of rice straw hydrolysates. Environmental Engineering Research. 20(3). 246-253. DOI: 10.4491/eer.2015.055

Ahn, W. S., Park, S. I. and Lee, S. Y. 2000. Production of Poly(3-Hydroxybutyrate) by Fed-Batch Culture of Recombinant *Escherichia coli* with a Highly Concentrated Whey Solution. Appl. Environ. Microbiol. 66(8). 3624-3627. DOI: 10.1128/aem.66.8.3624-3627.2000

Al-Kaddo, K. B., Mohamad, F., Murugan, P., Shun, T. J., Sudesh, K., Samian, M. R. 2020. Production of P(3HB-co-4HB) copolymer with high 4HB molar fraction by T Burkholderia contaminans Kad1 PHA synthase. Biochemical Engineering Journal. 153(107394). DOI: 10.1016/j.bej.2019.107394.

Al-Salem, S. M., Lettieri, P. and Baeyens, J., 2009. Recycling and recovery routes of plastic solid waste (PSW): A review. Waste Management. 29. 2625-2643. 10.1016/j.wasman.2009.06.004

Aldor, I. A. and Keasling, J. D., 2003. Process design for microbial plastic factories: metabolic engineering of polyhydroxyalkanoates. Curr. Opin. Biotechnol. 14(5). 475-483. DOI: 10.1016/j.copbio.2003.09.002

Alias, Z. and Tan, I. K. P., 2005. Isolation of palm oil-utilising, polyhydroxyalkanoate (PHA)-producing bacteria by an enrichment technique. Bioresource Technology. 96. 1229-1234. DOI: 10.1016/j.biortech.2004.10.012

Alves, L. P. S. Almeida, A.T., Cruz, L. M., Pedrosa, F.O., de Souza, E. M., Chubatsu, L.S., Müller-Santos, M., Valdameri, G. 2017. A simple and efficient method for poly-3-hydroxybutyrate quantification in diazotrophic bacteria within 5 minutes using flow cytometry. Brazilian Journal of Medical and Biological Research. 50(1). 1414-1431. DOI: 10.1590/1414-431X20165492

Ambriz-Aviña, V., Contreras-Garduño, J. A., and Pedraza-Reyes, M. (2014). Applications of Flow Cytometry to Characterize Bacterial Physiological Responses. BioMed. Research International. 2014. DOI: 10.1155/2014/461941

Ampe, F., Léonard, D. and Lindley, N. D., 1998. Repression of Phenol Catabolism by Organic Acids in Ralstonia eutropha. Appl Environ Microbiol, 64(1), 1-6. DOI: 10.1128/aem.64.1.1-6.1998

Anjum, A., Zuber, M., Zia, K. M., Noreen, A., Anjum, M. N., Tabasum. S. 2016. Microbial production of polyhydroxyalkanoates (PHAs) and its copolymers: A review of recent advancements. International Journal of Biological Macromolecules, 89, 161-174. DOI: 89. 10.1016/j.ijbiomac.2016.04.069.

Aramvash, A., Shahabi, Z. A., Aghjeh, S. D. and Ghafari, M. D., 2015. Statistical physical and nutrient optimization of bioplastic polyhydroxybutyrate production by *Cupriavidus necator*. Int. J. Environ. Sci. Technol. 12. 2307-2316. DOI: 10.1007/s13762-015-0768-3

Aramvash, A., Zavareh, F. M. and Banadkuki, N. G., 2018. Comparison of different solvents for extraction of polyhydroxybutyrate from *Cupriavidus necator*. Eng Life Sci. 18(1). DOI: 10.1002/elsc.201700102

Arber, W., 2000. Genetic variation: molecular mechanisms and impact on microbial evolution. FEMS Microbiology Reviews. 24(1). 1-7. DOI: 10.1111/j.1574-6976.2000.tb00529.x

Arikawa, H., Sato, S., Fujiki, T. and Matsumoto, K. 2017. Simple and rapid method for isolation and quantitation of polyhydroxyalkanoate by SDS-sonication treatment. J. Biosci. Bioeng. 124(2). 250-254.

Arrigucci, R. and Pozzi, G. 2017. Identification of the chain-dispersing peptidoglycan hydrolase LytB of Streptococcus gordonii. PLoS One. 12(4). e0176117. DOI: 10.1371/journal.pone.0176117.

Arutchelvi, J., Muniyasamy, S., Arkatwar, A. S., Doble, M., Bhaduri, S., Uppara, P. V. 2008. Biodegradation of polyethylene and polypropylene. Indian Journal of Biotechnology. 7. 9-22. DOI: 10.1016/j.polymdegradstab.2021.109662

Aurrekoetxea, J., Sarrionandia, M. A. and Urrutibeascoa, I. 2001. Effects of recycling on the microstructure and the mechanical properties of isotactic polypropylene. Journal of Materials Science. 36. 2607-2613. DOI: 10.1023/A:1017983907260

Azubuike, C. C., Edwards, M. G., Gatehouse, A. M. R. and Howard, T. P., 2020. Applying Statistical Design of Experiments To Understanding the Effect of Growth Medium Components on *Cupriavidus necator* H16 Growth. Appl. Environ. Microbiol. 86(17). DOI: 10.1128/AEM.00705-20

Babic, A., Berkmen, M. B., Lee, C. A. and Grossman, A. D., 2011. Efficient Gene Transfer in Bacterial Cell Chains. mBio. 2(2). DOI: 10.1128/mBio.00027-11

Babos, G. Rydz, J., Kawalec, M., Klim, M., Fodor-Kardos. A., Trif, L., Feczkó, T. 2020. Poly(3-Hydroxybutyrate)-Based Nanoparticles for Sorafenib and Doxorubicin Anticancer Drug Delivery. Int J Mol Sci., 21(19). 7312. DOI: 10.3390/ijms21197312.

Baekeland, L. H., 1909. The synthesis, constitution and uses of Bakelite. The Journal of Industrial and Engineering Chemistry. 1(3). 149-161. DOI: 10.1021/ie50003a004

Balaban, N. Q., Merrin, J., Chait, R., Kowalik, L., Leibler, S. 2004. Bacterial persistence as a phenotypic switch. Science. 305(5690). 1622-1625. DOI: 10.1126/science.1099390

Ball, P. 2002. Catalyst gets cracking. Nature. 106. DOI: 10.1038/news020729-5

Basak, N., and Meena, S. S. (2022). Microbial biodegradation of plastics: Challenges, opportunities, and a critical perspective. Frontiers of Environmental Science & Engineering. 16:12. DOI: 10.1007/s11783-022-1596-6

Bassas Galià, M., 2010. Isolation and Analysis of Storage Compounds. In: Timmis K.N. (eds) Handbook of Hydrocarbon and Lipid Microbiology. Berlin. Springer. Berlin. Heidelberg. DOI: 10.1007/978-3-540-77587-4_292

Bátori, V., Åkesson, D., Zamani, A., Taherzadeh, M. J., & Sárvári Horváth, I. (2018). Anaerobic degradation of bioplastics: A review. Waste Management. 80. 406-413. DOI: 10.1016/j.wasman.2018.09.040

Benarroch, J. M., and Asally, M. (2020). The Microbiologist's Guide to Membrane Potential Dynamics. Trends in Microbiology. 28(4). 304-314. DOI: 10.1016/j.tim.2019.12.008

Bhatia, S. K. Kim, J. H., Kim, M. S., Kim, J., Hong, J. W., Hong, Y. G., Kim, H. J., Jeon, J. M., Kim, S. H., Ahn, J., Lee, H., Yang, Y. H. 2018. Production of (3-hydroxybutyrate-co-3-hydroxyhexanoate) copolymer from coffee waste oil using engineered *Ralstonia eutropha*. Bioprocess Biosyst Eng. 41. 229-235. DOI: 10.1007/s00449-017-1861-4

Bhuwal, A. K. Singh, G., Aggarwal, N. K., Goyal, V., Yadav, A. 2013. Isolation and Screening of Polyhydroxyalkanoates Producing Bacteria from Pulp, Paper, and Cardboard Industry Wastes. International Journal of Biomaterials, 2013. 752821. DOI: 10.1155/2013/752821

Biddlestone, F., Harris, A., Hay, N. and Hammond, T., 1996. The physical ageing of amorphous poly(hydroxybutyrate). Polymer International. 39(3). 221-229. DOI: 10.1002/(SICI)1097-0126(199603)39:3<221::AID-PI511>3.0.CO;2-O

Bio-Cat. 2021. Production Animal Enzyme Solutions. Available at: https://www.bio-cat.com/products-markets/enzymes/animal-nutrition-2/animal-nutrition/

Björklund, M., and Marguerat, S. (2017). Editorial: Determinants of Cell Size. Frontiers in Cell and Developmental Biology. 5. DOI: 10.3389/fcell.2017.00115

Blount, Z. D. 2015. The unexhausted potential of *E. coli*. eLife, 4. e05826. DOI: 10.7554/eLife.05826

Boey, J. Y. Mohamad, L., Khok, Y. S., Tay, G. S., Baidurah, S. 2021. A Review of the Applications and Biodegradation of Polyhydroxyalkanoates and Poly(lactic acid) and Its Composites. Polymers (Basel). 13(10). 1544. DOI: 10.3390/polym13101544.

Bonartsev, A. P. Bonartseva, G. A., Reshetov, I. V., Kirpichnikov, M. P., Shaitan, K. V. 2019. Application of Polyhydroxyalkanoates in Medicine and the Biological Activity of Natural Poly(3-Hydroxybutyrate). ACTA NATURAE. 11(2). 4-16. DOI: 0.32607/20758251-2019-11-2-4-16.

Bonnet, M., Lagier, J. C., Raoult, D. and Khelaifia, S. 2020. Bacterial culture through selective and non-selective conditions: the evolution of culture media in clinical microbiology. New Microbes New Infect. 34(100622). DOI: 10.1016/j.nmni.2019.100622.

Brandl, H., Gross, R. A., Lenz, R. W. and Fuller, R. C. 1988. *Pseudomonas oleovorans* as a Source of Poly(β-Hydroxyalkanoates) for Potential Applications as Biodegradable Polyesters. APPLIED AND ENVIRONMENTAL MICROBIOLOGY. 54(8). 1977-1982. DOI: 10.1128/aem.54.8.1977-1982.1988.

Braskem, 2018. Linear Low Density Polyethylene SLL118. Available at: https://www.braskem.com.br/europe/product-search?p=247 (Accessed April 2021).

Bresnan, S. Sznajder, A., Hauf, W., Forchhammer, K., Pfeiffer, D., Jendrossek, D. 2016. Polyhydroxyalkanoate (PHA) Granules Have no Phospholipids. Scientific Reports, 6(26612). DOI: 10.1038/srep26612

Bresan, S. and Jendrossek, D., 2017. New Insights into PhaM-PhaC-Mediated Localization of Polyhydroxybutyrate Granules in Ralstonia eutropha H16. Appl. Environ. Microbiol. 83(12). e00505-17. DOI: 10.1128/AEM.00505-17.

Brigham, C. J. and Sinskey, A. J., 2012. Applications of Polyhydroxyalkanoates in the Medical Industry. International Journal of Biotechnology for Wellness Industries. 1. 53-60. DOI: 10.6000/1927-3037.2012.01.01.03

Brown, A. P., Kroon, J. T., Topping, J. F., Robson, J. L., Simon, W. J. , Slabas, A. R. 2011. Components of complex lipid biosynthetic pathways in developing castor (*Ricinus communis*) seeds identified by MudPIT analysis of enriched endoplasmic reticulum. J. Proteome Res. 10(8). 3565-77. DOI: 10.1021/pr2002066

Brown, D. R. (2019). Nitrogen Starvation Induces Persister Cell Formation in Escherichia coli. Journal of Bacteriology, 201(3). DOI: 10.1128/JB.00622-18

Brown, B., Immethun, C. and Saha, R. 2020. *Rhodopseudomonas palustris* CGA009 polyhydroxybutyrate production from a lignin aromatic and quantification via flow cytometry. Bioresource Technology Reports. 11(100474). DOI: 10.1016/j.biteb.2020.100474

Bryant, J., Chewapreecha, C. and Bentley, S. D., 2012. Developing insights into the mechanisms of evolution of bacterial pathogens from whole-genome sequences. Future Microbiology, 7(11), 1283-1296. DOI: 10.2217/fmb.12.108

Bucci, D. Z., Tavares, L. T. and Sell, I., 2005. PHB packaging for the storage of food products. Polymer Testing. 24(5). 564-571. DOI: 10.1016/j.polymertesting.2005.02.008

Bucci, D. Z., Tavares, L. B. B. and Sell, I., 2007. Biodegradation and physical evaluation of PHB packaging. Polymer Testing. 26(7). 908-915. DOI: 10.1016/j.polymertesting.2007.06.013

Budde, C. F. Mahan, A. E., Lu, J., Rha, C., Sinskey, A. J. 2010. Roles of Multiple Acetoacetyl Coenzyme A Reductases in Polyhydroxybutyrate Biosynthesis in *Ralstonia eutropha* H16. J. Bacteriol. 192(20). 5319-5328. DOI: 10.1128/JB.00207-10

Budde, C. F. Riedel, S. L., Hübner, F., Risch, S., Popović, M. K., Rha, C., Sinskey, A. J., 2011. Growth and polyhydroxybutyrate production by Ralstonia eutropha in emulsified plant oil medium. Appl. Microbiol. Biotechnol. 89(5). 1611-1619. DOI: 10.1007/s00253-011-3102-0.

Bugnicourt, E., Cinelli, P., Lazzeri, A. and Alvarez, V., 2014. Polyhydroxyalkanoate (PHA): Review of synthesis, characteristics, processing and potential applications in packaging. eXPRESS Polymer Letters, 8(11), 791-808. DOI: 10.3144/expresspolymlett.2014.82

Cánovas, V. Garcia-Chumillas, S., Monzó, F., Simó-Cabrera, L., Fernández-Ayuso, C., Pire, C., Martínez-Espinosa, R. M. 2021. Analysis of Polyhydroxyalkanoates Granules in *Haloferax mediterranei* by Double-Fluorescence Staining with Nile Red and SYBR Green by Confocal Fluorescence Microscopy. Polymers. 13(10). 1528. DOI: 10.3390/polym13101582.

Castro, L. M. Foong, C. P., Higuchi-Takeuchi, Morisaki, K., Lopes, E. F., Numata, K., Mota, A. J. 2021. Microbial prospection of an Amazonian blackwater lake and whole-genome sequencing of bacteria capable of polyhydroxyalkanoate synthesis. Polymer Journal. 53. 191-202. DOI: 10.1038/s41428-020-00424-4.

Cavalheiro, J. M. B. T. Raposo, R. S., de Almeida M. C., Cesário, M. T., Sevrin C, Grandfils, C, da Fonseca, M. M., 2012. Effect of cultivation parameters on the production of poly(3-hydroxybutyrate-co-4-hydroxybutyrate) and poly(3-hydroxybutyrate-4-hydroxybutyrate-3-hydroxyvalerate) by *Cupriavidus necator* using waste glycerol. Bioresource Technology. 111. 391-397. DOI: 10.1016/j.biortech.2012.01.176

Chan, B. P. and Leong, K. W., 2008. Scaffolding in tissue engineering: general approaches and tissue-specific considerations. Eropean Spine Journal. 17(4). 467-479. DOI: 10.1007/s00586-008-0745-3

Chen, T., Cai, T., Jin, Q. and Ji, J., 2015. Design and fabrication of functional polycaprolactone. e-Polymers, 15(1), 3-13. DOI: 10.1016/j.envint.2019.104938.

Chen, Q., Allgeier, A., Yin, D. and Hollert, H., 2019. Leaching of endocrine disrupting chemicals from marine microplastics and mesoplastics under common life stress conditions. Environmental International. 130. 104938. DOI: 10.1016/j.envint.2019.104938

Chen, X., Chen, G., Wang, G. Zhu, P., Gao, C. 2020. Recent Progress on 3D-Printed Polylactic Acid and Its Applications in Bone Repair. Advanced Engineering Materials, 22(4). DOI: 10.1002/adem.201901065

Chernozem, R.V., Guselnikova, O., Surmeneva, M.A., Postnikov, P.S., Abalymov, A.A. Parakhonskiy, B.V., De Roo, N., Depla, D. Skirtach, A.G., Surmenev, R.A. 2020. Diazonium chemistry surface treatment of piezoelectric polyhydroxybutyrate scaffolds for enhanced osteoblastic cell growth. Applied Materials Today. 20(100758). DOI: 10.1016/j.apmt.2020.100758

Chiu, M. H. and Prenner, E. J., 2011. Differential scanning calorimetry: An invaluable tool for a detailed thermodynamic characterization of macromolecules and their interactions. J. Pharm. Bioallied. Sci. 3(1). 39-59. DOI: 10.4103/0975-7406.76463

Choi, P. J., Cai, L., Frieda, K. and Xie, X. S., 2008. A stochastic single-molecule event triggers phenotype switching of a bacterial cell. Science. 322(5900). 442-226. DOI: 10.1126/science.1161427

Chu, D., and Barnes, D. J. (2016). The lag-phase during diauxic growth is a trade-off between fast adaptation and high growth rate. Scientific Reports. 6. DOI: 10.1038/srep25191

Claudio, L., 2012. Our Food: Packaging and Public Health. Environ Health Perspect., 120(6), a232-a237. DOI: 10.1289/ehp.120-a232.

Cooper, M. S., Hardin, W. R., Petersen, T. W., and Cattolico, R. A. (2010). Visualizing "green oil" in live algal cells. Journal of Bioscience and Bioengineering. 109(2). 198-201. DOI: 10.1016/j.jbiosc.2009.08.004

Cossarizza, A., Chang, H. D., Radbruch, A., Akdis, M., Andrä, I., Annunziato, F., Bacher, P., Barnaba, V., Battistini, L., Bauer, W. M., Baumgart, S., Becher, B., Beisker, W., Berek, C., Blanco, A., Borsellino, G., Boulais, P. E., Brinkman, R. R., Büscher, M., Busch, D. H., Zimmermann, J. (2017). Guidelines for the use of flow cytometry and cell sorting in immunological studies. European journal of immunology. 47(10). 1584–1797. DOI: 10.1002/eji.201646632

Cózar, A., Martí, E, Duarte C., M, García-de-Lomas, J., van Sebille, E, Ballatore, T. J., Eguíluz, V. M., González-Gordillo, J. I., Pedrotti, M. L., Echevarría, F., Troublè, R., Irigoien, X. 2017. The Arctic Ocean as a dead end for floating plastics in the North Atlantic branch of the Thermohaline Circulation. Sci Adv, 3(4). e1600582. DOI: 10.1126/sciadv.1600582.

Dagnon, K. L., Thellen, C., Ratto, J. A. and D'Souza, N. A., 2010. Physical and Thermal Analysis of the Degradation of Poly(3-Hydroxybutyrate-co-4-Hydroxybutyrate) Coated Paper in a Constructed Soil Medium. Journal of Polymers and the Environment, 18, 510-522. 10.1007/s10924-010-0231-y

Dai, X. and Zhu, M., 2018. High Osmolarity Modulates Bacterial Cell Size through Reducing Initiation Volume in Escherichia coli. mSphere, 3(5). e00430-18. DOI: 10.1128/mSphere.00430-18.

Danimer Scientific, 2021. Danimer Scientific and Eagle Beverage to Produce Biodegradable Drinking Straws. Available at: https://danimerscientific.com/2020/11/17/danimer-scientific-and-eagle-beverage-to-produce-biodegradable-drinking-straws/ (Accessed 20/1/2023).

de Boer, P. A., Crossley, R. E. and Rothfield, L. I. 1989. A division inhibitor and a topological specificity factor coded for by the minicell locus determine proper placement of the division septum in *E. coli*. Cell, 56(4), 646-649. DOI: 10.1016/0092-8674(89)90586-2

de Eugenio, L. I. Galán, B., Escapa, I. F., Maestro, B., Sanz, J. M., García, J. L., Prieto, M. A. 2010. The PhaD regulator controls the simultaneous expression of the pha genes involved in polyhydroxyalkanoate metabolism and turnover in *Pseudomonas putida* KT2442. Environmental Microbiology. 12(6). 1591-1603. DOI: 10.1111/j.1462-2920.2010.02199.x.

de Jong, I. G., Haccou, P. and Kuipers, O. P., 2011. Bet hedging or not? A guide to proper classification of microbial survival strategies. Bioessays. 33(3) 215-223. DOI: 10.1002/bies.201000127

Deanin, R. D. and Bai, Z. Z., 1984. Polycaprolactone as a permanent plasticizer for poly(vinyl chloride). Journal of Vinyl Technology. 48(799). DOI: 10.1002/vnl.730060107

Dennis, D., McCoy, M., Stangl, A., Valentin, H. E., Wu, Z. 1998. Formation of poly(3-hydroxybutyrate-co-3-hydroxyhexanoate) by PHA synthase from *Ralstonia eutropha*. Journal of Biotechnology. 64(2-3). 177-186. DOI: doi: 10.1016/s0168-1656(98)00110-2

Deutscher, J. 2008. The mechanisms of carbon catabolite repression in bacteria. Curr. Opin. Microbiol. 11(2), 87-93. DOI: 10.1016/j.mib.2008.02.007

Dey, P. and Rangarajan, V. 2017. Improved fed-batch production of high-purity PHB (poly-3 hydroxybutyrate) by *Cupriavidus necator* (MTCC 1472) from sucrose-based cheap substrates under response surface-optimized conditions. 3 Biotech. 7(5). 310. DOI: 10.1007/s13205-017-0948-6

Di Lorenzo, M. L., Longo, A. and Androsch, R. 2019. Polyamide 11/Poly(butylene succinate) Bio-Based Polymer Blends. Materials. 12(17). 2833. DOI: 10.3390/ma12172833

Dimroth P. Mechanisms of sodium transport in bacteria. 1990. Philos. Trans. R. Soc. Lond. B. Biol. Sci. 326. 1236. 465-77. DOI: 10.1098/rstb.1990.0025

Divyashree, M. S., Shamala, T. R. and Rastogi, N. K. 2009. Isolation of polyhydroxyalkanoate from hydrolyzed cells of Bacillus flexus using aqueous two-phase system containing polyethylene glycol and phosphate. Biotechnology and Bioprocess Engineering. 14(4). 482-489. DOI: 10.1007/s12257-008-0119-z

Dong, Z. and Sun, X., 2000. A new method of recovering polyhydroxyalkanoate from *Azotobacter chroococcum*. Chinese Science Bulletin. 45. 252-256. DOI: 10.1007/BF02884685

Doyle, C., Tanner, E. T. and Bonfield, W., 1991. In vitro and in vivo evaluation of polyhydroxybutyrate and of polyhydroxybutyrate reinforced with hydroxyapatite. Biomaterials. 12(9). 841-847. DOI: 10.1016/0142-9612(91)90072-i

Drzyzga, O. and Prieto, A. 2019. Plastic waste management, a matter for the 'community'. Microb. Biotechnol. 12(1). 66-68. DOI: 10.1111/1751-7915.13328

DSMZ. 2007. Nutrient Agar. Available at: https://www.dsmz.de/microorganisms/medium/pdf/DSMZ_Medium1.pdf (Accessed 2 November 2022).

Du, G. and Yu, J., 2002. Green Technology for Conversion of Food Scraps to Biodegradable Thermoplastic Polyhydroxyalkanoates. Environ. Sci. Technol. 36(24). 5511-5516. DOI: 10.1021/es011110o

Du, S. and Lutkenhaus, J., 2019. At the heart of bacterial cytokinesis: the Z ring. Trends Microbiol. 27(9). 781-791. DOI: 10.1016/j.tim.2019.04.011

Dutt, K. and Soni, R. K., 2013. A review on synthesis of value added products from polyethylene terephthalate (PET) waste. Polymer Science Series B. 55(7-8). 430-452. DOI: 10.1134/S1560090413070075

Egan, A. J. F., Cleverley R. M., Peters, K., Lewis, R. J., Vollmer W. 2017. Regulation of bacterial cell wall growth. FEBS Journal. 284(6). 851-867. DOI: 10.1111/febs.13959

Eggers, J., and Steinbüchel, A. (2013). Poly(3-Hydroxybutyrate) Degradation in *Ralstonia eutropha* H16 Is Mediated Stereoselectively to (S)-3-Hydroxybutyryl Coenzyme A (CoA) via Crotonyl-CoA. Journal of Bacteriology. 195(14). 3213-3223. DOI: 10.1128/JB.00358-13

El-Hadi, A., Schnabel, R., Straube, E., Müller, G., and Henning, S. (2002). Correlation between degree of crystallinity, morphology, glass temperature, mechanical properties and biodegradation of poly (3-hydroxyalkanoate) PHAs and their blends. Polymer Testing. 21(6). 665-674. DOI: 10.1016/S0142-9418(01)00142-8

Evans, K., Stone, V., Chen, L., Ge, X., and Xu, P. (2014). Systematic study of genes influencing cellular chain length in Streptococcus sanguinis. Microbiology, 160(2),. 307-315. DOI: 10.1099/mic.0.071688-0

Fabra, M. J., Lopez-Rubio, A. and Lagaron, J. M. 2013. High barrier polyhydroxyalcanoate food packaging film by means of nanostructured electrospun interlayers of zein. Food Hydrocolloids. 32(1). 106-114. DOI: 10.1016/j.foodhyd.2012.12.007

Favaro, L. Basaglia, M., Rodriguez, J. E. G., Morelli, A., Ibraheem, O., Pizzocchero, V., and Casella, S. 2019. Bacterial Production of PHAs from Lipid-Rich by-Products. APPLIED FOOD BIOTECHNOLOGY. 6(1). 45-52. DOI: 10.22037/afb.v6i1.22246

Fernández-Castané, A., Li, H., Thomas, O. R. T. and Overton, T. W., 2018. Development of a simple intensified fermentation strategy for growth of *Magnetospirillum gryphiswaldense* MSR-1: Physiological responses to changing environmental conditions. New Biotechnology. 46. 22-30. DOI: 10.1016/j.nbt.2018.05.1201

Fiorese, M. L., Freitas, F., Pais, J., Ramos, A. M., de Aragão, G. M. F. and Reis, M. A. M., 2009. Recovery of polyhydroxybutyrate (PHB) from *Cupriavidus necator* biomass by solvent extraction with 1,2-propylene carbonate. Eng. Life Sci. 9(6). 454-461. DOI: 10.1002/elsc.200900034

Fleige, C., Kroll, J. and Steinbüchel, A., 2011. Establishment of an alternative phosphoketolase-dependent pathway for fructose catabolism in *Ralstonia eutropha* H16. Applied Microbial and Cell Physiology. 91. 769-776. DOI: 10.1007/s00253-011-3284-5

Franz, A., Rehner, R., Kienle, A., & Grammel, H. (2012). Rapid selection of glucose-utilizing variants of the polyhydroxyalkanoate producer *Ralstonia eutropha* H16 by incubation with high substrate levels. Letters in applied microbiology. 54(1). 45–51. DOI: 10.1111/j.1472-765X.2011.03171.x

Fukui, T. and Doi, Y., 1997. Cloning and Analysis of the Poly(3-Hydroxybutyrate-co-3-Hydroxyhexanoate) Biosynthesis Genes of Aeromonas caviae. JOURNAL OF BACTERIOLOGY. 179(15). 4821-4830. DOI: 10.1128/jb.179.15.4821-4830.1997

Fukui, T., Shiomi, N. and Doi, Y., 1998. Expression and Characterization of (R)-Specific Enoyl Coenzyme A Hydratase Involved in Polyhydroxyalkanoate Biosynthesis by *Aeromonas caviae*. Journal of Bacteriology. 180(3). 667-673. DOI: 10.1128/jb.180.3.667-673.1998

Fukui, T., Ohsawa, K., Mifune, J., Orita, I., Nakamura, S. 2011. Evaluation of promoters for gene expression in polyhydroxyalkanoate-producing *Cupriavidus necator* H16. Appl. Microbiol. Biotechnol. 89(5):1527-36. DOI: 10.1007/s00253-011-3100-2

Fukui, T., Mukoyama, M., Orita, I., Nakamura, S. 2014. Enhancement of glycerol utilization ability of *Ralstonia eutropha* H16 for production of polyhydroxyalkanoates. Applied microbiology and biotechnology. 98. DOI: 10.1007/s00253-014-5831-3.

Furrer, P., Hany, R., Rentsch, D., Grubelnik, A., Ruth, K., Panke, S., Zinn, M. 2007. Quantitative analysis of bacterial medium-chain-length poly([R]-3-hydroxyalkanoates) by gas chromatography. J. Chromatogr. A. 1143(1-2). 199-206. DOI: 10.1016/j.chroma.2007.01.002

Gahlawat, G. and Soni, S. K. 2017. Valorization of waste glycerol for the production of poly (3-hydroxybutyrate) and poly (3-hydroxybutyrate-co-3-hydroxyvalerate) copolymer by Cupriavidus necator and extraction in a sustainable manner. Bioresource Technology. 243. 492-501.

Gan, Z. and Zhang, H. 2019. PMBD: a Comprehensive Plastics Microbial Biodegradation Database. Database. 1(11). baz119. DOI: 10.1093/database/baz119

Garg, R. P., Yindeeyoungyeon, W., Gilis, A., Denny, T. P., Van Der Lelie, D., Schell, M. A. 2000. Evidence that *Ralstonia eutropha* (Alcaligenes eutrophus) contains a functional homologue of the *Ralstonia solanacearum* Phc cell density sensing system. Molecular Microbiology. 38(2). 359-367. 10.1046/j.1365-2958.2000.02131.x

Gazzotti, S., Felice, B. D., Ortenzi, M. A., and Parolini, M. (2022). Approaches for Management and Valorization of Non-Homogeneous, Non-Recyclable Plastic Waste. International Journal of Environmental Research and Public Health. 19(16). DOI: 10.3390/ijerph191610088

Germanov, E. S. Marshall, A. D., Bejder, L., Fossi, M. C., Loneragan, N. R. 2018. Microplastics: No Small Problem for Filter-Feeding Megafauna. Trends in Ecology and Evolution. 33(4). 227-232. DOI: 10.1016/j.tree.2018.01.005

Goh, Y. S. and Tan, I. K. P. 2021. Polyhydroxyalkanoate production by antarctic soil bacteria isolated from CaseyStation and Signy Island. Microbiological Research. 167. 211-219. DOI: 10.1016/j.micres.2011.08.002

González-Villanueva, M. Galaiya, H., Staniland, P., Staniland, J., Savill, I., Wong, T. S., Tee, K. L. 2019. Adaptive Laboratory Evolution of Cupriavidus necator H16 for Carbon Co-Utilization with Glycerol. International Journal of Molecular Science, 20(22). 5737. DOI: 10.3390/ijms20225737

GOV.UK. 2023. Regulations: Waste Electrical and Electronic Equipment (WEEE). Available at: https://www.gov.uk/guidance/regulations-waste-electrical-and-electronic-equipment#contact-us. (Accessed 28/2/2023)

Green, P. R., Kemper, J., Schechtman, L., Guo, L., Satkowski, M., Fiedler, S., Steinbüchel, A., Rehm, B. H. 2002. Formation of Short Chain Length/Medium Chain Length Polyhydroxyalkanoate Copolymers by Fatty Acid beta-Oxidation Inhibited *Ralstonia eutropha*. Biomacromolecules. 3. 208-213. DOI: 10.1021/bm015620m

Griebel, R., Smith, Z. and Merrick, J. M. 1968. Metabolism of poly(β-hydroxybutyrate). I. Purification, composition, and properties of native poly(β-hydroxybutyrate) granules from *Bacillus megaterium*. Biochemistry. 7(10). 3676-3681. DOI: 10.1021/bi00850a047

Grillo, R. Pereira, Ado E, de Melo, N. F., Porto, R. M., Feitosa, L. O., Tonello, P. S., Dias Filho, N. L., Rosa, A. H., Lima, R., Fraceto L. F. 2011. Controlled release system for ametryn using polymer microspheres: Preparation, characterization and release kinetics in water. Journal of Hazardous Materials. 186(2-3). 1645-1651. DOI: 10.1016/j.jhazmat.2010.12.044

Grousseau, E. Blanchet, E., Déléris, S., Albuquerque, M. G., Paul, E., and Uribelarrea, J. 2014. Phosphorus limitation strategy to increase propionic acid flux towards 3-hydroxyvaleric acid monomers in *Cupriavidus necator*. Bioresource Technology. 153. 206-215. DOI: 10.1016/j.biortech.2013.11.072

Gu, L. and Ozbakkaloglu, T. 2016. Use of recycled plastics in concrete: A critical review. Waste Manag. 51. 19-42. DOI: 10.1016/j.wasman.2016.03.005

Guerranti, C. Martellini, T., Perra, G., Scopetani, C., and Cincinelli, A. 2019. Microplastics in cosmetics: Environmental issues and needs for global bans. Environ. Toxicol. Pharmacol. 68. 75-79. DOI: 10.1016/j.etap.2019.03.007

Gupta, B., Revagade, N. and Hilborn, J., 2007. Poly(lactic acid) fiber: An overview. Prog. Polym.32. 455-482. DOI: 10.1016/j.progpolymsci.2007.01.005

Gurselt, I., Yagmurlu, F., Korkusuz, F. and Hasirci, V., 2002. In vitro antibiotic release from poly(3-hydroxybutyrate-co-3-hydroxyvalerate) rods. J. Microencapsul. 19(2). 153-164. DOI: 10.1080/02652040110065413. PMID: 11837970.

Gutierrez, M. Choi, M. H., Tian, B., Xu, J., Rho, J. K., Kim, M. O., Cho, Y. H., Yoon, S. C. 2013. Simultaneous Inhibition of Rhamnolipid and Polyhydroxyalkanoic Acid Synthesis and Biofilm Formation in Pseudomonas aeruginosa by 2-Bromoalkanoic Acids: Effect of Inhibitor Alkyl-Chain-Length. PLOS ONE, 8(9). DOI: 10.1371/journal.pone.0073986

Gutt, B., Kehl, K., Ren, Q. and Boesel, L. F. 2016. Using ANOVA Models To Compare and Optimize Extraction Protocols of P3HBHV from *Cupriavidus necator*. Ind. Eng. Chem. Res., 55(39), 10355-10365. DOI: 10.1021/acs.iecr.6b02694

Hampson, J. W. and Ashby, R. D. 1999. Extraction of Lipid-Grown Bacterial Cells by Supercritical Fluid and Organic Solvent to Obtain Pure Medium Chain-Length Polyhydroxyalkanoates. JAOCS. 76(11). 1371-1374. DOI: 10.1007/s11746-999-0152-x

Han, J., Shi, J., Xie, Z., Xu, J., and Guo, B. (2019). Synthesis, Properties of Biodegradable Poly(Butylene Succinate-co-Butylene 2-Methylsuccinate) and Application for Sustainable Release. Materials. 12(9). DOI: 10.3390/ma12091507

Harris, L. K., and Theriot, J. A. (2018). Surface Area to Volume Ratio: A Natural Variable for Bacterial Morphogenesis. Trends in microbiology. 26(10). 815. DOI: 10.1016/j.tim.2018.04.008

Hastings, G., Ohta, H., Niwa, S., and Boeree, N. 1992. Development of a degradable composite for orthopaedic use: in viva biomechanical and histological evaluation of two bioactive degradable composites based on the polyhydroxybutyrate polymer. Biomaterials, 13(8). 491-496. DOI: 0142-9612(92)90099-A

Havens, K. J., Bilkovic, D. M., Stanhope, D. M. and Angstadt, K. T., 2014. Fishing gear with degradable component. United States of America, Patent No. US8938908B2.

Heinrich, D. Madkour, M. H., Al-Ghamdi, M. A., Shabbaj, I. I., Steinbüchel, A. 2012. Large scale extraction of poly(3-hydroxybutyrate) from *Ralstonia eutropha* H16 using sodium hypochlorite. AMB Express. 2(59). DOI: 10.1186/2191-0855-2-59

Hejazi, P., Vashegani-Ferahani, E. and Yamini, Y., 2003. Supercritical fluid disruption of *Ralstonia eutropha* for poly(beta-hydroxybutyrate) recovery. Biotechnology Progress. 19(5). 1519-1523. DOI: 10.1021/bp034010q

Henriquez, T., Wirtz, L., Su, D., and Jung, H. (2021). Prokaryotic Solute/Sodium Symporters: Versatile Functions and Mechanisms of a Transporter Family †. International Journal of Molecular Sciences. 22(4). DOI: 10.3390/ijms22041880

Hermawan, S. and Jendrossek, D., 2007. Microscopical investigation of poly(3-hydroxybutyrate) granule formation in Azotobacter vinelandii. FEMS Microbiology Letters. 266(1). 60-64. DOI: 10.1111/j.1574-6968.2006.00506.x

Higuchi-Takeuchi, Mieko & Morisaki, Kumiko & Numata, Keiji. (2016). A Screening Method for the Isolation of Polyhydroxyalkanoate-Producing Purple Non-sulfur Photosynthetic Bacteria from Natural Seawater. Frontiers in Microbiology. 7. DOI: 10.3389/fmicb.2016.01509.

Hill, N. S., Buske, P. J. and Levin, P. A., 2013. A Moonlighting Enzyme Links *Escherichia coli* Cell Size with Central Metabolism. PLoS Genet. 9(7). 10.1371/journal.pgen.1003663

Hillenbrand, P., Maier, K., Cramer, P. and Gerland, U., 2016. Inference of gene regulation functions from dynamic transcriptome data. eLife. 5. e12188. DOI: 10.7554/eLife.12188

Hitchen, S. M. and Dean, J. R. 1993. Properties of supercritical fluids: Applications of Supercritical Fluids in Industrial Analysis. In: Dean, J.R. (eds) Applications of Supercritical Fluids in Industrial Analysis. Springer. Dordrecht. DOI: 10.1007/978-94-011-2146-0_1

Hogema, B. M. Arents, J. C., Inada, T., Aiba, H., van Dam, K., Postma, P. W. 1997. Catabolite repression by glucose 6-phosphate, gluconate and lactose in Escherichia coli. Mol Microbiol . 24(4). 857-867. DOI: 10.1046/j.1365-2958.1997.3991761.x

Hongsriphan, N., Pinpueng, A. 2019. Properties of Agricultural Films Prepared from Biodegradable Poly(Butylene Succinate) Adding Natural Sorbent and Fertilizer. J. Polym. Environ. 27. 434–443. DOI: 10.1007/s10924-018-1358-5

Hopewell, J., Dvorak, R. and Kosior, E., 2009. Plastics recycling: challenges and opportunities. Phil. Trans. R. Soc. B. 346. 2115-2126. DOI: 10.1098/rstb.2008.0311

Horng, Y. T., Chien, C. C., Wei, Y. H., Chen, S. Y., Lan, J. C., Sun, Y. M., Soo, P. C. Functional cis-expression of phaCAB genes for poly(3-hydroxybutyrate) production by Escherichia coli. Lett Appl Microbiol. 2011 May;52(5):475-83. doi: 10.1111/j.1472-765X.2011.03029.x

Hu, D. Chung, A. L., Wu, L. P., Zhang, X., Wu, Q., Chen, J. C., Chen, G. Q. 2011. Biosynthesis and characterization of polyhydroxyalkanoate block copolymer P3HB-b-P4HB. Biomacromolecules, 12(9), 3166-3173. DOI: 10.1021/bm200660k.

Huang, P., Furutate, S., Mizuno, S. and Tsuge, T. 2019. Thermal degradation behavior of bacterial poly(3-hydroxybutyrate-co-3-mercaptopropionate). Polymer Degradation and Stability, 165, 35-42. DOI: doi.org/10.1016/j.polymdegradstab.2019.04.016.

Huff, J. and Infante, P. F. 2011. Styrene exposure and risk of cancer. Mutagenesis. 26(5). 583-584. DOI: 10.1093/mutage/ger033

Huh, D. and Paulsson, J. 2011. Non-genetic heterogeneity from stochastic partitioning at cell division. Nat. Genet. 43(2). 95-100. DOI: 10.1038/ng.729

Ibrahim, M. H. A. and Steinbüchel, A. 2010. High-Cell-Density Cyclic Fed-Batch Fermentation of a Poly(3-Hydroxybutyrate)-Accumulating Thermophile, *Chelatococcus* sp. Strain MW10. Applied and Environmental Microbiology. 76(23). 7890-7895. DOI: 10.1128/AEM.01488-10

Ienczak, J. L., Quines, L. K., de Melo, A. A., Brandellero, M., Mendez, C. R., Schmidell, W., Aragao, G. 2011. High cell density strategy for poly(3-hydroxybutyrate) production by *Cupriavidus necator*. Brazillian Journal of Chemical Engineering. 28(4). 585-596. DOI: 10.1590/S0104-66322011000400004

Ienczak, J. L., Schmidt M., Quines L. K., Zanfonato, K., da Cruz Pradella, J. G., Schmidell, W., de Aragao G. M. 2016. Poly(3-Hydroxybutyrate) Production in Repeated fed-Batch with Cell Recycle Using a Medium with low Carbon Source Concentration. Appl. Biochem. Biotechnol. 178(2). 408-417. DOI: 10.1007/s12010-015-1883-9

Ikehata, K. and Liu, Y., 2011. Land Disposal of Wastes. In: Encyclopedia of Environmental Health. Elsevier. 353-361. DOI: 10.1016/B978-0-444-52272-6.00521-3

Irdahayu, N. M. N. M., Shantini, K., Huong, K.-H., Vigneswari, S., Aziz, N.A., Azizan, M.N.M. and Amirul, A.A.A. 2017. En route to economical eco-friendly solvent system in enhancing sustainable recovery of poly(3-hydroxybutyrate-co-4-hydroxybutyrate) copolymer. Eng. Life Sci. 17. 1050-1059. DOI: 10.1002/elsc.201600217

Irorere, V. U., Smyth, T. J., Cobice, D., McClean, S., Marchant, R., Banat, I. M. 2018. Fatty acid synthesis pathway provides lipid precursors for rhamnolipid biosynthesis in *Burkholderia thailandensis* E264. Appl. Microbiol. Biotechnol. 102(14). 6163-6174. DOI: 10.1007/s00253-018-9059-5.

Isak, I. Patel, M., Riddell, M., West, M., Bowers, T., Wijeyekoon, S, Lloyd, J. 2016. Quantification of polyhydroxyalkanoates in mixed and pure cultures biomass by Fourier transform infrared spectroscopy: comparison of different approaches. Letters in Applied Microbiology. 63(2).139-146. DOI: 10.1111/lam.12605

Isemori, Y. Tajima, K., Tanaka, S., Yu, F., Ishida, K., Inoue, Y. 2006. Effects of pH of Fermentation Medium on Biosynthesis of Poly[(3-hydroxybutyrate)-co- (3-mercaptopropionate)] by *Wautersia eutropha*. Macromolecular Bioscience. 6. 818-826. DOI: 10.1002/mabi.200600133

Jabeen, N., Majid, I. and Nayik, G. A., 2015. Bioplastics and food packaging: A review. Cogent Food and Agriculture.1(1). DOI: 10.1080/23311932.2015.1117749.

Jacobs, C. and Shapiro, L., 1999. Bacterial cell division: A moveable feast. Proc. Natl. Acad. Sci. 96. 5891-5893. DOI: 10.1073/pnas.96.11.589

Jacquel, N. Lo, C., Wei, Y., Wu, H., & Wang, S. S. 2008. Isolation and purification of bacterial poly(3-hydroxyalkanoates). Biochemical Engineering Journal. 39(1). 15-27. DOI: 10.1016/j.bej.2007.11.029

Jambeck, J. R. Geyer, R., Wilcox, C., Siegler, T. R., Perryman, M., Andrady, A., Narayan, R., Law, K. L., 2015. Plastic waste inputs from land into the ocean. Science. 347(6223). 768-771. DOI: 10.1126/science.1260352

Jarute, G., Kainz, A., Schroll, G., Baena, J. R., Lendl, B. 2004. On-line determination of the intracellular poly(beta-hydroxybutyric acid) content in transformed *Escherichia coli* and glucose during PHB production using stopped-flow attenuated total reflection FT-IR spectrometry. Anal. Chem. 76(21), 6353-6358. DOI: 10.1021/ac049803l

Jendrossek, D., 2009. Polyhydroxyalkanoate granules are complex subcellular organelles (carbonosomes). J. Bacteriol. 191(10). 3195-3202. DOI: 10.1128/JB.01723-08

Jeon, J. M., Brigham, C. J., Kim, Y. H., Kim, H. J., Yi, D. H., Kim, H., Rha, C., Sinskey, A. J., Yang, Y H. 2014. Biosynthesis of poly(3-hydroxybutyrate-co-3-hydroxyhexanoate) (P(HB-co-HHx)) from butyrate using engineered Ralstonia eutropha. Appl. Microbiol. Biotechnol. 98(12). 5461-9. DOI: 10.1007/s00253-014-5617-7

Juengert, J. R., Patterson, C. and Jendrossek, D., 2018. Poly(3-Hydroxybutyrate) (PHB) Polymerase PhaC1 and PHB Depolymerase PhaZa1 of *Ralstonia eutropha* Are Phosphorylated *In Vivo*. Applied and Environmental Microbiology. 84(13). DOI: 10.1128/AEM.00604-18

Kachrimanidou, V., Kopsahelis, N., Vlysidis, A., Papanikolaou, S., Kookos, I. K., Monje Martínez, B., Escrig Rondán, M. C., and Koutinas, A. A. 2016. Downstream separation of poly(hydroxyalkanoates) using crude enzyme consortia produced via solid state fermentation integrated in a biorefinery concept. Food and Bioproducts Processing. 100. 323-334. DOI: 10.1016/j.fbp.2016.08.002

Kacmar, J., Carlson, R., Balogh, S. J. and Srienc, F. 2005. Staining and quantification of poly-3-hydroxybutyrate in *Saccharomyces cerevisiae* and *Cupriavidus necator* cell populations using automated flow cytometry. Cytometry Part A. 69(1). 27-35. DOI: 10.1002/cyto.a.20197

Kampeerapappun, P. and Phanomkate, N. 2013. Slow Release Fertilizer from Core-Shell Electrospun Fibers. Chiang Mai Journal of Science. 40(4). 775-782.

Kang, Y., Liu, H., Genin, S., Schell, M. A., Denny, T. P. 2002. *Ralstonia solanacearum* requires type 4 pili to adhere to multiple surfaces and for natural transformation and virulence. Molecular Microbiology. 46(2). 427-437. 10.1046/j.1365-2958.2002.03187.x

Kapritchkoff, F. M., Viotti, A. P., Alli, R. C., Zuccolo, M., Pradella, J. G., Maiorano, A. E., Miranda, E. A., Bonomi, A. 2006. Enzymatic recovery and purification of polyhydroxybutyrate produced by *Ralstonia eutropha*. Journal of Biotechnology. 122(4). 453-462. DOI: 10.1016/j.jbiotec.2005.09.009

Karmann, S. Follonier, S., Bassas-Galia, M., Panke, S., and Zinn, M., 2016. Robust at-line quantification of poly(3-hydroxyalkanoate) biosynthesis by flow cytometry using a BODIPY 493/503-SYTO 62 double-staining. Journal of Microbiological Methods. 131. 166-171. DOI: 10.1016/j.mimet.2016.10.003

Kawakami, K., Largaespada, D. A. and Ivics Z. 2017. Transposons as Tools for Functional Genomics in Vertebrate Models. Trends Genet. 33(11). 784-801. DOI: 10.1016/j.tig.2017.07.006

Kawashima, Y., Orita, I., Nakamura, S., & Fukui, T. (2015). Compositional regulation of poly(3-hydroxybutyrate-co-3-hydroxyhexanoate) by replacement of granule-associated protein in *Ralstonia eutropha*. Microbial Cell Factories. 14. DOI:10.1186/s12934-015-0380-8

Kay, A. R. (2017). How Cells Can Control Their Size by Pumping Ions. Frontiers in Cell and Developmental Biology. 5. DOI: 10.3389/fcell.2017.00041

KEEG. 2021. GENOME: Cupriavidus necator H16. https://www.genome.jp/entry/T00416. (Accessed 29/4/2022)

Kelley, A. S. and Srienc, F. 1999. Production of two phase polyhydroxyalkanoic acid granules in *Ralstonia eutropha*. International Journal of Biological Macromolecules. 25. 61-67. DOI: 10.1016/S0141-8130(99)00016-1

Kermona, A. and Piotrowska, M. 2020. Polyurethane Recycling and Disposal: Methods and Prospects. Polymers.12(8). DOI: 10.3390/polym12081752

Keskin, G. Kizil, G., Bechelany, M., Pochat-Bohatier, C. and Öner, M. 2017. Potential of polyhydroxyalkanoate (PHA) polymers family as substitutes of petroleum based polymers for packaging applications and solutions brought by their composites to form barrier materials. Pure Appl. Chem. 89(12). 1841-1848. DOI: 10.1515/pac-2017-0401

Khanna, S. and Srivastava, A. K., 2005. Repeated batch cultivation of *Ralstonia eutropha* for Poly (beta-hydroxybutyrate) production. Biotechnol. Lett. 27(18). 1401-1403. DOI: 10.1007/s10529-005-0689-1

Khlebodarova, T. M. and Likoshvai, V. A., 2018. Persister Cells – a Plausible Outcome of Neutral Coevolutionary Drift. Sci Rep. 8. 14309. DOI: 10.1038/s41598-018-32637-2

Khosravi-Darani, K., Vasheghani-Farahani, E. and Shojaosadati, Y. Y. 2004. Effect of process variables on supercritical fluid disruption of *Ralstonia eutropha* cells for poly(R-hydroxybutyrate) recovery. Biotechnology Progress. 20(6). 1757-1765. DOI: 10.1021/bp0498037

Kichise, T., Fukui, T., Yoshida, Y., and Doi, Y. (1999). Biosynthesis of polyhydroxyalkanoates (PHA) by recombinant *Ralstonia eutropha* and effects of PHA synthase activity on *in vivo* PHA biosynthesis. International Journal of Biological Macromolecules. 25(1-3). 69-77. DOI:10.1016/S0141-8130(99)00017-3

Kichise, T., Taguchi, S. and Doi, Y. 2002. Enhanced Accumulation and Changed Monomer Composition in Polyhydroxyalkanoate (PHA) Copolyester by *In Vitro* Evolution of *Aeromonas caviae* PHA Synthase. Appl. Environ. Microbiol. 68(5). 2411-2419. DOI: 10.1128/AEM.68.5.2411-2419.2002

Kida, T., Kimura, T., Eno, A., Janchai, K., Yamaguchi, M., Otsuki, Y., Kimura, T., Mizukawa, T., Murakami, T., Hato, K., & Okawa, T. (2021). Effect of Ultra-High-Molecular-Weight Molecular Chains on the Morphology, Crystallization, and Mechanical Properties of Polypropylene. Polymers. 13(23). DOI: 10.3390/polym13234222

Klinke, S., de Roo, G., Witholt, B. and Kessler, B. 2000. Role of phaD in Accumulation of Medium-Chain-Length Poly(3-Hydroxyalkanoates) in *Pseudomonas oleovorans*. APPLIED AND ENVIRONMENTAL MICROBIOLOGY. 66(9). 3705-3710. DOI: 10.1128/aem.66.9.3705-3710.2000

Knoll, M., Hamm, T.M., Wagner, F., Martinez, V., and Pleiss, J. (2009). The PHA Depolymerase Engineering Database: A systematic analysis tool for the diverse family of polyhydroxyalkanoate (PHA) depolymerases. BMC Bioinformatics. 10. 89 - 89. DOI: 10.1186/1471-2105-10-89

Knowles, J., Hastings, G., Ohta, H., Niwa, S., and Boeree, N. (1992). Development of a degradable composite for orthopaedic use: In vivo biomechanical and histological evaluation of two bioactive degradable composites based on the polyhydroxybutyrate polymer. Biomaterials. 13(8). 491-496. DOI: 10.1016/0142-9612(92)90099-A

Kobayashi, T. Shiraki M, Abe T, Sugiyama A, Saito T. 2003. Purification and Properties of an Intracellular 3-Hydroxybutyrate-Oligomer Hydrolase (PhaZ2) in *Ralstonia eutropha* H16 and Its Identification as a Novel Intracellular Poly(3-Hydroxybutyrate) Depolymerase. JOURNAL OF BACTERIOLOGY. 185(12). 3485-3490. DOI: 10.1128/JB.185.12.3485-3490.2003

Kolibachuk, D., Miller, A. and Dennis, D. 1999. Cloning, Molecular Analysis, and Expression of the Polyhydroxyalkanoic Acid Synthase (phaC) Gene from *Chromobacterium violaceum*. APPLIED AND ENVIRONMENTAL MICROBIOLOGY. 68(8). 3561-3565. DOI: 10.1128/aem.65.8.3561-3565.1999

Koller, M. Hesse, P, Bona, R, Kutschera, C, Atlić, A, Braunegg, G. 2007. Potential of various archae- and eubacterial strains as industrial polyhydroxyalkanoate producers from whey. Macromol. Biosci. 12(7). 218-226. DOI: 10.1002/mabi.200600211

Koller, M., Niebelschütz, H. and Braunegg, G. 2013. Strategies for recovery and purification of poly[(R)-3-hydroxyalkanoates] (PHA) biopolyesters from surrounding biomass. Engineering in life sciences. 13. 549-562. DOI: 10.1002/elsc.201300021

Koller, M. 2014. Poly(hydroxyalkanoates) for Food Packaging: Application and Attempts towards Implementation. APPLIED FOOD BIOTECHNOLOGY. 1(1). 3-15. DOI: 10.22037/afb.v1i1.7127

Koller, M., 2018. A Review on Established and Emerging Fermentation Schemes for Microbial Production of Polyhydroxyalkanoate (PHA) Biopolyesters. Fermentation. 4(30). DOI: 10.3390/fermentation4020030

Köse, G. T., Korkusuz, F., Özkul, A., Soysal, Y., Özdemir, T., Yildiz, C., and Hasirci, V., 2005. Tissue engineered cartilage on collagen and PHBV matrices. Biomaterials. 26(25), 5187-5197. DOI: 10.1016/j.biomaterials.2005.01.037

Kotte, O., Volkmer, B., Radzikowski, J. L. and Heinemann, M., 2014. Phenotypic bistability in *Escherichia coli's* central carbon metabolism. Molecular Systems Biology, 10(7). 736. DOI: 10.15252/msb.20135022

Kourmentza, C., Plácido J., Venetsaneas, N., Burniol-Figols, A., Varrone, C., Gavala, H. N., Reis M. A. M. 2017. Recent Advances and Challenges towards Sustainable Polyhydroxyalkanoate (PHA) Production. Bioengineering. 4(2). 55. DOI: 10.3390/bioengineering4020055

Kragh, K. N., Hutchison, J. B., Melaugh, G., Rodesney, C., Roberts, A. E., Irie, Y., Jensen, P. Ø., Diggle, S. P., Allen, R. J., Gordon, V., Bjarnsholt, T. 2016. Role of Multicellular Aggregates in Biofilm Formation. American Society for Microbiology, 7(2). e00237. DOI: 10.1128/mBio.00237-16

Krebs, H. A. 1935. Metabolism of amino-acids. Biochemical Journal. 29(7). 1620-1644.

Kurian, N. S., & Das, B. (2021). Comparative analysis of various extraction processes based on economy, eco-friendly, purity and recovery of polyhydroxyalkanoate: A review. International Journal of Biological Macromolecules.183. 1881-1890. DOI: 10.1016/j.ijbiomac.2021.06.007

La Rosa, R., de la Peña, F., Prieto, M. A., and Rojo, F. 2014. The Crc protein inhibits the production of polyhydroxyalkanoates in *Pseudomonas putida* under balanced carbon/nitrogen growth conditions. Environ Microbiol. 16(1). 278-290. DOI: 10.1111/1462-2920.12303

Labet, M. and Thielemans, W. 2009. Synthesis of polycaprolactone: a review. Chem. Soc. Rev. 38(12). 3484-3504. DOI: 10.1039/b820162p

Ladd, M. and Bordoni, B., 2022. Genetics, Transposons. Treasure Island (FL): StatPearls Publishing.

Lakshman, K. and Shamala, T. R., 2006. Extraction of polyhydroxyalkanoate from Sinorhizobium meliloti cells using Microbispora sp. culture and its enzymes. Enzyme and Microbial Technology, 39(7), 1471-1475. DOI: 10.1007/s10098-013-0630-6

Lakshmanan, S. and Murugesan T. 2013. The chlor-alkali process: Work in Progress. Clean Technologies and Environmental Policy. 16. 225–234. DOI: 0.1007/s10098-013-0630-6

Lau, N. S., Tsuge, T. and Sudesh, K., 2011. Formation of new polyhydroxyalkanoate containing 3-hydroxy-4-methylvalerate monomer in *Burkholderia sp*. Appl. Microbiol. Biotechnol. 89. 1599-1609.

Lebreton, L., Slat, B., Ferrari, F., Sainte-Rose, B., Aitken, J., Marthouse, R., Hajbane, S., Cunsolo, S., Schwarz, A,, Levivier, A., Noble, K., Debeljak, P., Maral, H., Schoeneich-Argent, R., Brambini, R.,

Reisser, J. 2018. Evidence that the Great Pacific Garbage Patch is rapidly accumulating plastic. Scientific Reports, 8(1). 4666. DOI: 10.1038/s41598-018-22939-w

Lebreton, L., van der Zwet, J., Damsteeg, JW. Slat, B. Andrady, A., Reisser, J. 2017. River plastic emissions to the world's oceans. Nature Communications, 8. 15611. DOI: 10.1038/ncomms15611.

Legat, A., Gruber, C., Zangger, K., Wanner, G., Stan-Lotter, H. 2010. Identification of polyhydroxyalkanoates in *Halococcus* and other haloarchaeal species. Appl. Microbiol. Biotechnol. 87(3). 1119-1127. DOI: 10.1007/s00253-010-2611-6

Lens, P. N. L. and Hemminga, M. A. 1998. Nuclear magnetic resonance in environmental engineering: Principles and applications. Biodegradation. 9(6). 393-409. DOI: 10.1023/a:1008316031421

Lewis, K., 2010. Persister cells. Annu. Rev. Microbiol. 64. 357-372. DOI: 10.1146/annurev. micro.112408.134306

Li, Z., Xin, X., Xiong, B., Zhao, D.., Zhang, X, Bi, C. 2020. Engineering the Calvin–Benson–Bassham cycle and hydrogen utilization pathway of *Ralstonia eutropha* for improved autotrophic growth and polyhydroxybutyrate production. Microb. Cell. Fact. 19(1). 228. DOI: 10.1186/s12934-020-01494-y

Lleo, M. M., Canepari, P., and Satta, G. (1990). Bacterial cell shape regulation: Testing of additional predictions unique to the two-competing-sites model for peptidoglycan assembly and isolation of conditional rod-shaped mutants from some wild-type cocci. Journal of Bacteriology. 172(7). 3758-3771. DOI: 10.1128/jb.172.7.3758-3771.1990

López-Abelairas, M., García-Torreiro, M., Lú-Chau, T., Lema, J., & Steinbüchel, A. 2015. Comparison of several methods for the separation of poly(3-hydroxybutyrate) from *Cupriavidus necator* H16 cultures. Biochemical Engineering Journal. 93. 250-259. DOI: 10.1016/j.bej.2014.10.018

Luklinska, Z. B. and Bonfield, W. 1997. Morphology and ultrastructure of the interface between hydroxyapatite-polyhydroxybutyrate composite implant and bone. JOURNAL OF MATERIALS SCIENCE: MATERIALS IN MEDICINE. 8. 379-383. DOI: 10.1023/A:1018589018205

Lusher, A. L., Tirelli, V. and Officer, R. 2015. Microplastics in Arctic polar waters: the first reported values of particles in surface and sub-surface samples. scientific reports, 5. 14947. DOI: 10.1038/srep14947

Lütke-Eversloh, T., Bergander, K., Luftmann, H. and Steinbüchel, A. 2001. Biosynthesis of Poly(3-hydroxybutyrate-co-3-mercaptobutyrate) as a Sulfur Analogue to Poly(3-hydroxybutyrate) (PHB). Biomacromolecules. 2. 1061-1065. DOI: 10.1021/bm015564p

Madison, L. L. and Huisman, G. W. 1999. Metabolic Engineering of Poly(3-Hydroxyalkanoates): From DNA to Plastic. Microbiol. Mol. Biol. Rev. 63(1). 21-53. DOI: 10.1128/mmbr.63.1.21-53.1999

Madkour, M. H., Heinrich, D., Alghamdi, M. A., Shabbaj, I. I., Steinbüchel, A. 2013. PHA Recovery from Biomass. Biomacromolecules. 14. 2963-2972. DOI: 10.1021/bm4010244.

Maehara, A., Doi, Y., Nishiyama, T., Takagi, Y., Ueda, S., Nakano, H., Yamane, T. 2001. PhaR, a protein of unknown function conserved among short-chain-length polyhydroxyalkanoic acids producing bacteria, is a DNA-binding protein and represses *Paracoccus denitrificans* phaP expression in vitro. FEMS Microbiology Letters. 200(1). 9-15. DOI: 10.1111/j.1574-6968.2001.tb10685.x

Maehara, A., Taguchi, S., Nishiyama, T., Yamane, T., Doi, Y. 2002. A Repressor Protein, PhaR, Regulates Polyhydroxyalkanoate (PHA) Synthesis via Its Direct Interaction with PHA. J. Bacteriol. 184(14). 3992-4002. DOI: 10.1128/JB.184.14.3992-4002.2002

Maestro, B. and Sanz, J. M. 2017. Polyhydroxyalkanoate-associated phasins as phylogenetically heterogeneous, multipurpose proteins. Microb. Biotechnol. 10(6). 1323-1337. DOI: 10.1111/1751-7915.12718

Magdouli, S., Brar, S. K., Blais, J. F. and Tyagi, R. D. 2015. How to direct the fatty acid biosynthesis towards polyhydroxyalkanoates production?. Biomass and Bioenergy. 74. 268-279. DOI: 10.1016/j.biombioe.2014.12.017

Maitz, M. F. 2015. Applications of synthetic polymers in clinical medicine. Biosurface and Biotribology, 1(3), 161-176. DOI: 10.1016/j.bsbt.2015.08.002

Mak, C. W., Yeung, K. C.-F. and Chan, K. M. 2019. Acute toxic effects of polyethylene microplastic on adult zebrafish. Ecotoxicology and Environmental Safety. 182. 109442. DOI: 10.1016/j.ecoenv.2019.109442

Mancic, L., Pontón, P. I., Letichevsky, S., Costa, A. M., Marinkovic, B. A., and Rizzo, F. C. 2016. Application of silane grafted titanate nanotubes in reinforcing of polyamide 11 composites. Composites Part B: Engineering. 93. 153-162. DOI: 10.1016/j.compositesb.2016.03.028

Mansfield, D. A., Anderson, A. J. and Naylor, L. A. 1995. Regulation of PHB metabolism in *Alcaligenes eutrophus*. Canadian Journal of Microbiology. 41(13). DOI: 10.1139/m95-166

Mansilla, M. C., Cybulski, L. E., Albanesi, D. and de Mendoza, D., 2004. Control of Membrane Lipid Fluidity by Molecular Thermosensors. JOURNAL OF BACTERIOLOGY. 186(20). 6681-6688. DOI: 10.1128/JB.186.20.6681-6688.2004

Marciniak, P. and Możejko-Ciesielska, J. 2021. What Is New in the Field of Industrial Wastes Conversion into Polyhydroxyalkanoates by Bacteria?. Polymers (Basel). 13(11). 1731. DOI: 10.3390/polym13111731

Martin, D. P. and Williams, S. F. 2003. Medical applications of poly-4-hydroxybutyrate: strong flexible absorbable biomaterial. Biochemical Engineering Journal. 16(2). 97-105. DOI: 10.1016/S1369-703X(03)00040-8

Martinez, S. and Déziel, E. 2020. Changes in polyhydroxyalkanoate granule accumulation make optical density measurement an unreliable method for estimating bacterial growth in *Burkholderia thailandensis*. Canadian Journal of Microbiology. 66(3). 256-262. DOI: 10.1139/cjm-2019-0342

Martino, L., Cruz, M. V., Scoma, A., Freitas, F., Bertin, L., Scandola, M., and Reis, M. A. 2014. Recovery of amorphous polyhydroxybutyrate granules from *Cupriavidus necator* cells grown on used cooking oil. Int. J. Biol. Macromol. 71. 117-123. DOI: 10.1016/j.ijbiomac.2014.04.016

Matsumoto, K., Nakae, S., Taguchi, K., Matsusaki, H., Seki, M., Doi, Y. 2001. Biosynthesis of Poly(3-hydroxybutyrate-co-3-hydroxyalkanoates) Copolymer from Sugars by Recombinant *Ralstonia eutropha* Harboring the phaC1Ps and the phaGPs Genes of *Pseudomonas sp*. 61-3. Biomacromolecules. 2. 934-939. DOI: 10.1021/bm0155367

McAdam, B., Fournet, M. B., McDonald, P. and Mojiccevic, M., 2020. Production of Polyhydroxybutyrate (PHB) and Factors Impacting Its Chemical and Mechanical Characteristics. Polymers (Basel). 12(12). DOI: 10.3390/polym12122908

McLain, V. C., 2007. Final Report on the Safety Assessment of Polyethylene. International Journal of Toxicology. 26. 115-127. DOI: 10.1080/10915810601163962

Megazyme Ltd. 2023a. D-Fructose/D-Glucose Assay Kit. Available at: https://www.megazyme.com/d-fructose-d-glucose-assay-kit. (Accessed 10/2/2023)

Megazyme Ltd. 2023b. D-Gluconic Acid/D-Glucono-δ-lactone Assay Kit. Available at: https://www.megazyme.com/d-gluconic-acid-d-glucono-delta-lactone. (Accessed 10/2/2023)

Merck KGaA, 2022(a). Meat extract. Available at: https://www.sigmaaldrich.com /GB/en/product/sial/70164 (Accessed 24 5 2022).

Merck KGaA, 2022(b). Peptone from soybean, enzymatic digest. Available at: https://www.sigmaaldrich.com/GB/en/product/sial/70178 (Accessed 24/5/2022).

Merklein, M. and Hagenah, H., 2012. The Effect of Thermoforming of PLA-PHBV Films on the Morphology and Gas Barrier Properties. Key Engineering Materials. 504-506. 1135-1138. DOI: 10.4028/www.scientific.net/KEM.504-506.1135

Mezzolla, V., D'Urso, O. F. and Poltonieri, P. 2018. Role of PhaC Type I and Type II Enzymes during PHA Biosynthesis. Polymers. 10(8). DOI: 10.3390/polym10080910.

Micro Powders, Inc., 2015. BIOSCRUB®. Available at: http://www.mpipersonalcare.com/ViewProducts.aspx?id=38andfp=main (Accessed 2021)

Miguel, O. and Iruin, J. J. 1999. Evaluation of the transport properties of Poly(3-hydroxybutyrate) and its 3-hydroxyvalerate copolymers for packaging applications. Macromolecular Symposia. 144(1), 427-438. DOI: 10.1002/masy.19991440140

MirelTM, 2021. Product Information. Available at: http://www.mirelplastics.com/product-information/

Miyaue, S., Suzuki, E., Komiyama, Y., Kondo, Y., Morikawa, M., & Maeda, S. 2018. Bacterial Memory of Persisters: Bacterial Persister Cells Can Retain Their Phenotype for Days or Weeks After Withdrawal From Colony–Biofilm Culture. Frontiers in Microbiology. 9. DOI: 10.3389/fmicb.2018.01396

Mohandas, S. P., Balan, L., Gopi, J., Anoop, B., Mohan P., S., Philip, R., Cubelio, S. S., and Singh, I. B. 2021. Biocompatibility of polyhydroxybutyrate-co-hydroxyvalerate films generated from Bacillus cereus MCCB 281 for medical applications. International Journal of Biological Macromolecules. 176. 244-252. DOI: 10.1016/j.ijbiomac.2021.02.006

Moreno, R., Martínez-Gomariz, M., Yuste, L., Gil, C., Rojo, F. 2009. The *Pseudomonas putida* Crc global regulator controls the hierarchical assimilation of amino acids in a complete medium: evidence from proteomic and genomic analyses. Proteomics. 9(11). 2910-2928. DOI: 10.1002/pmic.200800918

Mozejko-Ciesielska, J., Szacherska, K. and Marciniak, P. 2019. Pseudomonas Species as Producers of Eco-friendly Polyhydroxyalkanoates. Journal of Polymers and the Environment. 27(4). 1151-1166. DOI: 10.1007/s10924-019-01422-1

Mravec, F., Obruca, S., Krzyzanek, V., Sedlacek, P., Hrubanova, K., Samek, O., Kucera, D., Benesova, P., Nebesarova. 2016. J. Accumulation of PHA granules in *Cupriavidus necator* as seen by confocal fluorescence microscopy. FEMS Microbiol. Lett. 363:10. DOI: 10.1093/femsle/fnw094

Murchison, H., Larrimore, S., Hull, S. and Curtiss, R. I., 1982. Isolation and characterization of Streptococcus mutans mutants with altered cellular morphology or chain length. Infect. Immun. 38(1), 282-291. DOI: 10.1128/iai.38.1.282-291.1982

Murugan, P., Chhajer, P., Kosugi, A., Arai, T., Brigham, C. J., Sudesh, K. 2016. Production of P(3HB-co-3HHx) with Controlled Compositions by Recombinant *Cupriavidus necator* Re2058/pCB113 from Renewable Resources. CSAWAC. 44(9). 1085-1260. doi.org/10.1002/clen.201500714

Murugesan, S. and Iyyaswami, R., 2017. Low frequency sonic waves assisted cloud point extraction of polyhydroxyalkanoate from *Cupriavidus necator* Author links open overlay panel. Journal of Chromatography B. 1060. 207-214. DOI: 10.1016/j.jchromb.2017.06.009

Myers, J. A., Curtis, B. and Curtis, W. 2013. Improving accuracy of cell and chromophore concentration measurements using optical density. BMC Biophys. 6(4). DOI: 10.1186/2046-1682-6-4

Nafchi, A. M., Maradpour, M., Saeidi, M. and Alias, A. K. 2013. Thermoplastic starches: Properties, challenges,and prospects. Starch. 65(1-2). 61-72. DOI: 10.1002/star.201200201

Nakajima, H., Dijkstra, P. and Loos, K., 2017. The Recent Developments in Biobased Polymers toward General and Engineering Applications: Polymers that Are Upgraded from Biodegradable Polymers, Analogous to Petroleum-Derived Polymers, and Newly Developed. Polymers. 9(10). DOI: 10.3390/polym9100523

Needhidasan, S., Samuel, M. and Chidambaram, R. 2014. Electronic waste – an emerging threat to the environment of urban India. Journal of Environmental Health Science and Engineering. 12(36). DOI: 10.1186/2052-336X-12-36

Neis, E. P. J. G., Dejong, C. H. C. and Rensen, S. S. 2015. The Role of Microbial Amino Acid Metabolism in Host Metabolism. Nutrients. 7(4). 2930-2946. DOI: 10.3390/nu7042930

Neves, A. and Müller, J. 2012. Use of enzymes in extraction of polyhydroxyalkanoates produced by *Cupriavidus necator*. Biotechnology Progress. 28(6). 1575-1580. DOI: 10.1002/btpr.1624

Newman, J. C. and Verdin , E., 2019. β-hydroxybutyrate A Signalling Metabolite. Annual review of nutrition. 37(1). 51-76. DOI: 10.1146/annurev-nutr-071816-064916

Ng, K., Wong, Y., Tsuge, T., & Sudesh, K. (2011). Biosynthesis and characterization of poly(3-hydroxybutyrate-co-3-hydroxyvalerate) and poly(3-hydroxybutyrate-co-3-hydroxyhexanoate) copolymers using jatropha oil as the main carbon source. Process Biochemistry. 46(8). 1572-1578. DOI: 0.1016/j.procbio.2011.04.012

NIBIB, 2017. Biomaterials. Available at: https://www.nibib.nih.gov/science-education/science-topics/biomaterials (Accessed 15/ 3/2021).

Norman, T. M., Lord, N. D., Paulsson, J. and Losick, R., 2015. Stochastic Switching of Cell Fate in Microbes. Annu. Rev. Microbiol. 69. 381-403. DOI: 10.1146/annurev-micro-091213-112852

Novikov, L. N., Novikova, L. N., Mosahebi, A., Wiberg, M., Terenghi, G., and Kellerth, J. 2002. A novel biodegradable implant for neuronal rescue and regeneration after spinal cord injury. Biomaterials. 23. 3369-3376. DOI: 10.1016/S0142-9612(02)00037-6

Nwinyi, O. C. and Owolabi, T. A., 2019. Scanning electron microscopy and Fourier transmission analysis of polyhydroxyalkanoates isolated from bacteria species from abattoir in Ota, Nigeria. Journal of King Saud University - Science, 285-298. DOI: 10.1016/j.jksus.2017.08.003

Nwoko, Q. A., and Okeke, I. N. (2021). Bacteria autoaggregation: How and why bacteria stick together. Biochemical Society Transactions, 49: 3. 1147-1157. DOI: 10.1042/BST20200718

Nygaard, D., Yashchuk, O. and Hermida, É. B., 2019. Evaluation of culture medium on poly(3-hydroxybutyrate) production by *Cupriavidus necator* ATCC 17697: application of the response surface methodology. Heliyon. 5(3). e01374. DOI: 10.1016/j.heliyon.2019.e01374

Obeso, J. I., Gómez-Botrán, J. L., Olivera, E. R. and Luengo, J. M., 2015. The phasin PhaF controls bacterial shape and size in a network-forming strain of *Pseudomonas putida*. Journal of Biotechnology. 199. 17-20. DOI: 10.1016/j.jbiotec.2015.01.022

Obruca, S., Sedlacek, P., Krzyzanek, V., Mravec, F., Hrubanova, K., Samek, O., Kucera, D., Benesova, P., and Marova, I. 2016. Accumulation of Poly(3-hydroxybutyrate) Helps Bacterial Cells to Survive Freezing. PLoS ONE. 11(6). DOI: 10.1371/journal.pone.0157778

Ogawa, T. 1992. Effects of Molecular Weight on Mechanical Properties of Polypropylene. Journal of Applied Polymer Science. 44. 1869-1871.

Ogunsona, E., Ojogbo, E. and Mekonnen, T. 2018. Advanced material applications of starch and its derivatives. European Polymer Journal. 108. 570-581. DOI: 10.1016/j.eurpolymj.2018.09.039

Oldewurtel, E. R., Kitahara, Y. and van Teeffelen, S. 2021. Robust surface-to-mass coupling and turgor-dependent cell width determine bacterial dry-mass density. PNAS, 118(32). e2021416118. DOI: 10.1073/pnas.2021416118

Orman, M. A. and Brynildsen, M. P., 2015. Inhibition of stationary phase respiration impairs persister formation in *E. coli*. Nat. Commun. 6. 7983. DOI: 10.1038/ncomms8983

Otake, Y., Kobayashi, T., Asabe, H., Murakami, N. and Ono, K. 1995. Biodegradation of low-density polyethylene, polystyrene, polyvinyl chloride, and urea formaldehyde resin buried under soil for over 32 years. Journal of Applied Polymer Science, 56, 1789-1796. DOI: 10.1002/app.1995.070561309

Ou, F., McGoverin, C., Swift, S., and Vanholsbeeck, F. (2017). Absolute bacterial cell enumeration using flow cytometry. Journal of applied microbiology. 123(2). 464–477. DOI: 10.1111/jam.13508

Ozbudak, E. M., Thattai, M., Lim, H. N., Shraiman, B. I., Van Oudenaarden, A. 2004. Multistability in the lactose utilization network of *Escherichia coli*. Nature. 427. 737-740. DOI: 10.1038/nature02298

Pachekoski, W. and Belem, L. (2009). Thermal, Mechanical and Morphological Properties of Poly (Hydroxybutyrate) and Polypropylene Blends After Processing. Materials Research-ibero-american Journal of Materials. 12. DOI: 10.1590/S1516-14392009000200008

Page, W. J. and Knosp, O. 1989. Hyperproduction of Poly-Hydroxybutyrate during Exponential Growth of *Azotobacter vinelandii* UWD. Appl. Environ. Microbiol. 55(6). 1334-1339. DOI: 10.1128/aem.55.6.1334-1339.1989

Pagliano, G., Galletti, P., Samorì, C., Zaghini, A., and Torri, C. 2021. Recovery of Polyhydroxyalkanoates From Single and Mixed Microbial Cultures: A Review. Front. Bioeng. Biotechnol. 9. DOI: 10.3389/fbioe.2021.624021

Pan, H., Wang, J., Wu, H., Li, Z., & Lian, J. (2021). Synthetic biology toolkit for engineering *Cupriviadus necator* H16 as a platform for CO_2 valorization. Biotechnology for Biofuels. 14. DOI: 10.1186/s13068-021-02063-0

Papenfort, K. and Bassler, B. L., 2016. Quorum sensing signal–response systems in Gram-negative bacteria. Nat. Rev. Microbiol. 14(9). 576-588. DOI: doi.org/10.1038/nrmicro.2016.89

Park, S. J., Jang, Y. A., Noh, W., Oh, Y. H., Lee, H., David, Y., Baylon, M. G., Shin, J., Yang, J. E.., Choi, S. Y., Lee, S. H., Lee, S. Y. 2015. Metabolic Engineering of *Ralstonia eutropha* for the Production of Polyhydroxyalkanoates From Sucrose. Biotechnology and Bioengineering, 112(3). 638-643. DOI: 10.1002/bit.25469

Passanha, P., Kedia, G., Dinsdale, R. M., Guwy, A. J., and Esteves, S. R. 2014. The use of NaCl addition for the improvement of polyhydroxyalkanoate production by *Cupriavidus necator*. Bioresource Technology. 63. 287-294. DOI: 10.1016/j.biortech.2014.04.068

Paulsson, J., 2005. Models of stochastic gene expression. Physics of Life Reviews. 2(2). 157-175.

Pederson, E. N., McChalicher, C. W., Srienc, F. 2006. Bacterial synthesis of PHA block copolymers. Biomacromolecules. 7(6). 1904-11. DOI: 10.1021/bm0510101.

Pederson, E. N., McChalicher, C. W. J. and Srienc, F., 2006. Bacterial Synthesis of PHA Block Copolymers. Biomacromolecules. 7(6). 1904-1911. DOI: 10.1021/bm0510101

Pereira, Si., Sanchez Rodriguez, R., Rieumont Briones, J., Cabrera, J. (2008). Synthesis of biodegradable polyhydroxyalcanoate copolymer from a renewable source by alternate feeding. Polymer Engineering & Science. 48. 2051 - 2059. DOI: 10.1002/pen.21178.

Perkins, W.G., Capiati, N.J. and Porter, R.S. (1976), The effect of molecular weight on the physical and mechanical properties of ultra-drawn high density polyethylene. Polym. Eng. Sci. 16. 200-203. DOI:

Petrović, E. K. and Hamer, L. K., 2018. Improving the Healthiness of Sustainable Construction: Example of Polyvinyl Chloride (PVC). Buildings. 8(2). 28. DOI: 0.3390/buildings8020028

Pfeiffer, D., Wahl, A. and Jendrossek, D., 2011. Identification of a multifunctional protein, PhaM, that determines number, surface to volume ratio, subcellular localization and distribution to daughter cells of poly(3-hydroxybutyrate), PHB, granules in *Ralstonia eutropha* H16. Molecular Microbiology. 82(4). 936-951. DOI: 10.1111/j.1365-2958.2011.07869.x

Pfeiffer, D. and Jendrossek, D., 2012. Localization of Poly(3-Hydroxybutyrate) (PHB) Granule-Associated Proteins during PHB Granule Formation and Identification of Two New Phasins, PhaP6 and PhaP7, in *Ralstonia eutropha* H16. J. Bacteriol. 194(21). 5909-5921. DOI: 10.1128/JB.00779-12

Phithakrotchanakoon, C., Champreda, V., Aiba, S. A. and Pootanakit, T., 2015. Production of Polyhydroxyalkanoates from Crude Glycerol Using Recombinant *Escherichia coli*. J. Polym. Environ. 23(1). 38-44. DOI: 10.1007/s10924-014-0681-8

Phithakrotchanakoon, C., Champreda, V., Aiba. S., Pootanakit, K., Tanapongpipat, S. 2013. Engineered *Escherichia coli* for Short-Chain-Length Medium-Chain-Length Polyhydroxyalkanoate Copolymer Biosynthesis from Glycerol and Dodecanoate. Biosci. Biotechnol. Biochem, 77(6), 1262-1268. DOI: 10.1271/bbb.130073

Picard, E., Gerard, J-F. Espuche, E. (2013). Reinforcement of the Gas Barrier Properties of Polyethylene and Polyamide Through the Nanocomposite Approach: Key Factors and Limitations. Oil & Gas Science and Technology. 70. DOI: 10.2516/ogst/2013145.

Pierucci, O., 1978. Dimensions of *Escherichia coli* at various growth rates: model for envelope growth. Journal of Bacteriology, 135(2). 559-574. DOI: 10.1128/jb.135.2.559-574.1978

Piuri M, Sanchez-Rivas C, Ruzal SM. 2005. Cell wall modifications during osmotic stress in *Lactobacillus casei*. J Appl Microbiol. 98(1). 84-95. DOI: 10.1111/j.1365-2672.2004.02428.x

Plaitakis, A., Kalef-Ezra, E., Kotzamani, D., Zaganas, I., Spanaki, C. The Glutamate Dehydrogenase Pathway and Its Roles in Cell and Tissue Biology in Health and Disease. Biology (Basel). 2017. 6(1). 11. DOI: 10.3390/biology6010011

Plastics Europe, 2018. Plastics - the Facts 2018. Available at: https://www.plasticseurope.org/application/files/6315/4510/9658/Plastics_the_facts_2018_AF_web.pdf (Accessed 7 8 2021).

Plastics Europe, 2020. Plastics - The Facts 2020. Available at: https://plasticseurope.org/knowledge-hub/plastics-the-facts-2020/ (Accessed 9 3 2021).

Plastics Europe, 2021. POLYOLEFINS. Available at: https://www.plasticseurope.org/en/about-plastics/what-are-plastics/large-family/polyolefins (Accessed 7 07 2021).

Poh, L., Wu, Q., Chen, Y., Narimissa, E. (2022). Characterization of industrial low-density polyethylene: a thermal, dynamic mechanical, and rheological investigation. Rheologica Acta. 61. DOI: 10.1007/s00397-022-01360-1.

Pötter, M., Müller, H., Reinecke, F., Wieczorek, R., Fricke, F., Bowien, B., Friedrich, B., Steinbüchel, A. 2004. The complex structure of polyhydroxybutyrate (PHB) granules: four orthologous and paralogous phasins occur in *Ralstonia eutropha*. Microbiology (Reading). 150(7). 2301-2311. DOI: 10.1099/mic.0.26970-0

Pradella, J. G., Lenczak, J. L., Delgado, C. R. and Taciro, M. K. 2012. Carbon source pulsed feeding to attain high yield and high productivity in poly(3-hydroxybutyrate) (PHB) production from soybean oil using *Cupriavidus necator*. Biotechnol. Lett., 34(6), 1003-1007. DOI: 10.1007/s10529-012-0863-1

Prata, J. C., 2018. Airborne microplastics: Consequences to human health?. Environ. Pollut. 234. 115-126. DOI: 10.1016/j.envpol.2017.11.043

Pries, A., Priefert, H., Krüger, N. and Steinbüchel, A. 1991. Identification and characterization of two Alcaligenes eutrophus gene loci relevant to the poly(beta-hydroxybutyric acid)-leaky phenotype which exhibit homology to ptsH and ptsI of *Escherichia coli*. J. Bacteriol. 173(18). 5843-5853. DOI: 10.1128/jb.173.18.5843-5853.1991

Prieto, A., Escapa, I. F., Martínez, V., Dinjaski, N., Herencias, C., de la Peña, F., Tarazona, N., Revelles, O. 2016. A holistic view of polyhydroxyalkanoate metabolism in *Pseudomonas putida*. Environmental Microbiology. 18(2). 341-357. DOI: 10.1111/1462-2920.12760

PSAC. 2021. Facts about Canada's Oil and Natural Gas Industry: Fractional Distilation. Available at: https://oilandgasinfo.ca/patchworks/fractional-distillation/ (Accessed 10/7/2021).

Puchalski, M., Szparaga, G., Biela, T., Gutowska, A., Sztajnowski, S., and Krucińska, I. 2018. Molecular and Supramolecular Changes in Polybutylene Succinate (PBS) and Polybutylene Succinate Adipate (PBSA) Copolymer during Degradation in Various Environmental Conditions. Polymers, 10(3). DOI: 10.3390/polym10030251

Puls, J., Wilson, S. A. and Hölter, D., 2011. Degradation of Cellulose Acetate-Based Materials: A Review. Environ. 19(1). 152-165. DOI: 10.1007/s10924-010-0258-0

Pye, J. E. and Roth, C. B. 2011. Two simultaneous mechanisms causing glass transition temperature reductions in high molecular weight freestanding polymer films as measured by transmission ellipsometry. Phys. Rev. Lett. 107(23). 235701. DOI: 10.1103/PhysRevLett.107.235701

Qi, L., Wu, L., He, R., Cheng, H., Liu, B., & He, X. (2019). Synergistic toughening of polypropylene with ultra-high molecular weight polyethylene and elastomer-olefin block copolymers. RSC Advances. 9(41). 23994-24002. DOI: 10.1039/c9ra01073d

Radecka, I., Irorere, V., Jiang, G., Hill, D., Williams, C., Adamus, G., Kwiecień, M., Marek, A. A., Zawadiak, J., Johnston, B., and Kowalczuk, M. 2016. Oxidized Polyethylene Wax as a Potential Carbon Source for PHA Production. Materials. 9(5). DOI: 10.3390/ma9050367

Ramprasad, C., Teja, H. C., Gowtham, V., and Vikas, V. (2022). Quantification of landfill gas emissions and energy production potential in Tirupati Municipal solid waste disposal site by LandGEM mathematical model. MethodsX, 9. DOI: 10.1016/j.mex.2022.101869

Ramsay, J. A., Berger, E., Ramsay, B. A. and Chavarie, C. 1990. R Recovery of poly-3-hydroxyalkanoic acid granules by a surfactant-hypochlorite treatment. Biotechnology Techniques. 4(4). 221-226. DOI: 10.1007/BF00158833

Ranriamahefa, S., Renard, E., Guérin, P. and Langlois, V. 2003. Fourier Transform Infrared Spectroscopy for Screening and Quantifying Production of PHAs by Pseudomonas Grown on Sodium Octanoate. Biomacromolecules. 4(4). 1092-1097. DOI: 10.1021/bm034104o

Raskin, D. M. and de Boer, P. A. J., 1999. Rapid pole-to-pole oscillation of a protein required for directing division to the middle of *Escherichia coli*. Proc. Natl. Acad. Sci. 96. 4971-4976. DOI: 10.1073/pnas.96.9.4971

Reis, E. C. C., Borges, A. P. B., Fonseca, C. C., Martinez, M. M. M., Eleotério, R. B., Morato, G. O., & Oliveira, P. M. 2010. Biocompatibility, osteointegration, osteoconduction, and biodegradation of a hydroxyapatite-polyhydroxybutyrate composite. Brazilian Archives of Biology and Technology.53(4). DOI: 10.1590/S1516-89132010000400010

Reyes Ruiz, L. M., Wlliams, C. L. and Tamayo, R. 2020. Enhancing bacterial survival through phenotypic heterogeneity. PLoS Pathog.16(5). DOI: 10.1371/journal.ppat.1008439

Riedel, S. L., Lu, J., Stahl, U. and Brigham, C. J., 2014. Lipid and fatty acid metabolism *in Ralstonia eutropha*: relevance for the biotechnological production of value added products. Applied Microbiology and Biotechnology. 98(4). 1469-1483. DOI: 10.1371/journal.ppat.1008439

Riis, V. and Mai, W. 1988. Gas chromatographic determination of poly-β-hydroxybutyric acid in microbial biomass after hydrochloric acid propanolysis. Journal of Chromatography A. 445. 285-289. DOI: 10.1016/S0021-9673(01)84535-0

Rivera-Briso, A.L. and Serrano-Aroca, Á. 2018. Poly (3-Hydroxybutyrate-co-3-Hydroxyvalerate): Enhancement strategies for advanced applications. Polymers. 10(7). DOI: 732. doi:10.3390/ polym10070732

Rojas, E., Theriot, J. A. and Huang, K. C., 2014. Response of *Escherichia coli* growth rate to osmotic shock. PNAS, 111(21). DOI: 10.1073/pnas.1402591111

Rojo, F., 2010. Carbon catabolite repression in *Pseudomonas*: optimizing metabolic versatility and interactions with the environment. FEMS Microbiology Reviews, 34(5), 658-684. DOI: 10.1111/j.1574-6976.2010.00218.x

Roos, Y. H., 2009. Glass Transition Temperature and Its Relevance in Food Processing. Annual Review of Food Science and Technology. 1. 469-496. DOI: 0.1146/annurev.food.102308.124139

Rossii, S., Azghani, A. O. and Omri, A., 2004. Antimicrobial efficacy of a new antibiotic-loaded poly(hydroxybutyric-co-hydroxyvaleric acid) controlled release system. Journal of Antimicrobial Chemotherapy. 54(6). 1013-1018. DOI: 10.1093/jac/dkh477.

Sabharwal, P. K., Chattopadhyay, S. and Singh, H., 2018. Preparation and characterization of antimicrobial, biodegradable, triclosan-incorporated polyhydroxybutyrate-co-valerate films for packaging applications. Journal of Applied Polymer Science. 135(44). DOI: 10.1002/app.46862

Santhanam, A. and Sasidharan, S., 2010. Microbial production of polyhydroxy alkanotes (PHA) from Alcaligens s and Pseudomonas oleovorans using different carbon sources. AFRICAN JOURNAL OF BIOTECHNOLOGY, 9(21), 3144-3150.

Santolin, L., Waldburger, S., Neubauer, P., & Riedel, S. L. (2021). Substrate-Flexible Two-Stage Fed-Batch Cultivations for the Production of the PHA Copolymer P(HB-co-HHx) With *Cupriavidus necator* Re2058/pCB113. Frontiers in Bioengineering and Biotechnology. 9. DOI: 10.3389/fbioe.2021.623890

Saranya V, Poornimakkani, Krishnakumari MS, Suguna P, Binuramesh C, Abirami P, Rajeswari V, Ramachandran KB, Shenbagarathai R. 2012. Quantification of Intracellular Polyhydroxyalkanoates by Virtue of Personalized Flow Cytometry Protocol. Curr. Microbiol. 65(5). 589-594. DOI: 10.1007/s00284-012-0198-0

Savenkova, L., Gercberga, Z., Muter, O., Nikolaeva, V., Dzene, A., and Tupureina, V. 2002. PHB-based films as matrices for pesticides. Process Biochemistry. 37(7). 719-722. DOI: 10.1016/S0032-9592(01)00263-1

Schwartz, E., Henne, A., Cramm, R., Eitinger, T., Friedrich, B., and Gottschalk, G. 2003. Complete nucleotide sequence of pHG1: a *Ralstonia eutropha* H16 megaplasmid encoding key enzymes of H(2)-based ithoautotrophy and anaerobiosis. J. Mol. Bio. 332(2). 369-383. DOI: 0.1016/S0022-2836(03)00894-5

Sedlacek, P., Slaninova, E., Enev, V., Koller, M., Nebesarova, J., Marova, I., Hrubanova, K., Krzyzanek, V., Samek, O., Obruca, S. 2019. What keeps polyhydroxyalkanoates in bacterial cells amorphous? A derivation from stress exposure experiments. Appl. Microbiol. Biotechnol. 103(4). 1905-1917. DOI: 10.1007/s00253-018-09584-z

Segura, D. and Espín, G., 2004. Inactivation of pycA, encoding pyruvate carboxylase activity, increases poly-β-hydroxybutyrate accumulation in *Azotobacter vinelandii* on solid medium. Applied Genetics and Molecular Biotechnology. 65. 414-418. DOI: 10.1007/s00253-004-1611-9

Segura, D., Guzmán, J. and Espín, G., 2003. *Azotobacter vinelandii* mutants that overproduce poly-beta-hydroxybutyrate or alginate. Appl. Microbiol. Biotechnol. 63(2). 159-163. DOI: 10.1007/s00253-003-1397-1

Sen, S. K. and Raut, S., 2015. Microbial degradation of low density polyethylene (LDPE): A review. Journal of Environmental Chemical Engineering. 3(1). 462-473. DOI: 10.1016/j.jece.2015.01.003

Sendra, M., Staffieri, E., Yeste, M. P., Moreno-Garrido, I., Gatica, J. M., Corsi, I., and Blasco, J. 2019. Are the primary characteristics of polystyrene nanoplastics responsible for toxicity and ad/absorption in the marine diatom *Phaeodactylum tricornutum*?. Environmental Pollution. 249. 610-619. DOI: 10.1016/j.envpol.2019.03.047

Senuma, W., Takemura, C., Hayashi, K., Ishikawa, S., Kiba, A., Ohnishi, K., Kai, K., & Hikichi, Y. 2020. The putative sensor histidine kinase PhcK is required for the full expression of phcA encoding the global transcriptional regulator to drive the quorum-sensing circuit of *Ralstonia solanacearum* strain OE1-1. Molecular Plant Pathology. 21(12). 1591-1605. DOI: 10.1111/mpp.12998

Shamala, T. R., Divyashree, M. S., Davis, R., Latha Kumari, K. S., N. Vijayendra, S. V., & Raj, B. 2009. Production and characterization of bacterial polyhydroxyalkanoate copolymers and evaluation of their blends by fourier transform infrared spectroscopy and scanning electron microscopy. Indian J. Microbiol. 49(3). 251-258. DOI: 0.1007/s12088-009-0031-z

Sharma, P. K., Fu, J., Spicer, V., Krokhin, O. V., Cicek, N., Sparling, R., & Levin, D. B. 2016. Global changes in the proteome of *Cupriavidus necator* H16 during poly-(3-hydroxybutyrate) synthesis from various biodiesel by-product substrates. AMB Express. 6. DOI: 10.1186/s13568-016-0206-z

Sharpe, M. E., Hauser, P. M., Sharpe, R. G. and Errington, J., 1998. *Bacillus subtilis* Cell Cycle as Studied by Fluorescence Microscopy: Constancy of Cell Length at Initiation of DNA Replication and Evidence for Active Nucleoid Partitioning. Journal of Bacteriology. 180(3). 547-555. DOI: 10.1128/jb.180.3.547-555.1998

Shimizu, R., Dempo, Y., Nakayama, Y., Nakamura, S., Bamba, T., Fukusaki, E., and Fukui, T. 2015. New Insight into the Role of the Calvin Cycle: Reutilization of CO_2 Emitted through Sugar Degradation. Scientific Reports. 5. DOI: 10.1038/srep11617

Shishatskaya, E.I., Volova, T.G., Efremov, S.N., Puzyr, A. P., Mogil'naya, O. A. 2002. Tissue Response to Biodegradable Suture Threads Made of Polyhydroxyalkanoates. Biomedical Engineering. 36. 210-217. DOI: 10.1023/A:1021184119268

Shishatskaya, E. I., Volova, T. G., Puzyr, A. P., Mogilnaya, O. A., Efremov, S. N. 2004. Tissue response to the implantation of biodegradable polyhydroxyalkanoate sutures. J. Mater. Sci. Mater. Med. 15(6). 719-728. DOI: 10.1023/b:jmsm.0000030215.49991.0d

Shishatskaya, E. I., Voinova, O. N., Goreva, A. V., Mogilnaya, O. A., Volova, T. G. 2008. Biocompatibility of polyhydroxybutyrate microspheres: in vitro and in vivo evaluation. Journal of materials science. Materials in medicine. 19(6). 2493–2502. DOI: 10.1007/s10856-007-3345-6

Shrivastav, A., Mishra, S. K., Shethia, B., Pancha, I., Jain, D., and Mishra, S. 2010. Isolation of promising bacterial strains from soil and marine environment for polyhydroxyalkanoates (PHAs) production utilizing Jatropha biodiesel byproduct. International Journal of Biological Macromolecules. 47(2). 283-287. DOI: 10.1016/j.ijbiomac.2010.04.007

Shubhra, Q. T. H. and Alam, A. K. M. M. 2013. Mechanical properties of polypropylene composites A review. Journal of Thermoplastic Composite Materials. 26(3). 362-391. DOI: 10.1177/0892705711428

Shum-Tim, D., Stock, U., Hrkach, J., Shinoka, T., Lien, J., Moses, M. A., Stamp, A., Taylor, G., Moran, A. M., Landis, W., Langer, R., Vacanti, J. P., and Mayer, J. E. 1999. Tissue Engineering of Autologous Aorta Using a New Biodegradable Polymer. Ann. Thorac. Surg. 68(6). DOI: 2299-2304. 10.1016/S0003-4975(99)01055-3

Singhvi, M. S., Zinjarde, S. S. and Gokhale, D. V. 2019. Polylactic acid: synthesis and biomedical applications. Journal of Applied Microbiology. 127(6). 1612-1626. DOI: 10.1111/jam.14290

Siracusa, V., Genovese, L., Munari, A. and Lotti, N., 2017. How Stress Treatments Influence the Performance of Biodegradable Poly(Butylene Succinate)-Based Copolymers with Thioether Linkages for Food Packaging Applications. Materials (Basel). 10(9). DOI: 10.3390/ma10091009

Sky, 2021. Sky Ocean rescue. Available at: https://www.skyoceanrescue.com/ (Accessed 22 08 2021).

Smith, M., Love, D., Rochman, C. M. and Neff, R. A., 2018. Microplastics in Seafood and the Implications for Human Health. Curr. Environ. Health. Rep. 5(3). 375-386. DOI: 10.1007/s40572-018-0206-z

Sodian, R., Sperling, J. S., Martin, D. P., Stock, U., Mayer, J. E. Jr., Vacanti, J.. P. 1999. Tissue Engineering of a Trileaflet Heart Valve—Early In Vitro Experiences with a Combined Polymer. Tissue Engineering. 5(5). DOI: 489-494. 10.1089/ten.1999.5.489

Solis, M. and Silveira, S. 2020. Technologies for chemical recycling of household plastics - A technical review and TRL assessment. Waste Manag.105. 128-138. DOI: 10.1016/j.wasman.2020.01.038

Solopova, A., Weissing, F. J., Bachmann, H., Teusink, B., Kok, J., & Kuipers, O. P. 2014. Bet-hedging during bacterial diauxic shift. Proc. Natl. Acad. Sci. USA. 111(20). 7427-7432. DOI: 10.1073/pnas.1320063111

Song, J. H., Murphy, R. J., Narayan, R. and Davies, G. B. H. 2009. Biodegradable and compostable alternatives to conventional plastics. Phil. Trans. R. Soc. B. 364. 2127-2139. DOI: 10.1098/rstb.2008.0289

Sperber, A. M. and Herman, J. K., 2017. Metabolism Shapes the Cell. Journal of Bacteriology.199(11). DOI: 10.1128/JB.00039-17

Spitslsky , Z. and Bleha, T., 2004. Elastic properties of poly(hydroxybutyrate) molecules. Macromol. Biosci. 4(6). 609-609. DOI: 10.1111/jam.14290

Stern, C., Frick, A. and Weickert, G. (2007), Relationship between the structure and mechanical properties of polypropylene: Effects of the molecular weight and shear-induced structure. J. Appl. Polym. Sci. 103. 519-533. DOI: 10.1002/app.24156

Stevenson, K., McVey, A., Clark, I., Swain, P. S., Pilizota, T. 2016. General calibration of microbial growth in microplate readers. Scientific Reports. 6. 38828. DOI: 10.1038/srep38828

Stratford, J. P., Edwards, C. L. A., Ghanshyam, M. J., Malyshev, D., Delise, M. A.., Hayashi, Y., Asally, M. 2019. Electrically induced bacterial membrane-potential dynamics correspond to cellular proliferation capacity. Proc. Natl. Acad. Sci. USA. 116(19). 9552-9557. DOI: 10.1073/pnas.1901788116.

Stubbe, J., Tian, J., He, A., Sinskey, A. J., Lawrence, A. G., Liu, P. 2005. Nontemplate-dependent polymerization processes: polyhydroxyalkanoate synthases as a paradigm. Annu. Rev. Biochem. 74. 433-480. DOI: 10.1146/annurev.biochem.74.082803.133013

Sun, Z., Ramsay, J. A., Guay, M., Ramsay, B. A. 2007. Fermentation process development for the production of medium-chain-length poly-3-hyroxyalkanoates. Appl. Microbiol. Biotechnol. 75:3. 475-485. DOI: 10.1007/s00253-007-0857-4

Szatmári, D., Sárkány, P., Kocsis, B., Nagy, T., Miseta, A., Barkó, S., Longauer, B., Robinson, R. C., and Nyitrai, M. (2020). Intracellular ion concentrations and cation-dependent remodelling of bacterial MreB assemblies. Scientific Reports. 10. DOI: 10.1038/s41598-020-68960-w

Sznajder, A. and Jendrossek, D., 2014. To Be or Not To Be a Poly(3-Hydroxybutyrate) (PHB) Depolymerase: PhaZd1 (PhaZ6) and PhaZd2 (PhaZ7) of *Ralstonia eutropha*, Highly Active PHB Depolymerases with No Detectable Role in Mobilization of Accumulated PHB. Appl. Environ. Microbiol. 80(16). 4936-4946. DOI: 10.1128/AEM.01056-14

Tachibana, Y., Masuda, T., Funabashi, M. and Kunioka, M., 2010. Chemical Synthesis of Fully Biomass-Based Poly(butylene succinate) from Inedible-Biomass-Based Furfural and Evaluation of Its Biomass Carbon Ratio. Biomacromolecules. 11(10). 2760-2765. DOI: 10.1021/bm100820y

Tamer, I. M., Moo-Young, M. and Chisti, Y. 1998. Disruption of *Alcaligenes latus* for Recovery of Poly(β-hydroxybutyric acid): Comparison of High-Pressure Homogenization, Bead Milling, and Chemically Induced Lysis. Ind. Eng. Chem. Res. 37(5). 1807-1814. DOI: 10.1021/ie9707432

Tanadchangsaeng, N. and Yu, J., 2012. Microbial synthesis of polyhydroxybutyrate from glycerol: gluconeogenesis, molecular weight and material properties of biopolyester. Biotechnol. Bioeng. 109(11). 2808-2818. DOI: 10.1002/bit.24546

Tchieu, J. H., Norris, V., Edwards, J. S. and Saier Jr, H. 2001. The Complete Phosphotransferase System in *Escherichia coli*. J. Mol. Microbiol. Biotechnol. 3(3). 329-346.

Thompson, R. C., Swan, S. H., & Moore, C. J. (2009). Our plastic age. Philosophical Transactions of the Royal Society B: Biological Sciences. 364. 1526. 1973-1976. DOI: 10.1098/rstb.2009.0054

Tian, J., Sinskey, A. J. and Stubbe, J., 2020. Kinetic Studies of Polyhydroxybutyrate Granule Formation in *Wautersia eutropha* H16 by Transmission Electron Microscopy. Journal of Bacteriology. 187(11). 3814-3824. DOI: 10.1128/JB.187.11.3814-3824.2005

Tikhomirova, T. S., Taraskevich, M. S., Ponomarenko, O. V. 2018. The role of laboratory-scale bioreactors at the semi-continuous and continuous microbiological and biotechnological processes. Appl. Microbiol. Biotechnol.102(17). 7293-7308. DOI: 10.1007/s00253-018-9194-z

Tokiwa, Y., Calabia, B. P., Ugwu, C. U. and Aiba, S. 2009. Biodegradability of Plastics. Int. J. Mol. Sci. 10(9). 3722-3742.

Toro, E. and Shapiro, L. 2010. Bacterial chromosome organization and segregation. Cold Spring Harb Perspect Biol. 2(2). a000349. DOI: 0.1101/cshperspect.a000349

Tribelli, P. M. and López, N. I.,2011. Poly(3-hydroxybutyrate) influences biofilm formation and motility in the novel Antarctic species *Pseudomonas extremaustralis* under cold conditions. Extremophiles. 15(5). 541-547. DOI: 10.1007/s00792-011-0384-1

Tripathi, L., Wu, P., Chen, J., & Chen, Q. (2012). Synthesis of Diblock copolymer poly-3-hydroxybutyrate -block-poly-3-hydroxyhexanoate [PHB-b-PHHx] by a ß-oxidation weakened *Pseudomonas putida* KT2442. Microbial Cell Factories, 11, 44. DOI: 10.1186/1475-2859-11-44

Trunk, T., Khalil, H. S. and Leao, J. C., 2018. Bacterial autoaggregation. AIMS Microbiol. 4(1). 140-164.

Tsang, J. 2017. Bacterial plasmid addiction systems and their implications for antibiotic drug development. Postdoc J. 5(5). 3-9.

Tyo, K. E., Zhou, H. and Stephanopoulos, G. N. 2006. High-Throughput Screen for Poly-3-Hydroxybutyrate in *Escherichia coli* and *Synechocystis* sp. Strain PCC6803. Appl. Environ. Microbiol. 72(5). 3412-3417. DOI: 10.1128/AEM.72.5.3412-3417.2006

Uchino, K. and Saito, T., 2006. Thiolysis of Poly(3-hydroxybutyrate) with Polyhydroxyalkanoate Synthase from *Ralstonia eutropha*. The Journal of Biochemistry. 139(3). 615-621. DOI: 10.1093/jb/mvj069

Uchino, K., Saito, T. and Jendrossek, D. 2008. Poly(3-Hydroxybutyrate) (PHB) Depolymerase PhaZa1 Is Involved in Mobilization of Accumulated PHB in *Ralstonia eutropha* H16. APPLIED AND ENVIRONMENTAL MICROBIOLOGY. 74(4). 1058-1063. DOI: 10.1128/AEM.02342-07

Universal Recycling, 2021. Equestrian Surfaces. Available at: https://www.universalrecyclingcompany.co.uk/equestrian-surfaces/ (Accessed 7 8 2021).

University of Stuttgart, 2009. The PHA Depolymerase Engineering Database. Available at: http://www.ded.uni-stuttgart.de/ (Accessed 26 8 2021).

USEPA. 1997. NEW CHEMICALS ENVIRONMENTAL TECHNOLOGY INITIATIVE AUTOMOTIVE REFINISHING INDUSTRY ISOCYANATE PROFILE. Washington D.C.: U.S. Environmental Protection Agency.

van Boxtel, C., van Heerden, J. H., Nordholt, N., Schmidt, P., & Bruggeman, F. J. 2017. Taking chances and making mistakes: non-genetic phenotypic heterogeneity and its consequences for surviving in dynamic environments. Journal of the Royal Society. 14(132). 2017014. DOI: 10.1098/rsif.2017.0141

Vandewijngaarden, J., Wauters, R., Murariu, M. 2016. Poly(3-hydroxybutyrate-co-3-hydroxyhexanoate)/Organomodified Montmorillonite Nanocomposites for Potential Food Packaging Applications. J. Polym. Environ. 24. 104-118. DOI: 10.1007/s10924-016-0751-1

Verlinden, R. A., Hill, D. J., Kenward, M. A., Williams, C. D., Radecka, I. 2007. Bacterial synthesis of biodegradable polyhydroxyalkanoates. Journal of Applied Microbiology. 102. 1437-1449. DOI: 10.1111/j.1365-2672.2007.03335.x

Vidal-Mas, J., Resina-Pelfort Haba, E., Comas, J., Manresa, A., Vives-Rego, J. 2001. Rapid flow cytometry – Nile red assessment of PHA cellular content and heterogeneity in cultures of Pseudomonas

aeruginosa 47T2 (NCIB 40044) grown in waste frying oil. Antonie van Leeuwenhoek. 80(1). 57-63. DOI: 10.1023/a:1012208225286

Vijaranakul, U., Nadakavukaren, M. J., Wilkinson, B. J., & Jayaswal, R. K. (1995). Increased cell size and shortened peptidoglycan interpeptide bridge of NaCl-stressed *Staphylococcus aureus* and their reversal by glycine betaine. Journal of Bacteriology. 177(17). 5116-5121. DOI: 10.1128/jb.177.17.5116-5121.1995

Villano, M., Beccari, M., Dionisi, D., Lampis, S., Miccheli, A., Vallini, G., and Majone, M. 2010. Effect of pH on the production of bacterial polyhydroxyalkanoates by mixed cultures enriched under periodic feeding. PROCESS BIOCHEMISTRY. 45(5). 714-723. DOI: 10.1016/j.procbio.2010.01.008

Virolle, C., Goldlust, K., Djermoun, S., Bigot, S., and Lesterlin, C. 2020. Plasmid Transfer by Conjugation in Gram-Negative Bacteria: From the Cellular to the Community Level. Genes (Basel). 11(11). DOI: 10.3390/genes11111239

Vizcaino-Caston, I., Kelly, C. A., Fitzgerald, A. V., Leeke, G. A., Jenkins, M., and Overton, T. W. 2016. Development of a rapid method to isolate polyhydroxyalkanoates from bacteria for screening studies. Journal of Bioscience and Bioengineering. 121:1. 101-104. DOI: 10.1016/j.jbiosc.2015.04.021

Voloshin, S. A. and Kaprelyants, A. S., 2004. Cell-cell interactions in bacterial populations. Biochemistry (Mosc). 69(11). 1268-1275. DOI: 10.1007/s10541-005-0072-9

Wahl, A., Schuth, N., Pfeiffer, D., Nussberger, S., Jendrossek, D. 2012. PHB granules are attached to the nucleoid via PhaM in Ralstonia eutropha. BMC Microbiol. 12. 262. DOI: 10.1186/1471-2180-12-262

Wang, Z., Itoh, Y., Hosaka, Y., Kobayashi, I., Nakano, Y., Maeda, I., Umeda, F., Yamakawa, J., Nishimine, M., Suenobu, T., Fukuzumi, S., Kawase, M., and Yagi, K. 2003. Mechanism of enhancement effect of dendrimer on transdermal drug permeation through polyhydroxyalkanoate matrix. Journal of Bioscience and Bioengineering, 96(6), 537-540. DOI: 10.1016/S1389-1723(04)70146-2

Wang, Y., Yang, F., Wu, Q., Cheng, Y., Yu, P. H., Chen, J., and Chen, G. 2005. Effect of composition of poly(3-hydroxybutyrate-co-3- hydroxyhexanoate) on growth of fibroblast and osteoblast. Biomaterials. 26(7). 755-761. DOI: 10.1016/j.biomaterials.2004.03.023

Wang, Y., Bian, Y.-Z., Wu, Q. and Chen, G.-Q., 2008. Evaluation of three-dimensional scaffolds prepared from poly(3-hydroxybutyrate-co-3-hydroxyhexanoate) for growth of allogeneic chondrocytes for cartilage repair in rabbits. Biomaterials. 29. 2858-2868. DOI: 10.1016/j.biomaterials.2008.03.021

Wang, Q., Yu, H., Xia, Y., Kang, Z., and Qi, Q. 2009. Complete PHB mobilization in Escherichia coli enhances the stress tolerance: a potential biotechnological application. Microbial cell factories. 8(47). DOI: 10.1186/1475-2859-8-47

Wang, Y., Chen, R., Cai, J., Liu, Z., Zheng, Y., Wang, H., Li, Q., and He, N. 2013. Biosynthesis and Thermal Properties of PHBV Produced from Levulinic Acid by *Ralstonia eutropha*. PLoS ONE. 8(4). DOI: 10.1371/journal.pone.0060318

Wang, Y., Yin, J., & Chen, G. (2014). Polyhydroxyalkanoates, challenges and opportunities. Current Opinion in Biotechnology. 30. 59-65. DOI: 10.1016/j.copbio.2014.06.001

Wang, X., Oehmen, A., Freitas, E. B., Carvalho, G., and Reis, M. A. 2017. The link of feast-phase dissolved oxygen (DO) with substrate competition and microbial selection in PHA production. Water Reseach. 112. 269-278. DOI: 10.1016/j.watres.2017.01.064

Wang, D., Luo, F., Shen, Z., Wu, X., Qi, Y. (2017). A study on the crystallization behavior and mechanical properties of poly(ethylene terephthalate) induced by chemical degradation nucleation. RSC Adv. 7. 37139-37147. DOI: 10.1039/C7RA06823A

Wang, X., Bengtsson, S., Oehmen, A., Carvalho, G., Werker, A., and Reis, M. A. 2019. Application of dissolved oxygen (DO) level control for polyhydroxyalkanoate (PHA) accumulation with concurrent nitrification in surplus municipal activated sludge. N. Biotechnol. 25(50). 37-43. DOI: 10.1016/j.nbt.2019.01.003

Wang, J., Ma, W., Fang, Y., Zhang, H., Liang, H., Liu, H., Wang, T., Chen, S., Ji, J., Wang, X. 2021. Engineering the Outer Membrane Could Facilitate Better Bacterial Performance and Effectively Enhance Poly-3-Hydroxybutyrate Accumulation. Applied and Environmental Microbiology. 87(23). e0138921. DOI: 10.1128/aem.01389-21

Warnecke, T., and Gill, R. T. (2005). Organic acid toxicity, tolerance, and production in *Escherichia coli* biorefining applications. Microbial Cell Factories. 4. 25. DOI: 10.1186/1475-2859-4-25

Waters, C. M. and Bassler, B. L. 2005. Quorum sensing: cell-to-cell communication in bacteria. Annu. Rev. Cell. Dev. Biol. 21. 319-346. DOI: 10.1146/annurev.cellbio.21.012704.131001

Webb, C., and Kamat, S. P. (1993). Improving fermentation consistency through better inoculum preparation. World journal of microbiology & biotechnology. 9(3). 308–312. DOI: 10.1007/BF00383069

Wen, Q., Ji, Y., Hao, Y., Huang, L., Chen, Z., Sposob, M. (2018). Effect of sodium chloride on polyhydroxyalkanoate production from food waste fermentation leachate under different organic loading rate. Bioresource Technology. 267. 133-140. DOI: 10.1016/j.biortech.2018.07.036

Westerholm, M., Müller, B., Isaksson, S. and Schnürer, A. 2015. Trace element and temperature effects on microbial communities and links to biogas digester performance at high ammonia levels. Biotechnology for Biofuels. 8. DOI: 10.1186/s13068-015-0328-6

Westfall, C. S. and Levin, P. A., 2018. Comprehensive analysis of central carbon metabolism illuminates connections between nutrient availability, growth rate, and cell morphology in *Escherichia coli*. PLoS Genet. 14(2). e1007205. DOI: 10.1371/journal.pgen.1007205

Wong, Y., Brigham, C. J., Rha, C., Sinskey, A. J., and Sudesh, K. 2012. Biosynthesis and characterization of polyhydroxyalkanoate containing high 3-hydroxyhexanoate monomer fraction from crude palm kernel oil by recombinant *Cupriavidus necator*. Bioresource Technology. 121. 320-327. DOI: 10.1016/j.biortech.2012.07.015

Woodruff, M. A. and Hutmacher, D. W., 2010. The return of a forgotten polymer - Polycaprolactonein the 21st century. Progress in Polymer Science. 35(10). 1217-1256. DOI: 0.1016/j.progpolymsci.2010.04.002

Wu, H., Fan, Z., Jiang, X., Chen, J., and Chen, Q. 2016. Enhanced production of polyhydroxybutyrate by multiple dividing *E. coli*. Microbial Cell Factories. 15. DOI: 10.1186/s12934-016-0531-6

Xu, J., Guo, B., Yang, R., Wu, Q., Chen, G., and Zhang, Z. 2002. *In situ* FTIR study on melting and crystallization of polyhydroxyalkanoates. Polymer. 43(25). 6893-6899. DOI: 10.1016/S0032-3861(02)00615-8

Xu, X., Li, X., Peng, S., Xiao, J., Liu, C., Fang, G., Chen, K. C., and Chen, G. 2010. The behaviour of neural stem cells on polyhydroxyalkanoate nanofiber scaffolds. Biomaterials. 31(14). 3967-3975. DOI: 10.1016/j.biomaterials.2010.01.132

Xu, S. Y., Zhang, H., He, P. J., Shao, L. M. 2011. Leaching behaviour of bisphenol A from municipal solid waste under landfill environment. Environ. Technol. 32(11-12). 1269-77. DOI: 10.1080/09593330.2010.535175

Yang, T. H., Kim, T. W., Kang, H. O., Lee, S. H., Lee, E. J., Lim, S.. C, Oh, S. O., Song, A. J., Park, S. J., Lee, S. Y. 2010. Biosynthesis of Polylactic Acid and Its Copolymers Using Evolved Propionate CoA Transferase and PHA Synthase. Biotechnology and Bioengineering. 105(1). 150-160. DOI: 10.1002/bit.22547.

Yang, Y. H., Brigham, C., Willis, L., Rha, C., Sinskey, A.. 2011. Improved detergent-based recovery of polyhydroxyalkanoates (PHAs). Biotechnol. Lett. 33(5). 937-942. DOI: 10.1007/s10529-010-0513-4

Yasotha, K., Aroua, M. K., Ramachandran, K. B. and Tan, I. K. P., 2006. Recovery of Medium-Chain-Length Polyhydroxyalkanoates (PHAs) Through Enzymatic Digestion Treatments and Ultrafiltration. Biochemical Engineering Journal. 30(3). 260-288. DOI: 10.1016/j.bej.2006.05.008

Yin, J., Wang, H., Fu, X. Z., Gao, X., Wu, Q., Chen, G. Q. 2015. Effects of chromosomal gene copy number and locations on polyhydroxyalkanoate synthesis by *Escherichia coli* and *Halomonas* sp. Appl. Microbiol. Biotechnol. 99. 5523-5534. DOI: 0.1007/s00253-015-6510-8.

York, G. M., Junker, B. H., Stubbe, J. and Sinskey, A. J., 2001. Accumulation of the PhaP Phasin of *Ralstonia eutropha* Is Dependent on Production of Polyhydroxybutyrate in Cells. J. Bacteriol. 183(14). 4217-4226. DOI: 10.1128/JB.183.14.4217-4226.2001

Zainab-L, I., Uyama, H., Li, C., Shen, Y. and Sudesh, K. 2018. Production of Polyhydroxyalkanoates From Underutilized Plant Oils by *Cupriavidus necator*. Clean – Soil, Air, Water. 46. 1700542. DOI: 10.1002/clen.201700542

Zhang, S., Narrlöw, O., Wawrzynczyk, J. and Dey, E. S. 2004. Poly(3-Hydroxybutyrate) Biosynthesis in the Biofilm of *Alcaligenes eutrophus*, Using Glucose Enzymatically Released from Pulp Fiber Sludge. Appl. Environ. Microbiol. 70(11). 6776-6782. DOI: 10.1128/AEM.70.11.6776-6782.2004

Zhang, L., Shi, Z. Y., Wu, Q. and Chen, G. Q., 2009. Microbial production of 4-hydroxybutyrate, poly-4-hydroxybutyrate, and poly(3-hydroxybutyrate-co-4-hydroxybutyrate) by recombinant microorganisms. Appl. Microbiol. Biotechnol. 84(5). 909-916. DOI: 10.1007/s00253-009-2023-7

Zhang, L., Chiang, W. C., Gao, Q., Givskov, M., Tolker-Nielsen, T., Yang, L., Zhang, G.. 2012. The catabolite repression control protein Crc plays a role in the development of antimicrobial-tolerant subpopulations in *Pseudomonas aeruginosa* biofilms. Microbiology. 158(12). 3014-3019. DOI: 10.1099/mic.0.061192-0

Zhang, W., Chen, C., Cao, R., Maurmann, L., and Li, P. 2015. Inhibitors of Polyhydroxyalkanoate (PHA) Synthases: Synthesis, Molecular Docking, and Implications. ChemBioChem. 16(1). 156-166. DOI: 10.1002/cbic.201402380

Zhang, Z., Zhang, Q., Guan, S., & Shi, H. (2020). Quantitative Connection between Cell Size and Growth Rate by Phospholipid Metabolism. Cells. 9(2). DOI: 10.3390/cells9020391

Zhao, Y., Rao, Z., Xue, Y., Gong, P., Ji, Y., and Ma, Y.2015. Biosynthesis, property comparison, and hemocompatibility of bacterial and haloarchaeal poly(3-hydroxybutyrate-co-3-hydroxyvalerate). Sci. Bull. 60(22). 1901-1910. DOI: 10.1007/s11434-015-0923-8

Zhu, K. and Rock, C. O., 2008. RhlA Converts β-Hydroxyacyl-Acyl Carrier Protein Intermediates in Fatty Acid Synthesis to the β-Hydroxydecanoyl-β-Hydroxydecanoate Component of Rhamnolipids in *Pseudomonas aeruginosa*. J. Bacteriol. 190(9). 3147-3154. DOI: 10.1128/JB.00080-08

Zia, K. M., Bhatti, H. N. and Bhatti, I. A. 2007. Methods for polyurethane and polyurethane composites, recycling and recovery: A review. Reactive and Functional Polymers. 67. 675-692. DOI: 10.1016/j.reactfunctpolym.2007.05.004

Zinn, M., Weilenmann, H.-.-U., Hany, R., Schmid, M. and Egli, T. 2003. Tailored Synthesis of Poly([R]-3-hydroxybutyrate-co-3-hydroxyvalerate) (PHB/HV) in *Ralstonia eutropha* DSM 428. Acta. Biotechnol. 23(2-3). 309-316. DOI. 10.1002/abio.200390039

Chapter 8 Appendix 1

8.1 Full data corresponding to section 3.1

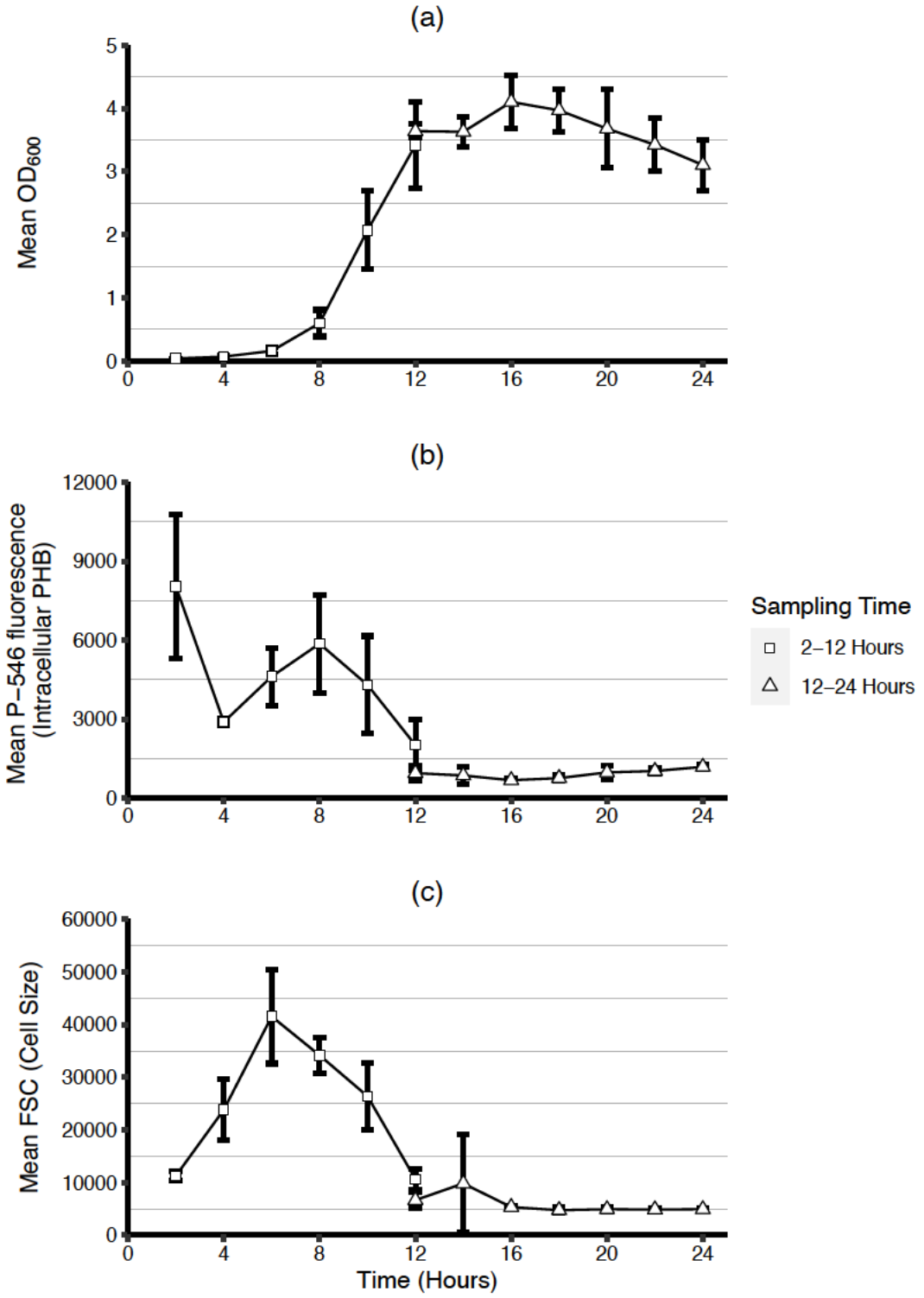


Figure 8.1 - The mean OD_{600}, mean P-546 fluorescence (Intracellular PHB) and mean FSC (cell size) determined by flow cytometry for *C. necator* grown in 0.8% (w/v) ME seed cultures. The experiment was conducted in two independent experiments covering Cells were stained with SYTO62 (1 µM) and P-546 (1µM). Error bars represent SD. n=4.

8.2 Full data corresponding to section 3.2

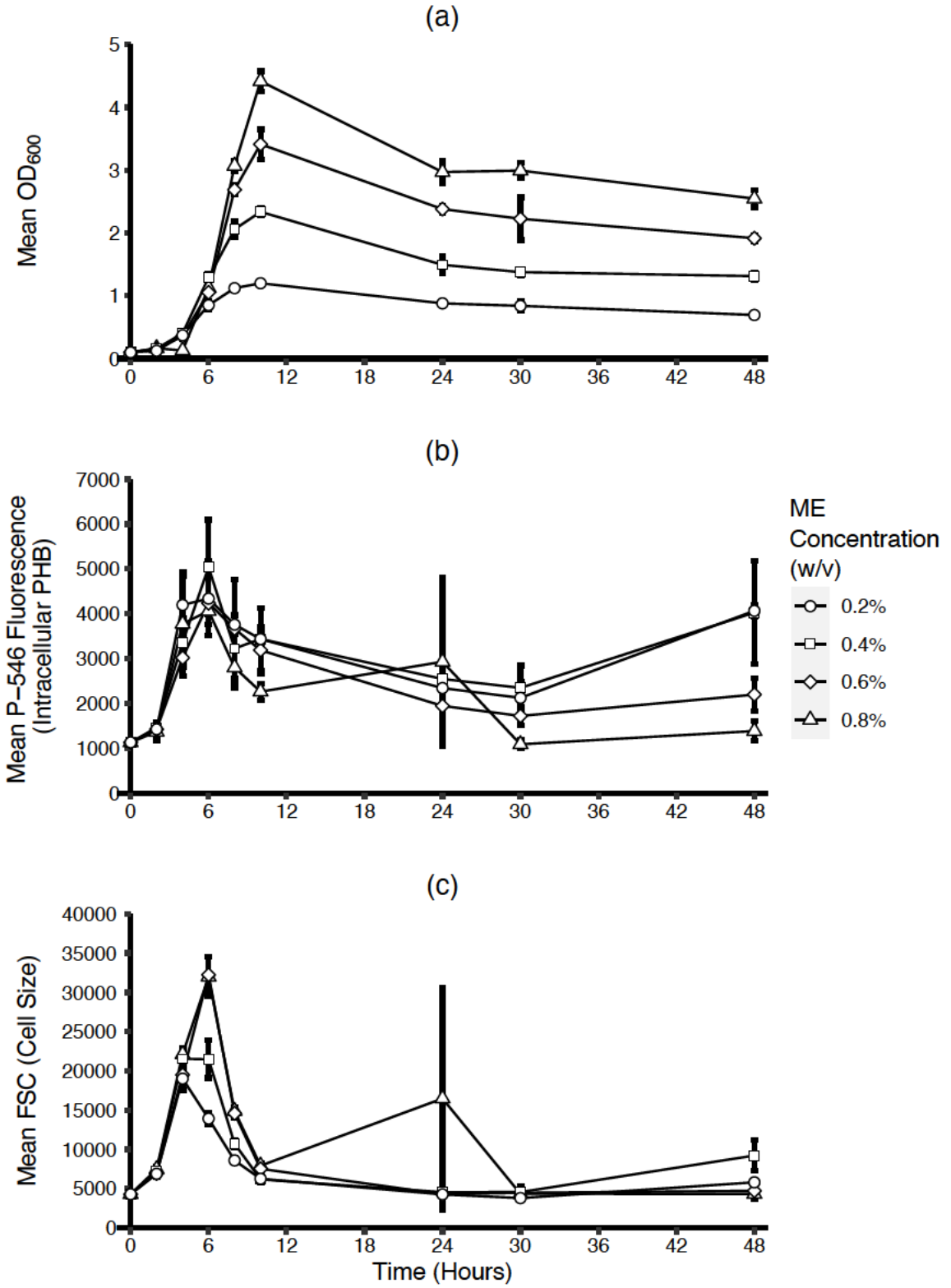


Figure 8.2 - Graphs displaying the (a) mean OD_{600}, (b) mean P-546 fluorescence (Intracellular PHB) content and (c) mean FSC (cell size) of *C. necator* cultures grown in 0.2, 0.4, 0.6 and 0.8% (w/v) ME. Error bars represent SD. n=3.

8.3 Raw data corresponding to section 3.3

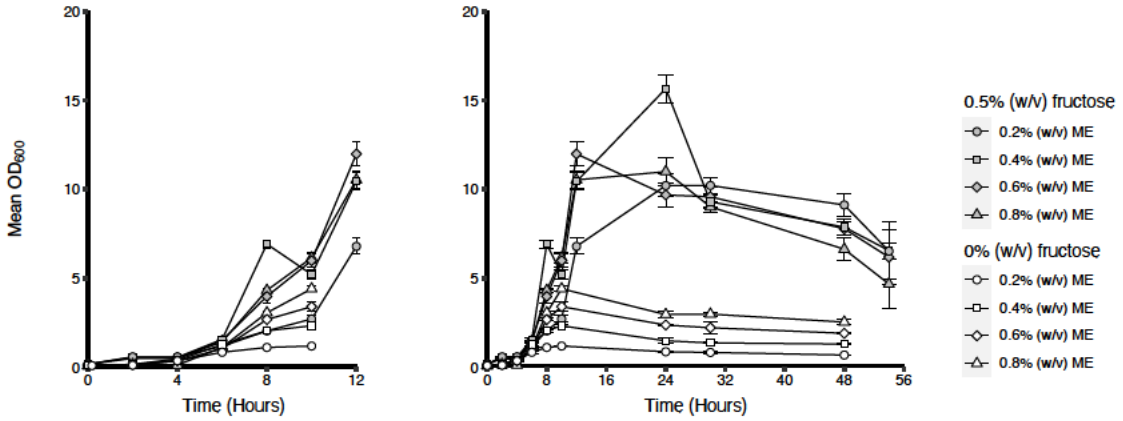


Figure 8.3 - Graphs displaying the mean OD_{600} of *C. necator* cultures grown in 0.2%, 0.4%, 0.6% and 0.8% (w/v) ME with and without 0.5% (w/v) fructose supplementation. Error bars represent SD. n=3 biological replicates.

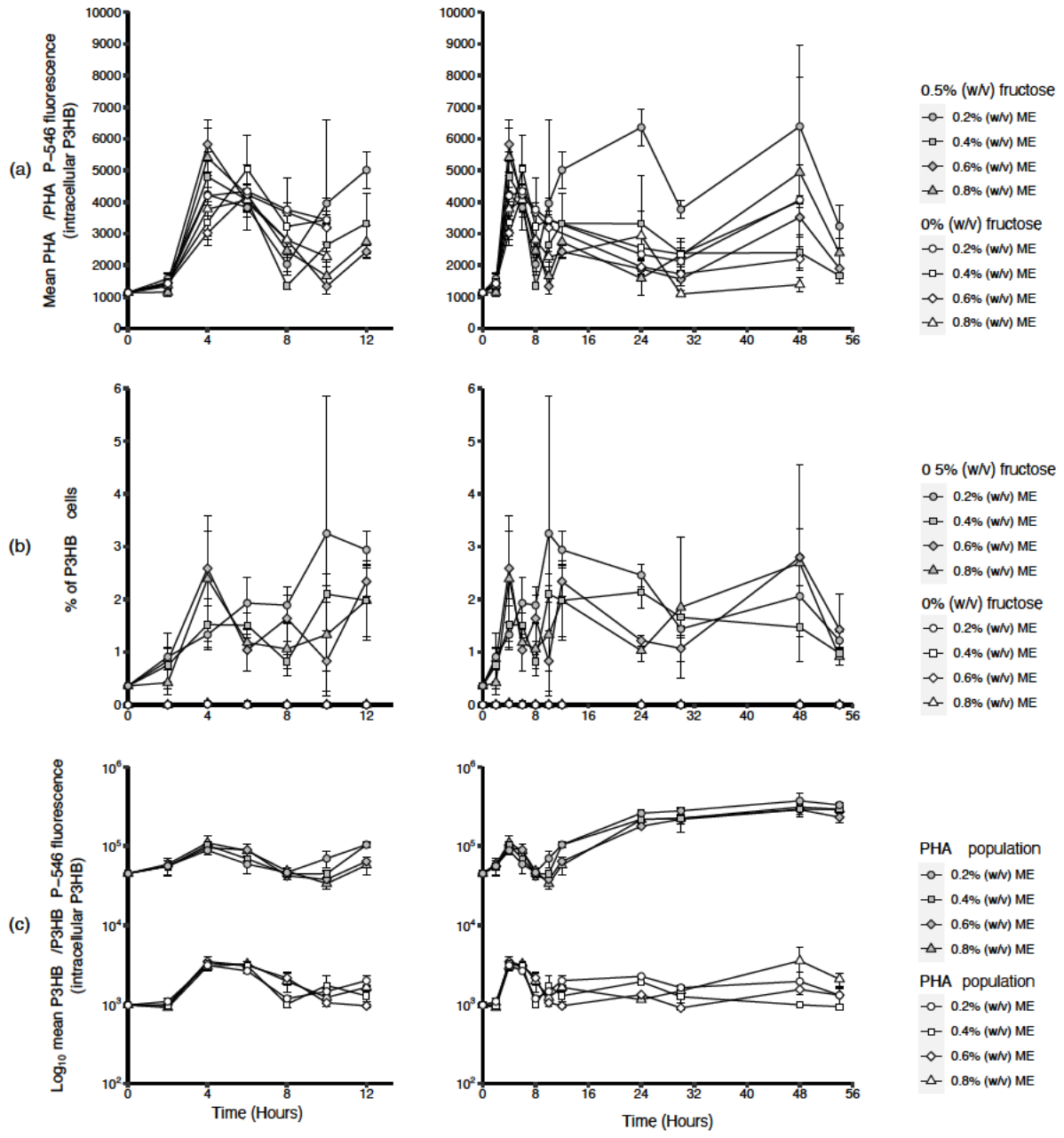


Figure 8.4 - Graphs displaying data for *C. necator* cultures grown in 0.2%, 0.4%, 0.6% and 0.8% (w/v) ME with (a) mean P3HB^{++} P-546 fluorescence (P3HB) and (b) mean percentage of P3HB^{++} cells comparing cultures with and without fructose supplementation and (c) mean P3HB^{+}/P3HB^{++} fluorescence which displays data for cultures only with 0.5% (w/v) fructose. Error bars represent SD. n=3 biological replicates.

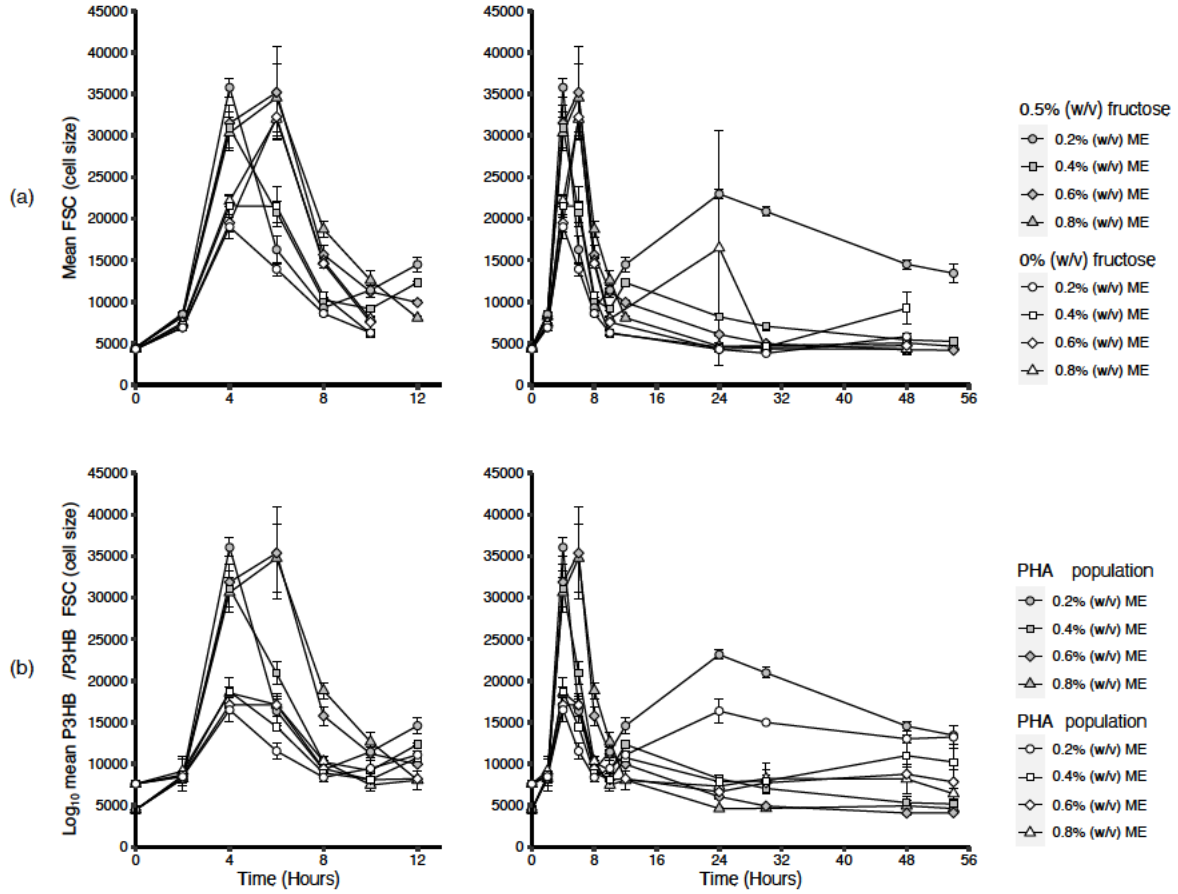


Figure 8.5 - Graphs displaying data for *C. necator* cultures grown in 0.2%, 0.4%, 0.6% and 0.8% (w/v) ME displaying (a) mean overall FSC comparing cultures with and without 0.5% (w/v) fructose supplementation and (b) mean $P3HB^{+}/P3HB^{++}$ FSC for cultures supplemented with 0.5% (w/v) fructose only. Error bars represent SD. n=3 biological replicates.

8.4 Full data corresponding to section 3.3

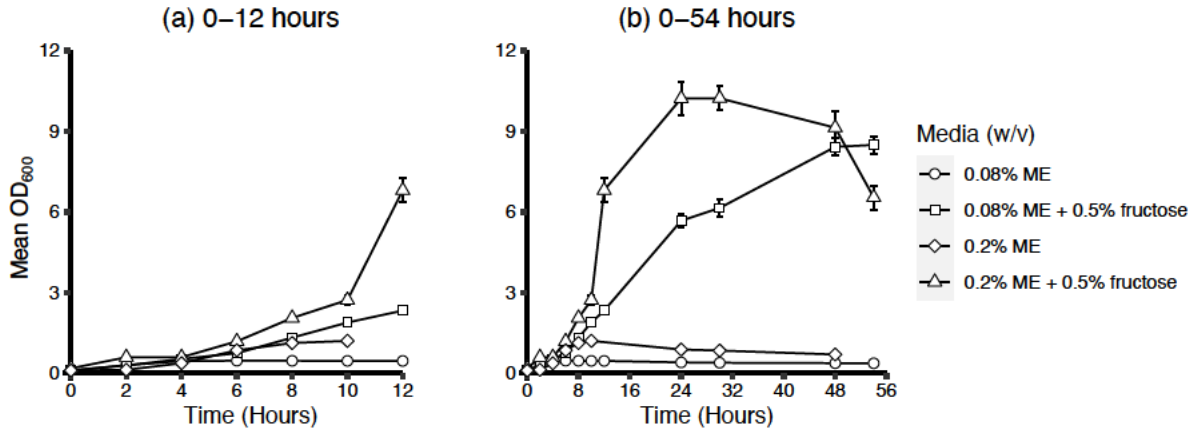


Figure 8.6 – Full OD_{600} data for *C. necator* cultures grown in 0.08% and 0.2% (w/v) ME with and without 0.5% (w/v) fructose supplementation. Error bars represent SD. n = 3 biological replicates.

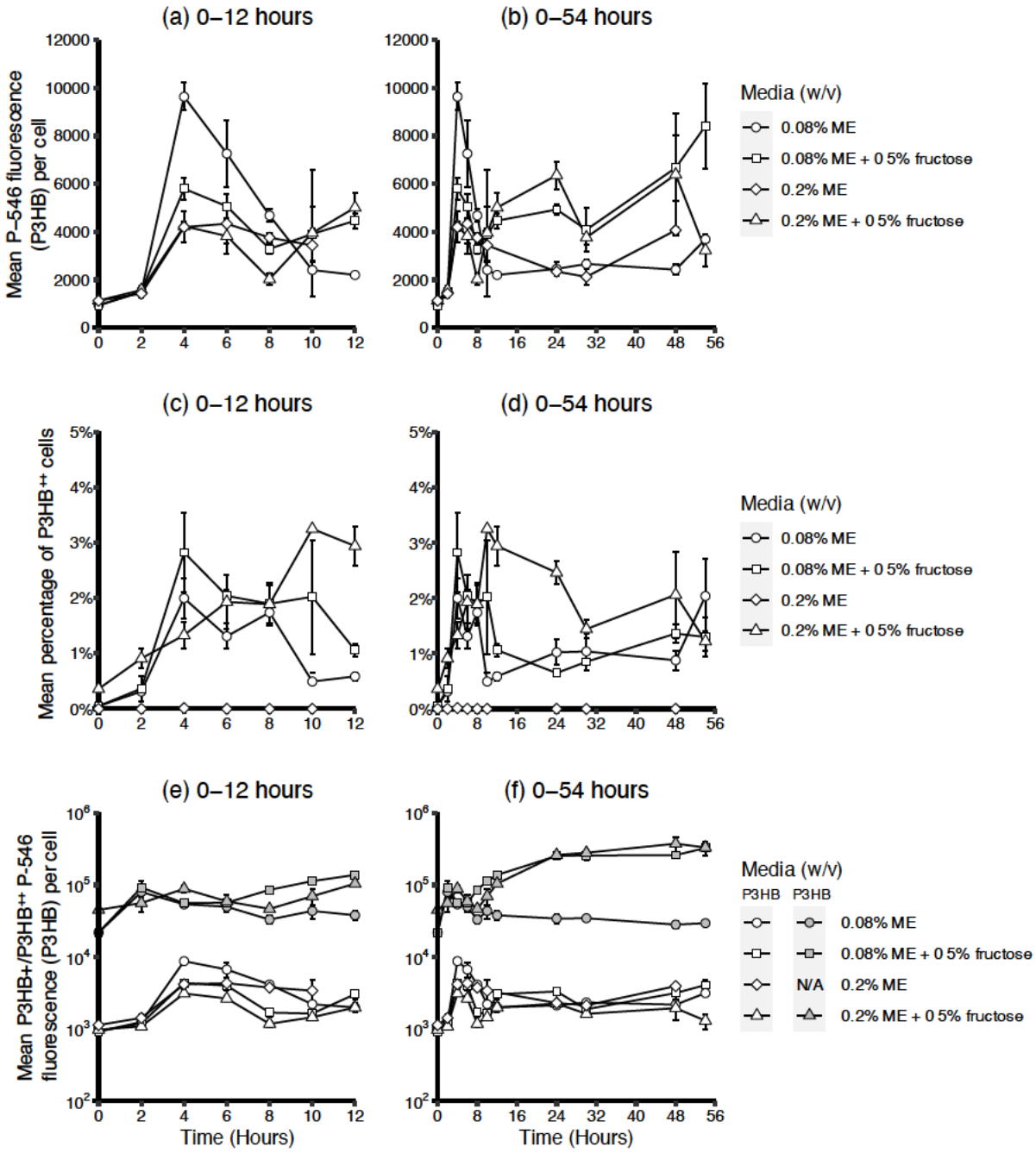


Figure 8.7 – Full data representing mean P-546 (P3HB) per cell (a), mean percentage of P3HB^{++} cells (b) and mean P3HB^{+} and P3HB^{++} P-546 fluorescence (P3HB) (c), for *C. necator* cultures grown in 0.08% and 0.2% (w/v) ME with and without 0.5% (w/v) fructose supplementation. Error bars represent SD. n = 3 biological replicates.

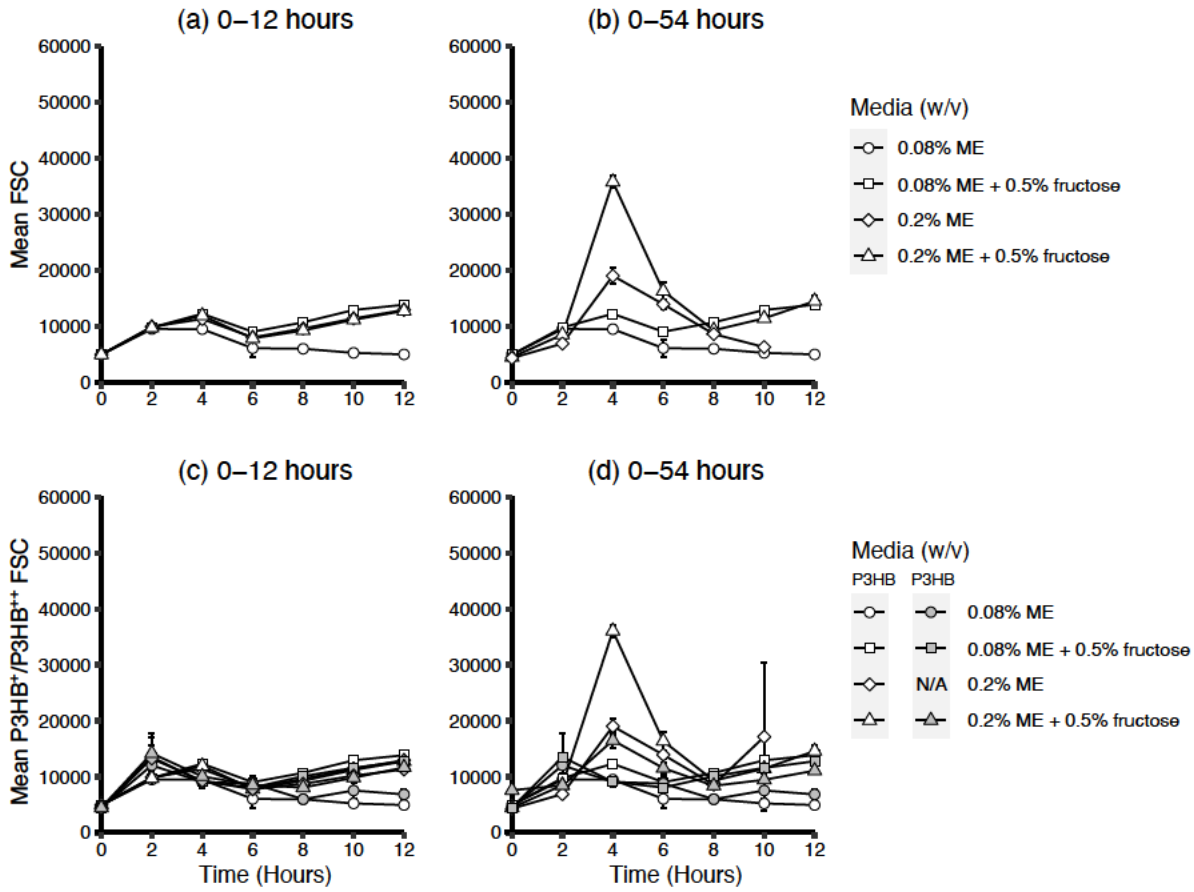


Figure 8.8 – Full data for mean overall (a) and P3HB^{+}/P3HB^{++} (b) FSC (cell size) data for *C. necator* cultures grown in 0.08% and 0.2% (w/v) ME with and without 0.5% (w/v) fructose supplementation. Error bars represent SD. n = 3 biological replicates.

8.5 Full data corresponding to section 3.5

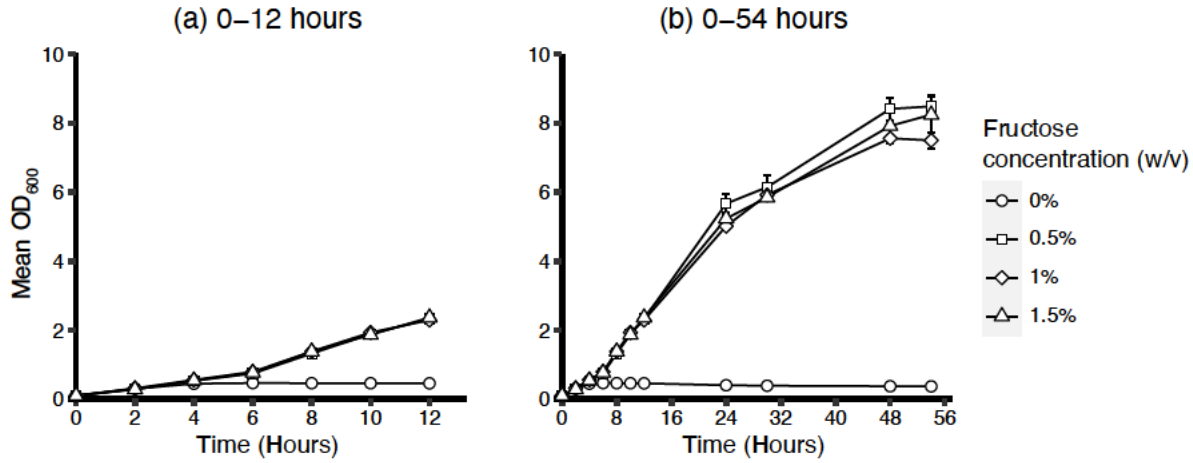


Figure 8.9 – Full OD_{600} data for *C. necator* cultures containing 0.08% (w/v) and supplemented with 0%, 0.5%, 1%, 1.5% (w/v) fructose. Error bars represent SD. n = 3 biological replicates.

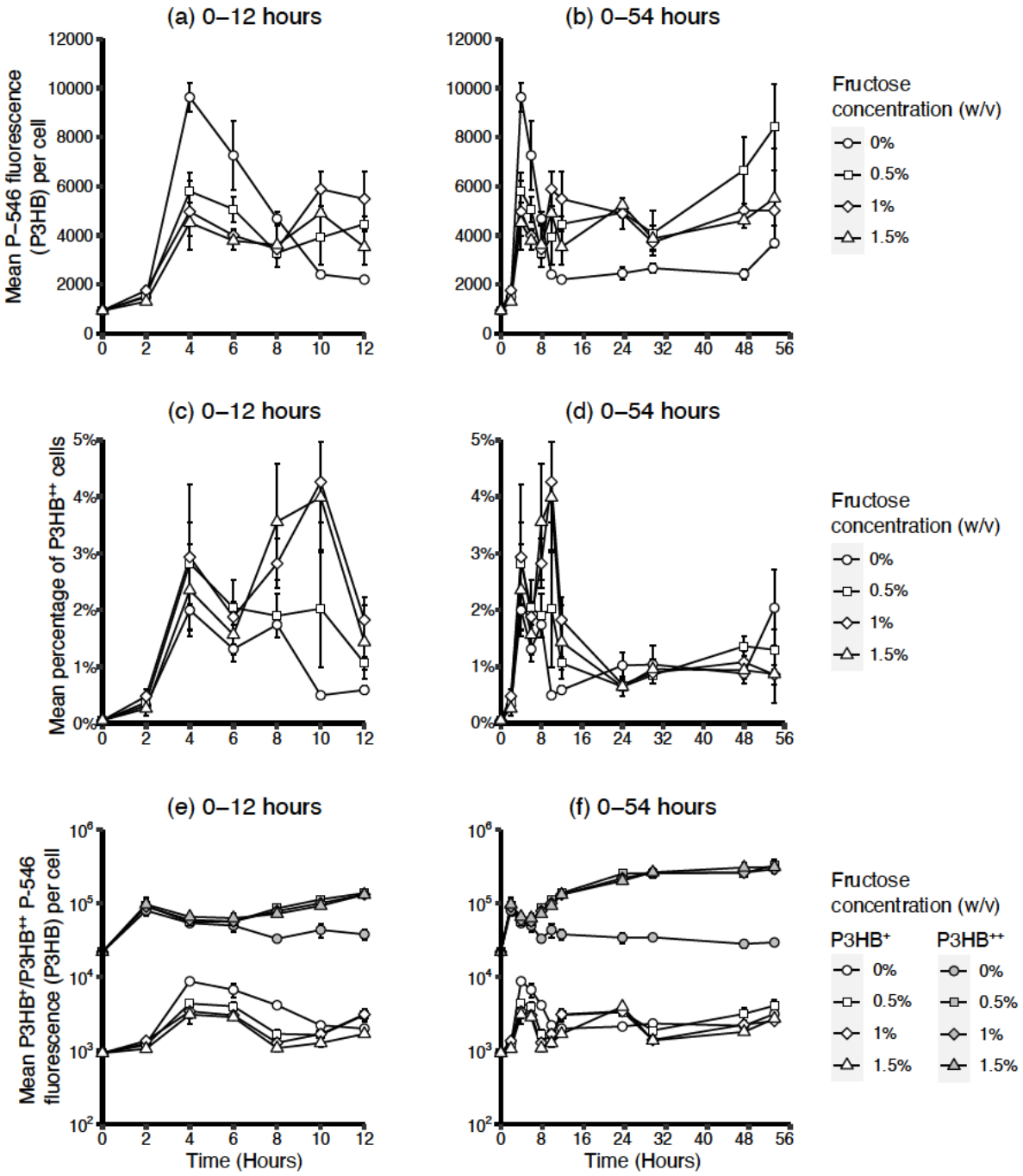


Figure 8.10 - Full data representing mean P-546 (P3HB) per cell (a), mean percentage of P3HB^{++} cells (b) and mean P3HB^{+} and P3HB^{++} P-546 fluorescence (P3HB) (c) for *C. necator* cultures containing 0.08% (w/v) and supplemented with 0%, 0.5%, 1%, 1.5% (w/v) fructose. Error bars represent SD. n = 3 biological replicates.

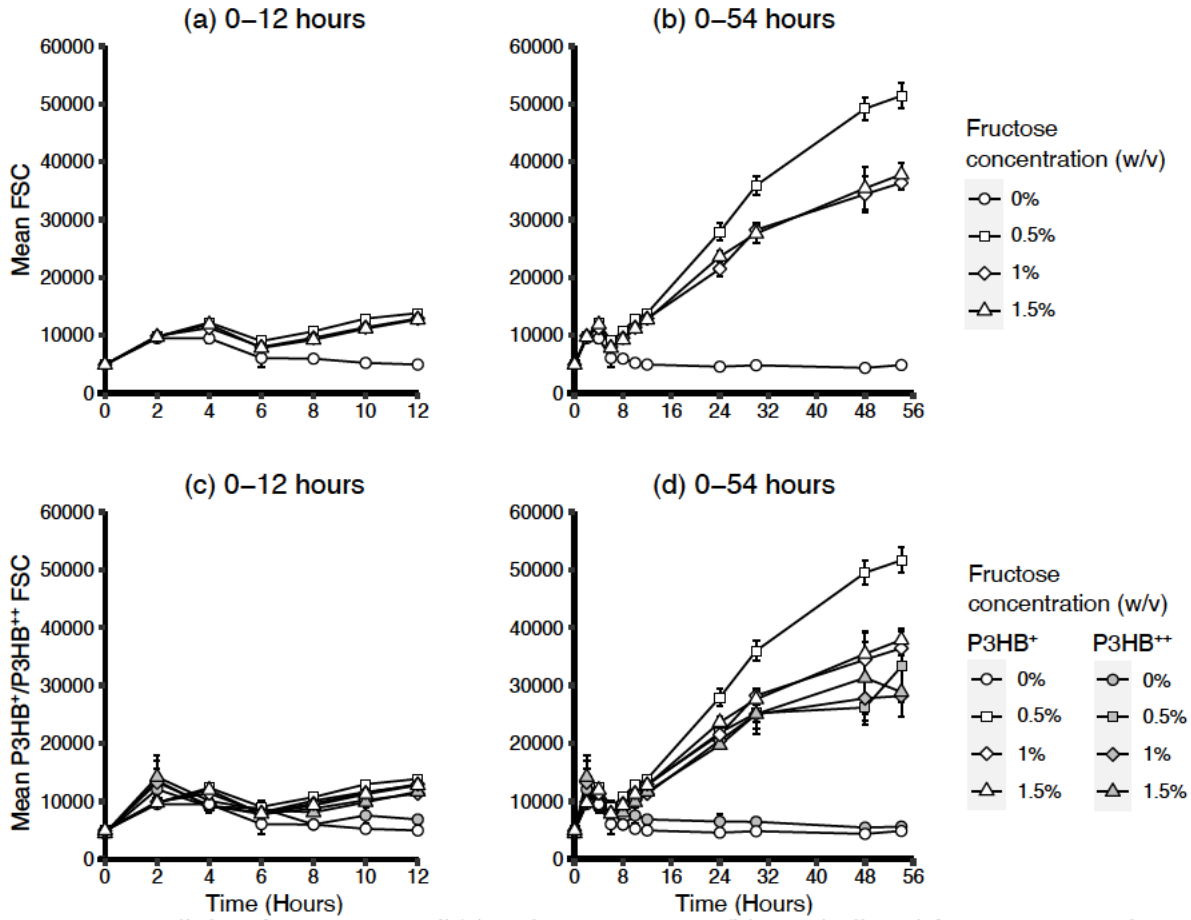


Figure 8.11 - Full data for mean overall (a) and P3HB^{+}/P3HB^{++} (b) FSC (cell size) for *C. necator* cultures containing 0.08% (w/v) and supplemented with 0%, 0.5%, 1%, 1.5% (w/v) fructose. Error bars represent SD. n = 3 biological replicates.

8.6 Full data corresponding to section 3.6

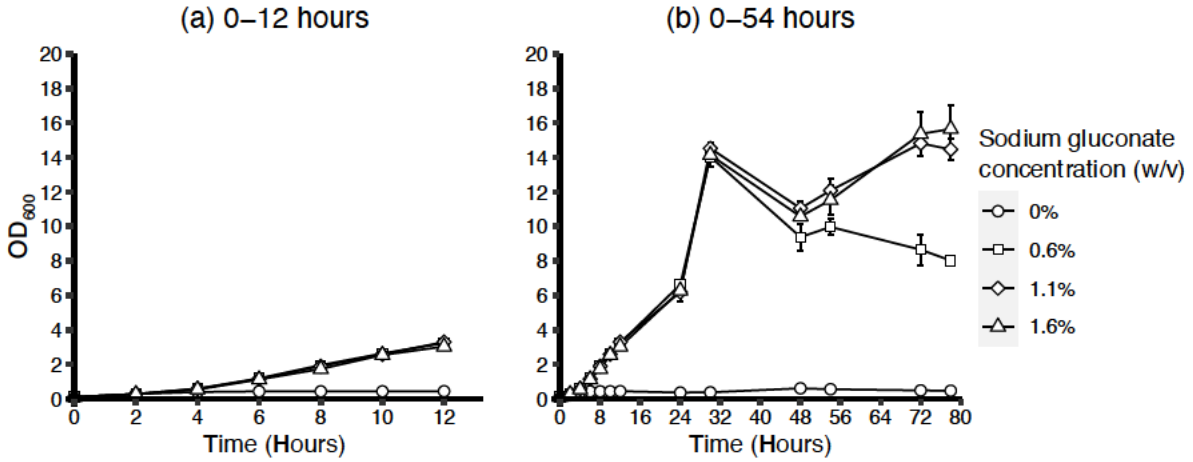


Figure 8.12 – Full OD_{600} data for *C. necator* cultures containing 0.08% (w/v) ME and supplemented with 0%, 0.6%, 1.1% and 1.6% (w/v) sodium gluconate. Error bars represent SD. n = 3 biological replicates.

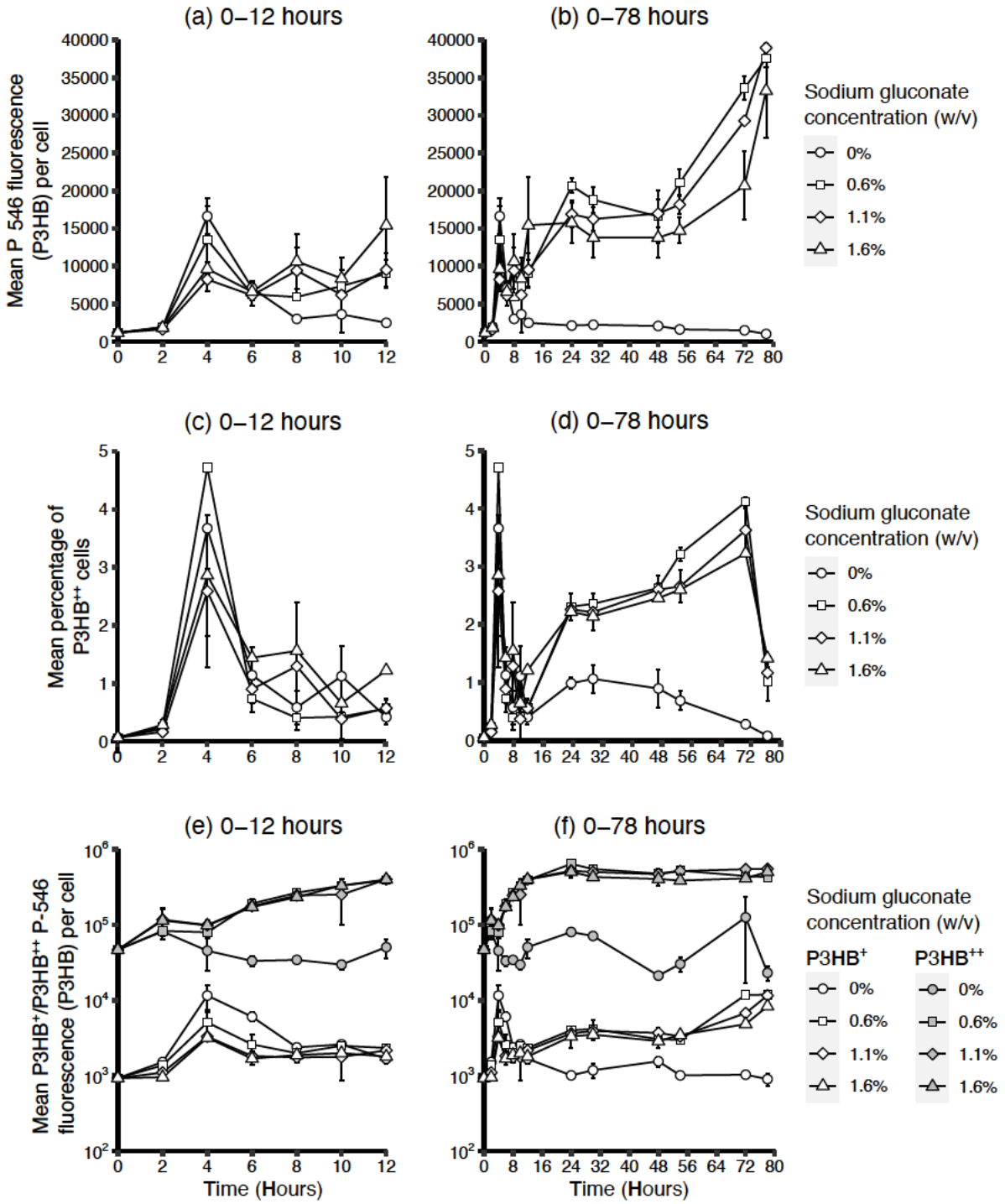


Figure 8.13 - Full data representing mean P-546 (P3HB) per cell ((a) and (b)), mean percentage of P3HB^{++} cells ((c) and (d)) and mean P3HB^{+} and P3HB^{++} P-546 fluorescence (P3HB) ((e) and (f)) for *C. necator* cultures containing 0.08% (w/v) ME and supplemented with 0%, 0.6%, 1.1% and 1.6% (w/v) sodium gluconate. Error bars represent SD. n = 3 biological replicates.

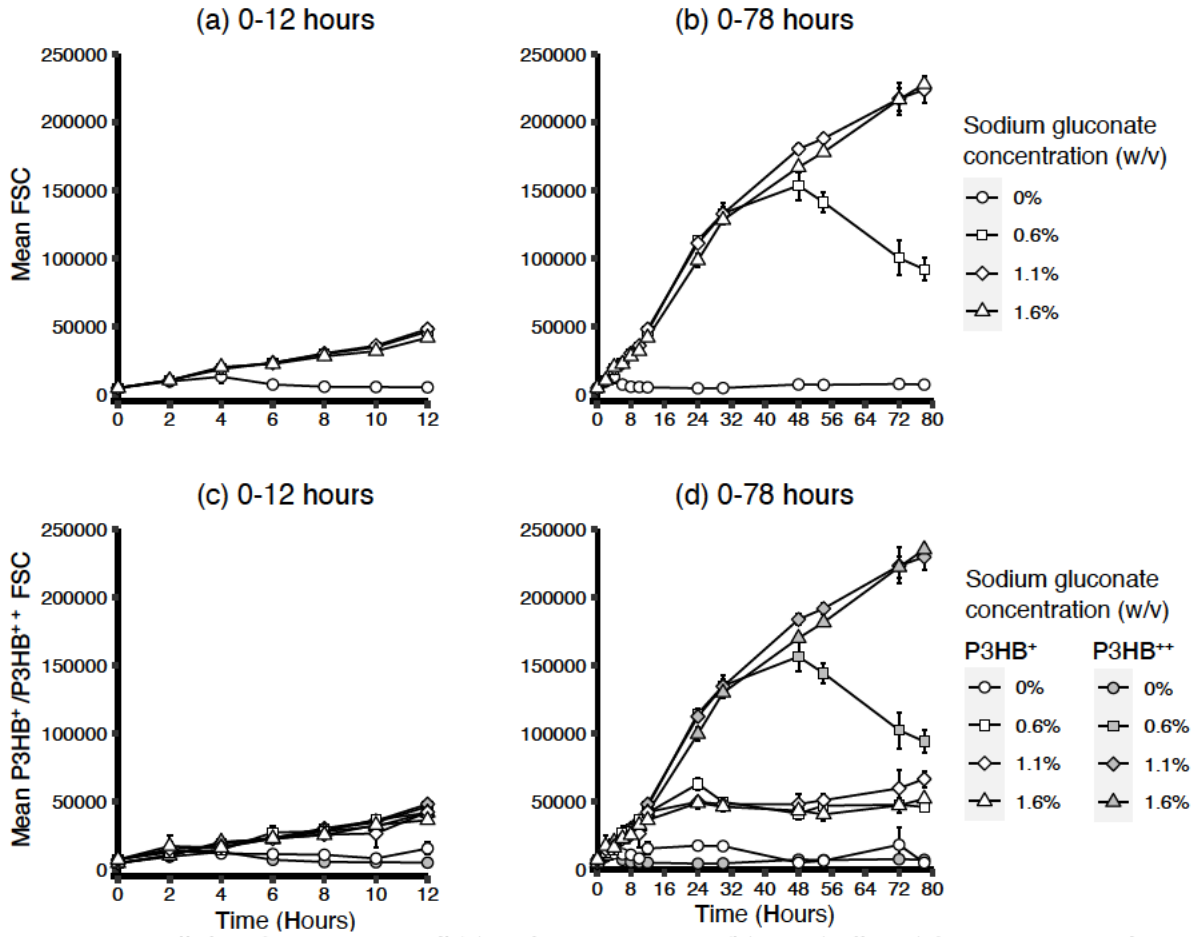


Figure 8.14 - Full data for mean overall (a) and P3HB^{+}/P3HB^{++} (b) FSC (cell size) for *C. necator* cultures containing 0.08% (w/v) ME and supplemented with 0%, 0.6%, 1.1% and 1.6% (w/v) sodium gluconate. Error bars represent SD. n = 3 biological replicates.

8.7 Full data corresponding to fructose and sodium gluconate comparisons in section 3.6

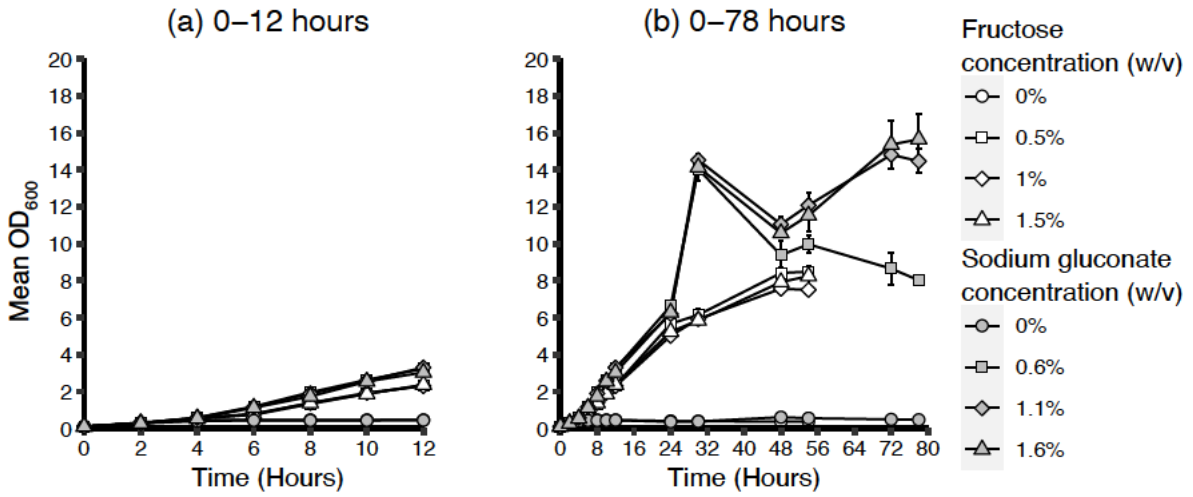


Figure 8.15 - Full OD_{600} data for *C. necator* cultures containing 0.08% (w/v) ME and supplemented with 0%, 0.6%, 1.1% and 1.6% (w/v) sodium gluconate or 0%, 0.5%, 1% and 1.5% (w/v) fructose. Error bars represent SD. n = 3 biological replicates

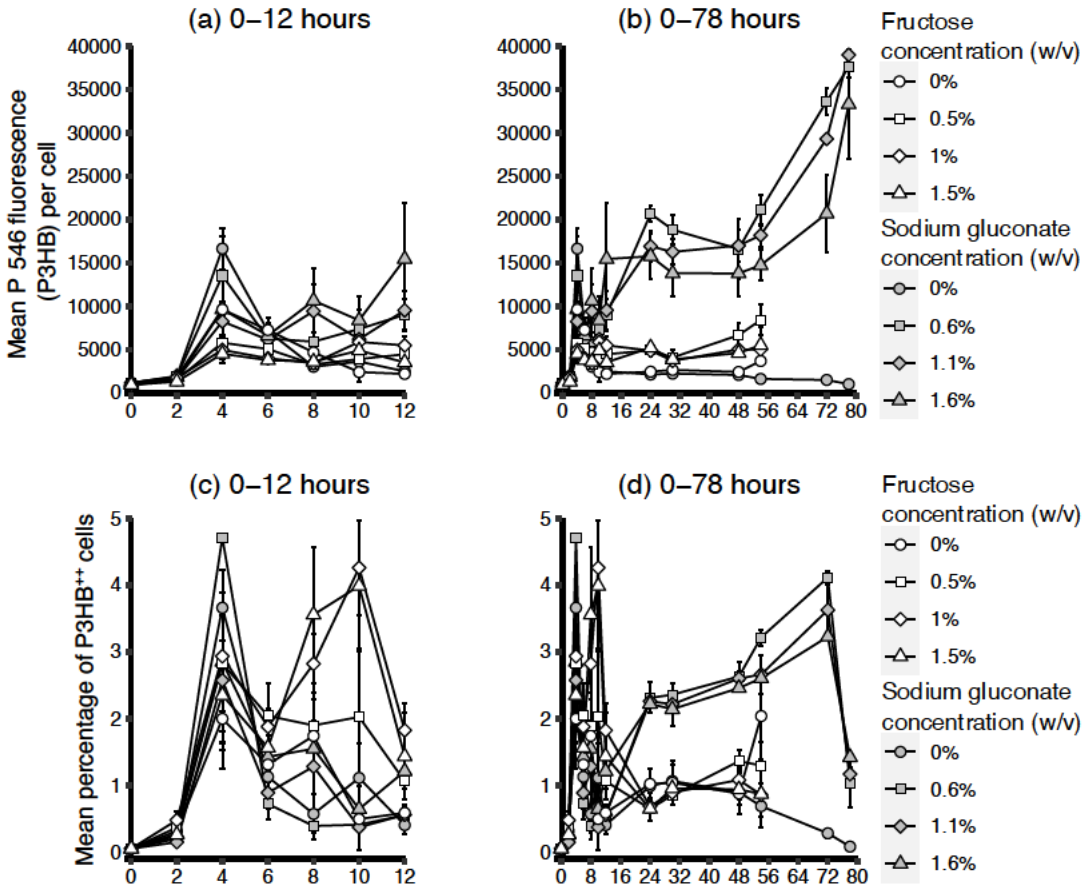


Figure 8.16 – Full data representing mean P-546 (P3HB) per cell ((a) and (b)), mean percentage of P3HB^{++} cells ((c) and (d)) for *C. necator* cultures containing 0.08% (w/v) ME and supplemented with 0%, 0.6%, 1.1% and 1.6% (w/v) sodium gluconate or 0%, 0.5%, 1% and 1.5% (w/v) fructose. Error bars represent SD. n = 3 biological replicates.

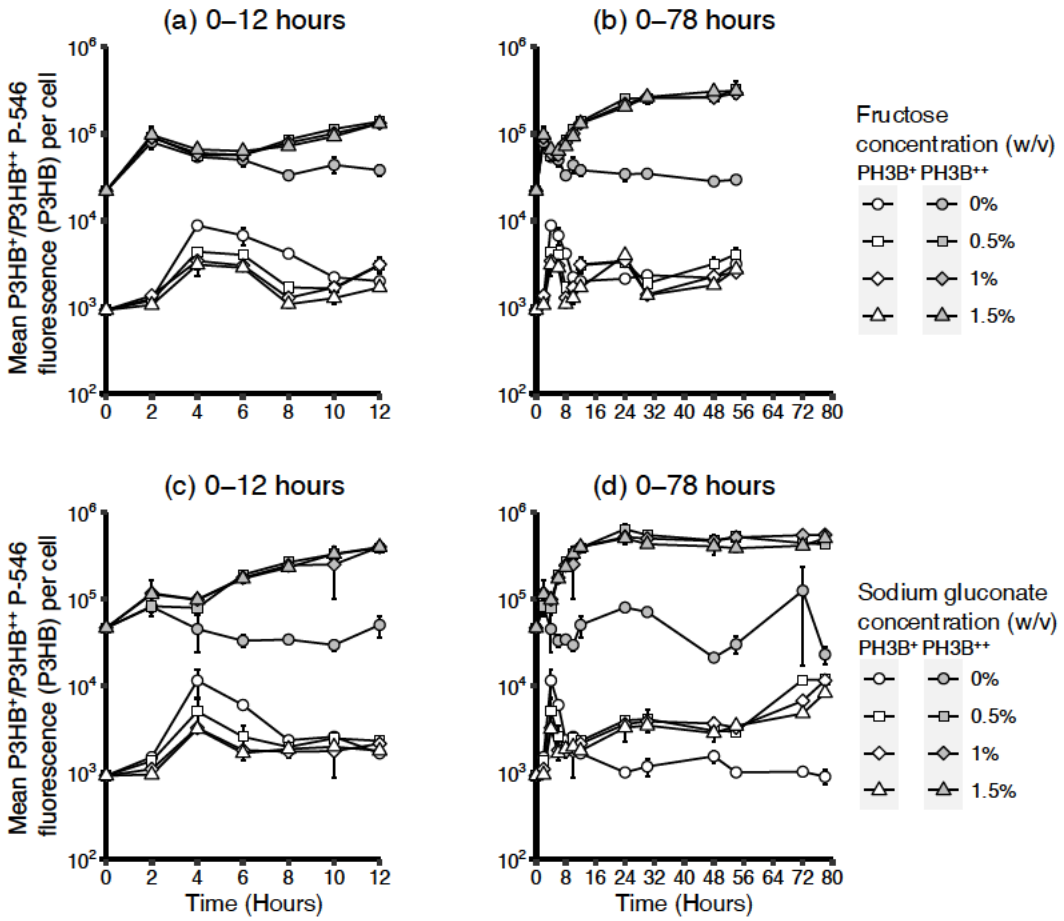


Figure 8.17 - Full data representing mean P3HB^{+}/P3HB^{++} P-546 (P3HB) per cell ((a) and (b)), mean percentage of P3HB^{++} cells ((c) and (d)) for *C. necator* cultures containing 0.08% (w/v) ME and supplemented with 0%, 0.6%, 1.1% and 1.6% (w/v) sodium gluconate. Error bars represent SD. n = 3 biological replicates.

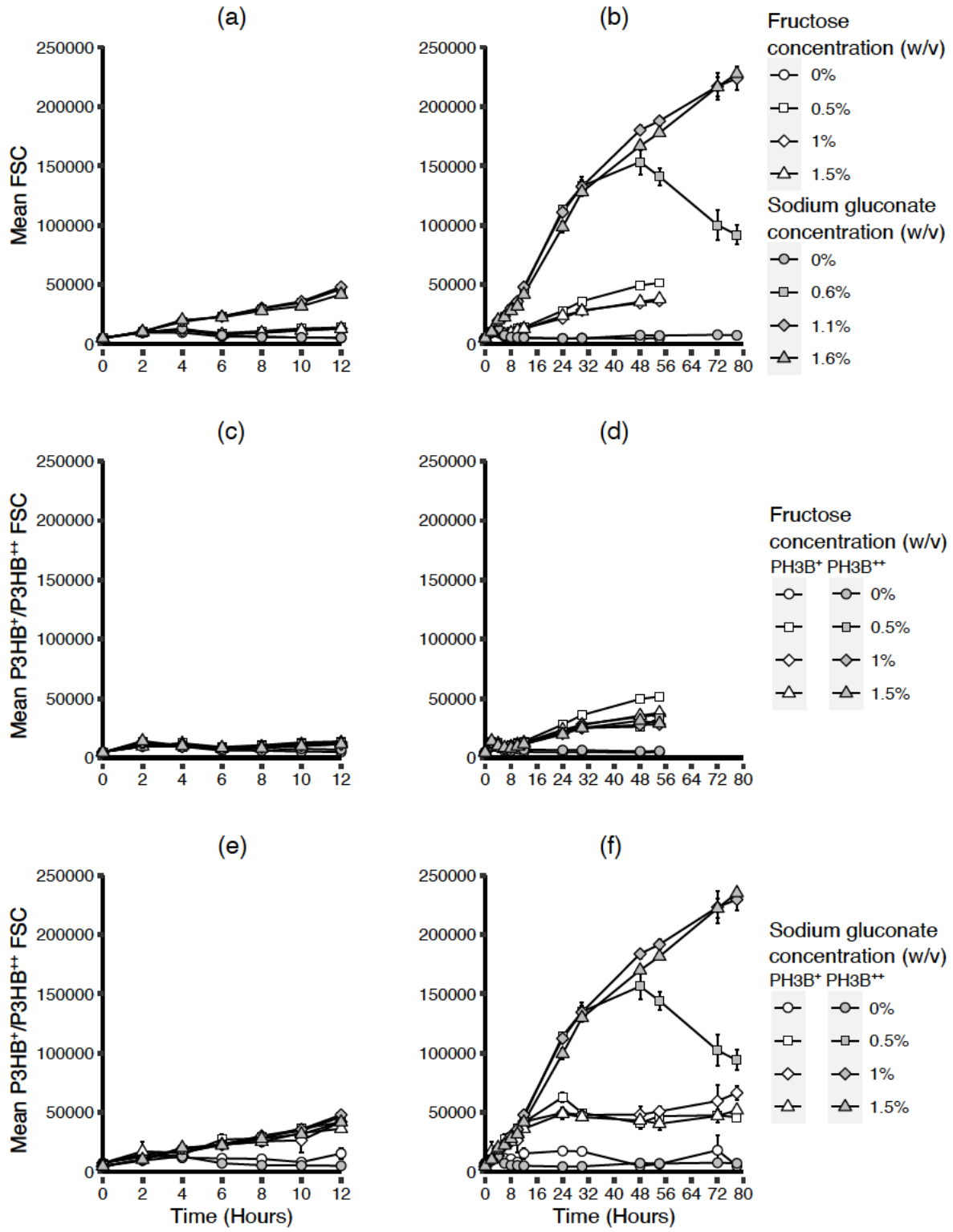


Figure 8.18 - Full data for mean overall FSC (cell size) ((a) and (b)) and mean P3HB⁺/P3HB⁺⁺ FSC (cell size) for *C. necator* cultures containing 0.08% (w/v) ME and supplemented with 0%, 0.6%, 1.1% and 1.6% (w/v) sodium gluconate ((c) and (d)) or 0%, 0.5%, 1% and 1.5% (w/v) fructose ((e) and (f)). Error bars represent SD. n = 3 biological replicates.

8.8 Full data corresponding to section 3.7

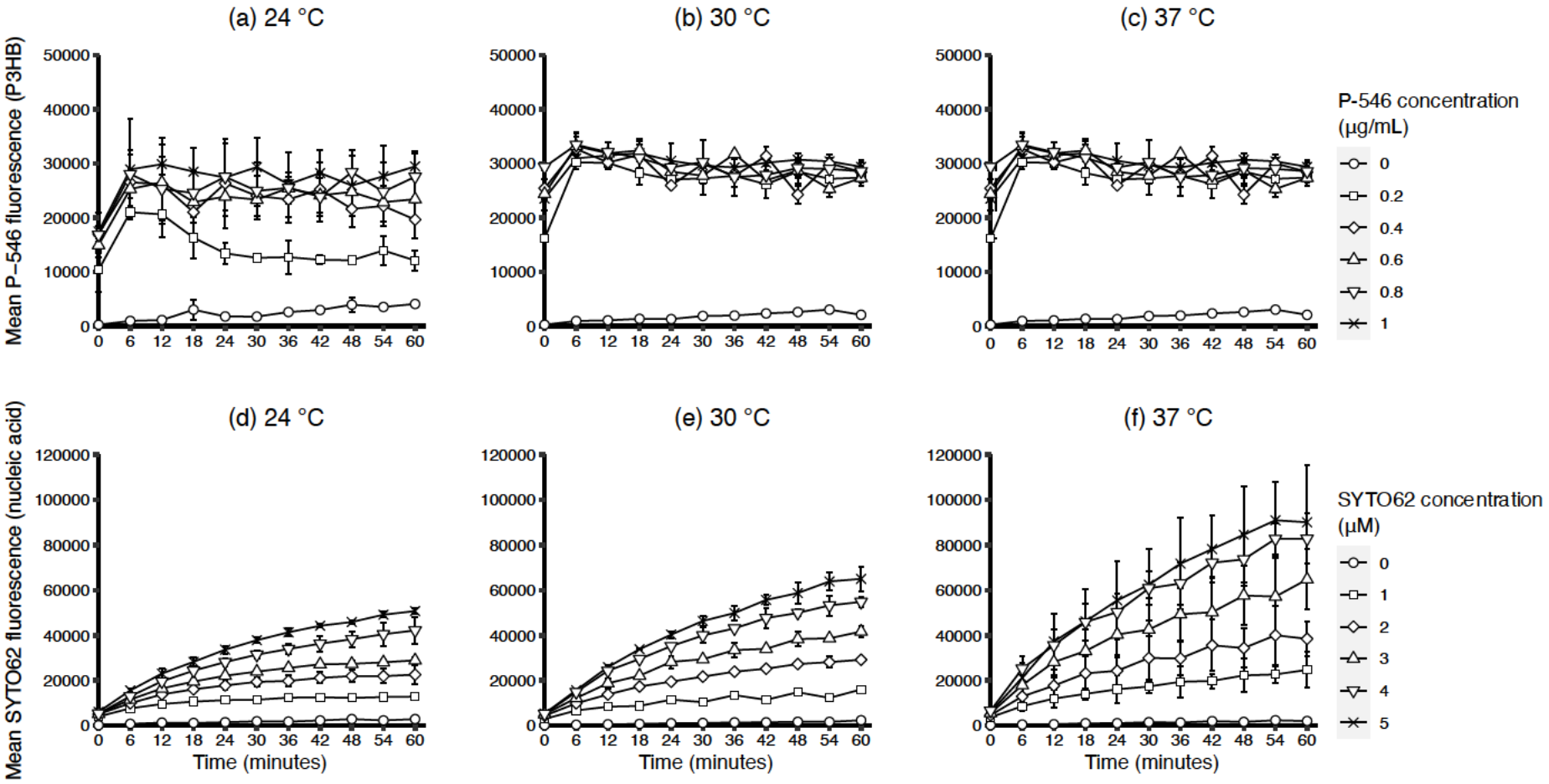


Figure 8.19 – Graphs displaying full data for SYTO62 and P-546 staining optimisations. Cultures used contained *C. necator* grown for 72 hours in 0.08% (w/v) ME supplemented with 0.6% (w/v) sodium gluconate.

8.9 Full data corresponding to section 3.8

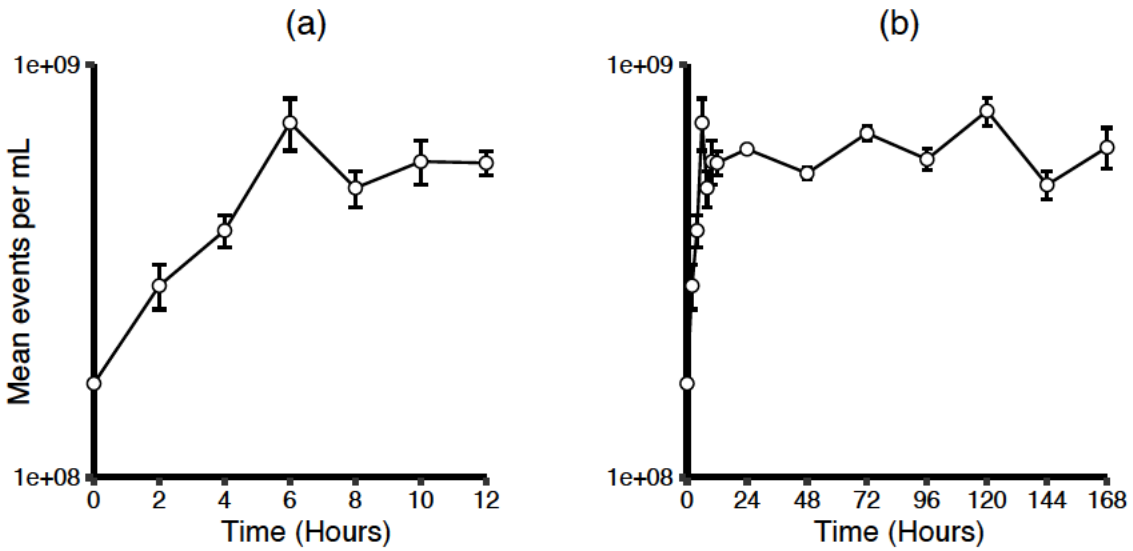


Figure 8.20 – Full data showing mean events per mL for *C. necator* cultures grown in 0.08% (w/v) ME and supplemented with 0.6% (w/v) sodium gluconate. Error bars represent SD. n = 3 biological replicates.

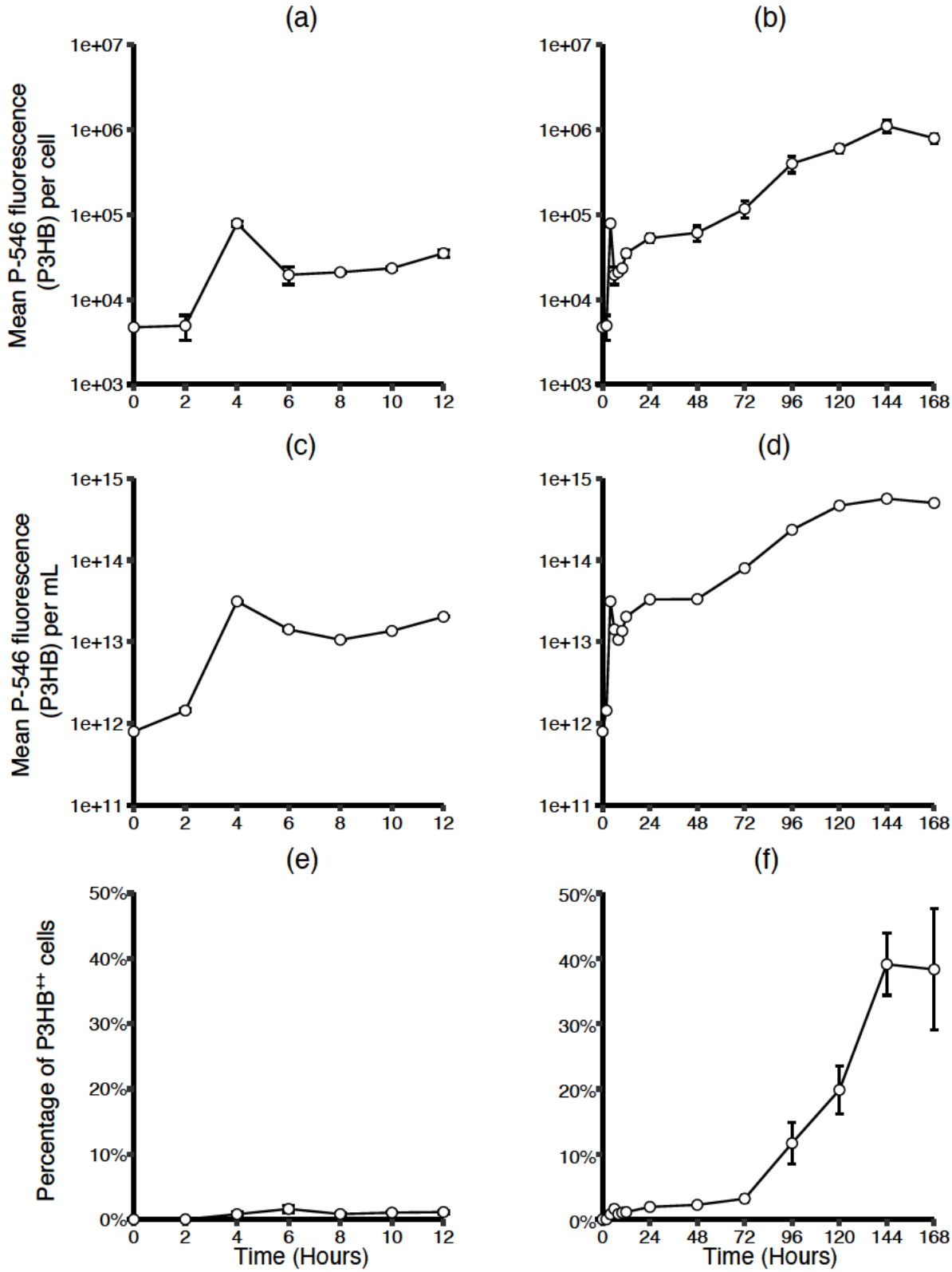


Figure 8.21 – Full data showing mean P-546 fluorescence per cell ((a) and (b)) and per mL ((c) and (d)) in addition to the mean percentage of P3HB^{++} cells for *C. necator* cultures grown in 0.08% (w/v) ME and supplemented with 0.6% (w/v) sodium gluconate. Error bars represent SD. n = 3 biological replicates.

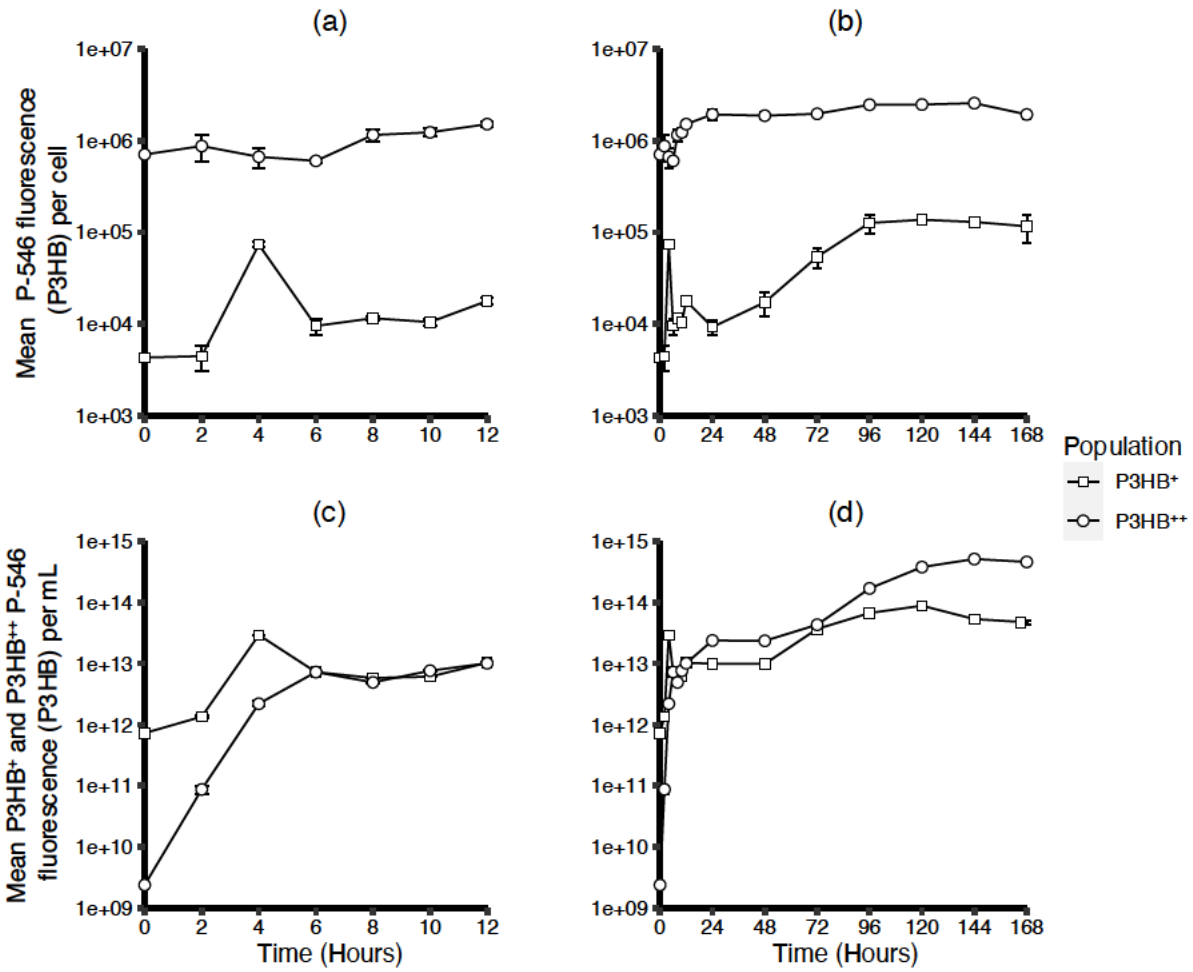


Figure 8.22 – Full data showing the mean P-546 fluorescence (P3HB) per cell ((a and (b)) and per mL ((c) and (d)) for *C. necator* cultures grown in 0.08% (w/v) ME and supplemented with 0.6% (w/v) sodium gluconate. Error bars represent SD. n = 3 biological replicates.

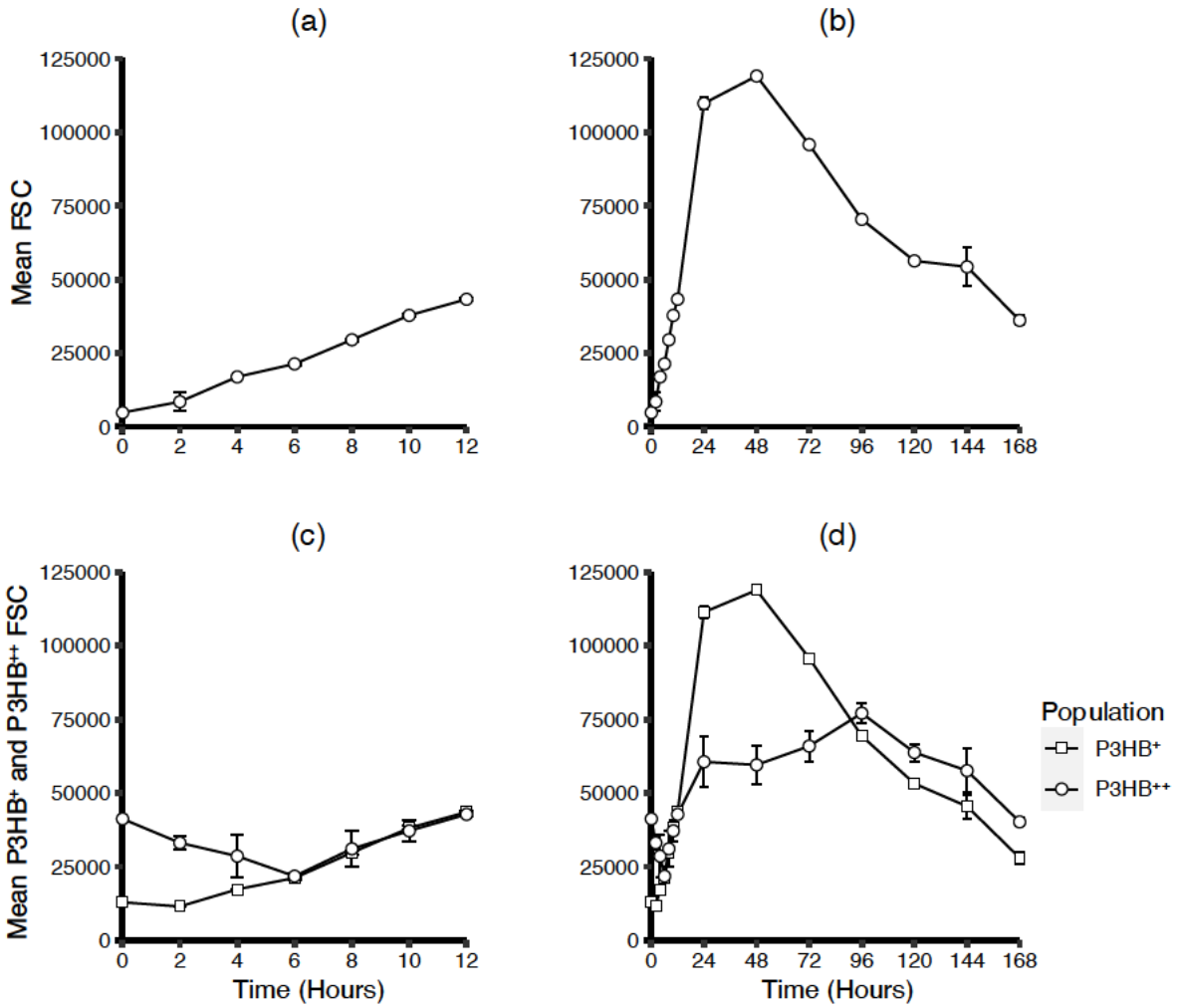


Figure 8.23 – Full data showing mean overall FSC (cell size) and P3HB^{+}/P3HB^{++} FSC (cell size) for *C. necator* cultures grown in 0.08% (w/v) ME and supplemented with 0.6% (w/v) sodium gluconate. Error bars represent SD. n = 3 biological replicates.

8.10 Full data corresponding to section 3.9

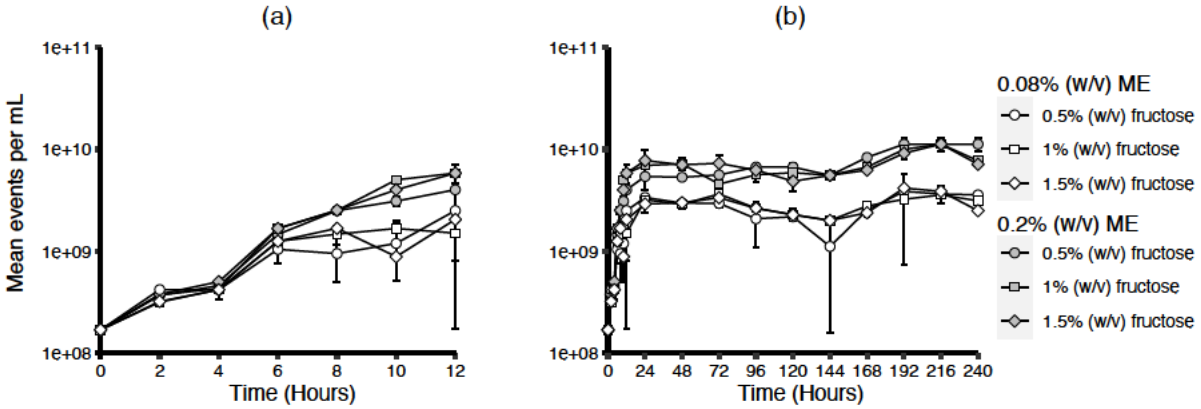


Figure 8.24 – Full mean events per mL for *C. necator* cultures containing either 0.08% or 0.2% (w/v) ME and supplemented with 0.5%, 1% and 1.5% (w/v) fructose. Error bars represent SD. n = 2 biological replicates.

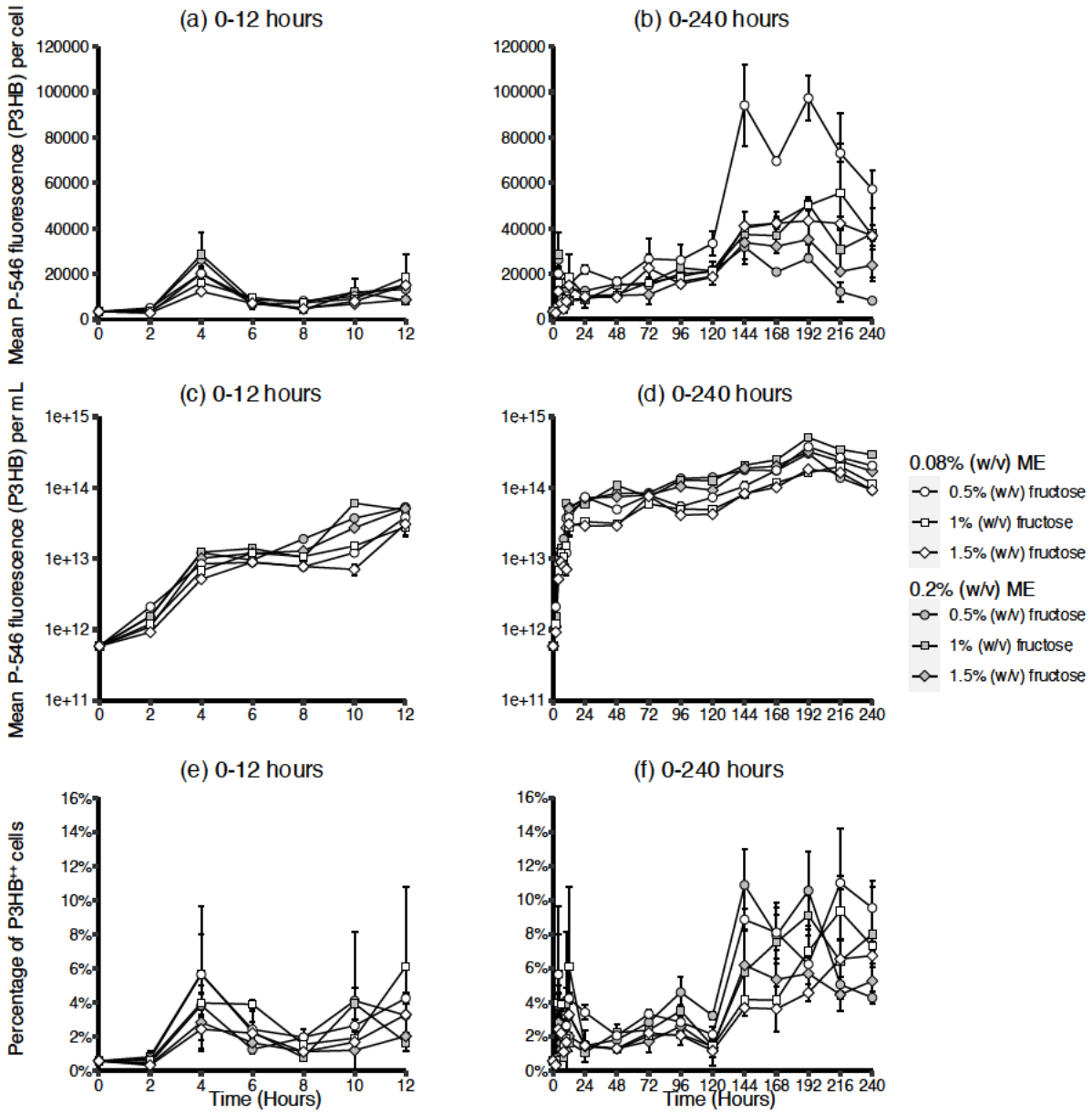


Figure 8.25 – Full data showing mean P-546 fluorescence per cell ((a) and (b)) and per mL ((c) and (d)) and the mean percentage of P3HB^{++} cells for *C. necator* cultures containing either 0.08% or 0.2% (w/v) ME and supplemented with 0.5%, 1% and 1.5% (w/v) fructose. Error bars represent SD. n = 2 biological replicates.

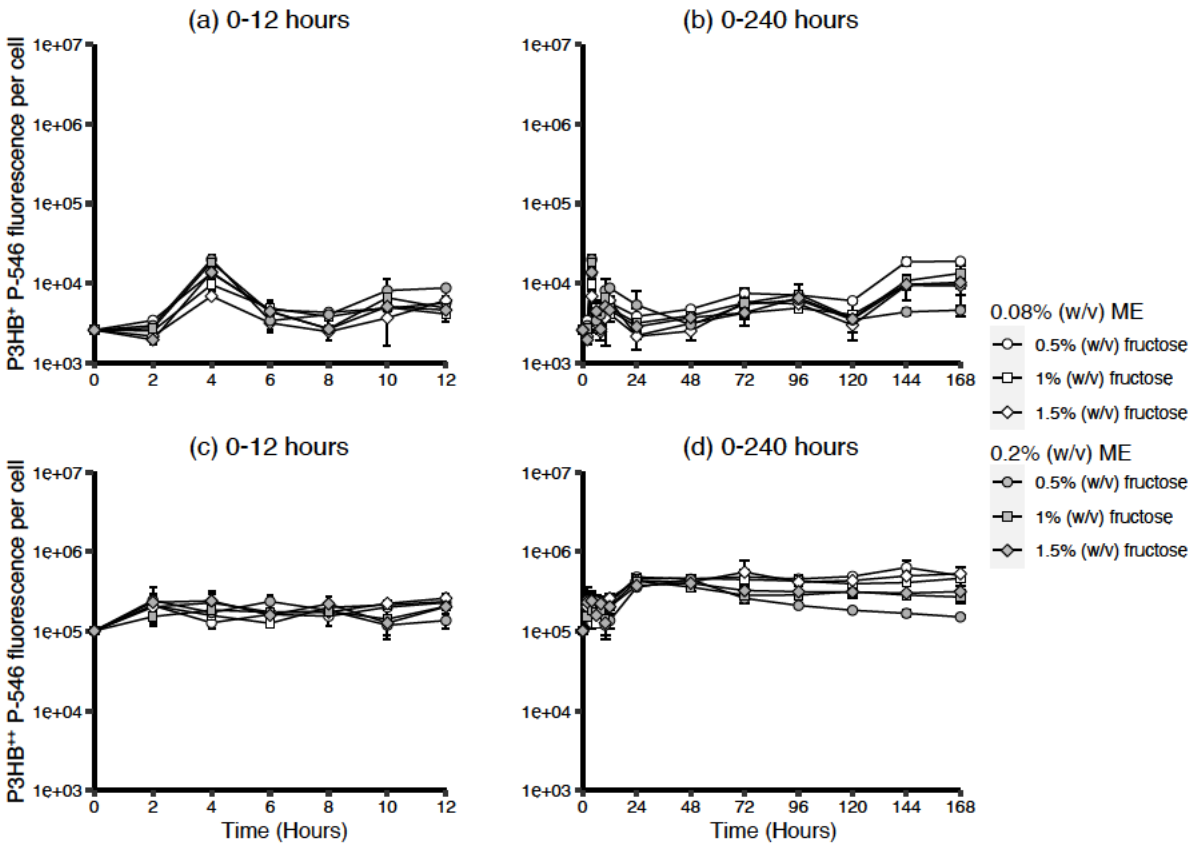


Figure 8.26 – Full data showing mean P3HB^{+} ((a) and (b)) P3HB^{++} ((c) and (d)) P-546 fluorescence per cell for *C. necator* cultures containing either 0.08% or 0.2% (w/v) ME and supplemented with 0.5%, 1% and 1.5% (w/v) fructose. Error bars represent SD. n = 2 biological replicates.

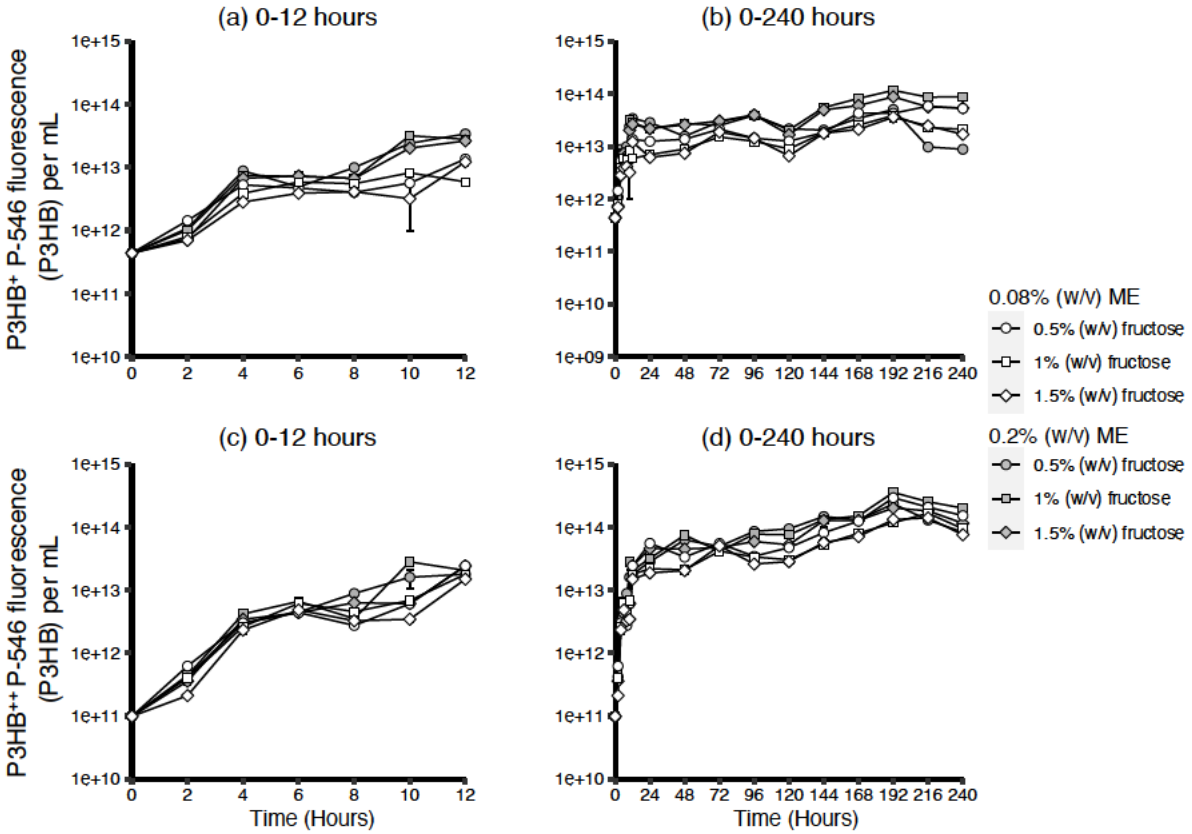


Figure 8.27 – Full data showing mean P3HB^{+} ((a) and (b)) P3HB^{++} ((c) and (d)) P-546 fluorescence per mL for *C. necator* cultures containing either 0.08% or 0.2% (w/v) ME and supplemented with 0.5%, 1% and 1.5% (w/v) fructose. Error bars represent SD. n = 2 biological replicates.

,

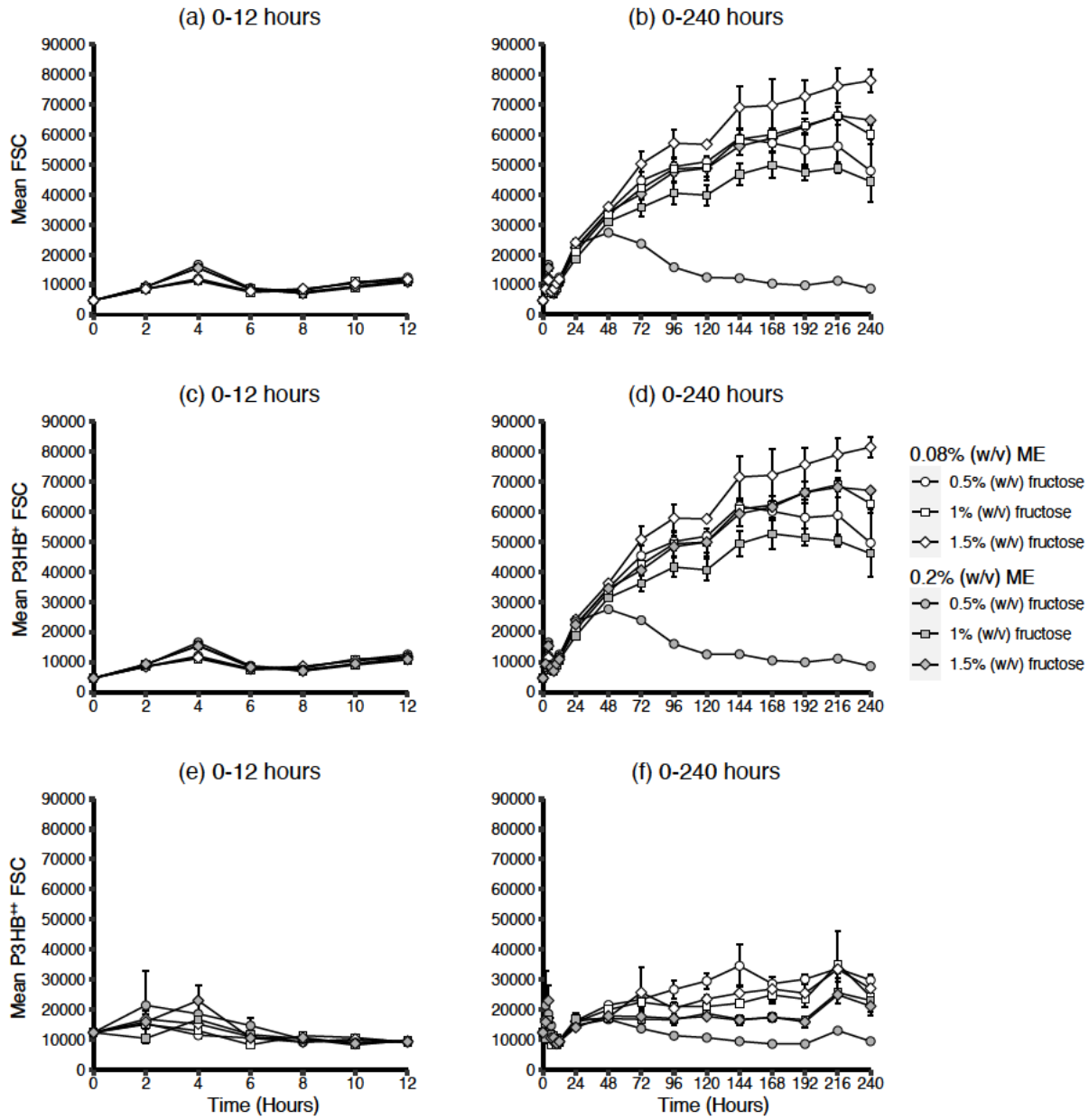


Figure 8.28 – Full data showing mean FSC (cell size) for the overall population ((a) and (b)) and the P3HB^{+} ((c) and (d)) and P3HB^{++} ((e) and (f)) populations for *C. necator* cultures containing either 0.08% or 0.2% (w/v) ME and supplemented with 0.5%, 1% and 1.5% (w/v) fructose. Error bars represent SD. n = 2 biological replicates.

8.11 Comparisons between fructose and sodium gluconate supplementation corresponding to section 3.9

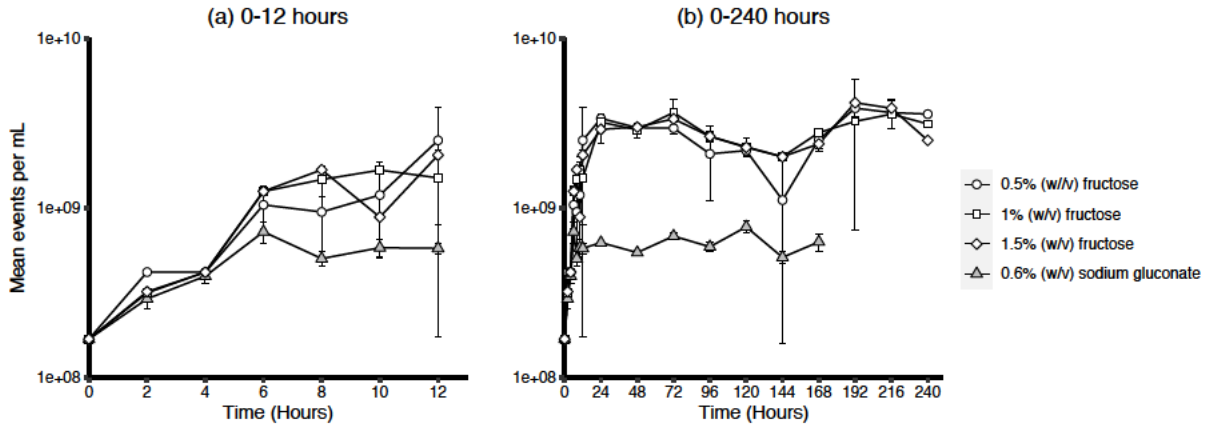


Figure 8.29 - Full data showing comparisons of flow cytometry events per mL at 24 hours for 0.08% (w/v) *C. necator* supplemented with 0.5%, 1% and 1.5% (w/v) fructose or 0.6% (w/v) sodium gluconate. Error bars represent SD. n = 2 biological replicates for fructose supplemented cultures and n = 3 for sodium gluconate supplemented cultures.

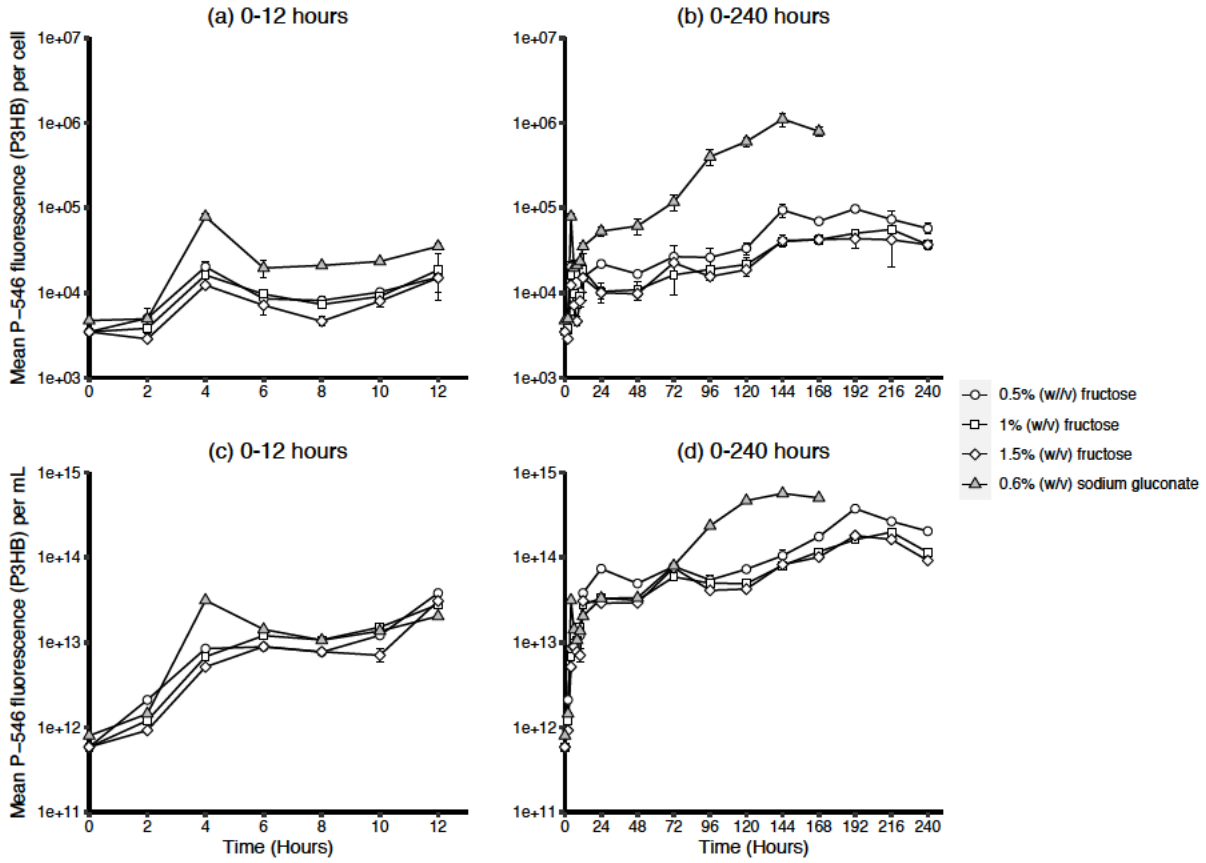


Figure 8.30 - Full data showing comparisons of mean P-546 fluorescence per cell ((a) and (b)) and per mL ((c) and (d)) at 168 hours for 0.08% (w/v) *C. necator* supplemented with 0.5%, 1% and 1.5% (w/v) fructose or 0.6% (w/v) sodium gluconate. Error bars represent SD. n = 2 biological replicates for fructose supplemented cultures and n = 3 for sodium gluconate supplemented cultures.

Chapter 9 - Appendix 2 (raw data corresponding to chapter 4)

9.1 Raw data corresponding to section 4.2

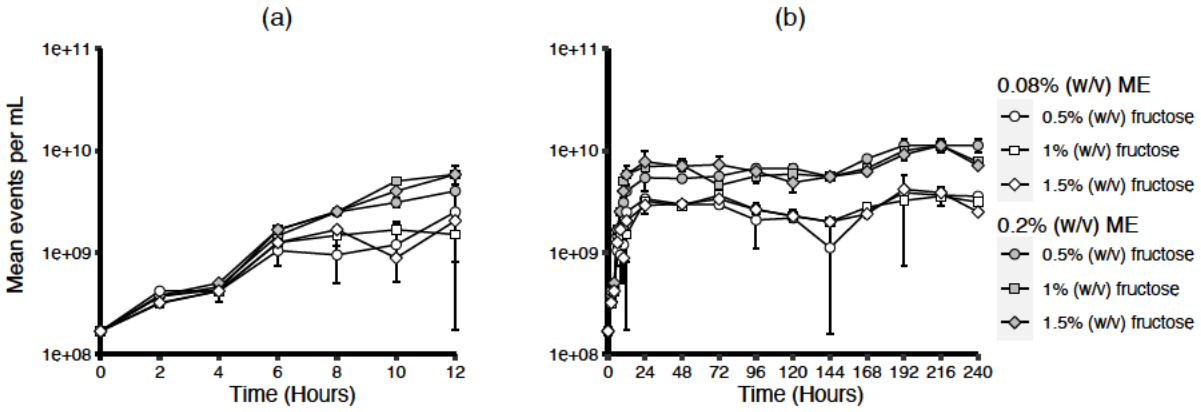


Figure 9.1 – Full mean events per mL data for *C. necator* cultures containing 0.08%, 0.2% or 0.4% (w/v) and supplemented with 0.5% (w/v) fructose at 0 hours and either 0.6% or 1.2% (w/v) sodium gluconate at 24 hours. Error bars represent SD. n = 2 biological replicates.

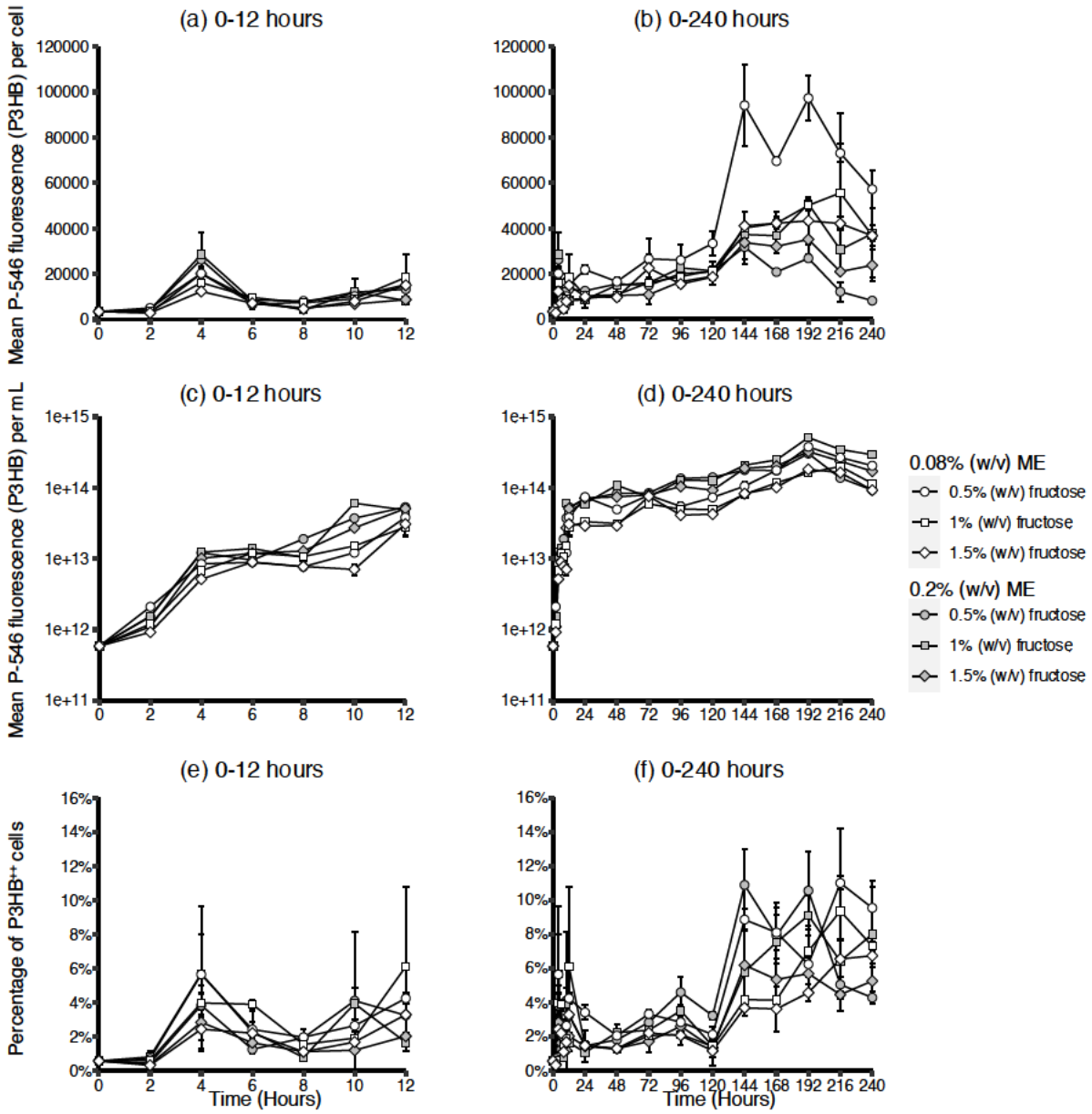


Figure 9.2 – Full data for P-546 fluorescence (P3HB) per cell ((a) and (b)) and per mL ((c) and (d)) in addition to the percentage of P3HB^{++} cells ((e) and (f)) for *C. necator* cultures containing 0.08%, 0.2% or 0.4% (w/v) and supplemented with 0.5% (w/v) fructose at 0 hours and either 0.6% or 1.2% (w/v) sodium gluconate at 24 hours. Error bars represent SD. n = 2 biological replicates.

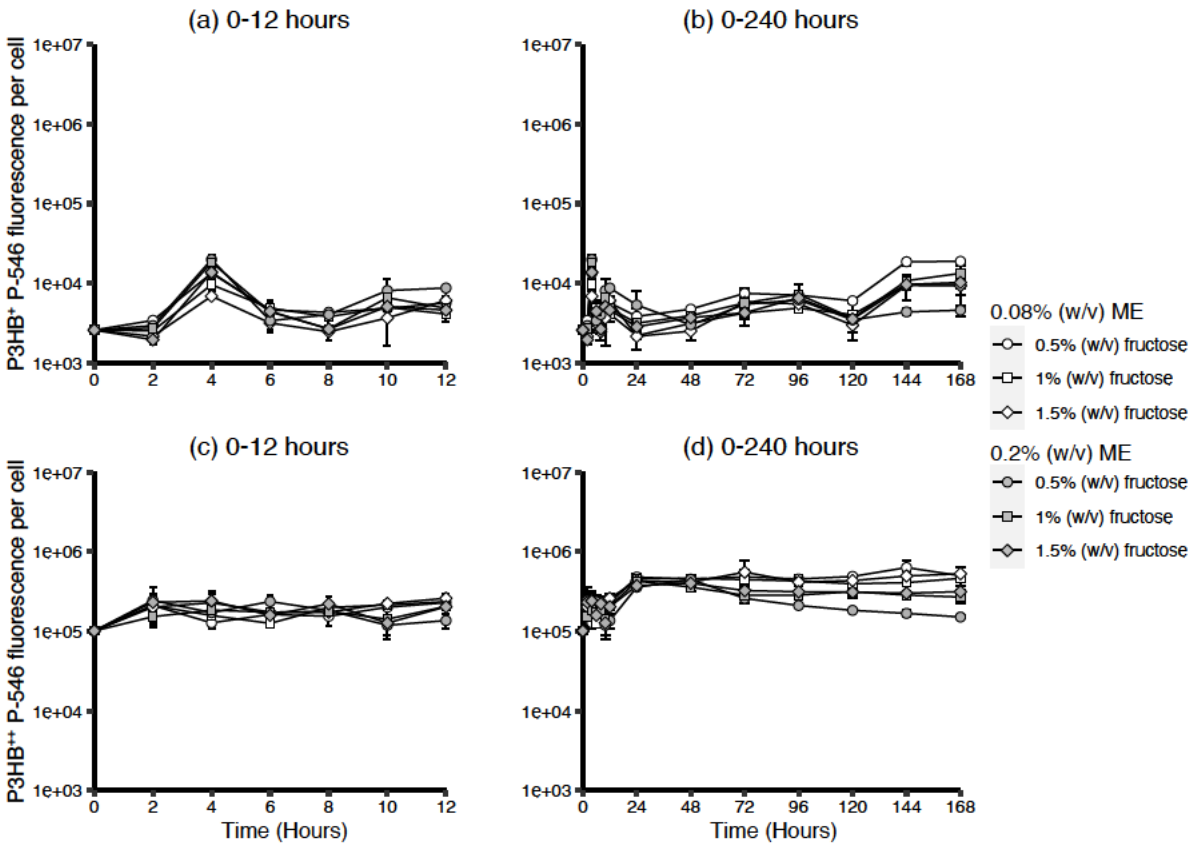


Figure 9.3 – Full data displaying P-546 fluorescence (P3HB) per cell for the P3HB^{+} and P3HB^{++} populations for *C. necator* cultures containing 0.08%, 0.2% or 0.4% (w/v) and supplemented with 0.5% (w/v) fructose at 0 hours and either 0.6% or 1.2% (w/v) sodium gluconate at 24 hours. Error bars represent SD. n = 2 biological replicates.

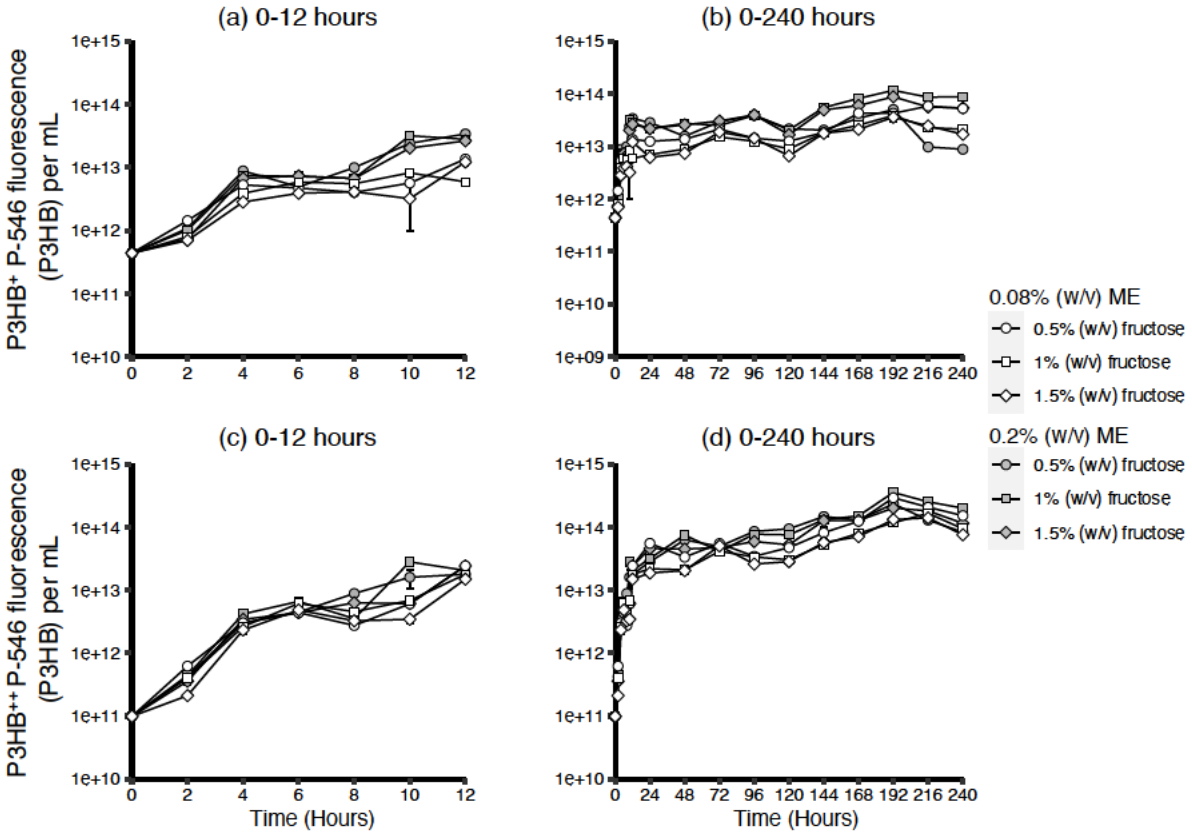


Figure 9.4 - Full data displaying P-546 fluorescence (P3HB) per mL for the P3HB^{+} and P3HB^{++} populations for *C. necator* cultures containing 0.08%, 0.2% or 0.4% (w/v) and supplemented with 0.5% (w/v) fructose at 0 hours and either 0.6% or 1.2% (w/v) sodium gluconate at 24 hours. Error bars represent SD. n = 2 biological replicates.

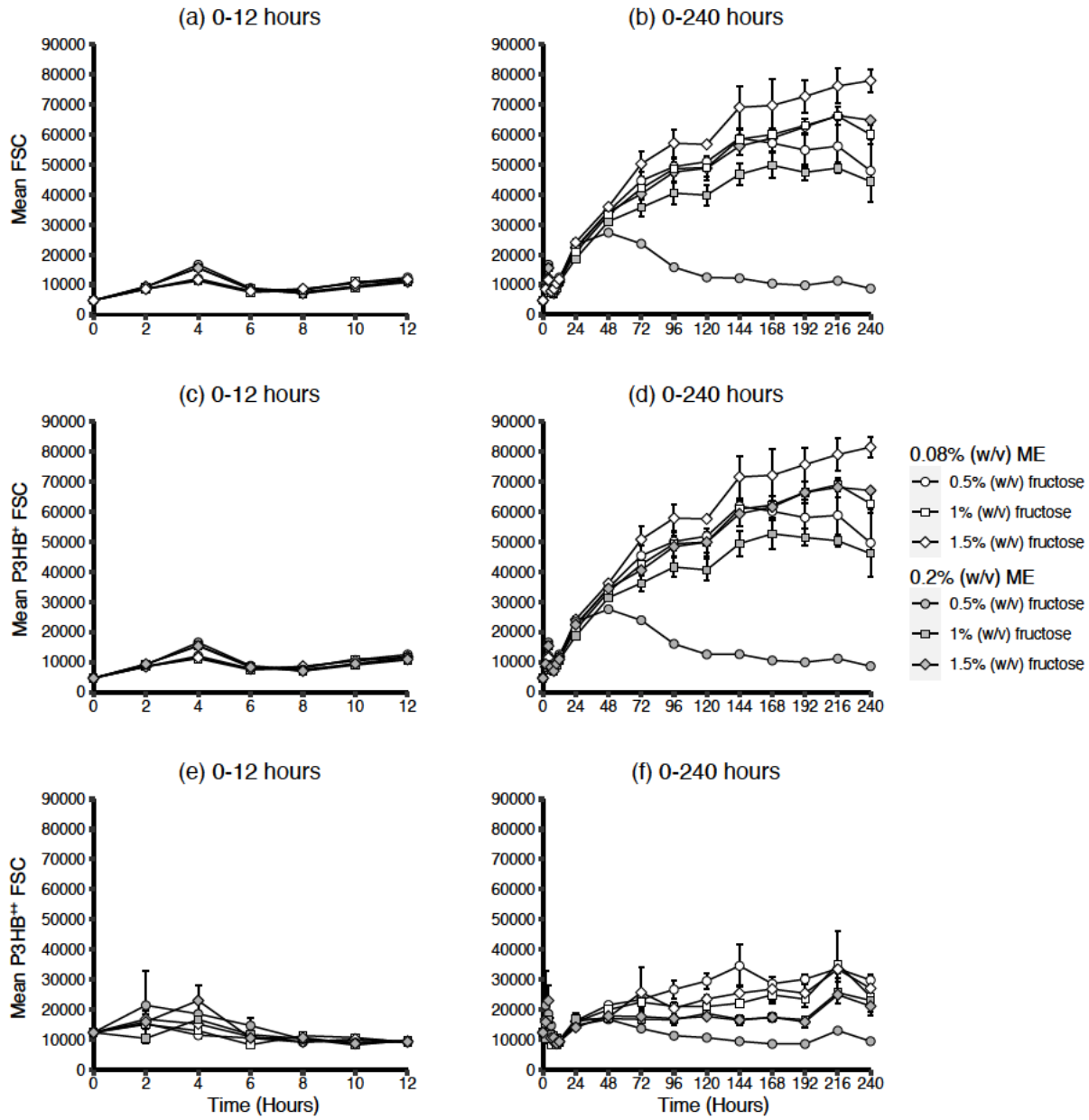


Figure 9.5 - Full data showing mean FSC (cell size) for the overall population ((a) and (b)) and the P3HB^{+} ((c) and (d)) and P3HB^{++} ((e) and (f)) populations for *C. necator* cultures containing 0.08%, 0.2% or 0.4% (w/v) ME and supplemented with 0.5% (w/v) fructose at 0 hours and either 0.6% or 1.2% (w/v) sodium gluconate at 24 hours. Error bars represent SD. n = 2 biological replicates.

9.2 Raw data corresponding to section 4.3

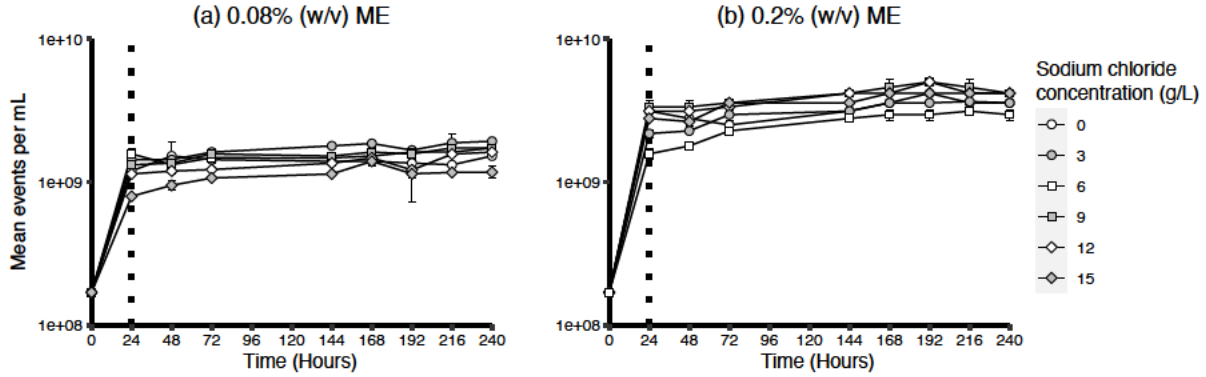


Figure 9.6 - Full mean events data for *C. necator* cultures grown in media containing either 0.08% or 0.2% (w/v) ME, 0, 3, 6, 9, 12 or 15 g/L sodium chloride and supplemented with 0.5% (w/v) fructose at 0 hours and 0.6% (w/v) sodium gluconate at 24 hours. Error bars represent SD. n = 3 biological replicates.

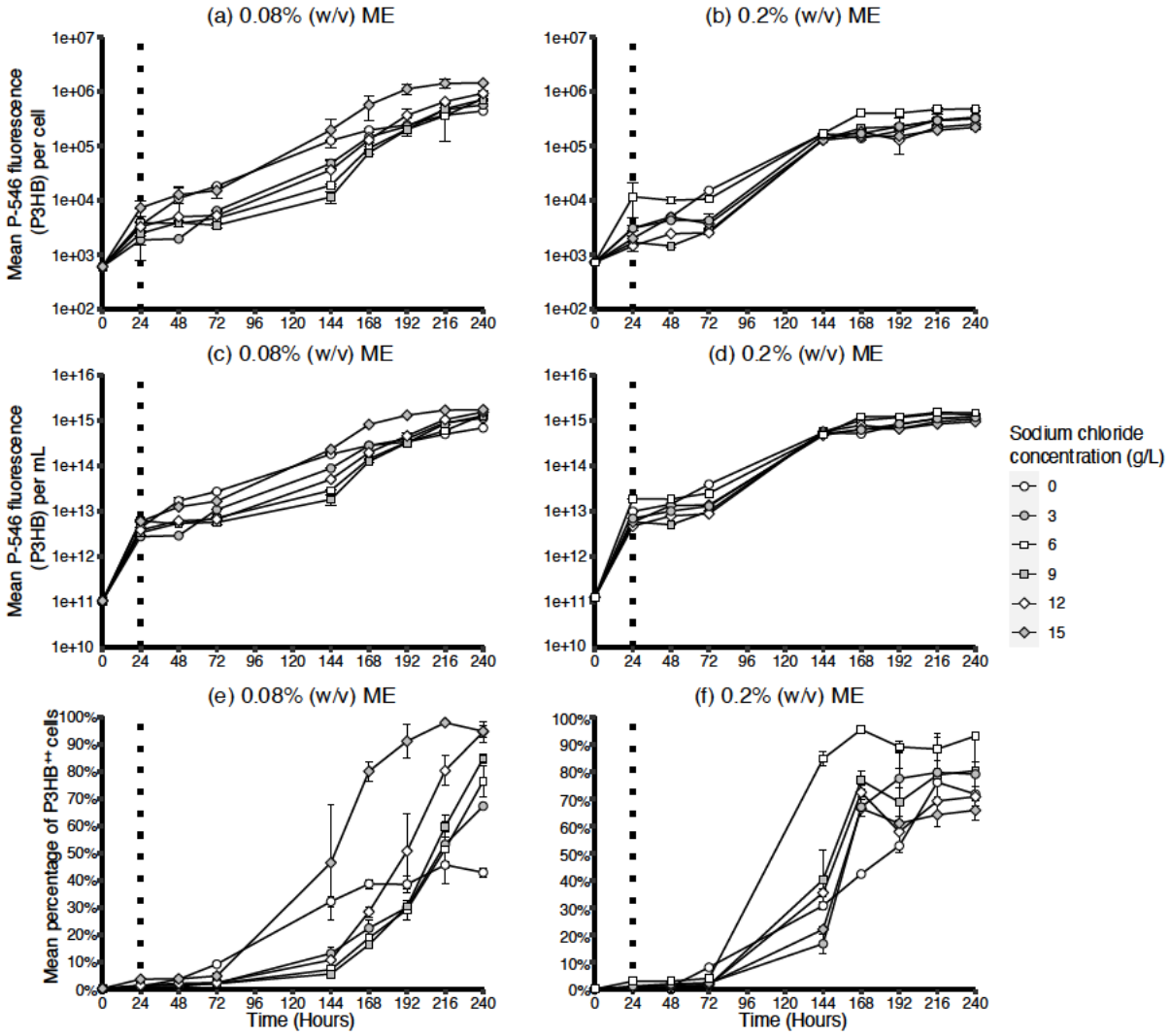


Figure 9.7 - Full data for P-546 fluorescence (P3HB) per cell ((a) and (b)) and per mL ((c) and (d)) in addition to the percentage of P3HB^{++} cells ((e) and (f)) for *C. necator* cultures grown in media containing either 0.08% or 0.2% (w/v) ME, 0, 3, 6, 9, 12 or 15 g/L sodium chloride and supplemented with 0.5% (w/v) fructose at 0 hours and 0.6% (w/v) sodium gluconate at 24 hours. Error bars represent SD. n = 3 biological replicates.

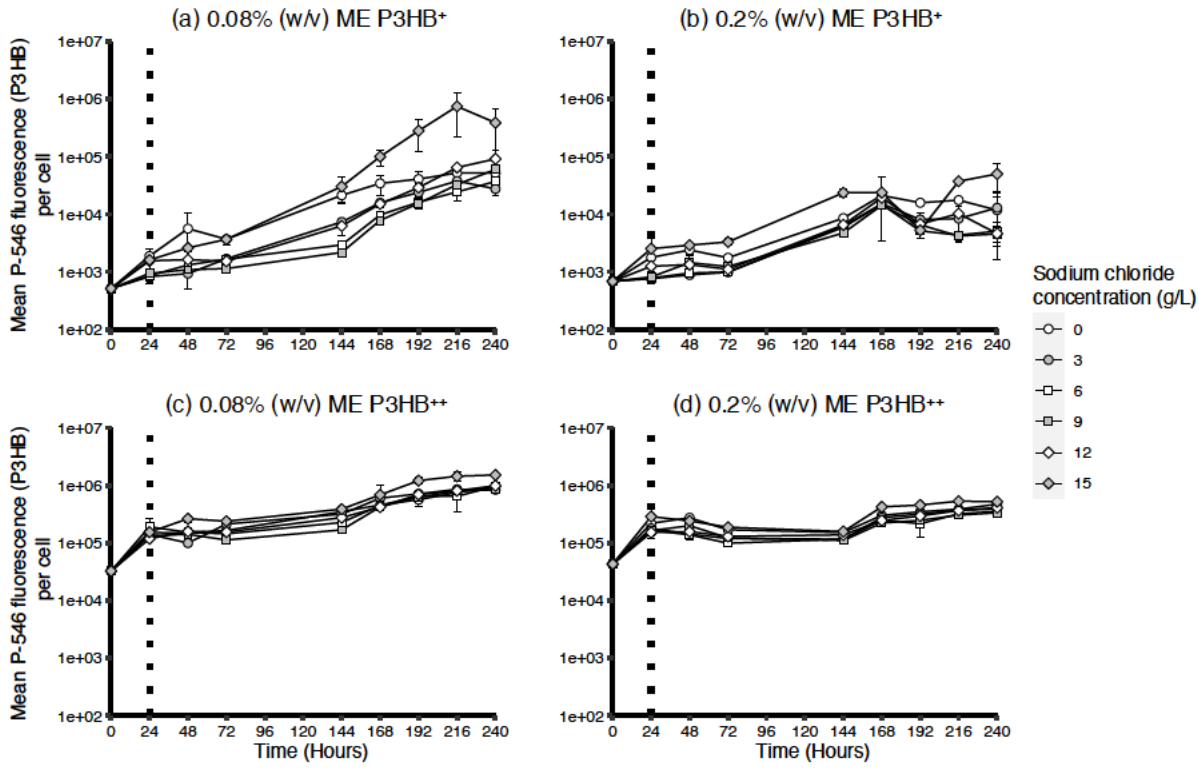


Figure 9.8 – Full data displaying P-546 fluorescence (P3HB) per cell for the P3HB^{+} and P3HB^{++} populations for *C. necator* cultures containing either 0.08% or 0.2% (w/v) ME, 0, 3, 6, 9, 12 or 15 g/L sodium chloride and supplemented with 0.5% (w/v) fructose at 0 hours and 0.6% (w/v) sodium gluconate at 24 hours. Error bars represent SD. n = 3 biological replicates.

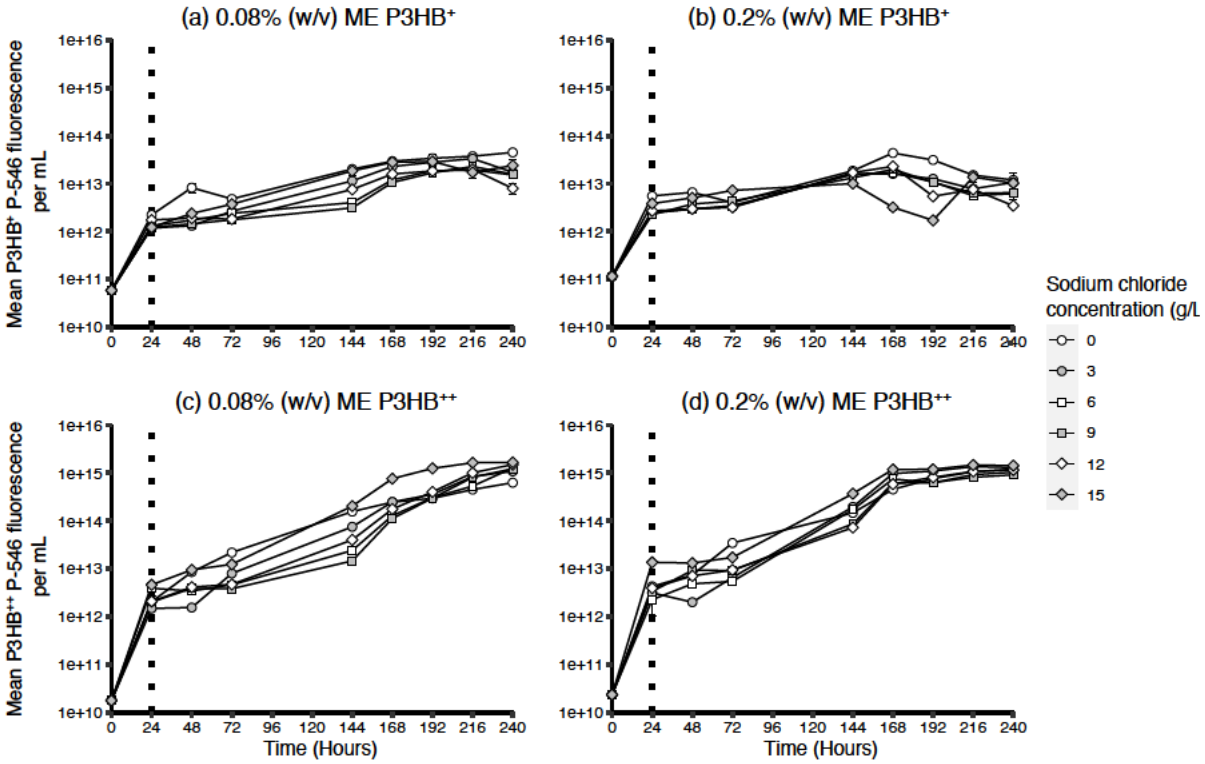


Figure 9.9 - Full data displaying P-546 fluorescence (P3HB) per cell for the P3HB^{+} and P3HB^{++} populations for *C. necator* cultures containing either 0.08% or 0.2% (w/v) ME, 0, 3, 6, 9, 12 or 15 g/L sodium chloride and supplemented with 0.5% (w/v) fructose at 0 hours and 0.6% (w/v) sodium gluconate at 24 hours. Error bars represent SD. n = 3 biological replicates.

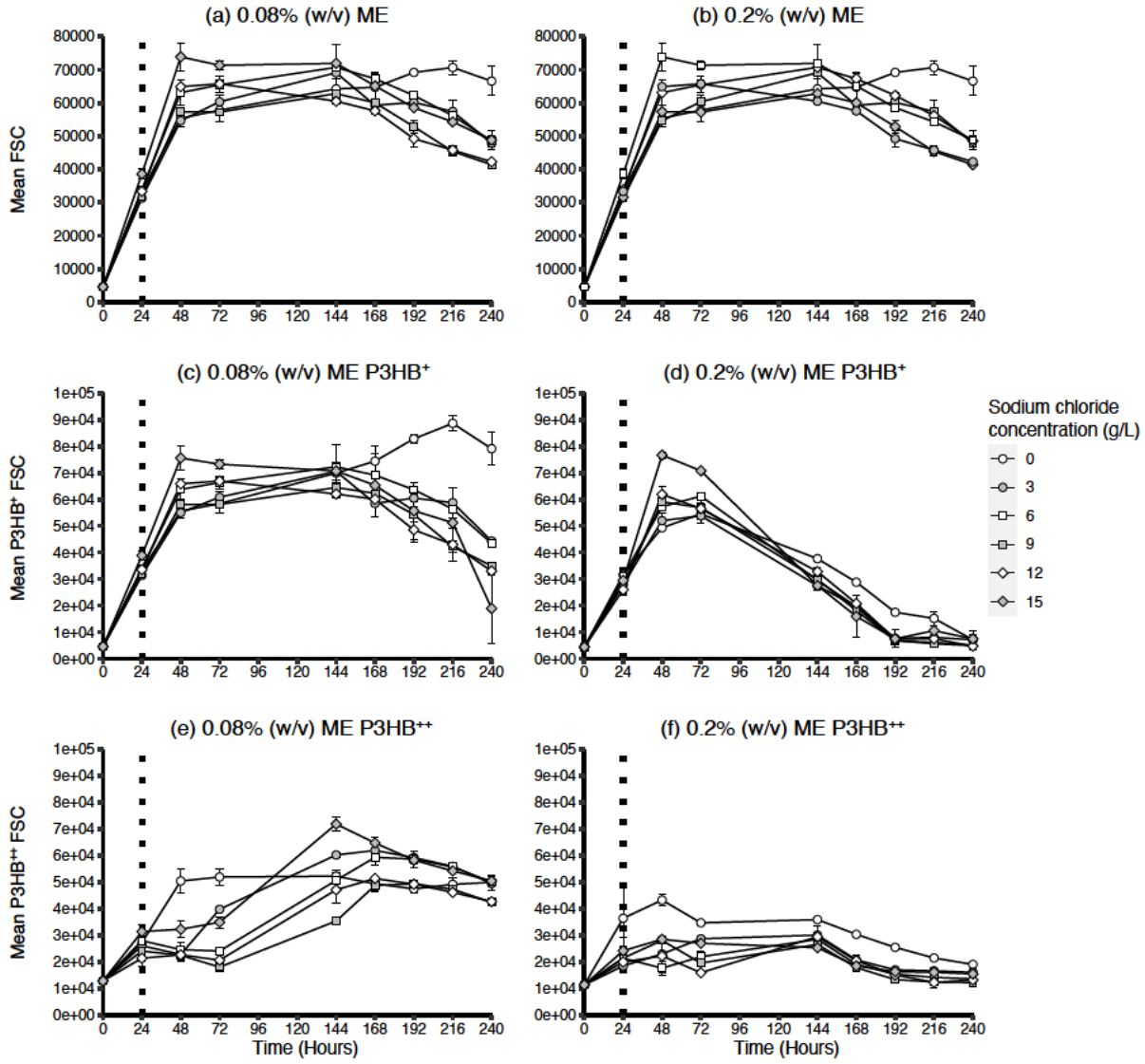


Figure 9.10 - Full data showing mean FSC (cell size) for the overall population ((a) and (b)) and the P3HB^{+} ((c) and (d)) and P3HB^{++} ((e) and (f)) populations for *C. necator* cultures containing either 0.08% or 0.2% (w/v) ME, 0, 3, 6, 9, 12 or 15 g/L sodium chloride and supplemented with 0.5% (w/v) fructose at 0 hours and 0.6% (w/v) sodium gluconate at 24 hours. Error bars represent SD. n = 3 biological replicates.

9.3 Full data corresponding to section 4.4

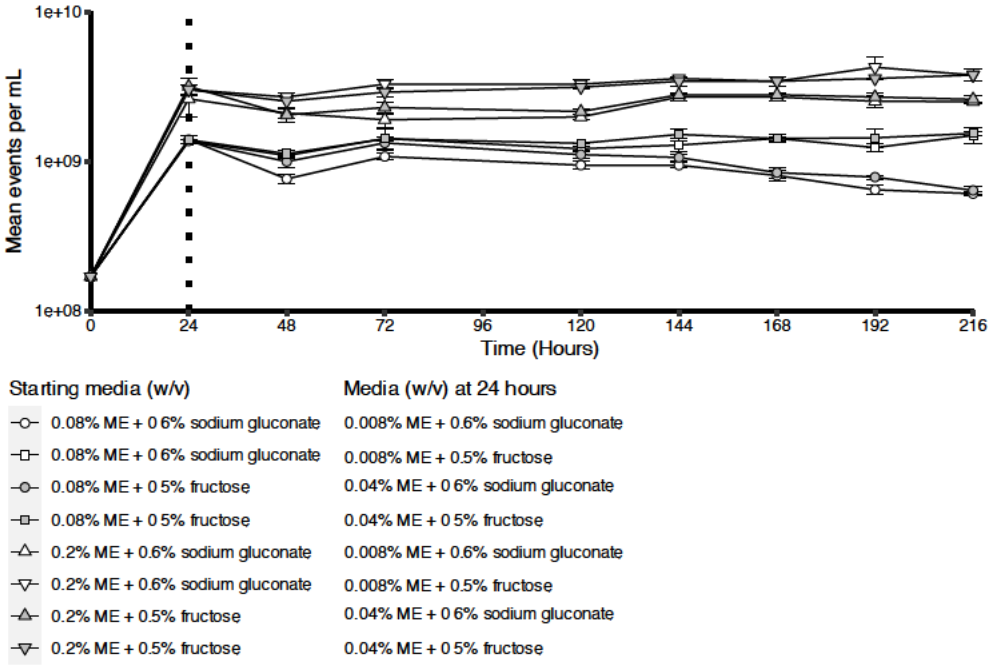


Figure 9.11 – Full mean events per mL data for *C. necator* cultures grown initially in either 0.08% or 0.2% (w/v) ME up to 24 hours when the growth media was changed to either 0.008% or 0.04% (w/v) ME. Media before and after 24 hours was supplemented with either 0.5% (w/v) fructose or 0.6% (w/v) sodium gluconate. Error bars represent SD. n = 3 biological replicates.

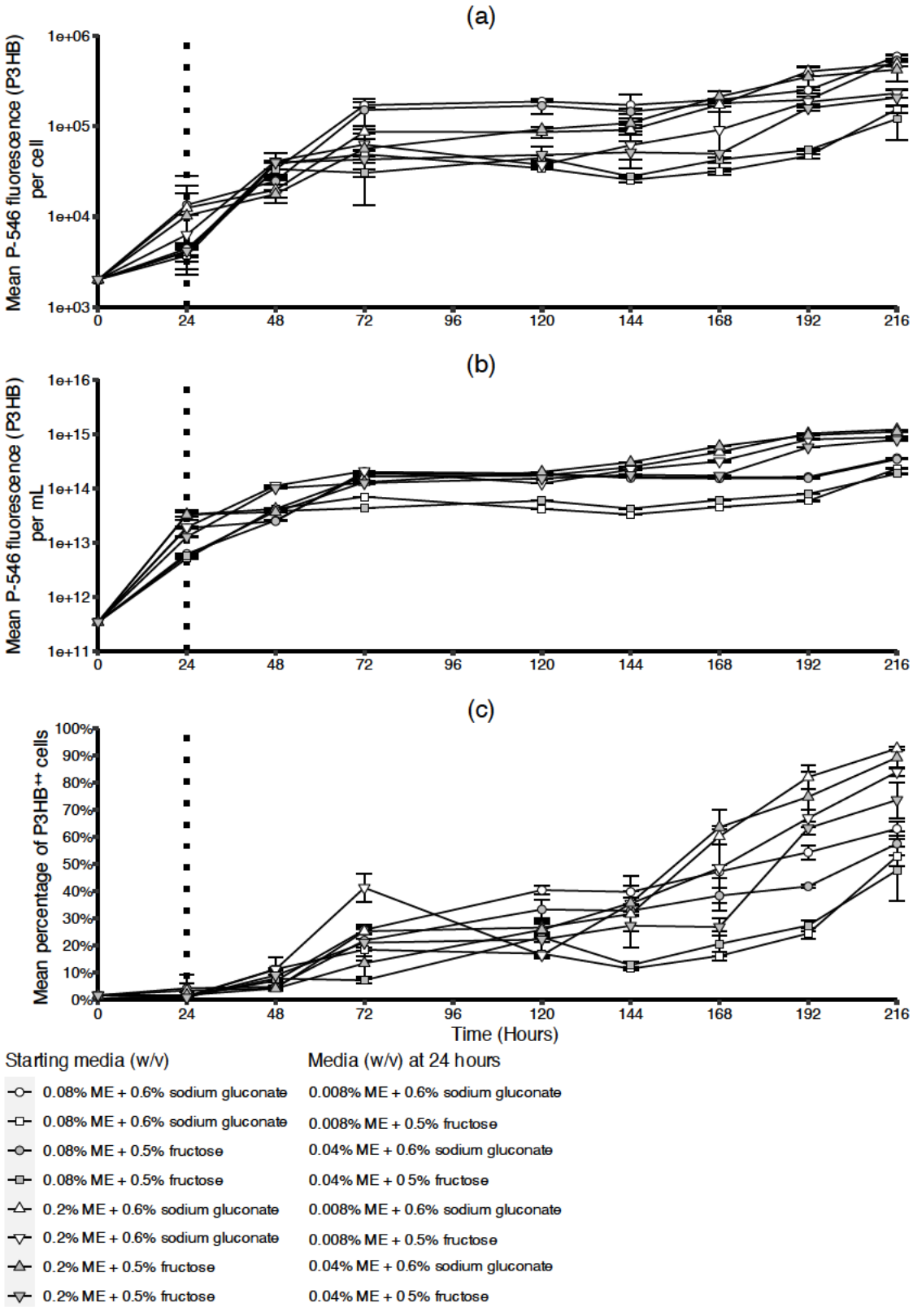


Figure 9.12 - Full data for P-546 fluorescence (P3HB) per cell ((a) and (b)) and per mL ((c) and (d)) in addition to the percentage of P3HB^{++} cells ((e) and (f)) for *C. necator* cultures grown initially in either 0.08% or 0.2% (w/v) ME up to 24 hours when the growth media was changed to either 0.008% or 0.04% (w/v) ME. Media before and after 24 hours was supplemented with either 0.5% (w/v) fructose or 0.6% (w/v) sodium gluconate. Error bars represent SD. n = 3 biological replicates.

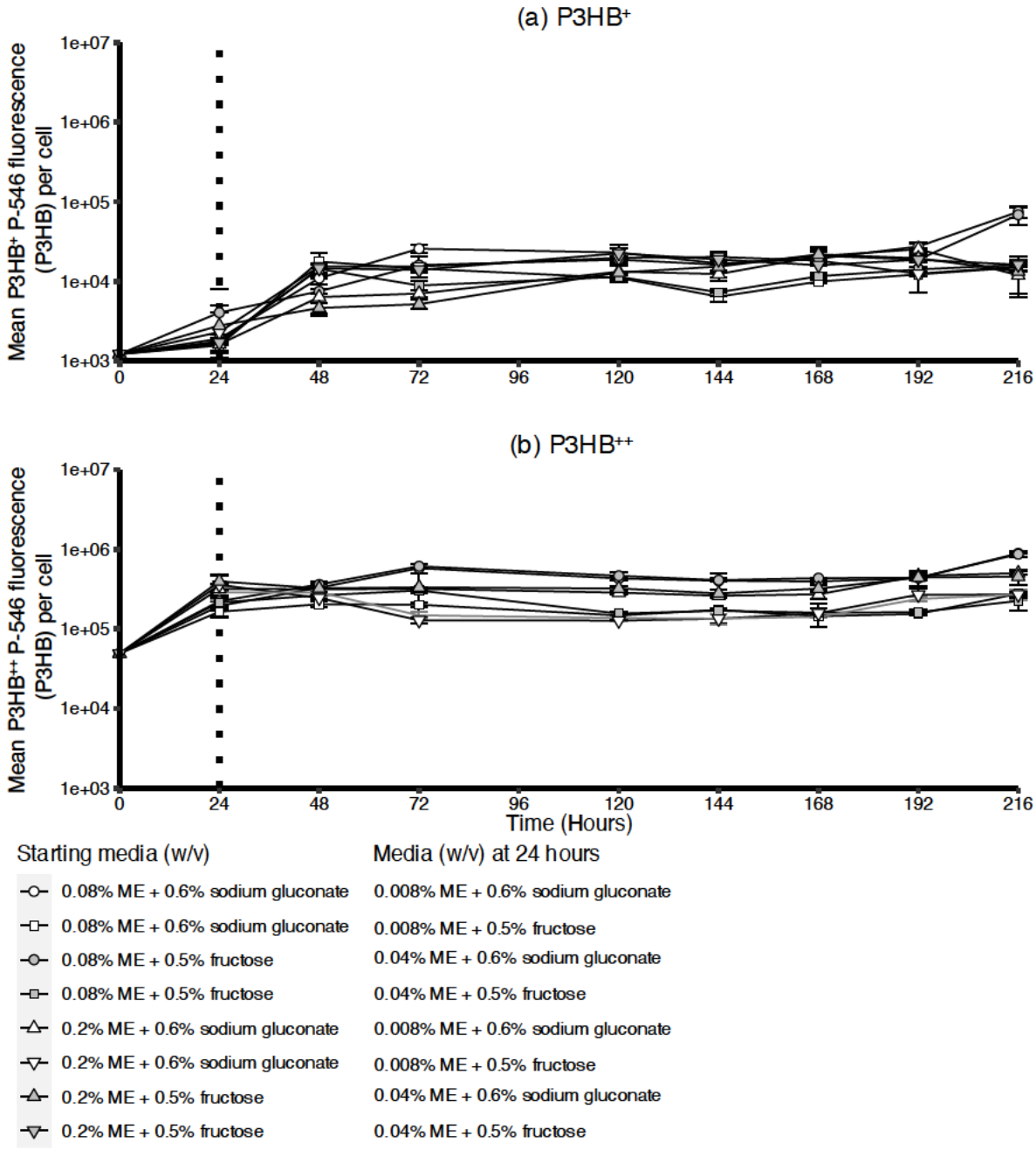


Figure 9.13 - Full data displaying P-546 fluorescence (P3HB) per cell for the P3HB^{+} and P3HB^{++} populations for *C. necator* cultures grown initially in either 0.08% or 0.2% (w/v) ME up to 24 hours when the growth media was changed to either 0.008% or 0.04% (w/v) ME. Media before and after 24 hours was supplemented with either 0.5% (w/v) fructose or 0.6% (w/v) sodium gluconate. Error bars represent SD. n = 3 biological replicates.

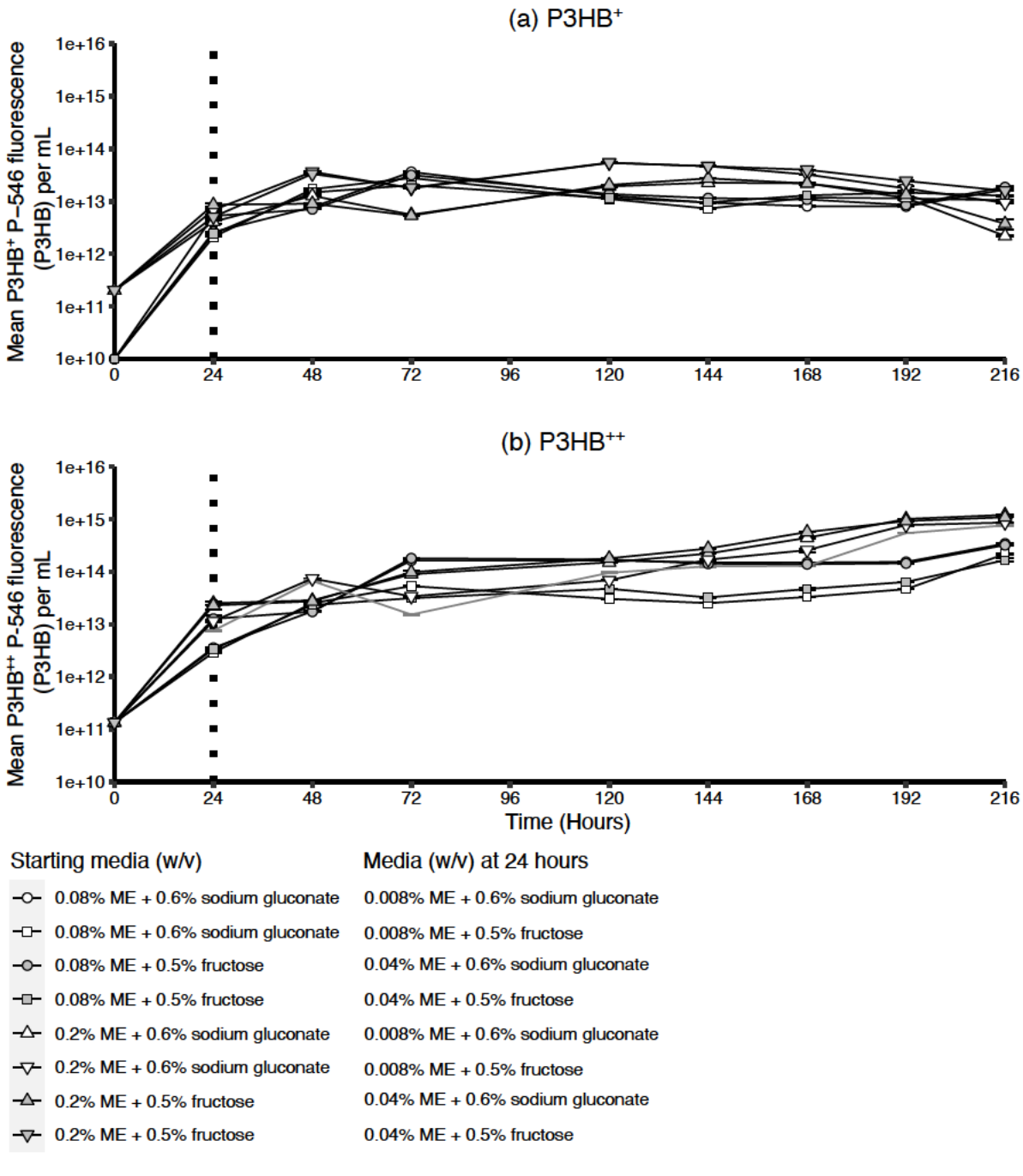


Figure 9.14 - Full data displaying P-546 fluorescence (P3HB) per mL for the P3HB^{+} and P3HB^{++} populations for *C. necator* cultures grown initially in either 0.08% or 0.2% (w/v) ME up to 24 hours when the growth media was changed to either 0.008% or 0.04% (w/v) ME. Media before and after 24 hours was supplemented with either 0.5% (w/v) fructose or 0.6% (w/v) sodium gluconate. Error bars represent SD. n = 3 biological replicates.

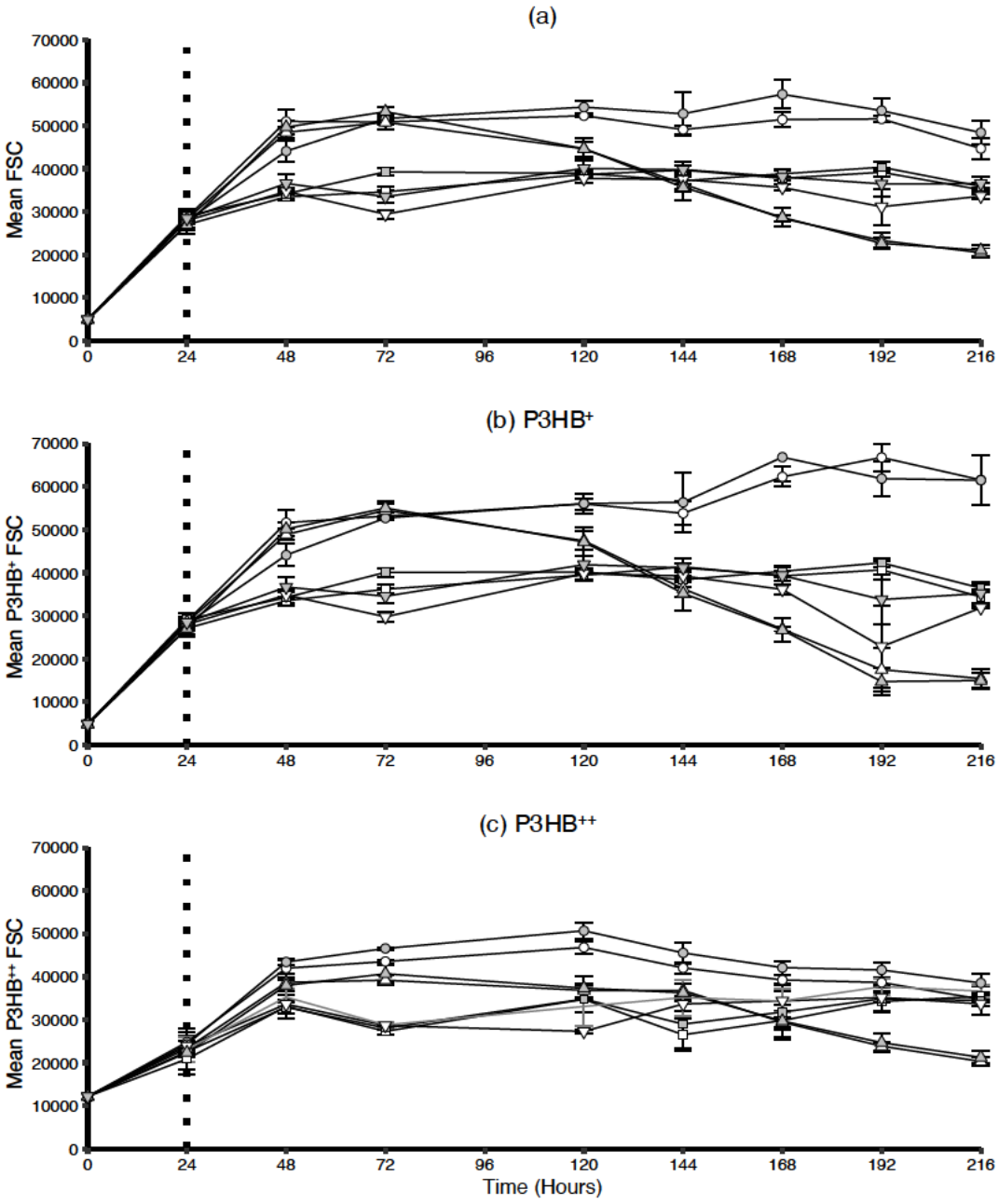


Figure 9.15 - Full data showing mean FSC (cell size) for the overall population ((a) and (b)) and the P3HB$^+$ ((c) and (d)) and P3HB^{++} ((e) and (f)) populations for *C. necator* cultures grown initially in either 0.08% or 0.2% (w/v) ME up to 24 hours when the growth media was changed to either 0.008% or 0.04% (w/v) ME. Media before and after 24 hours was supplemented with either 0.5% (w/v) fructose or 0.6% (w/v) sodium gluconate. Error bars represent SD. n = 3 biological replicates.

9.4 Data corresponding to section 4.5

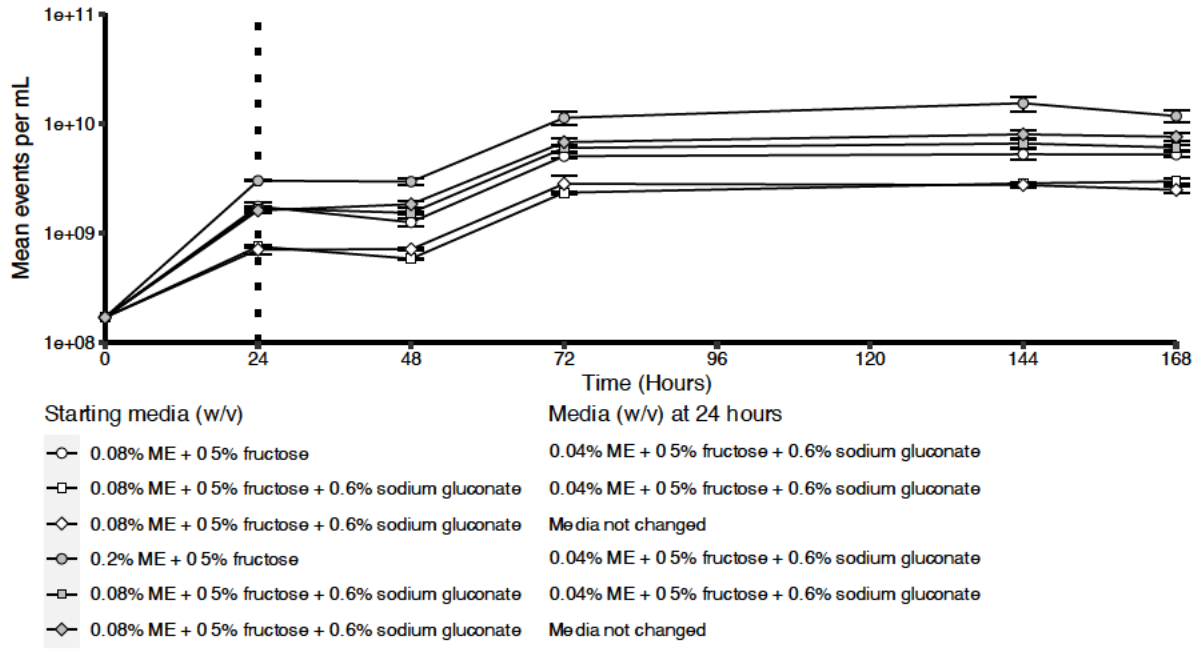
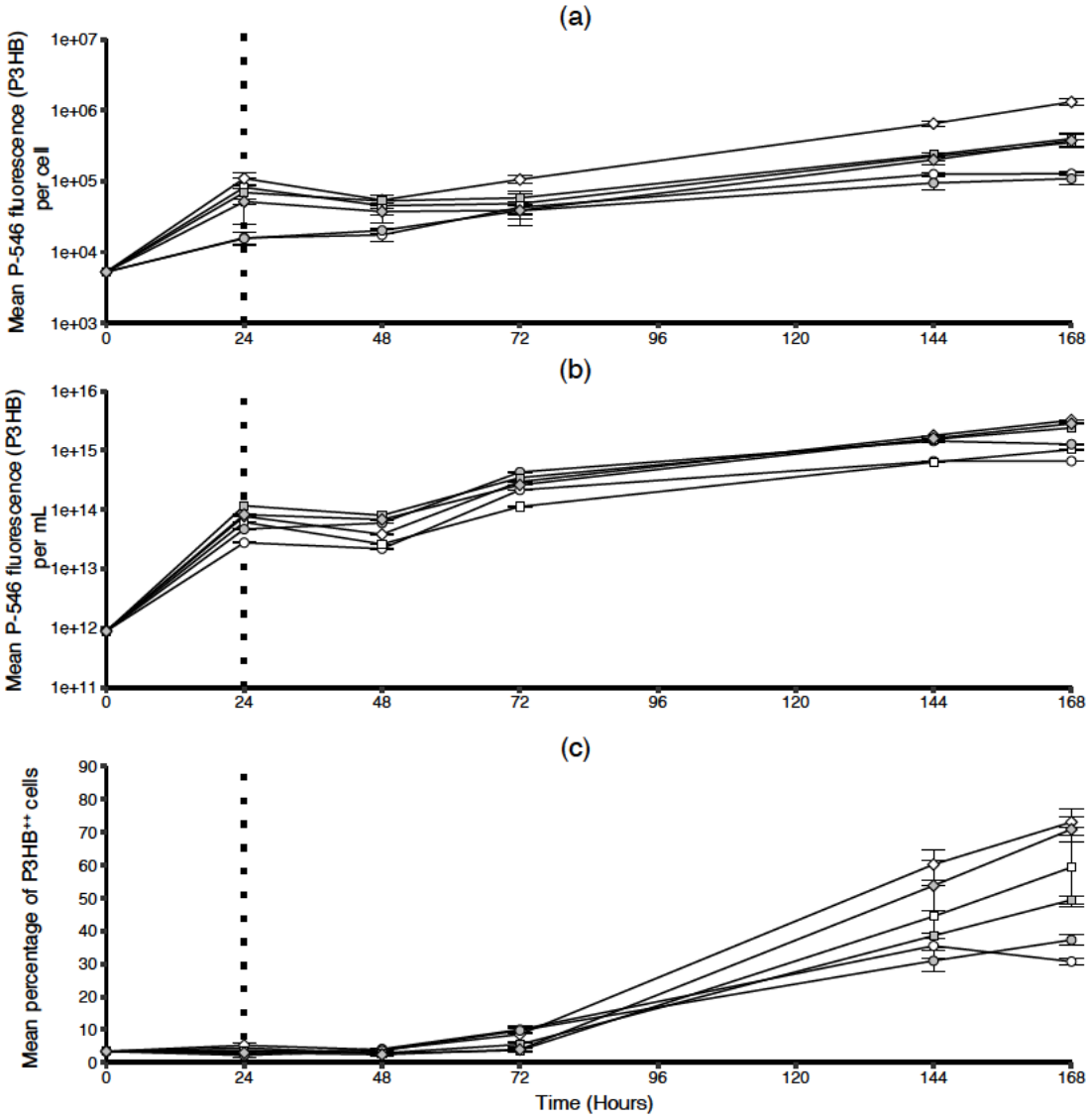


Figure 9.16 – Full mean events data for *C. necator* cultures initially containing 0.08% or 0.2% (w/v) ME and supplemented with 0.5% (w/v) fructose, 0.6% (w/v) sodium gluconate or both. Media was either changed or not changed or replaced with 0.04% (w/v) ME and supplemented with both 0.5% (w/v) fructose and 0.6% (w/v) sodium gluconate. Error bars represent SD. n = 3 biological replicates.



Starting media (w/v)	Media (w/v) at 24 hours
0.08% ME + 0.5% fructose	0.04% ME + 0.5% fructose + 0.6% sodium gluconate
0.08% ME + 0.5% fructose + 0.6% sodium gluconate	0.04% ME + 0.5% fructose + 0.6% sodium gluconate
0.08% ME + 0.5% fructose + 0.6% sodium gluconate	Media not changed
0.2% ME + 0.5% fructose	0.04% ME + 0.5% fructose + 0.6% sodium gluconate
0.08% ME + 0.5% fructose + 0.6% sodium gluconate	0.04% ME + 0.5% fructose + 0.6% sodium gluconate
0.08% ME + 0.5% fructose + 0.6% sodium gluconate	Media not changed

Figure 9.17 - Full data for P-546 fluorescence (P3HB) per cell ((a) and (b)) and per mL ((c) and (d)) in addition to the percentage of P3HB^{++} cells ((e) and (f)) for *C. necator* cultures initially containing 0.08% or 0.2% (w/v) ME and supplemented with 0.5% (w/v) fructose, 0.6% (w/v) sodium gluconate or both. Media was either changed or not changed or replaced with 0.04% (w/v) ME and supplemented with both 0.5% (w/v) fructose and 0.6% (w/v) sodium gluconate. Error bars represent SD. n = 3 biological replicates.

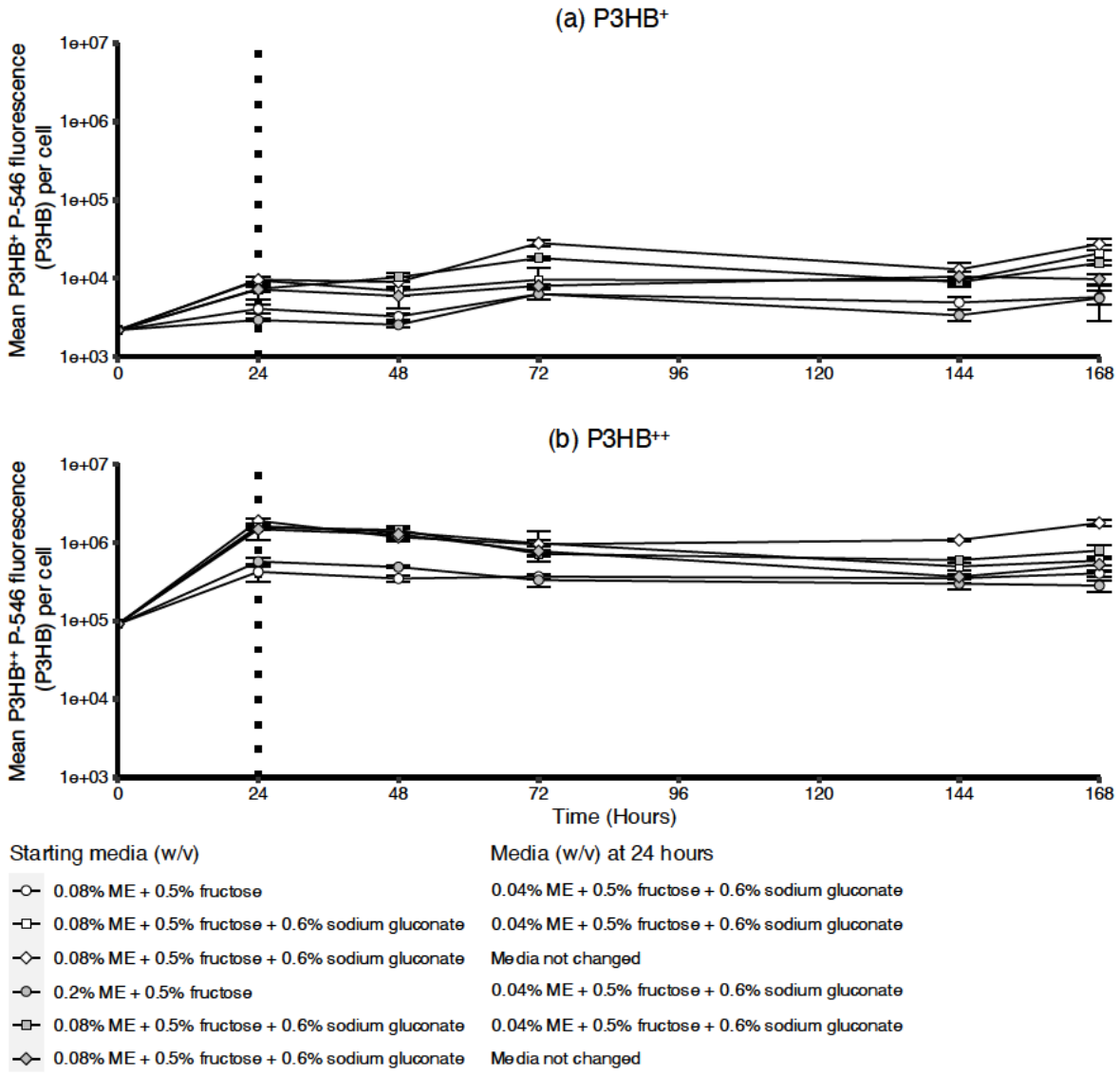


Figure 9.18 - Full data displaying P-546 fluorescence (P3HB) per cell for the P3HB^{+} and P3HB^{++} populations for *C. necator* cultures initially containing 0.08% or 0.2% (w/v) ME and supplemented with 0.5% (w/v) fructose, 0.6% (w/v) sodium gluconate or both. Media was either changed or not changed or replaced with 0.04% (w/v) ME and supplemented with both 0.5% (w/v) fructose and 0.6% (w/v) sodium gluconate. Error bars represent SD. n = 3 biological replicates.

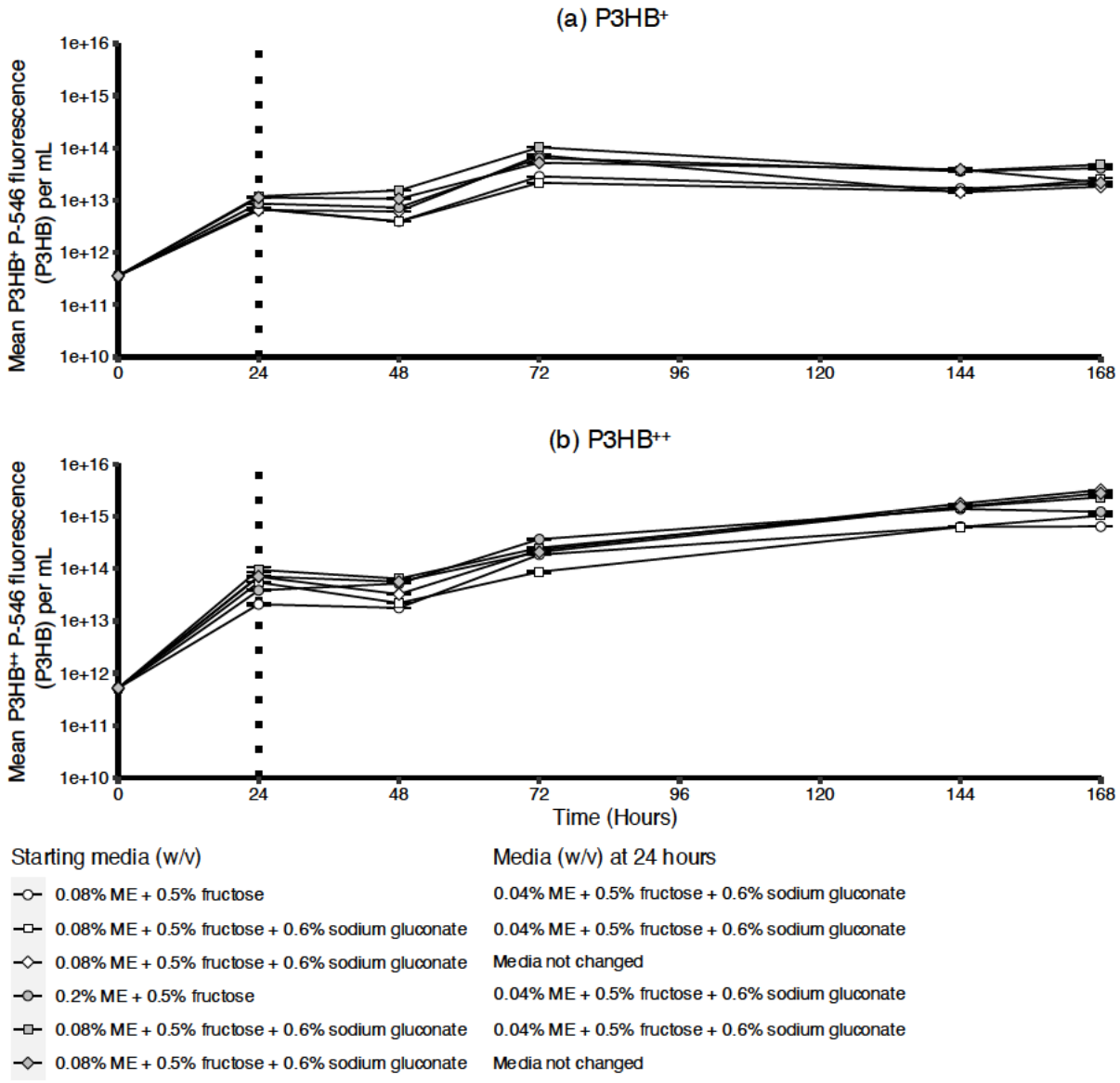


Figure 9.19 - Full data displaying P-546 fluorescence (P3HB) per mL for the P3HB^{+} and P3HB^{++} populations for *C. necator* cultures initially containing 0.08% or 0.2% (w/v) ME and supplemented with 0.5% (w/v) fructose, 0.6% (w/v) sodium gluconate or both. Media was either changed or not changed or replaced with 0.04% (w/v) ME and supplemented with both 0.5% (w/v) fructose and 0.6% (w/v) sodium gluconate. Error bars represent SD. n = 3 biological replicates.

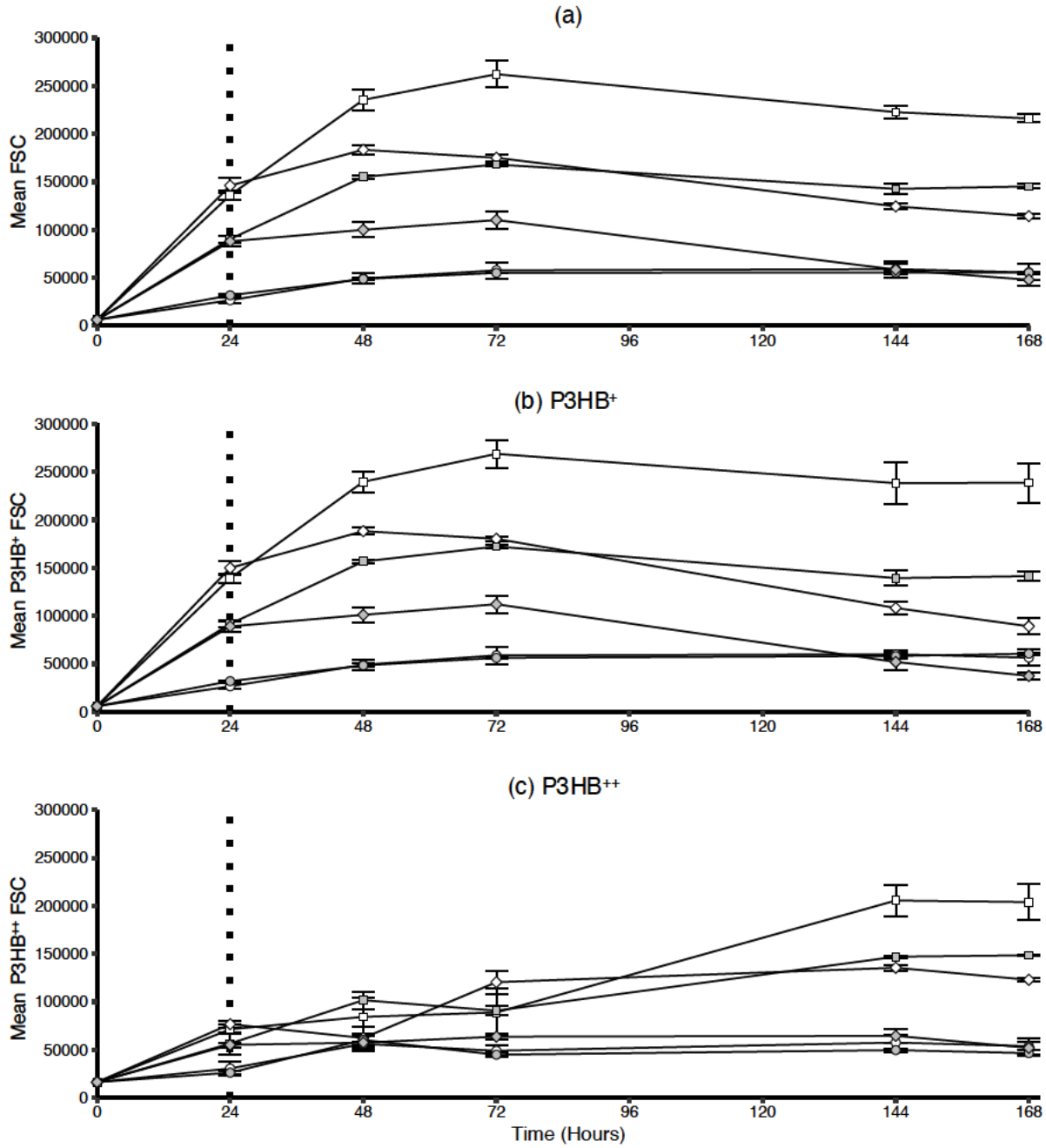


Figure 9.20 - Full data showing mean FSC (cell size) for the overall population ((a) and (b)) and the P3HB^{+} ((c) and (d)) and P3HB^{++} ((e) and (f)) populations for *C. necator* cultures initially containing 0.08% or 0.2% (w/v) ME and supplemented with 0.5% (w/v) fructose, 0.6% (w/v) sodium gluconate or both. Media was either changed or not changed or replaced with 0.04% (w/v) ME and supplemented with both 0.5% (w/v) fructose and 0.6% (w/v) sodium gluconate. Error bars represent SD. n = 3 biological replicates.